To the Graduate Council:

I am submitting herewith a dissertation written by Shawn A. Hawkins entitled "The rRNAt/rDNA ratio as a measure of nitrite oxidizing activity." I have examined the final electronic copy of this dissertation for form and content and recommend that it be accepted in partial fulfillment of the requirements for the degree of Doctor of Philosophy, with a major in Civil Engineering.

Kevin G. Robinson

Major Professor

We have read this dissertation
and recommend its acceptance:

Alice. C. Layton

Gary S. Sayler

Gregory D. Reed

Acceptance for the Council:

Anne Mayhew

Vice Chancellor and Dean of
Graduate Studies

(Original signatures are on file with official student records)

THE rRNAt/rDNA RATIO AS A MEASURE OF NITRITE OXIDIZING ACTIVITY

A Dissertation

Presented for the

Doctor of Philosophy Degree

The University of Tennessee, Knoxville

Shawn Allen Hawkins

December 2005

Copyright © 2005 by Shawn A. Hawkins

All rights reserved.

DEDICATION

This work is dedicated,
in loving memory,
to my mother
BARBARA HAWKINS

ACKNOWLEDGEMENTS

I would like to acknowledge the guidance of my major professor Dr. Kevin Robinson, who contributed significantly to the scholarly merit of this dissertation. I would like to express gratitude to Dr. Alice Layton, who helped me formulate my research ideas and critically reviewed my experimental designs and results. I would like to thank Dr. Gary Sayler, who, in addition to serving on my committee, provided funding for a large portion of my research. I would like to thank Dr. Gregory Reed for serving on my committee. At the Center for Environmental Biotechnology, I received a great deal of "bench top" help from Victoria Garrett: thank you. Tom Carson helped me put together the final electronic version of this document: thank you. I would like to thank Dr. Merve Oguz and John Shubzda for their friendship and encouragement.

I want to thank my parents, Mike and Barbara Hawkins, for instilling in me the work ethic required to achieve this goal.

I would not have completed this degree without the loving, unquestioning support of my wife, Dr. Pamela Hawkins. Her sacrifices and companionship made this achievement possible.

ABSTRACT

A bench scale nitrification reactor (BSNR) containing nitrite oxidizing bacteria (NOB) of the genus *Nitrobacter* ($\approx 1 \times 10^{10}$/L; 5 - 22% of bacteria) was used to assess the ribosomal RNA transcript (rRNAt) to ribosomal RNA gene (rDNA) ratio as an in-situ nitrite oxidizing activity metric. A quantitative PCR detection system was developed that amplified a 143 base pair sequence within the *Nitrobacter* spp. 16S - 23S intergenenic spacer region. The resulting real-time PCR (rDNA) and real-time RT-PCR (rRNAt) assays were specific, accurate, and sensitive, requiring three replicate nucleic acid extracts to reliably detect a true 2-fold concentration difference in BSNR mixed liquor samples. These assays were used to establish upper (1.8) and lower (0.69) ratio prediction intervals ($\alpha = 0.10$) for the BSNR operating at high nitrification efficiency. These intervals served as benchmarks when the ratio was measured in all subsequent experiments. It was hypothesized that during NOB inhibition the ratio would decline below 0.69 and during unlimited nitrite oxidation exceed 1.8.

When the *Nitrobacter* rRNAt/rDNA ratio was measured in a batch nitrite oxidation experiment, the metric value increased monotonically from a lower limit less than 0.10 during nitrite starvation to an upper limit greater than 3.0 eight hours after unlimited nitrite oxidation began. The ratio declined monotonically back to 0.10 within 4 hours of nitrite exhaustion. Because of the slow *Nitrobacter* grow rate, the rDNA concentration ($\approx 6 \times 10^9$ copies/L) did not change appreciably. Thus, the metric response was mediated by rRNAt abundance that varied as the growth prospect changed from unfavorable (nitrite starvation: $\approx 5 \times 10^8$ copies/L), to favorable (excess nitrite: $\approx 3 \times 10^{10}$ copies/L), and back to unfavorable (nitrite starvation: $\approx 5 \times 10^8$ copies/L). This demonstrated that quantitative PCR is better suited to detect activity as opposed population changes in slow growing bacteria.

Batch inhibition experiments supported a hypothesized negative monotonic correlation between the *Nitrobacter* rRNAt/rDNA ratio and the inhibitor concentration and fraction inhibition level. For all the compounds studied, the ratio was significantly

reduced (< 0.69) after 4.5 hours of exposure to concentrations that extensively inhibited nitrite oxidation. However, the response varied at the same inhibition level for the different inhibitors investigated. For 3,5-DCP (an uncoupler), the ratio dropped below 0.69 at concentrations that did not significantly reduce nitrite oxidation rates, suggesting that the metric is particularly sensitive to growth inhibitors. When this compound induced near complete inhibition of nitrite oxidation, the ratio dropped to ≈ 0.06. For azide and H^+, the ratio fell below 0.69 only if unlimited nitrite oxidation rates were reduced by ≥ 80%. When nitrite oxidation was completely inhibited by a sudden pH change to 5.0, the ratio fell to ≈ 0.3. A pH change to 4.5 also stopped nitrite oxidation, but the ratio did not decline. This indicated that the metric response can be disrupted if rRNAt processing is inhibited.

Though widely reported as an NOB inhibitor in the literature, free ammonia did not significantly reduce nitrite oxidation rates while ammonia oxidizing bacteria were inhibited. However, nitrite oxidation was significantly inhibited at low free ammonia concentrations if the ammonia oxidizing bacteria were allowed to remain active. This was accompanied by a low (≈ 0.10) rRNAt/rDNA ratio.

In a staged BSNR inhibition experiment, the *Nitrobacter* rRNAt/rDNA ratio accurately reflected nitrite oxidizing activity. The ratio dropped significantly (< 0.69) 22 hours before the nitrification efficiency fell below 90%. When nitrite oxidizing activity was later recovered, the ratio increased significantly (> 0.69) before this was apparent in the reactor soluble nitrogen data.

In summary, a wide range of experiments suggested the rRNAt/rDNA ratio was an effective monitor of in-situ nitrite oxidation activity. The metric could possibly be used to identify, remediate, and forecast nitrification and N-removal instability during wastewater treatment.

TABLE OF CONTENTS

CHAPTER 1.0 INTRODUCTION 1
1.1 Current Problems 1
1.2 Research Proposal 3
1.3 Research Goals and Objectives 6

CHAPTER 2.0 LITERATURE REVIEW 8
2.1 Nitrification 8
2.1.1 Stoichiometry and substrates 8
2.1.2 Phylogeny 10
2.1.3 Dominant nitrifier genera in wastewater treatment systems 12
2.2 Nitrifiers Grow Slowly With Low Yield 13
2.2.1 Factors that contribute to low growth rate and yield 14
2.2.2 Nitrifier growth rates control single sludge reactor design 17
2.3 Nitrifier Inhibition 18
2.3.1 AOB vs. NOB: which nitrifier is more susceptible to inhibition? 18
2.3.2 Selective inhibitors of ammonia and nitrite oxidation 20
2.3.3 Propensity for nitrite buildup during wastewater treatment 21
2.3.4 Nitrifier substrates may be inhibitory 22
2.3.5 Oxygen limitations 26
2.4 Alternate N-Conversion Pathways Promoting Partial Nitrification 27
2.4.1 Denitritification 28
2.4.2 Anaerobic ammonia oxidation 29
2.4.3 Summary 31
2.5 Molecular Enumeration of Bacterial Population and Activity 31
2.5.1 The polymerase chain reaction 32
2.5.2 The limitations of enumerative data 36
2.5.3 Activity assessments using the polymerase chain reaction 37
2.6 Mechanistic Aspects of Bacterial Activity 39
2.6.1 RNA/DNA and rRNA/rDNA ratios 40
2.6.2 Ribosomal gene transcript 40
2.7 Summary 47

CHAPTER 3.0 MATERIALS AND METHODS 48
3.1 Overview of Experimental Approach 48
3.2 Bench Scale Nitrification Reactor 50
3.2.1 Seed 50
3.2.2 Influent composition 52
3.2.3 Reactor construction and operating technique 53

3.2.4 Temperature 53
3.2.5 pH 54
3.2.6 Oxygen 54
3.3 *Nitrobacter hamburgensis* Culture 55
3.4 Analytical Measurements 55
3.4.1 Suspended solids 55
3.4.2 Nitrogen 56
3.5 Electrolytic Respirometry 57
3.6 Nucleic Acid Extraction 58
3.6.1 DNA 58
3.6.2 RNA 59
3.7 Clone Library Construction 61
3.7.1 PCR amplification 61
3.7.2 Cloning 61
3.7.3 Plasmid extraction 62
3.7.4 Sequencing 63

CHAPTER 4.0 DETECTION SYSTEM DESIGN AND EVALUATION 64
4.1 Introduction 64
4.2 Identifying a BNSR NOB 64
4.2.1 Clone library of BSNR bacterial 16S - 23S ISR sequences 65
4.2.2 Which NOB is dominant in the BSNR? 67
4.3 *Nitrobacter* Specific 16S - 23S ISR Real-Time PCR Primers 68
4.3.1 Initial alignment and primer design guidelines 68
4.3.2 *Nitrobacter hamburgensis* ISR sequence diversity 69
4.3.3 *Nitrobacter* specific PCR primers 70
4.4 Primer Melting Temperature and Specificity 71
4.4.1 Temperature gradient PCR 72
4.4.2 Specificity 72
4.5 *Nitrobacter* Specific 16S - 23S ISR Real-Time PCR Probe 73
4.6 Real-Time PCR Optimization 74
4.6.1 *Nitrobacter* rDNA standards 74
4.6.2 Optimization 75
4.7 Real-Time RT-PCR Optimization 77
4.7.1 *Nitrobacter* rRNAt standards 77
4.7.2 Optimization 82
4.8 PCR Efficiency and Inhibition Evaluations 83
4.8.1 Real-time PCR 83
4.8.2 Real-time RT-PCR 85
4.8.3 Summary 87
4.9 Sample Volume and Real-Time PCR Statistical Power Analyses 88

4.9.1 Real-time PCR 88
4.9.2 Real-time RT-PCR 92
4.10 *Nitrobacter* as a Dominant Nitrite Oxidizer in the BSNR 94
4.11 Summary 98

CHAPTER 5.0 *NITROBACTER* rRNAt/rDNA RANGE AND DYNAMICS 100
5.1 Introduction 100
5.2 BSNR *Nitrobacter* rRNAt/rDNA Prediction Intervals 101
5.2.1 Method 102
5.2.2 Results 102
5.2.3 Summary 113
5.3 The *Nitrobacter* rRNAt/rDNA Ratio Range and Rate of Change 113
5.3.1 Hypotheses 114
5.3.2 Experiment execution and objectives 115
5.3.3 Results 116
5.4 Summary 126

CHAPTER 6.0 BATCH RESPIROMETRIC INHIBITION EXPERIMENTS 128
6.1 Introduction 128
6.1.1 Experimental approach 129
6.1.2 Overview of the inhibition assay 131
6.1.3 Hypotheses 133
6.2 3,5-DCP 135
6.2.1 The inhibition mechanism 135
6.2.2 3,5-DCP dose-response curve 139
6.2.3 3,5-DCP inhibition experiments with RNA and DNA extractions 143
6.2.4 Summary 150
6.3 Azide 152
6.3.1 The inhibition mechanism 152
6.3.2 Azide dose-response curve 155
6.3.3 Azide inhibition experiments with RNA and DNA extractions 158
6.3.4 Summary 164
6.4 H^+ 166
6.4.1 The inhibition mechanism 166
6.4.2 H^+ dose-response curve 168
6.4.3 H^{+-} inhibition experiments with RNA and DNA Extractions 170
6.4.4 Summary 181
6.5 *Nitrobacter* rRNAt/rDNA Ratio Response to Different Inhibitors 181
6.6 Inhibition Experiment Quality Control 185
6.7 Summary 186

CHAPTER 7.0 BATCH AMMONIA INHIBITION EXPERIMENTS 189
7.1 Introduction 189
7.2 Free Ammonia Inhibition of Nitrite Oxidation 189
7.2.1 The inhibition mechanism 189
7.2.2 Preliminary free ammonia inhibition experiments 190
7.3 Inhibition of Nitrite Oxidation during High AOB Activity 192
7.3.1 Hypothesis for NOB inhibition during high AOB activity 192
7.3.2 Method 192
7.3.3 Results 193
7.4 Summary 208

CHAPTER 8.0 BSNR INHIBITION EXPERIMENT 209
8.1 Introduction 209
8.2 Overview of the BSNR Inhibition Experiment 210
8.2.1 Phase 1 - the pH control system is disabled 211
8.2.2 Phase 2 - the pH setpoint is changed to 8.0 214
8.2.3 Phase 3 - the pH setpoint is changed to 7.2 215
8.3 Results 215
8.3.1 Phase 1 220
8.3.2 Phase 2 226
8.3.3 Phase 3 231
8.4 Summary 238

CHAPTER 9.0 CONCLUSIONS AND IMPLICATIONS 242
9.1 Conclusions 242
9.2 Implications 246

REFERENCES 250

APPENDIXES 281
Appendix A Quantitative PCR Primer and Probe Design Data 282
Appendix B Quantitative PCR Optimization Data 324
Appendix C Quantitative PCR Quality Control Data 333
Appendix D *Nitrobacter* rRNAt/RNA Ratio Range and Rate of Change Data 342
Appendix E Batch Respirometric Inhibition Experiment Data 352
Appendix F BSNR Inhibition Experiment Data 375

VITA 383

LIST OF TABLES

Table 1 Heterotrophic and nitrifier substrate electron work potential. 14

Table 2 Free ammonia inhibition of ammonia and nitrite oxidation. 23

Table 3 Nitrifier oxygen half saturation coeffcients. 26

Table 4 Molecular investigations of bacterial activity using RNA/DNA and rRNA/rDNA ratios and rRNAt abundance. 41

Table 5 A list of BSNR influent constituents and their concentrations. 52

Table 6 Summary of toal bacterial rDNA and *Nitrobacter* rDNA copy abundance in replicate BSNR DNA extracts 95

Table 7 *Nitrobacter* rRNAt, rDNA, and the rRNAt/rDNA ratio in the BSNR over the 11 week time period used to establish ratio prediction intervals..... 104

Table 8 Sample descriptions for the experiment used to assess the range and dynamics of the *Nitrobacter* rRNAt/rDNA ratio. 116

Table 9 Nitrite and *Nitrobacter* molecular data for the experiment used to assess the range and dynamics of the *Nitrobacter* rRNAt/rDNA ratio (Figure 13). 119

Table 10 The effect of the classical respiratory chain uncouplers 2,4-DNP, (C)CCP, and FCCP on *Nitrobacter*. 136

Table 11 *Nitrobacter* molecular data for a respirometric inhibition experiment with 3,5-DCP (Figure 17; Experiment I). 146

Table 12 *Nitrobacter* molecular data for a respirometric inhibition experiment with 3,5-DCP (Figure 17; Experiment II). 147

Table 13 The effect of azide (% inhibition) on *Nitrobacter* cell free extract and whole cell activity. 154

Table 14 *Nitrobacter* molecular data for a respirometric inhibition experiment with azide (Figure 20; Experiment III). 161

Table 15 *Nitrobacter* molecular data for a respirometric inhibition experiment with azide (Figure 20; Experiment IV). 162

Table 16 *Nitrobacter* molecular data for a respirometric inhibition experiment with acid (Figure 24; Experiment V). 176

Table 17 *Nitrobacter* molecular data for a respirometric inhibition experiment with acid (Figure 24; Experiment VI). 177

Table 18 BSNR NOB inhibition experiments with free ammonia. 191

Table 19 The results for two batch respirometric inhibition experiments using the BSNR biomass and ammonia doses. 196

Table 20 *Nitrobacter* molecular data for a respirometric inhibition experiment with ammonia (Figure 29; Experiment VII). 205

Table 21 Outline of the BSNR inhibition experiment conducted in three phases initiated by perturbations of the reactor pH control system.. 211

Table 22 Timing of the sample events during the BSNR inhibition experiment..... 216

Table 23 pH, DO, MLSS, soluble nitrogen concentrations, and the nitrification efficiency during the BSNR inhibition experiment. 217

Table 24 *Nitrobacter* molecular data during the BSNR inhibition experiment..... 218

Table A-1 Cloned BSNR DNA sequences (clone library 1) generated with the conserved bacterial PCR primers 1055f and 23Sr.. 283

Table A-2 Blastn (Altschul et al., 1990; Altschul et al., 1997) sequence analysis results for Table A-1.. 292

Table A-3 A ClustalX percent identify matrix for the 16S portion of the sequences in Table A-1 and the major phylogenic branches of the nitrifiers. 300

Table A-4 Cloned *Nitrobacter hamburgensis* DNA sequences generated with the conserved bacterial primers 1055f and 23Sr (clone library 2).. 306

Table A-5 A melting temperature analysis for potential forward and reverse primers from regions 13 and 16, respectively, of the *Nitrobacter* 16S - 23S ISR (Figure A-3).. 308

Table A-6 The results of a secondary structure and specificity analysis of primers from regions 13 and 16 of the *Nitrobacter* 16S - 23S ISR (Figure A-3).. 310

Table A-7 Cloned BSNR DNA sequences generated with *Nitrobacter* specific primers (Table A-5) (clone library 3). 315

Table A-8 Cloned *Nitrobacter hamburgensis* DNA sequences generated with *Nitrobacter* specific primers (Table A-5) (clone library 4).. 316

Table A-9 A melting temperature analysis of potential real-time PCR antisense probe sequences within region 16 of the *Nitrobacter* 16S - 23S ISR (Figure A-3). 317

Table A-10 A secondary structure and specificity analysis of potential real-time PCR antisense probe sequences (Table A-9).. 320

Table C-1 Quantitative PCR results for dilutions of a BSNR DNA and RNA extract..... 334

Table C-2 Quantitative PCR results for BSNR DNA and RNA extracts from different mixed liquor sample volumes. 336

Table C-3 A statistical summary of the *Nitrobacter* rDNA and rRNAt data in Table C-2.. 339

Table C-4 ANOVA comparisons of the *Nitrobacter* rDNA and rRNAt data in Table C-2 and Table C-3..... 340

Table C-5 Total bacterial rDNA and *Nitrobacter* rDNA gene copy number in replicate BSNR DNA extracts. 341

Table D-1 Soluble nitrogen, nitrification efficiency, and MLVSS in the BSNR over the 11 week time period used to establish *Nitrobacter* rRNAt/rDNA upper and lower prediction intervals..... 343

Table D-2 Quantitative PCR results for the 11 week period used to establish BSNR *Nitrobacter* rRNAt/rDNA prediction intervals. 344

Table D-3 Quantitative PCR results for an experiment that evaluated the *Nitrobacter* rRNAt/rDNA ratio range and dynamics..... 348

Table E-1 Results for batch respirometric inhibition experiments using the inhibitor 3,5-DCP..... 353

Table E-2 Quantitative PCR results for a 3,5-DCP respirometric inhibition experiment (Experiment I) (Figure 17-A)..... 355

Table E-3 Quantitative PCR results for a 3,5-DCP respirometric inhibition experiment (Experiment II) (Figure 17-B). 357

Table E-4 Results for batch respirometric inhibition experiments using the inhibitor azide. 359

Table E-5 Quantitative PCR results for an azide respirometric inhibition experiment (Experiment III) (Figure 20-A). 361

Table E-6 Quantitative PCR results for an azide respirometric inhibition experiment (Experiment IV) (Figure 20-B). 363

Table E-7 Results for batch respirometric inhibition experiments using the inhibitor H^+ (sudden acidic pH changes). 365

Table E-8 Quantitative PCR results for an H^+ (acid) respirometric inhibition experiment (Experiment V) (Figure 24-A). 367

Table E-9 Quantitative PCR results for an H^+ (acid) respirometric inhibition experiment (Experiment VI) (Figure 24). 369

Table E-10 Quantitative PCR results for an ammonia respirometric inhibition experiment (Experiment VII) (Figure 29)..... 371

Table F-1 Quantitative PCR results for a BSNR inhibition experiment (Figure 36). 376

LIST OF FIGURES

Figure 1 Diagram comparing standard reduction potentials for nitrifier and heterotrophic substrate electrons..... 15

Figure 2 Diagram of a dual labeled linear probe for real-time PCR including signal (FAM) and quencher (BHQ-1) fluorophore structures. 34

Figure 3 Schematic diagram (A - F) of a real-time PCR cycle illustrating fluorescent signal generation via Taq polymerase exonuclease digestion of a dual labeled linear probe during primer extension..... 35

Figure 4 Outline of the experimental approach used to evaluate the rRNAt/rDNA ratio as an NOB activity metric. 49

Figure 5 Schematic diagram of the BSNR. 51

Figure 6 A PCR inhibition investigation of the optimized *Nitrobacter* rDNA real-time PCR detection system. 84

Figure 7 A PCR inhibition investigation of the optimized *Nitrobacter* rRNAt real-time RT-PCR detection system.. 86

Figure 8 A test of the discriminatory power of the *Nitrobacter* rDNA real-time PCR assay. 90

Figure 9 A test of the discriminatory power of the *Nitrobacter* rRNAt real-time RT-PCR assay. 93

Figure 10 Nitrogen (A) and MLVSS and molecular data (B) collected from the BSNR over the 11 week time period used to establish upper and lower *Nitrobacter* rRNAt/rDNA ratio prediction intervals..... 103

Figure 11 An empirical distribution function (A: operating day indicated) and boxplot (B) of *Nitrobacter* rRNAt/rDNA ratio data collected during 10 weeks of continuous high nitrification efficiency (≥ 90%)..... 110

Figure 12 Respirograms for six vessels (A - F) in the experiment used to assess the *Nitrobacter* rRNAt/rDNA ratio range and dynamics for change. 117

Figure 13 A composite respirogram with overlaying nitrite data (A) and *Nitrobacter* rDNA, rRNAt, and rRNAt/rDNA ratio data (B) for six vessels (Figure 12) in the experiment used to assess the *Nitrobacter* rRNAt/rDNA ratio range and dynamics for change..... 118

Figure 14 Outline of the experimental approach used to evaluate the *Nitrobacter* rRNAt/rDNA ratio response to mechanistically distinct inhibitors. 130

Figure 15 The results of a respirometric inhibition experiment using 3,5-DCP 140
Figure 16 The effect of 3,5-DCP on BSNR nitrite oxidation-dependent respiration rates 142
Figure 17 The effect of 3,5-DCP on the *Nitrobacter* rRNAt and rDNA concentrations during two batch respirometric inhibition experiments (Experiment I and Experiment II). 144
Figure 18 The effect of 3,5-DCP on the *Nitrobacter* rRNAt/rDNA ratio 151
Figure 19 The effect of azide on BSNR nitrite oxidation-dependent respiration rates 156
Figure 20 The effect of azide on the *Nitrobacter* rRNAt and rDNA concentrations during two batch respirometric inhibition experiments (Experiment III and Experiment VI). 159
Figure 21 The effect of azide on the *Nitrobacter* rRNAt/rDNA ratio 165
Figure 22 The effect of pH changes on BSNR nitrite oxidation-dependent respiration rates 169
Figure 23 Variability in NOB adaptive potential following inhibition with acid doses 171
Figure 24 The effect of a sudden change to low pH (H^+ dose) on the *Nitrobacter* rRNAt and rDNA concentrations during two batch respirometric inhibition experiments (Experiment V and Experiment VI). 174
Figure 25 The effect H^+ on the *Nitrobacter* rRNAt/rDNA ratio 180
Figure 26 The effect of mechanistically distinct inhibitors on the *Nitrobacter* rRNAt/rDNA ratio 182
Figure 27 An examination of the residual nitrite oxidation activity in BSNR samples during batch respirometric inhibition experiments when the fraction inhibition exceeded 0.50 184
Figure 28 A plot of paired NOR and OUR inhibition calculations from the 3,5-DCP, azide, and H^+ respirometric inhibition experiments 187
Figure 29 An evaluation of NOB inhibition at high ammonia concentrations with inhibited and uninhibited AOB present. 194
Figure 30 Soluble nitrogen data for vessel 5 during a preliminary ammonia inhibition experiment with uninhibited AOB. 199
Figure 31 The effect of ammonia doses on *Nitrobacter* rDNA and rRNAt 204
Figure 32 The effect of reduced pH on aerobic activity during ammonia oxidation in unbuffered media 213

Figure 33 The response of various operational parameters after disabling the BSNR pH control system to initiate phase 1 of a staged inhibition experiment..... 221

Figure 34 The response of various operational parameters after enabling the BSNR pH control system at a setpoint of 8.0 to initiate phase 2 of a staged inhibition experiment..... 227

Figure 35 The response of various operational parameters after changing the BSNR pH control system setpoint from 8.0 to 7.2 to initiate phase 3 of a staged inhibition experiment..... 232

Figure 36 The overall response of various operational parameters during a staged BSNR inhibition experiment 239

Figure 37 Schematic diagram illustrating inferences for the NOB activity level given different ranges of *Nitrobacter* rRNA/rDNA ratio value when complete nitrification is promoted at 30°C. 247

Figure A-1 A phylogram of clone library 1 (Table A-1) that includes the major phylogenic branches of nitrifying bacteria as outgroups. 302

Figure A-2 Two tRNA sequences identified in the clone 1-20 DNA sequence (Table A-1) using tRNAscan-SE version 1.21. 303

Figure A-3 A ClustalX alignment of the 16S - 23S ISRs for clone 1-20 (Table A-1), *Nitrobacter* spp., and two closely related α-Proteobacteria..... 304

Figure A-4 Electrophoresis gel images of temperature gradient PCR products using *Nitrobacter* specific primers (Table A-5) and DNA extracts from either the BSNR mixed liquor (A) or a *N. hamburgensis* mixtrophic culture (B)..... 312

Figure A-5 Electrophoresis gel images of temperature gradient PCR products using *Nitrobacter* specific primers (Table A-5) and DNA extracts from either the BSNR mixed liquor (A) or a *N. hamburgensis* mixtrophic culture (B)..... 313

Figure A-6 Electrophoresis gel images documenting cloning of PCR products obtained with *Nitrobacter* specific primers (Table A-5) and either BSNR (b) or *N. hamburgensis* (n) DNA extracts.. 314

Figure B-1 Threshold cycle (A) and light yield (B) versus annealing temperature/Mg^{2+} gradients for real-time PCR reactions using the *Nitrobacter* detection system with Quantitect® Probe PCR mastermix (Qiagen; Valencia, CA)..... 325

Figure B-2 Threshold cycle (A) and light yield (B) versus annealing temperature/Mg^{2+} gradients for real-time PCR reactions using the *Nitrobacter* detection system with Platinum® Quantitative PCR SuperMix-UDG (Invitrogen; Carlsbad, CA).. 326

Figure B-3 Threshold cycle (A) and light yield (B) versus annealing temperature/Mg^{2+} gradients for real-time PCR reactions using the *Nitrobacter* detection system with HotMasterMix (Eppendorf; Hamburg, Germany).. 327

Figure B-4 Threshold cycle (A and light yield (B) versus plasmid copy number/Mg^{2+} gradients for real-time PCR reactions using the *Nitrobacter* detection system with Quantitect® Probe PCR mastermix (Qiagen; Valencia, CA)..... 328

Figure B-5 Threshold cycle (A) and fluorescent light yield (B) for real-time PCR reactions (mean ± standard deviation of 3 reactions) with the *Nitrobacter* rDNA detection system and a 10^6 copies/μL standard..... 329

Figure B-6 Threshold cycle (A) and fluorescent light yield (B) for real-time PCR reactions (mean ± standard deviation of 3 reactions) with the *Nitrobacter* rDNA detection system and a 10^6 copies/μl standard..... 330

Figure B-7 Electrophoresis gel images that document linearization of a plasmid containing a BSNR *Nitrobacter* clone.. 331

Figure B-8 Electrophoresis gel image used to evaluate the integrity of an artificial *Nitrobacter* rRNAt stock solution.. 332

CHAPTER 1.0

INTRODUCTION

1.1 Current Problems

Nitrification is the chemolithotrophic oxidation of ammonia to nitrate, an aerobic biochemical process conducted in two sequential stages: ammonia $\xrightarrow{1^{st}\ Stage}$ nitrite $\xrightarrow{2^{nd}\ Stage}$ nitrate. Each stage is performed by different bacterial genera capable of either ammonia or nitrite oxidation. No known bacteria perform both stages for growth purposes (Watson et al., 1989; Hooper et al., 1997). Nitrification is promoted at municipal and industrial wastewater treatment plants (WWTPs) to meet effluent limits that are promulgated to relieve adverse effects ammonia discharge has on receiving water quality (EPA, 1993). For example, ammonia creates a large oxygen demand (4.57 mg O_2/mg NH_4^+-N) that can lower the dissolved oxygen (DO) concentration in receiving waters. The impact can be severe in instances where wastewater discharge contributes significantly to receiving stream flow and the in-stream conditions promote nitrification (USGS, 1999). Another concern is toxicity to aquatic life caused by the free form of ammonia (NH_3) (Arthur et al., 1987). Acute toxicity occurs in fish at free ammonia concentrations between ≈ 0.1 - 10 mg-N/L), while chronic exposure criteria range between ≈ 0.5 - 50 µg-N/L, depending on the pH and temperature (EPA, 1993). In some receiving waters nitrogen is the macronutrient limiting algae blooms, so ammonia or nitrate in wastewater effluents can contribute to eutrophication (EPA, 1993; USGS, 1999). To protect receiving water quality in this circumstance, nitrification is promoted as the initial step in nitrogen removal via denitrification (Benefield and Randall, 1985).

The slow growth rate of nitrifiers controls the design solid retention time (SRT) of single sludge carbon oxidation/nitrification reactors (Grady et al., 1999) that are the favored means for implementing nitrification (EPA, 1993). Since nitrification is recognized as an unstable process (Balmelle et al., 1992; Wagner, et al., 1996; Mobarry et al., 1996; Jonsson et al., 2000) that is sensitive to inhibition (Blum and Speece, 1991;

Dalzell et la., 2002) which can further lower nitrifier growth rates (Hockenbury and Grady, 1977), safety factors are added to the design SRT of these reactors (Grady et al., 1999). The addition of safety factors translates into capital and operating costs which could be partially allayed if nitrification efficiency could be improved.

Nitrification efficiency is controlled by the rates of ammonia and/or nitrite oxidation; however, the overall rate of nitrification is most often limited by ammonia oxidation (Grady et al., 1999). Further, ammonia oxidizing bacteria (AOB) are more sensitive to inhibiting compounds than the nitrite oxidizing bacteria (NOB) (Tomlinson et al., 1966; Hockenbury and Grady, 1977; Wang and Reed, 1984; Blum and Speece, 1991). Thus, nitrite buildups do not normally occur as nitrification efficiency declines. However, specific factors that selectively inhibit the NOB and produce nitrite buildups are: low DO (Jayamohan et al., 1988; Bernet et al., 2001; Bae et al., 2002; Ruiz et al., 2003; Garrido et al. ,1997), aeration patterns/duration (Turk and Mavinic, 1989a; Yoo et al., 1999; Pollice et al., 2002; Peng et al., 2004; Fux et al., 2003), influent COD/N ratio (Tseng et al., 1998), low/high/changing pH (Suthersan and Ganczarczyk, 1986; Bae et al., 2002), high free ammonia concentrations (Anthonisen et al., 1976; Suthersan and Ganczarczyk, 1986; Turk and Mavinic, 1989a), high/low temperatures (Randall and Buth, 1984a; Randall and Buth, 1984b; Bae et al., 2002), and short SRT (Hellinga et al. 1998; Pollice et al., 2002; Balmelle et al., 1992). Effluent nitrite is undesirable since this compound is linked to gastric cancer (EPA, 1993), is toxic to fish (Henze, 1991), contributes to WWTP chorine demand (Philips and Verstraete, 2000), and may inhibit AOB (Stein and Arp, 1998a; Anthonisen et al., 1976). Further, nitrite buildup may be a symptom of impending ammonia oxidation failure (Randall and Buth, 1984a; Randall and Buth, 1984b) and sludge bulking (Philips et al., 2002) Since the AOB provide the sole lithotrophic substrate for the NOB (nitrite), the NOB activity level is sensitive to factors that adversely affect both ammonia and nitrite oxidation. Thus, research on how to identify and remediate poor nitrification efficiency should focus on the NOB.

The tendency for incomplete nitrification at high ammonia concentrations, and the fact that nitrification limits nitrogen removal efficiency via denitrification (Shammas,

1986; Jayamohan et al., 1988), has led to investigations of nitrogen removal from highly nitrogenous wastewaters thorough partial nitrification (encompassing only ammonia oxidation) followed by denitritification (the use of nitrite as a terminal electron acceptor). Notable benefits of partial nitrification/denitritification include a 25% reduction in the oxygen demand for ammonia removal, a 40% reduction in the carbon requirement for nitrogen removal, 63% higher nitrogen removal rates, and lower biomass production (Voets et al., 1975; Turk and Mavinc, 1987). Interestingly, denitritification is also unstable, with NOB acclimation (increasing nitrite oxidation activity) jeopardizing these benefits (Turk and Mavinic, 1989a; Turk and Mavinic, 1989b; Villaverde et al., 2000). New reactor designs for partial nitrification/denitritification have been implemented that better limit NOB activity (Hellinga et al., 1998), but this requires short SRTs and high temperatures that are not feasible at many WWTPs.

Partial nitrification is also promoted for anaerobic ammonia oxidization (anammox) using a mixture of ammonia oxidizers and newly discovered bacteria that oxidize ammonia with nitrite as the terminal electron acceptor (Jetten et al., 1999). This is an even more efficient pathway for nitrogen removal than denitritification. However, the NOB are direct competitors of the anaerobic ammonia oxidizers, so conditions must be stringently maintained that limit NOB activity (Kuenen and Jetten, 2001).

In summary, improving the efficiency of nitrification (for ammonia removal) and partial nitrification (for nitrogen removal) could result in significant costs savings for wastewater treatment. Because NOB activity levels reflect the efficiency of both processes, quantifying the activity of these bacteria may help identify and remediate instability in both scenarios and thereby improve the cost effectiveness of wastewater treatment.

1.2 Research Proposal

Research in the last decade has been, in part, a quest to identify and enumerate the nitrifiers (mainly the AOB) in activated sludge. Fluorescent in-situ hybridization (FISH) of ribosomal nucleic acid (rRNA) has been a prominent and useful technique, revealing the spatial organization of nitrifiers in mixed liquor flocs and biofilms (Wagner et al.,

1995; Wagner et al., 1998; Juretschko et al., 1998). However, enumeration with FISH has been controversial, since bacterial RNA content varies with past growth conditions (Oda et al., 2000) and growth rate (Poulsen et al., 1993), and quantification of slow growing (Kämpher et al., 1996) and/or starved bacteria (Wagner et al., 1993) is difficult. Recently, quantitative PCR was used to enumerate NOB in activated sludge (Dionisi et al., 2002; Harms, et al. 2003) via the ribosomal RNA gene (rDNA). This technique provides truly enumerative data with high sample throughput and eliminates the need for pure cultures in assay development.

Though enumeration of populations may help improve wastewater treatment performance, for example through improved modeling capabilities (Burrell et al., 1998; Wagner et al., 1998; Oerther et al., 1999), this data will not adequately address the problem of identifying nitrification and denitritification/anammox instability. This assessment is based first on the fact that NOB activity may rapidly or gradually change during inhibition and acclimation, while the population remains relatively unchanged (Turk and Mavinic, 1989b; Bernet et al., 2001). Second, enumerative data require substrate conversion rates to infer activity levels. This would not be reliable in denitritification or anammox reactors where simultaneous nitrite oxidation and reduction occur. Third, FISH and real-time PCR have poor resolving ability for population changes of slow growing bacteria. For example, a recent study of the nitrite oxidizer *Nitrospira* indicated real-time PCR poorly discriminated 2- or even 5-fold differences in rDNA copy number (Dionisi et al., 2003). Thus, enumerative data is useful, but appears better suited to detect large, presumably long term nitrite oxidizer population changes, particularly since these bacteria are such slow growers (Watson et al., 1989; Ehrich et al., 1995).

Though NOB population changes may be difficult to detect, identifying nitrite oxidizing activity changes, and hence declining nitrification and denitritification or anammox efficiency may be feasible. This is because the ribosomal RNA transcript abundance (rRNAt) has been found to vary greatly (more than 2-fold) during growth and catabolic activity changes in fast growing bacteria such as *Escherichia coli* (Cangelosi and Brabant, 1997; Licht et al., 1999; Oerther et al., 2000) and *Acinetobacter*

species/strains (Oerther et al., 2000; Oerther et al., 2002; Stroot and Oerther, 2003), as well as slow growing bacteria such as *Mycobacterium tuberculosis* (Cangelosi et al., 1996) and an anammox organism (Schmid et al., 2001). Since both catabolic and anabolic activities are intimately tied to the protein synthesis rate and number of ribosomes in bacteria (Stevenson and Schmidt, 1998), these results are understandable. Further, the ribosome construction rate increases approximately with the square root of growth rate, but is limited by the rate of rRNA transcription (via ribosomal protein autogenous transcription control) (Zengel and Lindahl, 1994). Interestingly, ribosomal RNA transcription may in turn be regulated by the energy charge of the cell through the initiating nucleotide triphosphate (NTP) concentration (Gaal et al., 1997), which in the case of NOB would link back to nitrite oxidizing activity. All of these factors indicate the ribosomal transcript would be an excellent activity indicator for the NOB.

Ribosomal transcript abundance has not been evaluated in NOB, nor has quantitative PCR been used to measure this parameter. Though Cangelosi and Brabant (1997) recommended that rRNAt levels should be interpreted through normalization to the rDNA gene copy number, an rRNAt/rDNA type ratio has not been investigated as an activity metric. This type of ratio may improve on the limited success others have had using rRNA/rDNA ratios as indicators of microbial activity (Muttray and Mohn, 1998; Muttray and Mohn, 2000; Muttray et al., 2001; Ka et al., 2001; Milner et al., 2001), since abundance of the rRNAt changes faster and over a larger range than rRNA (Cangelosi et al., 1996; Cangelosi and Brabant, 1997; Licht et al., 1999; Oerther et al., 2000; Schmid et al., 2001). Also, an rRNAt/rDNA ratio may be more appropriate for NOB since some slow growing bacteria retain a high number of ribosomes during starvation and inhibition (Morita, 1993; Wagner et al., 1995; Morgenroth et al., 2000).

In summary, the need for a species specific in-situ indicator of nitrite oxidizing activity could be met by an rRNAt/rDNA type ratio. Real-time PCR would be well suited for such a study, since one detection system could be used to quantify both the rRNAt and rDNA concentrations using primers targeting the 16S - 23S intergenic spacer region (ISR) of NOB genera.

1.3 Research Goals and Objectives

This research was formulated on the premise that an in-situ indicator of NOB activity could be used to improve application of complete and partial nitrification during wastewater treatment. The overall goal was to develop and test the rRNAt/rDNA ratio as a species specific indicator of in-situ NOB activity, with the main hypothesis being that this metric could be used to infer nitrite oxidizing activity levels (independent of other indicators) and predict future treatment performance. The tasks to accomplish this goal were organized into 3 phases. In phase 1, the range and dynamics of the NOB rRNAt/rDNA ratio were examined. In phase 2, the hypothesis that the metric would decline monotonically with increasing inhibitor concentration and fraction inhibition was tested. In phase 3, the ratio was measured during a staged inhibition event in a bench scale reactor. The specific objectives of this study were to:

1. Establish a bench scale nitrification reactor (BSNR) promoting complete nitrification to provide the study with enriched nitrifying biomass.
2. Identify a dominant NOB in the BSNR and design a real-time PCR detection system for the 16S - 23S ISR of this organism; this would allow the NOB rRNAt levels and rRNAt/rDNA ratio to be studied under a variety of conditions favorable and unfavorable for nitrite oxidation.
3. Test the specificity, accuracy, and sensitivity of the quantitative PCR assays for the BSNR biomass.
4. Establish upper and lower prediction intervals for the rRNAt/rDNA metric in the BSNR; these intervals would be used for baselines comparison purposes.
5. Investigate the range and dynamics of the NOB rRNAt/rDNA ratio following transitions between nitrite starvation and unlimited nitrite oxidation; this would determine whether the metric could indicate unusually low or high nitrite oxidation activity in the BSNR, and how well the metric would forecast future reactor performance, which would be limited by the metric's rate of change.

6. Evaluate the rRNAt/rDNA ratio during batch NOB inhibition experiments with mechanistically distinct inhibitors; this would indicate whether the metric's response would be effective across the wide range of inhibitors that affect nitrite oxidation.
7. Assess whether the metric value could be used to predict future nitrification efficiency in the BSNR by measuring the ratio during a staged inhibition experiment.

CHAPTER 2.0

LITERATURE REVIEW

2.1 Nitrification

2.1.1 Stoichiometry and substrates

Nitrifying bacteria aerobically use inorganic nitrogen as an electron donor and reductant energy source (Madigan et al., 2000). The stoichiometry and free energy yields for ammonia and nitrite oxidation are (Atlas and Bartha, 1997; Madigan et al., 2000):

(1) $NH_4^+ + 1.5O_2 \rightarrow NO_2^- + 2H^+ + H_2O$

$\Delta G^{0\prime} \approx$ -280 kJ/reaction (79%)
STAGE 1 – ammonia oxidization

(2) $NO_2^- + 0.5O_2 \rightarrow NO_3^-$

$\Delta G^{0\prime} =$ -74.1 kJ/reaction (21%)
STAGE 2 – nitrite oxidation

Stage 1 and 2 are designated nitritification and nitratification, respectively (Prakasam and Loehr, 1972). AOB are the "nitrosifyers", oxidizing ammonia to nitrite; NOB are the true "nitrifiers", oxidizing nitrite to nitrate (Madigan et al., 2000). However, the term "nitrifiers" is commonly used to refer to these bacteria as a group (Teske et al., 1994), and this is the convention adopted herein. Genus names distinguish ammonia ("Nitroso"; e.g. *Nitrosomonas europaea*) from nitrite ("Nitro"; e.g. *Nitrobacter winogradskyi*) oxidizing bacteria (Madigan et al., 2000).

Two important stoichiometric characteristics of nitrification are the consumption of oxygen and production of acidity, both of which must be carefully accounted for in the design of wastewater treatment reactors (Grady et al., 1999). The nitrifiers consume 4.57 mg O_2/mg N, with ammonia oxidation consuming 3.43 mg O_2/mg N and nitrite oxidation consuming 1.14 mg O_2/mg N. In medium strength domestic wastewater (220 mg

BOD_5/L and 25 mg NH_4^+-N/L) nitrification accounts for approximately 35% of the oxygen demand required for wastewater treatment. Ammonia oxidation produces 2 moles of hydrogen ions for every mole of ammonia oxidized, which is equivalent to a alkalinity consumption of 7.1 mg $CaCO_3$/mg NH_4^+-N. Thus, nitrification can consume all of the influent alkalinity during wastewater treatment, so pH control may be required to prevent pH drops that can otherwise inhibit both ammonia and carbon oxidation (Tchobanoglous and Burton, 1991; Grady et a., 1999).

Though "ammonia" loosely designates the most reduced, inorganic form of nitrogen, two inter-convertible forms exist: free ammonia (NH_3), an unionized gas that likely serves as the AOB substrate (Suzuki et al., 1974), and the ammonium ion (NH_4^+; Equation 3). Ammonium is the predominant form at pHs and temperatures of interest in wastewater treatment. The free ammonia concentration is a function of the total ammonia concentration, the ratio of the ammonia and water ionization constants (K_b/K_w), pH (Equation 4), and temperature (Equation 5) (Anthonisen et al., 1976). Thus, as the pH and temperature increase, the proportion of the total ammonia in the free form increases. However, at pHs below 8.5, ammonia gas losses from even highly nitrogenous wastewaters are negligible (Ford et al., 1980). Thus, nitrification and denitrification are more cost effective for removing ammonia and nitrogen from wastewater rather than air stripping at high pH (EPA, 1993; Siegrist, 1996). It is the free form of ammonia that is linked to aquatic toxicity (EPA, 1993) and NOB inhibition (Anthonisen et al., 1976).

(3) $$NH_4^+ \Leftrightarrow NH_3 + H^+$$

(4) $$NH_3\,(mg/L) = \frac{\text{Total ammonia}\,(mg/L)\times 10^{pH}}{(K_b/K_w)+10^{pH}}$$

(5) $$K_b/K_w = e^{(6{,}334/273+°C)}$$

Two inter-convertible forms also exist for nitrite (Equation 6), the nitrite ion (NO_2^-) and free nitrous acid (NO_2H), the latter likely serving as the NOB substrate (O'Kelly et al., 1970). The concentration of free nitrous acid (Equation 7) varies as a

function of the total nitrite concentration, the nitrous acid ionization constant (K_a), and temperature (Equation 8) (Anthonisen et al., 1976). As the pH declines, the proportion of total nitrite concentration in the free form increases notably and may cause AOB inhibition (Anthonisen et al., 1976).

(6) $$NO_2H \Leftrightarrow NO_2^- + H^+$$

(7) $$NO_2H\,(mg/L) = \frac{NO_2^-\,(mg/L)}{K_a \times 10^{pH}}$$

(8) $$K_a = e^{(-2{,}300/273 + °C)}$$

2.1.2 Phylogeny

The nitrifiers were originally categorized phenotypically in the family *Nitrobacteraceae* (Watson et al., 1989), being discriminated by the ability to utilize inorganic nitrogen as an energy source. AOB were classified into five genera based on cell morphology: *Nitrosomonas*, *Nitrosococcus*, *Nitrosospira*, *Nitrosolobus*, and *Nitrosovibrio* (Koops et al., 1991). Four NOB genera were delineated using cell ultrastructure characteristics: *Nitrobacter*, *Nitrococcus*, *Nitrospira*, and *Nitrospina* (Bock and Koops, 1992).

Phylogeny is now inferred with DNA sequences and once functionally distinct microorganisms, such as the nitrifiers, are known to be unrelated. Nearly all of the chemolithotrophic nitrifiers are members of the largest Eubacteria kingdom, Proteobacteria (Head et al., 1993; Teske et al., 1994) which contains gram negative bacteria categorized into five subdivisions (α, β, χ, δ, and ε) that entail high phenotypic and physiologic diversity (Madigan et al., 2000). The exception is *Nitrospira* (Watson et al., 1986; Ehrich et al., 1995), which forms a separate phylum containing NOB as well as non-nitrifiers (Ehrich et al., 1995; Daims et al., 2001). Twenty five species of AOB and eight species of NOB have been cultured, but it is apparent from in-situ studies that the number of species and strains in the environment is much higher (Koops and Pommerening-Röser, 2001; Hermanssen and Lindgren, 2002).

Ammonia oxidizers

Nearly all identified chemolithotrophic AOB occur in the β-subdivision of Proteobacteria. The marine ammonia oxidizer *Nitrosococcus oceanus* and the extreme halophile *Nitrosococcus halophilus* belong to the γ-subdivision (Juretschko et al., 1998). Another member of the genus *Nitrosococcus mobilis* clusters with *Nitrosomonas* in the β-subdivision, indicating a taxonomic error (Teske et al., 1994). Pommerening-Röser et al. (1996) phylogenetically organized the β subclass into six lines of decent: *Nitrosomonas marina*, *Nitrosomonas oligotropha*, *Nitrosomonas europaea, Nitrosomonas mobilis*, *Nitrosomonas communis*, and *Nitrosospira*. However, Purkhold et al (2000) indicate *N. mobilis* should be merged with *N. europaea*.

Nitrite oxidizers

Most cultured NOB belong to the α-, δ-, and γ-subdivisions of Proteobacteria. None occur in the β-subdivision containing nearly all known AOB (Teske et al., 1994). *Nitrobacter* contains three (Bock and Koops, 1992) or four (Grundmann et al. 2000) species and forms a tightly grouped, highly related (> 99% 16S rDNA similarity) cluster in the α-subdivision (Teske et al., 1994; Orso et al., 1994). Individual strains must be identified using digests of the 16S - 23S ISR (Navarro et al., 1992b; Grundmann et al., 2000) or DNA homology (Bock et al., 1983; Navarro et al., 1992a). *Nitrospina* and *Nitrococcus* are halophiles found in the δ- and γ-subdivisions, respectively. *Nitrospira* was recently found distinct enough to constitute a separate phylum (an earlier analysis by Teske et al. (1994) indicated δ-subclass relatedness). Daims et al. (2001) conducted a comprehensive phylogenetic study on *Nitrospira* that revealed four monophyletic lines of descent. Their phylogenic tree displayed coverage for 16S rDNA probe sequences designed to detect *Nitrospira* NOB. The highly unique *Nitrospira* 16S rDNA sequence has aided identification and enumeration in activated sludge using FISH and competitive and real-time PCR (Dionisi et al., 2002; Harms et al., 2003; Schramm et al., 1999). Thus, there appears to be significant divergence between *Nitrospira* and the classic NOB genus *Nitrobacter*. Divergence between the NOB genera is also suggested by the fact that they may utilize different nitrite oxidizing enzyme systems (Watson et al., 1986).

2.1.3 Dominant nitrifier genera in wastewater treatment systems

Research suggests that specific treatment venues may favor different genera and species of AOB/NOB, relating perhaps to different growth kinetics, oxygen and substrate affinities, and varying sensitivity to environmental perturbations (Juretschko et al., 1998). Culture based techniques (e.g. MPN and selective plating) cannot be used to identify or enumerate dominant nitrifiers in wastewater treatment biomass.

Ammonia oxidizers

A total of 122 clones, originating from PCR amplification of activated sludge in 11 WWTPs with primers for the ammonia monooxygenase gene (*amoA*), revealed that all putative AOB were affiliated with the β-subclass Proteobacteria (Purkhold et al., 2000). Representatives of all major clusters were found, though *Nitrosospira* occurred at only two plants, one established with seed sludge from the other. Research has revealed relatively few occurrences of *Nitrosospira*-like AOB in activated sludge; exceptions are Hiorns et al (1995) and Coskuner and Curtis (2002). However, Hiorns et al (1995) indicate that *Nitrosospira* are ubiquitous in the environment, and that enrichment of environmental samples is selective for nitrosomonads. Of the β-subclass AOB, *N. eutropha* may dominate SHARON type reactor systems (Logemann et al., 1998). The γ-subclass remains conspicuously absent from wastewater treatment reactors.

Nitrite oxidizers

Nitrobacter spp. were once thought to be the dominate nitrite oxidizers in activated sludge reactors (Benefield and Randall, 1985; Tchobanoglous and Burton, 1992; Grady et al., 1999), likely because this genus was isolated using culture-based techniques such as plating and MPN assays (e.g. Ford et al., 1980). However, when Wagner et al. (1996) analyzed 9 WWTPs, a drinking water biofilm, and constructed wetlands using in-situ hybridization specific for *Nitrobacter* 16S rRNA, these researchers found no samples with detectable *Nitrobacter*, even though *Nitrobacter* had been cultured from one of the treatment systems. Juretschko et al. (1998) isolated only one NOB (*Nitrobacter*) from an activated sludge sample, despite the fact that *Nitrobacter* was

below in-situ detection limits and *Nitrospira* represented as much as 9% of all mixed liquor bacteria.

It has been suggested that *Nitrospira*, rather than *Nitrobacter*, is the dominant NOB in a variety of environments, including biological wastewater treatment reactors (Burrell et al., 1998). *Nitrospira* spp. have been detected in nitrifying biofilms from two reactors with different influent ammonia and salt concentrations (Daims et al., 2000; Daims et al., 2001), in a biological nutrient removal plant located in Queensland, Australia (and a nitrite-oxidizing sequencing batch reactor seeded with mixed liquor from this plant) (Burrell et al., 1998), in an intermittently aerated nitrification/denitrification animal waste processing reactor (Juretschko et al., 1998), in both industrial and municipal type activated sludge (Dionisi et al., 2002), in a freshwater aquaria filter (Hovanec et al., 1998), an oligotrophic reactor (Schramm, et al. 1998), and in groundwater receiving livestock wastewater (Cho and Kim, 2000). However, Mobarry et al. (1996) found *Nitrobacter* in a bench scale reactor, and Coskuner and Curtis (2002) were able to detect both *Nitrobacter and Nitrospira* in mixed liquor samples. Sadén and Dalhammer (2000) found detectable *Nitrobacter* in mixed liquor samples from several WWTPs in Sweden. Also, *Nitrobacter* appeared dominant in a bench scale reactor treating high ammonia landfill leachate (Calli et al., 2003), while Schramm et al. (1996) reported *Nitrobacter* in a trickling filter biofilm treating eel aquaculture water.

2.2 Nitrifiers Grow Slowly With Low Yield

The presence of nitrification in wastewater treatment reactors is not reflected by a large accumulation of biomass, but rather by the accumulation of the end product nitrate, and by the extra oxygen consumption and alkalinity demands these bacteria place on the treatment system (Grady et al., 1999). This is a result of their low yield, so that even when highly nitrogenous, low C/N wastewater is degraded, nitrifiers coexist with heterotrophic bacteria (Burrell et al., 1998). In municipal wastewater treatment reactors, the nitrifiers likely make up only a small percentage (≈ 1 - 5 %) of total bacteria (Dionisi et al., 2003). This has long been recognized as a particular limitation in modeling

nitrification using only the mixed liquor suspended solids concentration (Sharma and Ahlert, 1976). Slow growth rates, another nitrifier characteristic, are important since this determines the design SRT of single sludge carbon oxidation and nitrification reactors (Grady et al., 1999).

2.2.1 Factors that contribute to low growth rate and yield

Small number and work potential of substrate electrons

Figure 1 illustrates the aerobic work potential of an intermediate in heterotrophic catabolism (α-ketoglutarate), a biosynthetic intermediate (NADPH), and the nitrifier substrates (hydroxylamine (NH_2OH), an intermediate in ammonia oxidation, and nitrite) (Stryer, 1995; Poughon et al., 2001). The diagram emphasizes that the electron transfer potential from α-ketoglutarate is 2.2 and 3.6 times that of the electrons in hydroxylamine and nitrite, respectively, and that the nitrifier intermediates do not possess sufficient potential to directly reduce $NADP^+$. The low work potential contributes to poor free energy yield (Table 1). Since α-ketoglutarate is only an intermediate in heterotrophic metabolism, the $\Delta G°'$ for its oxidation is only a fraction of the total energy yield for an organic molecule (e.g. the energy yield for glucose is ≈ 687 kcal/mol). Thus, both the low electron work potential, and the small number of electrons available per substrate molecule, contributes to low nitrifier yields.

Table 1 Heterotrophic and nitrifier substrate electron work potential.

Substrate			$\Delta E'_0$ (mV) (O_2 as oxidant: $E°'$ 820 mV)	$\Delta G°'$ (kcal/mol)
oxidant/reductant	E'_0 (mV)	n[1]		
α–ketogluterate/succinate + CO_2	-670	2	1,490	-69
NADPH + H^+/$NADP^+$	-320	2	1,140	-53
NH_2OH/NO_2^-	+127	4	693	-64
NO_2^-/NO_3^-	+408	2	412	-19

1 Number of electrons transferred (the net electrons transferred for ammonia oxidation is 4: Poughon et al., 2001).

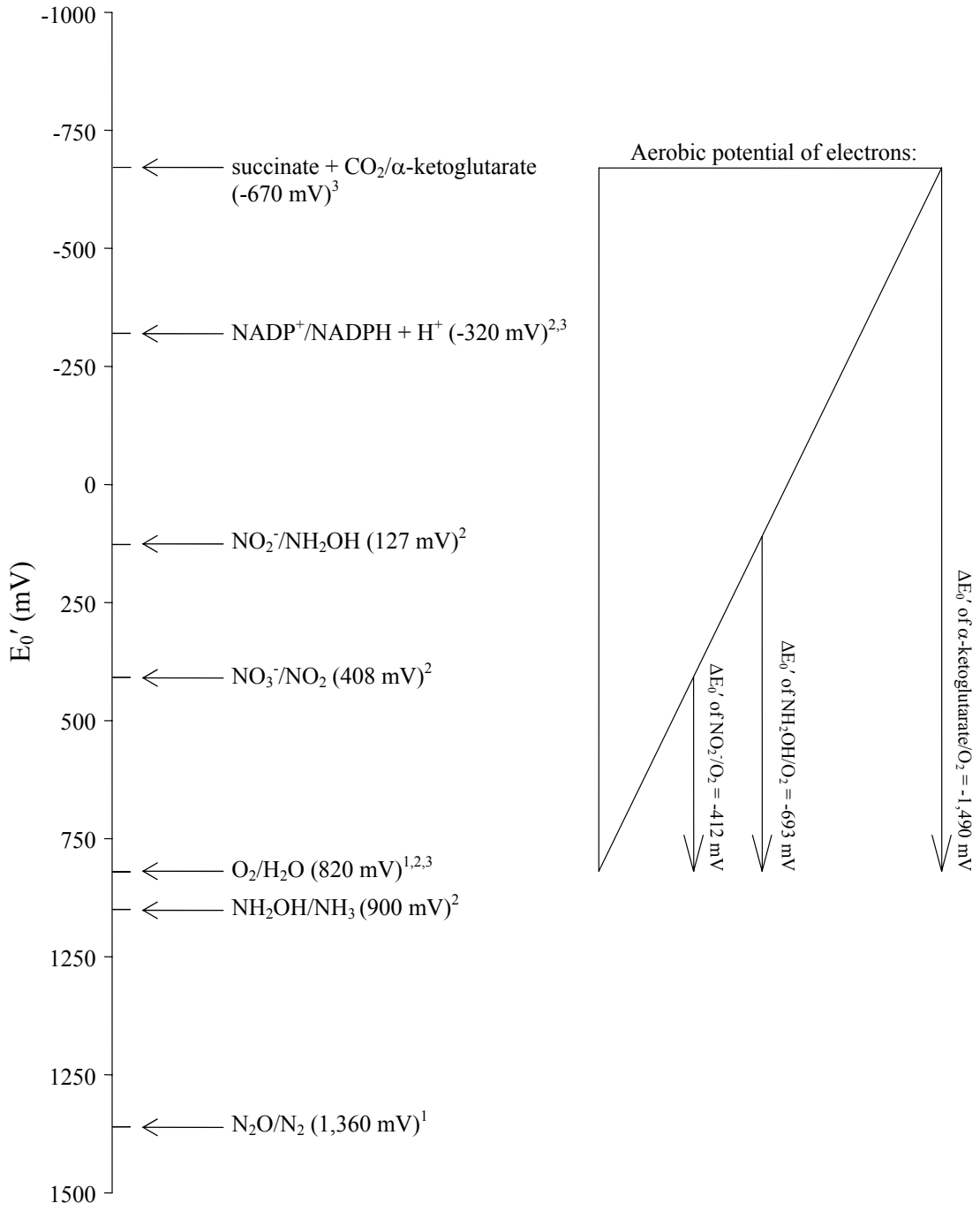


Figure 1 Diagram comparing standard reduction potentials for nitrifier and heterotrophic substrate electrons.

1 Madigan et al. (2000).
2 Poughon et al. (2001).
3 Stryer (1995).

Potential energy costs of reverse electron flow

Biosynthetic reactions seem to require the reduced form of the coenzyme $NADP^+$ (NADPH) (Madigan et al., 2000; Stryer, 1995). Organic substrates typically possess E_0' lower than this electron carrier (Figure 1), so heterotrophs are capable of conserving reducing power by transferring electrons from substrate molecules and their intermediates to $NADP^+$ (Madigan et al., 2000). Depending on the needs of the organism (maintenance versus growth), electrons may be donated to the respiratory chain (by NADH) to liberally generate free energy (ATP), or to biosynthetic intermediates with high thermodynamic efficiency (by NADPH). For heterotrophs this split in the electron flow pathway, which Rittmann and McCarty (2001) designate f_e^0 (energy production) and f_s^0 (cell synthesis) ($f_e^0 + f_s^0 = 1$), is decisively in favor of cell synthesis.

Nitrifying bacteria utilize substrates with higher E_0' than the typical anabolic electron carrier (Figure 1). Thus, reverse electron flow may be required to place low potential substrate electrons in a more energized state against a thermodynamic energy gradient during chemolithoautototrophic growth. This could be accomplished at the expense of the proton motive force generated by the AOB and NOB electron transport chains (Bock and Wagner, 2001). The large free energy demand and inefficiency of reverse electron flow could create a shunt directing nearly all substrate electrons to oxygen, which would make the nitrifier f_e^0 large (Rittmann and McCarty, 2001). However, NADH synthesis may the primary (i.e. ATP-independent) energy conservation reaction in *Nitrobacter*, obviating the need for reverse electron flow, though it is unclear how this occurs (Bock and Wagner, 2001).

High reductive energy expense for carbon fixation

Heterotrophs use reduced carbon for growth (oxidation state ≈ 0). This limits reductive power expenditures to synthesize the carbon backbones of organic molecules during cell growth. Conversely, the nitrifiers may typically be autotrophic, requiring oxidized inorganic carbon for growth. A caveat is that several *Nitrobacter* species/strains growth faster mixotrophically than autotrophically, and some even grow heterotrophically, albeit very slowly, indicating that reduced carbon could be obtained

from simple organic compounds (Bock, 1976; Steinmüller and Bock, 1976; Bock et al., 1983; Bock et al., 1990). However, it is unknown how well the nitrifiers compete for organic compounds in wastewater treatment systems, and these organisms definitely utilize the Calvin cycle and/or phosphoenol-pyruvate carboxylase to reduce inorganic carbon when this is required (Bock and Wagner, 2001). An approximation for Calvin cycle growth stoichiometry is presented below (Madigan et al., 2000):

(9) $6CO_2 + 12\ NADPH + 18\ ATP \rightarrow C_6H_{12}O_6(PO_3H_2) + 12\ NADP + 18\ ADP + 17\ Pi$

It can be seen that for each carbon assimilated, 12 NADPH are consumed along with 18 ATP. Thus, autotrophic growth carries heavy free energy and reductive power demands that may lower nitrifier yield. Also, low growth rate is a characteristic of autotrophic metabolism (Madigan et al., 2000).

2.2.2 Nitrifier growth rates control single sludge reactor design

The SRT is the dominant factor affecting the capabilities of a biological wastewater treatment reactor, and the value of this parameter must exceed the growth rate of particular groups of microorganisms desired in the reactor or they will be washed out (Benefield and Randall, 1985; Grady et al., 1999). The SRT, in turn, largely determines the size of the reactor, and thus is a key driving force in the construction and operating cost of wastewater treatment facilities (Grady et al., 1999). When nitrification is required, the slow nitrifier growth rate is used to determine the minimum SRT of single sludge reactors (Grady et al., 1999). Grady et al. (1999) recommend three multiplicative safety factors when nitrification is promoted that account for peak ammonia loading effects, DO concentration, and for general "uncertainty." Since nitrification is recognized as an inherently unstable process, particularly if the wastewater is poorly characterized with respect to potential inhibiting compounds, the effect of promoting nitrification is a large (2- to 5-fold) increase in the design SRT. Since nitrification remains prone to inhibition, even this design accommodation seems insufficient to promote consistent high

nitrification efficiency. It has long been recognized that if nitrification efficiency could be improved, the cost savings would be large (Hockenbury and Grady, 1977).

2.3 Nitrifier Inhibition

Nitrifiers are more susceptible to specific inhibiting compounds that heterotrophs (Koopman and Bitton, 1986; Blum and Speece, 1991; Dalzell et al., 2002), particularly in industrial WWTPs (Jonsson et al., 2000). Inhibition can further reduce the already low nitrifier growth rates (Hockenbury and Grady, 1977) and lead to reactor washout with complete loss of ammonia oxidation (Grady et al., 1999). Undoubtedly, this contributes to nitrification being recognized as an inherently unstable process that is difficult to maintain and reestablish following inhibition (Balmelle et al., 1992; Wagner et al., 1996; Mobarry et al., 1996; Johnsson et al., 2000). It is generally accepted that AOB are more susceptible to inhibition than NOB, and since the ammonia oxidation rate typically limits the overall rate of nitrification (Grady et al., 1999), AOB appear to be the "weak link" in nitrification (Hockenbury and Grady, 1977). However, a propensity for NOB inhibition under certain operating conditions has also been noted, particularly when the DO concentration is low. Further, AOB and NOB inhibition events can lead to ammonia and nitrite buildup, which can exacerbate poor performance.

2.3.1 AOB vs. NOB: which nitrifier is more susceptible to inhibition?

Tomlinson et al. (1966) conducted one of the first investigations of nitrifier inhibition using settled activated sludge from a pilot-scale plant and industrially and agriculturally important inhibitors (organic chemicals, fungicides, and heavy metals). Nitrite oxidation was, in general, less susceptible to inhibition than ammonia oxidation, except for chlorate, cyanide, hydrazine sulfate, 2,4-dinitrophenol, and azide. Phenolic and nitrogenous organo-sulfur compounds were appreciably toxic to the AOB and/or NOB. In the case of the phenolic compounds this may indicate the nitrifiers are particularly sensitive to uncouplers (Escher et al., 1996). An important finding was that while heavy metals inhibited pure cultures of *N. europaea*, much greater concentrations were required to inhibit ammonia oxidation when activated sludge was used as the

inoculant, presumably because the toxic effect was ameliorated by adsorption. This was not true for short term inhibition caused by organic compounds such as phenolics, although adaptation and/or degradation by heterotrophs appeared to decrease the inhibitory effect (also observed by Gernaey et al., 1999).

Hockenbury and Grady (1977) investigated 52 organic compounds (including 13 industrially significant compounds in terms of production) to determine whether they inhibited nitrification. The compounds were screened at 100 mg/L and those exhibiting nitrification inhibition (20) were retested for the effect on nitrite oxidation. Only a small number inhibited nitrite oxidation (p-nitrobenzaldehyde, p-nitroaniline, and n-methylaniline), but at concentrations higher than those required to inhibit ammonia oxidation. The finding that nitrite oxidation was less sensitive to inhibition than ammonia oxidation was supported by their literature review of pure culture inhibition studies (*Nitrosomonas* and *Nitrobacter* spp) covering 34 compounds. Thirty were more inhibitory to *Nitrosomonas*, two affected both *Nitrosomonas* and *Nitrobacter* (2,4-DNP and aminoguanidine), while only two were specifically inhibitory to *Nitrobacter* (nitrourea and quinacrine).

Williamson and Johnson (1981) and Wang and Reed (1984) used "*Nitrobacter*" as a test organism for inhibition. Although Williamson and Johnson (1981) demonstrated that nitrite oxidation was particularly sensitive to an uncoupler (2,4,5-TCP), Wang and Reed (1984) later concluded that AOB would be a more sensitive indicator in tests designed to detect inhibiting compounds.

In summary, several researchers have indicated AOB are more sensitive to chemical inhibition than NOB. For both AOB and NOB, phenolic compounds appear to be particularly inhibitory (Strotmann and Eglsäer, 1995), perhaps because these compounds inhibit growth (Escher et al., 1996). However, an interesting observation is that since ammonia oxidation provides the nitrite oxidizer with a primary lithotrophic substrate, NOB activity is ultimately affected by both AOB and NOB inhibition. Hence, NOB activity could be used as an indicator of future nitrification instability, whether this originated as NOB or AOB inhibition.

2.3.2 Selective inhibitors of ammonia and nitrite oxidation

Allylthiourea (ATU-$C_4H_8N_2S$) selectively inhibits AOB. The mechanism appears to be chelation of copper from the active site of AMO (Bédard and Knowles, 1989; Stein and Arp, 1998a), which likely explains observations of Tomlinson et al. (1966) that copper alleviated thiourea inhibition. Both Čech et al. (1984) and Chudoba et al. (1992) found that 8.6 μM (1 mg/L) of ATU completely suppressed nitrification in bench scale activated sludge reactors. Pollard et al. (1998) utilized 172 μM ATU to inhibit autotrophic growth during batch tests. Chandran (1999) incubated samples of a nitrifier enrichment to determine optimum ATU/ammonium concentration for complete AOB inhibition: 17 μM ATU and a small dose of NH_4^+-N resulted in sustained AOB inhibition after an incubation time of 1 hour (no NOB inhibition was detected at this concentration). Ginestet et al. (1998) also performed an investigation of AOB inhibition using a nitrifier enrichment. Instantaneous AOB inhibition was achieved at an ATU concentration of 86 μM. Though ATU does not inhibit hydroxylamine oxidation in the AOB (an intermediate in the oxidation of ammonia to nitrite), hydrazine appears to specifically inhibit hydroxylamine oxidation (Sharma and Ahlert, 1977).

Chlorate was reported to selectively inhibit NOB (Voets et al., 1975). However, when Chandran (1999) incubated an enriched nitrifying culture with 10 mM chlorate both ammonium and nitrite oxidation were inhibited. Ginestet et al. (1998) noted that chlorate acted too slowly and nonspecifically for use in rapid kinetic assays, and demonstrated that azide was a powerful, selective inhibitor of nitrite oxidation. These researchers observed a 75% reduction in oxygen consumption at 2,800 and 0.98 μM azide for ammonia and nitrite oxidizing activity, respectively. Further, they observed that 24 μM instantly and completely inhibited nitrite oxidation with no apparent affect on ammonia oxidation or heterotrophic activity (endogenous oxygen uptake rate). Chandran (1999) also found that a sodium azide concentration of 24 μM selectively inhibited NOB without adversely affecting the maximum specific ammonia oxidation rate, though higher concentrations inhibited both nitrite and ammonia oxidation. Sánchez et al., (2001) and Guisasola et al., (2005) confirmed that 24 μM inhibited nitrite oxidation.

2.3.3 Propensity for nitrite buildup during wastewater treatment

Though the NOB are less sensitive to chemical inhibition than the AOB, NOB can be inhibited by a wide variety of operational and environmental factors which lead to nitrite buildup: low DO (Jayamohan, et al., 1988; Bernet, et al., 2001; Bae et al., 2002; Ruiz et al., 2003: reviewed in Section 2.3.5), pH (Suthersan and Ganczarczyk, 1986; Bae et al., 2002; Garrido et al., 1997), free ammonia (many: e.g. Anthonisen et al, 1976; Suthersan and Ganczarczyk, 1986; Turk and Mavinic, 1989a), free hydroxylamine (Yang and Alleman, 1992), heavy metal toxicity (Randall and Buth, 1984b), low/high temperature (Randall and Buth, 1984a; Randall and Buth, 1984b; Bae et al., 2002; Balmelle et al., 1992; Hellinga, et al. 1998), aeration patterns/duration (Turk and Mavinic, 1989a; Yoo et al., 1999; Pollice et al., 2002; Peng et al., 2004; Fux et al., 2003), influent COD/N ratio (Tseng et al., 1998), and shortened SRT (Alleman, 1985; Hellinga, et al. 1998; Pollice et al., 2002). Further, nitrite buildup may precede ammonia oxidation failure (Randall and Buth, 1984a; Randall and Buth, 1984b) and sludge bulking (Philips et al., 2002). Bench scale municipal wastewater treatment research at the University of Tennessee (Hawkins, 2000; Parker, 2001) illustrated nitrite buildup (NOB inhibition) during a variety of environmental perturbations (low temperature, low DO, and influent wastewater strength increases). The propensity for NOB inhibition when the free ammonia concentration is high, and the propensity for AOB inhibition following nitrite buildup, emphasize that accumulation of the nitrifier substrates can exacerbate poor nitrification efficiency (Section 2.3.4). However, many factors, including the free ammonia concentration, have been more or less anecdotally linked to nitrite buildup (Philips et al., 2002). Though the mechanisms leading to nitrite accumulation are often not clear, a recent review of the causes of nitrite buildup indicates pH, dissolved oxygen concentration, volatile fatty acids, and reactor operational factors are likely most important (Philips et al., 2002). NOB activity may be a better marker for predicting future nitrification performance, since nitrite buildup also lowers nitrification efficiency, and may precede ammonia oxidation failures.

2.3.4 Nitrifier substrates may be inhibitory

Free ammonia

Anthonisen et al. (1976) conducted a thorough review of free ammonia inhibition of nitrification, suggesting ranges for the inhibitory effect on NOB (0.08 to 0.8 mg NH_3-N/L) and AOB (8 to 124 mg NH_3-N /L). In the ensuing years, many researchers have investigated free ammonia inhibition of the NOB, typically in attempts to promote denitritification (Section 2.4.1), though the results have been ambiguous (Table 2). For example, Ford et al. (1980) reported poor nitrification performance only above 5.8 mg NH_3-N/L (well in excess of the Anthonisen et al. (1976) threshold), complete NOB inhibition at 24 mg NH_3-N/L initially, but subsequent NOB acclimation to 56 mg NH_3-N/L. When Suthersan and Ganczarczyk (1986) exposed a nitrifying sludge to high free ammonia concentrations in an attempt to promote denitritification, NOB acclimated to 2.5 mg NH_3-N/L. These researchers indicated that the free ammonia concentration, pH, time of exposure, and biomass concentration were important factors in determining the time required before acclimation occurred. A prolonged study of nitrite buildup via free ammonia exposure (Turk and Mavinc, 1987; Turk and Mavinic, 1989a) ended with a poor forecast for denitritification stability due to NOB acclimation (up to 20 - 40 mg NH_3-N/L) (Turk and Mavinic, 1989b).

A concern in many of the investigations that implicated free ammonia as the root cause of nitrite buildup was the lack of a control for AOB activity (Table 2) which would hold the free ammonia concentration fixed. Two recent publications investigated free ammonia inhibition of nitrite oxidation after inhibiting the AOB with ATU (Section 2.3.2). Chung et al. (2005) but did not detect substantial NOB inhibition (> 53%) at 82 mg NH_3-N/L. Fux et al. (2003) did not detect significant short term NOB inhibition (≤ 10%) at free ammonia concentrations as high as 80 mg-N/L. These researchers attributed nitrite buildup at high free ammonia concentrations to limited DO supply (short aeration cycles) and designed a sequencing batch reactor for denitritification using this principle (Section 2.4.1).

Table 2 Free ammonia inhibition of ammonia and nitrite oxidation.

System	Inhibition	NH_3 (mg-N/L)	Were AOB inhibited as a control?	Reference
Nitrite buildup in agricultural, industrial, and municipal WWTPs and in soil	NOB - threshold	0.08 - 0.8	No	Anthonisen et al., 1976
	AOB - threshold	8 - 124	-	
AOB and NOB enrichments; DO > 1.5 mg/L	NOB - acclimated; (conflicting results)	17 - 38	No	Wong-Chong and Loehr, 1978
Bench scale reactors treating industrial wastewater	Poor nitrification performance	> 5.8	No	Ford et al., 1980
Nitrifier enrichment; high pH/NH_3 interactions; fed batch assay; DO > 6 mg/L	Initial NOB inhibition > 50%	> 0.8	No	Suthersan and Ganczarczyk, 1986
	Full NOB acclimation	≥ 2.1		
Pre-denitrifying plug flow bench scale system with mixed biomass; artificial wastewater and landfill leachate	Denitritification initially successful	5	No	Turk and Mavinic, 1987, 1989a, 1989b
	Denitritification failed due to acclimation	≥ 40		
Two-stage anaerobic-aerobic process; potato starch wastewater; limited batch tests; (NH_3 controlled via oxygen supply to reactors)	High NOB inhibition	> 0.8	No	Abeling and Seyfried, 1992
	AOB inhibition threshold	> 5.8		
Nitrifier enrichment; NH_3 poorly correlated with nitrite buildup in batch assays; pH 7.5, DO = 0.5 - 6.0 mg/L	Transient nitrite accumulation of > 35% of added ammonia	≥ 3	No	Yang and Alleman, 1992
Unacclimated nitrifier enrichment (frozen subsamples); mineral synthetic substrate, pH 8.1, DO = 2.5 mg/L, 25°C	High NOB inhibition	≥ 3	No	Balmelle et al., 1992
	AOB inhibition threshold	> 6		

Table 2 Continued.

System	Inhibition	NH_3 (mg-N/L)	Were AOB inhibited as a control?	Reference
Unacclimated bench scale nitrifying reactor; mixed culture; glucose/NH_4 growth media	NOB inhibition threshold (NO_2^- buildup, batch tests)	3.3	No	Bae et al., 2002
SHARON and SBR reactors treating digester effluent; batch tests at 30°C, pH 8.1 ± 0.4	≤ 10% NOB inhibition	24 - 80	Yes	Fux et al. (2003)
Plug flow biofilm reactor; nitrifier enrichment; batch assays of biofilm NOB activity	Nitrite accumulation in reactor and in batch assays	0.3 - 5.0	No	Yun and Kim (2003)
NH_3 effect on aerobic granule formation; sequencing batch reactor at different N/COD	AOB	> 9.2	-	Yang, et al., 2004
	NOB	< 9.2	No	
Suspended and attached biomass in a pilot scale reactor treating livestock wastewater; batch tests used aliquots of each biomass type; oxygen limitations were more significant than the potential inhibitory effect of free ammonia	Complete inhibition with oxygen limitation (batch)	8 - 16	Yes	Chung et al. (2005)
	≈ 30-50 % inhibition, no oxygen limitation (batch)	82		
	High NOB activity (in pilot scale reactor)	37		

In summary, free ammonia appears to mainly affect the NOB. However, a comprehensive study of free ammonia as an inhibiting factor for nitrite oxidation (including controls for the DO concentration and AOB activity) appears to be missing from the literature. Such a study seems particularly warranted since high nitrite concentrations appear to inhibit ammonia oxidation.

Free nitrous acid

Anthonisen et al. (1976) also investigated free nitrous acid inhibition of nitrification and proposed that concentrations between 0.06 and 0.8 mg HNO_2-N/L inhibited ammonia oxidation. Much higher concentrations are required to completely inhibit nitrite oxidation (Wong-Chong and Loehr, 1978: 2.65 mg HNO_2^-N/L). Abeling and Seyfield (1992) indicated that 0.04 mg NHO_2-N/L inhibited denitrification. Fux et al. (2003) observed 20 to 25% reductions in AOB activity at 0.16 mg HNO_2-N/L (pH 7, 30°C), while Hellinga et al. (1998) observed 50% inhibition at 0.2 mg HNO_2-N/L at pH 7 (total nitrite concentrations of several hundred mg-N/L at pH 6 - 8). Others have indicated that the total nitrite concentration must be exceedingly high before inhibition occurs. For example, Prakasam and Loehr (1972) observed threshold levels of nitrite inhibition for ammonia oxidation exceeding 1,000 mg NO_2^--N/L. Chandran (1999) observed no effect on either the maximum specific substrate utilization rate or substrate affinity constant of AOB at nitrite-N levels up to 100 mg/L. Turk and Mavinic (1987) did not observe ammonia oxidation inhibition at 115 mg NO_2^--N/L.

Stein and Arp (1998b) showed specific loss of AOB activity in *N. europaea* due to nitrite toxicity that mechanistically affected ammonia monooxygenase (AMO), but that did not occur in the presence of AMO substrates. Previous research had shown that *N. europaea* ended ammonium oxidation in batch assays when nitrite accumulated to 20 - 25 mM, thereby protecting AMO activity (Stein and Arp, 1998a). The onset of nitrite inhibition in the absence of ammonia occurred at 5 mM NO_2^- for *N. europaea* (70 mg NO_2-N/L) (Stein and Arp, 1998b).

2.3.5 Oxygen limitations

AOB possess a lower oxygen affinity constant than the NOB (Table 3), so DO limitations can lead to nitrite buildup. Bernet et al. (2001) simulated NOB and AOB growth using oxygen affinity constants of 0.3 and 1.1 mg/L, respectively, and predicted AOB would outgrow NOB by a factor of two when the DO concentration was 0.5 mg/L. Garrido et al. (1997) used these same oxygen affinity constants to successfully model a stable nitrite buildup in a biofilm airlift suspension reactor when the DO was 1 to 2 mg/L. When the DO concentration was reduced in a coculture of *N. winogradskyi* and *N. europaea*, *N. winogradskyi* succumbed to low DO effects first (Laanbroek and Gerards, 1993). Under the oxygen limited condition, 90 to 99% of all oxygen appeared to be scavenged by *N. europaea*, while *N. hamburgensis* cell counts were significantly lower under oxygen limiting conditions (Laanbroek and Gerards, 1993). Nitrite buildup and NOB washout was obtained in a *N. europaea*/*N. hamburgensis* coculture after imposing sudden oxygen limitation. However, when *N. hamburgensis* was allowed to adapt to low DO, nitrite buildup did not occur (Laanbroek et al., 1994).

Table 3 Nitrifier oxygen half saturation coefficients.

System studied	Environmental parameters	Oxygen Affinity Constant, (mg/L)		Reference
		AOB	NOB	
nitrifier enrichment	25°C	0.74 ± 0.02	1.75 ± 0.01	Guisasola, et al., 2005
SHARON reactor	35°C	1.45	1.1	Hellinga et al., 1998
nitrifier enrichment	20°C	0.63	1.32	Jayamohan et al., 1988
activated sludge	20°C	0.6	1.3	Wisemann, 1994
nitrifier enrichment (saline media)	30°C	1.66	3.0	Sánchez et al., 2001
N. europaea	30°C; pH 7.8	0.48 - 0.64	-	Hollocher et al., 1982
Nitrobacter agilis	30°C; pH 7.5	-	0.48 - 0.64	
"ammonia oxidizers"	-	0.50	-	Rittmann and McCarty, 2001
"nitrite oxidizers"	-	-	0.68	
N. europaea/*N. winogradskyi*	25°C; pH 7.5	0.03 - 0.48	0.70 - 5.32	Laanbroek and Gerards, 1993

Researchers have concluded that low DO concentration was an important factor in nitrite buildup within a variety of reactor types. Garrido et al. (1997) found that stable nitrite buildup (50%) occurred in a biofilm airlift suspension reactor when the DO was gradually reduced to 1 - 2 mg/L. Bernet et al. (2001) obtained stable nitrite accumulation (≈ 90% of influent ammonia) in a stirred biofilm reactor (nitrifier enrichment) if the DO was held at 0.5 mg/L. Bae et al. (2002) found that low DO favored nitrite accumulation in batch experiments. Pollice et al. (2002) found that lowering the SRT to 10 days in a batch reactor containing a nitrifier enrichment completely inhibited NOB when the DO was 2.0 mg/L. These researchers also demonstrated that intermittent aeration (aeration 10 minutes every 20 minutes, DO 2.0 - 0.0 mg/L) led to sustained nitrite buildup at SRTs between 3 and 24 days. Ruiz et al. (2003) found that as the DO was systematically lowered a stable nitrite accumulation occurred at 0.7 mg O_2/L in a bench scale CSTR. However, below 0.5 mg/L AOB activity was also inhibited. Hanaki et al. (1990) found that for a CSTR containing a nitrifier enrichment, influent ammonia was oxidized to nitrite when the DO concentration (0.5 mg/L) and SRT (4 days) were low. Interestingly, these researchers found that the addition of glucose to the influent, and presumably heterotrophic competition for oxygen, reduced the ammonia oxidation efficiency even if the bulk DO concentration was maintained at 0.5 mg/L. Thus, Hanaki et al. (1990) proposed that organic loading likely increases the oxygen affinity constants measured for the nitrifiers in WWTPs, versus the values obtained with pure AOB and NOB cultures.

2.4 Alternate N-Conversion Pathways Promoting Partial Nitrification

The literature documents a propensity for poor nitrification performance due to a wide range of inhibiting factors (Section 2.3). This, along with the slow growth rate and low yield of nitrifiers (Section 2.2), make these bacteria susceptible to reactor washout that exacerbates poor nitrification and denitrification performance. Though beneficial for ammonia and nitrogen removal when implemented consistently, nitrification is expensive because of high oxygen consumption, while denitrification following complete nitrification is costly because of the high oxidative potential of nitrate (excess sludge

production), and because the addition of easily degradable compounds is often required (e.g. methanol). Due to these limitations, attention has not only focused on improving the reliability of nitrification, but has lead to investigations of more efficient N-conversion pathways that promote partial nitrification (suppression of nitrite oxidation). However, processes that suppress NOB activity are not well understood (Fux et al., 2002), making the implementation of these new nitrogen(N)-conversion pathways unreliable.

2.4.1 Denitritification

Denitritification, the use of nitrite as a terminal electron acceptor, was investigated as an alternate N-conversion pathway for wastewater treatment in the 1980s in reactor configurations that promoted free ammonia inhibition of the NOB (Suthersan and Ganczarczyk, 1986; Turk and Mavinc, 1987; Turk and Mavinic, 1987a). These studies revealed that partial nitrification followed by denitritification offered benefits over complete nitrification followed by denitrification including a 25% reduction in the oxygen demand for ammonia removal, a 40% reduction in the carbon requirement for N-removal, a 63% increase in N-removal rates, and lower biomass production. However, these early attempts at denitrification failed because NOB adapted to high free ammonia concentrations (Turk and Mavinic, 1989b). Currently, two reactor types are being investigated to promote denitritification for highly nitrogenous wastewaters.

CSTR

The single reactor for high ammonium removal over nitrite (SHARON; Hellinga et al., 1998) is a newer technique to accomplish partial nitrification/full denitritification. SHARON uses a small complete-mix stirred tank reactor (CSTR) and selective pressure to washout the slower growing NOB: high temperature (30 - 40°C), high pH (7 - 8), and low SRT (< 2 days). Changes from nitrification to denitritification are accomplished by simply turning the air supply on and off. Thus, competition for oxygen may also limit NOB activity. The reactor pH is particularly important because this affects AOB and NOB growth rates and potential free nitrous acid inhibition of ammonia oxidation. Acidity produced by ammonia oxidation can be economically counterbalanced by dosing the reactor with methanol rather than NaOH, which both produces the needed alkalinity

and removes nitrogen as N_2. However, this works well only if bicarbonate is the predominant counter ion for ammonium (Schmidt et al., 2003). Oxygen and carbon requirements are lower than for complete nitrification followed by denitrification (Hellinga et al., 1998, Fux et al., 2002). However, NOB acclimation remains a concern in the effort to maintain these benefits (Hellinga et al., 1998). The process is not viable for many highly nitrogenous wastewaters produced at lower temperatures.

SBR

A competing design for implementation of sustained denitritification is the sequencing batch reactor (SBR) which has demonstrated 90% nitrogen removal in a full scale reactor (Fux et al., 2003). In the SBR, short aerobic/anaerobic cycles were used to promote nitrite buildup. Though NOB inhibition could have resulted from free ammonia inhibition or oxygen limitations, batch tests indicated free ammonia was not an important inhibiting factor. A batch reactor appears well suited for denitritification of sludge digester or filter press effluents, since these waste streams are intermittently generated and idle periods between waste additions may promote nitrite accumulation (Morgenroth et al., 2000). However, the long term effectiveness of the process may be limited by NOB acclimation.

2.4.2 Anaerobic ammonia oxidation

Anaerobic ammonia oxidation (anammox) was discovered in a denitrifying fluidized bed reactor (Mulder et al., 1995) and subsequently shown to be biologically mediated (van de Graaf et al., 1995). ^{15}N studies revealed that the product N_2 contained nitrogen atoms from nitrite and ammonium (van de Graaf, et al., 1997) and that nitrite was used as a terminal electron acceptor for ammonia oxidation. The same researchers found that reducing power for autotrophic growth was obtained by oxidizing a small amount of nitrite to nitrate. Kuenen and Jetten (2001) provided the following simplified stoichiometry for energy production and growth:

(10) Catabolic reaction $NH_4^+ + NO_2^- \rightarrow N_2 + 2H_2O$ [$\Delta G^{\circ\prime} = -357 kJ\ mol^{-1}$]

(11) Anabolic reaction $CO_2 + 2NO_2^- + H_2O \rightarrow CH_2O$ (biomass) $+ 2NH_3^-$

Oxygen was found to reversibly inhibit anammox at low concentrations (> 0.5% saturation; Strous et al., 1997b). Strous et al. (1999b) reported the maximum specific ammonia oxidation rate (45 ± 5 nmol/mg protein/min), minimum doubling time (11 days), and biomass yield (0.66 ± 1 mol C/mol ammonia) at pH 8 and 40°C for anammox. Although traditional AOB can oxidize ammonia anaerobically (Bock et al., 1995; Schmidt and Bock, 1997), the rates for anammox are ≈ 20-fold higher (Jetten et al., 1999). The very slow growth rate and low yield of these bacteria emphasize sludge retention in anammox wastewater treatment reactors and are manifested in the 3 to 6 months required to establish sufficient biomass in these reactors (van Dongen et. al., 2001; Strous and Jetten, 2004). Since anammox bacteria grow much more slowly than the NOB with which they compete for nitrite, the competitive edge provided to anammox bacteria must be strictly maintained, particularly since high nitrite concentrations (> 100 mg-N/L) are toxic to these bacteria (Strous et al., 1999b).

Ecologically, AOB and anammox may aid one another at anoxic/oxic interfaces, with AOB oxidizing a portion of the ammonia present, thereby keeping the oxygen concentration low, inhibiting NOB activity, and providing substrate and an anoxic environment for the anammox bacteria. Since several Plactomycetes have been found in reactors treating highly nitrogenous wastewater (Candidatus *Brocadia anammoxidans*, Strous et al., 1999a; Candidatus *Kuenenia stuttgartiensis*, Schmid et al., 2000; Candidatus *Scalindua brodae* and Candidatus *Scalindua wagneri*; Schmid et al., 2003), it is apparent that this ecological niche can be created in WWTPs (Siegrist et al., 1998; Egli et al., 2001; Dapena-Mora et al., 2004). The apparent diversity of bacteria that perform anammox highlights the potential usefulness of this process for making wastewater treatment more cost effective. NOB are of interest in anammox systems because they are natural competitors of these bacteria.

In the completely autotrophic nitrogen removal over nitrite (CANON) process aerobic ammonia oxidizers and anaerobic ammonia oxidizers simultaneously oxidize ammonia to dinitrogen gas and produce a small amount of nitrate (Sliekers et al., 2002).

This makes the process more economically appealing than denitritification because less oxygen is required for ammonia removal and the external reducing agent is completely eliminated. Improvements in oxygen transfer rates may improve nitrogen conversion rates (Sliekers et al., 2003). However, CANON reactors may be susceptible to competition from NOB including *Nitrobacter* and *Nitrospira spp.* when placed under realistic fluctuations in influent oxygen supply (Third et al., 2001).

2.4.3 Summary

NOB activity reduces the advantages denitritification and anammox processes provide for N-removal by competing for nitrite. Thus, the NOB activity level reflects the success of efforts to promote both complete nitrification and these alternate N-removal processes. An in-situ indicator of nitrite oxidizer activity would be useful to improve both complete and partial nitrification, and in either case significant economic benefits could be obtained through reduced capital and operational costs for wastewater treatment.

2.5 Molecular Enumeration of Bacterial Population and Activity

As indicated previously, even when highly nitrogenous wastewater with a low C/N ratio is degraded, nitrifying bacteria coexist with heterotrophic bacteria (Burrell et al., 1998). In WWTPs with a high C/N ratio, the nitrifiers make up only a small percentage (≈ 1 - 5 %) of total bacteria (Dionisi et al., 2003). In fact, it is likely that the most widely used biomass measures, the mixed liquor suspended solids (MLSS) and volatile suspended solids (MLVSS), display variations that exceed the nitrifier portion of the total suspended solids. This has long been recognized as a limitation in modeling nitrifier population and activity variations, since activity estimates are based on the suspended solids concentration (Sharma and Ahlert, 1977; Ford et al., 1980). More specifically, efforts to determine in-situ nitrifier kinetic parameters such as the maximum specific growth rate, as well as efforts to calibrate wastewater treatment models at WWTPs have been hampered. Uncertainty in these parameters likely contributes to the nitrification instability, which continues despite the fact that reactor design explicitly accommodates nitrifier growth rates with added safety factors (Section 2.2.2). A new

molecular technique, quantitative PCR, may provide improved modeling of nitrifier populations and activity and is reviewed below. After considering the limitations of enumerative data, quantitative RT-PCR is reviewed, since this technique may also be used to provide species specific activity information.

2.5.1 The polymerase chain reaction

The polymerase chain reaction (PCR) was conceived in 1983 (Mullis, 1990) and first performed using the Klenow fragment of DNA polymerase I from *E. coli* (Saiki et al., 1985). This reaction, which amplifies a DNA sequence, was made practical and highly specific when the heat stable polymerase from *Thermus aquaictus* (*Taq*) was introduced (Saiki et al., 1988). Quantitative application of the PCR (i.e. to measure the initial copy number of a DNA sequence) has been demonstrated using techniques that detect the accumulation of the amplicon (kinetic PCR, Higuchi et al., 1993; real-time PCR, Heid et al., 1996). Endpoint detection techniques are less reliable for quantitative purposes due to small differences in reaction components, cycling parameters, and the tendency for the PCR product to re-anneal and thereby complete with the primers (Freeman et al., 1999; Hermansson and Lindgren 2001). A stepping stone between continuous monitoring and endpoint detection was competitive PCR (Zimmermann and Mannhalter, 1996), which was recently used to enumerate NOB in a subsurface mine via the nitrite oxidoreductase gene (Hirayama et al., 2005) and in activated sludge via the 16S rDNA gene (Dionisi et al., 2002). Since the vast majority of microorganisms appear to be uncultivable, including certain nitrifying strains (Hermansson and Lindren, 2001), PCR based enumeration of bacteria represents an indispensable tool for study in the fields of applied and environmental microbiology.

The real-time version of quantitative PCR offers a broader detection range than competitive PCR, and eliminates the need for post PCR processing which can be a source of error and contamination (Sharkey et al., 2004). One real-time method utilizes fluorescent probes complementary to the PCR product that are digested as the reaction proceeds (Livak, et al., 1995). Thus, an advantage of real-time PCR over kinetic PCR, which uses an intercalating dye to nonspecifically bind to accumulating DNA, is the

increased specificity the probe sequence offers (Heid et al., 1996; McPherson and Møller, 2000). Real-time PCR technology is mainly based to two competing probe designs, both of which contain integral chemical fluorophores and quenchers: molecular beacons and linear dual labeled probes. Molecular beacons place the fluorophore and quencher in close proximity by placing them at opposite ends of a relatively long oligonucleotide that forms a hairpin structure. Linear dual labeled probes place the fluorophore and quencher in close proximity by simply having them bracket a short probe sequence (Figure 2). In intact probes, the quencher absorbs fluorophore emissions so long as the molecules are within 10 to 100 Å of one another (Molecular Probes, 2001). For both probe designs, PCR product is detected via unquenched fluorophore produced when the probe is cleaved during the extension phase of the PCR by the 3′ → 5′ exonuclease activity of *Taq* polymerase (Figure 3) (Holland et al., 1991). Quantification occurs with amplification plots of light yield versus cycle number after a threshold fluorescence value is established to identify the emergence of the exponential phase of amplification from background fluorescence values (Heid et al., 1996). The point at which a particular amplification plot crosses the threshold value determines the threshold cycle (C_T). Quantification often occurs by referencing the sample C_T with those for a series of external or internal standards (Heid et al., 1996). This greatly increases the sensitivity and range of quantitative PCR (Heid et al., 1996).

Recently, real-time PCR has been used to enumerate bacteria in environmental samples, which may reflect enhanced nucleic acid extraction efficiency for these samples (Sharkey et al., 2004). One application has been the enumeration of the catabolic genes involved in degradative pathways: carazole 1,9a-dioxygenase genes in soil samples (Widada, et al., 2001), MTBE degrading bacteria in laboratory and field soil and groundwater (Hristova et al., 2001), *Methylocyctis*, a trichloroethylene-degrading bacterium in groundwater (Kikuchi et al., 2002), and proteolytic genes in soil samples (Bach et al., 2002). Another application is detection of pathogens: *Clavibacter michiganensis* (Bach et al., 2003), enterococci and human adenoviruses in sewage and environmental samples (He and Jiang, 2005), and *Listeria monocytogens* in water and

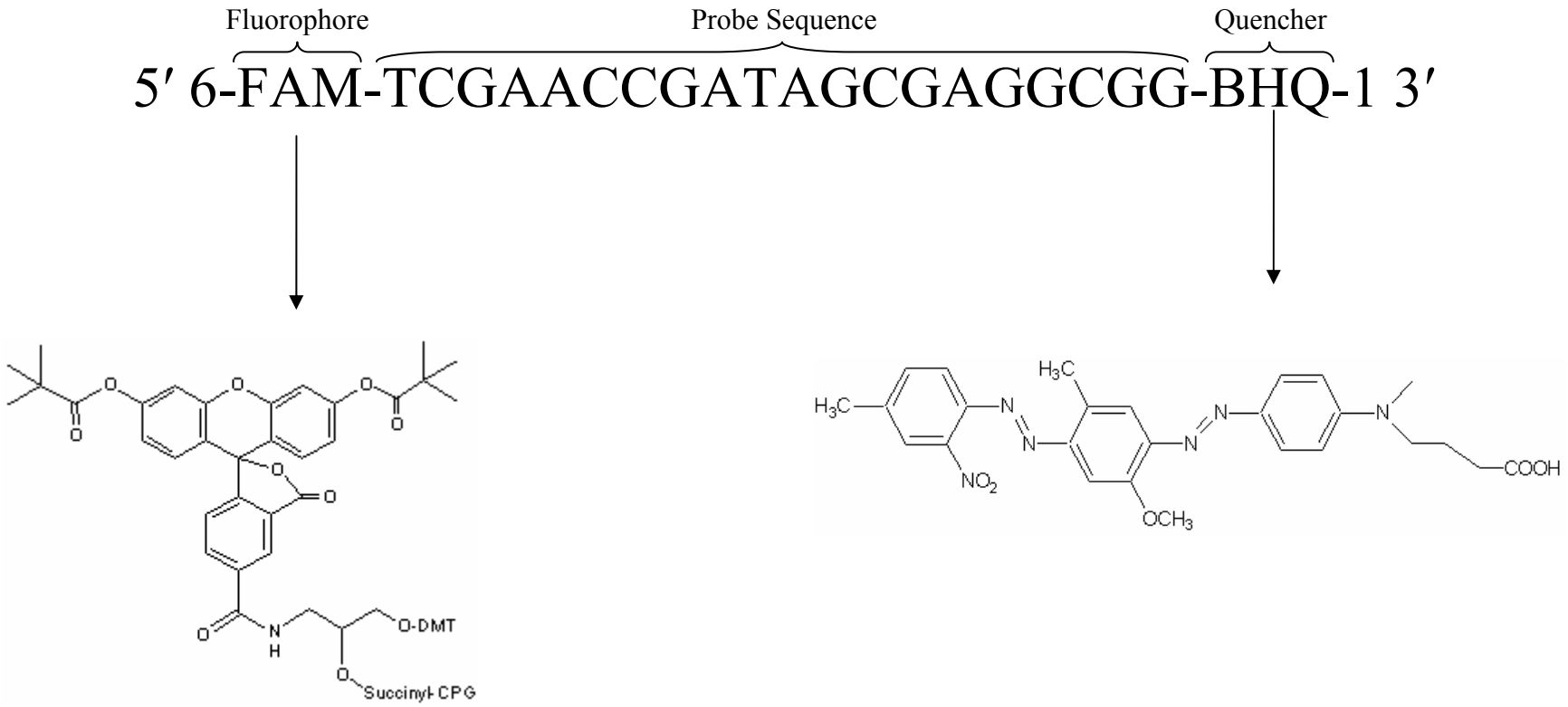


Figure 2 Diagram of a dual labeled linear probe for real-time PCR including signal (FAM) and quencher (BHQ-1) fluorophore structures (Biosearch Technologies, Novato, CA: the fluorophore structures shown are prior to incorporation onto the oligonucleotide).

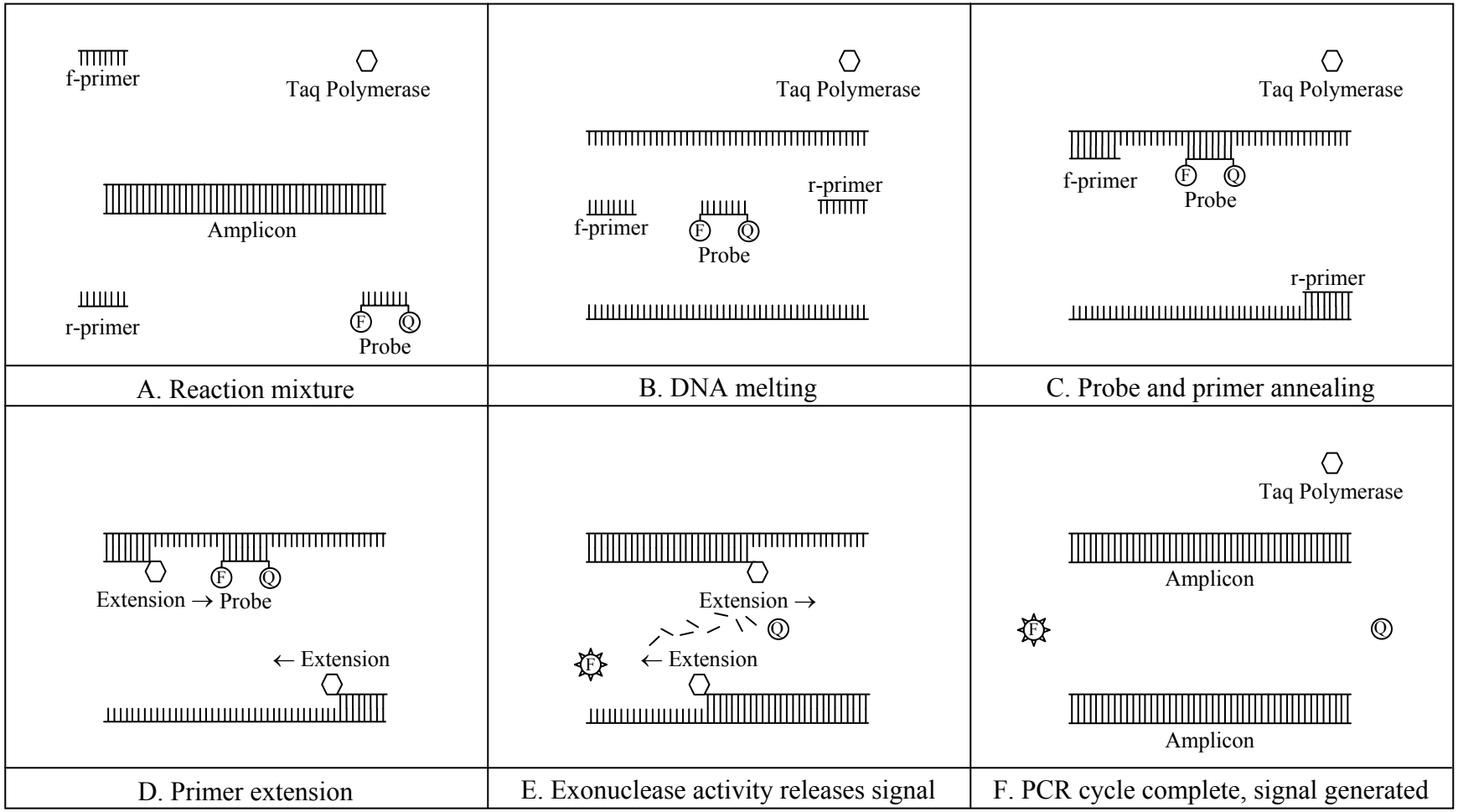


Figure 3 Schematic diagram (A - F) of a real-time PCR cycle illustrating fluorescent signal generation via Taq polymerase exonuclease digestion of a dual labeled linear probe during primer extension (F = fluorophore; Q = quencher).

milk/milk products (Nogva et al., 2000). Nitrifying bacteria (mainly the AOB) have been enumerated with real-time PCR on a limited basis. The AOB have been quantified in arable soil samples (Hermansson and Lindren, 2001), while the NOB 16S rDNA and AOB *amoA* genes have been quantified in activated sludge samples (Dionisi et al., 2002; Harms et al., 2003). Recently, real-time PCR of the AOB *amoA* gene detected the rise of a competitive dominant relationship between two distinct AOB subpopulations (Layton et al., 2005). However, for slow growing bacteria such as the NOB, the reproducibility of the technique may be poor because these bacteria are a low percentage of the total bacteria biomass (Dionisi et al., 2003). Dionisi et al. (2003) found that 22 and 5 replicate reactions were required to detect 2- and 5-fold increases in *Nitrospira* rDNA concentration in low biomass activated sludge samples. Though their findings for total bacterial rDNA abundance were better (3 replicates required to detect a 2-fold difference), this and other quantitative molecular techniques, such as FISH, appear unsuitable for detecting short term population changes in the NOB, which display doubling times greater than 8 hours (Watson et al., 1989; Ehrich et al., 1995). Also, though enumeration of genes such as *amoA* and rDNA can provide function-specific detection, enumeration, and phylogenic information for nitrifier subpopulations (Aoi et al., 2004a; Arki et al., 2004), no information is provided for in-situ activity, which is needed in the case of the NOB to detect and thus help prevent nitrification and N-removal instability.

2.5.2 The limitations of enumerative data

It has been suggested that new molecular based enumerative techniques could be linked with observed activity to improve wastewater treatment modeling (Burrell et al., 1998; Wagner et al., 1998; Oerther et al., 1999). However, it is unclear how well this effort will address nitrification instability since nitrifiers, and particularly the NOB, may respond to stress with decreased activity rather than a sharp decline in cell number (Turk and Mavinic, 1989b; Bernet et al., 2001; Laanbroek et al., 1994). For the alternate N-conversion pathways reviewed in Section 2.4, enumerative data could not be reliably linked to substrate conversion rates, since a variety of nitrite interconversions mediated

by different subpopulations could occur simultaneously. As previously indicated, the NOB are slow growers, with a doubling time in excess of 8 hours, so enumerative data may be less useful in meeting the need to identify and remediate nitrification and N-removal instability. However, another molecular technique, RT-PCR, can provide subpopulation specific activity information.

2.5.3 Activity assessments using the polymerase chain reaction

The reverse transcription-PCR (RT-PCR) reaction can be used to enumerate mRNA and rRNA. This technique takes advantage of reverse transcriptase (RT), an enzyme typically possessed by retroviruses, but also found in other types of viruses and even *E. coli* (Madigan et al., 2000). RT has three main catalytic abilities (Madigan et al., 2000): (1) constructing single stranded copy DNA (cDNA) using an RNA template, (2) synthesizing double stranded DNA using a DNA template, and (3) ribonuclease activity wherein the RNA part of a RNA/DNA hybrid is degraded. Moloney murine leukemia virus (MMLV-RT), avian myeloblastosis virus (AMV-RT), and more recently a thermostable RT/DNA polymerase from *Thermus thermophilus* (r*Trh*) have been used in RT-PCR procedures to quantify mRNA transcripts (Freeman et al., 1999). In fact, r*Trh* possess DNA polymerase processivity comparable to *Taq* polymerase (Sellner and Turbett, 1998). Generally these enzymes have been cloned and genetically engineered so that they are RNase H negative, since this activity interferes with the polymerase for formation of the RNA:DNA hybrid (Sharkey et al., 2004). An important difference in these RT enzymes is the temperature for optimum activity: 37, 42, and 60-70ºC for MMLV-RT, AMV-RT and rTth-RT (polymerase activity 60-94 ºC), respectively. Using a higher temperature during the RT step has been suggested as a means of avoiding unspecific primer annealing during gene specific cDNA construction (Freeman et al., 1996). A more stringent RT reaction has also been shown to prevent primer and mRNA secondary structures that interfere with gene quantification. In any case, once cDNA copies are made, PCR is used for amplification (Freeman et al., 1999; Bustin et al., 2000).

RT-PCR has been characterized as highly sensitive, having been used to detect transcripts of β-actin (constitutively expressed) and interleukin 2 from a single mouse thymoma cell (Chiocchia and Smith, 1997). While the technique's sensitivity is appealing, Freeman et al., (1999) note in a review of quantitative RT-PCR that success depends on the quantification strategy and choice of standards. Freeman et al. (1999) also note that variability in the RT-PCR reaction is common. Several techniques exist to quantify RT transcripts including competitive, kinetic, and real-time PCR (Freeman et al., 1999; Sharkey et al., 2004). The use of end point quantification is discouraged (Freeman et al., 1999), and kinetic amplification offers the reduced possibility of heteroduplex formation to which competitive PCR is prone (Sharkey et al., 2004). Gibson et al. (1995) first utilized real-time PCR to quantify mRNA transcripts following RT.

Recently RT-PCR has been used in a variety of environmental microbiology applications. RT-PCR has been used to detect expression of genes involved in biodegradative processes such as chlorocatcehol dioxygenase (Meckenstock et al., 1998) and *nahAc* for phenanthrene degradation (Marlowe et al., 2002), as well as for overall bacterial growth (rRNA) in contaminated soil amended with nutrients (Ka et al., 2001). In addition, RT-PCR has been used to detect the presence of pathogens or pathogenic activity: *Vibrio cholerae*, (Lyon, 2001), *Bacillus anthracis*, (Makino et al., 2001), *Vibrio vulnificus*, (Fischer-Le Saux et al., 2002), and *Clostridium botulinum*, (Sharkey et al., 2004). Muttray et al. (2001) utilized RT-PCR to measure the rRNA/rDNA ratio as an activity measure in a resin acid degrading bacterium. Though the ribosomal RNA and gene transcript copy number have been investigated as bacteria activity indicators (reviewed in Section 2.6), the research to date has not utilized real-time RT-PCR which could improve the detection range and measurement sensitivity.

For the AOB, RT-PCR followed by DGGE was used to assess the distribution and activity of β-subclass ammonia oxidizers in compost and composted materials (Kowalchuk et al., 1999). Several researchers have recently measured transcripts for the *amoA* gene in attempts to correlate transcript abundance with activity (Bollman et al., 2005; Aoi et al., 2004a; Aio et al., 2004b). Bollmann et al. (2005) observed that *amoA*

transcripts decreased over a 12 day time period following the onset of starvation, but increased within 4 hours of the addition of ammonia, while rRNA levels stayed constant. However, no activity investigations could be identified utilizing RT-PCR of NOB specific rRNA or the catabolic gene for nitrite oxidation (nitrite oxidoreductase).

2.6 Mechanistic Aspects of Bacterial Activity

Protein synthesis is the essence of bacterial activity and is intimately tied to both the rate of ribosome synthesis (Gaal et al., 1997) and the relative cellular ribosome content (Stevenson and Schmidt, 1998). Ribosomes are the protein manufacturing centers of cells, composed of large (50S) and small (30S) subunits. In *E. coli*, the 50S and 30S subunits are composed of two rRNAs (23S & 5S)/≈34 r-proteins and one rRNA (16S)/≈21 r-proteins, respectively (Zengel and Lindahl, 1994). Ribosomes may represent as much as 50% of the dry weight of fast growing cells (Zengel and Lindahl, 1994). Bacterial RNA content varies with growth condition and history (Oda et al., 2000) and growth rate (Poulsen et al., 1993). The ribosome construction rate increases approximately with the square root of growth rate, but is limited by the rate of rRNA transcription via ribosomal protein autogenous transcription control (Zengel and Lindahl, 1994). The rRNA transcription rate may in turn be regulated by the energy charge of the cell, and thus metabolic activity, through the initiating nucleotide concentration (Gaal et al., 1997). Eigener (1975) provided evidence that the energy charge (ATP concentration) could function as "part of the regulating factors in the metabolism *Nitrobacter*."

A key aspect of the bacterial cell response to changes in the surrounding environment involves the translational machinery (rRNA, tRNA, translation factors, etc.), and in particular the rRNA (Molin and Givskov, 1999). In their review, Molin and Givskov (1999) note that bacteria responded immediately to favorable changes in the surrounding environment (increase in nutrients) by increasing the rRNA transcription rate which caused the cellular ribosome content to rise. For example, Holmstrøm et al. (1999) observed mRNAs encoding the translation factor EF-T using in-situ RT-PCR and found that abundance was related to bacterial growth activity in *Salmonella typhimurium*. In

the case of unfavorable changes (nutrient depletion or inhibition), rRNA synthesis is decreased and the cellular ribosome content falls. In general, other cellular synthesis rates respond more slowly (Molin and Givskov, 1999).

2.6.1 RNA/DNA and rRNA/rDNA ratios

The previous observations may explain the success of RNA/DNA and rRNA/rDNA ratios as bacterial activity indicators (Table 4). Kerkhof and Ward (1993) conducted a literature review and found that the RNA/DNA ratio ranged from 2 to 10 at growth rates (μ) from 0.20 to 1.75 hr^{-1} in fast growing bacteria. For a slow growing marine denitrifier, they found the ratio ranged linearly from 2.0 to 2.7, while rRNA/rDNA ratio ranged nonlinearly from 0.5 to 1.5 (μ = 0.01 - 0.12 hr^{-1}). The RNA/DNA ratio ranged between 0.5 and 3.0 at μ = 0.1 - 0.7 hr^{-1} for resin acid degraders, while the rRNA/rDNA ratio ranged from 9 to 70 during batch growth of one of the isolates (Muttray and Mohn, 1998).

Species-specific probes were used to measure resin acid degrader activity with the rRNA/rDNA ration of both *Sphingomonas* (Muttray and Mohn, 2000) and *Pseudomonas* isolates in mixed culture (Muttray et al., 2001). Using rRNA/rDNA quantified with universal 16S primers in competitive PCR and RT-PCR reactions, Ka et al. (2001) found that the rRNA/rDNA ratio for total bacteria ranged from 9 to 275 after nutrient addition to artic soil contaminated with total petroleum hydrocarbons. However, the rDNA concentration did not change significantly. Milner et al. 2001 used fluorometry (RNA & DNA) and oligonucleotide probes (rRNA and rDNA) to quantify RNA/DNA and rRNA/rDNA ratios for buffered and unbuffered batch growth of *Listeria monocytogenes*. The ratios broadly reflected activity.

2.6.2 Ribosomal gene transcript

Molecular ratios using the total rRNA can be insensitive for some bacteria such as *Vibrio* species (Flaerdh et al., 1992), *Desulfobacter latus* (Fukui et al., 1996), and the slow growing *Mycobacteria tuberculosis* (Cangelosi et al. 1996) which maintain high rRNA content even upon starvation. Further, the rRNA content of the β-subclass AOB

Table 4 Molecular investigations of bacterial activity using RNA/DNA and rRNA/rDNA ratios and rRNAt abundance.

Reference	Metric	Target Microorganism	Application	Measurement Technique[1]	Summary of Results[2]
Kerkhof and Ward (1993)	RNA/DNA; rRNA/rDNA	*Psuedomonas stutzeri* Zobell; cited results for others	RNA/DNA and rRNA/rDNA to detect growth rates	EtBr Fluorescence of DNA & RNA; Hybridization^{DIG} of rDNA and rRNA	• RNA/DNA (linear) 2.0-2.7, rRNA/rDNA (nonlinear) 0.5-1.5: $\mu \approx 0.01 - 0.12$ hr^{-1} • RNA/DNA cited in the literature ranged from 2-10: $\mu \approx 0.2 - 1.75$ hr^{-1}
Cangelosi et al. (1996)	rRNAt; rRNA	*Mycobaterium tuberculosis*	Assay for rapid detection of antibiotic resistant strains	Hybridization^{AR}; RT-PCR amplification with gel imaging	• rRNAt abundance was low in antibiotic susceptible cells but not in resistant cells • rRNAt levels varied more quickly and over a larger range than RNA
Cangelosi and Brabant (1997)	rRNAt, rRNA: (relative hybridization signal per OD_{600}; normalized densitometer values)	*Escherichia coli*	Uninhibited and inhibited batch experiments	Hybridization^{AR}; DNA Probe Sandwich Hybridization	• rRNAt responded quicker & over larger range than rRNA during batch growth • rRNAt declined quickly on exposure to nutrient deprivation and uncouplers • chloramphenicol removed the uncoupler response; rifampin did not slow the decline of the uncoupler response
Muttray and Mohn (1998)	RNA/DNA; rRNA/rDNA	Various resin acid degrader isolates and *Escherichia coli*	Growth rate vs. RNA/DNA; batch growth of a resin acid degrading bacteria	Spectrophotometric quantification of total RNA & DNA; Hybridization^{AR}	• Positive correlation between exponential phase growth rate and RNA/DNA for all but one resin acid degrader and *E. coli*: RNA/DNA = 0.5 - 3; μ = 0.1-0.7 hr^{-1}; varied among strains at the same μ • rRNA/rDNA ranged from 9 to 70 during batch growth of a resin acid degrader

Table 4 Continued.

Reference	Metric	Target Microorganism	Application	Measurement Technique[1]	Summary of Results[2]
Licht et al. (1999)	rRNAt; rRNA (23S)	*Escherichia coli*	Growth in a mouse cecum contents and the cecum mucus layer	FISH; Northern blots[AR]	• rRNAt responded quicker & over larger range than rRNA in batch growth • inhibition by mouse intestinal contents indicated as inability to process rRNAt; ring shaped rRNAt FISH phenotype
Muttray and Mohn (2000)	rRNA/rDNA	*Sphingomonas* sp. Dha-33	rRNA/rDNA, growth rate, activity relations	Hybridization[AR]	• rRNA/rDNA varied from 18-42 at μ = 0.04-0.17 hr^{-1} in a CSTR • rRNA/rDNA increased from ≈ 0.1-1.6 during batch growth on resin acid; RNA/DNA varied from 1 - 7.
Oerther et al. (2000)	rRNA; rRNAt; rRNAt/rRNA; (relative hybridization signal also normalized to OD_{600} or volatile suspended solids)	*Escherichia coli; Acinetobacter calcoaceticus*	Pure culture batch growth experiments in LB media & filtered wastewater; *Acinetobacter* spp. in bench and full scale reactors	FISH; Hybridization[AR]	• Growth in LB media showed a faster and more substantial response for rRNAt versus rRNA • Variability in individual *Acinetobacter* cell response to filtered municipal WW • Change in growth attitude detectable in bench and full scale reactors
Ka et al. (2001)	rRNA/rDNA	Bacteria (conserved primers)	Response to nutrient addition	Competitive PCR and RT-PCR	• Increase in rRNA/rDNA (9 to 275) after nutrient addition to arctic soil contaminated with hydrocarbons

Table 4 Continued.

Reference	Metric	Target Microorganism	Application	Measurement Technique[1]	Summary of Results[2]
Milner et al. (2001)	RNA/DNA; rRNA/rDNA	*Listeria monocytogens*	pH controlled & uncontrolled batch growth	Total RNA & DNA by Fluorescence; Hybridization[AR]	• RNA/DNA = 2-12.5 & rRNA/rDNA = 2-19 (unbuffered growth); RNA/DNA = 2-35 & rRNA/rDNA = 2-38 (buffered growth) • rRNA greatest near end of exponential phase, declined greatly upon entering stationary phase
Muttray et al. (2001)	rRNA/rDNA	*Pseudomonas abietaniphila* BKME-9 (a resin acid degrader)	Resin acid toxicity in pulp and paper mill effluent, pH spike inhibition	Competitive PCR and RT-PCR	• Ratio increased (220 - 1200) with growth rate (0.036 - 0.352 hr^{-1}) (chemostat) • During batch growth, ratio was 275 during early exponential phase, < 25 in stationary phase • Ratio responded to DO limitation and alkaline pH spike, concomitantly rose as activity subsequently increased
Oerther et al. (2001)	rRNA	*Gordonia spp.* (formerly *Norcardia amarae*)	Correlation with filamentous foaming at a WWTP	FISH; Antibody staining; Hybridization[AR]	• Increase in *Gordonia* rRNA from 0.25 to 1.4% of total rRNA (hybridization) • Suggested increase in VSS from 4% to more than 32% (antibody staining)
Schmid et al. (2001)	rRNAt; rRNA (16S & 23S)	Candidatus *Brocadia anammoxidans*	Oxygen inhibition	FISH	• rRNAt decreased upon oxygen exposure quicker and to a much greater extent than 16S rRNA and 23S rRNA

Table 4 Continued.

Reference	Metric	Target Microorganism	Application	Measurement Technique[1]	Summary of Results[2]
Oerther et al. (2002)	rRNAt; rRNA; (relative hybridization signal normalized to OD_{600})	2 *Acinetobacter johnsonii* strains	Micronutrient effects on growth	Hybridization[AR]	• rRNAt responded more quickly than rRNA when upshifts in growth rate occurred after dilution to fresh media and when micronutrient supplements were added to synthetic wastewater
Stroot and Oerther (2003)	rRNAt (average object fluorescent signal)	*Acinetobacter calcoaceticus*	Response to 4 different filtered primary effluents	FISH	• High rRNAt during chloramphenicol inhibition • Assertion that high fluorescent signals for cells exposed to filtered primary effluent indicated growth inhibition that prevented rRNAt processing

1 DIG - Digoxygenin probes; AR - autoradiographic probes; (EtBr) ethidium bromide.
2 μ = specific growth rate.

remained high during periods of low activity caused by starvation (Morita, 1993; Morgenroth et al., 2000) and/or inhibition (Wagner, et al. 1995). However, there is evidence that the ribosomal transcript would be an effective substitute (Table 4).

The premature rRNA transcript (rRNAt) regulates the ribosome construction rate (Zengel and Lindahl, 1994) and there is good evidence from a broad range of bacterial species that rRNAt abundance may respond more quickly and significantly to changing growth conditions than mature rRNA (Table 4). Ribosomal gene transcript abundance was first used to rapidly identify antibiotic susceptibility in *Mycobacterium tuberculosis* strains (Cangelosi et al., 1996). Ribosomal transcripts remained abundant in resistant strains but rapidly disappeared from susceptible strains, while rRNA changed little in susceptible cells. Cangelosi and Brabant (1997) could not detect rRNAt in stationary phase *E. coli*, but on dilution into fresh media the per cell equivalent of rRNAt increased > 50-fold during outgrowth. The relative rRNA abundance increased only 5-fold over the same time course. Likewise, on transition from exponential to stationary phase, the per cell equivalent of rRNAt declined much more rapidly and to a greater extent than rRNA. Importantly, these researchers also observed significant declines in rRNAt following nutrient deprivation and inhibition with uncouplers (dinitrophenol, KH_2AsO_4, and m-chlorophenylhydrazone), whereas there was no effect on mature rRNA. These researchers suggested utilizing the rRNAt abundance to provide activity information on specific bacteria subpopulations by normalizing the rRNAt concentration to more stable population markers such as rRNA or rDNA. However, investigations of rRNAt/rDNA type ratios could not be identified in the literature.

Since the publication of Cangelosi and Bradant (1997), relatively few subsequent investigators have utilized rRNAt abundance as the basis for an in-situ activity metric (Table 4). Schmid et al. (2001) demonstrated that after 1 hour of anammox inhibition with oxygen, the rRNAt FISH signal fell to only 8% of its original strength, whereas the signal strength for 16S and 23S rRNA remained strong after 4 hours. Oerther et al. (2000) observed a 12-fold increase in the per cell equivalent of *E. coli* rRNAt ≈ 45 minutes after transfer of an overnight culture into fresh LB media, but the change in

rRNA was only 4-fold. The rRNAt/rRNA ratio increased from approximately 0.1 to 0.25 over a growth cycle. These researchers observed more muted changes for *Acinetobacter calcoaceticus* batch growth, but a more significant response for rRNAt (5-fold increase in 15 minutes) versus rRNA (2.5 fold increase in 3 hours) was maintained. Further, these researchers utilized the relative rRNAt abundance to show diauxic growth of this organism on filtered wastewater, as well as changes in activity during bench scale SBR treatment of filtered wastewater, and differences in the activity level of *Acinetobacter* spp. in the return activated sludge versus aeration basin of a full scale WWTP. The rRNAt levels were also shown to vary over a wider range and more quickly than rRNA in *Acinetobacter johnsonii* (Oerther et al., 2002). Licht et al. (1999) utilized FISH and northern blots to show that the relative *E. coli* 16S rRNAt abundance increased to a greater extent (11-fold) than the level of mature 23S rRNA (3-fold) during transition to a higher growth rates. These researchers suggested that an *E coli* growth inhibitor was present in mouse cecum contents that prevented precursor rRNAt processing, so that the relative rRNAt abundance exceeded that found in much slower growing *E. coli* within the mouse cecal mucus layer. Abnormally high rRNAt levels were also found by Cangelosi and Brabant (1997) and Oerther et al. (2000) for *E. coli* and *A. calcoaceticus* cells treated with chloramphenicol, which inhibits rRNA maturation. Stroot and Oerther (2003) indicated that unknown inhibitors in wastewater can cause abnormally high rRNAt levels.

Relatively few studies of rRNAt abundance have been conducted in wastewater treatment applications (Schmid et al., 2001; Oerther et al., 2000; Oerther et al., 2002; Stroot and Oerther, 2003). None of the studies reviewed utilized rRNAt/rDNA type ratios, which would appear superior to the rRNAt/rRNA type ratio investigated by Oerther et al. (2000), since this would provide a more concrete measure of the cell number for normalization. In addition, all of the studies reviewed utilized hybridization techniques rather than quantitative RT-PCR. Quantitative PCR could improve the usefulness of the rRNAt/rDNA metric by improving the detection limit for rRNAt and hence the range of the activity metric. Finally, no studies of rRNAt abundance have been

conducted for NOB, which are of interest in promoting greater nitrification and N-removal efficiency in wastewater treatment.

2.7 Summary

Specific enumerative data will likely improve understanding and modeling of nitrification activity; however, the Literature Review revealed the need for a basic, but *species specific* snapshot of nitrifier activity. No such indicator has been investigated for NOB, which are the nexus of interest in promoting traditional nitrification and in realizing the benefits of alternate N-conversion pathways. Such an indicator might serve to detect and diagnose the cause of AOB and NOB inhibition in traditional wastewater treatment applications. For the more efficient N-conversion processes, the indicator could detect and diagnose NOB adaptation.

The mechanistic underpinnings of cell growth lie in the protein synthesis rate and link with cell ribosome and rRNA content. RNA/DNA and rRNA/rDNA ratios have been used to monitor species specific activity, but not for nitrifying bacteria. There is clear evidence that incorporating the ribosomal transcript into a ratio would the improve sensitivity of this type of activity metric. Thus, the rRNAt/rDNA ratio could serve as a species specific indicator of NOB activity.

CHAPTER 3.0

MATERIALS AND METHODS

3.1 Overview of Experimental Approach

The rRNAt/rDNA ratio was evaluated in a bench scale nitrification reactor (BSNR) and in batch assays using mixed liquor samples from this reactor (Figure 4). The first task was to establish the BSNR, which is described in Section 3.2. After the reactor was well established, a 16S - 23S ISR clone library was constructed using conserved primers specific for bacteria. This allowed a dominant NOB in the reactor to be identified (*Nitrobacter* genus). Using stringent guidelines for real-time PCR primer and probe sequences, a new quantitative PCR system was designed targeting *Nitrobacter* ribosomal operon and ribosomal transcript. Experiments were then performed to ensure these assays were specific, accurate, and sensitive. The protocols for nucleic acid extraction and cloning are presented in Sections 3.6 and 3.7, respectively. Also, the culturing techniques for *Nitrobacter hamburgensis*, which was used to study intra-strain ISR sequence diversity, is described in Section 3.3.

After the detection systems were developed and tested (Chapter 4.0), the rRNAt/rDNA metric's utility was examined in three phases. In phase 1, the range and dynamics of the ratio were studied. First, upper and lower prediction intervals were established for the metric in the BSNR while high nitrification efficiency was maintained. This was a pivotal aspect of the research, since all other measures of the ratio were compared principally against the metric's lower prediction interval in the BSNR. Second, the upper and lower limiting values for the ratio were evaluated during nitrite starvation and unlimited nitrite oxidation, respectively, in a batch respirometric experiment. This established the range of possible ratio values, as well as the metric rate of change. In the second phase of the study, the rRNAt/rDNA response was measured in batch respirometric inhibition assays. This indicated whether the metric's response to different types of inhibitors was the same, and whether during significant nitrite oxidation

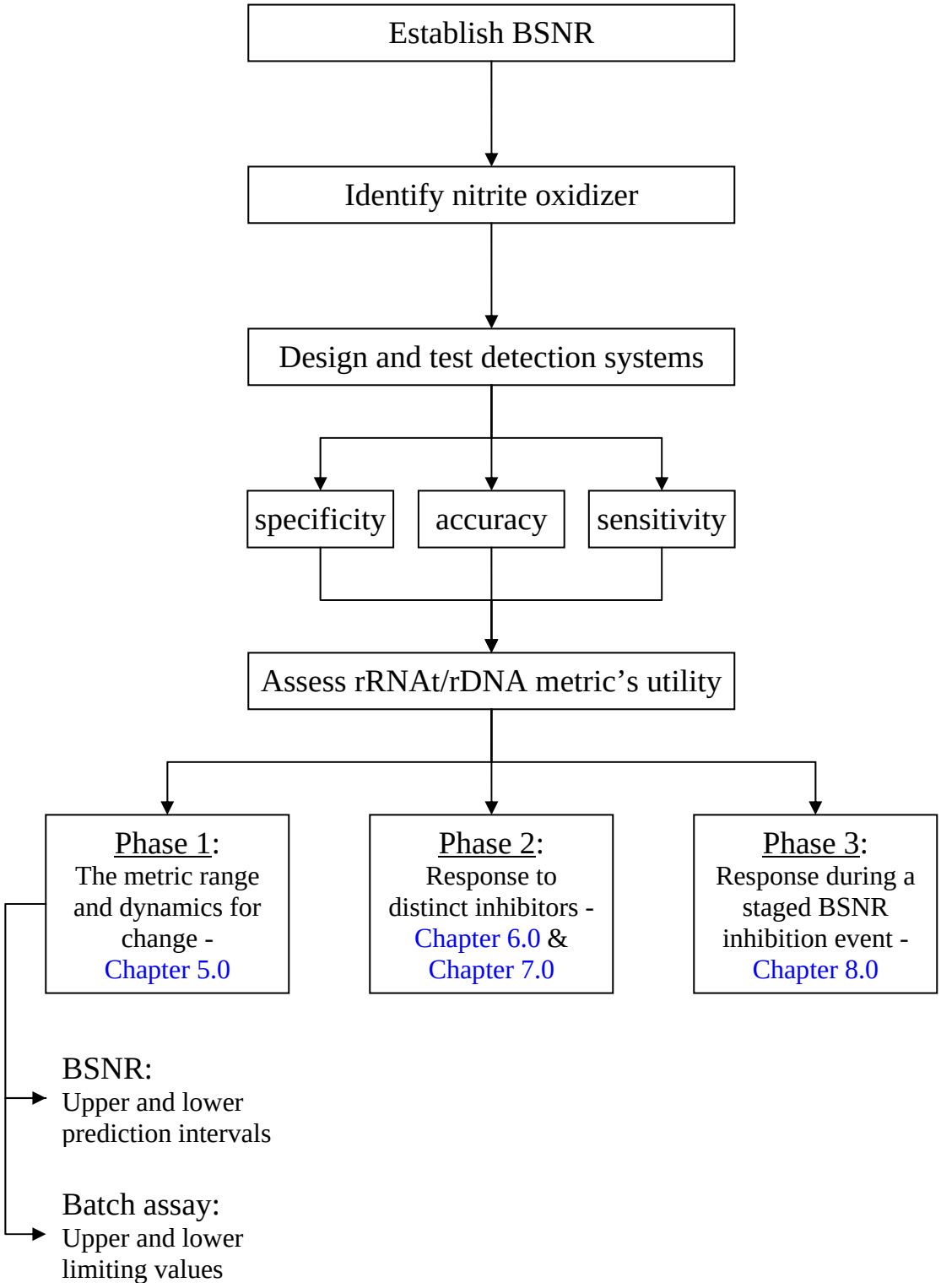


Figure 4 Outline of the experimental approach used to evaluate the rRNAt/rDNA ratio as an NOB activity metric.

inhibition the metric consistently declined below the lower BSNR prediction interval. The respirometer used in these studies is described in Section 3.5. In phase 3, the diagnostic and predictive usefulness of the metric was evaluated in a staged BSNR inhibition event. The design details of the experiments performed in the phase 1 - 3 experiments are provided in Chapters 5 - 8. The mixed liquor solids and nitrogen analysis protocols used in these experiments are described in Section 3.4.

3.2 Bench Scale Nitrification Reactor

The BSNR system was constructed to provide this study with a source of enriched nitrifying biomass (Figure 5), but could exemplify any full scale reactor treating highly nitrogenous wastewater with a low C:N ratio. The enrichment provided a practical benefit in that NOB activity could be easily evaluated using respirometry because of the low heterotrophic oxygen demand.

3.2.1 Seed

Bioscience, Inc. (Bethlehem, PA) markets microbial cultures with specific enzymatic capabilities (Microcat® Microbial and Chemical Additives). One product line, designated XNL/XNC, is marketed to municipal, industrial, and food processing wastewater treatment facilities that require continuous high nitrification performance. XNL/XNC, which are in liquid suspension/concentrated slurry forms, purportedly combine highly enriched but mixed nitrifying bacteria populations to yield enhanced nitrification and reseeding effect during performance lapses. The products are typically metered into activated sludge reactors to curb the effects of poor nitrification performance. Although the Bioscience product was chosen to seed the BSNR, similar commercial nitrifier cultures were available from Remediation Resources (Brampton, Ontario, Canada), Ecological Laboratories (Cape Coral, FL, USA), and Star Biological (Dallas, TX, USA). The widespread availability of these products is a testament to the difficulty in maintaining high nitrification efficiency. A 200 ml sample of XNC was used to seed the BSNR.

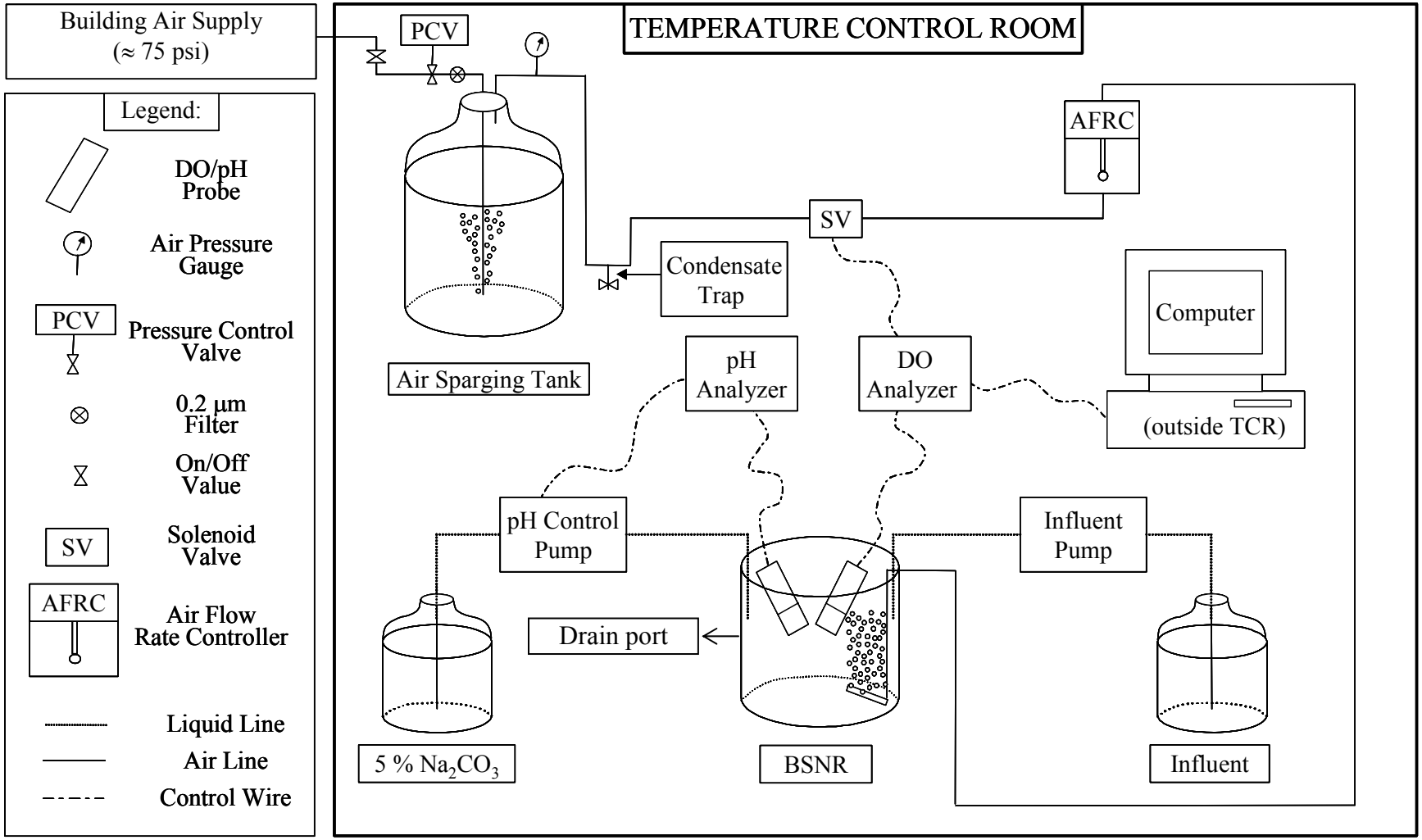


Figure 5 Schematic diagram of the BSNR.

3.2.2 Influent composition

The BSNR influent composition is provided in Table 5. The high ammonia concentration (1,500 mg-N/L) is similar to that found in sludge digester effluents (Graja and Wilderer, 2001), landfill leachate (Egli et al., 2001), and many different types of industrial wastewaters such as rendering plant effluent (Juretschko et al, 1998). The micronutrient composition is based on past nitrifier enrichments that served as surrogates for activated sludge during modeling studies (Hall and Murphy, 1980; Copp and Murphy, 1995; Kim and Chang, 1999). However, one important difference between the influent composition used in this and the referenced studies was the phosphate level, which in most nitrifier enrichment media reviewed greatly exceeded nutrient demand, serving mainly to control the reactor pH via buffering. The BSNR was equipped with a pH control system that eliminated the need for a high buffer capacity. Also, a buffered influent would have hindered a study of pH inhibition (Chapter 6.0).

The BSNR was initially seeded and operated for several months with unsterilized influent containing 1,000 mg-N/L provided as $(NH_4)_2CO_3$. However, chemical precipitation problems in the influent feed lines resulted in a switch to $(NH_4)_2SO_4$ which

Table 5 A list of BSNR influent constituents and their concentrations.

Constituent[1]	Influent composition	Influent Concentration
deionized water	1 L	-
1 M K_2HPO_4	1.5 ml	1.5 mM
1 M KH_2PO_4	24 ml	1.5 mM
1 M $MgSO_4$	12 ml	750 µM
1 M $CaCl_2$	3.2 ml	200 µM
30 mM $FeSO_4$/50 mM EDTA	5.3 ml	9.9 µM/16.6 µM
10 mM $CuSO_4$	0.8 ml	0.5 µM
$(NH_4)_2SO_4$	113 grams	53.6 mM (1,500 mg NH_4-N/L)

1 Certified A.C.S. (Fisher Scientific; Fair Lawn, NJ) or A.R.G. (Mallinckrodt, Paris, KY) chemicals were used for stock solutions prepared in class A volumetric glassware with deionized water (stored in the dark at 30°C).

eliminated this problem. Also, after the switch to $(NH_4)_2SO_4$, the influent and influent lines were sterilized after large (16L) batches of influent were prepared. This eliminated potential microbial growth in the influent lines and storage tank.

3.2.3 Reactor construction and operating technique

A 10 Liter Plexiglass® reactor contained the culture (Hawkins, 2000). The top and bottom plates were 12″ (30.48 cm) square and ½″ (1.27 cm) thick. A 12″ (30.48 cm) long section of 10″ (25.4 cm) inside diameter tube (½" thick) was permanently bonded to the bottom plate. The contents were mixed by placing the reactor on a 12″ (30.48 cm) square magnetic stir plate (Model 547035, Barnstead/Thermolyne, Dubuque, IO). A 3" (7.62 cm) Teflon® coated stir bar was turned at speed setting 7 for vigorous mixing. To avoid photo inhibition (Sharma and Ahlert, 1977), the reactor was housed in a dark, temperature control room. Since it was necessary to enter the room for extended periods of time with full lighting, the reactor was wrapped with 1/8" aluminum clad foam.

The reactor was operated in continuous-fed batch mode. Influent flowed at 1 L/day through opaque Neoprene® tubing (Masterflex P/N P-06404-13, Cole Parmer Instrument Company, Vernon Hills, IL) via a digital standard drive peristaltic pump (Model 7523-50, Cole Parmer Instrument Company, Vernon Hills, IL). When combined with the base adjusting solution flow (≈ 0.35 L/day), this caused the reactor volume to increase from 10 to ≈ 12.7 liters every 48 hours, at which point the reactor was drained back to 10 Liters. The flow rate and operating scheme provided a SRT of 10 days (typical for municipal WWTPs promoting nitrification: Grady et al, 1999) as well as 2.6 liters of fresh reactor mixed liquor for experiments outside the reactor every 48 hours.

3.2.4 Temperature

The BSNR was housed in a temperature control room (TCR; Model NSCP2S, Norlake Scientific, Hudson, WI) maintained at 30°C. Foam insulation surrounded the reactor to buffer against temperature fluctuations during heating and cooling cycles.

3.2.5 pH

The BSNR was equipped with a pH control system consisting of a dual input pH analyzer (Model WDP300, Walchem Corporation, Holliston, MA) and a flat surface glass electrode (Model WEL-PHF-NN, Walchem Corporation, Holliston, MA) that minimized biofouling. The reactor was operated at a pH setpoint of 7.20. When the pH fell below the set point, a relay in the controller energized a pump (P/N 10570105B2A126, Barnant Company, Barrington, IL) that injected a 5% Na_2CO_3 solution into the reactor. This raised the pH back to the setpoint at which time the controller shut off power to the pump. The metering pump, with a stroke volume 0.16 mL and at speed setting 1.5 (5 - 6 strokes/min), was capable of adjusting the pH quickly, and maintained the pH between ≈ 7.19 and 7.25.

3.2.6 Oxygen

Compressed air (≈ 800 cm^3/minute) was filtered through a 0.2 μm, 37 mm inline bacterial air vent (Uniflo-50T, Gelman Sciences, Ann Arbor, MI) and then sparged through deionized water in a 25 liter Nalgene® polyethylene carboy. The humidified air traveled thorough a condensate trap to a flow rate controller containing two direct reading flowtubes (Model 082-02G, Aalborg Instruments, Orangeburg, NY). Air was split through the two tubes (≈ 400 cm^3/min each) before continuing to a stainless steel fine bubble diffuser located at the bottom of the reactor. A constant airflow rate was achieved by supplying air to the flow rate controller at a set pressure (10 psig) using an inline backpressure controller (Model 100HR, Controlair, Amherst, NH).

The DO concentration was measured with a dual input DO analyzer (Model D53, GLI International, Milwaukee, WI) equipped with a three-electrode Clark type probe (Model 5500, GLI International, Milwaukee, WI). The analyzer contained independent relays that were programmable in setpoint control mode and controlled power to a solenoid valve located immediately upstream of the flow path splitter (Hawkins, 2000). With a set point of 6.5, the reactor received air continuously at 800 cm^3/min, which

maintained the DO between ≈ 3 and 5 mg/L. This is above the oxygen affinity constants for nitrifying bacteria (Table 3).

3.3 *Nitrobacter hamburgensis* Culture

A second source of biomass for the study was a *Nitrobacter hamburgensis* culture, which was used to assess intra-strain 16S - 23S ISR diversity after this NOB genus was found in a BSNR clone library (ISR diversity may vary within prokaryotic species) (Navarro et al., 1992b). Though archived at the UT Center for Environmental Biotechnology, this organism was originally acquired from the Deutsche Sammlung von Mikroorganismen Zellkulturen (DSMZ - DSM 10229). This bacteria was cultured in DSMZ media 756a (mixotrophic *Nitrobacter* media) and 756c (autotrophic *Nitrobacter* media) at 30°C. However, growth could not be established in the autotrophic media within three months. Growth in the mixotrophic media occurred in approximately one month, and thereafter nitrite was exhausted with concomitant growth in less than one week. The cultures were checked for heterotrophic contamination using agar plates (Bock and Koops, 1992) as new batches of media were seeded. Contamination was never detected.

3.4 Analytical Measurements

3.4.1 Suspended solids

Mixed liquor volatile suspended solids (MLVSS) were analyzed with method 2540 E: Fixed and Volatile Solids Ignited at 550°C (APHA, 1998). A mixed liquor sample was dispensed onto a pre-ignited 47 mm, 1.5 micron glass fiber filter (typically Proweigh®; Environmental Express; Mt. Pleasant, SC) in a vacuum flask assembly. After drying for at least one hour at 103°C, the filter was placed in a 550°C muffle furnace for at least 15 minutes. The MLVSS concentration was calculated using the following equation:

$$\text{mg volatile suspended solids/L} = \left(\frac{W_{FWDS} - W_{FWA}}{V} \right) \times 1{,}000$$

where :

(12)

W_{FWDS} = weight of filter with dried solids (mg)

W_{FWA} = weight of filter with ash (mg)

V = volume of sample (L)

3.4.2 Nitrogen

Ammonia

When the available sample size was not limiting, Standard Method 4500 D: Ammonia-Selective Electrode Method (APHA, 1998) was used to determine ammonia concentrations in 100 ml samples. An Orion 250A analyzer equipped with a model 95-12 probe (Orion Research, Boston, MA) was utilized in this procedure.

Ion chromatography was used to quantify ammonia when high accuracy was required or if only small sample volumes were available. A DX-500 ion chromatograph (IC) (Dionex Corporation; Sunnyvale, CA) equipped with an Ionpac® NGI primary guard column (P/N 39567), an Ionpac® CS12 guard column (P/N 44002), and an Ionpac® CS12 cation exchange column (P/N 44001) was used to perform the analysis. Auto-suppression recycle mode was used with a cation self regenerating suppressor-ultra (CSRS-Ultra, P/N 53948) and 20 mM methane-sulfonic acid eluent at 1 ml/min. An AS-40 auto sampler avoided retention time variation and improved sample throughput and analytical accuracy. Samples were filtered (typically Acrodisc® 25 mm or 13 mm 0.45 μm; Pall Gelman Laboratory, Ann Arbor, MI), then introduced into the IC eluent stream through a 25-μL sample loop for separation and subsequent quantification using the conductivity signal. Concentrations were typically evaluated in triplicate using ammonia ion standards spanning 5 to 6 concentrations. All ammonia samples were preserved with concentrated sulfuric acid (2 μl acid per mL of sample: ≈ pH 2) and stored at 4°C until analysis.

Nitrate/Nitrite

Anion samples were filtered (typically Acrodisc® 25 mm or 13 mm 0.45 μm; Pall Gelman Laboratory, Ann Arbor, MI) and stored at 4°C until analysis using standard method 4110 B: Ion Chromatography with Chemical Suppression of Eluent Conductivity (APHA, 1998). A DX-500 IC (Dionex Corporation, Sunnyvale, CA) equipped with an Ionpac® AS9-HC 4 mm guard (P/N 51786) and anion exchange (P/N51891) column was used for the analysis. The IC was run in auto-suppression recycle mode with an anion self regenerating suppressor-ultra (ASRS-Ultra, P/N 53946) using 9 mM Na_2CO_3 eluent at 1 mL/min. An AS-40 auto sampler performed injections through a 25 μL sample loop. Concentrations were typically evaluated in triplicate based on standards spanning 5 to 6 concentrations.

3.5 Electrolytic Respirometry

A BI 2000 electrolytic respirometer (Bioscience; Bethlehem, PA) was used in batch respirometric assays of BSNR mixed liquor samples. Briefly, oxygen was supplied intermittently to a hermetically sealed and vigorously mixed vessel in response to pressure drops within the vessel. The pressure drop was sensed by a switch leg immersed in a dilute solution of sulfuric acid that sealed the vessel. Oxygen was liberated to the vessel atmosphere by passing electric current through the acid. The cumulative oxygen consumption was tallied for a set time interval (typically 0.1 hrs) using the current setting (typically 75 mA) and the total time current was applied to the element during the time interval. The respirometer included a temperature controlled water bath which was maintained at 30 ± 1°C. During respirometric experiments, vessels were covered with an opaque cloth to avoid photo inhibition of the nitrifying bacteria (Sharma and Ahlert, 1977).

Before conducing experiments with the BSNR biomass, the oxygen transfer capacity of the respirometer was evaluated with activated sludge (obtained from a local municipal WWTP) that had been completely inhibited with copper sulfate. After verifying that the oxygen demand was ≈ 0 mg/L/hr, 1.0013 grams of Na_2SO_3 and 0.0158

grams of $CoCl_2 \cdot 6H_2O$ were added to the inhibited mixed liquor sample. Since sulfite is an oxygen scavenger which rapidly reacts with any oxygen present in solution, oxygen consumption in the vessel was limited only by the mass transfer capacity of the respirometer. A linear regression through the cumulative oxygen uptake data estimated the maximum transfer capacity at 26.3 mg O_2/L/hr ($R^2 > 0.99$). This experiment demonstrated the respirometer accurately measured oxygen consumption since the added sodium sulfite stoichiometrically required 126 mg oxygen and the total demand was 125 mg. In experiments with the BSNR biomass, the oxygen transfer capacity of the instrument was not allowed to exceed 80% of the total capacity of the instrument (≈ 21 mg/L/hr) in an effort to ensure that oxygen did not limit NOB and/or AOB activity. The DO concentration was observed mid-experiment on several occasions with high oxygen demand (> 10 mg/L/hr); the concentration was always near saturating levels (8 mg/L).

3.6 Nucleic Acid Extraction

3.6.1 DNA

Sample collection and storage

Mixed liquor samples were collected (≈ 5 ml, typically in triplicate) in preweighed sterile 15 ml centrifuge tubes. The tubes were reweighed after sample collection to establish the sample volumes (based on water density). In addition to ensuring the sample volumes were measured accurately, this procedure removed potential sample bias created by attempts to withdraw exact sample volumes. The tubes were centrifuged for 15 minutes at 3,000 × *g*, the supernatant discarded, and the pellet was frozen at -80°C.

Lysis, extraction, and DNA extract storage

DNA was extracted from the pellets using the Fast DNA kit (Q-BIOgene, Carlsbad, CA, USA) with slight modifications of the manufacturer's protocol (Dionisi et al., 2002). The samples were unfrozen and then centrifuged at 3,000 rpm for 15 minutes at room temperature. Excess supernatant was removed with a pipette, the pellet was resuspended in 800 µl of the kit CLS-TC solution, then transferred to a lysing tube

containing a ¼" sphere and garnet matrix. Cells were immediately lysed in a homogenizer (FastPrep 120; Q-BIOgene) at speed 4 for 20 seconds. The lysate was chilled on ice for five minutes and centrifuged at 10,000 - 14,000 × *g* for 15 minutes at 4°C. The supernatant was combined with 600 µl of glass milk binding matrix and gently mixed for 10 minutes at room temperature. The binding matrix was separated from the supernatant and then resuspended in 500 µl of 80% (v/v) ethanol, transferred to a Spin™ module (Q-BIOgene), spun down, and a second 500 µl 80% ethanol wash was completed. DNA was eluted by resuspending the binding matrix in 100 µl of 10 mM Tris-HCl (pH 8), incubating the suspension at room temperature for 5 - 10 minutes, and centrifuging it at 10,000 × *g* for 1 minute. A second elution was performed for a total extraction volume of 200 µl. When required, the DNA concentration was determined with a calibrated fluorometer (Hoefer DyNA® Quant 200; Amersham Biosciences; Piscataway, NJ) at the University of Tennessee Molecular Biology Resource Facility (MBRF). The DNA extracts were stored at -80°C as 1:5 dilutions in 10 mM TRIS HCl at pH 8.0.

3.6.2 RNA

Sample collection and storage

Mixed liquor samples (≈ 3 ml, typically in triplicate) were placed directly into 2 volumes of RNAprotect™ for Bacteria (Cat. No. 76506; Qiagen, Inc.; Valencia, CA, USA) contained in sterile 15 ml pre-weighted centrifuge tubes. RNAprotect™ freezes the expression profile at the moment of sampling by preventing transcript degradation and gene induction (Qiagen, 2001a). Immediately after the samples were collected they were mixed and incubated 5 to 10 minutes at room temperature. Following incubation, the tubes were re-weighed to determine the sample volume, centrifuged for 15 minutes at 3,000 × *g*, and then stored at -80°C after the supernatant had been decanted. The pellets were stored no longer than 28 days prior to extraction.

Lysis, extraction, and RNA extract storage

An enzymatic lysis protocol for gram positive bacteria was followed (Qiagen, 2001b). The samples were retrieved from - 80°C storage and centrifuged for 5 minutes at 3,000 × *g*. All but a trace (≈ 25 µl) of the supernatant was removed with a pipette. The pellets were resuspended in 200 µl of lysozyme solution, transferred to sterile micro centrifuge tubes, and vortexed 10 seconds every minute for 10 minutes. Stock lysozyme (250 mg/ml: Sigma-Genosys; The Woodlands, TX; catalog number L7651) was prepared in RNase free water, stored in single use aliquots at -20°C for up to two weeks, and diluted in RNase free TE buffer (10 mM Tris·Cl, 1 mM EDTA pH 8.0) immediately prior to use. To complete lysis, 700 µl of the buffer RLT (RNeasy Mini Kit component; Qiagen, Inc.; Valencia, CA) was added and the solution was vortexed. Particulate matter was removed by centrifuging the lysate for 2 minutes at 14,000 × *g*. The supernatant was then transferred to a sterile centrifuge tube for immediate extraction.

RNA was extracted from the lysate supernatant using the RNeasy Mini Kit (Cat. No. 74104; Qiagen, Inc.; Valencia, CA). Pure ethanol (500 µl) was added to the lysate and the solution was mixed with a pipette. The mixture was applied to the kit's mini spin columns, centrifuged for 30 seconds at ≥ 10,000 × *g*, and the supernatant discarded. The column was washed with 350 µl of the kit's buffer RW1 and an on-column DNase digestion was performed (Cat. No. 79254; Qiagen). DNase I in Buffer RDD (80 µl) was pipetted onto the column which was then incubated at room temperature for 25 to 30 minutes. The column was rinsed with 350 µl of the kit's buffer RW1, transferred to a fresh collection tube, and rinsed twice with 500 µl aliquots of the kit's RPE solution. The column was placed into a fresh micro centrifuge tube and centrifuged for 2 minutes at 14,000 × *g* to remove all traces of the ethanol. Elution occurred into a RNase free centrifuge tube using two 30 µl aliquots of RNA storage buffer (Cat. No. 7001; Ambion, Inc.; Austin, TX). Multiple, single use, 1:5 dilutions of the RNA extracts were made using storage buffer immediately after elution. The remaining extract and dilutions were frozen at -80°C. Elution and dilution into the storage buffer, and the practice of discarding the 1:5 working dilutions after they were unfrozen, minimized the potential for

RNA degradation. Quantitative PCR is likely dependent on an undegraded, high quality RNA extract (Bustin, 2002).

3.7 Clone Library Construction

3.7.1 PCR amplification

Ready-To-Go beads (Amersham Pharmacia Biotech, Piscatawa, NJ) were employed in 25 µl reactions containing 21 µl of 0.2 µM filtered HPLC grade water (fHPLC: Fischer Scientific, catalog number W5-4), 1 µl of each primer (10 µM), and 2 µl of dilute DNA extract. Typically, the reactions followed a touchdown PCR protocol consisting of: *Taq* activation at 95°C for 5 minutes, 10 touchdown cycles with melting at 95°C for 15 seconds, annealing at 65°C → 55°C for 45 seconds (-1°C per cycle), ending with extension at 72°C for 1 min, and followed by 19 cycles at 55°C with final extension at 72°C for 1 minute. The reactions were examined with agarose gel electrophoresis [1.5% (w/v) low EEO electrophoresis grade agarose (Fisher Scientific, Springfield, NJ) in 0.5% TBE with 1 µl (10 mg/ml) ethidium bromide (EtBr) per 10 mL of gel volume)] ran in 0.5% TBE at 100 V. PCR products were viewed with an AlphaImager™ 2000 (Alpha Innotech Corporation, San Leandro, CA; AlphaEase software version 4.6). Product bands were typically compared with the 1Kb Plus DNA molecular weight marker (Invitrogen, Carlsbad, CA).

3.7.2 Cloning

Fresh PCR products were cloned using the TOPO TA Cloning® Kit for Sequencing (Invitrogen, Carlsbad, CA). Amplicons were ligated into a linearized plasmid (pCR®4-TOPO) containing single 3′ thymidine overhangs and covalently bound topoisomerase enzyme. *Taq* polymerase from the PCR reaction added a single deoxyadenosine terminal residue at the 3′ end of the PCR product and thereby promoted high ligation efficiency with the vector. Cloning followed the manufacturer's suggested protocol in a 5 µl reaction mixture (1 µl of PCR product, 1 µl of the TOPO vector, 1 µl of salt solution, and 2 µl of 0.2 µM fHPLC water). The ligation reaction was incubated 5

minutes at room temperature, stored briefly on ice, and a 2 µl aliquot was added to freshly unfrozen One Shot® Chemically Competent *Escherichia coli* (Invitrogen, Carlsbad, CA). The cells were incubated on ice for 5 minutes, transformed with a heat shock at 42°C for 30 seconds, and immediately placed back on ice. SOC media (250 µl) was added prior to incubation at 37°C for one hour with horizontal shaking at 200 rpm. Typically, two cell suspension aliquots (20 and 50 µl) were spread onto Luria Bertani-Kanamycin agar plates (LB-Kan_{50}: 10g/L tryptone, 5 g/L yeast extract, 5 g/L NaCl, and 10 g/L of agar in 1 Liter of distilled water at pH 7.5 with 50 µg/ml kanamycin) and incubated overnight at 37°C. Since the pCR®4-TOPO vector insertion site disrupts the lethal *ccdB* gene, only bacteria that contained plasmids formed colonies. The colonies were selected with sterile toothpicks and grown overnight in a 1 ml LB-Kan_{50} solution (200 rpm horizontal shaking at 37°C). Sterile 40% glycerol (500 µl) was added to 500 µl of the overnight suspension, at which point the cells were placed in storage at -80°C. Typically, 80 to 100 distinct colonies were archived for each clone library. Clone sequencing often proceeded immediately, in which case a 20 µl aliquot of the overnight culture was regrown overnight in 10 mL of LB-Kan_{50} solution for plasmid purification.

3.7.3 Plasmid extraction

Purified plasmid DNA was extracted from clone cultures using the Wizard® Plus SV Miniprep DNA purification system (Promega, Madison, WI). One to two ml of the culture was transferred to a sterile 1.5 ml tube and centrifuged for five minutes at 10,000 × *g*. After discarding the supernatant, the cells were resuspended in 250 µl of the kit's cell resuspension solution. The cell suspension was augmented with 250 µl of the kit's cell lysis solution, mixed gently, and incubated at room temperature less than five minutes. Lysis was completed with 10 µl of the kit's alkaline protease solution. The lysate was neutralized with 350 µl of the kit's neutralization solution and cell debris was removed by centrifuging the mixture at room temperature for ten minutes at 14,000 x *g*. The lysate was placed in a filter spin column and centrifuged for 1 minute at 14,000 x *g*. The spin filter was washed twice, first with 750 and then 250 µl of the kit's column wash

solution. The spin column was transferred to a sterile 1.5 µl micro centrifuge tube for elution of the purified plasmid using two 50 µl aliquots of nuclease-free water. Plasmid DNA was quantified using a calibrated fluorometer at the MBRF and stored at - 80°C.

Prior to sequencing, plasmid preps were verified to contain an appropriately sized insert by digesting an aliquot of the prep for a minimum of 2 hours at 37°C in a restriction enzyme mix containing 15.5 µl of 0.2 µM fHPLC water, 2 µl of a 10X buffer solution (Buffer H, Fisher Scientific, Springfield, NJ), 0.5 µl of EcoR1 restriction enzyme (12 U/µl, Fisher Scientific, Springfield, NJ), and 2 µl of the plasmid DNA extract. Single inserts of the anticipated size were verified by subjecting the restriction enzyme digest to agarose gel electrophoresis and imaging as previously described (Section 3.7.1).

3.7.4 Sequencing

Plasmid DNA was sequenced at the MBRF. Sequence data was acquired with an Applied Biosystems (Foster City, CA) 3100 Genetic Analyzer using a 50 capillary array and the POP6 polymer. Dye terminator sequencing reactions were performed using Big Dye Terminator Reaction Mix (Applied Biosystems, Foster City, CA).

CHAPTER 4.0

DETECTION SYSTEM DESIGN AND EVALUATION

4.1 Introduction

A literature review revealed that NOB are a focus of interest in improving traditional nitrification and denitrification as well as more efficient N-conversion processes that rely on partial nitrification. The ribosomal gene to transcript ratio (rRNAt/rDNA) was proposed as a metric that could improve N-treatment efficiency by providing a species specific snapshot of the NOB activity level within biological reactors. To test this metric, NOB rDNA and rRNAt detection systems were required that were specific, sensitive, and accurate. Real-time PCR (rDNA) and real-time RT-PCR (rRNAt) were chosen to measure these parameters because quantitative PCR appeared to meet the required detection system characteristics while providing high sample throughput.

Information herein documents the development and testing of these detection systems for the BSNR. The target was the 16S - 23S intergenic spacer region (ISR), which was chosen because it would allow both ribosomal gene and transcript abundance to be quantified with the same primer and probe set. Further, the ISR could be PCR amplified with low bias using conserved bacteria specific primers located within the 16S and 23S genes. This would allow BSNR NOB to be identified with the 16S portion of cloned amplicons. Once a BSNR NOB was identified, the goal was to design and then test the detection systems to verify their specificity, sensitivity, and accuracy. These tasks preceded and aided the design and interpretation of experiments testing the effectiveness of the rRNAt/rDNA metric.

4.2 Identifying a BNSR NOB

Clone libraries were used to identify BSNR nitrite oxidizers. Mixed liquor DNA extracts were PCR amplified using conserved bacterial primers with broad specificity: 1055f (5′-ATGGCTGTCGTCAGCT-3′; Ferris et al., 1996) and 23Sr (5′-

GGGTTBCCCCATTCRG-3′; Borneman and Triplett, 1997). These primers were used because they enclosed the 16S - 23S ISR, minimized bias in identifying the NOB, and provided sufficient 16S rDNA sequence data to phylogenetically classify the clones.

4.2.1 Clone library of BSNR bacterial 16S - 23S ISR sequences

DNA was extracted from a 5 ml mixed liquor sample collected from the BSNR 50 days after the reactor was seeded, and approximately 32 days (> 3 SRTs) after the reactor had reached steady state nitrification efficiency (99.5 ± 0.5 % conversion of ammonia to nitrate). The operating condition of the BSNR at the time of this sampling event included an influent concentration of 1,000 mg/L NH_4^+-N provided as $(NH_4)_2CO_3$. DNA was extracted again from a 5 ml BSNR sample 131 days later, and 56 days following an influent change to 1,500 mg/L NH_4^+-N provided as $(NH_4)_2SO_4$ (Section 3.2.2). At this time, the reactor had been operating 33 days (> 3 SRTs) with steady state high nitrification efficiency (99.4 ± 0.3 % conversion of ammonia to nitrate). Thus, the reactor was well established prior to the two cloning events used to identify NOB within the reactor. Each DNA extract was diluted 1:50, PCR amplified with primers 1055f and 23Sr, and cloned. The 3′ portion of 40 cloned 16S rDNA genes were sequenced (Table A-1: 20 from each DNA extract) using the conserved primer 1492r (Lane, 1991) or M13r/M13f primers specific for the cloning vector. Each partial 16S sequence was subject to a BLASTn (Altschul et al., 1990; Altschul et al., 1997) search of GenBank® to identify phylogenic associates (Table A-2).

The BLASTn search indicated seven of the forty partial clone sequences were nitrifiers, a surprisingly small number (17.5%) given the highly selective characteristics of the reactor. Six clones (1-6, 1-7, 1-13, 1-29, 1-34, and 1-38) were highly similar to GenBank® entries for the 16S rDNA genes of *Nitrosomonas eutropha and/or Nitrosomonas europaea* (97-99% identity). BLAST 2 sequence comparisons (Tatusova and Madden, 1999) indicated the partial clone sequences shared 99% sequence identity (one base pair mismatches), with clone 1-7 also displaying a single deletion. Only one of the clones (1-20) was highly similar (99%) to a GenBank® entry for a NOB (*Nitrobacter spp.*). The high similarity (97 - 100%) between the cloned BSNR sequences and known

nitrifiers indicated links at the species or strain level (Stackbrandt and Goebel, 1994; Tourova, 2003).

To confirm these phylogenic assessments, the 16S portion of the partial clone sequences were grouped with 16S rDNA sequences from each of the major phylogenic branches of known nitrifiers. GenBank® sequences AF037106 (*Nitrosomonas europaea*) and M96395 (*Nitrosococcus oceanus*) represented AOB in the α- and γ-subdivisions of Proteobacteria, respectively. GenBank® sequences L11661 (*Nitrobacter winogradskyi*), L35504 (*Nitrospina gracilis*), L35510 (*Nitrococcus mobilis*), and X82558 (*Nitrospira moscoviensis*) represented NOB in the α-, δ-, and γ-subdivisions of Proteobacteria and the phylum *Nitrospira*, respectively. All of the sequences were truncated to include only that portion of the 16S rDNA sequence from the annealing site for 1055f to within approximately 5 base pairs of the 3′ 1492r primer annealing site. The sequences were aligned using ClustalX (version 1.83; Thompson et al., 1997) at the default program settings in multiple alignment mode (data not shown). A percent identity matrix was generated by drawing a NJ tree for the alignment (Table A-3). The tree was bootstrapped using the default program settings and displayed in phylogram format (Figure A-1) using TreeView Version 1.6.5 (http://taxonomy/zoology.gla.ac.uk/rod/rod.html). In Figure A-1, clones 1-6, 1-7, 1-13, 1-29, 1-34, and 1-38 clustered with the GenBank® sequence AF037106 (*N. europaea*), as anticipated. Further, BSNR clones taxonomically associated with α-proteobacteria (Table A-2: clones 1-1, 1-5, 1-12, 1-16, 1-20, 1-24, 1-27, 1-31, 1-35, 1-39, and 1-40) sub-grouped with L11661 (*Nitrobacter winogradskyi*), as expected. This indicated the phylogenetic analysis was accurate even though truncated 16S sequence data was used. Clone 1-20 shared low sequence similarity (≤ 92%) with all other library entries, including other α-proteobacteria, but ≈ 100% similarity with *Nitrobacter winogradskyi*. Table A-3 confirmed that all other library entries displayed low sequence similarity with known NOB. *Nitrospira*, *Nitrospina*, and *Nitrococcus* sequences displayed ≤ 84%, 87%, and 92% sequence similarity with the library entries, respectively. In summary, *Nitrobacter* was confirmed present in the BSNR biomass, so the 16S - 23S ISR of clone 1-20 was fully sequenced (Table A-1).

To properly design a real-time PCR detection system for the cloned *Nitrobacter* sequence, it was necessary to eliminate the 16S and 23S rDNA portions of the sequence data. Further, for specificity purposes it was necessary to identify tRNA genes, which are often found within the ISRs of bacterial ribosomal genes (Brosius et al., 1981; García-Martínez et al., 1999). The ISR for clone 1-20 was inferred and excised from the 16S and 23S rDNA sequences using a ClustalX multiple sequence alignment with published 16S - 23S ISRs for α-subclass Proteobacteria. Included were all GenBank® ISR sequences available for *Nitrobacter* spp. plus two close relatives (Grundmann et al., 2000; Willems et al., 2001): AJ279303 (*Nitrobacter hamburgensis* strain DSM 10299), AJ279304 (*Nitrobacter winogradskyi* strain DSM 10237), AJ005008 (*Nitrobacter sp.* strain DE30), AJ005009 (*Nitrobacter winogradskyi* strain '*agilis'*), AJ005010 (*Nitrobacter winogradskyi* strain ATCC 25391), AJ005011 (*Nitrobacter hamburgensis* strain X14), AJ005012 (*Nitrobacter vulgaris* strain Z), AJ005014 (*Nitrobacter sp.* strain LL), AJ005013 (*Rhodopseudomonas palustris* strain DSM 123), and Z35330 (*Bradyrhizobium japonicum* strain USDA110). To identify tRNA genes within the ISR, the excised sequence was analyzed with tRNAscan-SE version 1.21 (Lowe and Eddy, 1997; http://www.genetics.wustl.edu/eddy/tRNAscan-SE/), a publicly available web tool that combines a low false positive detection rate with a 98 - 99% true detection rate for tRNA genes. Two tRNA genes were identified with anticodon sequences for isoleucine and alanine (Figure A-2). These tRNA genes were also found in the previously published *Nitrobacter* ISR sequences.

4.2.2 Which NOB is dominant in the BSNR?

The attempt at "unbiased" cloning (i.e. using conserved primers) provided limited insight into the reactor's NOB population diversity and only 1 ISR sequence for real-time PCR primer/probe design. This was of concern since the ISR can be highly divergent (Jenson et al., 1993). Further, the clone library did not eliminate the possibility that other NOB, for example *Nitrospira* spp. (Burrell et al., 1998), were also present in the reactor. However, to examine the merits of the NOB rRNAt/rDNA ratio it only appeared necessary to study a dominant NOB population, not necessarily all NOB species present.

Thus, *Nitrobacter* was assumed to be a dominant NOB in the BSNR. A goal was set to design real-time PCR primers general enough to amplify all known *Nitrobacter spp.*, but specific enough to avoid amplifying all closely related α-Proteobacteria. Such a detection system seemed useful beyond the scope of this work, but could not be identified in the literature. Further, these design goals would minimize the risk associated with a lack of ISR sequence diversity from the BSNR mixed liquor for primer design. On the one hand, it seemed likely that if the resulting primers were general enough to detect all known *Nitrobacter* spp., they would amplify all *Nitrobacter* rDNA within the BSNR. On the other hand, if the resulting primers were specific enough to avoid detecting all published non-NOB α-Proteobacteria sequences, it seemed likely the primers would be specific enough to avoid cross reactivity with uncharacterized α-Proteobacteria in the BSNR. This last point was important since *Nitrobacter* spp. and other α-Proteobacteria share high rDNA sequence similarity (Orso et al., 1994; Grundmann et al., 2000; Willems et al., 2001), and 1 in 4 of the cloned sequences obtained from the BSNR was taxonomically associated with the α-Proteobacteria (Table A-2). Once the detection system was designed, it could be used to verify whether *Nitrobacter* was a dominant nitrite oxidizer in the reactor.

4.3 *Nitrobacter* Specific 16S - 23S ISR Real-Time PCR Primers

4.3.1 Initial alignment and primer design guidelines

A 16S - 23S ISR alignment was performed that included the BSNR *Nitrobacter* clone, all available *Nitrobacter spp*. ISRs, and two closely related nitrogen-fixing α-Proteobacteria (*Rhodopseudomonas palustris* and *Bradyrhizobium japonicum*: Orso et al., 1994). The alignment was divided into 20 regions that reflected *Nitrobacter* sequence conservation (Figure A-3). These regions were examined for possible real-time PCR detection systems using the following guidelines (Qiagen, 2002; Bustin, 2000):

1. regions 6 and 8 (Figure A-2), which were tRNA genes, were excluded
2. maximum consecutive base pairs (bp) in a primer or probe: 4

3. minimum/maximum primer and probe lengths: 16/27 bp
4. maximum purines contained in the final 5 base pairs of a primer: 3
5. maximum distance between probe and primer: 25 bp
6. minimum/maximum amplicon length: 65/200 bp
7. minimum/maximum primer melting temperature (T_m): 56 and 62°C
8. minimum/maximum probe T_m: 66 and 72°C

These guidelines narrowed the choice of the forward and reverse primers to regions 13 and 16, respectively, and the choice of the probe to an antisense sequence in region 16 (Figure A-3).

4.3.2 *Nitrobacter hamburgensis* ISR sequence diversity

N. hamburgensis was used to study *Nitrobacter* intrastrain ISR sequence diversity because Navarro et al. (1992b) indicated that significant ISR sequence diversity can be present even within prokaryotic species. *N. hamburgensis* was chosen because this species displayed the least ISR sequence similarity with the BSNR *Nitrobacter* clone (90%) and the most similarity (77%) with closely related α-Proteobacteria (Orso et al., 1994; Grundmann et al., 2000). Thus, in lieu of species/strain *Nitrobacter* sequence diversity in the BSNR, which unbiased cloning did not provide for primer design, the most distant relative in the genera provided insight into the intra-species ISR diversity. This was considered prudent since *Nitrobacter* tends to be present as consortia of different species and strains across diverse environments (Navarro et al., 1992a; Navarro et al., 1992b). This organism was obtained from the UT Center for Environmental Biotechnology and grown mixotropically (Section 3.3).

A 1 ml sample of a stationary phase mixotrophic *N. hamburgensis* culture was centrifuged and the cells were resuspended in 100 µl of 0.2 µm filter sterilized 10 mM TRIS-HCl at pH 8.0. A 2 µl aliquot of the suspension served as template in a touchdown PCR reaction with the conserved primers 1055f and 23Sr. The PCR products were subject to 1.5% agarose gel electrophoresis which revealed a single amplicon of the anticipated size. The PCR products were regenerated, cloned, and sequenced using the

primer 23Sr (designated clone library 2: Table A-4). This revealed the 3′ end of the 16S - 23S ISR (453 bp), including regions 13 through 16 (Figure A-3). A ClustalX alignment revealed some ISR sequence diversity (4 singe bp mismatches, no deletions or substitutions), with three mismatches occurring within regions 13 through 16. By accommodating this additional sequence diversity, it was reasoned that the resulting primer specificity would be improved for the genera as a whole.

4.3.3 *Nitrobacter* specific PCR primers

The sequence data in clone library 2 and Figure A-3 were combined, truncated to include only regions 13 thorough 16, and realigned using ClustalX for PCR primer design. All possible forward and reverse primers from regions 13 and 16, respectively, were considered that: presented no *Nitrobacter spp*. mismatches, at least one mismatch with the two closely related α-Proteobacteria, met the primer guidelines listed in Section 4.3.1 other than the T_m requirement, and provided room in the 5′ area of region 16 for at least one probe that met the guidelines in Section 4.3.1. These specifications yielded two forward and 26 reverse primer sequences that were investigated for T_m (Table A-5) and secondary structure potential (hairpins and self dimmers) at 37°C (Table A-6). Since the primers displayed negative free energy values for dimmer formation at 37°C, hairpin structures were further investigated at 60°C using MFOLD version 3.1 (Zuker, 2003) (Table A-6). In addition, the specificity of each primer was evaluated with BLASTn searches of GenBank® (Table A-6).

Both forward primers displayed optimal specificity (no GenBank® mismatches), and little potential to form stable secondary structures at 60°C. The primer designated NITISRf514-543 (5′-CCATTCACTATCTCCAGGTC-3′; Table A-6) was chosen because it violated only one minor structural objection and displayed an ideal T_m (60°C) at a common optimal Mg^{2+} concentration (3 - 4 mM) for real-time PCR (Qiagen, 2002). With two exceptions, none of the potential reverse primers displayed significant dimmer stability at RT incubation temperatures (45 - 55°C). Selectivity, matching T_m (60.8°C) to the chosen forward primer (Bustin, 2000), and an optimal DNA/RNA heteroduplex T_m at 3 mM Mg^{2+} (52.8°C: Qiagen, 2002) was used to select the reverse primer (NITISRr639-

660: 5′-TTGATTAGAAAGACCAGCTTGC-3′; Table A-6). This primer had only one exact match in GenBank® (Table A-6).

Because of the negative free energy values for self dimer formation at 37°C (Table A-6), both self and cross dimer potential was evaluated for the chosen primers using sequence complementarity plots using an online oligonucleotide analysis tool (http://oligos.qiagen.com/oligos/toolkit.php). These plots confirmed no significant potential for self dimer formation, but the 3′ complementarity score (4 consecutive matching base pairs) of the forward and reverse primers exceeded the default primer picking conditions in the Primer 3 software (Rozen and Skaletsky, 2000). Subsequently, the primer pair was analyzed with a 2-state hybridization model using nearest neighbor energy parameters at 60°C, Na^+ and Mg^{2+} concentrations of 50 and 3 mM, respectively, and a total nucleic acid concentration of 1 µM (Zuker, 2003, Mfold version 3.1: http://www.bioinfo.rpi.edu/applications/mfold). An estimated T_m of 10.6°C confirmed little propensity for cross primer dimer formation.

In summary, the chosen primers were highly specific for *Nitrobacter* and displayed excellent structural stability at ideal annealing and extension temperatures for quantitative PCR and reverse transcription (≈ 60° and 50°C, respectively: Qiagen, 2002). Further, the resulting amplicon was an ideal size (143 bp) for real-time PCR (Qiagen, 2002). The primer sequences displayed little potential for dimmer formation that can lower PCR efficiency (McPherson and Møller, 2000) and thereby deteriorate real-time PCR sensitivity (Rasmussen, 2001).

4.4 Primer Melting Temperature and Specificity

NITISRf514-543 and NITISRr639-660 were prepared on a 50 nM production scale using desalting purification by Sigma-Genosys (The Woodlands, TX). The dry primers were resuspended at 100 µM in 10 mM TRIS-HCl at pH 8.0, incubated on ice for 15 minutes, gently mixed, diluted in 100 µl aliquots at 10 µM, and stored at -20°C. To assure the primers performed optimally in tests of the *Nitrobacter* rRNAt/rDNA ratio, they were vetted for melting temperature and specificity using a BSNR DNA extract.

4.4.1 Temperature gradient PCR

Primer specificity and T_m were initially evaluated with temperature gradient PCR reactions using two templates: a 1:50 dilution of a 5 ml BSNR DNA extract, and a 1:10 dilution of a 1 ml stationary phase *N. hamburgensis* DNA extract. Each reaction contained 12.5 µl of Quantitect® Probe PCR mastermix (Qiagen; Valencia, CA), 5.5 µl of 0.2 µM fHPLC water, 1 µl of each primer (10 µM), and 5 µl of the DNA extract dilution. The reactions were conducted on a DNA Engine Tetrad PTC-225 thermocycler (MJ Research; Alameda, CA) using the following temperature protocol: 50°C for 2 minutes, 95°C for 15 minutes, 45 cycles at 94°C, with a 56 - 71°C gradient annealing/extension for 1 minute, all while the thermocycler lid was maintained at 100°C. The PCR products were subject to a 2% agarose gel electrophoresis which indicated that a single amplicon of the anticipated size (≈ 140 bp) was generated up to an annealing and extension temperature of approximately 68°C (Figure A-4). The reactions were repeated with the same protocol over a narrower temperature gradient (60 - 68°C); electrophoresis indicated an annealing and extension temperature optimum of slightly over 60°C (Figure A-5).

4.4.2 Specificity

To assure the specificity of the chosen primers, clone libraries were constructed using PCR products obtained from BSNR and *N. hamburgensis* DNA extracts (designated clone libraries 3 and 4, respectively). An attempt was initially made to construct clone libraries with a real-time PCR mastermix, which typically contains elevated salt concentrations that decrease primer specificity (McPherson and Møller, 2000). Specifically, the 62°C annealing and extension temperature reaction above was repeated to generate products for cloning (Figure A-6). However, the real-time PCR mastermix partially replaced dTTP with dUTP. This allows uracil-N-glycosylate (UNG) treatment of PCR reactions to eliminate carryover PCR contamination (McPherson and Møller, 2000), but made cloning inefficient with the UNG+ strain used for cloning. Hence, only one clone was obtained and sequenced (Table A-7: clone 4-10). The

reactions were repeated using PCR Ready to Go® beads (Amersham Pharmacia Biotech, Piscatawa, NJ) which were combined with 21.5 µl of 0.2 µM fHPCL water, 1 µl of the primers (10 µM), and 2.5 µl of the BSNR or *N. hamburgensis* DNA extract dilutions. A low annealing temperature (55°C) was used to increase the propensity for unspecific amplification in lieu of the high salt concentration found in real-time PCR mastermixes. The PCR products were again composed of single amplicons of the anticipated size (Figure A-6). Nine clones (4-1 - 4-9) were sequenced from the PCR reaction with the BSNR DNA extract (Table A-7), while five clones (5-1 - 5-5) were sequenced from the PCR reaction with the *N. hamburgensis* DNA extract (Table A-8). All of the clones contained the expected *Nitrobacter* ISR insert, indicating the primers were specific for *Nitrobacter* within the reactor.

4.5 *Nitrobacter* Specific 16S - 23S ISR Real-Time PCR Probe

The sequence data in clone libraries 3 and 4 were added to the data in Figure A-3 and aligned with ClustalX between the reverse and forward primers as a probe sequence selection guide. This allowed the ISR sequence diversity to be studied within the BSNR *Nitrobacter* population directly, which was expected to be somewhat divergent (Navarro et al., 1992b). This alignment confirmed it would be necessary to tolerate a single bp mismatch (C for T substitution) for clone 4-1 (highlighted in the potential probe sequences presented in Table A-9). Since only 1 in 10 BSNR clones contained a single internal bp mismatch with the potential probe sequences, this was considered acceptable, particularly since the probe would likely bridge the mismatch.

A T_m evaluation of all possible antisense probe sequences within the 5′ end of region 16 was conducted (Table A-9). Acceptable antisense sequences were qualified by eliminating those sequences with a 5′ G, which can quench the fluorophore signal (Qiagen, 2002). The remaining sequences were evaluated for secondary structure potential at 37°C and 60°C and for specificity using a BLASTn search of GenBank® (Table A-10). All probe sequences displayed good *Nitrobacter* specificity, exactly matching at most two non-NOB sequences in GenBank® (Table A-10). However, many

of the sequences were unacceptable because of a tendency to form stable secondary structures at ≈ 60°C. The sequence designated NITISRp610-629 was considered optimal because it: displayed the least secondary structure potential, had a T_m ≈ 8 - 10°C higher than the primer T_m at 3 mM Mg^{2+} (Qiagen, 2002; Bustin, 2000), was short (20 bp) and thus more selective, and had a lower G/C ratio than the other choices (Qiagen, 2002). This probe sequence did not display significant complementarity with itself or the chosen primers (data not shown).

A labeled probe [5′-6-FAMd(TCGAACCGATAGCGAGGCGG)BHQ-1-3′] with the Blackhole Quencher™ (BHQ) was obtained from Biosearch Technologies, Inc (Novato, CA). The probe was HPLC purified on a 200 nM production scale that yielded 17.83 nM. The dry probe was resuspended in 178.3 µl of 10 mM TRIS at pH 8.0 (100 µM), incubated 5 minutes at room temperature, and vortexed lightly to produce a probe stock solution that was stored at -20°C. Working solutions (10 µM; also stored at -20°C) were prepared as needed for several weeks of reactions by diluting the probe in PCR grade or 0.2 µm fHPLC water.

4.6 Real-Time PCR Optimization

Optimization of real-time and real-time RT-PCR reactions is essential for reliable gene and particularly transcript quantification (Bustin, 2000; Bustin, 2002). Thus, after constructing a series of *Nitrobacter* rDNA standards, the primer and probe set was optimized with respect to: the PCR mastermix used, the annealing and extension temperature, the Mg^{2+} concentration, and the primer and probe concentrations (McPherson and Møller, 2000; Qiagen, 2002).

4.6.1 *Nitrobacter* rDNA standards

The BSNR *Nitrobacter* clone was grown overnight in 35 ml LB-Kan_{50} cultures in 50 ml sterile tubes (37°C, 200 rpm horizontal shaking). Plasmids were extracted, linearized with an EcoR1 digest, and subject to electrophoresis in a 2% agarose gel that confirmed the preparation was free of significant genomic DNA and RNA contamination. The extract DNA concentration was then quantified with the PicoGreen® DNA detection

system (Molecular Probes; Eugene, OR). This assay yielded a standard curve with excellent linear fit (R^2 = 0.9988) through triplicate measures of eight PicoGreen® Lambda DNA standards. Using the standard curve and the average of seven fluorescence measurements of three plasmid preparation dilutions, the plasmid extract DNA concentration was inferred (114 ng/µl). The length of the plasmid (5,411 bp) was then used to compute the plasmid copy concentration (1.92 x 10^{10} copy/µl: Qiagen, 2002). A 10^9 copies/µl *Nitrobacter* rDNA standard was prepared by diluting 52 µl of the plasmid preparation into 948 µl of 0.2 µm fHPLC water. A 10^7 copies/µl standard was then prepared by diluting 100 µl of the 10^9 standard into 9.9 ml of 0.2 µm fHPLC water. Six 1:10 serial dilutions were then used to complete a *Nitrobacter* rDNA standard series down to 10^1 copies/µl. Aliquots of the *Nitrobacter* rDNA standards were frozen at -80°C and used no more than twice before discarding them to preserve the DNA integrity.

4.6.2 Optimization

The process used to optimize the Nitrobacter rDNA detection system consisted of four sequential stages: (1) a PCR mastermix/annealing temperature evaluation, (2) a $MgCl_2$ titration, which also included an evaluation of the newly prepared *Nitrobacter* rDNA standards, (3) a primer titration at two probe concentrations, and (4) a probe titration at the optimum primer concentrations.

Three PCR mastermixes were evaluated: Quantitect® Probe PCR mastermix (Qiagen; Valencia, CA), Platinum® Quantitative PCR SuperMix-UDG (Invitrogen; Carlsbad, CA), and HotMasterMix (Eppendorf; Hamburg, Germany). Each mastermix was tested across temperature and $MgCl_2$ gradients on a MJ DNA Engine Opticon™ (MJ Research; Waltham, MA) with identical software settings for baseline subtraction (average fluorescence for cycles 3-7) and threshold fluorescence (5 × fluorescence standard deviation for cycles 3-7) using a 10^6 copies/µl *Nitrobacter* rDNA standard as the template. Threshold cycle (C_T) and light yield (Y_L) were plotted on identical scales for the Qiagen, Invitrogen, and Eppendorf mastermixes as shown in Figure B-1, Figure B-2, and Figure B-3, respectively. C_T and Y_L were superior (lower and higher, respectively) with the Quantitect® mastermix. Y_L was adversely affected (lowered) at

annealing/extension temperatures above approximately 65°C for all the salt concentrations tested (Figure B-1). Salt additions improved (lowered) the C_T at annealing/extension temperatures above 61°C, but did not improve the results at annealing/extension temperatures below 61°C. Thus, the annealing/extension temperature was set at 61°C, the highest temperature at which salt additions were unnecessary for optimal C_T results.

In stage 2, *Nitrobacter* rDNA standards (10^1 - 10^5 copies/µL) and a Mg^{2+} (4 - 6 mM) gradient provided data for both a standards evaluation and an assessment of the optimum Mg^{2+} concentration for the reaction (Figure B-4). Linear regressions through the results displayed excellent fits ($R^2 > 0.993$) and high PCR efficiency (> 90% calculated with the calibration curve slope: Rasmussen, 2001). Thus, the *Nitrobacter* rDNA standards yielded good results and could be used with confidence in future experiments. The C_T was unaffected by the Mg^{2+} gradient, but Y_L was affected, with 4.0 mM Mg^{2+} being optimal (generally yielding more light). This was the concentration included in the Quantitect® mastermix, so it was not necessary to add Mg^{2+} to optimize the reaction

In stage 3, a primer gradient (all combinations of 400, 700, and 1000 nM of the reverse and forward primers) was tested at two probe concentrations (100 and 200 nM) using a 10^6 copies/µl *Nitrobacter* rDNA standard as template (Figure B-5). As expected, the C_T and Y_L were higher at the higher probe concentration, but no consistent effect was apparent at the different primer concentration combinations. Since 400 nM was suggested as an optimal primer concentration for the Quantitect® mastermix (Qiagen, 2002), and since lower and balanced primer concentrations tend to yield better results (Bustin, 2000), the primer concentrations were set at 400 nM.

In stage 4, a probe titration (100 - 400 nM x 100 nM) was tested with the 10^6 copies/µl *Nitrobacter* rDNA standard (Figure B-6). A nominal improvement in the C_T was noted (from 15.8 down to 15.3) as the probe concentration increased from 100 to 400 nM, whereas Y_L steadily increased, as expected. Because no significant improvement in

C_T was noted at the high probe concentrations, the concentration was set at 150 nM to economize the reactions.

The final reaction mix adopted for the study was: 12.5 µl of QuantiTect® Probe PCR mastermix (Qiagen; Valencia, CA), 5.125 µl of nuclease free H_2O, 400 nM of each primer (1µl), 150 nM of probe (0.375 µl), and 5 µl of template. The final temperature protocol adapted for the study was as follows: 50°C for 2 minutes, *Taq* activation at 95°C for 15 minutes, and 40 cycles with melting at 94°C for 15 seconds and annealing/extension at 61°C for 1 minute. The reactions were executed on an MJ DNA Engine Opticon thermocycler using the average fluorescence for cycles 3-7 for baseline subtraction and a manual threshold fluorescence setting of 0.005.

4.7 Real-Time RT-PCR Optimization

Real-time PCR optimization can be complicated by the RT step (Bustin, 2000). Thus, after producing an external series of *Nitrobacter* rRNAt standards, the optimized real-time PCR reaction was reassessed with the RT step.

4.7.1 *Nitrobacter* rRNAt standards

Choice and generation of a linear transcript target

The BSNR *Nitrobacter* clone was chosen as the starting point for rRNAt standard preparation because a long series of upstream (1,063) and downstream (243) bases were available beyond the forward and reverse primers, respectively. This characteristic is necessary to reproduce transcript secondary structure and thus RT efficiency using an artificial standard (Freeman et al., 1999). The use of DNA standards for quantitative RT-PCR is discouraged since they cannot account for variability in the RT reaction (Freeman et al., 1999; Sharkey et al., 2004).

The BSNR clone was grown overnight in 40 ml LB-Kan_{50} cultures in sterile 50 mL centrifuge tubes (37°C, 200 rpm horizontal shaking). The cells were pelleted at 10,000 x *g* for 20 minutes at 4°C and the plasmids extracted using the Wizard® *Plus* Midiprep DNA Purification System (Promega; Madison, WI) with elution in 300 µl of

nuclease free water. The DNA concentration was measured at the MBRF (362 ng/µl) and the extract was stored temporarily at -80°C.

To provide sufficient transcription template, the plasmid preparation was unfrozen and concentrated using an ethanol/salt precipitation (Sambrook and Russell, 2001). Briefly, $1/10^{th}$ volume of 3 M sodium acetate (prepared in diethyl pyrocarbonate (DEPC) treated water) was added to the plasmid extract, followed by 2 volumes of 100% ethanol. The solution was gently mixed, centrifuged at 12,000 × g for 15 minutes at room temperature, and the supernatant was aspirated. The pellet was washed with 2 volumes of 100% ethanol, centrifuged at 12,000 × *g* for 15 minutes at room temperature, and the supernatant was aspirated. The pellet was air dried at room temperature for 5 - 10 minutes and resuspended in DEPC water. The DNA concentration was measured twice at the MBRF (2.42 and 2.44 µg/µl).

To produce transcripts of a defined length, the plasmid prep was linearized using a *Spe1* restriction enzyme digest (Promega; Madison, WI). All digest components, except the restriction enzyme, were first combined [29.6 µl of DEPC H_2O, 4 µl of 10 X buffer B (Promega; Madison, WI), 0.4 µl of bovine serum albumin, and 4 µl of the concentrated plasmid], gently mixed with a pipette, and then 2 µl of *SpeI* (10 units/µl) was added to yield an enzyme to plasmid DNA ratio > 2 U/µl. The digestion proceeded for 4 hours at 37°C. A control reaction with no restriction enzyme was simultaneously performed.

The linearization and control reactions were electrophoresed on an agarose gel and periodically inspected with brief UV illumination to confirm separation of the cut plasmid. When the separation was sufficient (Figure B-7-Aa), the digested plasmid was removed from the gel with a sterile razor (Figure B-7-Ab), weighed to the nearest $1/10^{th}$ mg, and frozen at -80°C. Linear plasmid was recovered from the frozen agarose section using a gel extraction kit (QIAquick by Qiagen; Valencia, CA) following the manufacturer's micro centrifuge protocol. The plasmid was eluted in 50 µl of the kit EB buffer. The integrity of the recovered plasmid was confirmed since the plasmid migrated as a single, narrow band of the expected size during electrophoresis (≈ 5.5 Kb; Figure B-

7-C). The buffer was exchanged and the DNA was concentrated in DEPC H_2O using the ethanol/salt precipitation previously described.

Large scale transcription reaction

The linearized plasmid served as template in a large scale transcription reaction (T7 Ribomax™ Large Scale RNA Production System; Promega Corporation, Madison, WI) which included: 4 µl of 5X T7 transcription buffer, 6 µl of rNTPs (25 nM), 3.24 µl of the concentrated linear plasmid (1.17 µg), 4.76 µl of nuclease free water, and 2 µl of T7 RNA polymerase (to produce sense strand copies of the cloned rDNA insert). The reaction components were mixed gently and incubated four hours at 37 °C.

The transcription reaction was purified using the RNA cleanup protocol for the RNeasy® kit (Qiagen, Inc.; Valencia, CA). Briefly, the reaction was diluted in 100 µl of RNase free water and 350 µl of the kit's buffer RLT and vortexed. 250 µl of 100% ethanol was added, the solution was mixed by pipetting, placed onto the binding column, and centrifuged briefly at 12,000 x *g*. The supernatant was discarded and the column was washed with two 500 µl aliquots of the kit's RPE buffer. The column was centrifuged one minute at 12,000 x *g* in a fresh RNase free micro centrifuge tube to assure all traces of ethanol were removed. RNA was eluted with two 50 µl aliquots of RNA storage buffer (Cat. No. 7001; Ambion, Inc.; Austin, TX) after 1 minute incubations at room temperature.

DNase digestion

The partially purified RNA was subject to a rigorous RNase-free DNase digestion using the DNA-free™ system (Ambion, Inc.; Austin, TX) after the cleanup column eluant was diluted (10 dilutions at 1:10). These solutions were buffered with 10 µl of DNase buffer (100 mM Tris-HCl at pH 7.5, 25 mM $MgCl_2$, 1 mM $CaCl_2$), 2 µl of DNase I (2U/µl) was added, and then the mixtures were incubated for 1 hour at 37 °C. The reactions were terminated with 0.1 volume of the kit's DNase inactivation solution followed by vigorous vortexing and a two minute incubation at room temperature. The supernatant from the termination reactions were collected in two RNase free micro centrifuge tubes and concentrated using an ethanol/salt precipitation (Sambrook and

Russell, 2001). For the ethanol precipitation, 0.1 volume of 3M sodium acetate was added followed by 2.5 volumes of 100% ethanol and centrifugation for 15 minutes at 14,000 x *g* at 4°C. The ethanol was aspirated and the tube was washed with 2 volumes of 70% ethanol prepared in DEPC H_2O. The pellet was air dried at room temperature for 5 to 10 minutes and then resuspended in 50 µl of RNA storage buffer (Cat. No. 7001; Ambion, Inc.; Austin, TX). These solutions were combined to yield approximately 100 µl of a *Nitrobacter* rRNAt standard stock solution.

Quality control

The rRNAt stock solution was vetted for integrity, nucleic acid purity, and potential DNA contamination to assure that the *Nitrobacter* rRNAt concentration could be inferred accurately with dilutions of this solution.

Integrity

The integrity of the artificial transcript solution was evaluated with a 1.5% denaturing agarose gel using a standard electrophoresis protocol (Sambrook and Russell, 2001). A solution of 0.75 g of low EEO agarose in 36 ml of DEPC H_2O was boiled, cooled to 55°C, and augmented with 5 ml of 10X MOPS and 9 ml of 37% formaldehyde. The molten gel was cast in an electrophoresis apparatus previously cleaned with 1 M NaOH and rinsed with DEPC H_2O to remove potential RNase contamination. After the gel solidified, it was submerged in 1X MOPS solution and pre-run for 10 minutes. Salt gradients in the running buffer were avoided by recirculating the buffer between the electrophoresis terminal wells with a Masterflex LS standard drive pump (speed setting 1, fitted with Masterflex 95410-14 tubing from Cole Parmer). Once the gel was prepared, 10 µl of the rRNAt stock solution was diluted with 20 µl of RNA buffer (10 ml deionized formamide, 37% formaldehyde, 2.0 ml 10X MOPS) and incubated for 10 minutes at 65°C. The denatured RNA was cooled on ice for 2 minutes and 2 µl of RNA loading buffer (50% glycerol, 1mM EDTA, 0.4% bromophenol blue) and 1.5 µl of a 1 mg/ml EtBr solution was added. The gel was run two hours and photographed under UV light (Figure B-8). The transcript preparation had good integrity, migrating as a single ≈ 1500 bp band.

Purity

The nucleic acid purity of the *Nitrobacter* rRNAt standard stock solution was evaluated by determining the UV absorption ratio (A_{260}/A_{280}) for a dilution in 10 mM TRIS-HCl at pH 7.6 (to eliminate pH effects on the absorbance value). Also, a preliminary nucleic acid quantification was made using the A_{260} of a stock solution dilution in DEPC H_2O. Quartz cuvettes were pre-washed (0.1 M NaOH, 1mM EDTA) to eliminate potential RNase contamination, rinsed with DEPC H_2O, and dried at 80°C. The cuvettes were tare weighted, reweighed following addition of DEPC H_2O or buffer, and used to blank a spectrophotometer (Beckman Coulter DU 640B). The rRNAt stock solution (10 µl) was then added to the cuvettes and the absorbance values were recorded. The A_{260}/A_{280} ratio was 2.14, confirming high nucleic acid purity (Qiagen, 2002). Based on the A_{260} of 0.4734 for the water dilution, the undiluted RNAt stock solution contained 1.257 µg nucleic acid/µl (Qiagen, 2002).

Template contamination

Duplicate "no RT" control reactions were run with a 1:1,000 dilution of the RNA standard stock solution, a positive control (10^6 copies/µl *Nitrobacter* rDNA standard), and a negative control (DEPC H_2O). The mean C_T for the stock solution dilution was 24.8, while the C_T for the positive control was 14.3. No amplification occurred for the negative control. The contaminating template concentration was estimated in the stock solution dilution (9.68×10^2 copies/µL) and the positive control (1.31×10^6 copies/µL) using the 4 mM Mg^{2+} standard curve in Figure B-4 (accuracy was assured by the positive control result). To assess the template DNA contamination, the transcript size (1,518 bp) and A_{260} RNA quantification result were used to compute the transcript copy number in a 1:1,000 dilution of the RNA standard stock ($\approx 1.47 \times 10^9$ copy/µl). Since the rRNAt concentration greatly exceeded the template concentration, the contamination was insignificant.

Quantification of RNA stock solution and preparation of standard series

The RNA standard stock solution was quantified with the RiboGreen® RNA Quantification Reagent and Kit (Molecular Probes; Eugene, OR). Fluorescence

measurements for 1:1,000 and 1:2,000 dilutions of the RNA standard stock were averaged and used to compute the stock solution concentration. The RiboGreen® and spectrophotometric assays yielded similar results: 1,240 and 1,257 ng/µl, respectively. The results were averaged and used to compute the quantity of rRNAt standard stock solution (10.3 µl) required to prepare 1.5 ml of a 10^9 copies/µl standard. Successive 1:10 dilutions produced a 10^8 - 10^1 copies/µl standard series. The dilutions were mass based and made in an RNA buffer (Cat No. 7001; Ambion, Inc.; Austin, TX) to protect against base hydrolysis during storage. Single use aliquots of each standard were stored in non-stick RNase free tubes (Ambion, Inc.; Austin, TX) at -80°C.

4.7.2 Optimization

The newly created standards were evaluated with the *Nitrobacter* rRNAt detection system. The reaction included: 12.5 µl of QuantiTect® Probe RT-PCR mastermix (Qiagen; Valencia, CA), 4.875 µl of nuclease free H_2O, 400 nM of each primer (1µl), 150 nM of probe (0.375 µl), 0.25 µl of RT enzyme mix, and 5 µl of the 10^9 to 10^1 copies/µl standards. The temperature protocol was as follows: RT reaction at 50°C for 30 minutes, *Taq* activation at 95°C for 15 minutes, and 40 cycles with melting at 94°C for 15 seconds and annealing/extension at 61°C for 1 minute. The reactions were prepared at 32°C (on ice) to prevent RT enzyme activity prior to executing the reactions on an MJ DNA Engine Opticon thermocycler using the average fluorescence for cycles 3-7 for baseline subtraction and a manual threshold fluorescence setting of 0.005. Amplification was successful over 7 orders of magnitude (10^9 - 10^2) but not efficient for the 10^1 standard. This detection limit is within a commonly observed range for RT-PCR (5-500 copies; Bustin, 2000). A negative control (DEPC H_2O template) did not amplify. A linear fit of the 10^9 - 10^2 C_T results displayed excellent linearity (R^2 = 0.9996), while the slope (-0.2893) confirmed the RT/PCR efficiency was high (Rasmussen, 2001: 94.7%). Because the results were so favorable, leaving little room to improve the assay, the conditions used in this experiment were accepted as optimal.

4.8 PCR Efficiency and Inhibition Evaluations

PCR is subject to inhibition by a variety of factors principally associated with the DNA or RNA source material and extraction chemicals (McPherson and Møller, 2000). Inhibition can also affect the RT reaction in RT-PCR (Bustin, 2000; Qiagen, 2002). Dilution of the extracted template can be used to both diagnosis and remove RT and/or PCR inhibition by lowering the inhibitor concentration (McPherson and Møller, 2000).

Inhibition was investigated with the optimized *Nitrobacter* rDNA real-time PCR and *Nitrobacter* rRNAt real-time RT-PCR assays using BSNR DNA and RNA extracts, respectively. It was hoped that little or no inhibition would be evident for the extract dilutions, since this would allow a small dilution factor to be adopted for the study that would maximize the assay sensitivity (Dionisi et al., 2003). Further, the dilution series could be used to verify that similar RT and/or PCR amplification efficiency existed for the *Nitrobacter* rDNA and rRNAt standards and the BSNR DNA and RNA extracts, respectively. This would confirm that the *Nitrobacter* rDNA and rRNAt concentrations could be inferred accurately with the standards (Rasmussen, 2001; Qiagen, 2002).

4.8.1 Real-time PCR

PCR inhibition and amplification efficiency were investigated using a series of 1:2 dilutions of a BSNR DNA extract (1:2 - 1:1,024). The dilutions, as well as a *Nitrobacter* rDNA standards series (10^7 - 10^1 copies/µl), were analyzed in triplicate. The threshold cycle results were plotted versus the dilution fraction (e.g. 1:2 = 0.5) and the *Nitrobacter* rDNA standard concentration and fit with linear regressions to estimate the PCR efficiency (Figure 6A: assay data provided in Table C-1) (Rasmussen, 2001). For the *Nitrobacter* rDNA standards, the efficiency was 85% over six orders of magnitude, while for the BSNR DNA extract dilutions the efficiency was 91% over 2.5 orders of magnitude. Since the amplification efficiencies were similar, the standards could be used to infer the *Nitrobacter* rDNA concentration accurately (< 60% error up to 30 amplification cycles for a 6% amplification efficiency difference). The relative error for a true 2-fold difference in *Nitrobacter* rDNA due to the potential PCR efficiency

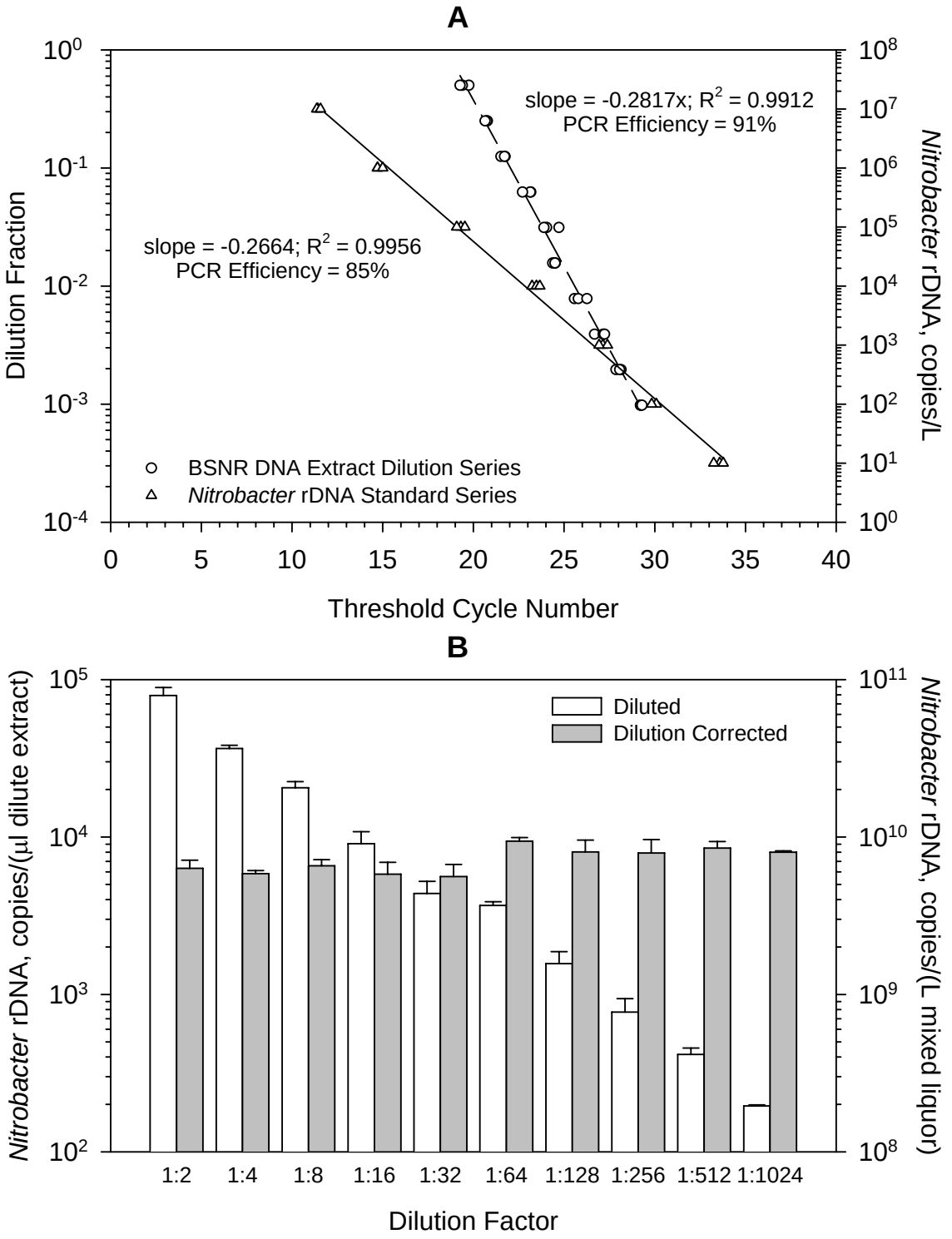


Figure 6 A PCR inhibition investigation of the optimized *Nitrobacter* rDNA real-time PCR detection system. A. Threshold cycle results for *Nitrobacter* rDNA standards and BSNR DNA extract dilutions. B. *Nitrobacter* rDNA concentration in the BSNR DNA extract dilutions

disparity would be much lower (< 3%). This effect was evaluated empirically by comparing the 1:2 and 1:256 dilution results ($7.91 \pm 1.18 \times 10^4$ and $7.72 \pm 1.46 \times 10^2$ *Nitrobacter* rDNA copies/µL, respectively: Table C-1). Since the 1:256 dilution concentration was smaller than the 1:2 dilution by a factor of 128, the 1:2 dilution concentration could be used to predict the 1:256 concentration (6.18×10^2 copies/µL). The actual result was only 20% higher than expected. This level of accuracy was considered acceptable for the purposes of the study, particularly since a small difference in rDNA concentration was anticipated during experiments that evaluated the rRNAt/rDNA ratio because of the slow *Nitrobacter* growth rate (Watson et al., 1989).

The high PCR efficiency and excellent linear fit through the dilution series data (Figure 6-A: $R^2 = 0.9912$) indicated the extract did not significantly inhibit the reaction (McPherson and Møller, 2000). Potential PCR inhibition was further examined by plotting the DNA extract dilution series results versus the dilution factor (Figure 6-B). A slight increase in the copies/(L mixed liquor) results was evident as the dilution exceeded 1:64. The average results for the 1:2 - 1:32 and 1:64 - 1:1,024 dilutions were 6.03 ± 0.4 and $8.37 \pm 0.6 \times 10^9$ copies/L, respectively. Though a small inhibitory effect (< 28%) was indicated, this could be negated by a decrease in assay reproducibility as the dilution is increased (Dionisi et al., 2003). Also, this could have resulted from the difference in the amplification efficiency of the standards and dilutions. Thus, a small dilution factor (1:5) was adopted as standard for BSNR DNA extracts in all future experiments. This would allay some of the inhibitory effect, if present, but maintain the assay sensitivity.

4.8.2 Real-time RT-PCR

Reverse transcription/PCR inhibition was investigated with a series of 1:2 dilutions of a BSNR RNA extract (1:2 - 1:1024). The dilution series and a series of 10^7 - 10^2 copies/µl *Nitrobacter* rRNAt standards were analyzed in triplicate with the optimized *Nitrobacter* rRNAt real-time PCR assay (Figure 7-A: assay data provided in Table C-1). The RT-PCR efficiency was 90% over five orders of magnitude for the standards and 98% over 2.5 orders of magnitude for the RNA dilutions. As for the *Nitrobacter* rDNA assay, this would produce only a small error in the relative *Nitrobacter* rRNAt results

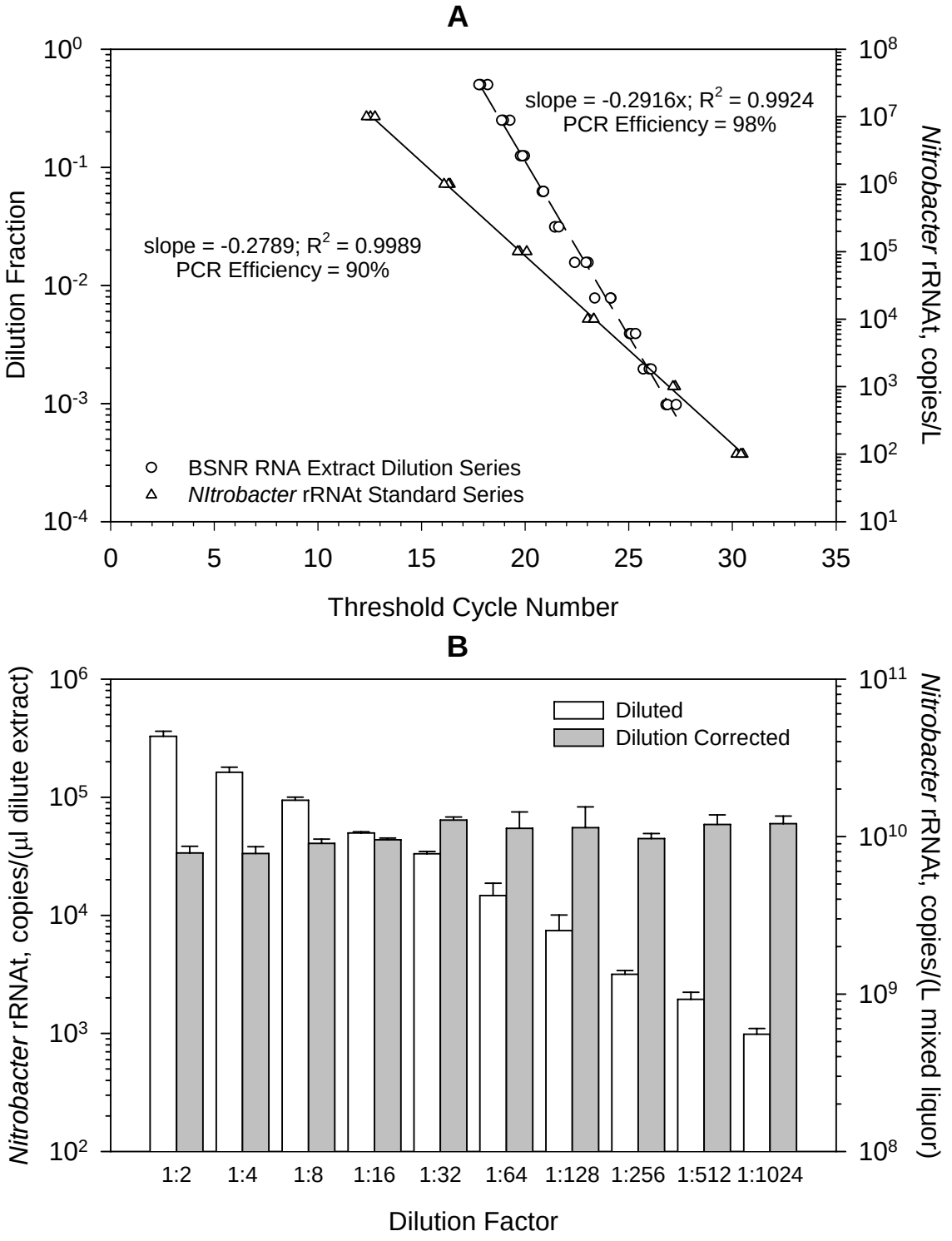


Figure 7 A PCR inhibition investigation of the optimized *Nitrobacter* rRNAt real-time RT-PCR detection system. A. Threshold cycle results for *Nitrobacter* rRNAt standards and BSNR RNA extract dilutions. B. *Nitrobacter* rRNAt concentration in the BSNR RNA extract dilutions.

when a true 2 order of magnitude difference existed between two samples. This was again evaluated empirically by comparing the 1:2 and 1:256 dilution results ($3.28 \pm 0.4 \times 10^5$ and $3.17 \pm 0.3 \times 10^3$ *Nitrobacter* rRNAt copies/μL, respectively: Table C-1). The predicted concentration in the 1:256 dilution (2.56×10^3 copies/μL) using the 1:2 result was only 22% lower than expected. This level of accuracy was considered acceptable for the purposes of the study since variations in the *Nitrobacter* rRNAt/rDNA ratio were expected to cover ≤ 2 orders of magnitude (Cangelosi and Brabant, 1997; Oether et al., 2000; Licht et al., 1999).

The high RT/PCR efficiency and excellent linear fit through the dilution series results (Figure 7-A: $R^2 = 0.9924$) confirmed the BSNR RNA extract did not significantly inhibit the RT or PCR reactions. As for the DNA extract, this was further explored by plotting the RNA extract dilution series results versus the dilution factor (Figure 7-B). This revealed a slight increase in copies/(L mixed liquor) results as the dilution factor exceeded 1:16. Average results for grouped dilutions 1:2 - 1:16 and 1:32 - 1:1024 were $8.57 \pm 0.9 \times 10^9$ and $1.15 \pm 0.9 \times 10^{10}$, respectively. Since the inhibition effect was small (< 26%), a small dilution factor (1:5) was also adopted as standard for all future measurements of *Nitrobacter* rRNAt. As for the *Nitrobacter* rDNA assay, this was anticipated to allay some inhibition, if present, but maintain the assay sensitivity.

4.8.3 Summary

BSNR nucleic acid extracts did not cause significant RT and/or PCR inhibition. This allowed a small dilution factor (1:5) to be adopted for mixed liquor DNA and RNA extracts prior to *Nitrobacter* rDNA and rRNAt quantification, which would maximize the assay sensitivity (Dionisi et al., 2003). Similar amplification efficiencies for the artificial *Nitrobacter* standards and *Nitrobacter* ribosomal genes and transcripts recovered in the reactor RNA and DNA extracts, respectively, indicated the assays would yield accurate results. Further, the relative accuracy for comparing samples was confirmed empirically. For consecutive 1:2 DNA extract dilutions, the *Nitrobacter* rDNA results overlapped only once (Figure 6-A), while the rRNAt results never overlapped (Figure 7-A). This

suggested that relatively few assays would be required to distinguish between samples possessing a true 2-fold difference in *Nitrobacter* rDNA or rRNA concentration. However, the dilution series results did not account for the variability nucleic acid extraction would contribute to the final results. Thus, a subsequent experiment was performed that analyzed the assay results across replicate nucleic acid extracts.

4.9 Sample Volume and Real-Time PCR Statistical Power Analyses

Planning for adequate statistical power should be involved in any rational approach to experimentation (Samuels, 1989). In regards to this study, a recent review (Dionisi et al., 2003) indicated that the variability of real-time PCR can lead to low sensitivity for detecting 2- or even 5-fold *Nitrospira* rDNA concentration differences in mixed liquor DNA extracts. Also, variability and difficulty with reproducibility are reported for real-time RT-PCR (Bustin, 2000; Bustin, 2002). Hence, a statistical power analysis was conducted on replicate BSNR mixed liquor DNA and RNA extracts to assess how many replicate extractions/real-time PCR assays would be required to detect true 2- to 5-fold differences in *Nitrobacter* rDNA or rRNAt abundance. Power analyses were designed that would empirically and theoretically test the sensitivity of the assays by quantifying *Nitrobacter* rDNA and rRNAt in nucleic acid extracted from different mixed liquor sample volumes (collected simultaneously). The copies/(µl extract) results were expected to be proportionately different according to the sample size, but the copies/(L mixed liquor) results were expected to be similar. This would also help determine whether the sample volume influenced the assay accuracy and reproducibility, so that standard sample volumes could be adopted for the study.

4.9.1 Real-time PCR

Twelve BSNR mixed liquor samples were collected simultaneously at four different volumes (3 replicates × ≈ 0.5, 1, 2, and 5 ml). DNA was extracted from the samples in separate extraction rounds that included one representative of each volume. The extracts were in turn quantified with five replicate *Nitrobacter* rDNA assays.

Sample volume effects

The results, both as copies/(µl extract) and copies/(L mixed liquor), are presented in Figure 8-A and Table C-2. As expected, the results in copies/(µl extract) increased as the extraction volume increased, from an overall average of $1.04 \pm 0.2 \times 10^4$ copies/µl for the ≈ 0.5 ml samples, to $3.14 \pm 0.6 \times 10^5$ copies/µl for the ≈ 5 ml samples. The results as copies/(L of mixed liquor) should have been the same across the different samples volumes. However, the results for the ≈ 0.5 ml samples ($4.37 \pm 1.0 \times 10^9$ copies/L) were clearly lower than for the large sample volumes ($9.79 \pm 5.6 \times 10^9$, $1.29 \pm 0.3 \times 10^{10}$, and $1.29 \pm 0.2 \times 10^{10}$ copies/L for the ≈ 1, 2, and 5 ml extraction volumes, respectively). This indicated the ≈ 0.5 ml sample volume did not yield accurate results, perhaps because DNA extraction was inefficient for such a small sample volume.

To assess the assay's variability, the log transformed copies/(L mixed liquor) data in Table C-2 (*Nitrobacter* rDNA) were analyzed to determine the mean, standard deviation, and coefficient of variation (CV) for the intra-assay and inter-extraction results by sample volume (Table C-3). The CVs for the 0.5, 1, and 2 ml inter-extractions results (1.08, 3.12, 1.37%) were notably higher than for the 5 ml samples (0.78%). This suggested that the 5 ml sample volume provided better inter-extraction reproducibility. There was little difference in the intra-assay CVs for the different samples (≈ 0.5%: Table C-3). However, for all the extracts the inter-extraction CV exceeded the intra-assay CVs. This indicated DNA extraction contributed to the measurement variability, contrary to a report by Dionisi et al. (2003). However, the finding that more mixed liquor biomass (larger sample volumes herein) improved the assay reproducibility was in agreement with their findings, since they reported more concentrated mixed liquor samples yielded better real-time PCR discriminatory power. Since a larger sample volume appeared to provide better accuracy, and the 5 ml sample seemed to provide better inter-extraction reproducibility, a 5 ml sample volume was adopted as standard for the study.

Statistical power analysis

In only one instance, the average copies/(µl extract) results for the different gross sample volumes overlapped; the exception occurred for a ≈ 1 ml DNA extract, for which

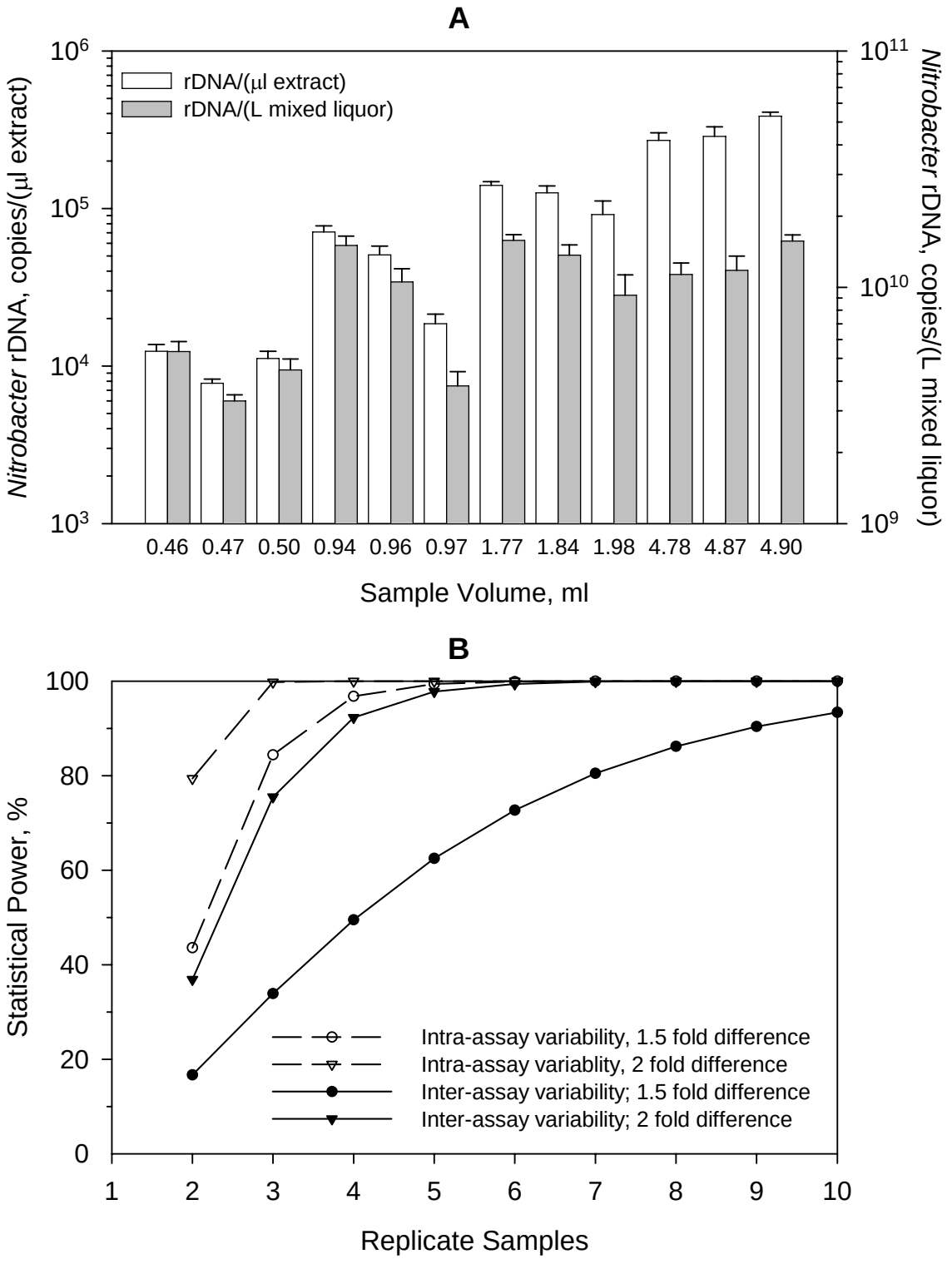


Figure 8 A test of the discriminatory power of the *Nitrobacter* rDNA real-time PCR assay. A. The *Nitrobacter* rDNA concentration in BSNR mixed liquor DNA extracts. B. A statistical power analysis of the detection system.

the *Nitrobacter* rDNA concentration overlapped with two of the ≈ 0.5 ml extracts (Figure 8-A). Aside from this apparent outlier, the data empirically indicated the assay could discriminate between two BSNR mixed liquor samples if the *Nitrobacter* rDNA concentration differed by approximately 2-fold. To quantify the assay discriminatory power more clearly, and judge the impact that DNA extraction had on the rDNA concentration estimate, a statistical power analysis was performed. For this analysis, the replicate real-time PCR standard deviation was estimated as the square root of the mean square error (0.0538) for an analysis of variance (ANOVA: Table C-4) of the replicate log transformed copies/(L mixed liquor) data in Table C-2. The standard deviation of the average assay result across replicate DNA extracts was similarly estimated (0.104) with an ANOVA of the 2 and 5 ml sample volume results in Table C-3 (since a larger volume seemed to produce better assay results). Subsequently, SamplePower^{TM} 2.0 (SPSS; Chicago, IL) was used to compute the statistical power for 2 - 10 replicate measurements of two independent groups that possessed one or the other standard deviation. The basis of comparison was a t-test with the effect size set at 1.5-, 2-, and 5-fold differences in the *Nitrobacter* rDNA concentration (0.18, 0.30, and 0.50 log scale differences; $\alpha = 0.05$; Tails = 2). For the 5-fold difference, only two samples would be required to obtain a statistical power ≥ 90%, regardless of the additional variability DNA extraction added to the concentration estimate. The effect of DNA extraction was also small for the 2-fold true difference, for which 3 replicates would be required to achieve reasonable statistical power (> 75%: Figure 8-B). However, if the true difference was reduced to 1.5-fold, 7 samples would be required to achieve more than 75% power considering the inter-extract standard deviation (Figure 8-B). If DNA extraction had not added variability, only two replicate real-time PCR assays would have been required for single sample extracts (Figure 8-B: inferred from the intra-assay result). Because of the expense and labor for replicate extractions, three (but a minimum of 2) replicate extracts were adopted as standard for the study. The number of assay replicates per extract was set at 3.

Dionisi et al. (2003) report the findings of a similar power analysis for real-time PCR bacterial and *Nitrospira* specific rDNA detection systems. These researchers found

that 3 replicate DNA extractions would be required to achieve a statistical power of 80% for a true 2-fold difference in bacterial rDNA gene copy number. However, their *Nitrospira* real-time PCR assay was much less sensitive, requiring 22 or 5 replicate assays to achieve a statistical power of 80% when a true 2- or 5-fold difference in *Nitrospira* rDNA existed (for low biomass samples akin to the BSNR). Thus, the *Nitrobacter* rDNA assay herein was comparable to their bacterial rDNA assay, but much more sensitive than the *Nitrospira* assay. Even so, the power analysis confirmed it would be difficult to detect *Nitrobacter* growth in short term experiments (< 12 hours), since the doubling time of this genera is often reported in excess of 12 hours (Watson et al., 1989), and only 1 copy of the *rrn* operon is present (Navarro, 1992a).

4.9.2 Real-time RT-PCR

A similar experiment was performed for the *Nitrobacter* rRNAt detection system. Nine BSNR mixed liquor samples were collected simultaneously at three different volumes (3 replicates × ≈ 1, 2, and 5 ml). RNA was extracted from the samples in separate rounds and quantified with five replicate assays.

Sample volume effects

The results, both as copies/(µl extract) and copies/(L mixed liquor), are presented in Figure 9-A and Table C-2. As expected, the copies/(µl extract) results increased as the extraction volume increased, from an overall average of $2.14 \pm 0.4 \times 10^5$ copies/µl for the ≈ 1 ml samples, to $9.71 \pm 0.7 \times 10^5$ copies/µl for the ≈ 5 ml samples. Further, the results as copies/(L of mixed liquor) were similar for the different extract volumes (1.35 ± 0.3, 1.46 ± 0.1, and $1.26 \pm 0.1 \times 10^{10}$ for the ≈ 1, 2, and 5 ml samples, respectively). Thus, the sample volume did not affect the reproducibility of the assay.

To assess the assay's variability, the log transformed copies/(L mixed liquor) data in Table C-2 were analyzed to determine the mean, standard deviation, and CV, both in terms of the intra-assay and inter-extraction results (Table C-3). The CV for the inter-extraction results of the 1 ml samples (0.90%) was higher than for the 2 and 5 ml samples (0.17 and 0.28%, respectively). Thus, the larger sample volumes appeared to provide

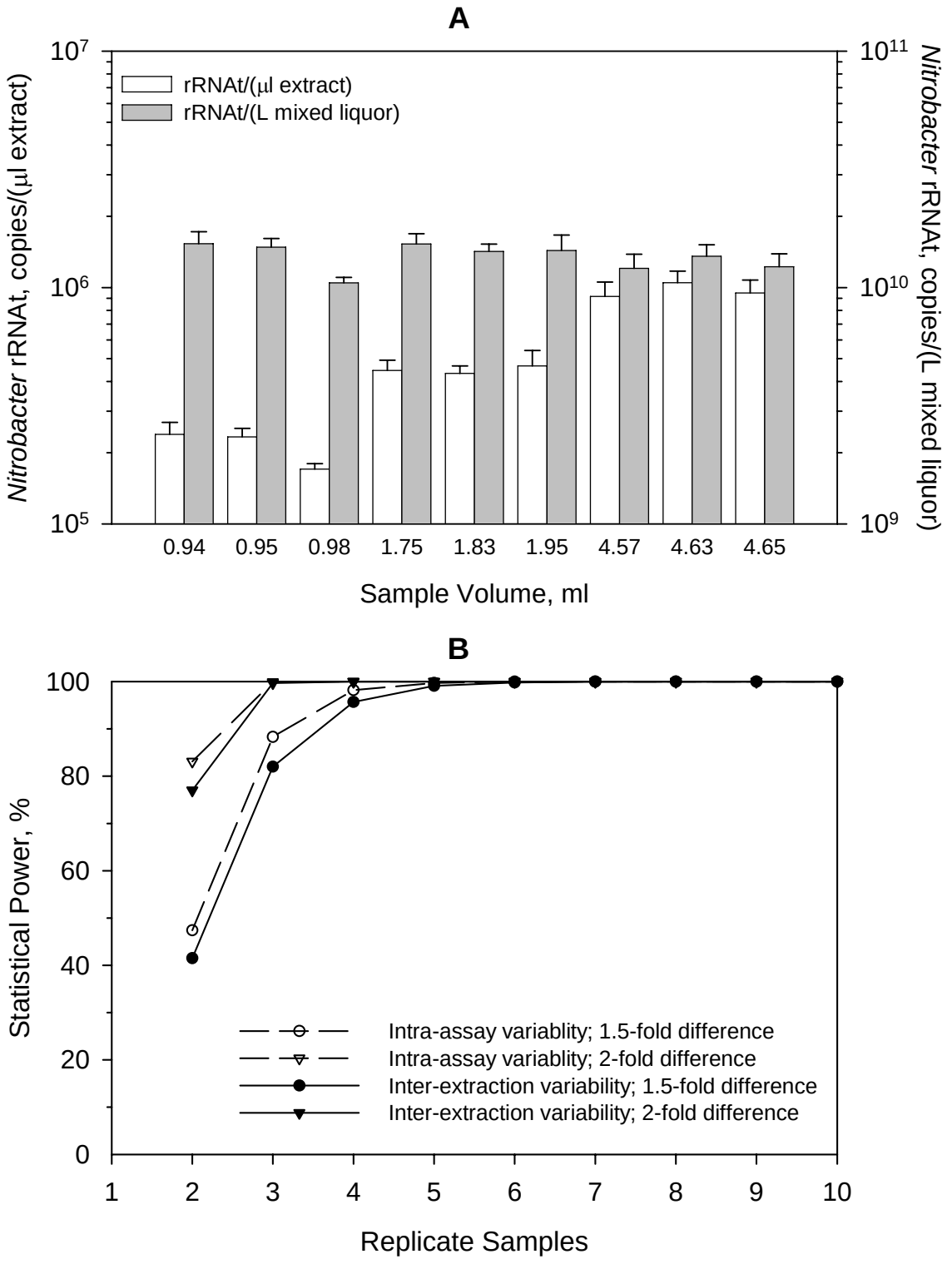


Figure 9 A test of the discriminatory power of the *Nitrobacter* rRNAt real-time RT-PCR assay. A. *Nitrobacter* rRNAt concentration in BSNR mixed liquor RNA extracts. B. A statistical power analysis of the detection system.

better inter-extraction reproducibility. However, the intra-assay CVs were approximately the same as the inter-extraction CVs (mean 0.48% and 0.45%, respectively). This suggested that RNA extraction had little impact on the final concentration estimate. Though the results suggested a larger sample volume may provide better reproducibility, a compromise of 3 ml was adopted as standard for the study. This allayed the cost of the RNA sample preservative required, but likely improved the assay reproducibility.

Statistical power analysis

None of the copies/(µl extract) results for the different sample volumes overlapped (Figure 9-A). This indicated that the *Nitrobacter* rRNAt assay could detect a true 2- to 2.5-fold difference in *Nitrobacter* rRNAt concentration with as few as 3 RNA extracts. To confirm the assay's sensitivity, a power analysis was conducted using the intra-assay standard deviation (0.0506) (estimated using the square root of the MSE for an ANOVA of the replicate assay data: Table C-4) and the inter-extraction standard deviation (0.0558) (similarly estimated with an ANOVA of the 1, 2, and 5 ml mean assay data: Table C-4). SamplePower™ 2.0 (SPSS; Chicago, IL) was used to compute the statistical power for 2 - 10 replicate measurements of two independent groups which possessed one or the other standard deviation as previously described. For the 5-fold difference, only two samples were required to obtain a statistical power ≥ 90%. For both the 1.5- and 2-fold differences, 3 replicate sample extractions would provide more than 80% power (Figure 9-B). The results indicated the *Nitrobacter* rRNAt assay was more sensitive than the *Nitrobacter* rDNA assay, and that RNA extraction had little effect on the measurement variability. Since the variation in the *Nitrobacter* rRNAt was expected to cover 1 - 2 orders of magnitude, 2 to 3 replicate sample extractions were adopted as standard for the study, along with 3 assay replicates for each replicate extract. The results indicated the assay would easily discriminate such large concentration differences.

4.10 *Nitrobacter* as a Dominant Nitrite Oxidizer in the BSNR

Three 5 ml mixed liquor samples were collected from the BSNR 508 days after the reactor had been seeded, and 401 days following the influent change to 1,500 mg/L

NH_4^+-N, to assess whether *Nitrobacter* was a dominant NOB in the then well established reactor. *Nitrobacter* rDNA was quantified with three replicate real-time PCR reactions (Table C-5: summarized in Table 6). In addition, total bacterial rDNA was quantified in triplicate with the bacterial rDNA real-time PCR detection system and protocol of Dionisi et al. (2003) for 1:5, 1:50, and 1:500 dilutions of the DNA extracts (Table C-5: summarized in Table 6). The dilution series results did not reveal PCR inhibition of the bacterial rDNA assay, since the concentration did not systematically increase as the dilution factor increased (McPherson and Møller, 2000). As expected, the mean bacterial rDNA copy abundance ($2.50 \pm 1.7 \times 10^{11}$ copies/L) exceeded that of *Nitrobacter* ($1.34 \pm 0.3 \times 10^{10}$ copies/L).

A *rrn* operon copy number database was consulted to estimate the number of ribosomal (*rrn*) operons that could be assumed to be present in the BSNR bacteria (Klappenbach, et al., 2001; http://rrndb.cme.msu.edu/). At the time this database was consulted, it contained 502 entries and was last updated on 02/04/2004. The average bacterial entry had 4.1 *rrn* operons per genome, though the number ranged from 1 to 15 (Klappenbach, et al., 2001). This information was used to confine the relative abundance of *Nitrobacter* in the BSNR by assuming the reactor harbored bacteria with an average *rrn* operon copy number equal to or less than the database average. An assumption that the copy number exceeded the database average did not appear reasonable, since the

Table 6 Summary of total bacterial rDNA and *Nitrobacter* rDNA copy abundance in replicate BSNR DNA extracts.

BSNR DNA Extract		Bacterial rDNA		*Nitrobacter* rDNA	
replicate	dilution	copies/L	mean	copies/L	mean
1	1:5	1.14E+11		1.06E+10	
	1:50	2.46E+11		-	
	1:500	1.35E+11		-	
2	1:5	1.48E+11		1.65E+10	
	1:50	4.07E+11	2.50E+11	-	1.34E+10
	1:500	2.08E+11		-	
3	1:5	1.51E+11		1.31E+10	
	1:50	6.20E+11		-	
	1:500	2.18E+11		-	

reactor was likely nitrifier enriched, and both *Nitrosomonas europaea* (Chain et al., 2003) and *Nitrobacter* species/strains (Navarro, 1992a) (both present in the reactor) possess only one *rrn* operon.

Nitrobacter rDNA constituted 5% of the total bacteria rDNA copies measured, and between from 11 - 22% of total bacteria in the reactor assuming the average bacteria possessed between 2 and 4.1 *rrn* operons/genome. The total *Nitrobacter* concentration in the BSNR ($\approx 9 \times 10^{10}$ bacteria/g MLVSS) was approximately 4.5 fold higher than the average for 10 municipal WWTPs in Sweden (Sandén and Dalhammar, 2000: measured with an amperometric immunosensor at $\approx 2 \times 10^{10}$/g). The result was an order of magnitude higher than the *Nitrospira* rDNA concentration in a bench scale reactor treating municipal wastewater with comparable solids content (2 day SRT, 260 mg MLVSS/L: $\approx 1 \times 10^{9}$ copies/L), but was similar to another reactor treating the same wastewater at a much higher solids concentration (20 day SRT, 2,610 mg/L: $\approx 1 \times 10^{10}$ copies/L) (Dionisi et al., 2003). In terms of the relative percentage of bacteria in the mixed liquor, only one estimate for *Nitrobacter* could not be found: Sánchez et al. (2001) indicated (using slot blot hybridization) that *Nitrobacter* and *Nitrospira* constituted 10% and 25%, respectively, of bacteria in a nitrifier enrichment. *Nitrospira* constituted 9% (Jurelsenko et al. 1998: using FISH) of total bacteria in an activated sludge system treating high ammonium, rendering plant effluent (≈ 4,000 mg-N/L). *Nitrospira* was < 5% of biofilm bacteria on a rotating biological contactor treating ammonium rich (500 mg-N/L) wastewater with low organic carbon (Egli et al., 1998). Using real-time PCR, Dionisi et al. (2003) estimated that *Nitrospira* constituted 1.5 - 4.3% of all bacteria in the previously mentioned bench scale reactors (assuming 3.6 *rrn*/genome). In comparison, *Nitrobacter* appeared more concentrated in the BSNR, particularly since the solids content (≈ 150 mg MLVSS/L) was much lower than in many of these other reactors. Also, *Nitrobacter* appeared to represent a relatively large percentage of total bacteria, thought the Sánchez et al. (2001) results were similar. Hence, *Nitrobacter* was likely a dominant NOB in the BSNR, and, as such, was an appropriate subject for a study of the NOB rRNAt/rDNA ratio.

The results indicate the BSNR clone library did not accurately present the bacterial composition of the reactor. *Nitrobacter* represented only 1 in 40 of the cloned sequences, despite comprising ≈ 1 in 5 or 10 bacteria in the reactor. Further, 33 of the 40 cloned rDNA sequences were non-nitrifiers (presumably heterotrophs), despite the highly selective and enriching characteristics of the BSNR. However, these are not unique observations. Okabe et al. (1999) demonstrated using FISH that a wide variety of non-nitrifier eubacteria (presumably heterotrophs) coexisted with AOB in an autotrophic nitrifying biofilm. For the abattoir WWTP activated sludge previously mentioned, Juretschko et al. (1998) found no AOB in 60 cloned rDNA sequences, despite the highly enriching and selective nature of the effluent, and the fact that ≈ 1 in 5 bacteria was an AOB. Also, while *Nitrospira* constituted approximately 9% of the mixed liquor bacteria in this reactor, only 2 of the 60 cloned sequences were contributed by this NOB. Similarly, Egli et al. (1998) found no NOB in 26 rDNA clones originating from a biofilm treating ammonium rich, reduced organic leachate, even though *Nitrospira* constituted up to 5% of biofilm bacteria. The poor recovery of NOB cloned sequence in this study may have been due to bias created by the "conserved" PCR amplification reaction used to create the clone libraries. Also, heterotrophic bacteria within the BSNR may have possessed several *rrn* operons/genome, which could have contributed to amplification bias.

With few exceptions, *Nitrobacter* has not been found to dominate bench- or full-scale wastewater treatment systems when molecular techniques have been utilized, though this organism has often been isolated using culture based enumerative techniques (Section 2.1.3). Interestingly, Fourattt et al. (2003) found that *Nitrobacter* was dominant in a nitrifier bioaugmentation product from Novozymes Biologicals. Since the BSNR was seeded with a similar product (Section 3.2.1), this could explain why *Nitrobacter* was dominant in the BSNR.

4.11 Summary

Although limited "unbiased" sequence diversity was obtained from the BSNR, a single clone indicated *Nitrobacter* was present in the reactor. This was important because it determined which NOB would be examined with respect to the proposed rRNAt/rDNA activity metric. Since this genus appeared to be a dominant nitrite oxidizer in the reactor, any failure of the rRNAt/rDNA ratio to correlate with nitrite oxidizing activity would not likely result from the confounding effects of other NOB sub-populations.

Conservative principles were used to design a quantitative PCR detection system targeting the *Nitrobacter* 16S - 23S ISR which allowed the ribosomal gene and transcript could to be quantified with the same primer and probe sequences. Once designed, the rRNAt and rDNA assays were found to be highly specific and free from PCR and RT inhibition when using BSNR nucleic acid extracts. Further, the assays appeared to yield accurate results using external standards. In so far as the assay reproducibility was concerned, it was shown both empirically and theoretically that approximately 3 replicate extracts could distinguish a true 2-fold concentration difference. The finding that the assays were specific, accurate, and sensitive was important since the proposed metric was a ratio of the measured quantities: to avoid inflating the metric variance, it was important to quantify both the numerator (rDNA) and quotient (rRNAt) reproducibility.

Because *Nitrobacter spp.* are slow growers with doubling times in excess of ≈ 12 hours (Watson et al., 1989), the sensitivity of the rDNA assay would likely make it difficult to detect short term population shifts, which was also true for both total bacteria and *Nitrospira* within full and bench scale wastewater treatment systems (Dionisi et al., 2002; Dionisi et al., 2003). However, the rRNAt assay should easily detect the large differences in expression typical of the ribosomal gene (Table 4). This was an important finding and could reflect a guiding principle for how molecular techniques would be most useful for engineers trying to improve wastewater treatment performance: molecular techniques may be better suited to study activity as opposed to population changes, particularly for slow growing microorganisms.

Based on the results herein, it appeared reasonable to assume that log transformed *Nitrobacter* rDNA and rRNAt concentration data were normally distributed with equal variance across replicate sample extracts. Using these assumptions, the *Nitrobacter* rDNA and rRNA results for replicate sample extracts could be analyzed with ANOVA and Tukey HSD comparisons. Conversely, since the rRNAt/rDNA metric constitutes a ratio, assumptions for its distribution should be avoided (Muttray et al., 2001). Instead, hypotheses would best consist of comparisons to an expected range (e.g. prediction intervals) or expected metric trends (increasing vs. decreasing) following activity changes. Since distribution assumptions cannot be made for the ratio, these hypotheses could be evaluated with nonparametric statistics (Helsel and Hirsch, 2002) after the ratio was computed with the overall *Nitrobacter* rDNA and rRNAt mean results. To display variability in the ratio estimate, the interquartile range of all possible ratio values give the rDNA and rRNAt results across replicate sample extracts could be used (Helsel and Hirsch, 2002). These approaches were taken in evaluating the *Nitrobacter* rDNA and rRNAt concentration data and the rRNAt/rDNA metric in Chapters 5, 6, 7, and 8 (Figure 4).

CHAPTER 5.0

NITROBACTER rRNAt/rDNA RANGE AND DYNAMICS

5.1 Introduction

Nitrite oxidizing activity is of prime interest since it controls both nitrification and denitritification efficiency. Moreover, nitrite oxidation affects NOB growth rates and likely the ribosomal transcription rates, though this has not been investigated. Generally, when nitrite oxidation activity is low, expected NOB growth potential would also be low, resulting in lower demand for protein, new ribosomes, and hence less abundant rRNA and rRNAt. Conversely, during high nitrite oxidation activity, more growth potential would be expected, resulting in higher demand for protein, new ribosomes, and hence more abundant rRNA and rRNAt (Cangelosi and Brabant, 1997). Thus, the usefulness of the rRNAt/rDNA ratio for the NOB would depend on whether changes in nitrite oxidation activity, from relatively high to low levels and vice versa, could be resolved in changing ratio values. To test this possibility, a batch nitrite oxidation experiment was performed with BSNR mixed liquor samples to estimate a lower limit for the *Nitrobacter* rRNAt/rDNA ratio, proposed to occur during nitrite starvation, as well as an upper limit, proposed to occur during unlimited nitrite oxidation. This would establish a range of "possible" ratio values that would indicate whether these extremes levels of nitrite oxidation activity could be inferred using the metric value.

In continuously fed wastewater treatment reactors, an intermediate range of nitrite oxidation activity, and hence NOB rRNAt/rDNA ratio values, may persist while the desired N-treatment efficiency is maintained. Conversely, changes in NOB activity toward the nitrite starvation and unlimited nitrite oxidation extremes may precede departures from high N-treatment efficiency. For example, in a denitritification reactor successfully promoting stable nitrite buildup, NOB acclimation may represent a change from generally low nitrite oxidation activity, reflected in a low "normal" range for the rRNAt/rDNA ratio, to initially unlimited nitrite oxidation activity (since excess nitrite

would be present). Conversely, when complete nitrification is promoted, NOB inhibition may represent a detrimental change from generally high nitrite oxidation activity, reflected in a high "normal" range for the rRNAt/rDNA ratio, to levels akin to nitrite starvation. In either case, declines in treatment performance would be expected if the adaptation/inhibition persisted. Thus, the usefulness of the proposed metric appeared to hinge not only on the range of "possible" ratio values, but also on a range of "normal" values while high efficiency was maintained in a reactor. If the range of "normal" reactor values could be distinguished from the upper and lower ratio limits, then detrimental changes in NOB activity might be detectable in WWTP reactors by monitoring the rRNAt/rDNA metric over time. The BSNR, in which high NOB activity was promoted, was used to evaluate this possibility. After setting a nitrification efficiency standard, lower and upper prediction intervals were computed for the *Nitrobacter* rRNAt/rDNA ratio. Though such prediction intervals were not established in previous investigations of bacterial molecular activity (Table 4), they could prove useful for screening normal from abnormal activity levels.

The time required for the ratio to transition between the upper and lower limiting values was also of interest. Though this occurred quickly for *E. coli* and *Acinetobacter* spp. (< 1 hour; Cangelosi and Brabant, 1997; Oerther et al., 2000), it was anticipated to take much longer for the slow growing NOB. This would impact the metric's usefulness, since an improvement in treatment efficiency would be realized with actions taken only after a detrimental NOB activity change was detected.

5.2 BSNR *Nitrobacter* rRNAt/rDNA Prediction Intervals

The BSNR was operated 539 days (432 days at the final influent composition specified in Section 3.2.2) prior to establishing prediction intervals for the *Nitrobacter* rRNAt/rDNA ratio. During the final 384 days of this time period, the nitrification efficiency (nitrate-N/(ammonia-N + nitrite-N + nitrate-N) × 100%) was typically high (evaluated 66 times: 98 ± 3%). Thus, the BSNR was well established with high nitrification efficiency before the prediction intervals were evaluated.

5.2.1 Method

Nitrification efficiency was monitored in the BSNR for 11 weeks using nitrogen samples collected three times per week. Mixed liquor samples were collected three times per week and analyzed for MLVSS, and weekly for three replicate DNA and RNA extractions. The objective was to establish lower and upper prediction intervals for the *Nitrobacter* rRNAt/rDNA ratio while the nitrification efficiency above 90%. It was hypothesized that during NOB inhibitory conditions, the ratio would fall below the lower prediction interval. This was tested during: nitrite starvation (Section 5.3), batch inhibition experiments with 3,5-DCP, azide, and H^+ (Chapter 6.0), a batch inhibition experiment at high ammonia concentrations (Chapter 7.0), and during a staged BSNR inhibition event (Chapter 8.0). Further, because NOB activity in the reactor was limited (excess nitrite was rarely present), it was hypothesized that during unlimited nitrite oxidation (when excess nitrite was present) the ratio would exceed the upper prediction interval (Section 5.3).

5.2.2 Results

Figure 10 presents BNSR data in consecutive operating days after the initial samples were collected to establish the ratio prediction intervals. The nitrogen, nitrification efficiency, and MLVSS data are provided in Table D-1. *Nitrobacter* rRNAt and rDNA data are presented in Table D-2 and summarized in Table 7 along with the rRNAt/rDNA ratio values. Table 7 also presents the statistical analysis results for the rDNA and rRNAt assay mean results after an ANOVA rejected the null hypothesis that the sample concentrations were all equal.

Soluble nitrogen

The highest ammonia concentration in the reactor occurred on day 1 (21.9 mg-N/L) and, in general, the concentration remained higher during days 1 - 33 (8.7 ± 4.8 mg-N/L) than during days 36 - 73 (0.5 ± 0.5 mg-N/L) (Figure 10-A). However, in all cases the concentrations were less than 2 % of the soluble nitrogen in the reactor. Thus, AOB activity was high throughout the 73 day time course of the experiment.

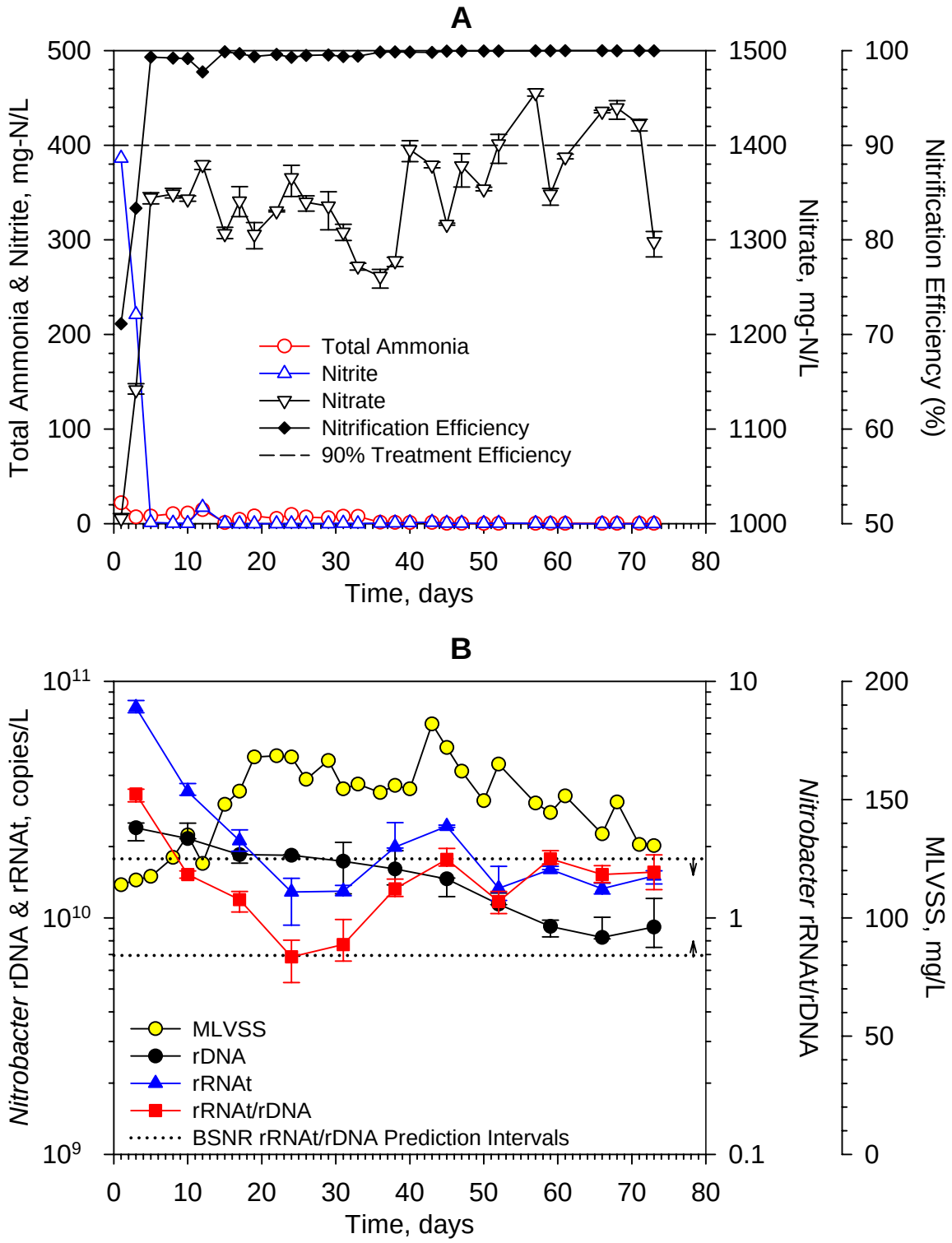


Figure 10 Nitrogen (A) and MLVSS and molecular data (B) collected from the BSNR over the 11 week time period used to establish upper and lower *Nitrobacter* rRNAt/rDNA ratio prediction intervals.

Table 7 *Nitrobacter* rRNAt, rDNA, and the rRNAt/rDNA ratio in the BSNR over the 11 week time period used to establish ratio prediction intervals.

Sample Day	*Nitrobacter* rDNA (copies/L)[1]			*Nitrobacter* rRNAt (copies/L)[1]			rRNAt[2] / rDNA
	Assay Mean	Statistical Analysis		Assay Mean	Statistical Analysis		
		Overall Mean	Tukey		Overall Mean	Tukey	
3	2.52E+10	2.35E+10	A	8.33E+10	7.84E+10	A	3.341
	2.41E+10			7.79E+10			
	2.12E+10			7.41E+10			
10	2.17E+10	2.28E+10	A	3.42E+10	3.48E+10	B	1.523
	2.52E+10			3.71E+10			
	2.17E+10			3.31E+10			
17	1.85E+10	1.81E+10	AB	-	2.16E+10	CDE	1.194
	1.86E+10			2.40E+10			
	1.70E+10			1.92E+10			
24	1.86E+10	1.84E+10	AB	1.50E+10	1.26E+10	F	0.684
	1.84E+10			9.63E+09			
	1.81E+10			1.31E+10			
31	2.10E+10	1.70E+10	ABC	1.25E+10	1.31E+10	F	0.771
	1.74E+10			1.38E+10			
	1.27E+10			1.31E+10			
38	1.93E+10	1.64E+10	ABC	1.99E+10	2.17E+10	CD	1.326
	1.61E+10			2.01E+10			
	1.38E+10			2.53E+10			
45	1.48E+10	1.39E+10	BCD	2.44E+10	2.46E+10	C	1.767
	1.23E+10			2.42E+10			
	1.46E+10			2.51E+10			
52	1.14E+10	1.19E+10	CDE	1.65E+10	1.39E+10	F	1.172
	1.28E+10			1.34E+10			
	1.14E+10			1.19E+10			
59	9.79E+09	9.11E+09	E	1.60E+10	1.62E+10	DEF	1.777
	9.22E+09			1.66E+10			
	8.32E+09			1.61E+10			
66	1.01E+10	8.84E+09	E	1.42E+10	1.35E+10	F	1.524
	8.29E+09			1.26E+10			
	8.15E+09			1.35E+10			
73	7.53E+09	9.60E+09	DE	1.59E+10	1.50E+10	F	1.559
	9.20E+09			1.51E+10			
	1.21E+10			1.39E+10			

1 Assay mean is the mean of triplicate Real Time or Real Time RT-PCR reactions for replicate DNA and RNA extracts (Table D-2). The overall mean is the average of the assay means. Log transformation made the assay mean data more symmetric and constant in variance. The log transformed assay mean data were analyzed with Tukey HSD multiple comparisons if ANOVA rejected the null hypothesis of sample equivalence ($\alpha = 0.05$). Samples not sharing a common letter are significantly different ($\alpha = 0.05$).

2 The rRNAt/rDNA metric was calculated with the overall rDNA and rRNAt means for each sample event.

The nitrite concentration was unexpectedly high on days 1 (386 mg-N/L) and 3 (221 mg-N/L), but low, as expected, from day 5 - 73 (< 1.5 mg-N/L, except for day 12 which was 17.2 mg-N/L) (Figure 10-A). The initial nitrite data likely document recovery from a previous NOB inhibition event, since excess nitrite was present but rapidly disappeared between days 1 and 5. No ammonia, nitrite, or nitrate data were available immediately prior to day 1 to assess this possibility.

Nitrate concentrations were somewhat low on days 1 (1,005 mg-N/L) and 3 (1,141mg-N/L), corresponding to the high nitrite levels (Figure 10-A). Thereafter, nitrate concentrations were high from day 5 - 73 (1,352 ± 51 mg-N/L). Thus, the nitrate data indicate that NOB activity was unusually high prior to day 5, since excess nitrite was converted to nitrate during this time period. Note that variability was expected in the nitrate data because of the reactor's continuous-fed batch style of operation (Section 3.2.3).

Nitrification efficiency

Nitrification efficiency was below the 90% standard on days 1 (71%) and 3 (83%) as a result of the high nitrite and low nitrate concentrations, but remained above 90% thereafter (> 98%) (Figure 10-A). Thus, the nitrification efficiency was at steady state between operating days 5 and 73, a time period covering more than 7 SRTs.

MLVSS

The MLVSS varied throughout the 11-week time period, despite mostly steady state nitrification efficiency (Figure 10-B). The minimum value (114 mg/L) occurred on day 1 but increased 32% to 168 mg/L by day 19. Between days 15 and 40 the volatile solids were relatively constant (159 ± 7 mg/L). An increase to the maximum value (182 mg/L) occurred between days 40 and 45. This was followed by a decline to 131 mg/L by day 73. The average MLVSS (149 ± 18 mg/L) was close to an expected value (150 mg VSS/L) calculated with typical biokinetic parameters for nitrification (Benefied and Randall, 1985: Y = 0.05 mg VSS/mg NH_4^+-N, decay rate = 0.05 day^{-1}) and assuming the BSNR could be modeled at steady state as a CSTR that converted all influent ammonia to nitrate at a SRT of 10 days. The average MLVSS was slightly higher (≈ 36%) than in a

10 L batch nitrifier enrichment reactor (≈ 110 mg/L) with the same SRT (10 days), but a lower influent ammonia concentration (500 mg NH_4^+-N/L: Pollice et al., 2002).

Nitrobacter rDNA

The *Nitrobacter* rDNA (and rRNAt) data are displayed as the median ± minimum/maximum assay mean in Figure 10-B (Table 7). The rDNA concentration decreased steadily from day 3 ($2.35 \pm 0.2 \times 10^{10}$ copies/L) to day 59 ($9.11 \pm 0.7 \times 10^{9}$ copies/L), a 61% decline (Table 7). The concentrations on days 66 and 73 (8.84 ± 1.1 and $9.60 \pm 2.3 \times 10^{9}$ copies/L, respectively) were similar to the level measured on day 59. To examine the significance of the overall downward trend evident in Figure 10-B, a Kendall-Theil robust line was constructed through the overall mean rDNA data (Table 7). The slope was significantly different than 0 (p-value < 0.0001) and indicated 2.2×10^{8} copies/L/day were lost from the reactor. The decline may have been in response to excess growth that occurred prior to and/or between days 1 and 5, since excess nitrite was converted to nitrate during this time. Overall, the *Nitrobacter* rDNA levels were similar to those found for *Nitrospira* rDNA in full scale municipal (12 samples collected monthly: $3 \pm 2 \times 10^{10}$ copies/L) and industrial (3 samples from summer months: $3 \pm 2 \times 10^{10}$ copies/L) WWTPs, even though the BSNR oxidized much more influent ammonia (≈ 1200 mg-N/L) than the municipal (≈ 20 mg-N/L) and industrial (45 mg-N/L) reactors (Dionisi et al., 2002). In the full scale reactors, the high NOB concentration relative to the amount of nitrite oxidized could reflect sludge recycle and hence high suspended solids concentrations. Dionisi et al., (2003) reported that *Nitrospira* rDNA abundance varied greatly (1.0×10^{9} to 3.6×10^{10} copies/L) in four bench scale reactors with widely different suspended solids concentrations (MLVSS = 350 mg/L to 2,100 mg/L) even though the reactors treated the same settled wastewater at similar nitrification efficiencies. It is also possible that the *Nitrobacter* yield in the BSNR was lower, since it was more strictly autotrophic that the referenced treatment systems.

ANOVA rejected the null hypothesis that the log transformed *Nitrobacter* rDNA measurements on days 3 to 73 were all equal (F = 20; p-value < 0.0001). Tukey HSD multiple comparisons identified 5 mean groups that reflected the significant overall

downward trend in this data (Table 7: Tukey groups A - E). Further, this analysis confirmed that between days 52 and 73, the rDNA measurements were not significantly different (Table 7; Tukey group E). Interestingly, the mean rDNA abundance and MLVSS data were not significantly correlated (Kendall's τ = -0.091; p-value = 0.697). This suggested *Nitrobacter* was a relatively small percentage of the reactor volatile suspended solids, despite the highly selective characteristics of the reactor.

Nitrobacter rRNAt

The *Nitrobacter* rRNAt concentration was highest while excess nitrite was present in the reactor on day 3 ($7.84 \pm 0.5 \times 10^{10}$ copies/L). Further, the transcript abundance was higher a week later on day 10 ($3.48 \pm 0.2 \times 10^{10}$ copies/L), than on any subsequent day when the nitrite concentration was also below 1 mg-N/L. Thereafter, between days 17 and 73, the rRNAt abundance varied between 1.26 and 2.46×10^{10} copies/L ($\approx$ 2-fold range). The only trend Figure 10-B suggested in the rRNAt abundance was a decrease over the first 2 to 4 weeks of the experiment (day 3 - 24). However, when the average rRNAt data from dates when the nitrification efficiency standard was met (day 10 - 73) were analyzed with a Kendall-Theil trend line the slope was not significantly different from 0 (p-value = 0.242). The lack of a significant trend in rRNAt abundance, given the decline in rDNA abundance, suggested that the transcript concentration will be inherently more variable than the gene concentration under steady state conditions. The ribosomal transcript was also more variable than rRNA, rDNA, and/or cell numbers (OD_{600}) in *E. coli* and *Acinetobacter* spp. while steady and non-steady state activity was observed (Licht et al., 1999; Cangelosi and Brabant, 1997; Oerther et al., 2000). Similarly, rRNA was more variable than rDNA and/or cell numbers in several other species of bacteria (Muttray and Mohn, 1998; Muttray et al. 2001; Milner et al., 2001).

ANOVA rejected the null hypothesis that the log transformed *Nitrobacter* rRNAt measurements on days 3 to 73 were all equal (F = 75; p-value < 0.0001). Tukey HSD comparisons identified 6 mean groups (Table 7: A - F), with days 3 and 10 constituting stand alone mean groups (Tukey groups A and B, respectively), while the remaining 9 days constituted four mean groups segregated over time (Tukey groups C - F). Half of

the data fell into a single group (Table 7: Group F) that included the final four measurements (days 52 to 73). The mean rRNAt abundance was not significantly correlated with MLVSS (Kendall's $\tau = 0.273$, p-value = 0.243) nor the mean rDNA data (Kendall's $\tau = 0.382$, p-value = 0.102). Overall, the BSNR *Nitrobacter* rRNAt range of values at steady state N-treatment performance (2-fold) was similar to that observed for *Pseudomonas abietaniphila* rRNA in a CSTR during steady state operation (Muttray et al., 2001: ≈ 4-fold range), but greater than rRNAt when measured as the % hybridization per VSS for *Acinetobacter* in a CSTR (Oerther et al., 2000: range ≈ 10 - 15%/mg/L). However, the latter measurements encompassed only 420 minutes of reactor operation.

Nitrobacter rRNAt/rDNA ratio

The *Nitrobacter* rRNAt/rDNA metric is displayed in Figure 10-B as the ratio of the rDNA and rRNAt overall means with error bars that correspond to the interquantile range of all possible ratios computed with the rDNA and rRNAt assay means (Table 7). In examining the results, the nitrification efficiency was used to qualify a proper range of metric data that could be used to establish prediction intervals reflecting high nitrification efficiency. Hence, the ratio measured on day 3 (3.3) was discarded and the 10 remaining ratio measurements made on days 10 - 73 (0.68 - 1.8), when the nitrification efficiency exceeded ≥ 90%, were combined. Though eliminated because of poor nitrification efficiency, the day 3 ratio was larger than those measured over the following 10 weeks (Figure 10-B). This may seem to contradict the general hypothesis discussed in Section 5.1 that low NOB activity would correspond to a low ratio, since the day with the lowest nitrification efficiency had the highest ratio. However, the nitrite concentration rapidly decreased between day 1 and 5 (386 to 1 mg-N/L), so during this time frame NOB oxidized all the nitrite that was generated from influent ammonia oxidation (no ammonia accumulated), plus the pool of nitrite present in the reactor on day 1. Thus, NOB activity was actually higher between days 1 and 5 than between days 8 and 73, and the rejection of the ratio datum for day 3 eliminated a measurement that corresponded to unusually high nitrite oxidation activity.

On days 10 - 17 and 38 - 73 the ratio varied little (1.2 - 1.8) despite the relatively high rRNAt abundance on day 10 and the significant decline in rDNA concentration during this time period. However, ratios for day 24 (0.68) and 31 (0.77) were notably lower than this range of values (Figure 10-B). To examine this further, an empirical distribution function was constructed for the log transformed ratio data (Figure 11-A). This figure contains equally spaced metric data along a linear cumulative frequency scale that assigned the smallest ratio (0.68) a cumulative frequency of 0, since no other ratio was smaller than this value, and the highest ratio (1.8) a value of 1, since all other ratios were smaller than this value (Iman et al., 1994). In between, the data were ordered from smallest to largest by the cumulative frequency (sample order number/total sample number) and connected by large or small vertical steps to emphasize the data distribution (Iman et al., 1994). The large step between the ratios measured on days 24 and 31 and the remaining data emphasize a gap in the distribution. Further, the day 24 and 31 results produced negative skew in a boxplot of the combined data (Figure 11-B). This indicated the data were not normally distributed, though an assumption of normality could not be rejected for such a small data set (10 observations: Shapiro Wilk W = 0.91; p-value = 0.31). Thus, the ratio varied significantly with a potentially non-normal distribution while the BSNR nitrification efficiency was at steady state.

Since future ratio measurements were predicted to either exceed or fall below a "normal" range of ratio values while steady state, high nitrification efficiency was maintained in the reactor, one sided upper and lower predictions intervals were appropriate for comparative purposes (Helsel and Hirsch, 2002). Further, these intervals were established nonparametrically (Helsel and Hirsch, 2002) to avoid assumptions for the ratio distribution (Muttray et al., 2001). The results indicated that new ratio measurements could be considered significantly lower than expected in the BSNR while high nitrification efficiency persisted for values < 0.69 ($\alpha = 0.10$). Conversely, a new ratio measurement could be considered larger than expected in the BSNR while high nitrification efficiency persisted for values > 1.8 ($\alpha = 0.10$). These prediction intervals were hypothesized to divide the range of possible ratio values into three zones as

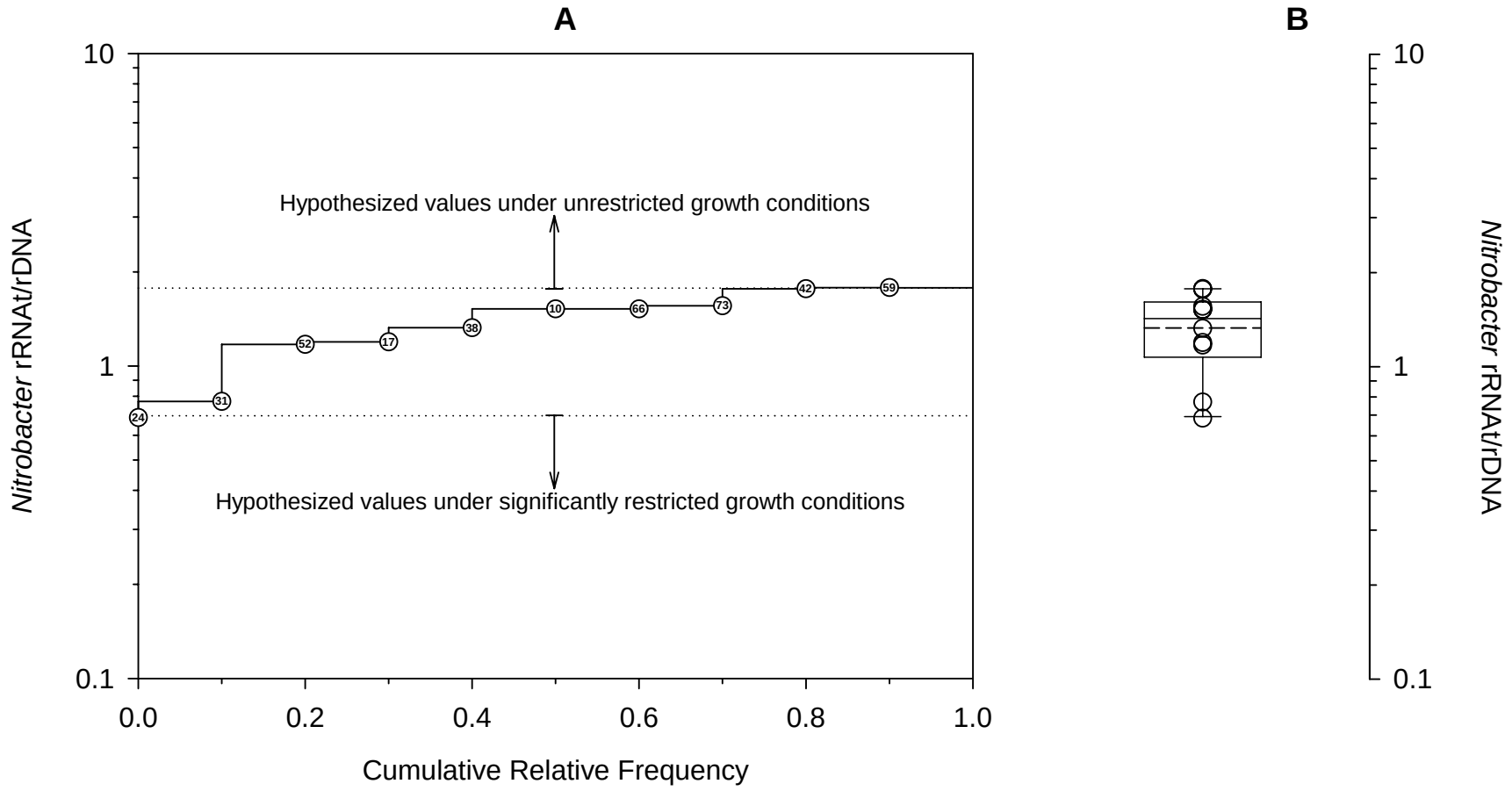


Figure 11 An empirical distribution function (A: operating day indicated) and boxplot (B) of *Nitrobacter* rRNAt/rDNA ratio data collected during 10 weeks of continuous high nitrification efficiency (≥ 90%). Within the empirical distribution function, upper (⋯) and lower (…) nonparametric prediction intervals ($\alpha = 0.10$) are annotated with hypotheses that are discussed in the text.

illustrated in Figure 11-A: (1) values larger than the upper prediction interval and corresponding, for example, to uninhibited nitrite oxidation activity with excess nitrite present, (2) "normal" values under uninhibited but restricted growth in the BSNR that mostly occurred between the lower and upper prediction intervals, and (3) low values below the lower prediction interval and corresponding to conditions where NOB activity was significantly repressed, such as during nitrite starvation or inhibition.

Since other researchers have not utilized a rRNAt/rDNA type ratio (Table 4), the range of values in Figure 11 could not be directly compared with results for other bacteria. In terms of the variation under steady state conditions in a reactor, the results herein (2.6-fold range) were lower than observed for the rRNA/rDNA ratio of a *P. abietaniphila* strain (Muttray et al., 2001: ≈ 500 - 2400; 5-fold range). Also, the results in this study indicated that during low NOB activity, fewer transcripts of the *Nitrobacter* ribosomal gene are quantifiable versus the gene itself. This was consistent with an investigation of *M. tuberculosis* rRNAt abundance when this organism was inhibited with rifampin (Cangelosi et al., 1996).

Other researchers have measured RNA/DNA and rRNA/rDNA type ratios for various species of bacteria in continuous cultures at different growth rates (Table 4). Though unexpected, some measurements of these ratios were less than 1: the rRNA/rDNA ratio in a *P. stutzeri* strain at low growth rates (Kerkhof and Ward, 1993: $\mu < 0.025$ hr^{-1}), the RNA/DNA ratio in two of five resin acid degrading isolates at low growth rates (Muttray and Mohn, 1998: $\mu \approx 0.1 - 0.3$ hr^{-1}), the rRNA/rDNA ratio of a *P. abietaniphila* strain inoculated into an activated sludge and subsequently starved for ≈ 3 days (Muttray et al., 2001), and the rRNA/rDNA ratio in *Listeria monocytogenes* after ≥ 40 hours of substrate starvation (Milner et al., 2001). Generally, rRNA/rDNA and RNA/DNA type ratios have been measured at values higher than 1. The rRNA/rDNA ratio, in particular, would be expected to exceed 1 since even slow growing bacteria possess hundreds or more likely thousands of ribosomes and only one or a few copies of the rDNA gene (Snyder and Champness, 2002). This was true for the rRNAt/rDNA ratio in a *Sphingomonas* isolate in continuous culture at $\mu = 0.04$-0.17 hr^{-1} (Muttray and Mohn,

2000: rRNA/rDNA = 18 - 42) and during a batch substrate oxidation experiment (Muttray and Mohn, 1998: rRNA/rDNA = 9 - 70). The rRNA/rDNA ratio was well above 1 for a *P. abietaniphila* strain in a continuous bioreactor (Muttray et al., 2001: rRNA/rDNA = 200 - 1200 at μ = 0.036 - 0.352 hr^{-1}), and for the total bacterial rRNA/rDNA ratio in a petroleum contaminated soil (Ka et al., 2001: rRNA/rDNA = 19 - 2001). Conversely, Oerther et al. (2000) measured the rRNAt/rRNA ratio and always found it to be less than 1, as expected, for both *E. coli* and *Acinetobacter*. In cited references, Kerkhof and Ward (1993) noted that the RNA/DNA ratios for *E. coli* (RNA/DNA $\approx$ 2 - 10; $\mu \approx$ 0.45 - 1.75 hr^{-1}), *S. typhimurium* (RNA/DNA $\approx$ 3 - 10; $\mu \approx$ 0.2 - 1.7 hr^{-1}), and *Aerobacter aerogenes* (RNA/DNA $\approx$ 3 - 9: $\mu \approx$ 0.2 - 1.25 hr^{-1}) were > 1 and complementary to their results for *P. stutzeri* at much lower growth rates (RNA/DNA $\approx$ 2.0 - 2.7: $\mu \approx$ 0.01 - 0.12 hr^{-1}). Though the RNA/DNA ratio is not useful for wastewater treatment purposes since a mixed culture is involved, the trend for a lower ratio with lower activity reflects the general hypotheses presented in Figure 11-A. Also, a review of these data clearly indicates that the type of ratio used affects the value and interpretation of the metric and that species specificity probably exists for different types of metabolic activity indicators. Thus, prediction intervals may be required to enhance the usefulness of these markers.

Cangelosi and Brabant (1997) observed that the activity information residing in ribosomal transcript abundance is likely most useful if expressed relative to a stable marker, such as the rDNA gene copy number. The results presented in Figure 10-B provide an indication that such a ratio will largely be determined by the transcript abundance, since the *Nitrobacter* rRNAt/rDNA ratio varied in parallel with the rRNAt concentration. Further, a significant correlation was found between the ratio and rRNAt (Kendall's τ = 0.564, p-value = 0.016), but not with rDNA (Kendall's τ = -0.055, p - value = 0.815). Even so, the significant decline in the *Nitrobacter* rDNA confirmed the need to normalize the rRNAt data to increase the metric's sensitivity. Further, this indicated that the gene abundance may be a more useful parameter for understanding

long term performance trends in N-removal reactors. As such, NOB rDNA may complement the short term activity data provided by the rRNAt/rDNA ratio.

5.2.3 Summary

The *Nitrobacter* rRNAt/rDNA ratio was measured in the BSNR over 10 consecutive weeks while high nitrification efficiency was maintained. These data were used to establish upper and lower nonparametric prediction intervals for the ratio that presumably reflected the high efficiency condition and, in general, high nitrite oxidation activity. The lower interval was intended for use as a baseline marker to predict declining nitrification efficiency in the BSNR (tested in Chapter 8.0). Further, both the lower and upper prediction intervals established reference points for NOB activity during batch assays with the BSNR biomass. During nitrite starvation, the *Nitrobacter* rRNAt/rDNA ratio was hypothesized to approach a limit below the lower BSNR prediction interval (Section 5.3). Similarly, when NOB activity was significantly inhibited with a variety of inhibitors, the ratio was hypothesized to drop below the lower BSNR prediction interval (Chapter 6.0 - Chapter 7.0). Conversely, during unlimited nitrite oxidation, the metric was hypothesized to approach a value that exceeded the upper BSNR prediction interval. This was tested during recovery from a staged BSNR inhibition event (Chapter 8.0) and in a batch nitrite oxidation assay (Section 5.3). Thus, the main intent in establishing these prediction limits was to aid the interpretation of the usefulness of the rRNAt/rDNA metric.

5.3 The *Nitrobacter* rRNAt/rDNA Ratio Range and Rate of Change

A batch nitrite oxidation experiment was performed with BSNR mixed liquor samples to estimate the *Nitrobacter* rRNAt/rDNA ratio range at minimum and maximum nitrite oxidation activity. The lower ratio limit was estimated during nitrite starvation, while the upper limit was estimated after a nitrite spike led to unlimited nitrite oxidation (i.e. nitrite was added well in excess of the NOB substrate affinity constant: ≈ 5.5 mg-N/L at 30° C, Rittmann and McCarty, 2001). The main objective for this experiment was to determine whether the range of possible *Nitrobacter* rRNAt/rDNA ratio values

exceeded the upper and lower prediction intervals established in the BSNR during steady state, high nitrification efficiency (Section 5.2). A metric value below the lower BSNR prediction interval would indicate decreased nitrite oxidation activity relative to the reactor meeting the 90% nitrification efficiency standard. Such a decrease in nitrite oxidation activity could occur during substrate starvation, for example during AOB inhibition, or if the NOB were directly inhibited. Further, since the nitrite oxidation activity level in the BSNR was relatively high but limited (excess nitrite was not typically present), it was anticipated that the upper prediction interval would be exceeded during unlimited nitrite oxidation. This would indicate that the ratio could be used to predict rising NOB activity in a denitritification or anammox reactor, though this was not specifically addressed in this study. Any remedial advantage the metric would offer in limiting the effects of NOB activity changes would depend on the time rate of change in the ratio. Hence, a second objective for this experiment was to place bounds on the metric response time.

5.3.1 Hypotheses

Because the NOB growth rate and yield are low (Section 2.2), *Nitrobacter* rDNA was not expected to increase significantly during the short period of unlimited nitrite oxidation in this experiment. Conversely, *Nitrobacter* rRNAt abundance was hypothesized to rise and fall significantly with nitrite oxidation activity and largely determine the *Nitrobacter* rRNAt/rDNA ratio. The following hypotheses were tested concerning the rRNAt concentration and the rRNAt/rDNA ratio:

I. During substrate starvation (minimum nitrite oxidation activity), the *Nitrobacter* rRNAt/rDNA ratio will fall below the lower prediction interval established in the BSNR (Section 5.2):

H_0: rRNAt/rDNA > 0.69

H_1: rRNAt/rDNA < 0.69

II. During maximum nitrite oxidation (with excess nitrite present), the *Nitrobacter* rRNAt/rDNA will exceed the upper prediction interval established in the BSNR (Section 5.2):

H_0: rRNAt/rDNA < 1.8

H_1: rRNAt/rDNA > 1.8

III. Following a transition from minimum to maximum nitrite oxidation activity, the *Nitrobacter* rRNAt concentration, and hence the *Nitrobacter* rRNAt/rDNA ratio, will increase monotonically over time:

H_0: Kendall's $\tau = 0$

H_1: Kendall's $\tau > 0$

IV. Following a transition from maximum to minimum nitrite oxidation activity, the *Nitrobacter* rRNAt concentration, and hence the *Nitrobacter* rRNAt/rDNA ratio, will decrease monotonically over time:

H_0: Kendall's $\tau = 0$

H_1: Kendall's $\tau < 0$

5.3.2 Experiment execution and objectives

The experiment was performed with six vessels that contained 400 ml of BSNR mixed liquor diluted into 500 ml of deionized water (vessels 1 - 6). Samples were collected from one of the vessels (vessel 1) following more than nine hours of nitrite starvation. Immediately thereafter, 70 ml of a 1,000 mg NO_2^--N/L solution was spiked into the vessels (final concentration 70.6 mg-N/L in vessel 1 and 68.6 mg-N/L in vessels 2 - 6) which were then sequentially sampled over the next 16 hours. The specific objectives were to: (1) estimate the *Nitrobacter* rRNAt/rDNA ratio lower and upper limits, (2) assess the time required for the metric to increase from the lower limit above the BSNR lower prediction interval, and (3) assess the time required for the ratio to decline back to the lower limit after nitrite exhaustion.

5.3.3 Results

The timing for twelve sampling events is described in Table 8 relative to the nitrite spike and the estimated start of nitrite oxidation. The first sample was collected immediately before nitrite was added to the vessels and followed more than nine hours of nitrite starvation. The next six samples were collected between 0.8 and 8.6 hours following the nitrite spike, or from 0.5 to 8.0 hours after nitrite oxidation was evident as an increasing oxygen uptake rate. A sample was taken as the nitrite was exhausted. Four more samples followed between 1 and 4 hours after the nitrite was exhausted.

The vessel respirograms are presented in Figure 12 (A - F). Time points nearest to the nitrite spike, the estimated beginning and end of nitrite oxidation, and the sample events are annotated. The respirometric data for all the vessels were averaged to create a composite respirogram which was overlain with nitrite data in Figure 13-A. Molecular data from the experiment is presented on the same time scale in Figure 13-B. The *Nitrobacter* rDNA and rRNAt data are provided in Table D-3 and summarized in Table 9 along with statistical analyses of the results. Table 9 also presents the nitrite and rRNAt/rDNA ratio results.

Table 8 Sample descriptions for the experiment used to assess the range and dynamics of the *Nitrobacter* rRNAt/rDNA ratio.

Sample Number	Vessel	Time, hrs		
		Relative to nitrite spike	Relative to start of substrate utilization	Previous period of nitrite starvation
1	1	-0.03	-	9
2	2	0.75	0.5	-
3	3	1.58	1	-
4	4	2.33	2	-
5	5	3.83	3.5	-
6	6	6.33	6	-
7	1	8.57	8	-
8	2	9.98	-	0
9	3	11.08	-	1
10	4	12.08	-	1
11	5	13.58	-	2
12	6	15.63	-	4

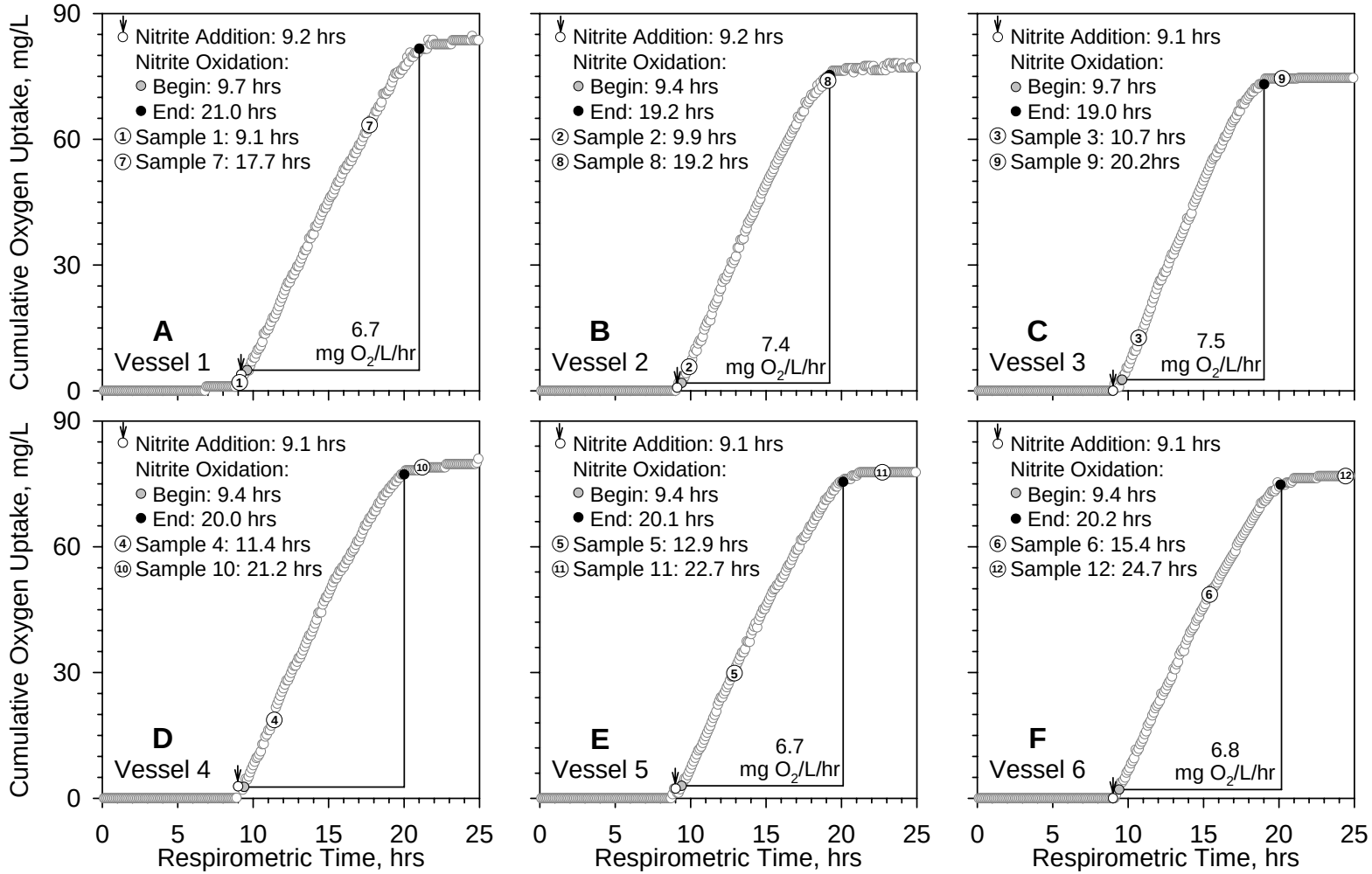


Figure 12 Respirograms for six vessels (A - F) in the experiment used to assess the *Nitrobacter* rRNAt/rDNA ratio range and dynamics for change.

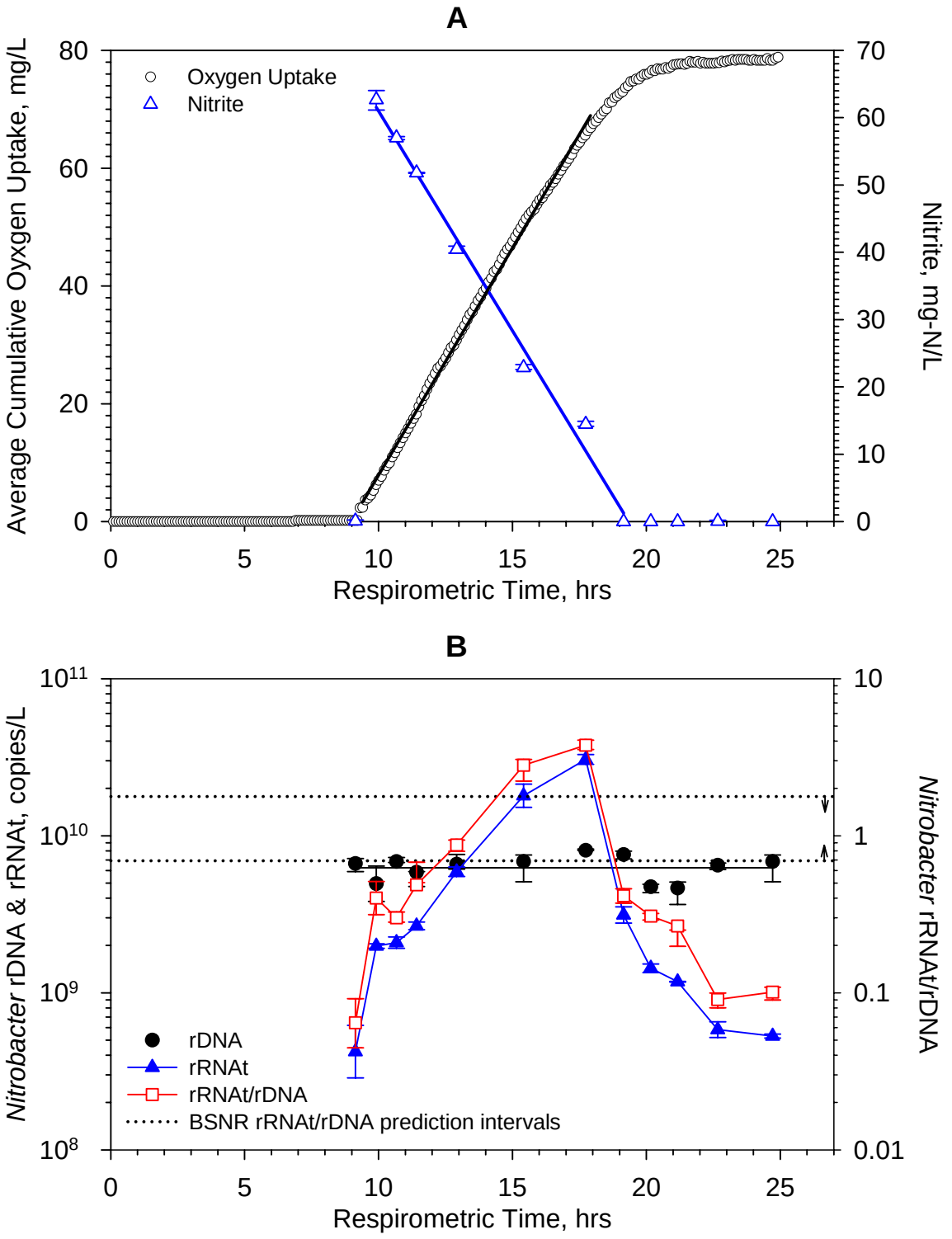


Figure 13 A composite respirogram with overlaying nitrite data (A) and *Nitrobacter* rDNA, rRNAt, and rRNAt/rDNA ratio data (B) for six vessels (Figure 12) in the experiment used to assess the *Nitrobacter* rRNAt/rDNA ratio range and dynamics for change.

Table 9 Nitrite and *Nitrobacter* molecular data for the experiment used to assess the range and dynamics of the *Nitrobacter* rRNAt/rDNA ratio (Figure 13).

Sample Event				Nitrite, mg/L	*Nitrobacter* rDNA (copies/L)[1]			*Nitrobacter* rRNAt (copies/L)[1]			rRNAt[2] / rDNA
Number	Vessel	Time (hrs): relative to nitrite spike	Time (hrs): period of starvation		Assay Mean	Statistical Analysis: Overall Mean	Statistical Analysis: Tukey	Assay Mean	Statistical Analysis: Overall Mean	Statistical Analysis: Tukey	
1	1	-0.03	> 9	0.1	6.65E+09 7.17E+09 5.91E+09	6.58E+09	ABCD	2.89E+08 6.21E+08 -	4.55E+08	F	0.069
2	2	0.75	-	62.7	- 6.41E+09 3.89E+09	5.15E+09	BCD	1.92E+09 2.06E+09 -	1.99E+09	CD	0.386
3	3	1.58	-	57.0	6.87E+09 6.78E+09 7.29E+09	6.98E+09	ABC	2.28E+09 1.93E+09 -	2.10E+09	CD	0.302
4	4	2.33	-	51.8	5.87E+09 5.98E+09 4.85E+09	5.57E+09	ABCD	2.83E+09 2.52E+09 -	2.67E+09	C	0.480
5	5	3.83	-	40.5	7.61E+09 6.15E+09 6.60E+09	6.79E+09	ABC	6.34E+09 5.53E+09 -	5.93E+09	B	0.874
6	6	6.33	-	22.9	7.63E+09 6.85E+09 5.09E+09	6.52E+09	ABCD	1.52E+10 2.13E+10 -	1.82E+10	A	2.797
7	1	8.57	-	14.5	8.30E+09 8.18E+09 8.05E+09	8.17E+09	A	2.86E+10 3.34E+10 -	3.10E+10	A	3.793

Table 9 Continued.

Sample Event				Nitrite, mg/L	*Nitrobacter* rDNA (copies/L)[1]			*Nitrobacter* rRNAt (copies/L)[1]			rRNAt[2] / rDNA
Number	Vessel	Time (hrs) relative to nitrite spike	Time (hrs) period of starvation		Assay Mean	Statistical Analysis Overall Mean	Statistical Analysis Tukey	Assay Mean	Statistical Analysis Overall Mean	Statistical Analysis Tukey	
8	2	9.98	-	0.0	7.13E+09 8.00E+09 7.60E+09	7.58E+09	AB	3.62E+09 2.78E+09 -	3.20E+09	BC	0.422
9	3	11.08	1	0.0	4.45E+09 5.08E+09 4.78E+09	4.77E+09	CD	1.35E+09 1.54E+09 -	1.44E+09	CD	0.303
10	4	12.08	1	0.0	3.69E+09 5.17E+09 4.69E+09	4.52E+09	D	1.19E+09 1.17E+09 -	1.18E+09	DE	0.261
11	5	13.58	2	0.1	6.47E+09 6.72E+09 6.10E+09	6.43E+09	ABCD	6.59E+08 5.23E+08 -	5.91E+08	EF	0.092
12	6	15.63	4	0.0	4.75E+09 6.64E+09 4.62E+09	5.33E+09	BCD	5.17E+08 5.48E+08 -	5.32E+08	F	0.100

1 Assay mean is the mean of triplicate Real Time or Real Time RT-PCR reactions for replicate DNA and RNA extracts (Table D-3). The overall mean is the average of the assay means. Log transformation made the assay mean data more symmetric and constant in variance. The log transformed assay mean data were analyzed with Tukey HSD multiple comparisons if ANOVA rejected the null hypothesis of sample equivalence ($\alpha = 0.05$). Samples not sharing a common letter are significantly different ($\alpha = 0.05$).

2 The rRNAt/rDNA metric was calculated with the overall rDNA and rRNAt means for each sample event.

Respirometric data

The initial oxygen uptake rate (OUR) was low in all the vessels. This continued into short lag times that followed the nitrite spikes (23 ± 7 minutes; range 15 - 32 minutes). Thereafter, the total oxygen consumed prior to the OUR falling back to ≈ 0 mg/L/hr was similar in all the vessels (76.7, 73.5, 70.5, 74.6, 72.5, and 72.3 mg/L, for vessels 1 - 6, respectively). The OUR (total oxygen consumed/time for nitrite oxidation) was linear and similar in all the vessels (7.0 ± 0.3 mg/L/hr; range 6.7 - 7.5 mg/L/hr). Thus, the vessels appeared to possess similar NOB populations. The respirometric data confirmed low aerobic activity prior to the nitrite spike, high aerobic activity following the nitrite addition, and low aerobic activity after the nitrite was exhausted.

Nitrite

The nitrite data overlay a composite respirogram in Figure 13-A. The concentration decreased over time at a near linear rate (6.53 mg NO_2^--N/L/hr, R^2 = 0.992). During nitrite oxidation, the OUR for the composite respirogram (7.71 mg O_2/L/hr) yielded a stoichiometry (1.18 mg O_2/mg NO_2^--N) very near the theoretical value (1.14 mg O_2/mg NO_2^--N). Thus, the nitrite data confirmed that nitrite oxidation was accurately monitored.

Nitrobacter rDNA

A linear regression through the *Nitrobacter* rDNA concentration data indicated that the gene abundance varied relatively little over the course of the experiment (6.20 ± 1.14 × 10^9 copies/L; range 4.52 - 8.17 × 10^9 copies/L). This was confirmed since the slope of a Kendall-Theil robust line through the average rDNA concentration and time data was not significantly different than 0 (p-value = 0.50). However, ANOVA of the log transformed *Nitrobacter* rDNA assay mean results (Table 9) rejected the null hypothesis that the sample event concentrations were all equal (F = 5.5; p-value = 0.0003). Four rDNA data groups were identified with a subsequent Tukey HSD analysis (Table 9). The rDNA concentration measured 8.6 hours after the nitrite spike in vessel 1 (8.17 ± 0.1 × 10^9 copies/L; Tukey group A) was significantly higher than was measured: 45 minutes after the nitrite spike in vessel 2 (5.15 ± 1.0 × 10^9 copies/L; Tukey groups B,C, and D), ≈

1 hour after substrate exhaustion in vessels 3 ($4.77 \pm 0.3 \times 10^9$ copies/L; Tukey groups C and D) and 4 ($4.52 \pm 0.8 \times 10^9$ copies/L; Tukey group D), and 4 hours after nitrite exhaustion in vessel 6 ($5.33 \pm 1.0 \times 10^9$ copies/L; Tukey groups C and D). However, in all cases samples taken from the same vessel at different times were not significantly different. Thus, although variability was present among the samples, the overall results showed no systematic tendency for the gene abundance to increase or decrease during more than 8 hours of unlimited nitrite oxidation. This result, and the small difference between the maximum and minimum average rDNA gene abundance (< 2-fold different), confirmed the *Nitrobacter* doubling time exceeds 8 hours (Watson et al., 1989). This sharply contrasts with the 1 to 2 order of magnitude rDNA increases observed in batch culture of heterotrophic bacteria over a similar time frame (Milner et al., 2001; Muttray et al., 2001). It also indicates that the sensitivity of quantitative PCR is such that growth will be difficult to detect for slow growing bacteria (Dionisi et al., 2003).

Nitrobacter rRNAt

The *Nitrobacter* rRNAt concentration varied over approximately 2 orders of magnitude and was independent of the rDNA concentration (Kendall's $\tau = 0.357$; p-value = 0.112). Before the nitrite spike, the transcript abundance was low at $4.55 \pm 2.0 \times 10^8$ copies/L. Following the nitrite spike, the transcript abundance increased over time so that after 8.6 hours the concentration had increased to $3.10 \pm 0.2 \times 10^{10}$ copies/L. After the nitrite was exhausted, the transcript abundance progressively decreased back down to $5.32 \pm 0.2 \times 10^8$ copies/L. The results were similar to those obtained in a preliminary experiment (data not shown), where after 15 hours nitrite starvation the *Nitrobacter* rRNAt abundance in a BSNR mixed liquor sample was low ($4.21 \pm 0.8 \times 10^8$ copies/L), but increased substantially after 7.7 hours of unlimited nitrite oxidation ($1.35 \pm 0.2 \times 10^{10}$ copies/L), and then decreased within 5 hours of nitrite exhaustion back to the original concentration ($5.88 \pm 1.0 \times 10^8$ copies/L). This is the first evidence that large differences in rRNAt exist in the slow growing NOB, though this was the case for two other slow growing bacteria (Cangelosi et al, 1996; Schimdt et, 2001). The results were similar to the large increase in *amoA* mRNA (≈ 15-fold in 6 hours) on exposure to excess ammonia

following a 72 hour starvation period (Aoi et al., 2004b). The magnitude of the change in this study (≈ 70-fold), though very large, was much less than that observed for *E. coli* rRNAt after a forced transition to stationary phase (≈ 1,000-fold decline) (Cangelosi and Brabant, 1997).

ANOVA of the log transformed rRNAt assay mean data (Table 9) rejected the null hypothesis that the sample events were equal ($F = 91$; p-value < 0.0001). Subsequent Tukey HSD multiple comparisons identified six significantly different mean groups in the 12 samples (Table 9: Groups A - F). The groupings confirm the transcript abundance significantly increased after the nitrite spike, and decreased following nitrite exhaustion. Further, this analysis indicated that *Nitrobacter* rRNAt abundance was similar before the nitrite spike ($4.55 \pm 2.0 \times 10^8$ copies/L) and after the nitrite was exhausted for 2 (5.91 ± 0.7 copies/L) and 4 hours ($5.32 \pm 0.2 \times 10^8$ copies/L). Also, the mean abundance measured 6.3 ($1.82 \pm 0.3 \times 10^{10}$ copies/L) and 8.6 ($3.10 \pm 0.2 \times 10^{10}$ copies/L) hours after the nitrite spike (vessels 6 and 1, respectively), were similar. This indicated that the transcript abundance was approaching an upper limit approximately 8 hours after starvation ended, which was similar to the time required for the relative *amoA* mRNA levels to increase to an upper limit (≈ 6 hours: Aoi et al., 2004b).

The *Nitrobacter* rRNAt concentration and respirometric time data were paired and divided into two phases to evaluate trends following the increase and decrease in nitrite oxidation activity. Phase 1 involved the transition from minimum activity, following more than 9 hours of nitrite starvation, through 8.0 hours of unlimited nitrite oxidation (samples 1 - 7). As hypothesized, the *Nitrobacter* rRNAt concentration increased monotonically during this time (Kendall's $\tau = 1$; p-value = 0.0002) with an accumulation rate of 2.78×10^9 *Nitrobacter* rRNAt copies/L/hr (the slope of a Kendall-Theil robust line). Phase 2 involved the transition from high nitrite oxidation activity, 8.6 hours after the nitrite spike, to low activity, 4 hours after the nitrite was exhausted. As hypothesized, the *Nitrobacter* rRNAt abundance decreased monotonically during this time (Kendall's $\tau = -1$; p-value = 0.0014). Further, the rate of decline upon nitrite exhaustion must have been very large initially, since at the moment of substrate depletion the rRNAt

concentration ($3.20 \pm 0.4 \times 10^9$ copies/L) was an order of magnitude less than previously measured while 15 mg NO_2^--N/L remained ($3.10 \pm 0.2 \times 10^{10}$ copies/L).

Nitrobacter rRNAt/rDNA

The *Nitrobacter* rRNAt/rDNA metric was highly correlated with the transcript abundance (Kendall's $\tau = 0.879$; p-value < 0.001), but not with the gene abundance (Kendall's $\tau = 0.295$; p-value < 0.189). This was clearly revealed in the parallel point to point fits of the rRNAt abundance and rRNAt/rDNA ratio data in Figure 13-B. Thus, the same trends observed for the *Nitrobacter* rRNAt concentration were also observed for the ratio: the metric increased monotonically after the transition from starved to unlimited nitrite oxidation (from 0.069 - 3.8; Kendall's t = 0.905; p-value = 0.014), and decreased monotonically during the transition from unlimited nitrite oxidation back to the starved state (from 3.8 - 0.10; Kendall's t = -0.867; p-value 0.0083). However, the ratio offered an advantage in that the results in this experiment could be compared directly with the steady state observations in the BSNR. The ratio value was smaller than the lower BSNR prediction interval (0.69) both before the nitrite spike (0.069) and after the added nitrite was exhausted (range from 0.42 - 0.092). Thus, as hypothesized, the metric was clearly lower during nitrite starvation than in the BSNR while high nitrification efficiency was maintained. Similarly, the ratio value was above the upper BSNR prediction interval (1.8) when samples were collected 6.3 and 8.6 hours after the nitrite spike (2.8 and 3.8, respectively). This was also hypothesized to occur because activity was limited in the BSNR, but unlimited in the batch experiment. The lowest (0.069) and highest (3.8) ratios were ≈ 55-fold different, and it appeared reasonable to assume these values approximated the upper and lower limits for the *Nitrobacter* rRNAt/rDNA metric.

The expression of the rRNAt relative to rDNA also allowed the relative changes in *Nitrobacter* rRNAt in this experiment to be compared with ribosomal transcript changes in other bacteria. For instance, Oerther et al., (2000) found that the *E. coli* rRNAt/OD_{600} and rRNA/OD_{600} ratios reached maximum values corresponding to 12-fold and 4-fold increases, respectively, after only 45 minutes in fresh LB medium. In a similar experiment, these researchers found that the rRNAt/OD_{600} ratio for *A.*

calcoaceticus peaked at a 5-fold increase after only 15 minutes in fresh LB media, while the rRNA/OD_{600} peaked at 3 hours. The *A. calcoaceticus* rRNAt levels (rRNAt/MLVSS) also peaked quickly after the fill cycle in a bench scale sequencing batch reactor treating filtered wastewater. Similar results were obtained for another *Acinetobacter* strain (Oerther et al., 2002). Cangelosi and Brabant (1997) measured a much larger increase in *E. coli* rRNAt/OD_{600} (50-fold) in less than 15 minutes in fresh media, while Licht et al. (1999) confirmed the *E. coli* transcript abundance peaked 1 hour after a transition to fresh media. In regards to the decline in the transcript abundance following a transition to a substrate starved state, this appeared to begin well before growth significantly slowed in *E coli* (Cangelosi and Brabant, 1997). Muttray and Mohn (2000) similarly found that the RNA/DNA ratio peaked early in exponential growth and declined rapidly during stationary phase for a *Sphingomonas* isolate, though the range of the metric (1 - 7) was clearly lower than measured in this study. However, the rate of decline following substrate starvation in this study (≈ 2 to 4 hours) was similar to the time required for the relative rRNAt hybridization signal to fall below detectable limits in a slow growing anammox bacterium inhibited with oxygen (Schmid et al., 2001). Thus, a salient conclusion that can be drawn from these comparisons is that the rRNAt concentration increases and decreases more slowly in *Nitrobacter* than in fast growing heterotrophic bacteria, but the magnitude of these changes are similar when normalized to estimates of the cell number. The fast increase in heterotrophic bacteria may be a function of the *rrn* copy number, which is higher in the bacteria referenced, perhaps to increase growth acceleration following a transition to favorable environments (Klappenbach et al., 2001).

The ATP content of *N. winogradskyi* was measured in a batch nitrite oxidation experiment by Eigener (1975). The ATP concentration increased slowly at first, but after the lag phase was complete, ATP increased exponentially despite the fact that both growth and substrate oxidation increased linearly. In this sense, the ATP concentration was similar to the rRNAt concentration measured herein. It is interesting to note that the ATP content in Eigener's study, like rRNAt/rDNA in this study, decreased quickly after

substrate exhaustion. As indicated in the literature review, the energy charge of the cell may be a regulatory factor in the rDNA transcript rate (Gaal et al., 1997).

Though the *Nitrobacte*r rRNAt/rDNA metric value clearly lagged nitrite oxidation activity changes, an emphasis on the time required for the metric to transition between the ratio's upper and lower limits should be tempered in the context of the expected values in the BSNR. The metric declined below the reactor's lower prediction interval less than one hour after the nitrite was exhausted, and increased above the lower prediction interval from a starved state in less than 4 hours. This indicated that the metric can be used to observe in-situ activity changes in *Nitrobacter* over a relatively short period of time, which would increase the usefulness of this parameter for remedial responses.

The range of the *Nitrobacter* rRNAt/rDNA metric (≈ 0.07 - 4.0) exceeds the range of values previously reported for the RNA/DNA metric for *P. stutzeri*, *Aerobacter aerogenes*, *S. typhimurium*, and *E. coli* (Kerkhof and Ward, 1993: ≈ 2 - 10), as well as several resin acid degrading bacteria (Muttray and Mohn, 1998: 0.5 - 3). Also, the range for *Nitrobacter* rRNAt/rDNA ratio was greater than the range reported for the rRNA/rDNA ratio for *P. stutzeri* (Kerkhof and Ward, 1993: 0.5 - 1.5) and resin acid degrading bacteria (Muttray and Mohn, 1998: 9 - 70). Though both the rRNA/rDNA and rRNAt/rDNA ratios offer the benefit of species specificity over the RNA/DNA ratio, the rRNAt/rDNA metric may be more sensitive because the range of possible values seems broader.

5.4 Summary

The difference between high nitrification performance conditions in the BSNR and both unlimited nitrite oxidation activity and substrate starvation were manifest in variations in the *Nitrobacter* rRNAt/rDNA ratio. In 10 independent observations of the ratio at high nitrification efficiency, the ratio varied between 0.68 and 1.8. During starvation, the ratio was much lower (0.069 - 0.10) than the lower prediction interval (0.69), and during unlimited nitrite oxidation the ratio attained higher values (> 3) than

the upper prediction interval (1.8). This suggests that the biometric has the capacity to detect declines in the reactor NOB activity that may precede poor nitrification efficiency. Furthermore, the results indicated that the ratio value should respond significantly and quickly to AOB inhibition, since this would create nitrite starvation. In this respect, is interesting to note that the decline in *Nitrobacter* rRNAt abundance in this study occurred much more quickly than that for *amoA* mrRNA in another nitrifier enrichment culture (Aoi et al., 2004b). This indicates that the NOB rRNAt/rDNA metric may be more sensitive to declining AOB activity (via nitrite starvation) than *amoA* mRNA.

CHAPTER 6.0

BATCH RESPIROMETRIC INHIBITION EXPERIMENTS

6.1 Introduction

A challenge to the rRNAt/rDNA metric's potential usefulness in improving nitrification and denitritification performance in wastewater treatment could be that many different inhibiting substances and/or environmental factors affect NOB activity (Section 2.3). Thus, an important aspect of proposing this metric to improve wastewater treatment performance was evaluating the parameter response to mechanistically distinct inhibitors. Does the metric response vary during different types of inhibition? Can the response at high inhibition levels be interpreted unequivocally? It was conceivable the metric would respond significantly to some types of inhibition, or perhaps be unresponsive to others because rRNAt processing was disrupted (Cangelosi et al., 1997; Licht et al., 1999; Stroot and Oerther et al., 2003).

These questions were addressed with batch respirometric inhibition experiments that mainly assessed whether, during inhibition, the *Nitrobacter* rRNAt/rDNA ratio consistently, significantly, and quickly declined below the lower BSNR prediction interval (Section 5.2). The ratio was expected to fall quickly below this limit after shock inhibition (caused by a variety of added inhibitors) because bacterial rDNA transcription is highly regulated (Gourse et al., 1996) and linked to broad growth outlook indicators such as the energy charge (Gaal et al., 1997). Although rDNA transcription regulation has not been studied for NOB, in general, and *Nitrobacter* specifically, it was reasoned that *Nitrobacter* rDNA transcription activity would decline in response to most inhibiting mechanisms due to diminished substrate utilization and growth potential. Ultimately, the demand for protein, and hence rRNA for ribosomes to make protein, would decline in the presence of an inhibitor and reflect a low rRNAt/rDNA ratio. Since NOB grow slowly, it seemed appropriate to base the inhibition assay on nitrite oxidation impacts rather than growth.

6.1.1 Experimental approach

An outline of the experimental approach used to evaluate these questions is provided in Figure 14. Inhibition was investigated using the BSNR biomass in batch experiments that measured a reduction in the nitrite oxidation rate, surrogately measured as a reduction in the oxygen uptake rate, following doses of four mechanistically distinct inhibitors: (1) 3,5-dichorophenol (DCP), which is generally viewed as an uncoupler (Escher and Schwarzenbach, 2002), (2) azide (N_3^-), which may inhibit nitrite oxidoreductase by chelating molybdenum (Ginestet et al., 1998) or alternately inhibit cytochrome oxidases involved in nitrite oxidation (López-Fiuza et al., 2002), (3) acid (H^+), which causes a drop in cytoplasmic pH that non-specifically inhibits enzyme activity, structurally damages cell membranes and macromolecules including DNA and protein, and/or interrupts cell transport processes (Maloney and Wilson, 1996; Dilworth and Glenn, 1999; Cotter and Hill, 2003), and (4) ammonia, which is widely reported to inhibit NOB in its free ammonia form (Table 2). The free ammonia investigation was anomalous (Figure 14) and is presented separately in Chapter 7.0.

The approach was to first generate dose-response curves for each inhibitor using preliminary experiments that did not evaluate the *Nitrobacter* rRNAt/rDNA ratio, but did verify that nitrite oxidation could be significantly inhibited (fraction inhibition > 0.74: quantified in Section 6.5). The dose-response curve was then used as a guide for two additional inhibition experiments that included DNA and RNA extractions. The intent was to evaluate the *Nitrobacter* rRNAt/rDNA ratio across a broad range of inhibition for the different inhibitors. The second inhibition experiment was complementary to the first experiment, which allowed the inhibitor/*Nitrobacter* rRNAt/rDNA ratio relationship to be more firmly established, or alternately was used to confirm any unusual results in the first experiment. Also, performing two experiments provided enough data to evaluate a hypothesized correlation between the metric and the inhibitor concentration and fraction inhibition level (Section 6.1.3). Whether the inhibitors elicited different metric responses at the same inhibition level was considered after combining the results across all inhibitors in one plot.

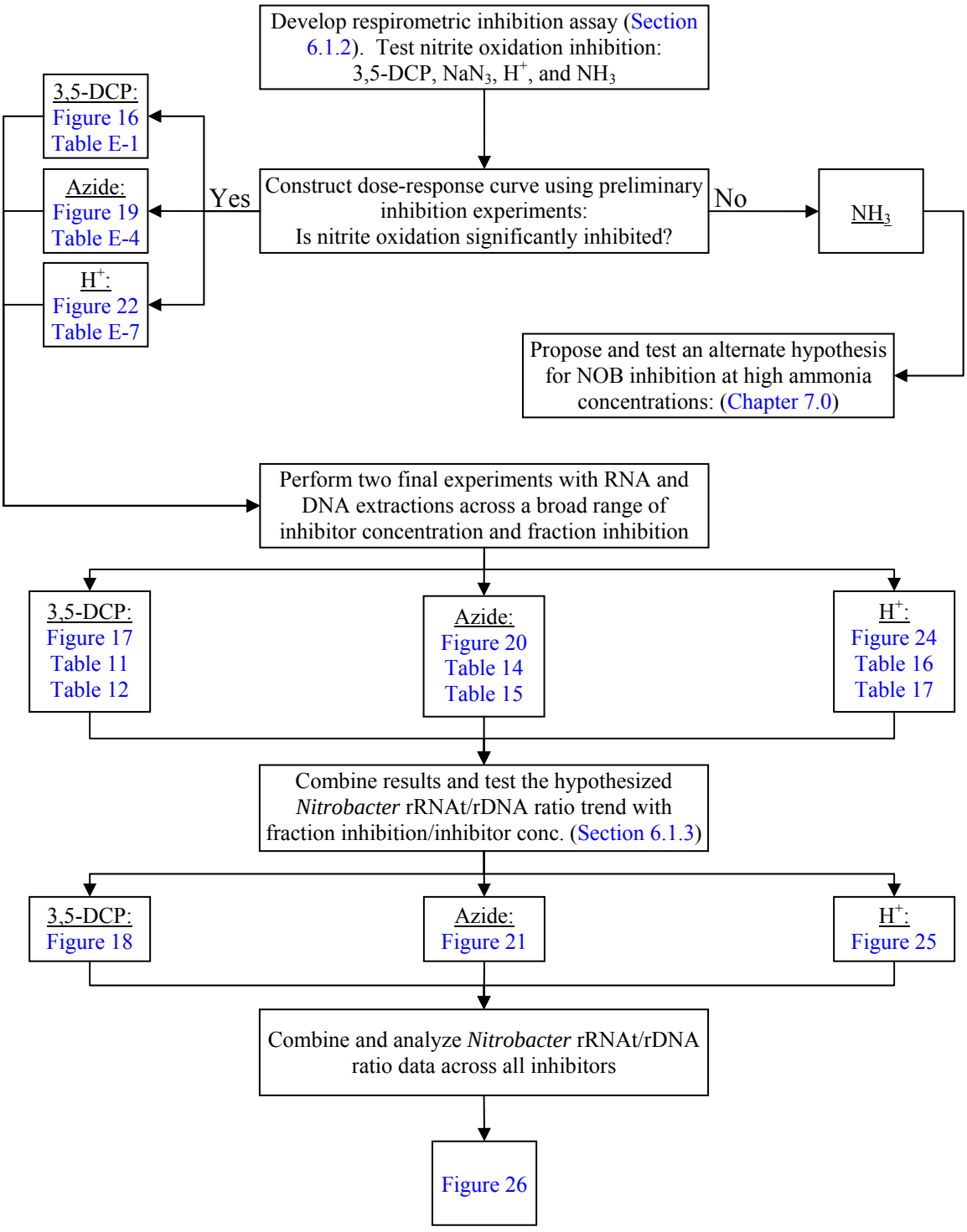


Figure 14 Outline of the experimental approach used to evaluate the *Nitrobacter* rRNAt/rDNA ratio response to mechanistically distinct inhibitors.

6.1.2 Overview of the inhibition assay

Establishing baseline conditions before and during the inhibition experiments

Four baseline conditions for the inhibition experiments were considered: (1) using fully adapted biomass, (2) beginning the experiments with initially uninhibited biomass, (3) accounting for or removing potentially confounding AOB and heterotrophic aerobic activity, and (4) establishing an upper baseline value for the *Nitrobacter* rRNAt/rDNA ratio prior to adding the inhibitor. The first two conditions were met by conducting the inhibition experiments after the BSNR was operated for more than one year and then only when high nitrification efficiency (≥ 95% removal of NH_4^+-N as NO_3^--N) existed. This level of efficiency was routinely observed.

The inhibition assay was designed to isolate an inhibitor's impact on NOB activity. Thus, a key aspect of establishing baseline conditions was removing or accounting for potentially confounding AOB and heterotrophic aerobic activity. For the nitrifier enriched BSNR biomass, this largely involved removing residual ammonia since exogenous heterotrophic substrates were absent. When the inhibition assay was first developed, AOB activity was minimized by diluting BSNR mixed liquor samples in deionized water (typically 50%) and then observing aerobic activity in the respirometer. Low background oxygen demand (< 0.5 mg/L/hr) was used to verify the absence of significant AOB/heterotrophic activity prior to beginning the assay. However, in using this procedure it was noted that the background oxygen utilization was insignificant soon after collecting the mixed liquor samples. This was presumably because: (1) there was little residual ammonia and nitrite in the reactor, and what was present was oxidized quickly in the respirometer, and (2) the BNSR biomass was nitrifier enriched, so the heterotrophic endogenous respiration rate was low. Though Hollocher et al. (1982) reported significant endogenous respiration for *N. agilis* and *N. europaea* (poly-β-hydroxybutyric acid oxidation), this did not occur with the BSNR biomass. After this observation was made, an alternative method was used to remove the potentially confounding AOB oxygen demand which simply involved shutting off the BSNR influent pump briefly (≤ 30 minutes). The end of AOB aerobic activity, and thus removal

of residual ammonia (< 5 mg-N/L), was indicated as a slight increase in the reactor pH (7.2 → 7.3). BSNR mixed liquor samples were immediately collected and diluted into nitrite solutions (final concentration 100 mg-N/L) to start the inhibition assay. This technique was used for most of the preliminary inhibition experiments and was always used for the final experiments that included DNA and RNA extractions. This procedure also promoted the upper baseline condition for the *Nitrobacter* rRNAt/rDNA ratio by avoiding significant periods of nitrite starvation.

A final aspect of establishing baseline conditions concerned the *Nitrobacter* rRNAt/rDNA ratio. It was reasoned that the inhibitor should be added only after the metric reached some baseline value. The baseline value could have been the metric's upper or lower limit (Chapter 5.0). Since the ratio was expected to drop in response to the presence of inhibitors, the upper limit was chosen as the baseline value. The upper limit was established by: (1) not exposing the mixed liquor samples to nitrite starvation for more than 15 minutes, and (2) by adding the inhibitor following several hours of nitrite oxidation at nitrite concentrations well in excess of the half saturation constant (≈ 1 - 11 mg NO_2^--N/L; Sharma and Ahlert, 1977, Hollocher et al., 1982). This baseline condition was verified by collecting RNA and DNA samples from a control vessel that did not receive inhibitor both before and after the inhibitor was added to the remaining vessels. These samples always had similar rRNAt/rDNA ratio results that exceeded the upper BSNR prediction interval (Section 5.2).

How inhibition was measured in the assay

The inhibition assay began after BSNR mixed liquor samples were exposed to nitrite and proceeded in two phases. In the first phase, nitrite oxidation proceeded without the inhibitor present and lasted approximately 4.5 hours, and was quantified with a linear regression fit of the final 4 hours of cumulative oxygen uptake and time data (Oxygen Uptake Rate 1 - OUR1). Eliminating the first 30 minutes of data assured that the respirometric vessel was fully equalized, that residual ammonia was completely removed, and that lags in NOB activity were complete. This phase ended when the inhibitor was added. After the vessel was resealed, the second phase began in which

potentially inhibited nitrite oxidation was quantified with a linear regression fit of an addition 4.5 hours of cumulative oxygen uptake and time data (OUR2). Typically, the first 30 minutes of this data was also excluded to assure that the respirometric vessel was fully equalized after it was resealed. The fraction inhibition was calculated as:

$$\text{Fraction Inhibition} = \frac{\text{OUR1} - \text{OUR2}}{\text{OUR1}} \tag{13}$$

where OUR1 = oxygen uptake rate during Phase 1
OUR2 = oxygen uptake rate during Phase 2

Each inhibition experiment included 4 to 6 identically prepared respirometric vessels which received different inhibitor doses. For quality control purposes, nitrite samples were often collected from each vessel at the start of the experiment, immediately before the inhibitor was added, and 4.5 hours later. For the final experiments with extractions, DNA and RNA samples were collected from one vessel immediately before the inhibitor was added, and from all of the vessels 4.5 hours later. Typically three, but a minimum of two replicate RNA and DNA samples were collected. An uninhibited control vessel was always used in the experiments that included DNA and RNA extractions, and frequently during the preliminary experiments.

6.1.3 Hypotheses

The experimental approach (Figure 14) and the assay (Section 6.1.2) were designed to assess the impact that inhibition had on *Nitrobacter* rRNAt abundance and hence the *Nitrobacter* rRNAt/rDNA ratio. The expected changes in these parameters can be summarized conceptually as follows: as the fraction inhibition/inhibitor dose increased, the *Nitrobacter* growth prospect would decrease the demand for protein and hence ribosomes, thereby lowering the requirement for rRNA and hence the rRNAt abundance. The expected changes were expressed as hypotheses, two of which (I and II) were evaluated for each inhibition experiment with extractions:

I. *Nitrobacter* rRNAt abundance will be higher in an uninhibited control vessel than in inhibited vessels:

H_0: Control vessel rRNAt abundance = inhibited vessel rRNAt abundance

H_1: Control vessel rRNAt abundance > inhibited vessel rRNAt abundance

II. In inhibited vessels, the *Nitrobacter* rRNAt/rDNA ratio will fall below the lower BSNR prediction interval (Section 5.2):

H_0: rRNAt/rDNA > 0.69

H_1: rRNAt/rDNA < 0.69

A final hypothesis (III) was expressed as an expected correlation between the *Nitrobacter* rRNAt/rDNA ratio and the fraction inhibition/inhibitor concentration and was evaluated using the combined data from two inhibition experiments (per inhibitor):

III. The *Nitrobacter* rRNAt/rDNA ratio will decrease monotonically with fraction inhibition and the inhibitor concentration:

H_0: Kendall's $\tau = 0$

H_1: Kendall's $\tau < 0$

Hypotheses were not made concerning *Nitrobacter* rDNA because gene abundance was not expected to vary significantly across vessels and over time during the inhibition assays. This conclusion was based on several factors. First, the vessels were assumed to be identical at the beginning of the experiments because they were prepared similarly at the same time and dilution rate. Second, the time between the inhibitor dose and sample collection (≈ 4.5 hours), along with the doubling time of *Nitrobacter* (minimum ≈ 8 hrs doubling time: Watson et al., 1989), indicated little growth potential existed during the assay, even in the uninhibited control vessel. Finally, the statistical power of the real-time PCR assay for *Nitrobacter* rDNA (Section 4.8) was poor for detecting < 2-fold differences given 2 or 3 replicate sample extracts. Similar assumptions have been made in past batch assays with nitrifiers, though these assays did not measure rDNA levels (e.g. Suthersan and Ganczarczyk, 1986; Bernet et al., 2001).

6.2 3,5-DCP

6.2.1 The inhibition mechanism

3,5-DCP is a hydrophobic ionogenic organic compound that partitions into biological membranes. Escher and Schwarzenbach (2002) classified this chemical as an uncoupler after observing high experimental effect concentrations using the Kinspec test system (accelerated membrane potential loss in isolated chromatophores of *Rhodobacter spaeroides*). The uncoupling mechanism likely involves a protonophoric shuttle system whereby phenoxide and phenol forms of 3,5-DCP repeatedly transport protons from the periplasm to the cytoplasm. This short-circuits oxidative phosphorylation by dissipating the ΔpH component of the proton motive force (Δp) (Stryer, 1995; Escher et al., 1996). Other factors contributing to inhibition may include low cytoplasmic pH (Kumar and Nicholas, 1983), hydrophobic effects that disrupt membrane/protein function (Walter et al., 1978), and protein precipitation (Williamson and Johnson, 1981).

The energy conservation mechanisms used by *Nitrobacter* are largely unknown (Bock and Wagner, 2001). Therefore, the mechanistic effect uncouplers have on nitrite oxidation and *Nitrobacter* growth activity are uncertain. However, a phenolic compound (2,4-dinitrophenol: 2,4-DNP) and three other classical mitochondrial uncouplers (carbonyl cyanide phenylhydrazone/chlorophenylhydrazone: CCP/CCCP; and carbonyl cyanide trifluoromethoxy-phenylhydrazone: FCCP) were used in tests of *Nitrobacter* cell free extracts, membrane vesicles, and artificial electron transport assemblages to discern energy conservation mechanisms (Table 10). This data indicates *Nitrobacter* is capable of respiratory control since low uncoupler doses generally stimulated NADH and oxygen consumption. Since *Nitrobacter* appears to be mainly autotrophic, a process that requires NADH based on basic thermodynamic considerations (Bock and Wagner, 2001), uncouplers likely lower the NOB growth efficiency. However, Table 10 indicates uncouplers inhibit nitrite oxidation before true uncoupling occurs, since nitrite oxidoreductase activity is affected at lower uncoupler concentrations. This effect may originate with branching in the *Nitrobacter* respiratory chain (Bock and Wagner, 2001).

Table 10 The effect of the classical respiratory chain uncouplers 2,4-DNP, (C)CCP, and FCCP on *Nitrobacter*.

Uncoupler	Concentration	Gross activity or oxidant/reductant system	% Effect on Activity		Preparation	Reference
			Decrease	Increase		
2,4-DNP	50 µM	ADP phosphorylation	0[1]	-	*Nitrobacter* cell free extract	Aleem and Nason, 1960
		Nitrite uptake	27	-	Washed *N. agilis* cells	Kumar and Nicholas, 1981
		Nitrate production	30	-		
		Oxygen uptake	20	-		
	100 µM	Nitrite uptake	63	-	Washed *N. agilis* cells	Kumar and Nicholas, 1981
		Nitrate production	66	-		
		Oxygen uptake	35	-		
		NO_2^-/O_2	40	-	*Nitrobacter* crude cell free extract	Aleem, 1977; Aleem and Sewell, 1984
		$NO_2^-/K_3Fe(CN)_6$	21	-		
		NO_2^-/NAD^+	100	-		
		$NADH/O_2$	8	-		
		$NADH/K_3Fe(CN)_6$	22	-		
		NADH/cyc c (horse)	0	-		
		$NADH/NO_3^-$(anaerobic)	-	9		
		Nitrite oxidase	41	-	*Nitrobacter* Membrane particles	O'Kelly et al., 1970
		Nitrite-cyc c reductase	12	-		
		NO_2^-/O_2	0	-	*N. winogradskyi* cells	Sundermyer and Bock, 1981; Freitag and Bock, 1990
		NO_2^-/NAD^+	100	-		
	400 µM	$NADH/NO_3^-$(anaerobic)	49	-	*Nitrobacter* crude cell free extract (inhibition measured as decrease in ATP formation)	Kiesow, 1964
	1.2 mM	$NADH/NO_3^-$(anaerobic)	83	-		
		$NADH/O_2$	84	-		
	1.6 mM	$NADH/O_2$	96	-		
		NO_2^-/O_2	90	-		

Table 10 Continued.

Uncoupler	Concentration	Gross activity or oxidant/reductant system	% Effect on Activity		Preparation	Reference
			Decrease	Increase		
CCCP	5 μM	Nitrite uptake	58	-	Washed *N. agilis* cells	Kumar and Nicholas, 1981
		Nitrate production	56	-		
		Oxygen uptake	70	-		
	10 μM	Whole cell respiration	70	-	Washed *N. agilis* cells	Kumar and Nicholas, 1983
		ΔΨ (membrane potential)	29	-		
		ΔpH (across membrane)	41	-		
		Δp (proton motive force)	32	-		
	50 μM	Whole cell respiration	100	-		
		ΔΨ (membrane potential)	35	-		
		ΔpH (across membrane)	65	-		
		Δp (proton motive force)	41	-		
	100 μM	NO_2^-/O_2	60		*Nitrobacter* crude cell free extract	Aleem, 1977; Aleem and Sewell, 1984
		$NO_2^-/K_3Fe(CN)_6$	46			
		NO_2^-/NAD^+	75			
		$NADH/O_2$	-	21		
		$NADH/K_3Fe(CN)_6$	11			
		NADH/cyc c (horse)	0			
		$NADH/NO_3^-$(anaerobic)		78		
CCP	200 μM	$NADH/O_2$	-	≈ 100	*N. winogradskyi* membrane vesicles	Cobley, 1976a; Cobley, 1976b
		NO_2^- ox.	≈ 66	-		
FCCP	0.27 μM	$K_3Fe(CN)_6$ proton pump	present	-	*N. winogradskyi* cells	Wetzstein and Ferguson, 1985
	0.4-2.6 μM	ΔpH (across membrane)	-	≈ 250-600	*N. agilis* cyc aa_3 vesicles; *N. agilis* proteoliposomes	Sone et al., 1983; Sone, 1986
		Oxygen uptake	present	-		

1 The uncouplers 2,4-DNP, thyroxine, and dicumarol in concentration as high as 50 μM failed to inhibit ATP formation, while higher concentration inhibited nitrite oxidation.

The mechanistic effect that uncouplers have directly on nitrite oxidation and the resulting energy conservation would depend on: (1) whether nitrite oxidation requires an initial energy input (Aleem, 1977; Aleem and Sewell, 1984) and (2) whether *Nitrobacter* extrudes protons for energy conservation via oxidative phosphorylation (Ferguson, 1982). The idea that nitrite oxidation requires energy input originated in inspection of the redox potential for the NO_2^-/NO_3^- couple (+430 mV) and the reduced/oxidized cytochrome c of *Nitrobacter* (+274 mV), and in the fact that uncouplers seem to inhibit nitrite oxidation directly (Aleem, 1968; Aleem, 1977). However, O'Kelly et al. (1970) demonstrated that nitrite oxidation in membrane vesicles of *N. agilis* was energy independent. This was later confirmed when nitrite oxidoreductase (Tanaka et al., 1983) and a membrane bound cytochrome c were isolated (Tanaka et al., 1993). Apparently, nitrite oxidation occurs in spite of seemingly unfavorable thermodynamics because the *Nitrobacter* cytochrome oxidase is particularly efficient at oxidizing cytochrome c (Tanaka et al., 1983; Bock and Wagner, 2001). In regards to proton pumping, this has been proposed to occur via nitrite oxidoreductase or the terminal cytochrome oxidase (Cobley, 1976b; Ferguson, 1982). Cobley (1976b) observed very low levels of alkalinization by *Nitrobacter* membrane vesicles during nitrite oxidation that was reversed by relatively high concentrations of the uncoupler CCP. However, Hollocher et al. (1982) could not demonstrate proton pumping with whole cells, spheroplasts, or everted vesicles of *N. agilis*. Further, Sone et al. (1983) could not demonstrate proton pumping after incorporating the *N. agilis* cytochrome oxidase into phospholipid vesicles; likewise, proteoliposomes prepared with *N. agilis* membranes did not pump protons (Sone, 1986). These findings suggested that neither the terminal cytochrome nor nitrite oxidoreductase extruded protons. However, Wetzstein and Ferguson (1985) were able to generate proton pumping at high H^+:O ratios using isoascorbate and ferro cyanide in *N. winogradskyi*, although this was not reported for nitrite oxidation. It would seem unusual to have a terminal cytochrome oxidase that is capable of pumping protons but that does not with a primary chemolithotrophic substrate. These results have not been reconciled (Bock and Wagner, 2001) and obscure the effect uncouplers have on *Nitrobacter*, particularly since respiratory control exists (Table 10).

In summary, 3,5-DCP may lower the energy efficiency of *Nitrobacter* cells, which is important given the high reduction potential of the NO_2^-/NO_3^- couple and the energy expense for carbon fixation. Since *Nitrobacter* was shown to maintain a narrow range of cytoplasmic pH (Kumar and Nicholas, 1983), a process that requires energy input, this effect is especially likely. Alternately, 3,5-DCP may interfere directly with one of the short electron transport chain components for nitrite oxidation (nitrite oxidoreductase, cytochrome c 550(s), or cytochrome oxidase).

6.2.2 3,5-DCP dose-response curve

Respirograms for a preliminary inhibition experiment with 3,5-DCP are provided in Figure 15 (this analysis serves as an example of the analytical technique). In this experiment, the BSNR mixed liquor was subsampled and immediately diluted with deionized water in respirometric vessels. The background OUR was negligible (< 0.5 mg/L/hr) and nitrite was added (100 mg-N/L) after 2.5 hours. After a short lag time (≈ 15 minutes), the oxygen uptake rate increased to similar and nearly constant values in all the vessels (OUR1 in Table E-1; dashed regression line in Figure 15), which indicated the added nitrite was oxidized at a near first order rate. Approximately 5 hours after the nitrite was added, 3,5-DCP doses were added to vessels 2 through 6. In vessels 1, 2, and 3, which received 0, 2, and 4 mg/L of 3,5-DCP, respectively, the oxygen uptake rate was essentially unaffected. In vessels 4, 5, and 6, which received 8, 16, and 31 mg/L, respectively, the subsequent oxygen uptake rates (OUR2 in Table E-1; solid regression lines in Figure 15) were very low (< 0.6 mg/L). The fraction inhibition ranged from 0.02 in the control vessel (vessel 1) to 0.98 in the vessel that received 16 mg/L (vessel 5) (Table E-1). The respirograms for vessels 1, 2, and 3 clearly indicated when the added nitrite was exhausted, since the OUR dropped to ≈ 0 mg/L/hr after a stoichiometric quantity of oxygen was consumed (≈ 114 mg O_2/100 mg NO_2^--N). In vessels 4, 5, and 6, no adaptation (increasing OUR over time) was observed within 10 to 15 hours after the inhibitor was added. Respiratory control was not evident since an increase in oxygen consumption did not occur at the low uncoupler doses and the stoichiometry was correct.

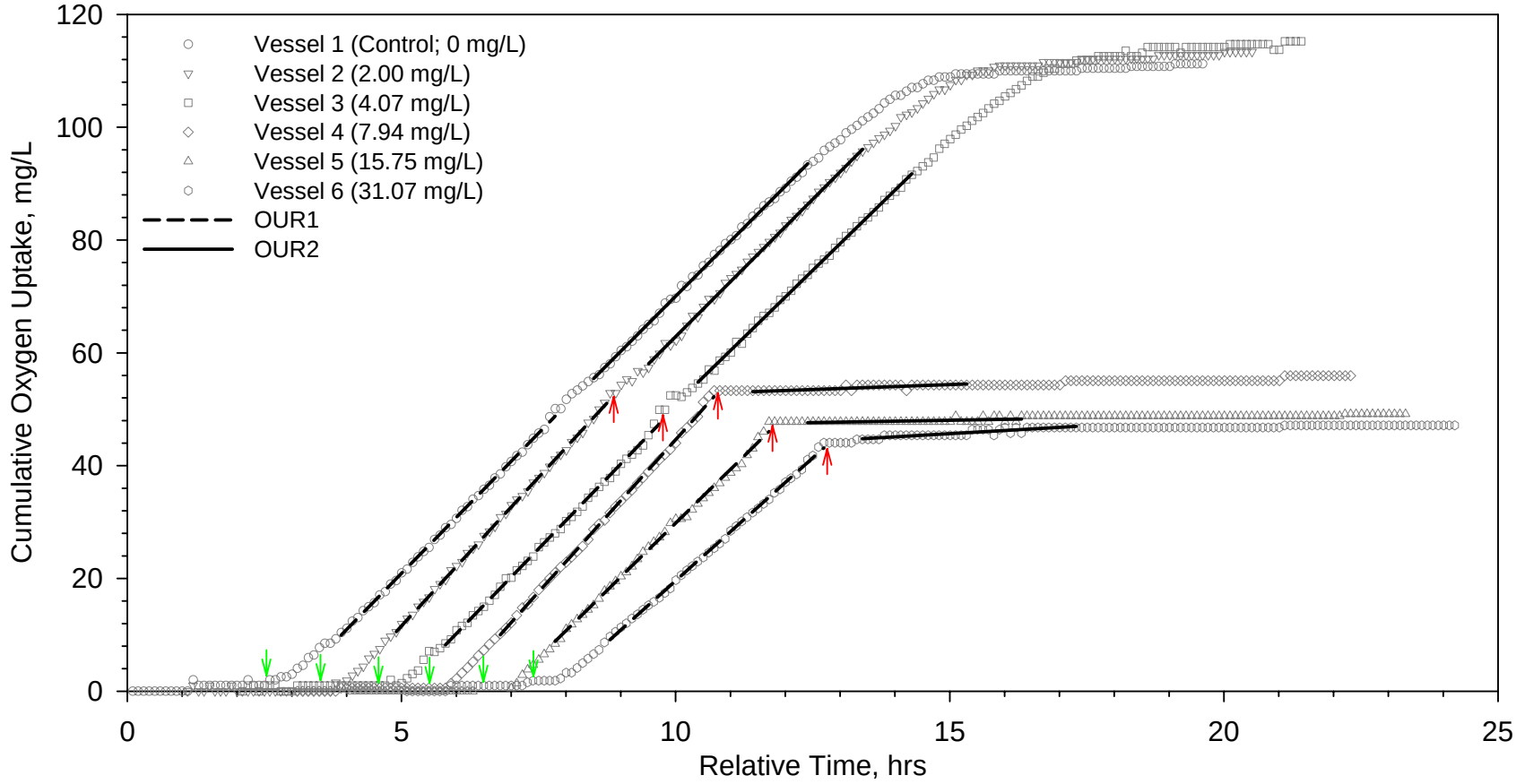


Figure 15 The results of a respirometric inhibition experiment using 3,5-DCP. Respirometric time for vessels 2 through 6 was offset by 1 to 5 hours, respectively, to make each respirogram clearly visible. Nitrite (downward arrows) and 3,5-DCP doses (upward arrows) were added at the time points indicated. Oxygen uptake rates were calculated using ≈ 4 hours of cumulative oxygen uptake and time data before (OUR1) and after (OUR2) the 3,5-DCP doses (amounts specified in the legend). The respirometric data are analyzed in Table E-1.

Five other preliminary inhibition experiments were conducted that included 28 3,5-DCP doses ranging between 2 and 31 mg/L (Table E-1). All the characteristics observed in Figure 15 were reproduced. In particular, the initial nitrite oxidation rates always displayed a linear profile (also observed by Wong-Chong and Loehr, 1978). Adaptation (increasing OUR) was always absent after the 3,5-DCP doses had been added.

The preliminary 3,5-DCP inhibition data were combined to generate a dose-response curve (Figure 16) which exhibited a threshold type relationship and a strong positive monotonic correlation (Kendall's $\tau = 0.83$; p-value < 0.001). At concentrations below 5 mg/L, the fraction inhibition was low (< 0.20). This quickly transitioned to high inhibition (> 0.95) at > 8 mg/L. Gendig et al. (2003) found that a 4 parameter Weibull model fit the 3,5-DCP inhibition data for an activated sludge. The preliminary 3,5-DCP data collected in this study were fit by a similar curve (4 parameter sigmoidal model) that was used to estimate the effective 3,5-DCP concentration inhibiting nitrite oxidation by 20, 50, and 80% (EC_{20}, EC_{50}, and EC_{80} = 6.09, 6.45, and 6.79 mg/L, respectively). The sharply uprising curve was indicated by the small EC_{20}/EC_{80} ratio (1.15): a 15 % increase in the 3,5-DCP concentration increased inhibition by a factor of 4.

Tang et al. (1992) reported an EC_{50} of 5.5 mg of 3,5-DCP/L for a nitrite oxidizer enrichment, only slightly lower than observed herein. A similar uncoupler (2,4,5-TCP) produced a lower IC_{50} value (3.5 mg/L) in a NOB enrichment (Williamson and Johnson, 1981). However, phenolic inhibition varies significantly with the extent of chlorination and pattern of substitution (Liu, 1981), so this comparison may not be warranted. The results could be compared with several 3,5-DCP inhibition studies of AOB and heterotrophic bacteria (Figure 16), which indicated that NOB are less sensitive to this compound than the AOB, but more sensitive than heterotrophic bacteria (especially at > 8 mg/L). This order of sensitivity has been observed for many other inhibitors (Tomlinson et al., 1966, Hockenbury and Grady, 1977, Blum and Speece, 1991). The BSNR nitrite oxidizers were approximately as sensitive to 3,5-DCP as *Vibrio fischeri* (LC_{50} = 5 mg/L; Strotmann and Eglasäer, 1995), which has long been used to test effluent toxicity (Microtox®; Bulich, 1986).

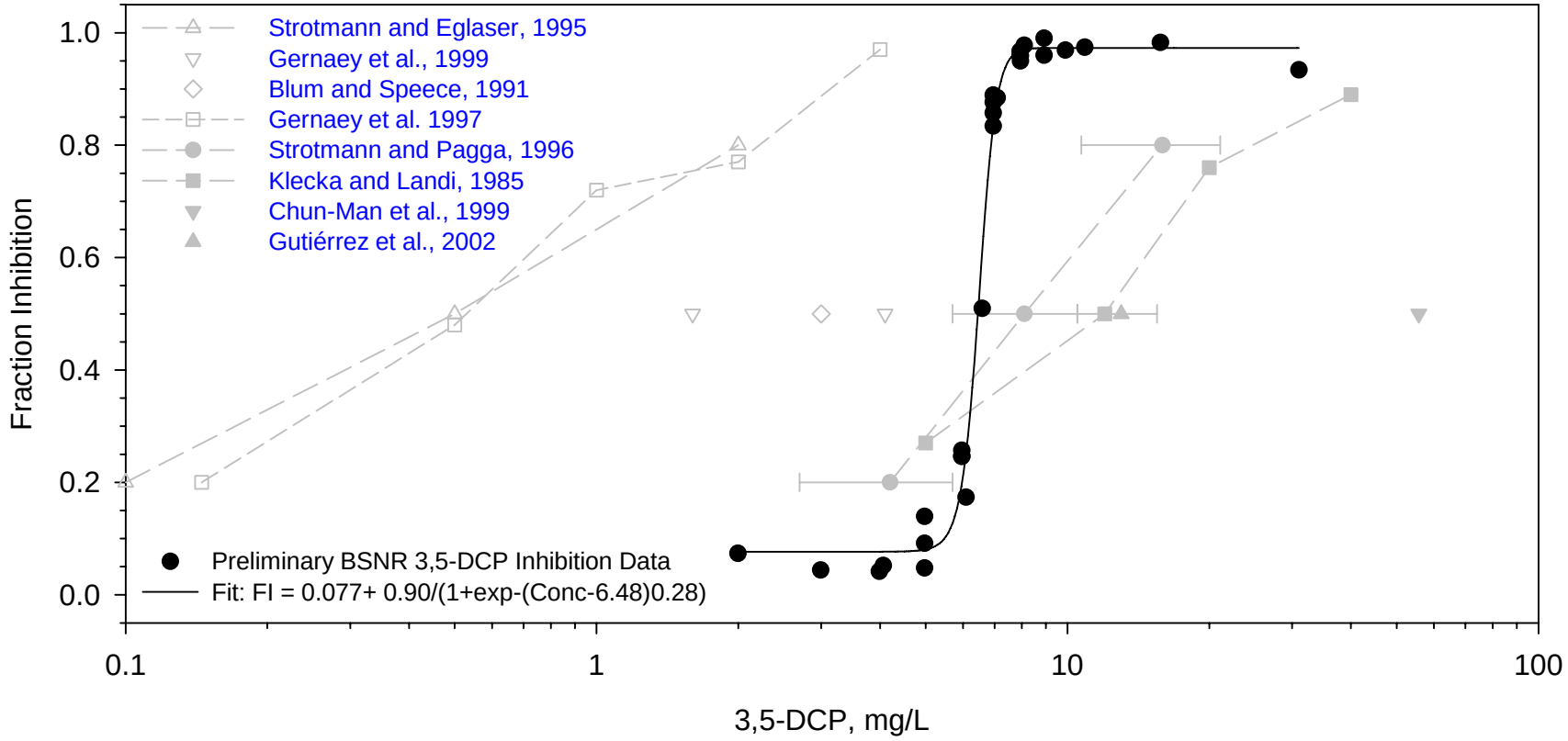


Figure 16 The effect of 3,5-DCP on BSNR nitrite oxidation-dependent respiration rates. Data from six preliminary inhibition experiments were fit with a four parameter sigmoid model using SigmaPlot® (adjusted R^2 = 0.9972; standard error = 0.04). The model equation is provided: FI = fraction inhibition, Conc = 3,5-DCP concentration in mg/L. A legend denotes published 3,5-DCP inhibition values for heterotrophs (closed gray symbols) and AOB (open gray symbols) that were plotted with point to point fits when more than one inhibition value was reported.

6.2.3 3,5-DCP inhibition experiments with RNA and DNA extractions

Two inhibition experiments (designated Experiments I and II) that included DNA and RNA extractions were conducted across a broad fraction inhibition range using the dose-response curve (Figure 16) as a guide. Analysis of the respirometric data from these experiments is provided in Table E-1. The *Nitrobacter* rDNA and rRNAt data are plotted in Figure 17 and summarized in Table 11 (Experiment I) and Table 12 (Experiment II) along with statistical analyses of the rDNA and rRNAt assay mean data (the *Nitrobacter* rRNAt/rDNA data is analyzed later with a separate plot that combines the results from Experiments I and II).

Nitrobacter rDNA

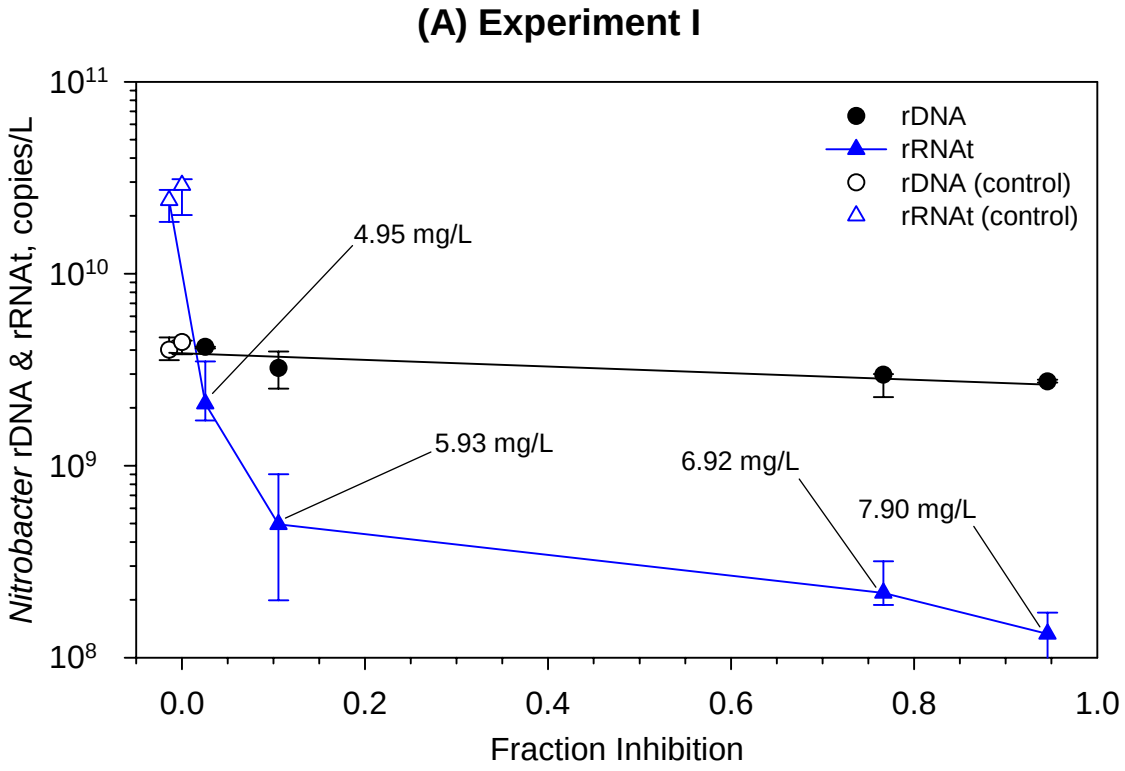
The 3,5-DCP doses had little or no effect on the Nitrobacter rDNA abundance (Figure 17). In Experiment I, the rDNA overall sample means ranged from 2.75 - 4.13 × 10^9 copies/L (Table 11: < 2-fold difference). In Experiment II, the range was 2.29 - 4.22 × 10^9 copies/L (Table 12: < 2-fold difference). Linear regression fits of the rDNA/fraction inhibition data in both experiments exhibited only shallow negative slopes (Figure 17). ANOVA of the log transformed rDNA assay mean data rejected sample equality in both Experiment I ($F = 7.4$, p-value = 0.002) and Experiment II ($F = 3.85$, p-value = 0.026), though a Tukey HSD analysis was unable to distinguish significant difference in Experiment II samples (Table 12). The declining trends and significant differences in rDNA data could indicate that growth inhibition occurred, but this appeared unlikely since the control vessel had the same gene abundance before and 4.5 hours after the inhibitor was added to the remaining vessels (compare the open symbols in Figure 17). Any rDNA differences in question were clearly small and inconsequential when compared to variations in the *Nitrobacter* rRNAt concentration.

Nitrobacter rRNAt

3,5-DCP systematically reduced the *Nitrobacter* rRNAt concentration (Figure 17). The highest doses in each experiment resulted in almost complete inhibition of nitrite oxidation (fraction inhibition > 0.95) and a two order of magnitude decline in rRNAt abundance relative to the control vessels. ANOVA of the log transformed assay mean

Figure 17 The effect of 3,5-DCP on the *Nitrobacter* rRNAt and rDNA concentrations during two batch respirometric inhibition experiments (Experiment I and Experiment II).

Nitrobacter rRNAt and rDNA data are displayed as the median ± minimum/maximum assay mean for replicate extractions (Experiment I: Table 11; Experiment II, Table 12). The sample type is distinguished: uninhibited controls (open symbols) versus samples from inhibited vessels (filled symbols). The 3,5-DCP dose is indicated with a line that points to the corresponding *Nitrobacter* rRNAt data point. Mean rDNA were fit with linear regressions. Median rRNAt assay mean data were fit with point to point lines.


(A) Experiment I
Nitrobacter rDNA & rRNAt, copies/L
Fraction Inhibition
rDNA
rRNAt
rDNA (control)
rRNAt (control)
4.95 mg/L
5.93 mg/L
6.92 mg/L
7.90 mg/L

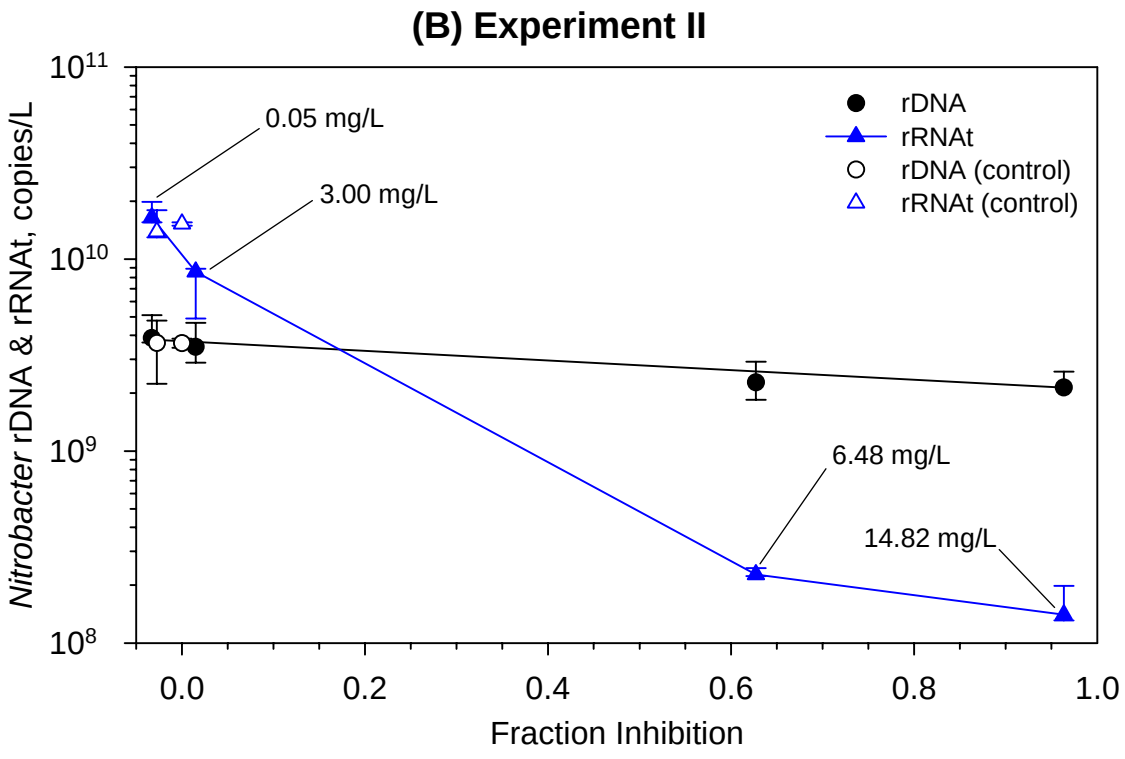

(B) Experiment II
Nitrobacter rDNA & rRNAt, copies/L
Fraction Inhibition
rDNA
rRNAt
rDNA (control)
rRNAt (control)
0.05 mg/L
3.00 mg/L
6.48 mg/L
14.82 mg/L

Table 11 *Nitrobacter* molecular data for a respirometric inhibition experiment with 3,5-DCP (Figure 17; Experiment I).

Sample		3,5-DCP (mg/L)	Fraction Inhibition	*Nitrobacter* rDNA (copies/L)[2]			*Nitrobacter* rRNAt (copies/L)[2]			rRNAt/rDNA[3]
				Assay Mean	Statistical Analysis		Assay Mean	Statistical Analysis		
Time[1]	Vessel				Overall Mean	Tukey		Overall Mean	Tukey	
Before Inhibitor Dose	1	-	-	4.90E+09	4.40E+09	A	3.11E+10	2.67E+10	A	6.080
				3.81E+09			2.02E+10			
				4.48E+09			2.89E+10			
After Inhibitor Dose	1	-	-0.01	3.55E+09	4.07E+09	A	2.73E+10	2.34E+10	A	5.737
				4.01E+09			2.41E+10			
				4.66E+09			1.86E+10			
	2	4.95	0.03	4.17E+09	4.13E+09	A	3.49E+09	2.44E+09	B	0.590
				4.08E+09			1.72E+09			
				4.15E+09			2.10E+09			
	3	5.93	0.11	2.52E+09	3.23E+09	AB	9.02E+08	5.32E+08	C	0.165
				3.93E+09			4.95E+08			
				3.23E+09			1.99E+08			
	4	6.92	0.77	3.00E+09	2.75E+09	B	3.18E+08	2.41E+08	CD	0.088
				2.28E+09			2.17E+08			
				2.98E+09			1.88E+08			
	5	7.90	0.95	2.71E+09	2.75E+09	B	1.72E+08	1.27E+08	D	0.046
				2.81E+09			1.33E+08			
				2.74E+09			7.70E+07			

1 Time indicates whether the sample was collected immediately before or ≈ 4.5 hours after the inhibitor was added.

2 Assay mean is the mean of triplicate Real Time or Real Time RT-PCR reactions for replicate DNA and RNA extracts (Table E-2). The overall mean is the average of the assay means. Log transformation made the assay mean data more symmetric and constant in variance. The log transformed assay mean data were analyzed with Tukey HSD multiple comparisons if ANOVA rejected the null hypothesis of sample equivalence ($\alpha = 0.05$). Samples not sharing a common letter are significantly different ($\alpha = 0.05$).

3 The rRNAt/rDNA metric was calculated with the overall rDNA and rRNAt means for each sample event.

Table 12 *Nitrobacter* molecular data for a respirometric inhibition experiment with 3,5-DCP (Figure 17; Experiment II).

Sample		3,5-DCP (mg/L)	Fraction Inhibition	*Nitrobacter* rDNA (copies/L)[2]			*Nitrobacter* rRNAt (copies/L)[2]			rRNAt/rDNA[3]
				Assay Mean	Statistical Analysis		Assay Mean	Statistical Analysis		
Time[1]	Vessel				Overall Mean	Tukey		Overall Mean	Tukey	
Before Inhibitor Dose	1	-	-	3.64E+09	3.65E+09	A	1.56E+10	1.53E+10	A	4.179
				3.45E+09			1.53E+10			
				3.85E+09			1.49E+10			
After Inhibitor Dose	1	-	-0.03	3.65E+09	3.56E+09	A	1.30E+10	1.49E+10	A	4.198
				4.78E+09			1.80E+10			
				2.24E+09			1.39E+10			
	2	0.50	-0.03	5.10E+09	4.22E+09	A	1.64E+10	1.73E+10	A	4.095
				3.68E+09			1.55E+10			
				3.88E+09			1.98E+10			
	3	3.00	0.01	2.89E+09	3.68E+09	A	8.89E+09	7.46E+09	B	2.029
				3.49E+09			8.58E+09			
				4.65E+09			4.91E+09			
	4	6.48	0.63	2.92E+09	2.35E+09	A	2.23E+08	2.32E+08	C	0.099
				1.85E+09			2.46E+08			
				2.28E+09			2.27E+08			
	5	14.82	0.96	2.59E+09	2.29E+09	A	1.31E+08	1.57E+08	C	0.068
				2.14E+09			1.41E+08			
				2.14E+09			1.98E+08			

1 Time indicates whether the sample was collected immediately before or ≈ 4.5 hours after the inhibitor was added.

2 Assay mean is the mean of triplicate Real Time or Real Time RT-PCR reactions for replicate DNA and RNA extracts (Table E-3). The overall mean is the average of the assay means. Log transformation made the assay mean data more symmetric and constant in variance. The log transformed assay mean data were analyzed with Tukey HSD multiple comparisons if ANOVA rejected the null hypothesis of sample equivalence ($\alpha = 0.05$). Samples not sharing a common letter are significantly different ($\alpha = 0.05$).

3 The rRNAt/rDNA metric was calculated with the overall rDNA and rRNAt means for each sample event.

data rejected the null hypothesis that the *Nitrobacter* rRNAt sample abundance was the same in Experiment I ($F = 93$; p-value < 0.0001) and Experiment II ($F = 419$; p-value < 0.0001). Subsequent Tukey HSD multiple comparisons identified four (Table 11) and three (Table 12) sample mean groups in Experiments I and II, respectively. For each experiment, the Tukey mean groups formed a coherent pattern with the sample mean descending as the fraction inhibition increased. Importantly, this analysis indicated no significant difference existed in *Nitrobacter* rRNAt abundance in the control vessel before and 4.5 hours after 3,5-DCP doses were added to the remaining vessels (compare the open symbols in Figure 17). Thus, prior to the inhibitor being added the *Nitrobacter* rRNAt concentration was high and unchanging. The data clearly confirmed Hypothesis I (Section 6.1.3) that the *Nitrobacter* rRNAt concentration would be higher in uninhibited versus significantly inhibited vessels. With respect to the general rRNAt response, Cangelosi and Brabant (1997) also observed sharp declines in rRNAt when *E. coli* was inhibited with uncouplers (1.25 mM 2,4-DNP, 50 mM KH_2AsO_4, and 50 μM CCCP). When they added uncouplers to complete growth media, the relative rRNAt decline was similar to the results obtained in this study (≈ 1.5 order of magnitude decline in 3 hours). However, growth and substrate utilization inhibition data were not provided by these researchers.

An unexpected result in Experiment I was that *Nitrobacter* rRNAt concentration in a vessel which received a low inhibitor dose (4.95 mg/L) was significantly lower than in the control vessel (Table 11). The unusual nature of this difference stemmed from the negligible inhibition observed in the dosed vessel (fraction inhibition = 0.03). This indicated that for *Nitrobacter* the rRNAt abundance was particularly sensitive to 3,5-DCP as a result of growth inhibition, though the ability to oxidize nitrite was not impacted. This would have important implications for applying the metric to improve wastewater treatment, and was exactly the type of seemingly unusual response that was of interest in this study.

To critically confirm the unexpected result obtained in Experiment I, two smaller 3,5-DCP doses (0.5 and 3.0 mg/L) were employed in Experiment II. These doses produced insignificant inhibition (fraction inhibition < 0.01) (Table 12). For the vessel

that received the 0.5 mg /L dose, the *Nitrobacter* rRNAt concentration was not significantly different from the control vessel concentration (Table 12). However, in the vessel which received 3.0 mg /L, the *Nitrobacter* rRNAt concentration was significantly lower than in the control vessel Thus, the result for Experiment I (seemingly low *Nitrobacter* rRNAt abundance during insignificant nitrite oxidation inhibition) was reproducible, but could be eliminated at a sufficiently low inhibitor dose.

The general phenomenon of growth inhibition while cells retain respiration (King and Dutka, 1986) is well reflected by the fact that standardized effluent toxicity tests exist for both respiration (ISO, 1986) and growth inhibition (Strotmann and Pagga, 1996). For denitrification, differential inhibition was observed in that active transport was strongly inhibited by uncouplers while the denitrification rate was not (Walter et al., 1978). Further, growth inhibition has been observed in *Nitrobacter* spp. while the ability to oxidize nitrite was not impacted. For instance, Yamanaka (1983) indicated that *N. agilis* was growth inhibited by 4 μM of paraquat, but that nitrite did not accumulate in an AOB/*N. agilis* mixed culture when this level of the herbicide was present. Others have observed this effect on *Nitrobacter* spp. when uncouplers were present. Freitag and Bock, (1990) reported that the uncoupling mechanism was active for *N. winogradskyi* at 100 μM 2,4-DNP, that it did not affect nitrite oxidation, but completely inhibited NADH formation. Aleem (1977) tested NADH oxidation by *Nitrobacter* electron transport particles using oxygen and nitrate as the terminal electron acceptors. For these experiments the ATP energy yields were practically zero in the presence of 5 μM CCCP, while the oxygen and nitrate consumption rates were increased 34 and 46%, respectively (a respiratory control response). Further, Aleem (1977) found that 2,4-DCP reduced oxygen consumption 19%, but reduced ATP formation by far more (62%). These findings are relevant to this study since NADH is required for *Nitrobacter* growth (Bock and Wagner, 2001). If the growth prospect for *Nitrobacter* was decreased by 3,5-DCP in the inhibition experiments, this would explain why the rRNAt concentration was lower in vessels that received this compound, even if the ability to oxidize nitrite was not impacted.

***Nitrobacter* rRNAt/rDNA**

The effect of 3,5-DCP on the *Nitrobacter* rRNAt/rDNA ratio was clearly mediated via an impact on the *Nitrobacter* rRNAt concentration. To examine this effect, the combined ratio data from Experiments I and II were plotted together against the backdrop of the preliminary dose response curve (Figure 18). It can be seen that the fraction inhibition observed in Experiments I and II (open circles) was in accord with the preliminary data (close circles). The rRNAt/rDNA metric decreased from values exceeding the upper BSNR prediction interval to values below the lower prediction interval at 3,5-DCP doses between 3 and 5 mg/L, though at 5 mg/L the fraction inhibition was negligible (0.03). Above 5 mg/L, the metric declined steadily and was well below the lower prediction interval as hypothesized (Section 6.1.3: hypothesis II). Further, the *Nitrobacter* rRNAt/rDNA ratio declined monotonically with fraction inhibition (Kendall's τ = -0.822; p-value = 0.0002) and 3,5-DCP concentration (Kendall's τ = -0.933; p-value = 0.0002) as hypothesized (hypothesis III: Section 6.1.3). Finally, it should be noted that in the control vessel the ratio was indeed the same before (Experiment I: 4; Experiment II: 6) and after (Experiment I: 4; Experiment II: 6) the inhibitor was added to the remaining vessels (see Table 11 and Table 12).

6.2.4 Summary

3,5-DCP, an electron transport chain uncoupler, elicited a monotonic decline in the *Nitrobacter* rRNAt/rDNA ratio as the concentration increased. The metric dropped below the lower BSNR prediction interval as the dose exceeded 5 mg/L, though nitrite oxidation was insignificantly inhibited (0.03) at that concentration. This result was hypothesized to reflect growth inhibition by 3,5-DCP, even as nitrite oxidation was unaffected, and has important implications for using the metric to improve wastewater treatment processes. In particular, it would seem the metric could provide early warning of poor reactor performance during NOB growth inhibition, since a reduction in nitrification efficiency would occur slowly as reactor washout occurred. Similarly, Tomlinson et al. (1966) suggested that the long term effect of heavy metals would be more severe than expected from short term inhibition tests because of growth inhibition.

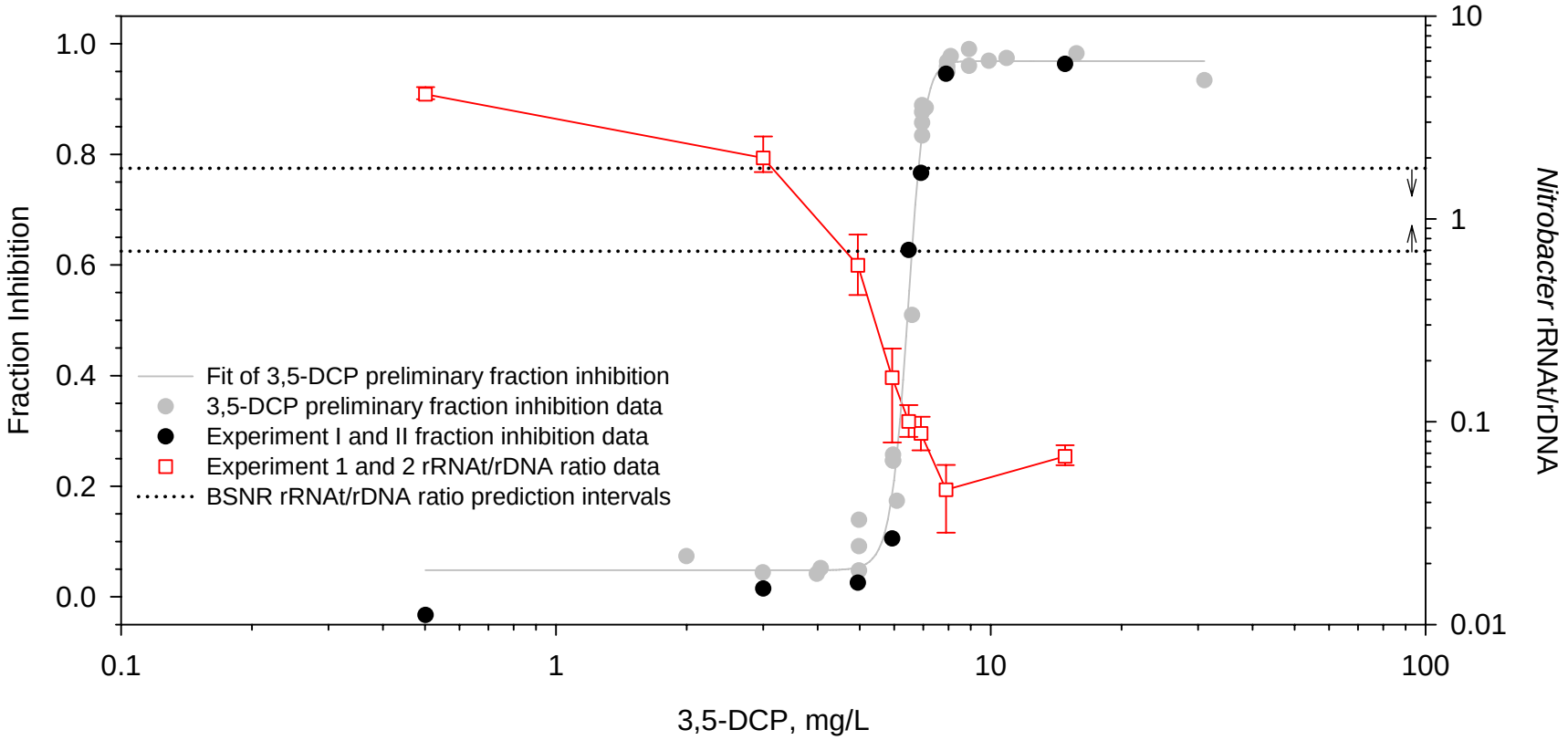


Figure 18 The effect of 3,5-DCP on the *Nitrobacter* rRNAt/rDNA ratio. *Nitrobacter* rRNAt/rDNA data are provided with a point to point fit (Table 11 and Table 12; error bars are the interquartile range of all possible ratios computed with the rRNAt and rDNA assay means). Horizontal reference lines indicate the upper (↓) and lower (↑) BSNR prediction intervals (Section 5.2). For perspective, the ratio data are plotted with the preliminary experiment dose/response data. Fraction inhibition results for Experiments I and II are distinguished and correspond to the ratio datapoints.

Further, the uncoupling mechanism was linked to growth inhibition in *Nitrobacter* membrane particles by Aleem (1977) who observed lower ATP yields with little effect on nitrite oxidation. Thus, it is possible to envision that a reduction in rRNAt transcription occurred upon 3,5-DCP exposure because electrons were directed away from carbon fixation and toward energy generation for maintenance purposes (Rittmann and McCarty, 2001). Interestingly, Aleem (1977) proposed that this split was regulated by the energy charge of the cell, which may also regulate the rDNA transcription rate (Gaal et al., 1999).

6.3 Azide

6.3.1 The inhibition mechanism

Azide is a classical inhibitor of the terminal cytochrome oxidase in mitochondria (Stryer, 1995). Mitochondrial cytochrome oxidase contains cytochromes a and a_3: cytochrome a accepts electrons from cytochrome c and transfers them to cytochrome a_3 where sequential oxygen reduction occurs (Stryer, 1995). In *Nitrobacter*, the terminal cytochrome oxidase for nitrite oxidation is type aa_3 (Sewell et al., 1972; Yamanaka et al., 1981) and similar enough to the mitochondrial enzyme that an evolutionary link to the organelle was proposed (Yamanaka, et al. 1984). Unionized azide inhibits type aa_3 cytochrome oxidases by reacting with the ferric form of heme a_3 thereby preventing enzyme turnover (Tsubaki and Yoshikawa, 1993; Stryer, 1995). The terminal oxidase is particularly critical in *Nitrobacter* because high activity is required to aid an otherwise energetically unfavorable transfer of electrons from nitrite to cytochrome c by nitrite oxidoreductase (Bock and Wagner, 2001). However, azide is capable of binding to other heme groups, for example those found in *E. coli* unbiquinol oxidase (Tsubaki et al., 1999), therefore NOB inhibition could also result from azide binding to other cytochrome containing electron transport chain components. However, since the concentration required to inhibit cytochrome oxidase in mitochondria ($EC_{50} \approx 1$ mM for mouse skeletal muscle cell respiration: Leary et al., 1998) is much higher than required to inhibit nitrite

oxidation (μM range: Ginestet et al., 1998), there is reason to suspect additional or different origins for the NOB inhibitory effect.

Azide is known to inhibit dissimilatory nitrate reductase enzymes which contain a molybdenum cofactor (Zumft, 1997). Molybdenum is essential for *Nitrobacter* growth (Finstein and Delwiche, 1965) and the nitrite oxidoreductase enzymes of both *N. winogradskyi* and *N. hamburgensis* utilize a molybdenum cofactor (Fukuoka et al., 1987; Krüger et al., 1987). In fact, nitrite oxidoreductase appears closely related to *E. coli* nitrate reductase (Kirstein and Bock, 1993). *Nitrobacter* has demonstrated nitrate reductase activity both in cell free extracts (Kiesow, 1964) and in strains of three species of whole cells (Bock et al., 1988; Freitag et al., 1987) that is mediated by nitrite oxidoreductase (Kukuoka et al., 1987). However, the inhibition threshold for denitrification occurs at much higher concentrations (mM range: Hamuda et al., 1995) than for nitrite oxidation. In a direct comparison of the inhibitory effects of milk analysis wastewater, López-Fiuza et al. (2002) found that denitrifiers, as well as methanogens and AOB, were much less sensitive to azide than NOB.

Consensus for which enzymatic system is affected was sought by comparing azide inhibition of *Nitrobacter* cell free extracts and whole cells (Table 13). Table 13 revealed a wide range of incipient inhibition for various components of the *Nitrobacter* respiratory chain. For example, in comparison with other enzymes, ATPase was relatively unaffected (6% at 100 μM). Thus, even though azide is known to inhibit mitochondrial and cell surface ATPase enzymes by stabilizing their inactive forms (Knowles and Nagy, 1999), the high NOB sensitivity is probably not associated with ATPase functionality. Likewise, NADH oxidation was relatively immune to azide when both oxygen (23% at 100 μM) and nitrate (0% at 100 μM) served as the terminal electron acceptor. In general, the effect on reducing power utilization was relatively low (Table 13). Kumar and Nicholas (1983) found that azide inhibited *N. agilis* respiration by 100%, removed 85% of the ΔpH component of the proton motive force, but left the ΔΨ component unaffected. Since ΔpH was a small component of the proton motive force, this effect also seems ancillary. Table 13 indicates that cytochrome oxidase is more

Table 13 The effect of azide (% inhibition) on *Nitrobacter* cell free extract and whole cell activity.

Azide (μM)	*Nitrobacter* cell free systems[1] (% inhibition)		% inhibition of NOB activity		Reference
0.3	-	-	nitrifier enrichment (respiration)	50	Ginestet et al., 1998
0.4	-	-	nitrifier enrichment (NO_2^-oxidation)	50	López-Fiuza et al., 2002
0.8	-	-	nitrifier enrichment (respiration)	75	Ginestet et al., 1998
4.4	*N. winogradskyi* nitrite oxidoreductase	28	-	-	Tanaka et al., 1983
8.8	*N. winogradskyi* nitrite oxidoreductase	42	-	-	Tanaka et al., 1983
24	-	-	nitrifier enrichment (respiration)	100	Ginestet et al., 1998
	-	-	nitrifier enrichment (respiration)	100	Guisasola, et al., 2005
	-	-	nitrifier enrichment (saline media)	100	Sánchez et al., 2001
44	*N. winogradskyi* nitrite oxidoreductase	61			Tanaka et al., 1983
50	-	-	*N. agilis* oxygen uptake	100	Kumar and Nicholas, 1983
	-	-	*N. agilis* ΔΨ (membrane potential)	0	
	-	-	*N. agilis* ΔpH (across membrane)	85	
	-	-	*N. agilis* Δp (proton motive force)	18	
	"nitrite oxidase"	100	-	-	O'Kelly et al., 1970
	"nitrite cytochrome c reductase"	70	-	-	
	"cytochrome oxidase"	28	-	-	
	NO_2^-/O_2	50		-	Aleem, 1977
100	NO_2^-/O_2	70	-	-	Aleem, 1977
	$NADH/NO_3^-$	0	-	-	
	$NADH/O_2$	23	-	-	
	N. winogradskyi ATPase activity	6	-	-	Hara et al., 1991
220	-	-	activated sludge NO_2^- oxidation rate	75	Tomlinson et al. 1966

sensitive than many enzymes (28% at 50 μM), but nitrite oxidoreductase is even more sensitive (100% at 50 μM, 28% at 4.4 μM). However, even nitrite oxidoreductase appears less susceptible than whole cell activity (50% at 0.3 μM), making the primary mechanism for azide inhibition of nitrite oxidation difficult to assess.

In summary, high azide sensitivity in *Nitrobacter* could not be traced to a single enzyme system, but could be due to simultaneous and perhaps synergistic effects on nitrite oxidoreductase and cytochrome oxidase, both of which are involved in the short (3 component) electron transport chain used to oxidize nitrite (Bock and Wagner, 2001). This would confirm that the azide inhibition mechanism is distinct from 3,5-DCP.

6.3.2 Azide dose-response curve

Seven preliminary respirometric inhibition experiments were conducted that included 30 doses of azide ranging from 10^{-7} - 10^{-3} M. These experiments were analyzed as previously described for 3,5-DCP and a dose-response curve was constructed (Figure 19; Table E-4).

The inhibition pattern obtained with azide was notably different from the one obtained with 3,5-DCP. For example, inhibition increased only gradually as the inhibitor dose was increased. Also, complete inhibition (fraction inhibition > 0.95) was more difficult to obtain with azide. The fraction inhibition was low (< 0.30) between 0.1 - 1.0 μM, rose to approximate 0.85 at 10 μM, but thereafter increased only slightly between 0.1 - 1.0 mM. The data displayed a strong positive monotonic correlation (Kendall's τ = 0.912; p-value < 0.001) and was well fit by a three parameter logistic model (Figure 19) which was used to compute the EC_{20}, EC_{50}, and EC_{80} values for azide: 0.57 μM, 1.84 μM, and 7.30 μM, respectively. The EC_{80}/EC_{20} ratio was 12.8 for azide, much higher than observed for 3,5-DCP (1.15). The disparate dose-response curves for these two inhibitors indicated their mechanisms are different.

Ginestet et al. (1998), López-Fiuza et al. (2002) and Tomlinson et al. (1966) investigated azide inhibition of nitrite oxidation using nitrifier enrichment cultures and activated sludge, respectively (Figure 19). Ginestet et al. (1998) and López-Fiuza et al.

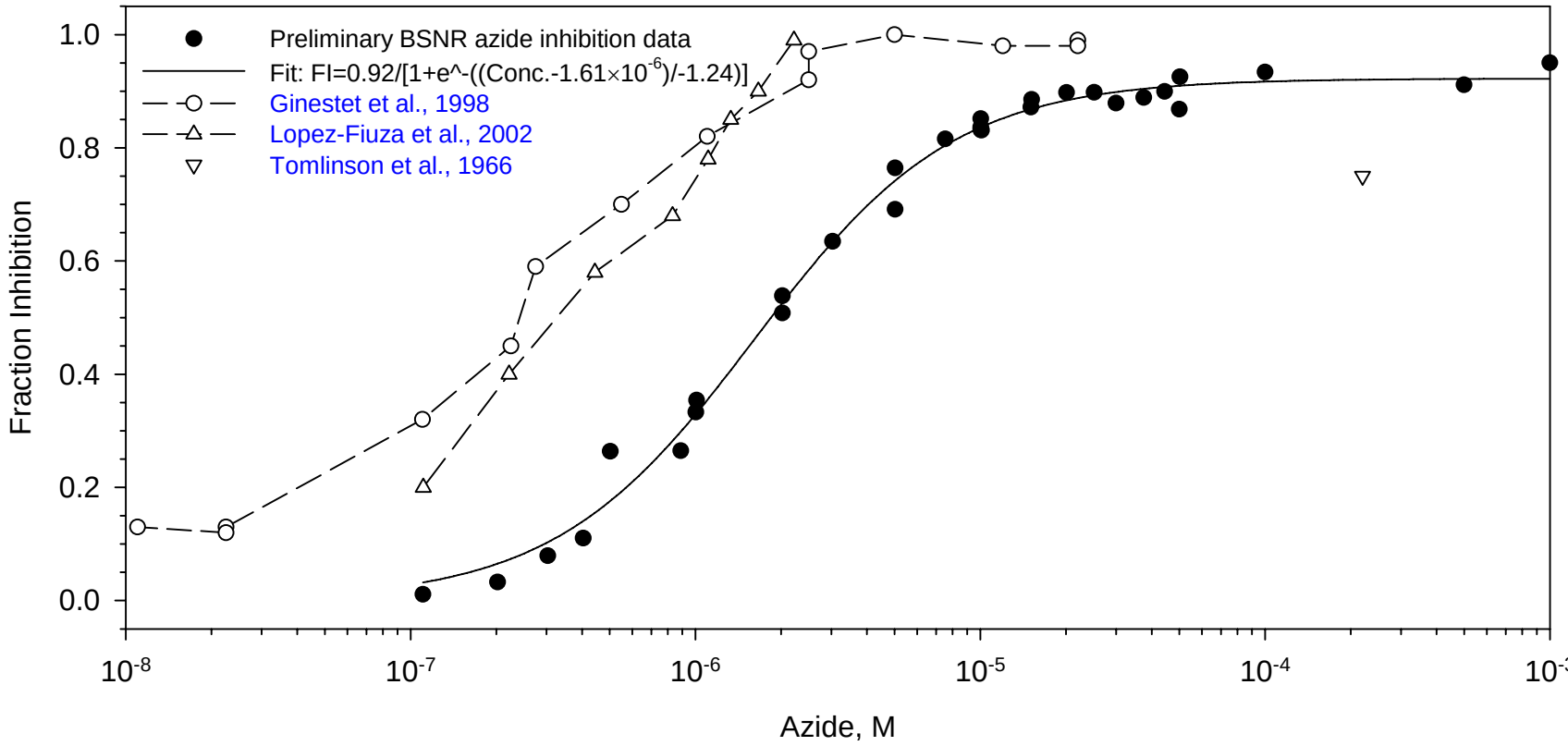


Figure 19 The effect of azide on BSNR nitrite oxidation-dependent respiration rates. Preliminary BSNR inhibition data were fit with a three parameter logistic model using SigmaPlot® (adjusted R^2 = 0.9986; standard error = 0.027). The model equation is provided in the legend: FI = Fraction Inhibition, Conc = N_3^- concentration in M.

(2002) estimated the EC_{50} of azide at 0.3 and 0.4 μM, respectively, while Tomlinson et al. (1966) observed 75% inhibition at a much higher concentration (220 μM). Kumar and Nicholas (1983) reported complete inhibition of *N. agilis* at 50 μM, but lower concentrations were not investigated. Ginestet et al. (1998) suggested 24 μM completely inhibited NOB without affecting AOB or heterotrophic activity. Subsequent investigations by Sánchez et al., (2001) and Guisasola et al., (2005) appear to confirm this. Thus, NOB were less sensitive to azide in this study than has been reported for nitrifier enrichments, though the result obtained by Tomlinson et al. (1996) indicate nitrite oxidation in activated sludge may be more resistance to azide.

Gutiérrez et al. (1996) identified many factors that contribute to variability in toxicity/inhibition determination in bacteria including: inocula used, effect measured, and the inhibition assay design. For nitrification inhibition evaluations, improved reproducibility was obtained when the same versus different biomass sources were used (Winther-Nielsen and Jansen, 1996). Thus, the difference between the results herein and those obtained by Ginestet et al. (1998) and López-Fiuza et al., (2002) could reflect differences in the inhibition assay design and the biomass sources. As an example, the tests in this study were conducted at 30°C, while the Ginestet et al. (1998) and López-Fiuza et al. (2002) investigations were conducted at 20°C and 25°C, respectively. Although they used nitrifier enrichments, their cultivation techniques were different and could have lead to functionally equivalent but different NOB populations (Fernandez et al., 2000). Also, the assay used in this investigation incorporated an extended period of high NOB activity prior to the inhibitor addition, unlike the Ginestet et al. (1998) and López-Fiuza et al., (2002) assays which contained little or no prior NOB activity. The high initial NOB activity could have resulted in more resilience when the azide was added. For example, the identified targets for azide inhibition, nitrite oxidoreductase and cytochrome oxidase, are both inducible (Bock and Wagner, 2001), so the extended period of high activity could have increased the cellular concentration of these enzymes and thereby increased resistance. Similarly, Ford et al. (1980) cited research indicating the AOB were more susceptible to inhibition during the lag versus log growth phases. Finally, it should be pointed out that the results obtained by López-Fiuza et al. (2002) and

Ginestet et al. (1998) are more disparate than thus far suggested. Azide induced NOB inhibition was similar in these studies, but the EC_{50} estimates for AOB were ≈ 3-fold different.

6.3.3 Azide inhibition experiments with RNA and DNA extractions

Two additional azide inhibition experiments (designated Experiments III and IV) were conducted using the dose-response curve (Figure 19) as a guide. Analysis of the respirometric data from these experiments is provided in Table E-4. The *Nitrobacter* rDNA and rRNAt data are plotted in Figure 20 and summarized in Table 14 (Experiment III) and Table 15 (Experiment VI) with statistical analyses of the assay mean data.

Nitrobacter rDNA

As was observed for 3,5-DCP, the azide doses had little or no effect on the *Nitrobacter* rDNA concentration (Figure 20). Regression lines through the rDNA/fraction inhibition data exhibited only shallow negative slopes (Figure 20). ANOVA did not reject the null hypothesis that the log transformed rDNA assay mean sample results were equal in Experiment III ($F = 3.0$; p-value 0.0543). However, ANOVA did reject equality in Experiment IV ($F = 14$; p-value = 0.0029). A subsequent Tukey HSD analysis indicated the concentration in the more inhibited vessels (fraction inhibition > 0.63: average 2.67×10^{-9} copies/L) was significantly (but slightly) lower than in the control and least inhibited vessels (average 4.94×10^{-9} copies/L). In both experiments, the control vessel rDNA concentration was the same before and 4.5 hours after azide was added to the remaining vessels (compare the open symbols in Figure 20). The potential rDNA decline was negligible compared with the *Nitrobacter* rRNAt variations.

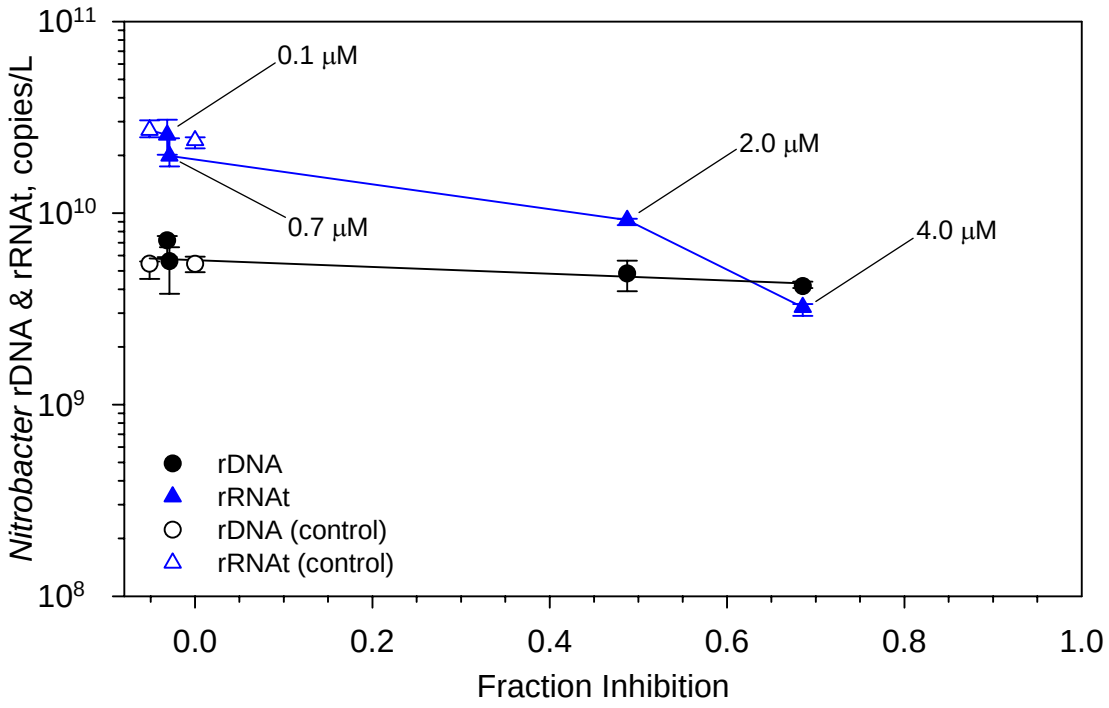
Nitrobacter rRNAt

Point to point fits of the *Nitrobacter* rRNAt data clearly indicated that transcript abundance declined as the azide dose and fraction inhibition increased (Figure 20). ANOVA of the log transformed *Nitrobacter* rRNAt assay mean data rejected the null hypothesis that the sample events were equal (Experiment III: $F = 135$; p-value < 0.0001; Experiment IV: $F = 134$; p-value < 0.0001) and subsequent Tukey HSD analyses

Figure 20 The effect of azide on the *Nitrobacter* rRNAt and rDNA concentrations during two batch respirometric inhibition experiments (Experiment III and Experiment VI).

Nitrobacter rRNAt and rDNA data are displayed as the median ± minimum/maximum assay mean for replicate extractions (Experiment III: Table 14; Experiment IV, Table 15). The sample type is distinguished: uninhibited controls (open symbols) versus samples from inhibited vessels (filled symbols). The azide dose is indicated with a line that points to the corresponding *Nitrobacter* rRNAt data point. Mean rDNA data were fit with linear regressions. Median rRNAt assay mean data were fit with point to point lines.

A. Experiment III



B. Experiment IV

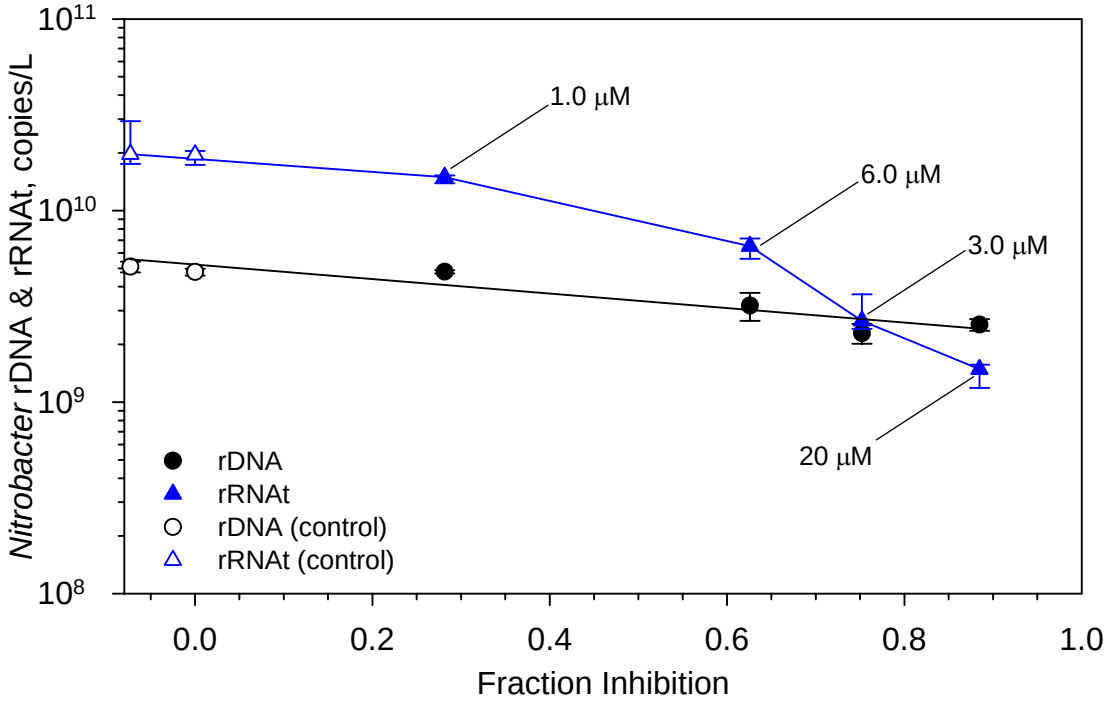


Table 14 *Nitrobacter* molecular data for a respirometric inhibition experiment with azide (Figure 20; Experiment III).

Sample		Azide (μM)	Fraction Inhibition	*Nitrobacter* rDNA (copies/L)[2]			*Nitrobacter* rRNAt (copies/L)[2]			rRNAt/rDNA[3]
				Assay Mean	Statistical Analysis		Assay Mean	Statistical Analysis		
Time[1]	Vessel				Overall Mean	Tukey		Overall Mean	Tukey	
Before Inhibitor Dose	1	-	-	5.44E+09	5.42E+09	-	2.40E+10	2.35E+10	A	4.341
				4.92E+09			2.49E+10			
				5.92E+09			2.18E+10			
After Inhibition Dose	1	-	-0.05	5.59E+09	5.19E+09	-	2.49E+10	2.75E+10	A	5.303
				5.43E+09			3.05E+10			
				4.53E+09			2.71E+10			
	2	0.101	-0.03	7.59E+09	6.90E+09	-	2.56E+10	2.55E+10	A	3.699
				5.89E+09			2.02E+10			
				7.20E+09			3.07E+10			
	3	0.704	-0.03	5.60E+09	5.34E+09	-	1.99E+10	2.07E+10	A	3.876
				6.64E+09			2.46E+10			
				3.79E+09			1.75E+10			
	4	2.01	0.49	5.64E+09	4.80E+09	-	9.34E+09	9.06E+09	B	1.889
				3.91E+09			8.65E+09			
				4.83E+09			9.19E+09			
	5	4.02	0.69	4.39E+09	4.20E+09	-	3.35E+09	3.16E+09	C	0.753
				4.15E+09			3.22E+09			
				4.06E+09			2.91E+09			

1 Time indicates whether the sample was collected immediately before or ≈ 4.5 hours after the inhibitor was added.

2 Assay mean is the mean of triplicate Real Time or Real Time RT-PCR reactions for replicate DNA and RNA extracts (Table E-5). The overall mean is the average of the assay means. Log transformation made the assay mean data more symmetric and constant in variance. The log transformed assay mean data were analyzed with Tukey HSD multiple comparisons if ANOVA rejected the null hypothesis of sample equivalence ($\alpha = 0.05$). Samples not sharing a common letter are significantly different ($\alpha = 0.05$).

3 The rRNAt/rDNA metric was calculated with the overall rDNA and rRNAt means for each sample event.

Table 15 *Nitrobacter* molecular data for a respirometric inhibition experiment with azide (Figure 20; Experiment IV).

Sample		Azide (μM)	Fraction Inhibition	*Nitrobacter* rDNA (copies/L)[2]			*Nitrobacter* rRNAt (copies/L)[2]			rRNAt/rDNA[3]
				Assay Mean	Statistical Analysis		Assay Mean	Statistical Analysis		
Time[1]	Vessel				Overall Mean	Tukey		Overall Mean	Tukey	
Before Inhibition Dose	1	-	-	4.98E+09	4.78E+09	A	2.05E+10	1.91E+10	A	4.003
				4.58E+09			1.96E+10			
				-			1.73E+10			
After Inhibition Dose	1	-	-0.07	4.76E+09	5.08E+09	A	1.97E+10	2.22E+10	A	4.362
				5.41E+09			2.93E+10			
				-			1.75E+10			
	2	1.00	0.28	4.88E+09	4.79E+09	A	1.50E+10	1.47E+10	A	3.069
				4.69E+09			1.52E+10			
				-			1.39E+10			
	3	3.01	0.63	2.66E+09	3.19E+09	B	5.61E+09	6.43E+09	B	2.014
				3.72E+09			7.15E+09			
				-			6.52E+09			
	4	6.02	0.75	2.56E+09	2.29E+09	B	2.41E+09	2.91E+09	C	1.270
				2.02E+09			3.65E+09			
				-			2.66E+09			
	5	20.1	0.88	2.72E+09	2.54E+09	B	1.19E+09	1.41E+09	D	0.557
				2.36E+09			1.49E+09			
				-			1.57E+09			

1 Time indicates whether the sample was collected immediately before or ≈ 4.5 hours after the inhibitor was added.

2 Assay mean is the mean of triplicate Real Time or Real Time RT-PCR reactions for replicate DNA and RNA extracts (Table E-6). The overall mean is the average of the assay means. Log transformation made the assay mean data more symmetric and constant in variance. The log transformed assay mean data were analyzed with Tukey HSD multiple comparisons if ANOVA rejected the null hypothesis of sample equivalence ($\alpha = 0.05$). Samples not sharing a common letter are significantly different ($\alpha = 0.05$).

3 The rRNAt/rDNA metric was calculated with the overall rDNA and rRNAt means for each sample event.

categorized the samples into 3 (A - C: Table 14) and 4 (A - D: Table 15) mean groups. In both experiments the control sample transcript abundance ($\approx 2 \times 10^{10}$ copies/L) was the same before and after azide doses were added to the remaining vessels. Thus, at the time azide was added, the transcript concentration was high and steady.

Vessels that were modestly inhibited with azide (fraction inhibition < 0.28) did not display a significantly lower *Nitrobacter* rRNAt concentration than the control vessels. However, when the fraction inhibition exceeded 0.49, rRNAt was significantly and progressively lowered. In Experiment III, the *Nitrobacter* rRNAt concentrations in vessels with fraction inhibition of 0.49 ($9.06 \pm 0.4 \times 10^9$ copies/L; 2.0 μM azide) and 0.69 ($3.16 \pm 0.2 \times 10^9$ copies/L; 4.0 μM azide) were significantly lower than in the control vessel ($2.75 \pm 0.3 \times 10^{10}$ copies/L). In Experiment IV, the *Nitrobacter* rRNAt concentrations in vessels with fraction inhibition of 0.63 ($6.43 \pm 0.8 \times 10^9$ copies/L; 3.0 μM azide), 0.75 ($2.19 \pm 0.7 \times 10^9$ copies/L; 6.0 μM azide), and 0.88 ($1.41 \pm 0.2 \times 10^9$ copies/L; 20 μM azide) were significantly lower than in the uninhibited control ($2.22 \pm 0.6 \times 10^{10}$ copies/L). In each experiment, the progressively more inhibited vessels contained less rRNAt. Thus, as hypothesized (Hypothesis I: Section 6.1.3), azide caused a significant decline in rRNAt abundance relative to the control vessel.

While the *Nitrobacter* rRNAt concentration was lowered by both 3,5-DCP and azide, the magnitude of the drop in the azide experiments was smaller and occurred at higher fraction inhibition values. For comparison, consider first Experiment IV in which the fraction inhibition caused by azide was 0.28 and 0.88 at 1 and 20 μM doses, respectively. Despite the 28% reduction in NOB activity, *Nitrobacter* rRNAt was not significantly lower than in the uninhibited control vessel (Table 15). When the fraction inhibition was 0.88, *Nitrobacter* rRNAt was ≈ 1 order of magnitude lower than in the control vessel (2.22×10^{10} versus 1.41×10^9 copies/L: Table 15). These results sharply contrast with those obtained in Experiment I. When the fraction inhibition was negligible (0.03: 5 mg/L 3,5-DCP), the *Nitrobacter* rRNAt concentration was an order of magnitude lower than in the control vessel (2.34×10^{10} versus 2.44×10^9 copies/L: Table 11). When inhibition was near complete in Experiment I (0.95: 7.9 mg 3,5-DCP/L), *Nitrobacter*

rRNAt abundance was two orders of magnitude lower than in the control vessel (2.34×10^{10} versus 1.27×10^{8} copies/L: Table 11).

***Nitrobacter* rRNAt/rDNA**

The *Nitrobacter* rRNAt/rDNA ratio data from Experiments III and IV are combined in Figure 21. A linear regression through the *Nitrobacter* rRNAt/rDNA ratio/azide concentration data indicated that the metric value dropped significantly as the azide dose increased from 1 to 20 μM. When the dose was ≤ 3.0 μM, which corresponded to fraction inhibition values ≤ 0.63, the metric value remained above the upper BSNR prediction interval, indicating that the growth prospective was not significantly diminished. Alternately, the metric response could have been delayed. However, as the azide dose increased to 20 μM, corresponding to a fraction inhibition of 0.88, the ratio fell below the lower BNSR prediction interval as hypothesized (Hypothesis II: Section 6.1.3). Further, the ratio value declined monotonically with fraction inhibition (Kendall's $\tau = -0.822$; p-value = 0.0002) and azide concentration (Kendall's $\tau = -0.844$; p-value < 0.0002) as expected (Hypothesis III: Section 6.1.3). However, in terms of the fraction inhibition value at which the metric fell below the lower BSNR prediction interval, the result was clearly much higher for azide (≈ 0.80) than 3,5-DCP (≈ 0.05).

6.3.4 Summary

Azide inhibition of nitrite oxidation activity caused a significant decline in *Nitrobacter* rRNAt abundance and hence in the *Nitrobacter* rRNAt/rDNA ratio. Unlike 3,5-DCP, this decline occurred only when NOB inhibition was high. The divergent response in the azide and 3,5-DCP inhibition experiments indicated that *Nitrobacter* rRNAt abundance was affected differently, at least in the short term, by mechanistically distinct inhibitors. More particularly, the azide results indicated that the metric may decline less and/or more slowly with some types of inhibition. This could be rationalized by considering the likely azide and 3,5-DCP mechanisms. Azide likely affects respiratory chain components directly, but there is no uncoupling of energy conservation, so potential remains for energy conservation, growth, and demand for rRNA. The more

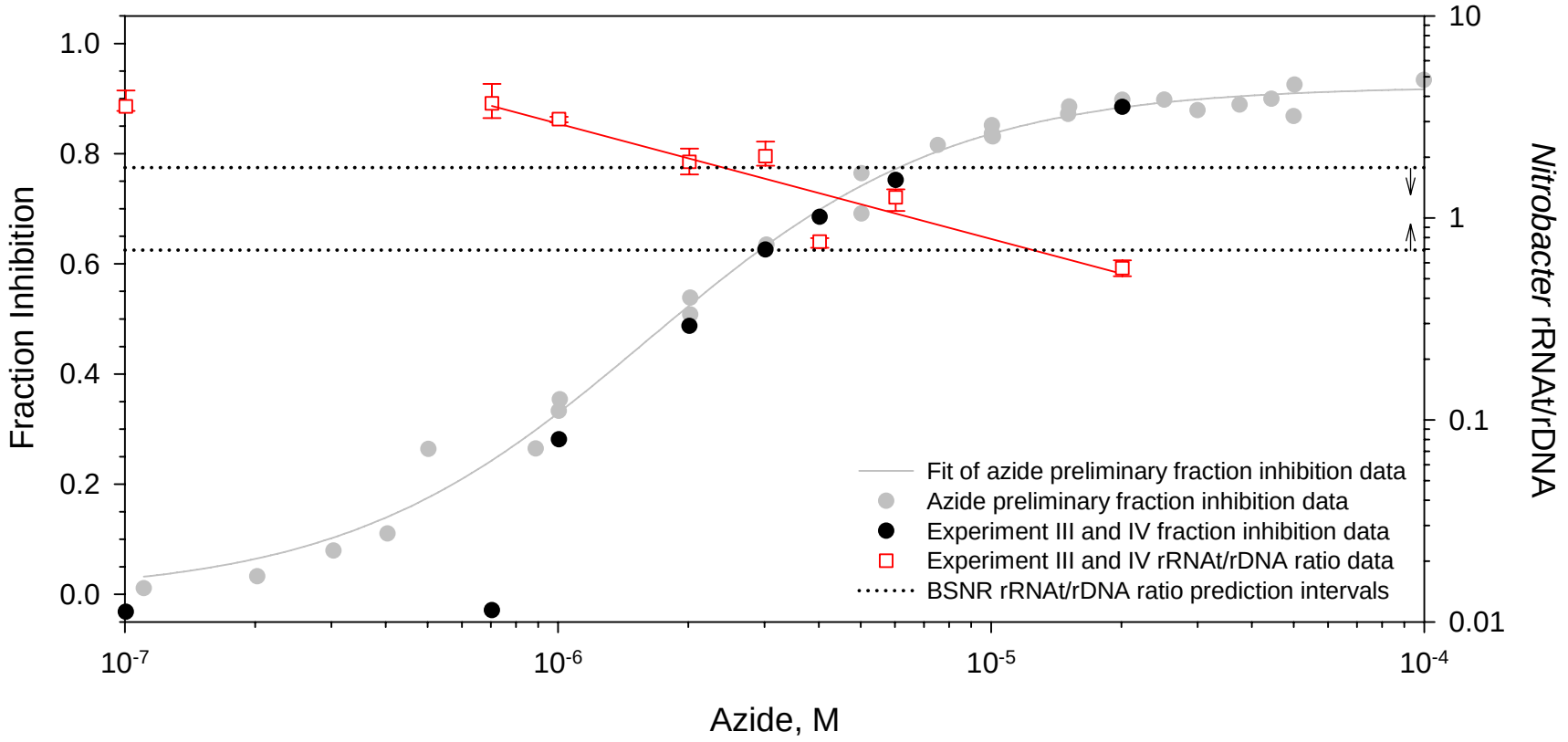


Figure 21 The effect of azide on the *Nitrobacter* rRNAt/rDNA ratio. *Nitrobacter* rRNAt/rDNA data are provided with linear regression fit for doses above 7 µM (Table 14 and Table 15; error bars are the interquartile range of all possible ratios computed with the rRNAt and rDNA assay means). Horizontal reference lines indicate the upper (↓) and lower (↑) BSNR prediction intervals (Section 5.2). For perspective, the ratio data are plotted with the preliminary experiment dose/response data. Fraction inhibition results for Experiments III and IV are distinguished and correspond to the ratio datapoints.

drastic decline in the *Nitrobacter* rRNAt/rDNA metric for 3,5-DCP likely reflected a disruption in energy conservation. Further, the difference in the metric response to these two inhibitors was reflected in dose response curve differences. Similar experiments testing bacterial RNA transcript abundance to mechanistically distinct inhibitors was not found in the literature, so a perspective on this observation and conclusion could not be established.

6.4 H^+

6.4.1 The inhibition mechanism

The mechanisms involved when bacteria succumb to low pH are not precisely known and likely vary among different phylogenetic groups. However, almost certainly it involves a drop in the cytoplasmic pH. Growth and respiratory inhibition can result as enzymes succumb non-specifically to low internal pH (Cotter and Hill, 2003). Cell death can ultimately result from membrane damage (Dilworth and Gleen, 1999).

It should be noted that a variety of bacteria exhibit stress responses to low pH that depend on the severity of the acid condition, the stress duration, and the concentration of energy sources (Shabala et al., 2002). The response to acid stress has been well studied in pathogenic bacteria including gram negative enterobacteria (Bearson et al., 1997) and gram positive bacteria (Cotter and Hill, 2003). This is because virulent strains of pathogenic bacteria must survive cyclical exposure to sudden acid stress on host entry (stomach acid) and when subject to phagocytosis. Recent reviews (Bearson et al., 1997; Cotter and Hill, 2003) of the strategies to survive low pH environments noted: (1) mechanisms to maintain internal pH (e.g. inducible amino acid decarboxylases, alkali production systems based on urea degradation, and proton pumping), (2) two component systems involving alternate sigma factors for expression of acid shock proteins that mediate DNA and protein repair (e.g. σ^s in *E. coli* for expression of RecA and DnaK), and (3) changes in the cell membrane that keep it intact at low pH. These systems have not been verified in *Nitrobacter*, but it seems likely the NOB possess such defensive

mechanisms since nitrification often lowers the surrounding environment's pH (Grady et al., 1999).

Several mechanisms for specific nitrite oxidation inhibition are possible at low pH. For example, nitrite exists in two interconvertible forms in solution, the nitrite ion and free nitrous acid (Section 2.1.1). The proportion of nitrite as free nitrous acid increases as the pH is lowered and Anthonisen et al. (1976) indicated NOB were inhibited by free nitrous acid between 0.07 - 0.8 mg HNO_2-N/L (≈ 3 - 30 mg NO_2^--N/L at pH 5.5). O'Kelly et al. (1970) observed nitrite oxidase inhibition in *N. agilis* cell free extracts at lower concentrations (1.4 - 9.8 μg HNO_2-N/L).

The reduction potential for the NO_2^-/NO_3^- pair decreases as the pH increases (414 and 328 mV at pH 6.8 and 9.0, respectively), whereas the reduction potential for intermediate electron acceptors may not be pH dependent (Aleem, 1977). Thus, as the pH is lowered a drop in cytoplasmic pH (Hollocher et al., 1982) could make nitrite oxidation energetically unfavorable.

Kumar and Nicholas (1983) confirmed that the $\Delta\Psi$ and ΔpH components of the proton motive force were dependent on external pH in *Nitrobacter*. They found that $\Delta\Psi$ contributed mostly to the proton motive force at pH > 7.5 because the intracellular pH remained constant (7.3 - 7.8) between pH 6.0 - 8.5. Interestingly, the proton motive force was highest at the lowest pH tested because the internal pH was maintained near 7.5. However, $\Delta\Psi$ was lowest at this point. Since nitrite oxidation may be aided by the $\Delta\Psi$ component of the proton motive force (Cobley, 1976a), this could make nitrite oxidation energetically unfavorable at low pH. Supporting this possibility is the fact that *Nitrobacter* has been shown to grow most efficiently at alkaline pH (Bock and Wagner, 2001) where $\Delta\Psi$ is higher (Kumar and Nicholas, 1983).

In summary, *Nitrobacter* is likely affected by several mechanisms following a sudden change to acid pH. The inhibitory mechanisms are less specific than described for 3,5-DCP and azide. Given the propensity for nitrification to lower the pH, particularly when buffering capacity is low in receiving waters (USGS, 1999) or in

wastewater treatment reactors (Grady et al., 1999), a study of the effects of low pH on the *Nitrobacter* rRNAt/rDNA ratio was considered pertinent.

6.4.2 H^+ dose-response curve

Seven preliminary respirometric inhibition experiments were conducted using sudden pH changes. Seventeen vessels were inhibited by adding acid to lower the pH from 7.2 to 7.0 - 4.4, while ten vessels were inhibited by adding base to raise the pH from 7.2 to 7.6 - 10.9 (to complete a pH-inhibition curve). The pH-inhibition curve was constructed (Figure 22) based on the analyses of the preliminary experiments in Table E-4. The fraction inhibition was low (< 0.25) if the pH remained between 6.1 and 8.7, high (> 0.75) after pH changes to below 5.5 or above 8.6, and complete (≈ 1.00) when the pH was below 5.0 or above 10.0. These pH activity limits are exceeded by *Nitrobacter* strains in extreme environments (Sorokin et al., 1998; Hankinson and Schmidt, 1988). For the acid doses, the fraction inhibition increased monotonically with H^+ (Kendall's τ = 0.839; $p < 0.0001$), but was less reproducible than with 3,5-DCP and azide.

Figure 22 is similar to a pH inhibition plot for nitrification presented by EPA (1993). Their plot, which contains a summary of mostly unacclimated results, indicates nitrification occurs between pH 5.5 and 10. However, results for habituated nitrifiers in their plot suggest that adaptation can lead to activity over a broader pH range. With this in mind, the short term results presented herein must be strictly associated with the conditions used to define inhibition. NOB with adaptive or evolved abilities are certainly active at very low pH (pH 4.0, de Boer et al., 1991; pH 3.2 - 4.3, Tarre and Green, 2004) and at least one *Nitrobacter* strain has been isolated that is active at pH 3.5 (Hankinson and Schmidt, 1988). Conversely, Ruiz et al. (2003) showed that ammonia oxidation ceased below pH 6.4, which could be related to scarcity of the substrate free ammonia as the pH declines (Section 2.1.1).

Surprisingly, adaptation occurred *during* the inhibition assays. In this respect, H^+ inhibition was distinct from 3,5-DCP and azide inhibition. This tendency for adaptation is demarcated with shading in Figure 22 and has been noted in a literature review of the nitrifiers (Ford et al., 1980). As the acid dose was increased to a final pH of 6.1 to 5.3,

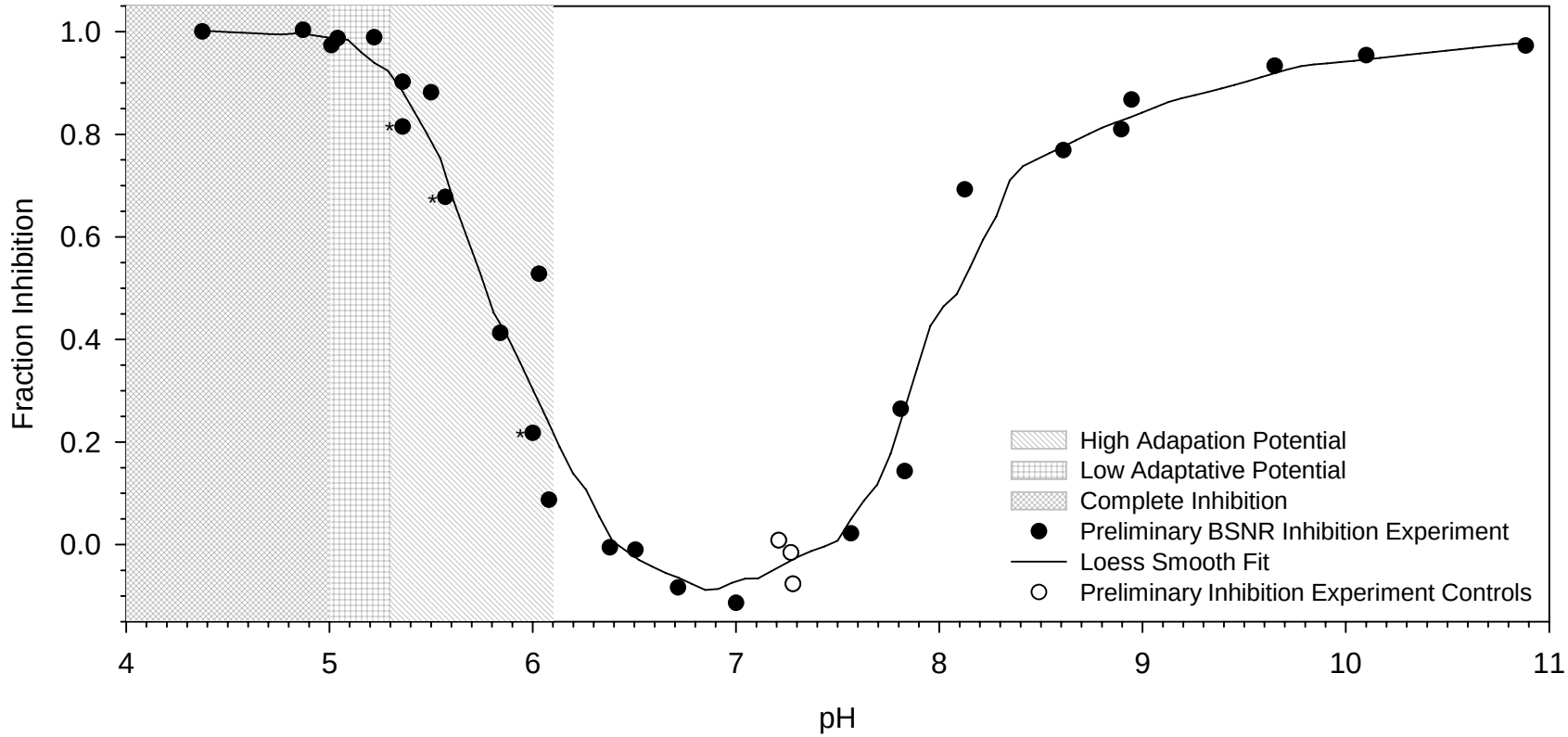


Figure 22 The effect of pH changes on BSNR nitrite oxidation-dependent respiration rates. The pH prior to acid or base addition was typically 7.2 - 7.3. The inhibition data were fit with a loess smooth using SigmaPlot® (sampling proportion 0.20, polynomial degree 1, nearest neighbor bandwidth method at 100 intervals). The preliminary inhibition experiments included control samples for which the pH was noted but not changed. Ranges of acid pH are demarcated with respect to the tendency for NOB adaptation (discussed in the text). Respirograms for the datapoints marked with "*" are plotted in Figure 23 to illustrate the adaptive response.

proportionately greater initial inhibition, longer lag times with no aerobic activity, and decreasing adaptive success generally occurred. When the pH was lowered to 5.3 - 5.0, lag times increased and little or no increase in the OUR occurred once a low level of activity resumed. Below pH 5.0, complete inhibition was observed. These findings are consistent with those of Suthersan and Ganczarczyk (1986) who observed that increasingly higher pH and NH_3 concentrations resulted in more severe NOB inhibition and longer recovery (lag) times.

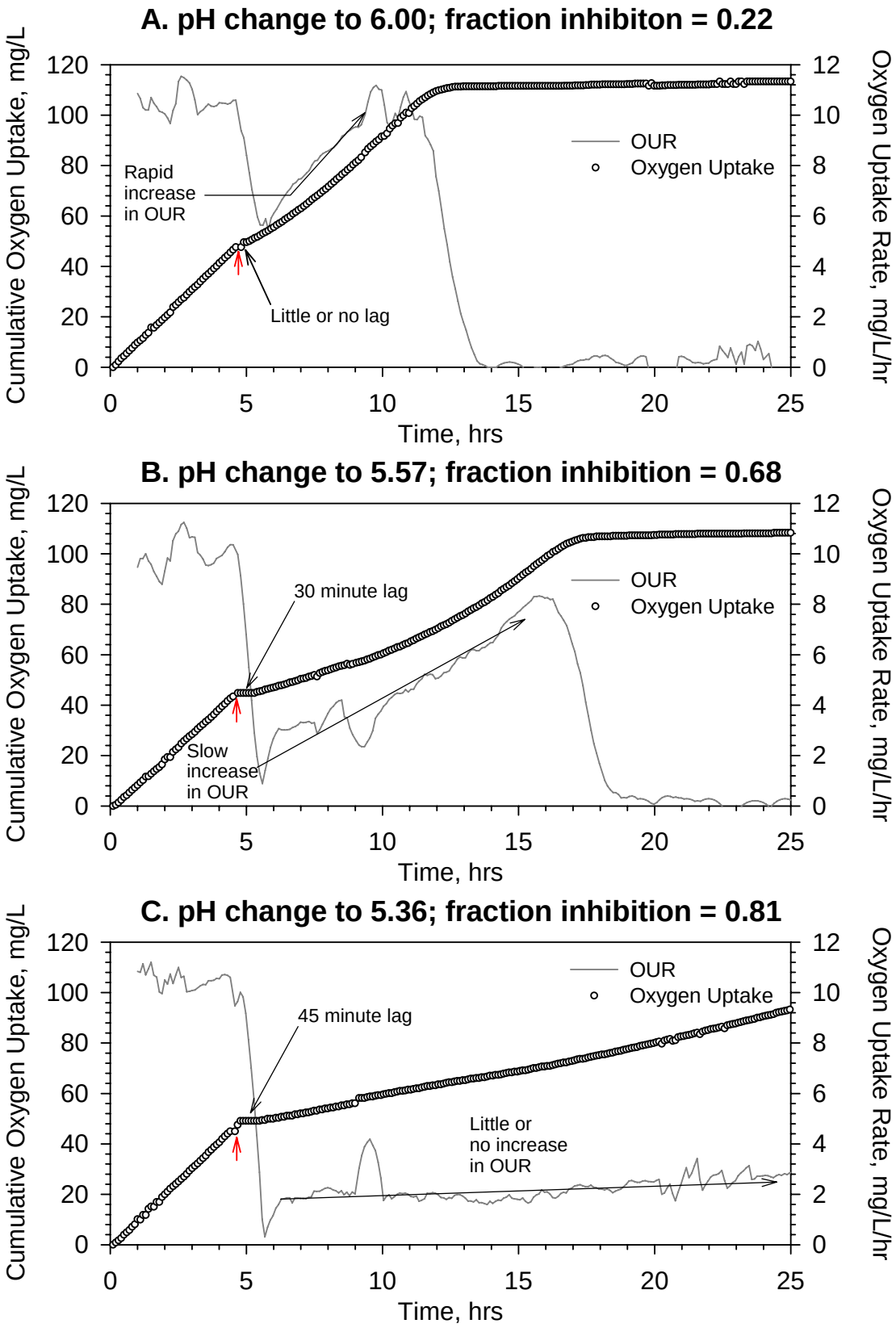
Typical adaptive responses are illustrated in Figure 23. In Figure 23-A, a pH change to 6.00 resulted in no initial absence in aerobic activity. The OUR increased rapidly to the level established prior to the acid dose before nitrite was depleted. In Figure 23-B, a pH change to 5.57 resulted in a lag period of 30 minutes during which no oxygen was utilized. Thereafter, the OUR increased slowly over time but did not regain the initial OUR before the nitrite was depleted. In Figure 23-C, a pH change to 5.36 resulted in a 45 minute lag period during which no oxygen was utilized. Thereafter, little or no increase in the OUR occurred once activity resumed (the nitrite was not depleted within 20 hours of the pH change). Thus, the results presented in Figure 22 are the average fraction inhibition values observed over a 4.5 hour time period after the H^+ dose.

Lags in *Listeria monocytogenes* activity (≈ 60 minutes) were tied to the synthesis of acid resistance proteins following acid doses, though the overall response strongly depended on substrate availability (Shabala et al., 2002). Thus, the design of the inhibition assay with excess nitrite present for several hours prior to the sudden pH change could have promoted short term adaptation in this study. Because the adaptive response was strong in the preliminary inhibition experiments, the final experiments (with DNA and RNA extractions) were conducted at pH < 6.0. Also, because *Nitrobacter* activity has been documented at very low pH, acid doses that resulted in pH ≈ 4.5 were investigated, though complete inhibition occurred at pH ≤ 5.0 (Figure 22).

6.4.3 H^{+-} inhibition experiments with RNA and DNA Extractions

Two acid inhibition experiments (designated Experiments V and VI) were performed with DNA and RNA extractions using the dose response curve in Figure 22 as

Figure 23 Variability in NOB adaptive potential following inhibition with acid doses. Respirometric data are provided for three preliminary assays distinguished in Figure 22 (A - C). At the time points indicated (↑) acid was added and resulted in the final pH and fraction inhibition noted. For each respirometric data point, the OUR was calculated using the previous one hour of cumulative oxygen uptake and time data and fit with a point to point line.


A. pH change to 6.00; fraction inhibiton = 0.22
Cumulative Oxygen Uptake, mg/L
Oxygen Uptake Rate, mg/L/hr
Time, hrs
OUR
Oxygen Uptake
Rapid increase in OUR
Little or no lag
B. pH change to 5.57; fraction inhibition = 0.68
30 minute lag
Slow increase in OUR
C. pH change to 5.36; fraction inhibition = 0.81
45 minute lag
Little or no increase in OUR

a guide. Analysis of the respirometric data is provided in Table E-7. The *Nitrobacter* rDNA and rRNAt data are plotted in Figure 24 and summarized in Table 16 (Experiment V) and Table 17 (Experiment VI) with statistical analyses of the sample assay mean data.

Nitrobacter rDNA

Though acid doses are capable of cell membrane destruction (Dilworth and Gleen, 1999), which would make DNA susceptible to degradation, this was not apparent in the *Nitrobacter* rDNA data from these experiments. Linear regression fits of the rDNA/fraction inhibition data in both experiments displayed insignificant slopes. In Experiment V, the *Nitrobacter* rDNA overall sample mean ranged only from 4.87 - 6.98 $\times 10^{-9}$ copies/L (Table 16), and in Experiment VI only from 6.18 - 8.99 $\times 10^{-9}$ copies/L (Table 17). ANOVA of the log transformed assay mean data did not reject the null hypothesis that the samples were equal in Experiment V ($F = 2.24$; p-value = 0.117), but a significant difference was indicated in Experiment VI ($F = 3.92$; p-value = 0.028), though in this case only two of the vessels were identified as being significantly different in the subsequent Tukey HSD comparisons (Table 17). The control sample rDNA was equal before and 4.5 hours after acid was added to the remaining vessels in both experiments (compare the open symbols in Figure 24). As with 3,5-DCP and azide experiments, the variability in gene abundance was inconsequential compared with the transcript variations.

Nitrobacter rRNAt

Point to point fits of the *Nitrobacter* rRNAt data in Experiments V and VI emphasized that the pH drop significantly lowered the *Nitrobacter* rRNAt concentration. Further, in both experiments the transcript abundance was affected in a systematic manner, with the abundance being high in the uninhibited control vessel ($\approx 1.6 \times 10^{10}$ copies/L), declining approximately one order of magnitude as the pH was dropped to near 5.0 ($\approx 1.9 \times 10^{9}$ copies/L), but surprisingly remaining high in vessels that were completely inhibited at pH 4.5 ($\approx 1.5 \times 10^{10}$ copies/L). This characteristic is strikingly different from the inhibition experiments with 3,5-DCP and azide, where a steady decline in rRNAt abundance was always evident with increasing inhibition/inhibitor dose.

Figure 24 The effect of a sudden change to low pH (H^+ dose) on the *Nitrobacter* rRNAt and rDNA concentrations during two batch respirometric inhibition experiments (Experiment V and Experiment VI).

Nitrobacter rRNAt and rDNA data are displayed as the median ± minimum/maximum assay mean for replicate extractions (Experiment V: Table 16; Experiment VI, Table 17). The sample type is distinguished: uninhibited controls (open symbols) versus samples from inhibited vessels (filled symbols). The final pH is indicated with a line that points to the corresponding *Nitrobacter* rRNAt data point. Mean rDNA data were fit with linear regressions. Median rRNAt assay mean data were fit with point to point lines.

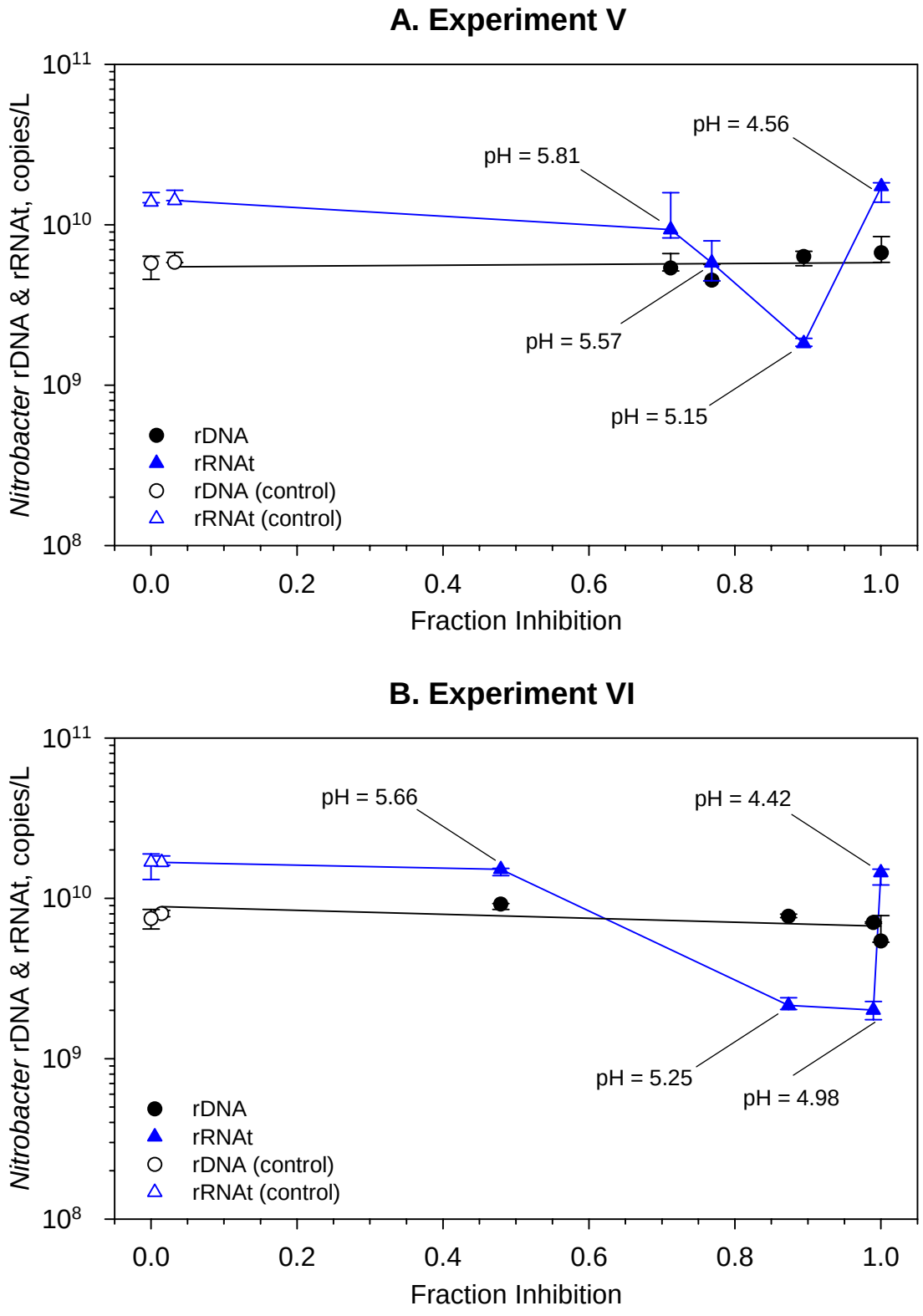

A. Experiment V
Nitrobacter rDNA & rRNAt, copies/L
10^11
10^10
10^9
10^8
pH = 4.56
pH = 5.81
pH = 5.57
pH = 5.15
rDNA
rRNAt
rDNA (control)
rRNAt (control)
0.0
0.2
0.4
0.6
0.8
1.0
Fraction Inhibition
B. Experiment VI
Nitrobacter rDNA & rRNAt, copies/L
10^11
10^10
10^9
10^8
pH = 5.66
pH = 4.42
pH = 5.25
pH = 4.98
rDNA
rRNAt
rDNA (control)
rRNAt (control)
0.0
0.2
0.4
0.6
0.8
1.0
Fraction Inhibition

Table 16 *Nitrobacter* molecular data for a respirometric inhibition experiment with acid (Figure 24; Experiment V).

Sample		H^+ (M) [pH]	Fraction Inhibition	*Nitrobacter* rDNA (copies/L)[2]			*Nitrobacter* rRNAt (copies/L)[2]			rRNAt/rDNA[3]
				Assay Mean	Statistical Analysis		Assay Mean	Statistical Analysis		
Time[1]	Vessel				Overall Mean	Tukey		Overall Mean	Tukey	
Before Inhibitor Dose	1	-	-	6.35E+09	5.56E+09	-	1.37E+10	1.45E+10	A	2.608
				5.74E+09			1.39E+10			
				4.57E+09			1.59E+10			
After Inhibitor Dose	1	3.94E-08 [7.41]	0.03	6.72E+09	6.13E+09	-	1.42E+10	1.49E+10	A	2.432
				5.83E+09			1.41E+10			
				5.82E+09			1.64E+10			
	2	1.56E-06 [5.81]	0.71	6.62E+09	5.71E+09	-	8.26E+09	1.11E+10	A	1.950
				5.36E+09			1.58E+10			
				5.15E+09			9.32E+09			
	3	2.69E-06 [5.57]	0.77	5.64E+09	4.87E+09	-	5.78E+09	6.06E+09	B	1.246
				4.50E+09			4.47E+09			
				4.46E+09			7.93E+09			
	4	7.08E-06 [5.15]	0.89	6.33E+09	6.23E+09	-	1.82E+09	1.84E+09	C	0.296
				6.82E+09			1.96E+09			
				5.55E+09			1.75E+09			
	5	2.79E-05 [4.56]	1.00	8.45E+09	6.98E+09	-	1.82E+10	1.65E+10	A	2.358
				5.82E+09			1.38E+10			
				6.67E+09			1.73E+10			

1 Time indicates whether the sample was collected immediately before or ≈ 4.5 hours after the inhibitor was added.

2 Assay mean is the mean of triplicate Real Time or Real Time RT-PCR reactions for replicate DNA and RNA extracts (Table E-8). The overall mean is the average of the assay means. Log transformation made the assay mean data more symmetric and constant in variance. The log transformed assay mean data were analyzed with Tukey HSD multiple comparisons if ANOVA rejected the null hypothesis of sample equivalence ($\alpha = 0.05$). Samples not sharing a common letter are significantly different ($\alpha = 0.05$).

3 The rRNAt/rDNA metric was calculated with the overall rDNA and rRNAt means for each sample event.

Table 17 *Nitrobacter* molecular data for a respirometric inhibition experiment with acid (Figure 24; Experiment VI).

Sample		H^+ (M) [pH]	Fraction Inhibition	*Nitrobacter* rDNA (copies/L)[2]			*Nitrobacter* rRNAt (copies/L)[2]			rRNAt/rDNA[3]
				Assay Mean	Statistical Analysis		Assay Mean	Statistical Analysis		
Time[1]	Vessel				Overall Mean	Tukey		Overall Mean	Tukey	
Before Inhibitor Dose	3	-	-	7.45E+09	7.48E+09	AB	1.68E+10	1.63E+10	A	2.178
				8.52E+09			1.31E+10			
				6.43E+09			1.88E+10			
After Inhibitor Dose	1	1.91E-07 [7.28]	0.01	7.66E+09	8.04E+09	AB	1.83E+10	1.71E+10	A	2.214
				8.88E+09			1.45E+10			
				8.38E+09			1.68E+10			
	2	4.57E-05 [5.66])	0.48	9.26E+09	8.99E+09	A	1.53E+10	1.48E+10	A	1.644
				9.15E+09			1.51E+10			
				8.50E+09			1.38E+10			
	3	1.78E-05 [5.25]	0.87	7.57E+09	7.76E+09	AB	2.40E+09	2.19E+09	B	0.283
				7.69E+09			2.15E+09			
				7.97E+09			2.02E+09			
	4	9.55E-04 [4.98]	0.99	6.97E+09	7.06E+09	AB	2.25E+09	2.01E+09	B	0.285
				7.12E+09			1.74E+09			
				-			-			
	5	2.63E-04 [4.42]	1.00	7.72E+09	6.18E+09	B	1.45E+10	1.39E+10	A	2.255
				5.21E+09			1.52E+10			
				5.37E+09			1.19E+10			

1 Time indicates whether the sample was collected immediately before or ≈ 4.5 hours after the inhibitor was added.

2 Assay mean is the mean of triplicate Real Time or Real Time RT-PCR reactions for replicate DNA and RNA extracts (Table E-9). The overall mean is the average of the assay means. Log transformation made the assay mean data more symmetric and constant in variance. The log transformed assay mean data were analyzed with Tukey HSD multiple comparisons if ANOVA rejected the null hypothesis of sample equivalence ($\alpha = 0.05$). Samples not sharing a common letter are significantly different ($\alpha = 0.05$).

3 The rRNAt/rDNA metric was calculated with the overall rDNA and rRNAt means for each sample event.

ANOVA of the log transformed *Nitrobacter* rRNAt assay mean data rejected the null hypothesis that transcript abundance was the same in the Experiment V ($F = 53$; p-value < 0.0001) and Experiment VI ($F = 190$; p-value < 0.0001) samples. Subsequent Tukey HSD comparisons were performed to delineate significant differences among the Experiment III (Table 16) and Experiment VI (Table 17) samples. In both experiments, the transcript abundance in uninhibited control samples was the same before and 4.5 hours after acid was added to the remaining vessels (compare the open symbols in Figure 24). This indicated that at the time the acid was added the transcript abundance in all the vessels was high and stable ($\approx 1.5 \times 10^{10}$ copies/L). However, samples from vessels in which the pH was lower than 5.0 were, in both experiments, not significantly different than in the control samples. Conversely, vessels with less severe pH changes exhibited systematically lower transcript abundance as the pH was lowered to near 5.0 (fraction inhibition 1.00). Because of this characteristic, hypothesis I (Section 6.1.3: that transcript abundance in significantly inhibited vessels would be lower than in an uninhibited control vessel) was not fully met for H^+.

Since this unusual result was produced in both experiments, it appeared the ability to process existing transcripts was impaired in *Nitrobacter* cells after a sudden pH change to ≈ 4.5. This effect has been observed in other bacteria. For instance, Cangelosi and Brabant (1997) observed that chloramphenicol, which inhibits rRNAt processing, halted rRNAt depletion in *E. coli* under a variety of growth limiting conditions. Stroot and Oerther (2003) also noted that rRNAt levels remained high in certain strains of *Acinetobacter calcoaceticus* after treatment with the antibiotic chloramphenicol, and inferred that unusually high rRNAt abundance upon *A. calcoaceticus* exposure to different municipal wastewaters indicated inhibiting compounds were present that prevented ribosome synthesis. Georgellis et al. (1992) observed that salt solutions inhibited processing of 5S rRNA, resulting in accumulation of the 9S rRNA precursor. Cangelosi et al. (1996) found that the antibiotics isoniazid or ethambutol did not elicit a decline in *M. tuberculosis* rRNAt. Licht et al. (1999) linked slow growth in *E. coli* to mouse intestinal content inhibition of rRNAt processing (abnormally high rRNAt

abundance at low growth rates). Because both mouse intestinal content and chloramphenicol cells gave ring shaped fluorescent signals during in-situ rRNAt hybridization, Licht et al. (1999) speculated that unprocessed transcripts were stuck in inhibited membrane bound endonucleases. Likewise, the low pH environment in this study may have affected endonuclease activity and hindered processing of existing transcripts. As previously mentioned, one mechanism for low pH inhibition is the lowered cytoplasmic pH that non-specifically inhibits enzyme activity.

***Nitrobacter* rRNAt/rDNA**

The *Nitrobacter* rRNAt/rDNA ratio displayed a clear trend with H^+ and fraction inhibition when the data from Experiments V and VI were combined (Figure 25). The ratio fell below the lower BSNR prediction interval after the pH was lowered to 5.3 - 5.0. Interestingly, this is the same pH range where short term adaptation to acid pH was less successful (Section 6.4.2; Figure 22). This transition from high to what could be considered unusually low ratio values occurred when the fraction inhibition was near 0.80. In this respect, the results for H^+ inhibition were similar to the results obtained with azide. Although the ratio was not much different than in the control vessels when the pH was lowered to 5.8 - 5.6 (fraction inhibition 0.48 - 0.77), these results could have been influenced by adaptation (Section 6.4.2; Figure 23).

Because of the unexpected *Nitrobacter* rRNAt results, there was no apparent difference in the ratio for the uninhibited control vessels and the most severely inhibited vessels at pH ≈ 4.5. Thus, the metric displayed a "U" shaped trend with decreasing pH so that the hypothesis that the ratio would fall below the BSNR lower prediction interval in inhibited vessels (hypothesis II: Section 6.1.3) was only partially met. However, hypothesis III (Section 6.1.3) was still met since the ratio declined monotonically with fraction inhibition (Kendall's τ = -0.714; p-value = 0.0071) and H^+ concentration (Kendall's τ = -0.857; p-value = 0.0009) down to pH 5.0. As previously indicated, other researchers have noted unusually high rRNAt abundance when activity was low, which would produce high rRNAt/rDNA values during low activity (Georgellis et al., 1992; Cangelosi and Brabant, 1997; Licht et al., 1999).

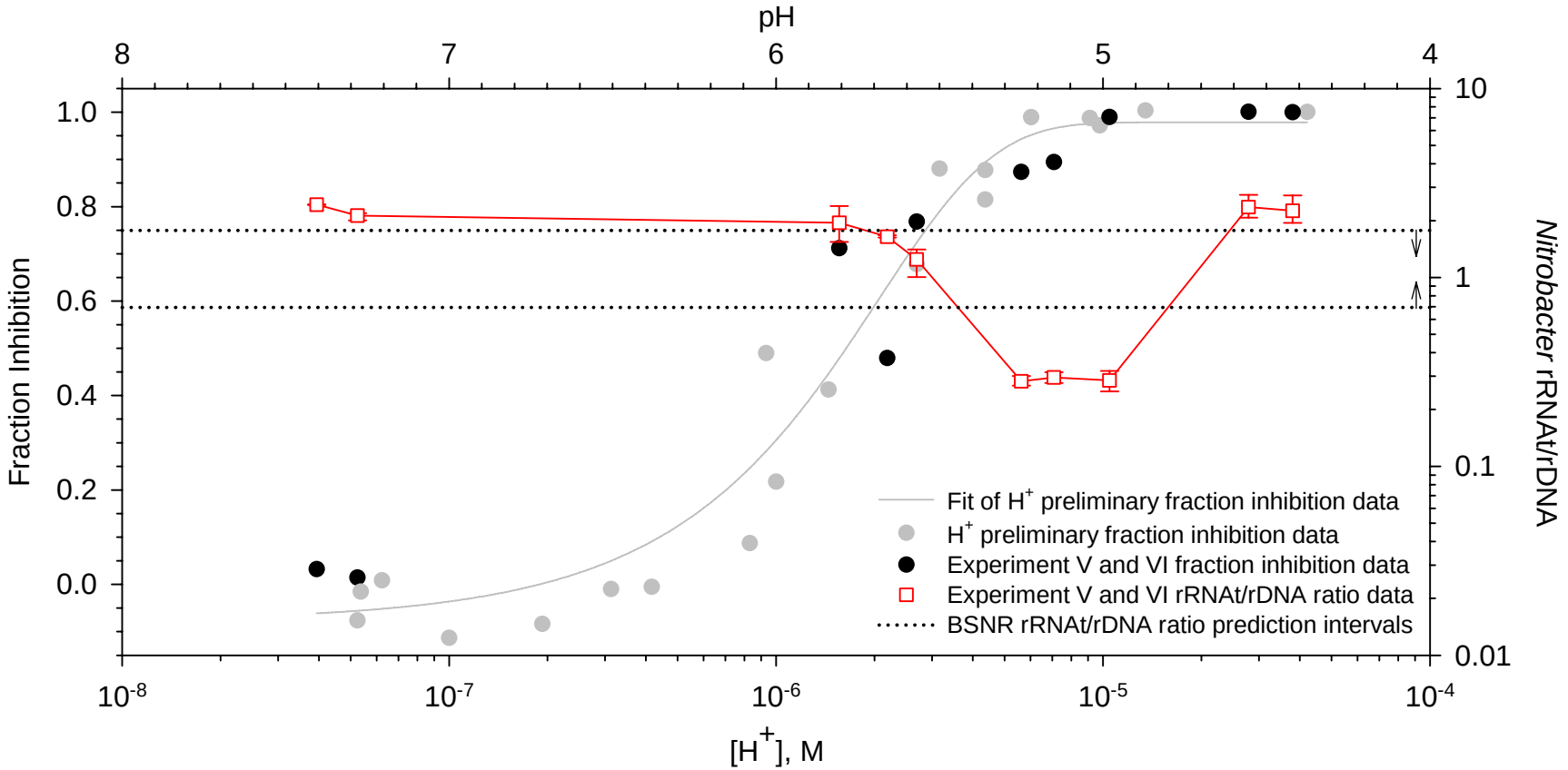


Figure 25 The effect H^+ on the *Nitrobacter* rRNAt/rDNA ratio. *Nitrobacter* rRNAt/rDNA data are provided with a point to point fit (Table 16 and Table 17; error bars are the interquartile range of all possible ratios computed with the rRNAt and rDNA assay means). Horizontal reference lines indicate the upper (↓) and lower (↑) BSNR prediction intervals (Section 5.2). For perspective, the ratio data are plotted with the preliminary experiment dose/response data fitted with a 4 parameter sigmoidal model (SigmaPlot®; adjusted $R^2 = 0.99$). Fraction inhibition results for Experiments V and VI are distinguished and correspond to the ratio datapoints.

6.4.4 Summary

Two respirometric inhibition experiments using acid doses confirmed that at very low pH (≈ 4.5), the expected drop in the *Nitrobacter* rRNAt/rDNA metric with increasing inhibition was disrupted. This trait distinguished the metric response to H^+ from 3,5-DCP and azide and illustrated that it is possible for the metric to exhibit high values while nitrite oxidation activity is low. This emphasizes the utility in measuring and using both rRNAt and rDNA measurements in the metric to assess NOB activity. Should an inhibitor enter a wastewater treatment system that disrupts the expected metric response (unusually low ratio values), the rDNA data could indicate, albeit more slowly, that inhibition was ongoing as reactor washout occurred (declining rDNA abundance). The results also emphasize that traditional indicators for nitrifier activity, such as effluent nitrite and nitrate, remain important. In short, the results for the H^+ inhibition experiments emphasize that the metric cannot be interpreted in a vacuum.

6.5 *Nitrobacter* rRNAt/rDNA Ratio Response to Different Inhibitors

The batch respirometric inhibition experiments were conducted to assess whether the *Nitrobacter* rRNAt/rDNA ratio consistently, significantly, and quickly declined during mechanistically distinct types of inhibition (Section 6.1). More generally, the experiments were designed to assess whether the metric was affected by different inhibition mechanisms, a seemingly important characteristic if this parameter is to be applied to improve nitrification and N-removal during wastewater treatment. In considering this assessment, results for the inhibitors 3,5-DCP, azide, and H^+ were examined on a single plot (Figure 26) so that the metric response at the same inhibition level could be directly compared.

A reasonable question to pose in examining Figure 26 is "at what fraction inhibition level should the *Nitrobacter* rRNAt/rDNA ratio be expected to drop below the lower BSNR prediction interval?" This question was prompted because the ratio fell below the lower BSNR prediction interval at vastly different fraction inhibition levels for 3,5-DCP (≈ 0.05) versus azide and H^+ (≈ 0.80). While others have proposed seemingly

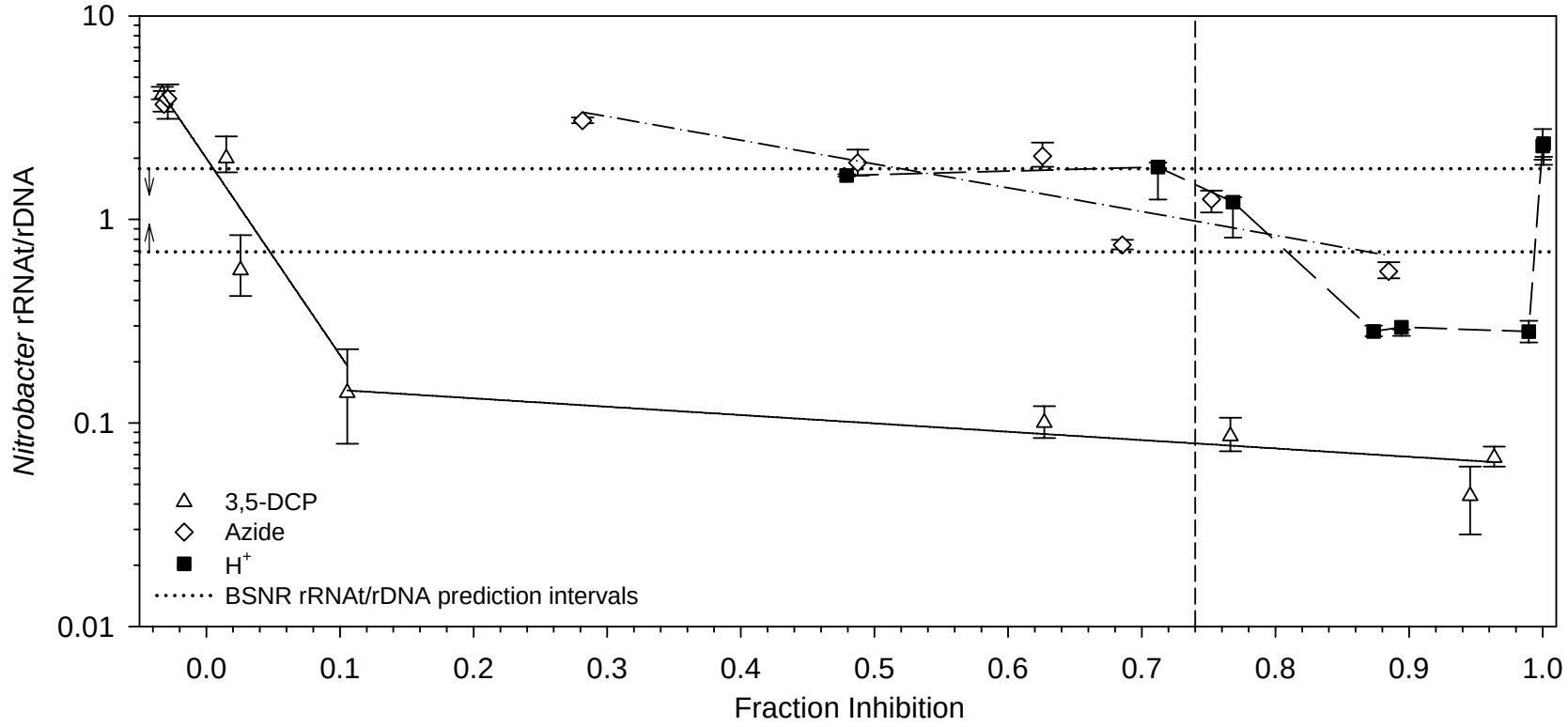


Figure 26 The effect of mechanistically distinct inhibitors on the *Nitrobacter* rRNAt/rDNA ratio. Eight results for the inhibitors 3,5-DCP, azide, and H^+ are plotted by fraction inhibition. The 3,5-DCP data are fit with two linear regression fits (———) to establish the data trend, the first through the fraction inhibition data ≤ 0.10, and the second through fraction inhibition data ≥ 0.10. The azide data are fit with a linear regression (— —) through seven data points for fraction inhibition data ≥ 0.28. All H^+ data are connected by a point to point fit (–·—·-). Horizontal reference lines indicate the upper (⇓) and lower (⇑) BSNR rRNAt/rDNA prediction intervals (Section 5.2). A vertical reference line (– – – –) indicates what could be considered a threshold for "significant" fraction inhibition as discussed in the text.

arbitrary fraction inhibition values as "significant" (e.g. 0.50: Suthersan and Ganczarczyk, 1986), the inhibition data herein were examined contextually by considering the residual nitrite oxidation activity (as mg O_2/L/hr) after the inhibitors had been added (OUR2 in Table E-1, Table E-4, and Table E-7). The residual OUR was corrected for dilution (OUR2V in Table E-1, Table E-4, and Table E-7) and compared directly with the rate of oxygen utilization required in the BSNR (by the NOB only) to maintain high nitrification efficiency. In order for the reactor to produce negligible effluent nitrite at an influent rate of 1,500 mg NH_4^+-N/day (assuming all the influent ammonia is oxidized to nitrite), NOB within the reactor would have to oxidize 62.5 mg NO_2^--N/hr, which corresponds to an oxygen demand of 71.4 mg O_2/hr. Because the reactor was operated in continuous-fed batch mode, the operating volume increased from 10 to 12.7 L every 48 hours (Section 3.2.3). Thus, nitrite buildup would be incipient in the BSNR if the NOB portion of the reactor oxygen demand fell below 5.6 mg O_2/L/hr. Rather than compare individual OUR2V data from the inhibition experiments with this value, all fraction inhibition data from the experiments that exceeded 0.50 were paired with the corresponding OUR2V data and fit with a linear regression (Figure 27). Using this fit, a fraction inhibition value of 0.74 corresponded to 5.6 O_2/L/hr. This provided an answer to posed question: because the lower BSNR prediction interval for the metric was established under high nitrification efficiency (i.e. while little nitrite was present in the reactor), the metric could reasonably be expected to decline below the lower BSNR prediction interval only if the fraction inhibition exceeded 0.74. This threshold was added to Figure 26 to allow the data to be examined not only in terms of the trends for different inhibitors, but also in terms of the total residual nitrite oxidation activity, and hence the potential impact on BSNR nitrification performance.

The data in Figure 26 indicate, unequivocally, that the *Nitrobacter* rRNAt/rDNA ratio can have different values at the same fraction inhibition level during short term (4.5 hours) exposure to mechanistically distinct inhibitors. For 3,5-DCP, the ratio data fell below the lower BSNR prediction interval at low fraction inhibition levels ($\approx$ 0.05), and thereafter fell from 0.2 to < 0.1 as the fraction inhibition increased to 0.95. Moreover, the

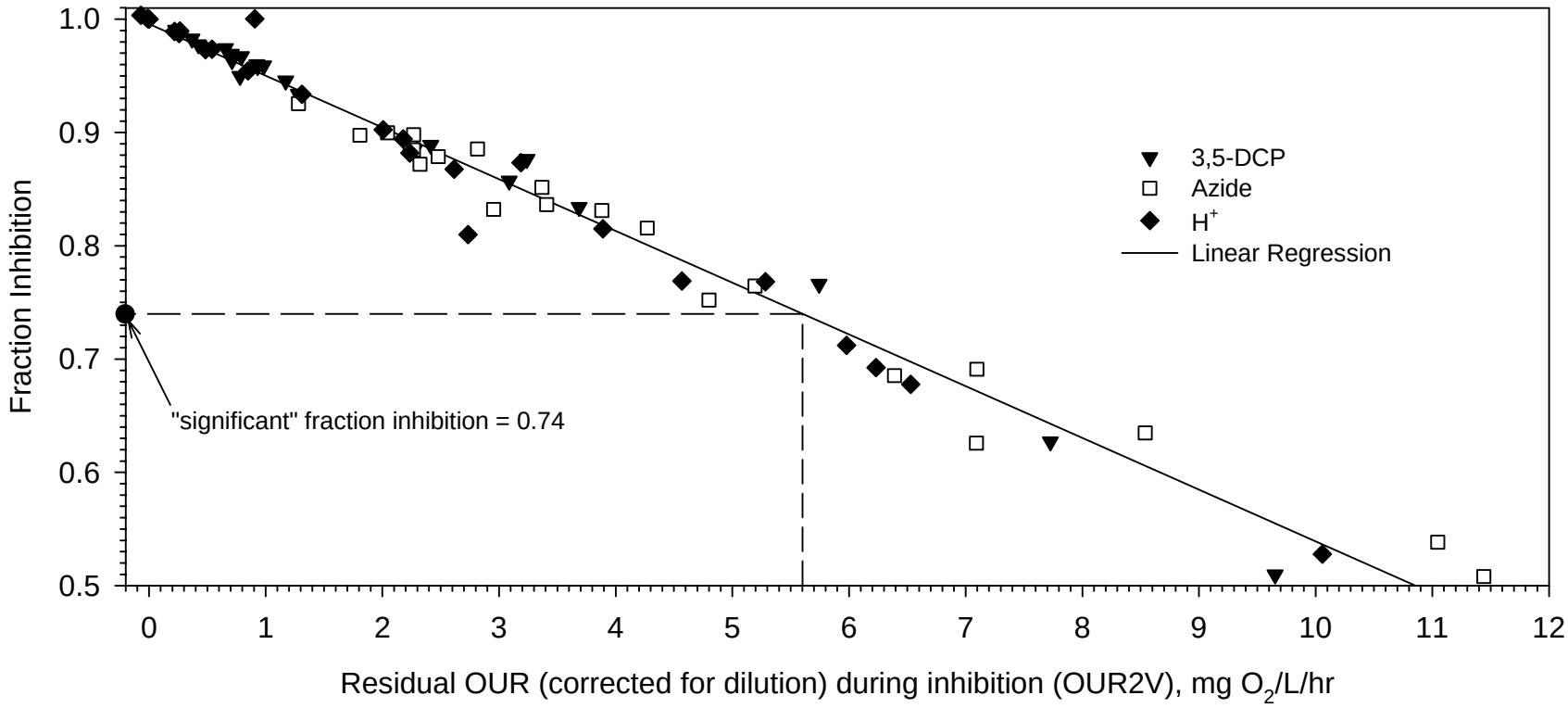


Figure 27 An examination of the residual nitrite oxidation activity in BSNR samples during batch respirometric inhibition experiments when the fraction inhibition exceeded 0.50. The collective data were fit with a linear regression that was subsequently used to infer a "significant" fraction inhibition level. Ostensibly, this fraction inhibition level represents a threshold of nitrite oxidation activity above which nitrite buildup would be expected to occur in the BSNR.

metric dropped to much lower values on exposure to 3,5-DCP (< 0.10 at fraction inhibition > 0.80) versus azide (0.6 at fraction inhibition ≈ 0.90) and H^+ (0.3 at fraction inhibition 0.85 - 1.00). Thus, most of the 3,5-DCP ratio observations were below the lower BSNR prediction interval even though the total residual nitrite oxidation activity would not result in a decrease in BSNR treatment performance. Conversely, the azide and H^+ ratio data fell below the lower BSNR prediction interval at much higher fraction inhibition values (> ≈ 0.80) that were interestingly near the threshold at which an adverse impact on BSNR performance could be expected. A final divergent aspect of the H^+ data was that at high doses the expected metric response disappeared.

6.6 Inhibition Experiment Quality Control

Although respirometric inhibition techniques have long been used for activated sludge toxicity testing (Koopman and Bitton, 1986), application for the nitrifiers is complicated by potential heterotrophic (King and Dutka, 1986) and nitrifier (Ginestet et al., 1998) endogenous respiration and by the fact that AOB provide nitrite for the NOB. To make respirometric activity assessments of nitrifiers discriminatory and accurate some researchers have used parallel reference cultures (Strotman and Eglsäer, 1995) or AOB and NOB specific inhibitors (Gernaey et al., 1997; Ginestet et al., 1998). However, even with these corrections the respirometric technique is ultimately a surrogate measure of activity (King and Dutka, 1986). Hence, other researchers have opted to use a decrease in the nitrite consumption rate or nitrate production rate to assess NOB inhibition (Hockenbury and Grady, 1977; Williamson and Johnson, 1981; Svenson et al., 2000, Grunditz and Dalhammer, 2001), though this provides much less descriptive data. Since the BSNR enrichment displayed insignificant endogenous respiration, and since excess ammonia was easily removed from BSNR samples prior to conducting the inhibition experiments, corrections for endogenous respiration and AOB aerobic activity were not made in this study. However, samples were frequently collected during the inhibition experiments at the start of the assays, immediately prior to inhibitor addition, and ≈ 4.5 hours later to assure that the respirometric technique was unbiased and accurate. These

samples were analyzed for nitrite and the resulting data was used to calculate the fraction inhibition independently as a decrease in the nitrite oxidation rate:

$$\text{Fraction Inhibition} = \frac{\text{NOR1} - \text{NOR2}}{\text{NOR1}} \quad (14)$$

where NOR1 = nitrite oxidation rate before inhibtor dose
NOR2 = nitrite oxidation rate after inhibitor dose

The NOR fraction inhibition results are provided in Table E-1, Table E-4, and Table E-7 for the 3,5-DCP, azide, and H^+ inhibition experiments, respectively. The results were combined with the respirometric fraction inhibition calculations (86 paired data) and fit with a linear regression (Figure 28). The slope was not significantly different from 1 (95% confidence interval: 0.99 to 1.04) and the intercept included the origin (95% confidence interval: -0.030 to +0.001). The root mean square error was low (0.04) and a residuals plots indicated homogeneity of variance (Figure 28). Further, the null hypothesis that the residuals were normally distributed about the regression line could not be rejected (Shapiro Wilk W Test: p-value = 0.569). Thus, it was concluded that the regression line was an appropriate fit of the paired NOR/OUR data, and from the line characteristics, the OUR based fraction inhibition calculations were seen to be unbiased and accurate.

6.7 Summary

The rRNAt/rDNA metric value dropped significantly and consistently when BSNR mixed liquor samples were exposed to three inhibitors. Literature reviews indicated these compounds were mechanistically distinct, and quality control testing indicated that the inhibition data for these substances was reliable. Since the metric was measured after only 4.5 hours exposure to the inhibitors, a significant response could be considered to occur quickly relative to reactor nitrification efficiency changes (investigated further in Chapter 8.0). Thus, the metric has potential utility in improving nitrification and N-removal during wastewater treatment by quickly signaling changes in

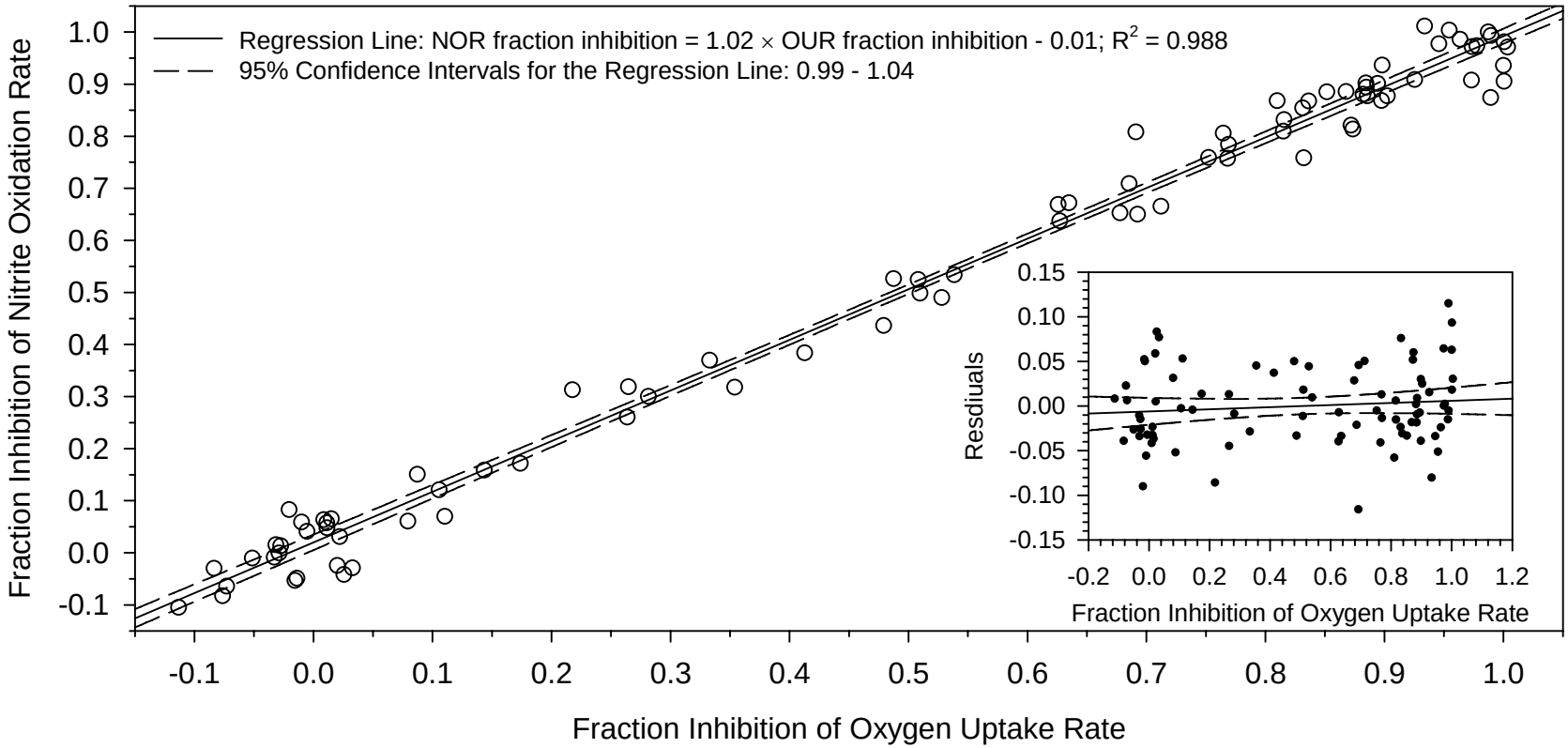


Figure 28 A plot of paired NOR and OUR inhibition calculations from the 3,5-DCP, azide, and H^+ respirometric inhibition experiments. The data were fit with a linear regression line and 95% confidence intervals for the line slope. The inset graph is a plot of the regression line residuals which were also fit with a linear regression and 95% confidence intervals for the slope.

the NOB activity level. Because the short term metric response varied for the different inhibitors, it may be possible to infer an unknown inhibitor's mechanistic effect based on the *Nitrobacter* rRNAt/rDNA metric behavior. For example, an unusually low ratio with concomitant high NOB activity followed by NOB washout (declining rDNA abundance) could indicate that a component in the influent wastewater affected growth processes. Conversely, washout at high ratio values could indicate rRNAt processing was inhibited. This could prove to be powerful information in narrowing the search for inhibiting substance in specific industrial discharges, particularly when combined with quantitative structure activity information (Escher and Schwarzenbach, 2002).

CHAPTER 7.0

BATCH AMMONIA INHIBITION EXPERIMENTS

7.1 Introduction

Free ammonia was one of four inhibitors used in batch respirometric inhibition experiments (Figure 14). However, this compound did not significantly inhibit nitrite oxidation in this study if the concentration was held constant by inhibiting the AOB. Subsequently, a study of NOB inhibition was conducted while the ammonia concentration was elevated, but with uninhibited AOB.

7.2 Free Ammonia Inhibition of Nitrite Oxidation

7.2.1 The inhibition mechanism

Ammonia exists in two forms (Section 2.1.1): the ammonium ion (NH_4^+), which is generally not perceived to be inhibitory, and unionized ammonia gas (free ammonia, NH_3), which is widely reported to inhibit NOB (Table 2), though a lack of consensus exists for this premise (Section 2.3.4). The two forms vary in proportion to one another with pH and temperature (Equations 3 - 5), but the ammonium ion is the dominant form at pH < 8.5 (pKa ≈ 9.25).

Although the mechanism for free ammonia inhibition of NOB and other bacteria is unknown, some possibilities have been investigated. Yang et al. (2004) linked free ammonia to decreased cell hydrophobicity and polysaccharide production. Thus, NOB inhibition could be caused or exacerbated by high free ammonia concentrations that interfere with the ability to form and incorporate into biofilms or flocs, which is a notable characteristic of some *Nitrobacter* strains (Watson et al., 1989). Since the NOB are especially slow growers, this could make them more susceptible to reactor washout. However, in batch inhibition assays this mechanism may be unimportant.

It is also possible that ammonia (and amines in general) inhibit NOB by collapsing the ΔpH component of the proton motive force (Dawes, 1986). In *N. agilis*, ΔpH was dissipated completely by > 140 mg-N/L at pH 7.0 (Kumar and Nicholas, 1983). However, the effect was only partial for the ΔΨ component at much higher ammonia concentrations (1,400 mg-N/L, pH 7.0). This indicated that NOB activity is possible even assuming a membrane potential is required for nitrite oxidation (Chen and Suzuki, 2004), and likely makes this mechanism ancillary.

As noted in Section 2.3.5, low DO, rather than free ammonia, has been linked to NOB inhibition when the total ammonia concentration is high. For example, a lack of significant short term nitrite oxidation inhibition was noted in batch tests by Fux et al. (2003) at high free ammonia concentrations (80 mg-N/L). These researchers attributed NOB inhibition to limited DO supply (short aeration periods) and designed a sequencing batch reactor based on this principle for denitritification (Section 2.4.1). Their premise can be construed to mean that high free ammonia correlates with low DO as a result of high AOB activity. However, many other researchers (Table 2: e.g. Yang and Alleman, 1992) have observed nitrite buildup in reactors with high free ammonia concentrations when the bulk DO was continuously high, and have assumed that DO could not limit nitrite oxidation since the NOB oxygen half saturation coefficient (Table 3) was exceeded.

In summary, the mechanism(s) for free ammonia inhibition of the nitrite oxidizers is almost wholly undescribed (Bock and Wagner, 2001), though the effect could be exacerbated by low DO concentration. Since a systematic batch study of free ammonia inhibition of the NOB was absent from the literature, one was undertaken in this study, but using appropriate controls for AOB activity (Table 2) at high bulk DO concentrations.

7.2.2 Preliminary free ammonia inhibition experiments

Preliminary respirometric inhibition experiments were conducted under the assumption that free ammonia significantly inhibited nitrite oxidation (Figure 14). The confounding effect of low DO was eliminated from concern by: (1) testing the DO concentration within respirometric vessels while the oxygen demand was high (> 10

mg/L/hr), which verified that the bulk DO concentration was at saturating levels, and (2) inhibiting AOB activity, which eliminated competition for oxygen, and also held the free ammonia concentration constant. Thus, a change in the inhibition assay design presented in Section 6.1.2 was the addition of 50 μM ATU to inhibit ammonia oxidation (Section 2.3.2). Additionally, to obtain high free ammonia concentrations, it was necessary to raise the pH at the beginning of the assay from the reactor setpoint (≈ 7.2) to 7.5 or 8.0. This was accomplished by adding 5 N NaOH. Since ammonia is a weak acid, it was also necessary to add NaOH with the doses to maintain the desired pH.

Surprisingly, free ammonia did not significantly inhibit nitrite oxidation (fraction inhibition > 0.74: defined in Section 6.5) even at very high free ammonia concentrations (72 mg-N/L: Table 18). In fact, the inhibition noted likely resulted, at least in part, from the pH changes (Suthersan and Ganczarczyk, 1986). A lack of free ammonia inhibition of NOB was also noted by Fux et al. (2003) and Chung et al. (2005) when ammonia oxidation was inhibited in their batch assays.

Table 18 BSNR NOB inhibition experiments with free ammonia.

Preliminary Experiment	pH Adjusted	pH after dose added	Ammonia Dose (mg-N/L)		Fraction Inhibition
			Ionized	Free	
1	No	7.26	49	0.7	0.07
		7.18	98	1.2	0.09
		7.12	147	1.6	0.14
		7.06	243	2.2	0.18
		6.94	475	3.3	0.19
2	Yes	7.49	196	4.9	0.49
		7.50	392	10.0	0.49
		7.49	588	14.6	0.47
		7.50	787	20.0	0.50
		7.49	980	24.4	0.49
3	Yes	8.00	93	7.5	0.52
		8.01	185	15.2	0.56
		7.99	370	29.1	0.54
		7.98	690	53.0	0.62
		7.99	913	71.9	0.58

7.3 Inhibition of Nitrite Oxidation during High AOB Activity

7.3.1 Hypothesis for NOB inhibition during high AOB activity

In response to the results presented in Table 18, an alternate hypothesis was tested in which high AOB activity was predicted to inhibit nitrite oxidation as a result of poor NOB competition for oxygen (Section 2.3.5). As previously noted, the DO concentration was measured at near saturating concentrations in the respirometric vessels, but there is evidence that NOB oxygen limitation can occur when the bulk DO concentration is high. For instance, microelectronic probes have demonstrated that the DO concentration within biomass flocs and biofilms can be much lower than in the bulk solution, even if the bulk DO is at saturating values (Schramm et al., 1996). Interestingly, nitrite and nitrate profiles along with FISH have indicated that NOB occupy the inner realm of flocs and biofilms relative to the AOB (Schramm et al., 1996; Okabe et al., 1999). This could make the NOB more susceptible to DO limitation during high aerobic activity, for instance, when excess ammonia is present. Further, some researchers have observed nitrite buildup at high DO concentrations that could have been caused by poor NOB competition for oxygen. For example, Yun and Kim (2003) operated an upflow bench scale biofilm reactor with enriched nitrifier biomass and found that at high DO concentrations (3.0 - 6.4 mg/L) NOB were largely inactive. They attributed this to high free ammonia concentrations in the initial stages of their reactor. However, nitrite buildup was eliminated after a progressive decrease in the ammonium loading rate. Thus, their results could alternately indicate that even at high bulk DO concentrations, the NOB were oxygen limited as a result of high AOB activity. Also, Peng et al. (2004) observed nitrite buildup in a SBR at bulk DO concentrations between 2 - 6 mg/L, and were able to use intermittent aeration to control the nitrite buildup.

7.3.2 Method

Two batch respirometric inhibition experiments were conducted to distinguish between NOB inhibition caused by free ammonia and high AOB activity. To

accommodate ammonia oxidation during these experiments, the inhibition assay in Section 6.1.2 was modified by seeding BSNR mixed liquor samples into 200 mM PO_4^{-3} buffer (pH = 7.2 ± 0.2; final concentration 100 mg NO_2^--N/L). The buffer prevented the pH from dropping more than 0.2 pH units while a 200 mg NH_4^+-N/L (total ammonia) dose was oxidized. The two experiments were identical, with each including five vessels that, in combination, isolated the potential inhibiting effect of the phosphate buffer, ATU, free ammonia, and high AOB activity on nitrite oxidation. The first experiment was preliminary and included frequent nitrogen sampling to document AOB and NOB activity trends. This experiment indicated NOB activity was significantly inhibited with ammonia present, but only if the ammonia was being oxidized. Subsequently, the experiment was repeated to confirm the preliminary results (designated Experiment VII; a continuation of the numbering from Chapter 6.0) and to test the hypothesis that the *Nitrobacter* rRNAt/rDNA ratio would be below the lower BSNR prediction interval (Section 5.2) as nitrite accumulated:

H_0: *Nitrobacter* rRNAt/rDNA during high AOB activity > 0.69

H_1: *Nitrobacter* rRNAt/rDNA during high AOB activity < 0.69

7.3.3 Results

The results for the experiments were virtually identical; therefore, respirometric data are analyzed only for Experiment VII (Figure 29). Table 19 contains the inhibition results for both the preliminary experiment and Experiment VII, and provides the vessel composition. Because of the large sample volume required for replicate DNA and RNA sampling in Experiment VII, nitrogen samples were not collected. Thus, nitrogen data are analyzed only for the preliminary experiment.

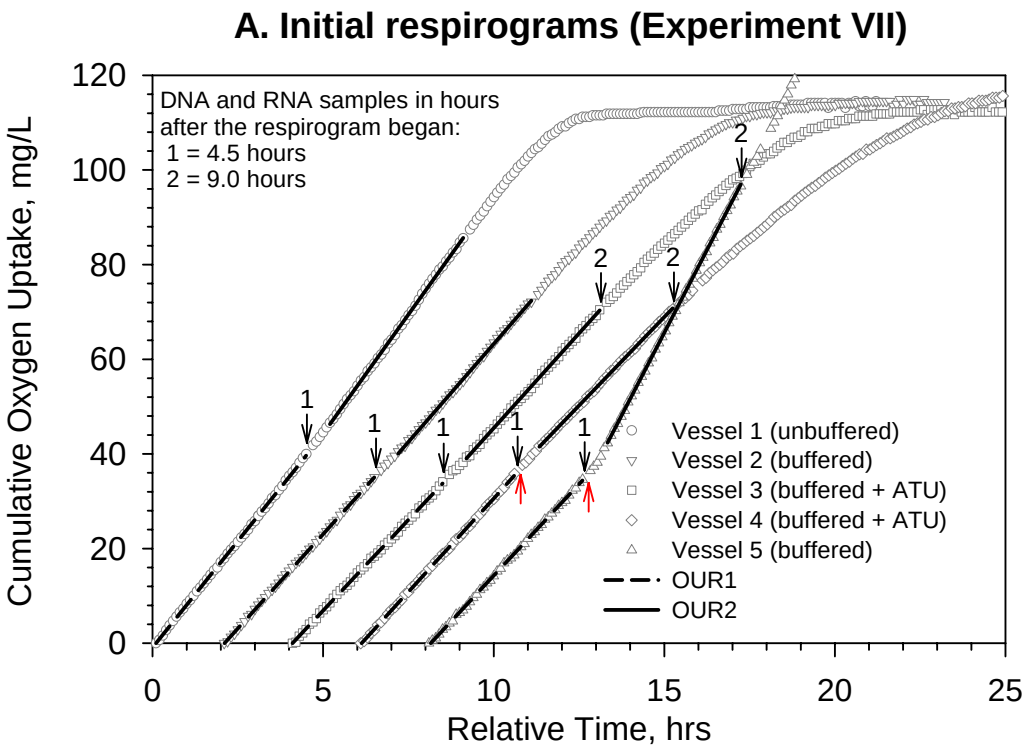
Respirometric data analysis: the first 10 hours of aerobic activity

A minimum of 10 hours of cumulative oxygen uptake data is presented for all vessels in Experiment VII in Figure 29-A. The initial oxygen uptake rate (OUR1) in an unbuffered vessel (vessel 1: 8.99 mg/L/hr) was 13% higher than in the remaining

Figure 29 An evaluation of NOB inhibition at high ammonia concentrations with inhibited and uninhibited AOB present.

A. Respirometric results for Experiment VII. Five vessels were prepared using 500 ml BSNR mixed liquor samples by diluting them into unbuffered (vessel 1) or buffered (200 mM PO_4^{-3}; vessels 2-5) nitrite solutions (final concentration 100 mg-N/L). The buffer alternately did (vessels 3 and 4) or did not (vessels 2 and 5) contain 50 μM ATU to inhibit AOB activity. Vessels 4 and 5 received doses of ammonia (final total ammonia concentration 200 mg-N/L) at the time indicated (↑). Aerobic activity was observed in all vessels simultaneously in a respirometer, but the respirograms have been offset in time to make each one clearly visible. Each respirogram was fit with linear regressions to established the oxygen uptake rates before (OUR1) and after (OUR2) ammonia was added to vessels 4 and 5 (fraction inhibition results provided in Table 19). DNA and RNA samples were collected at the time points indicated (↓). Vessels 1 - 4 did not display significant aerobic activity beyond the time frame presented.

B. The complete respirogram for vessel 5 is presented for both the preliminary experiment and Experiment VII (Table 19). The oxygen uptake rates were calculated as the slope of a best fit line through the previous 1 hour of cumulative oxygen uptake and time data. DNA and RNA samples were collected in Experiment VII at the time points indicated (↓). Ammonia (final total ammonia concentration 200 mg-N/L) was added at the time indicated (↑).


A. Initial respirograms (Experiment VII)
DNA and RNA samples in hours
after the respirogram began:
1 = 4.5 hours
2 = 9.0 hours
Vessel 1 (unbuffered)
Vessel 2 (buffered)
Vessel 3 (buffered + ATU)
Vessel 4 (buffered + ATU)
Vessel 5 (buffered)
OUR1
OUR2
Cumulative Oxygen Uptake, mg/L
Relative Time, hrs
0
20
40
60
80
100
120
0
5
10
15
20
25

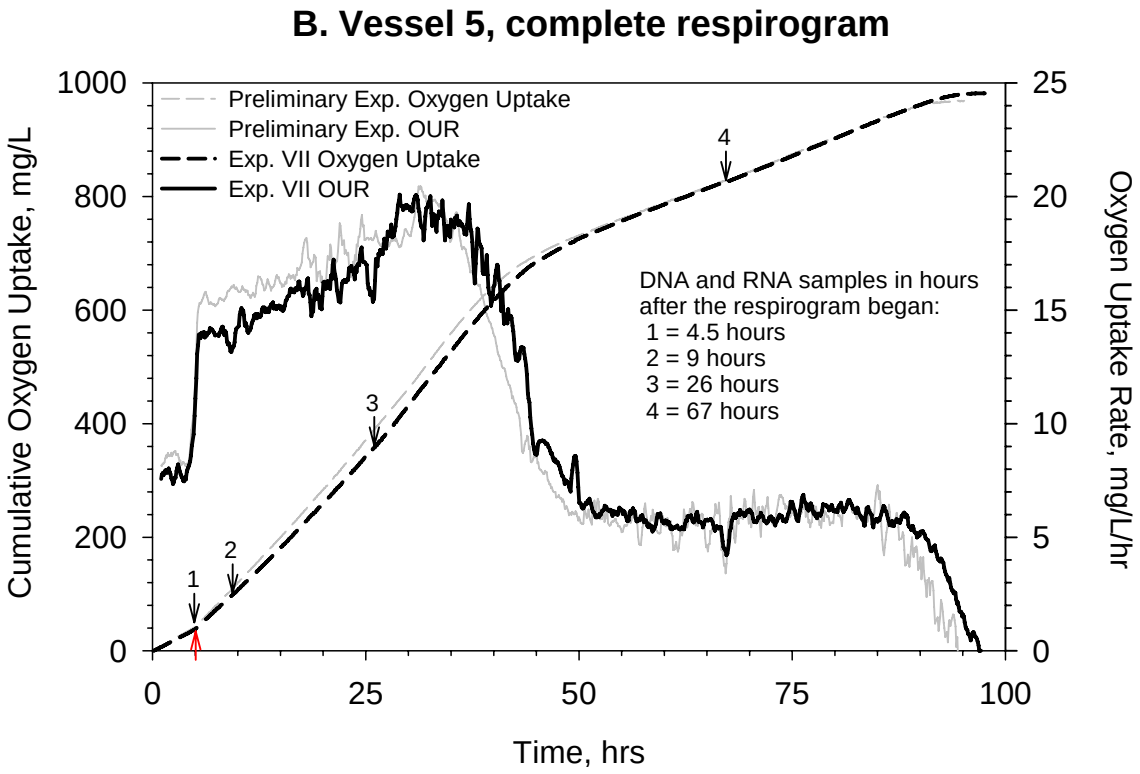

B. Vessel 5, complete respirogram
Preliminary Exp. Oxygen Uptake
Preliminary Exp. OUR
Exp. VII Oxygen Uptake
Exp. VII OUR
DNA and RNA samples in hours
after the respirogram began:
1 = 4.5 hours
2 = 9 hours
3 = 26 hours
4 = 67 hours
Cumulative Oxygen Uptake, mg/L
Oxygen Uptake Rate, mg/L/hr
Time, hrs
0
200
400
600
800
1000
0
5
10
15
20
25
0
25
50
75
100

Table 19 The results for two batch respirometric inhibition experiments using the BSNR biomass and ammonia doses.

Experiment (Figure)	Vessel	Dilution Media[1]		ATU[2]	OUR1[3]		Ammonia-N		OUR2[3]		Fraction Inhibition[4]		
		Unbuffered	Buffered		Slope	R^2	Total	Free	Slope	R^2	OUR	NOR	vs. vessel 1
Preliminary	1	✓	-	-	9.42	0.9996	-	-	10.15	0.9997	-0.08	-	-
	2	-	✓	-	8.35	0.9995	-	-	7.99	0.9994	0.04	-0.06	0.11
	3	-	✓	✓	8.12	0.9998	-	-	8.31	0.9996	-0.02	-0.01	0.14
	4	-	✓	✓	8.21	0.9997	200	2.63	7.73	0.9996	0.06	0.12	0.13
	5	-	✓	-	8.47	0.9998	200	2.63	15.42	1.0000	-0.82	1.51	0.10
Experiment VII (Figure 29)	1	✓	-	-	8.99	0.9995	-	-	10.08	0.9996	-0.12	-	-
	2	-	✓	-	7.91	0.9997	-	-	8.28	0.9995	-0.05	0.05	0.12
	3	-	✓	✓	7.62	0.9995	-	-	8.01	0.9996	-0.05	0.07	0.15
	4	-	✓	✓	7.89	0.9996	202	2.85	7.98	0.9998	0.05	0.11	0.12
	5	-	✓	-	7.77	0.9996	202	2.85	13.98	0.9999	-0.80	1.49	0.14

1 500 ml BSNR mixed liquor samples were diluted into 500 ml of deionized water with no pH adjustment or ≈200 mM PO_4^{-3} at pH 7.2, each containing 200 mg/L of nitrite-N.
2 500 µl of 0.1 M Allylthiourea added as an AOB inhibitor.
3 Oxygen uptake rates measured ≈ 4.5 hours before (OUR1) and ≈ 4.5 hours after (OUR2) ammonia doses: linear regression fit of the oxygen consumption data (mg/L/hr).
4 Fraction inhibition = [(OUR1-OUR2)/OUR1] or [(NOR1-NOR2)/NOR1] (obtained with nitrite samples); also shown is % difference between OUR1 in vessel 1 and vessels 2-5 (vs. vessel 1 column) which indicated the phosphate buffer slightly inhibited nitrite oxidation.

buffered vessels (vessels 2 - 5: range 7.62 - 7.91 mg/L/hr) (Table 19: note that similar results were obtained in the preliminary experiment). Thus, the phosphate buffer appeared to slightly inhibit nitrite oxidation. Increasing concentrations of a phosphate buffer were also reported to inhibit *N. agilis* cytochrome oxidase (98% reduction between 10 and 150 mM; Yamanaka et al., 1981).

Experiment VII included buffered vessels which did (vessels 3 and 4) and did not (vessels 2 and 5) contain 50 μM ATU. The initial OURs in the buffered vessels without ATU (7.91 and 7.77 mg/L/hr in vessels 2 and 5, respectively) were similar to the initial OURs in buffered vessels with ATU (7.62 and 7.89 mg/L/hr in vessels 3 and 4, respectively) (Table 19: note that similar results were obtained in the preliminary experiment). Thus, ATU did not affect NOB activity. This agreed with previous inhibition experiments in which 50 μM ATU completely inhibited AOB aerobic activity but had no effect on nitrite oxidation (data not shown; also, see Section 2.3.2).
Experiment VII included a buffered vessel that received ATU and a 200 mg-N/L dose of total ammonia after approximately 4.5 hours of nitrite oxidation (vessel 4: 2.85 mg NH_3-N/L). The respirogram for this vessel did not indicate a significant decrease occurred in aerobic activity after the ammonia addition (Figure 29-A) (Table 19 - fraction inhibition = 0.05: note that similar results were obtained in the preliminary experiment). Thus, free ammonia did not significantly inhibit nitrite oxidation. This was expected based on the results previously presented in Table 18.

The vessels that did not receive ammonia, or that contained inhibited AOB and received ammonia, consumed a stoichiometric amount of oxygen for nitrite oxidation (vessels 1 - 4; ≈ 114 mg/L O_2 for 100 mg NO_2^--N/L) prior to the OUR declining to ≈ 0 mg/L/hr. These vessels did not show significant aerobic activity beyond the time frames presented in Figure 29-A. This confirmed the absence of aerobic AOB activity in the buffered vessel with ATU (vessel 4) and also indicated that the respirometer accurately recorded oxygen consumption. Similar results were obtained in the preliminary experiment.

Conversely, the ammonia dose caused an immediate and substantial increase in the oxygen uptake rate in a buffered vessel with uninhibited AOB (vessel 5: Figure 29-B). The OUR increased from 7.77 to 13.98 mg/L/hr, an 80% increase (Table 19: note that similar results were obtained in the preliminary experiment). This increase was expected since the AOB were not inhibited.

Respirometric data analysis: Aerobic activity after 10 hours had elapsed (vessel 5)

Aerobic activity continued for several days following a 200 mg-N/L dose of total ammonia in the buffered vessel without ATU (Figure 29-B). In fact, oxygen consumption increased from approximately 14 to 20 mg/L/hr during the 33 hour time period which followed the ammonia dose. Oxygen utilization slowed between 37 and 50 hours into the assay, which was reflected by a smooth break in the cumulative oxygen uptake curve and a steady decrease in the OUR (from 20 down to 5 - 6 mg/L/hr). This decrease in aerobic activity suggested that ammonia was completely oxidized ≈ 50 hours after the dose was added. Thereafter, for a time period of ≈ 35 hours aerobic activity was lower than initially observed with just nitrite present (≈ 5 - 6 mg/L/hr). Oxygen utilization declined and then stopped after ≈ 95 hours.

These results suggested that the added ammonia and nitrite was oxidized to nitrate within approximately 90 hours of the ammonia spike. Interestingly, the OUR between 50 - 85 hours (≈ 5 - 6 mg/L/hr) was approximately 30% lower than the initial OUR in both the preliminary experiment and Experiment VII (Figure 29-B). This indicted that the long (40 hours) period of high AOB activity negatively impacted nitrite oxidation even after the ammonia was depleted (confirmed with the nitrogen data). Other researchers have found that NOB inhibition recovery was adversely affected by prolonged high AOB activity (Yun and Kim, 2003) and inhibitor exposure (Suthersan and Ganczarczyk, 1986).

N-data in a vessel with uninhibited AOB following an ammonia dose (vessel 5)

Nitrogen samples were collected frequently from vessel 5 during the preliminary experiment (Figure 30) and revealed that variations in aerobic activity evident in Figure 29-B corresponded to changes in AOB and NOB activity. This data was assumed to be representative of Experiment VII (see the similar OUR profiles in Figure 29-B).

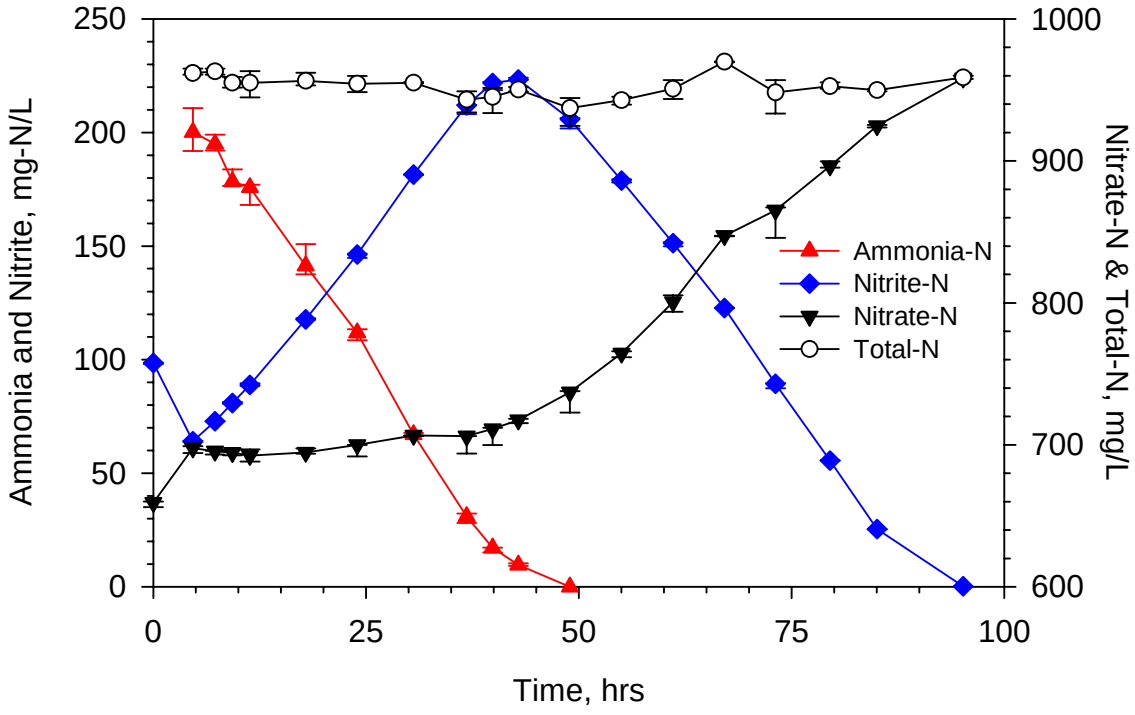


Figure 30 Soluble nitrogen data for vessel 5 during a preliminary ammonia inhibition experiment with uninhibited AOB.

Prior to the ammonia addition, nitrite decreased from 99 to 64 mg-N/L, while nitrate increased from 659 to 697 mg-N/L (Figure 30). Thus, the nitrite removed (≈ 35 mg-N/L) could be accounted for as nitrate produced (≈ 38 mg-N/L). Further, the stoichiometry for oxygen consumption (1.10 mg O_2/mg nitrite-N) was near the theoretical value for nitrite oxidation (1.14 mg O_2/mg nitrite-N). This indicated the respirometer accurately recorded a period of high NOB aerobic activity prior to the ammonia dose.

Ammonia was added at 4.6 hours and thereafter steadily decreased from 201 to 10 mg-N/L by 42.9 hours (Figure 30). When examined in context with the respirometric data (Figure 29-B), this confirmed that AOB activity increased substantially and almost immediately following the ammonia dose. After 42.9 hours, the ammonia oxidation rate slowed, and by 49.0 hours ammonia was undetectable. A Kendall-Theil best fit line through the ammonia data between 4.6 and 42.9 hours indicated the rate of change was -5.29 mg-N/L/hr (95% confidence interval: -5.86 to -4.59 mg-N/L/hr).

Concomitantly during this time frame (4.6 - 42.9 hours) nitrite increased from 64 to 223 mg-N/L (Figure 30). A Kendall-Theil best fit line through the nitrite data indicated the rate of change was +4.52 mg-N/L/hr (95% confidence interval: +3.92 to +4.78 mg-N/L/hr). Since more nitrite-N accumulated than was added as ammonia-N, NOB activity was clearly low during this time period. This assessment was confirmed by the nitrate concentration, which remained virtually unchanged (697 mg-N/L at 4.6 hours; 717 mg-N/L at 42.9 hours). Further, the slope of a Kendall-Theil best fit line through the nitrate data was not significantly different than 0 (0.21 mg-N/L/hr; 95% confidence limit: -0.52 to 0.42 mg-N/L/hr). Thus, of the ammonia that disappeared during this time frame (191 mg-N/L), 84% (159 mg-N/L) could be accounted for as accumulated nitrite, 10% (20 mg-N/L) could be accounted for as accumulated nitrate-N, and 6 % (12 mg-N/L) could not be accounted for but was likely consumed as an N-source for growth by the AOB (Grady et al., 1999). Similar N-losses have been reported for nitrifier enrichments in a biofilm reactor (5%; Bernet et al., 2001), in batch suspended growth reactors (3 - 7%; Pollice et al., 2002), and in a mixed culture treating potato starch wastewater (7%; Abeling and Seyfried, 1992). Thus, it appeared that while ammonia was present in the reactor, NOB activity was low, but only if the ammonia was being oxidized. This

inference was based on the results for vessel 4, in which NOB activity was not significantly inhibited by an identical ammonia dose when the AOB were inhibited with ATU.

The nitrite and nitrate data trends changed significantly between 39.9 and 55.0 hours, a time period that was concomitant with ammonia exhaustion and a decrease in the OUR (Figure 29-B). Nitrite data changed from increasing over time to decreasing over time, while the nitrate data increased significantly for the first time since ammonia was added to the vessel. Thus, the nitrogen and respirometric data taken together indicate that between 33.9 and 55.0 hours, a transition from low to high nitrite oxidation activity occurred that was concomitant with a change from high to low ammonia oxidation activity.

Between 55.0 - 85.1 hours, nitrite steadily disappeared while nitrate increased (Figure 30). The slope of a Kendall-Theil best fit through the nitrite data indicated the rate of change was -4.73 mg-N/L/hr (95% confidence limit: -4.24 to -5.36 mg-N/L/hr). A similar slope through the corresponding nitrate data indicated a rate of change of +5.33 mg-N/L/hr (95% confidence limit: + 4.85 to +5.98 mg-N/L/hr). During this same time period, the OUR was approximately 5.5 mg/L/hr (Figure 29-B). Thus, the stoichiometry for nitrite oxidation (1.16 mg O_2/mg NO_2^--N) and nitrate production (1.03 mg O_2/mg NO_3^--N) was near the theoretical value (1.14 mg O_2/mg NO_x^--N). The nitrite and nitrate data trends terminated with nitrite exhaustion between 85.1 and 95.2 hours (Figure 30). This was concomitant with the disappearance of aerobic activity from the vessel (Figure 29-B). Thus, between 55.0 - 85.1 hours, NOB activity was high but ended by 95.2 hours.

The nitrogen data was assessed by computing the total soluble nitrogen (NH_4^+-N + NO_2^--N + NO_3^--N: in effect a nitrogen mass balance), between 4.6 - 95.2 hours (Figure 30). The slope of a Kendall-Theil best fit line through these data was not different than 0 (p-value = 0.13). This indicated that the nitrogen measurements and NOB/AOB activity assessments were accurate.

The pattern for NOB recovery following high AOB activity presented in Figure 30 has been obtained by other researchers, though the interpretation of the inhibition factor(s) has varied. For example, Bae et al. (2002) describe their batch free ammonia

inhibition assay results as follows: "after … the free ammonia concentration was relatively low, the accumulated nitrite converted to nitrate quickly." Yun and Kim (2003) similarly reported that "batch kinetic analysis of ammonium and nitrite oxidation showed that nitrite oxidation activity was selectively inhibited in the presence of free ammonia", and further stated that "activity was recovered quickly as the free ammonia concentration decreased below the threshold inhibition concentration." Likewise, Balmelle et al. (1992) found that NOB inhibition occurred at both low and high DO concentrations (0.5 - 8.00 mg/L) and attributed this to initially high free ammonia concentrations in their batch assays. However, in all of these investigations AOB were not inhibited as a control prior to the assessment of free ammonia inhibition. Another interpretation of the results could have been that high AOB activity led to nitrite buildup by limiting the oxygen available for NOB.

Yang and Allemann (1992) studied the effects of DO (0.5 and 6.0 mg/L), pH (7.0, 7.5, 8.0, and 8.5), free ammonia, and free hydroxylamine on nitrite buildup with a nitrifier enrichment. Their study produced strikingly similar results to those in Figure 30 in that nitrite buildup occurred during high AOB activity, while NOB activity resumed as ammonia was depleted. Interestingly, this phenomenon occurred at both low and high DO values, though not consistently as the pH varied, suggesting that the pH change during their batch assay could have been an inhibitory factor (Suthersan and Ganczarczyk, 1986). They link nitrite buildup with free hydroxylamine, though an examination of the time course for nitrite buildup in their experiments revealed free hydroxylamine poorly coordinated with nitrite buildup. Surprisingly, they proposed that free hydroxylamine inhibited nitrite oxidation, but did not establish this in batch NOB inhibition studies with exogenously added hydroxylamine and inhibited AOB as a control. Hydroxylamine was not investigated as an NOB inhibitor in this study. Thus, it is possible that a buildup of this intermediate contributed to low NOB activity in vessel 5 in both experiments summarized in Table 19.

Experiment VII - Nitrobacter rDNA

The *Nitrobacter* rDNA concentration in samples collected from all vessels ≈ 4.5 hours after the assays began (immediately prior to the ammonia doses in vessels 4 and 5)

were similar (Figure 31). This was expected since each vessel was essentially prepared and treated identically up to this point in time (except for the absence of the buffer in vessel 1). The overall mean concentration ranged from 5.67 ± 0.5 to 8.85 ± 1.9 × 10^{9} copies/L in vessels 2 and 1, respectively, with the other vessels exhibiting intermediate overall means (Table 20). The overall mean in samples collected ≈ 9 hours after the assays began, or ≈ 4.5 hours after the ammonia spike to vessels 4 and 5, was approximately the same in vessel 3 (5.49 ± 1.2 × 10^{-9} copies/L), 4 (7.69 ± 2.1 × 10^{-9} copies/L) and 5 (5.91 ± 0.5 × 10^{-9} copies/L). Further, the overall mean did not change in vessel 5 when this vessel was sampled 26 hours (5.50 ± 0.6 × 10^{-9} copies/L) and 67 hours (5.15 ± 1.4 × 10^{-9} copies/L) after the assay began. Thus, the *Nitrobacter* ribosomal gene copy number did not significantly vary across different vessels at the same time during the experiment, or over time in the same vessel. This trend was confirmed with an ANOVA of the log transformed *Nitrobacter* rDNA assay means in Table 20, which did not reject the null hypothesis that the gene copy number was the same in each sample event (F = 2.06; p-value = 0.086).

Experiment VII - Nitrobacter rRNAt

ANOVA of the log transformed *Nitrobacter* rRNAt assay means in Table 20 rejected the null hypothesis that the samples were all equal (F = 38; p-value <0.0001). Subsequent Tukey HSD multiple comparisons delineated five groups (A - E: Table 20). No significant differences were found among samples taken 4.5 hours after the assays began. This was again expected since each vessel was essentially prepared and treated identically up to this point. At 4.5 hours, the *Nitrobacter* rRNAt concentration ranged from 1.44 ± 0.2 × 10^{10} to 7.36 ± 0.2 × 10^{9} copies/L in vessels 1 and 5, respectively. Thus, though the phosphate buffer slightly inhibited NOB aerobic activity, this was not readily apparent in the *Nitrobacter* rRNAt data. The concentrations ≈ 9 hours into the experiment in vessel 3 (6.49 ± 3.1 × 10^{9} copies/L) and 4 (8.56 ± 2.2 × 10^{9} copies/L) were not significantly different than the concentrations in these vessels 4.5 hours after the experiment started (Tukey group B: Table 20). This indicated that when the ammonia was added the rRNAt concentration in the vessels was stable and that the ammonia dose

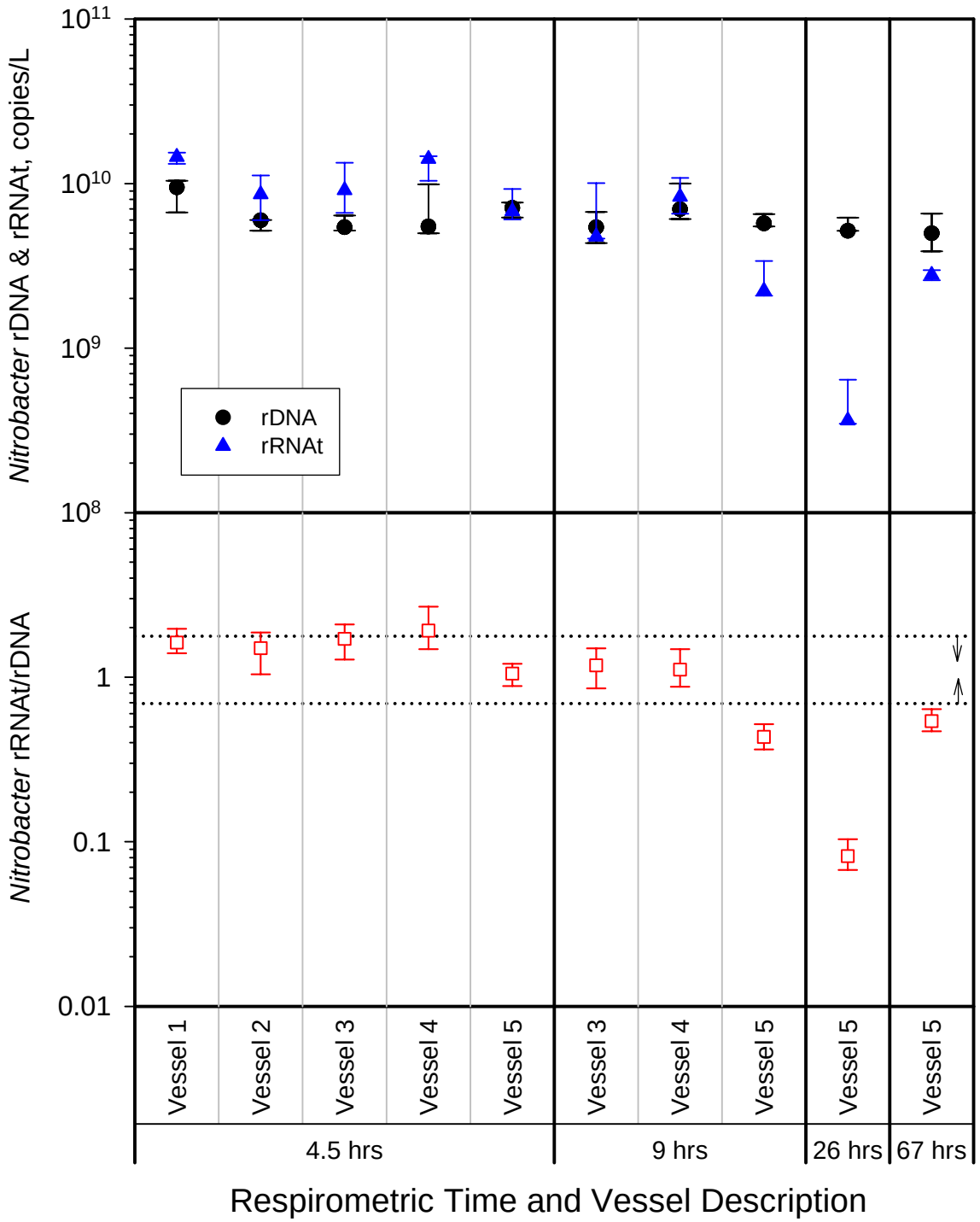


Figure 31 The effect of ammonia doses on *Nitrobacter* rDNA and rRNAt (Table 20: median ± minimum/maximum assay means) and the rRNAt/rDNA ratio (Table 20: error bars are the interquartile range of all possible ratios computed with the rRNAt and rDNA assay means) during a respirometric inhibition experiment (Figure 29-A). Reference lines indicate the upper (↓) and lower (↑) BSNR rRNAt/rDNA prediction intervals (Section 5.2).

Table 20 *Nitrobacter* molecular data for a respirometric inhibition experiment with ammonia (Figure 29; Experiment VII).

Sample[1]		NH_4^+ / NH_3 (mg-N/L)	Fraction Inhibition	*Nitrobacter* rDNA (copies/L)[2]			*Nitrobacter* rRNAt (copies/L)[2]			rRNAt / rDNA [3]
				Assay Mean	Statistical Analysis		Assay Mean	Statistical Analysis		
Time (hrs)	Vessel				Overall Mean	Tukey		Overall Mean	Tukey	
4.5	1	-/-	-	1.04E+10	8.85E+09	-	1.54E+10	1.44E+10	A	1.6
				6.68E+09			1.32E+10			
				9.48E+09			1.45E+10			
	2	-/-	-	6.01E+09	5.72E+09	-	1.12E+10	8.60E+09	AB	1.5
				5.17E+09			5.99E+09			
				5.98E+09			-			
	3	-/-	-	5.43E+09	5.67E+09	-	6.63E+09	9.71E+09	AB	1.7
				5.18E+09			9.11E+09			
				6.39E+09			1.34E+10			
	4	-/-	-	4.99E+09	6.79E+09	-	1.47E+10	1.30E+10	AB	1.9
				5.47E+09			1.04E+10			
				9.91E+09			1.41E+10			
	5	-/-	-	7.66E+09	6.99E+09	-	6.05E+09	7.36E+09	AB	1.1
				6.21E+09			6.78E+09			
				7.10E+09			9.26E+09			
9	3	-/-	-0.05	6.72E+09	5.49E+09	-	4.76E+09	6.49E+09	BC	1.2
				5.41E+09			1.01E+10			
				4.35E+09			4.63E+09			
	4	202/2.85	0.05	6.98E+09	7.69E+09	-	1.08E+10	8.56E+09	AB	1.1
				1.00E+10			8.31E+09			
				6.09E+09			6.56E+09			
	5	202/2.85	-0.80	5.72E+09	5.91E+09	-	2.08E+09	2.56E+09	D	0.43
				6.52E+09			2.23E+09			
				5.49E+09			3.38E+09			

Table 20 Continued.

Sample[1]		NH_4^+ / NH_3 (mg-N/L)	Fraction Inhibition	*Nitrobacter* rDNA (copies/L)[2]			*Nitrobacter* rRNAt (copies/L)[2]			rRNAt[3] / rDNA
				Assay Mean	Statistical Analysis		Assay Mean	Statistical Analysis		
Time (hrs)	Vessel				Overall Mean	Tukey		Overall Mean	Tukey	
26	5	-/-	-	6.19E+09 5.16E+09 5.16E+09	5.50E+09	-	6.42E+08 3.47E+08 3.64E+08	4.51E+08	E	0.082
67	5	-/-	-	4.98E+09 6.57E+09 3.88E+09	5.15E+09	-	2.59E+09 - 2.98E+09	2.78E+09	CD	0.54

1 Time indicates when the samples were collected as shown in Figure 29.

2 Assay mean is the mean of triplicate Real Time or Real Time RT-PCR reactions for replicate DNA and RNA extracts (Table E-10). The overall mean is the average of the assay means. Log transformation made the assay mean data more symmetric and constant in variance. The log transformed assay mean data were analyzed with Tukey HSD multiple comparisons if ANOVA rejected the null hypothesis of sample equivalence ($\alpha = 0.05$). Samples not sharing a common letter are significantly different ($\alpha = 0.05$).

3 The rRNAt/rDNA metric was calculated with the overall rDNA and rRNAt means for each sample event.

(vessel 4) did not significantly affect the *Nitrobacter* rRNAt concentration. However, *Nitrobacter* rRNAt abundance in the vessel with uninhibited AOB that received an identical ammonia dose was significantly lower than all other vessels 4.5 hours and 9.0 hours after the assay began (vessel 5, Tukey group D: $2.56 \pm 0.5 \times 10^9$ copies/L). Hence, in this vessel, where nitrite oxidation was inhibited, *Nitrobacter* rRNAt abundance had decreased. The impact worsened 27 hours into the assay since the rRNAt further dropped (vessel 5, Tukey group E: $4.51 \pm 1.7 \times 10^8$ copies/L). After the ammonia was oxidized and nitrite oxidation had resumed for 15 to 20 hours, the *Nitrobacter* rRNAt concentration increased, but not back to the same level observed prior to the ammonia addition (vessel 5, Tukey group CD: $2.78 \pm 0.3 \times 10^9$ copies/L). This indicated that the ammonia dose had a lasting negative effect on the *Nitrobacter* growth prospective.

In summary, the *Nitrobacter* rRNAt concentration broadly reflected nitrite oxidation activity during the experiment. Prior to ammonia addition, the abundance was high and similar in all vessels. When the transcript concentration was measured again 4.5 hours after an ammonia dose in the vessel with inhibited AOB (vessel 4), the abundance was unchanged, as was the rate of nitrite oxidation. In a vessel that received an identical ammonia dose but contained uninhibited AOB, the *Nitrobacter* rRNAt was significantly lowered after 4.5 hours, as was the rate of nitrite oxidation. This confirmed that nitrite oxidation and the rRNAt concentration were negatively impacted by high AOB activity, but not by free ammonia at ≈ 3 mg-N/L. The transcript abundance decreased further after nitrite oxidation had been inhibited 23.5 hours. Approximately 15 hours after nitrite oxidation resumed, the rRNAt concentration increased significantly, but not back to the level observed prior to the ammonia dose. This reflected the fact that the nitrite oxidation rate at this time was approximately 35% lower than initially observed.

***Nitrobacter* rRNAt/rDNA**

The *Nitrobacter* rRNAt/rDNA ratio was approximately the same in all vessels 4.5 hours after the assay began, ranging from 1.9 to 1.1 in vessels 1 and 5, respectively (Figure 29; Table 20). Approximately 9.0 hours after the experiment began, the ratio was higher than the BSNR lower prediction interval in the vessel that did not receive an

ammonia dose (vessel 3: 1.2) and in the vessel that received an ammonia dose but contained inhibited AOB (vessel 4: 1.1). As hypothesized, the *Nitrobacter* rRNAt/rDNA ratio was below the BSNR lower prediction interval in the vessel that received an ammonia dose and contained active AOB (vessel 5: 0.43). The ratio was even lower in this vessel near the apex of AOB activity (0.082), but rose again once AOB activity ended (0.54). However, the final ratio was below the lower BSNR lower prediction interval, confirming that the extended period of high AOB activity negatively impacted *Nitrobacter*, even as the excess nitrite was oxidized.

7.4 Summary

Free ammonia did not significantly inhibit nitrite oxidation in this study. Two subsequent experiments contrasted the effect of high ammonia oxidation activity and free ammonia concentration on nitrite oxidation. In these experiments, adding ammonia (≈ 3 mg NH_3-N/L) after AOB had been inhibited resulted in little or no NOB inhibition, though many investigations have indicated that this free ammonia concentration is inhibitory to unacclimated NOB (Table 2). When an identical ammonia dose was added to a vessel containing uninhibited AOB, the OUR increased substantially and variations in the oxygen demand and nitrogen data thereafter suggested that the added ammonia and nitrite were not oxidized at equal rates. Interestingly, at no time did the OUR closely approach the maximum oxygen exchange capacity of the respirometer (≈ 26 mg/L/hr: Section 3.5), which suggested that capacity existed to accommodate NOB activity. Nitrogen data confirmed that the NOB were significantly inhibited while the added ammonia was oxidized, though after the ammonia was depleted the accumulated nitrite was oxidized. Thus, the absence of nitrite oxidation after the ammonia addition appeared solely attributable to high AOB activity and not free ammonia. Though the mechanism for NOB inhibition was not clear, support exists for the hypothesis that the inhibition resulted from poor NOB competition for oxygen with highly active AOB, though this was not proven (free hydroxylamine could also have been inhibitory: Yang and Alleman, 1992). A low *Nitrobacter* rRNAt/rDNA ratio value reflected the inhibitory condition.

CHAPTER 8.0

BSNR INHIBITION EXPERIMENT

8.1 Introduction

The rRNAt/rDNA ratio was proposed as a new metric to improve nitrification and N-removal performance by providing a snapshot of the NOB activity level. To be useful in this respect, the metric must assume significantly different values during high and low NOB activity. This was shown to be the case in Chapter 5.0 by assessing the metric as the BSNR biomass transitioned from nitrite starvation to unlimited nitrite oxidation. In addition, the metric value must reflect that the desired operating condition is in jeopardy. This was demonstrated from the perspective of traditional nitrification by: (1) establishing a lower prediction interval for the *Nitrobacter* rRNAt/rDNA ratio in the BSNR during steady state, high nitrification efficiency (Section 5.2), and (2) observing that the metric dropped below this interval during nitrite starvation (Section 5.3) and NOB inhibition (Chapter 6.0 and Chapter 7.0).

While these experiments were successful, they did not directly test the intended application. To do this, a staged BSNR nitrification inhibition event was performed, during which it was hoped that the metric would accurately reflect nitrite oxidation activity as it varied. However, subtle aspects of the experiment were considered particularly important. For example, the initial inhibiting condition (lowered pH due to ammonia oxidation) was chosen not only because of its prevalence in deteriorating nitrification performance in full-scale WWTPs (Grady et al., 1999), but also because this would likely produce AOB inhibition, rather than direct NOB inhibition. This would provide an opportunity to demonstrate, as suggested in Section 5.4, that the NOB rRNAt/rDNA ratio would be sensitive to both AOB and NOB inhibition. In fact, this was one of the key reasons the NOB were chosen to test the rRNAt/rDNA metric as opposed to the AOB, since declining nitrification efficiency would be detected when caused by lapses in either ammonia or nitrite oxidation.

A staged reactor inhibition event would also provide an opportunity to answer a critical question that has not been adequately addressed: "Can the metric be used to *predict* changing NOB activity levels before changes in treatment performance occur?" It was hoped that the ratio would demonstrate a significant response by falling below the lower BNSR prediction interval *prior* to the decline in nitrification efficiency. Conversely, when NOB activity recovered, it was hoped that the ratio would rise above the lower prediction interval *prior* to improving nitrification efficiency. This would demonstrate whether the ratio could be used in a proactive manner during wastewater treatment, perhaps providing an opportunity to ameliorate undesired inhibition events. A favorable response would also indicate that NOB acclimation could be identified and limited in reactors promoting partial nitrification (Section 2.4). Such a comprehensive experiment of this type has not been performed previously with other biomarkers (Table 4).

Lastly, this experiment provided an opportunity to more fully explore free ammonia inhibition of the NOB, which has been used to promote partial nitrification (Section 2.4). If ideal conditions could be imposed on the reactor to promote free ammonia buildup, the free ammonia concentration could then be manipulated to assess whether a lack of NOB activity was truly due to free ammonia or due to highly active AOB.

8.2 Overview of the BSNR Inhibition Experiment

The inhibition event that was staged in the BSNR consisted of three phases. Each phase was initiated by a single manipulation of the reactor's pH control system, after which certain responses in the AOB and NOB activity levels were anticipated (Table 21). Although the inhibition event as a whole was controlled, the experiment could be considered analogous to a drop in influent alkalinity in a reactor treating highly nitrogenous wastewater (Grady et al., 1999). The planned scenario of ammonia followed by nitrite buildup is commonly observed in WWTPs (Anthonisen et al., 1976).

Table 21 Outline of the BSNR inhibition experiment conducted in three phases initiated by perturbations of the reactor pH control system. Expected responses and an interpretation of AOB and NOB activity are provided.

Phase	Perturbation	Expected Response	Interpretation
1	pH control disabled	Ammonia but not nitrite accumulates, nitrate declines	AOB inhibited; NOB substrate starved
2	pH control enabled at setpoint 8.0	Nitrate and accumulated ammonia decline, nitrite accumulates	AOB become active; NOB inhibited by high AOB activity
3	pH control setpoint lowered to 7.2	Excess ammonia oxidized, nitrate declines but then accumulates as excess nitrite is oxidized	NOB become active; the timing of this indicates the importance of NH_3 inhibition in Phase 2

To document activity and growth within the reactor, samples were frequently collected and analyzed for: MLVSS, soluble nitrogen (NH_4^+, NO_2^-, and NO_3^-), *Nitrobacter* rDNA, and *Nitrobacter* rRNAt (all DNA and RNA samples were collected and extracted in triplicate). To corroborate and refine AOB and NOB activity assessments, the pH and DO were monitored continuously with a YSI 556 Multiprobe (YSI, Yellow Springs, OH). This instrument also verified that the temperature setpoint (30°C) was maintained during changes in pH and biological activity (Hellinga et al., 1998). Based on the expected responses in AOB and NOB activity levels, hypotheses were developed for the molecular data during each phase of the experiment.

8.2.1 Phase 1 - the pH control system is disabled

To initiate phase 1, the reactor's pH control system was disabled. Acid equivalents produced by active AOB were expected to cause a pH decline that eventually inhibited the AOB resulting in ammonia buildup. Based on the work of Ruiz et al. (2003), nitrite buildup was not expected during phase 1, and this characteristic was assumed to indicate NOB activity was largely affected by nitrite starvation (i.e. AOB inhibition) as opposed to the declining pH. This expectation was also supported by

several batch experiments that tested the effect of small ammonia doses (final concentration ≈ 20 mg-N/L) on the aerobic activity of BSNR mixed liquor samples in unbuffered media. In these experiments, aerobic activity characteristically dropped near pH 6.3 and was negligible when pH 5.5 was attained. However, subsequent addition of nitrite demonstrated that the NOB were substrate limited rather than inhibited by the low pH.

The results of a typical experiment are provided in Figure 32. In this test, a BSNR mixed liquor sample was diluted 1:1 into a weak ammonia solution (final concentration 20 mg-N/L). At the start of the experiment the pH was 7.26, and over the next 3.8 hours aerobic activity was high (average OUR = 9.75 mg O_2/L/hr). At 3.8 hours, 33 mg O_2/L had been consumed and the pH had dropped to 6.26. Thereafter, between 4 and 10 hours after the ammonia dose, the OUR decreased and eventually dropped below 1 mg/L/hr, so that after 10 hours only 42 mg O_2/L had been consumed. The expected oxygen consumption based on the stoichiometry for nitrification (4.57 mg O_2/mg N) was 91 mg O_2/L. Between 10 and 43.3 hours, the OUR averaged 0.4 mg/L/hr and indicated that adaptation to the inhibiting condition was unlikely. After 43.3 hours, the pH was measured (5.54), and to distinguish between the NOB inhibitor factors (low pH versus nitrite limitation) nitrite was spiked into the vessel (final concentration 50 mg-N/L). After a lag time of 1.5 hours, the OUR increased significantly up to approximate 4 mg/L/hr, at which point the nitrite was apparently exhausted (evident as a sharp decline in OUR to ≈ 0 mg/L/hr). Thus, nitrification ended as the pH decreased from 6.3 - 5.5, but the limitation was due to inhibition of the AOB. Similar results were obtained by Ruiz et al. (2003) for a nitrifier enrichment: as the pH was systematically lowered in their reactor to 6.4, the failure of nitrification was signaled as effluent ammonia, but not nitrite, and a decline in the effluent nitrate concentration.

It should also be noted that the NOB H^+ inhibition experiments in Section 6.4 clearly demonstrated that nitrite oxidation was possible at pH 5.6 (see Figure 23). These results contradict the report by Bae et al. (2002) that the ammonia oxidation rate exceeds the nitrite oxidation rate when the pH is below 8.0.

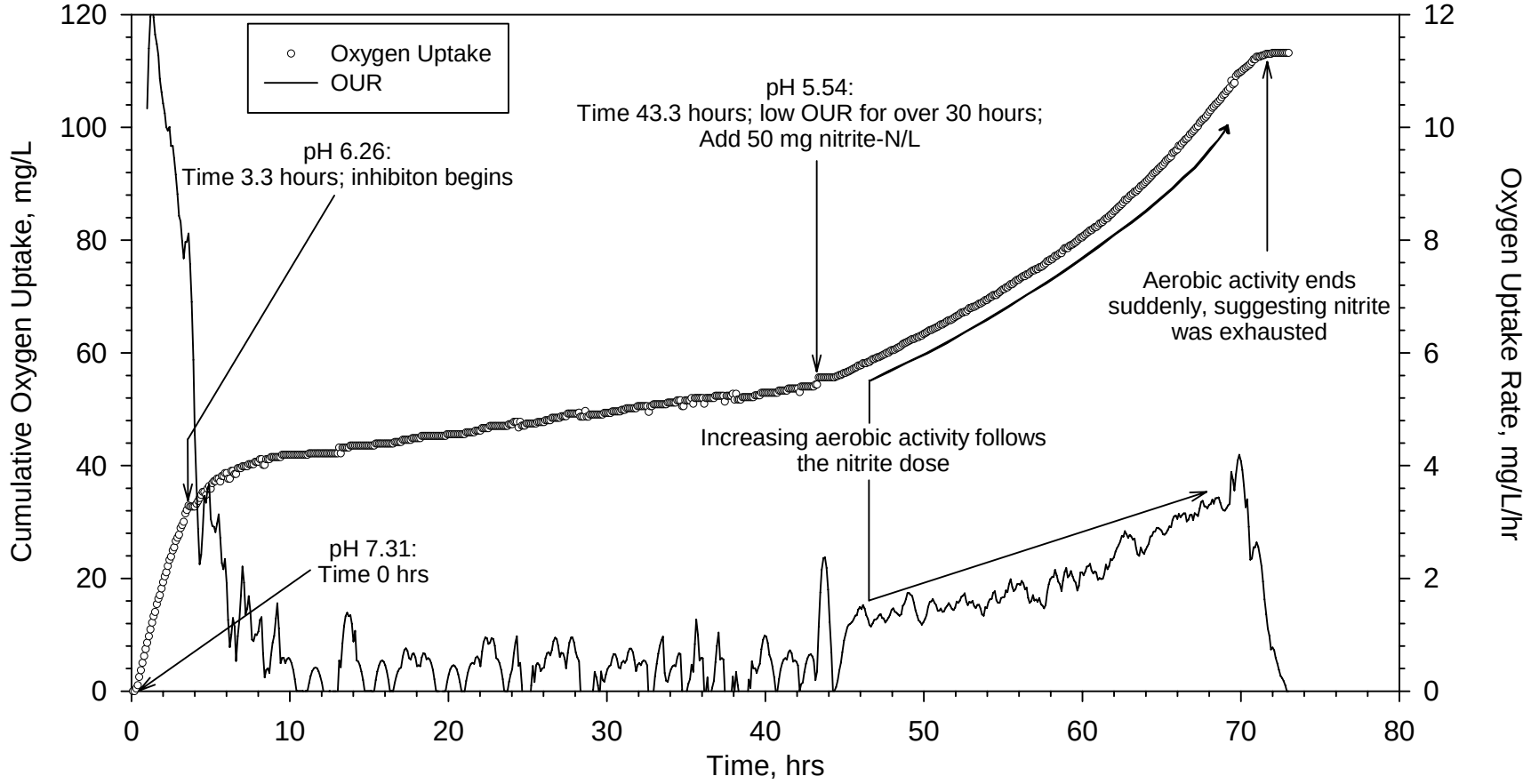


Figure 32 The effect of reduced pH on aerobic activity during ammonia oxidation in unbuffered media. The cumulative oxygen uptake and OUR data were monitored over time while the pH was measured at the time points indicated. After low aerobic activity prevailed for more than 30 hours, nitrite (50 mg-N/L) was added to the vessel.

In summary, both ammonia and nitrite oxidation were expected to decline after pH control was eliminated in phase 1. The poor *Nitrobacter* growth perspective was expected to decrease the demand for rRNAt, and hence lower the rRNAt/rDNA ratio. Reactor washout pressure was expected to reduce the *Nitrobacter* rDNA:

I. *Nitrobacter* rDNA, rRNAt, and rRNAt/rDNA will decrease monotonically:

H_0: Kendall's $\tau = 0$

H_1: Kendall's $\tau < 0$

II. *Nitrobacter* rRNAt/rDNA will fall below the lower BSNR prediction interval (Section 5.2).

H_0: rRNAt/rDNA > 0.69

H_1: rRNAt/rDNA < 0.69

8.2.2 Phase 2 - the pH setpoint is changed to 8.0

To initiate phase 2, the pH control system was enabled at a control setpoint of 8.0. This would convert a portion of the total ammonia accumulated during phase 1 to free ammonia (Equation 4) that reportedly inhibits NOB (Table 2), but would also remove the condition inhibiting AOB (low pH). Free ammonia and/or high AOB activity were expected to significantly limit NOB activity during phase 2. The *Nitrobacter* rDNA and rRNAt levels were expected to decline while the *Nitrobacter* rRNAt/rDNA ratio remained below the lower BSNR prediction interval:

I. *Nitrobacter* rDNA and rRNAt will decrease monotonically:

H_0: Kendall's $\tau = 0$

H_1: Kendall's $\tau < 0$

II. *Nitrobacter* rRNAt/rDNA will remain below the lower BSNR prediction interval (Section 5.1):

H_0: rRNAt/rDNA > 0.69

H_1: rRNAt/rDNA < 0.69

8.2.3 Phase 3 - the pH setpoint is changed to 7.2

To initiate phase 3, the pH control system setpoint was changed to 7.2. The timing of this event was carefully coordinated to assure that the pH change would lower the free ammonia concentration from values above what is typically reported as inhibitory (Table 2) to values that were clearly not inhibitory based on the batch free ammonia inhibition experiments (Table 18). Further, the AOB were expected to be highly active and mediate the pH setpoint change by producing acidity (the pH control system only raised the pH by adding a base: Section 3.2.5). Following the pH change, nitrite oxidation was expected to resume, but the timing of this event relative to the initiation of phase 3 would indicate whether free ammonia was a significant inhibitory factor in phase 2. Rising NOB activity levels, and hence the potential for growth and demand for *Nitrobacter* rRNAt, were the focus of the phase 3 hypotheses:

I. During accumulated nitrite removal, *Nitrobacter* rDNA, rRNAt, and rRNAt/rDNA will increase monotonically:

   H_0: Kendall's $\tau = 0$

   H_1: Kendall's $\tau > 0$

II. *Nitrobacter* rRNAt/rDNA will rise above the lower BSNR prediction interval:

   H_0: rRNAt/rDNA < 0.69

   H_1: rRNAt/rDNA > 0.69

8.3 Results

Thirty eight sample events were conducted in the BSNR inhibition experiment (Table 22). Reactor pH and DO (at the moment of sampling), MLSS, and nitrogen data are provided in Table 23. *Nitrobacter* rRNAt and rDNA results are summarized in Table 24 along with the results of a Tukey HSD analysis of the log transformed assay mean data conducted after ANOVA rejected the null hypothesis that the samples events were equal: rDNA ($F = 19$; p-value < 0.0001) and rRNAt ($F = 155$; p-value < 0.0001).

Table 22 Timing of the sample events during the BSNR inhibition experiment.

Sample Event		Total Elapsed Time		Elapsed Time in Phase		
Number	RNA/DNA samples[1]	Days	Hours	Time, hrs	Phase	pH setpoint
1	√	-	-0.08	-	-	7.2
2	√	0.09	2.06	2.06	1	pH control disabled
3	√	0.13	3.08	3.08		
4	√	0.17	4.02	4.02		
5	√	0.23	5.52	5.52		
6	√	0.34	8.09	8.09		
7		0.68	16.21	16.21		
8	√	1.03	24.68	24.68		
9		2.00	48.07	48.07		
10	√	3.00	72.12	72.12		
11		3.08	73.96	0.96	2	8.0
12		3.12	74.99	1.99		
13		3.21	77.00	4.00		
14	√	3.37	80.90	7.90		
15	√	3.87	92.98	19.98		
16	√	4.36	104.72	31.72		
17	√	4.88	117.07	44.07		
18		5.01	120.15	2.95	3	7.2
19		5.12	122.98	5.78		
20		5.25	126.02	8.82		
21	√	5.37	128.94	11.74		
22	√	5.80	139.15	21.95		
23	√	6.30	151.12	33.92		
24	√	6.79	162.96	45.76		
25		7.29	174.96	57.76		
26	√	7.79	187.05	69.85		
27		7.87	188.92	71.72		
28		7.96	190.95	73.75		
29		8.04	192.95	75.75		
30		8.12	194.95	77.75		
31		8.38	201.13	83.93		
32		8.79	211.07	93.87		
33		8.87	212.92	95.72		
34	√	9.87	236.95	119.75		
35		10.88	261.13	143.93		
36	√	11.88	285.13	167.93		
37		12.88	309.08	191.88		
38	√	13.86	332.76	215.56		

1 Indicates samples events that included analysis of *Nitrobacter* rDNA and rRNAt.

Table 23 pH, DO, MLSS, soluble nitrogen concentrations, and the nitrification efficiency during the BSNR inhibition experiment.

Sample		pH	DO, mg/L	MLSS, mg/L	Soluble Nitrogen, mg-N/L				Nitrification Efficiency, %[2]
					Ammonia		Nitrite	Nitrate	
Phase	Time, hrs				Total	Free[1]			
-	-	7.23	3.03	137	0.5	0.0	0.2	1298	99.95
1	2.06	6.86	3.32	140	0.8	0.0	0.0	1293	99.94
	3.08	6.69	3.89	134	1.4	0.0	0.0	1298	99.89
	4.02	6.66	5.68	143	3.6	0.0	0.0	1294	99.72
	5.52	6.68	6.12	140	12.8	0.0	0.0	1283	99.02
	8.09	6.62	6.08	139	28.7	0.1	0.0	1272	97.79
	16.2	6.32	6.13	136	79.8	0.1	0.0	1260	94.05
	24.7	5.99	6.29	134	136.6	0.1	0.0	1219	89.92
	48.1	5.60	6.36	120	286.5	0.1	0.0	1100	79.33
	72.1	5.60	6.31	107	402.5	0.1	0.0	995	71.20
2	0.96	8.00	4.83	104	393.2	29.3	0.8	972	71.16
	1.99	7.99	4.80	104	402.0	29.3	5.2	972	70.48
	4.00	8.01	4.79	106	394.2	30.0	8.4	974	70.76
	7.90	8.02	4.65	107	396.0	30.8	19.3	965	69.92
	20.0	8.00	4.12	108	371.2	27.7	59.2	914	67.99
	31.7	8.01	3.51	107	359.3	27.4	122.2	904	65.24
	44.1	8.02	2.33	112	300.8	23.4	212.0	847	62.30
3	2.95	7.48	1.96	108	270.5	6.4	237.0	827	61.97
	5.78	7.28	1.91	115	247.5	3.7	269.2	837	61.82
	8.82	7.25	1.62	120	223.3	3.2	302.3	838	61.45
	11.7	7.26	1.55	121	207.8	3.0	329.6	825	60.55
	22.0	7.26	1.02	122	129.3	1.9	418.2	767	58.34
	33.9	7.35	1.36	128	45.8	0.8	531.1	732	55.91
	45.8	7.25	3.75	130	5.3	0.1	580.9	713	54.86
	57.8	7.25	3.77	130	4.7	0.1	585.7	724	55.06
	69.9	7.29	3.35	130	4.4	0.1	558.2	735	56.65
	71.7	7.28	3.86	-	4.2	0.1	553.3	739	56.98
	73.8	7.28	3.57	-	0.0	0.0	554.7	753	57.57
	75.8	7.27	3.53	-	0.0	0.0	543.4	748	57.92
	77.8	7.28	3.45	-	0.0	0.0	543.6	769	58.57
	83.9	7.26	3.47	126	4.2	0.1	513.8	759	59.44
	93.9	7.28	3.37	-	0.0	0.0	478.1	799	62.57
	95.7	7.29	2.90	124	4.1	0.1	491.3	854	63.30
	120	7.29	3.10	123	3.7	0.1	362.5	962	72.44
	144	7.29	3.10	125	3.4	0.1	219.5	1102	83.18
	168	7.29	3.08	129	2.9	0.0	58.5	1150	94.93
	192	7.30	4.25	126	1.9	0.0	1.3	1198	99.73
	216	7.24	-	133	1.3	0.0	1.0	1198	99.81

1 Calculated with Equations 4 and 5 using the pH and total ammonia.

2 Calculated as: nitrate/(total ammonia + nitrite + nitrate) × 100%.

Table 24 *Nitrobacter* molecular data during the BSNR inhibition experiment.

Sample[1]		*Nitrobacter* rDNA (copies/L)[2]			*Nitrobacter* rRNAt (copies/L)[2]			$\frac{\text{rRNAt}}{\text{rDNA}}$[3]
Phase	Elapsed Time, hrs	Assay Mean	Statistical Analysis		Assay Mean	Statistical Analysis		
			Overall Mean	Tukey		Overall Mean	Tukey	
1	-0.1	7.53E+09	9.60E+09	BC	1.59E+10	1.50E+10	C	1.6
		9.20E+09			1.51E+10			
		1.21E+10			1.39E+10			
	2.1	1.21E+10	9.44E+09	BC	8.46E+09	5.85E+09	D	0.62
		8.42E+09			2.56E+09			
		7.80E+09			6.54E+09			
	3.1	1.42E+10	1.25E+10	AB	6.71E+09	5.76E+09	D	0.44
		1.28E+10			6.27E+09			
		1.06E+10			4.31E+09			
	4.0	8.87E+09	9.81E+09	BC	3.71E+09	3.28E+09	DE	0.27
		1.20E+10			3.67E+09			
		8.54E+09			2.45E+09			
	5.5	8.69E+09	9.67E+09	BC	1.68E+09	1.74E+09	EF	0.18
		9.34E+09			2.13E+09			
		1.10E+10			1.39E+09			
	8.1	8.02E+09	7.80E+09	BCD	4.65E+08	7.98E+08	GH	0.068
		1.11E+10			1.09E+09			
		4.30E+09			8.34E+08			
	24.7	9.83E+09	8.41E+09	BCD	5.19E+08	4.63E+08	GHIJ	0.052
		8.83E+09			4.11E+08			
		6.57E+09			4.60E+08			
	72.1	5.03E+09	4.69E+09	DEF	4.31E+08	3.78E+08	IJ	0.071
		5.28E+09			3.66E+08			
		3.77E+09			3.36E+08			
2	7.9	5.69E+09	5.47E+09	CDEF	7.20E+08	7.02E+08	GHI	0.12
		5.68E+09			7.53E+08			
		5.03E+09			6.34E+08			
	20.0	3.35E+09	3.37E+09	F	2.54E+08	2.78E+08	J	0.076
		3.66E+09			3.08E+08			
		3.12E+09			2.73E+08			
	31.7	4.34E+09	4.84E+09	DEF	4.66E+08	4.93E+08	GHIJ	0.087
		5.57E+09			6.05E+08			
		4.61E+09			4.07E+08			
	44.1	3.30E+09	3.17E+09	F	4.62E+08	4.72E+08	GHIJ	0.14
		3.47E+09			5.31E+08			
		2.73E+09			4.23E+08			

Table 24 Continued.

Sample[1]		*Nitrobacter* rDNA (copies/L)[2]			*Nitrobacter* rRNAt (copies/L)[2]			rRNAt[3] / rDNA
Phase	Elapsed Time, hrs	Assay Mean	Statistical Analysis		Assay Mean	Statistical Analysis		
			Overall Mean	Tukey		Overall Mean	Tukey	
3	11.7	5.51E+09	6.24E+09	CDE	9.46E+08	8.94E+08	FG	0.12
		7.17E+09			9.98E+08			
		6.06E+09			7.38E+08			
	22.0	4.53E+09	3.80E+09	EF	4.54E+08	3.64E+08	IJ	0.092
		3.84E+09			3.89E+08			
		3.03E+09			2.49E+08			
	33.9	5.80E+09	4.77E+09	DEF	3.91E+08	3.41E+08	IJ	0.071
		4.79E+09			3.46E+08			
		3.73E+09			2.86E+08			
	45.8	5.21E+09	4.81E+09	DEF	4.92E+09	5.79E+09	D	1.0
		5.60E+09			6.87E+09			
		3.62E+09			5.58E+09			
	69.9	7.79E+09	6.32E+09	CDE	2.26E+10	1.86E+10	BC	3.0
		6.13E+09			1.46E+10			
		5.03E+09			1.86E+10			
	120	1.22E+10	1.26E+10	AB	3.72E+10	3.40E+10	AB	2.4
		1.44E+10			3.19E+10			
		1.12E+10			3.30E+10			
	168	1.74E+10	1.84E+10	A	4.87E+10	4.88E+10	A	2.6
		1.88E+10			4.91E+10			
		1.91E+10			4.86E+10			
	216	1.20E+10	1.18E+10	AB	1.48E+10	1.79E+10	BC	1.5
		1.17E+10			1.51E+10			
		1.16E+10			2.39E+10			

1 See Table 22.

2 Assay mean is the mean of triplicate Real Time or Real Time RT-PCR reactions for replicate DNA and RNA extracts (Table F-1). The overall mean is the average of the assay means. Log transformation made the assay mean data more symmetric and constant in variance. The log transformed assay mean data were analyzed with Tukey HSD multiple comparisons if ANOVA rejected the null hypothesis of sample equivalence ($\alpha = 0.05$). Samples not sharing a common letter are significantly different ($\alpha = 0.05$).

3 The rRNAt/rDNA metric was calculated with the overall rDNA and rRNAt means for each sample event.

8.3.1 Phase 1

The data collected after the BSNR control system was disabled are presented in Figure 33 in stacked plots that contain identical x-axes. It should be noted that 0.3 hours of pH, DO, and temperature data were collected prior to disabling the pH control system at 0 hours. Also, the initial nitrogen and genetic data points are displayed at -0.08 hours since these samples were collected immediately before the pH control system was disabled. These were the final samples used to establish the prediction intervals for the *Nitrobacter* rRNAt/rDNA ratio in the reactor (Section 5.2). Thus, prior to the pH control system being disabled, the BSNR had operated with high nitrification efficiency for over 10 weeks.

pH, DO, and temperature

Though the temperature was unaffected in phase 1 (29.9 ± 0.3 °C), the pH and DO varied significantly. Immediately after the pH control system was disabled, a steep drop in the reactor pH (-0.17 pH units/hr) occurred as AOB initially continued to produce acid equivalents (Figure 33-A). After 3.5 hours, the decline stabilized temporarily at pH 6.7 (see the inset in Figure 33-A), but then dropped again at a lower rate (-0.04 pH units/hr) for 20 additional hours. Between 30 and 50 hours after phase 1 was initiated, this rate of decline slowed until a pH of ≈ 5.60 was attained. Thereafter, pH 5.6 was maintained until phase 1 ended.

Prior to disabling the pH control system, the DO was approximately 2.9 mg/L. Once phase 1 began, the concentration increased gradually to 3.5 mg/L over the course of 3 hours. The DO increased sharply thereafter, from 3.5 to 6.2 mg/L between 3 and 4 hours after phase 1 began (see the inset in Figure 33-A). The DO then remained at ≈ 6.2 until phase 1 ended.

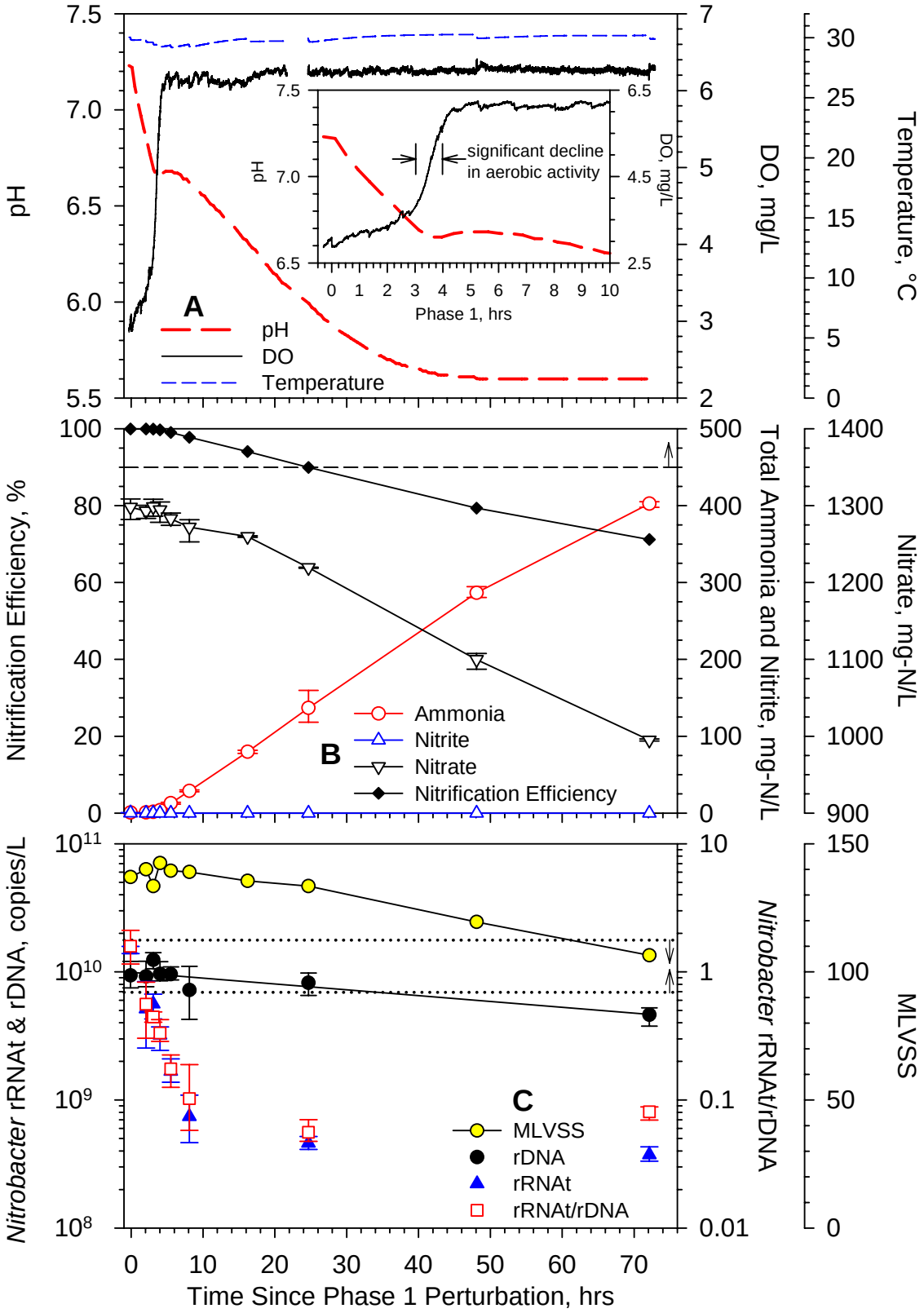
The main biochemical reaction in the BSNR was nitrification, so a drop in nitrification activity would be expected to increase the bulk DO concentration. Further, ammonia oxidation produces acidity, so a decline in the ammonia oxidation rate would be expected to stabilize the pH, though the influent pH, which was approximately 5.6, would

Figure 33 The response of various operational parameters after disabling the BSNR pH control system to initiate phase 1 of a staged inhibition experiment.

A. Temperature, pH, and DO data. An inset plot of the pH and DO data within the first 10 hours of disabling the pH control system is provided.

B. Soluble nitrogen data (as mg-N/L) are presented along with the nitrification efficiency. A horizontal reference line indicates 90% nitrification efficiency.

C. The MLVSS along with the *Nitrobacter* rDNA and rRNAt concentrations and the rRNAt/rDNA ratio. For the rDNA and rRNAt data, the median ± minimum/maximum assay mean are presented (Table 24). The rRNAt/rDNA ratio is displayed with error bars corresponding to the interquartile range of all possible ratio combinations of the rDNA and rRNAt assay means (Table 24). Horizontal reference lines (·····) indicate the upper (⇓) and lower (⇑) *Nitrobacter* rRNAt/rDNA ratio prediction intervals established in Section 5.2.


pH
DO, mg/L
Temperature, °C
A
pH
DO
Temperature
significant decline
in aerobic activity
Phase 1, hrs
Nitrification Efficiency, %
Total Ammonia and Nitrite, mg-N/L
Nitrate, mg-N/L
B
Ammonia
Nitrite
Nitrate
Nitrification Efficiency
Nitrobacter rRNAt & rDNA, copies/L
Nitrobacter rRNAt/rDNA
MLVSS
C
MLVSS
rDNA
rRNAt
rRNAt/rDNA
Time Since Phase 1 Perturbation, hrs

slowly lower the pH. With this in mind, the slow rise in the bulk DO concentration between 0 to 3 hours likely represented a gradual decrease in the nitrification rate, while the steep rise in the bulk DO between 4 and 5 hours indicated a significant and rapid decline in ammonia oxidation. This assessment is confirmed by the disruption of the initial high rate of pH decline (from 7.2 to 6.7: -0.17 pH units/hr) that occurred between 3 and 4 hours after phase 1 began (see the inset in Figure 33-A). Taken together, the pH and DO data indicate that between 3 and 4 hours after pH control was eliminated, nitrification ended in the reactor. Since the smaller rate of pH decline (-0.04 pH units/hr between 10 - 30 hours) occurred while the bulk DO concentration remained high, the decline was likely due to the acidic influent.

Soluble nitrogen

The total ammonia concentration increased steadily from less than 1 mg-N/L after 2.1 hours to 28.7 mg-N/L after 8.1 hours (Figure 33-B). Over this time period the total ammonia increased monotonically (Kendall's $\tau = 1$; p-value = 0.0014), indicating that the reactor treatment performance was declining. However, 8.1 hours after pH control had been eliminated the total ammonia concentration represented only 2% of soluble nitrogen in the reactor. Thus, it would have been difficult to justify a prediction of deteriorating treatment performance using only the total ammonia trend at that time. After 16.2 and 24.7 hours, the effluent ammonia was 6% (80 mg-N/L) and 10% (137 mg-N/L) of the soluble nitrogen, respectively. Thus, the nitrification efficiency specification used in Section 5.2 to establish the *Nitrobacter* rRNAt/rDNA ratio prediction intervals was maintained for ≈ 1 day after the pH control system was disabled. After 72 hours without pH control, the total ammonia concentration (403 mg-N/L; 41% of soluble nitrogen) clearly indicated an inhibition event was ongoing. A Kendall-Thiel trend line was used to estimate the total ammonia accumulation rate during Phase 1: +5.85 mg-N/L/hr (approximately the influent ammonia rate). Since the pH was low while the ammonia accumulated, the free ammonia concentration was insignificant (< 0.2 mg-N/L).

Nitrite concentrations remained below 0.1 mg-N/L throughout phase 1 (Figure 33-B), suggesting that AOB may have been inhibited prior to the NOB (Ruiz et al.,

2003). Nitrate concentrations dropped from 1,298 mg-N/L to 995 mg-N/L during phase 1 (Figure 33-B). The rate of nitrate decline, as well as ammonia accumulation, suggested that these concentrations were controlled hydraulically in the absence of nitrification. Thus, a nitrogen mass balance was formulated under the assumption that AOB activity ended 4 hours after the pH control system was disabled (this time corresponded to a significant increase in the reactor's bulk DO concentration and the end of the initial high rate of pH decline: see the inset in Figure 33-A). Using the ammonia (3.6 mg-N/L) and nitrate (1,294 mg-N/L) measured at this time, along with the influent flow rate (1 L/day at 1,500 mg NH_4^+-N/L) and the sample and wastage volumes which were carefully recorded, the nitrate decline and ammonia accumulation were projected forward (assuming only washout) to the end of phase I. The results (982 mg NO_3^--N/L; 377 mg NH_4^+-N/L) agreed well with the final phase I measurements (995 mg nitrate-N/L; 402 mg ammonia-N/L). Thus, the nitrogen data supported the assessment that ammonia oxidation largely ended in the BSNR within 4 hours of disabling the pH control system.

MLVSS

As Figure 33-C illustrates, the MLVSS steadily dropped from approximately 140 to 107 mg/L by the end of phase 1. The decline in reactor solids was estimated assuming growth was negligible and losses were hydraulically controlled beginning with the measurement made at 4 hours (143 mg/L). The projected concentration at the end of phase 1 (106 mg/L MLSS) agreed with measurement (107 mg/L), indicating that growth largely ended in the reactor soon after the pH control was disabled.

Nitrobacter rDNA

The *Nitrobacter* rDNA samples collected during the first 24 hours of phase 1 were not significantly different (see Table 24: Tukey HSD group B), displaying an average of 9.61×10^9 copies/L (range $1.25 \pm 0.2 \times 10^{10}$ - $7.80 \pm 3.4 \times 10^9$ copies/L). However, the last sample taken in Phase 1 ($4.69 \pm 0.8 \times 10^9$ copies/L) was significantly lower than all the first 5 rDNA measurements. A linear regression thorough the rDNA data (Figure 33-C) displayed a slight negative slope, but the downward trend that had been hypothesized (Section 8.2.1) was not significant (Kendall's τ = -0.50; p-value =

0.54). This was likely because of poor statistical power since the MLSS was only reduced by 25% during phase 1, and the real-time RT-PCR assay appeared insensitive for such small differences with only three replicates per sample event (Section 4.9.1).

Nitrobacter rRNAt

Nitrobacter rRNAt displayed a negative monotonic correlation with time over the first 8 hours of phase 1 (Kendall's $\tau = -1$; p-value = 0.0014) at a Kendall-Thiel slope of -1.43×10^9 copies/L/hr. Further, the absolute decline in abundance was very large during this time period, from $1.50 \pm 0.1 \times 10^{10}$ copies/L measured immediately before the pH control system was disabled, to $7.98 \pm 3.2 \times 10^8$ copies/L 8.1 hours later. Tukey HSD comparisons of the log transformed assay mean data revealed that two hours after the pH control system was disabled, the transcript concentration had significantly declined ($5.85 \pm 3.0 \times 10^9$ copies/L: Table 24, Tukey group D), though the DO and pH data indicated activity was present until approximately 3 hours into phase 1. Thus, the *Nitrobacter* rRNAt concentration quickly delineated a potential inhibitory condition (loss of pH control) much sooner than the nitrogen data (≈ 16 hours) and even before the pH and DO data. Over the entire time course of phase I, the transcript concentration declined monotonically (Kendall's $\tau = -1$; p-value < 0.0001) as hypothesized and was lowest in the last sample taken ($3.78 \pm 0.5 \times 10^8$ copies/L). The drop was more significant than observed for *P. abietaniphila* rRNA (≈ 20 fold) over the course of 0.5 to 2 hours in a CSTR following a pH change to 12.5 from the setpoint 6.5 (Muttray et al., 2001). However, the decline in rRNA concentration those researchers observed was likely heavily influenced by cell lysis and a concomitant 10-fold drop in rDNA (Muttray et al., 2001).

Nitrobacter rRNAt/rDNA

The rRNAt/rDNA metric was largely determined by *Nitrobacter* rRNAt abundance. Thus, the ratio exhibited the hypothesized monotonic decline during phase 1 (Kendall's $\tau = -1$; p-value = 0.0014; Section 8.2.1). Figure 33-C reveals that the ratio declined below lower BSNR prediction interval (as hypothesized: Section 8.2.1) after only 2.1 hours, and remained below this interval throughout the remainder of phase 1.

The results demonstrated that the metric can be used to predict lapses in treatment performance, since the metric dropped below the lower prediction interval 22 hours before the nitrification efficiency fell below 90%. The values attained during substrate starvation (Section 5.3: ≈ 0.07 - 0.10) and during batch inhibition experiments with 3,5-DCP (Section 6.2.3: ≈ 0.05 - .010) were similar to the lowest values attained during phase 1 (≈ 0.05), which indicate that the metric can be accurately measured in a variety of severely inhibiting conditions.

The relative change in the *Nitrobacter* rRNAt/rDNA ratio herein (31-fold) was larger that for a rRNA/rDNA metric used to infer activity of a *P. abietaniphila* strain in a CSTR following a pH change from 6.5 to 12.5 (Muttray et al., 2001: from 330 - 1600, a 5-fold change). Further, the changes herein were larger than in the rRNAt/rRNA ratio for *Acinetobacter* spp. in two lab scale sequencing batch reactors treating filtered wastewater (≈ 0.04 - 0.08) (Oerther et al., 2000). The rRNAt/rRNA ratio for *Acinetobacter* spp. also varied over a much smaller range in transition from the aeration basin to the return sludge basin of a full scale WWTP (≈ 0.23 - 0.35) (Oerther et al., 2000). This suggests that the rRNAt/rDNA ratio has a broader range than metrics previously utilized to detect in-situ bacterial activity.

8.3.2 Phase 2

The data collected after the pH control system was enabled at a control setpoint of 8.0 are presented in Figure 34 in stacked plots with identical x-axes. This setpoint was maintained for 44.3 hours. It should be noted that the initial nitrogen and molecular data points in Figure 34 are displayed at -0.9 hours because these are the final samples collected during phase 1.

pH, DO, and temperature

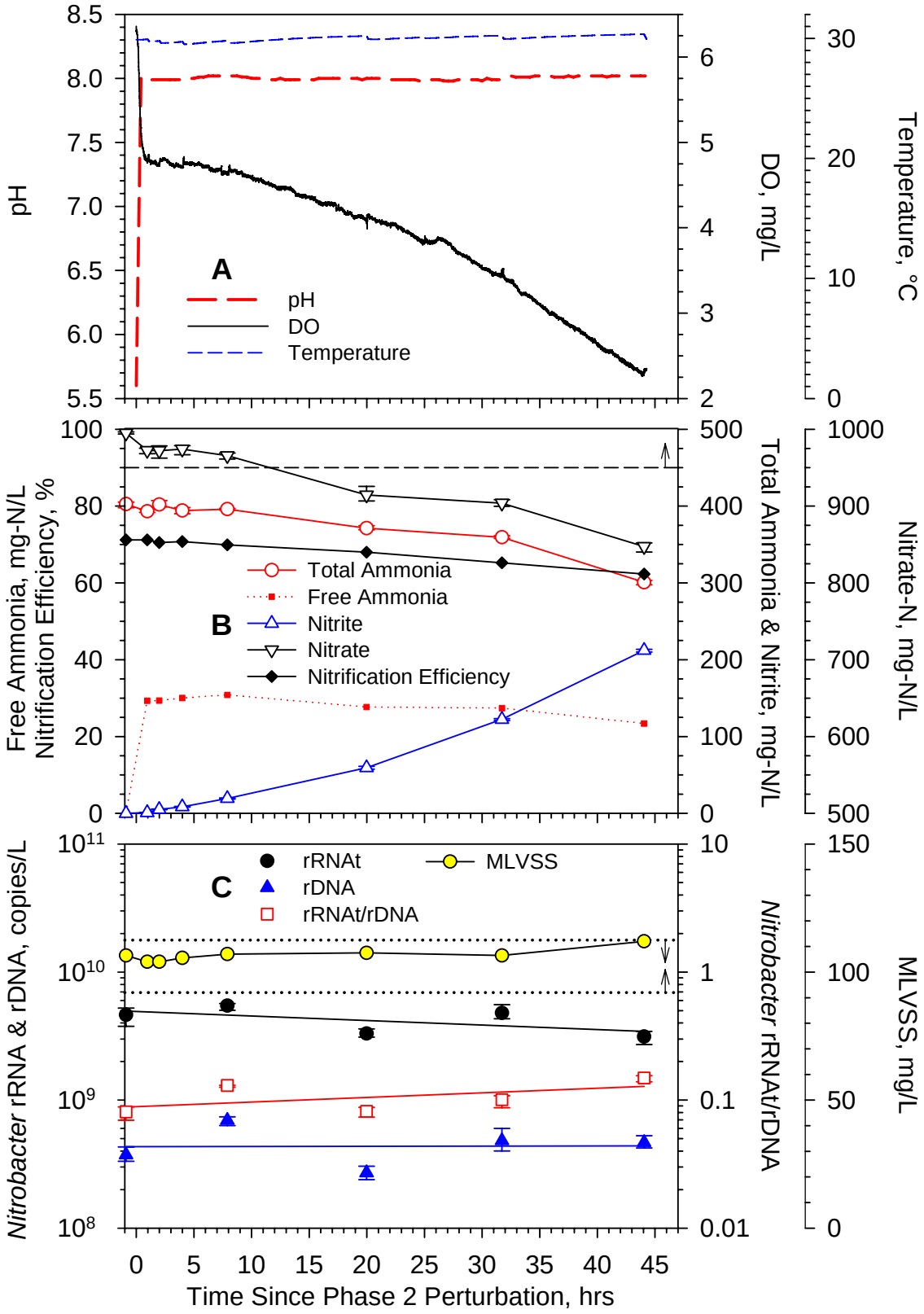
The pH control system attained the new setpoint quickly (within 15 minutes) and maintained it within a narrow range throughout phase 2 (8.00 +/- 0.01) (Figure 34-A). The DO concentration fell sharply (from 6.3 to 4.8 mg/L), but not as quickly (within 1.1 hours) (Figure 34-A). Thereafter, the DO declined to ≈ 2.25 mg/L after 44 hours at pH

Figure 34 The response of various operational parameters after enabling the BSNR pH control system at a setpoint of 8.0 to initiate phase 2 of a staged inhibition experiment.

A. Temperature, pH, and DO data.

B. Soluble nitrogen data (as mg-N/L) are presented along with the nitrification efficiency. A horizontal reference line indicates 90% nitrification efficiency.

C. The MLVSS along with the *Nitrobacter* rDNA and rRNAt concentrations and the rRNAt/rDNA ratio. For the rDNA and rRNAt data, the median ± minimum/maximum assay mean are presented (Table 24). The rRNAt/rDNA ratio is displayed with error bars corresponding to the interquartile range of all possible ratio combinations of the rDNA and rRNAt assay means (Table 24). Horizontal reference lines (·····) indicate the upper (⇓) and lower (⇑) *Nitrobacter* rRNAt/rDNA ratio prediction intervals established in Section 5.2.


A
pH
DO
Temperature
pH
DO, mg/L
Temperature, °C
B
Total Ammonia
Free Ammonia
Nitrite
Nitrate
Nitrification Efficiency
Free Ammonia, mg-N/L
Nitrification Efficiency, %
Total Ammonia & Nitrite, mg-N/L
Nitrate-N, mg-N/L
C
rRNAt
rDNA
rRNAt/rDNA
MLVSS
Nitrobacter rRNA & rDNA, copies/L
Nitrobacter rRNAt/rDNA
MLVSS, mg/L
Time Since Phase 2 Perturbation, hrs

8.0, with the concentration dropping more quickly toward the end of phase 2 (note the concave shape of the DO data trend in Figure 34-A). This suggested aerobic activity began concomitantly with the pH change and increased gradually over time. Thus, an increase in ammonia oxidation occurred soon after pH control was initiated. During phase 2, the temperature remained at the setpoint (30 ± 0.2 °C), despite the significant increase in bacterial activity.

Soluble nitrogen

While the total ammonia concentration increased rapidly when pH control was disabled (Figure 33-B), the trend for increasing ammonia concentration ended abruptly as pH control was enabled (Figure 34-B). During the first 8 hours of phase 2, the total ammonia concentration remained approximately constant (Table 23: 396 ± 17 mg-N/L). Thereafter, the concentration decreased to 301 mg-N/L after 44 hours at pH 8.0. This indicated that during the first 8 hours of phase 2, the ammonia oxidization rate approximately equaled the influent ammonia flow rate, but toward the end of phase 2, the ammonia oxidizing activity exceeded the influent rate. Thus, AOB activity increased substantially immediately after pH control system was enabled, and the total AOB activity level appeared to increase as phase 2 proceeded.

As the pH increased from 5.6 to 8.0, the free ammonia concentration increased from 0.1 to 30 mg-N/L due to a rapid acid/base equilibrium reaction (Figure 34-B) (see equations 3 - 5: Section 2.1.1). Thereafter, the concentration decreased gradually to 23.4 mg-N/L after 44 hours at pH 8.0 due to a drop in the total ammonia concentration. This free ammonia concentration range is well above most previously reported threshold levels for unacclimated NOB inhibition (Table 2: ≈ 1 - 5 mg-N/L). Though Anthonisen et al., 1976, Abeling and Seyfried, 1992, Balmelle et al., 1992, and Yang et al., 2004 indicate that such high free ammonia concentrations potentially inhibit AOB activity (Table 2), there was no evidence for significant AOB inhibition during phase 2. Since significant volatile losses of ammonia gas due to air stripping do not occur at < pH 8.5 (Ford et al., 1980), the decrease in the ammonia concentration can be attributed to AOB activity.

During phase 2, the nitrite concentration increased from below detection limits near the end of phase 1 to 212 mg-N/L at the end of phase 2 (Figure 34-B). Further, the accumulation rate appeared to increase as phase 2 proceeded, since the data trend curved upward slightly over time. Thus, the nitrite data indicate ammonia was oxidized by AOB during phase 2, but the NOB remained largely inactive.

The nitrate concentration decreased steadily when pH control was absent in the reactor (Figure 33-B). This trend was disrupted for the first 8 hours of phase 2, during which time the concentration remained relatively constant (Table 23: 971 ± 4.0 mg-N/L) (Figure 34-B). Thereafter, the nitrate concentration decreased significantly down to 847 mg-N/L at approximately the same rate noted during phase 1. Since the nitrate concentration declined during most of phase 2, NOB activity remained low.

MLVSS

After the pH control system was disabled, a MLVSS decline indicated little or no growth occurred in the reactor (Figure 33-C). However, when the control system was enabled this trend was halted (Figure 34-C). Thereafter, the MLVSS remained relatively unchanged for 44 hours (Table 23: 107 ± 3 mg/L). These results, in combination with the ammonia data, suggested that AOB growth occurred after pH control was enabled. Since the MLVSS concentration remained unchanged, this further suggested that the biomass previously lost hydraulically was replaced by AOB biomass. However, the variability apparent in the MLVSS during steady state nitrification efficiency (Section 5.2) indicated this interpretation of the results may be anecdotal.

Nitrobacter rDNA

The phase 2 *Nitrobacter* rDNA concentrations were not significantly (Table 24: Tukey group F). This was supported by a linear regression through rDNA data (Figure 34-C) and in that the MLVSS remained relatively constant during phase 2. Though this contradicted the hypothesis that the *Nitrobacter* rDNA concentration would decline during phase 2 (Section 8.2.2), the abundance at the end of phase 2 was the lowest observed in the experiment ($3.17 \pm 0.4 \times 10^9$ copies/L). Further, when the phase 1 and phase 2 data were combined, a significant monotonic decline was present (Kendall's τ = -

0.697; p-value = 0.001). Thus, the hypothesized decline in *Nitrobacter* rDNA abundance occurred, but poorly reflected the low NOB activity that was present in phases 1 and 2.

Nitrobacter rRNAt

Nitrobacter rRNAt remained low after the pH control system was enabled (Table 24: 2.78 to 7.02 $\times$ 10^8 copies/L. A linear regression through the data (Figure 34-C) did not indicate the significant downward trend that had been hypothesized (Section 8.2.2) was present. However, the transcript abundance remained low relative to the concentration measured immediately prior to the start of phase 1 (1.50 $\times$ 10^{10} copies/L), corroborating the evident lack of NOB activity.

Nitrobacter rRNAt/rDNA

A linear regression through the rRNAt/rDNA ratio data (Figure 34-C) also indicated that the metric changed little during phase 2, contrary to the hypothesis for a monotonic decline (Section 8.2.2) (Figure 34-C). However, the values (Table 24: range 0.076 - 0.14) were well below the lower BSNR prediction interval during all of phase 2 as hypothesized (Section 8.2.2). Thus, the metric reflected the fact that little nitrite oxidation activity occurred during phase 2.

8.3.3 Phase 3

To initiate phase 3, the pH setpoint was lowered from 8.0 to 7.2 to suddenly reduce the free ammonia concentration. Thus, if free ammonia had been significantly inhibiting NOB activity in phase 2, resumption in nitrite oxidation would be expected soon after phase 3 began.

pH, DO, and temperature

To avoid data loss from the multiprobe the instrument was removed from the reactor so accumulated data could be downloaded between 22.7 and 24.7 hours into phase 3 (hence the 2 hour gap in the DO data presented in Figure 35-A). At this time, the instrument was recalibrated for the DO concentration and pH.

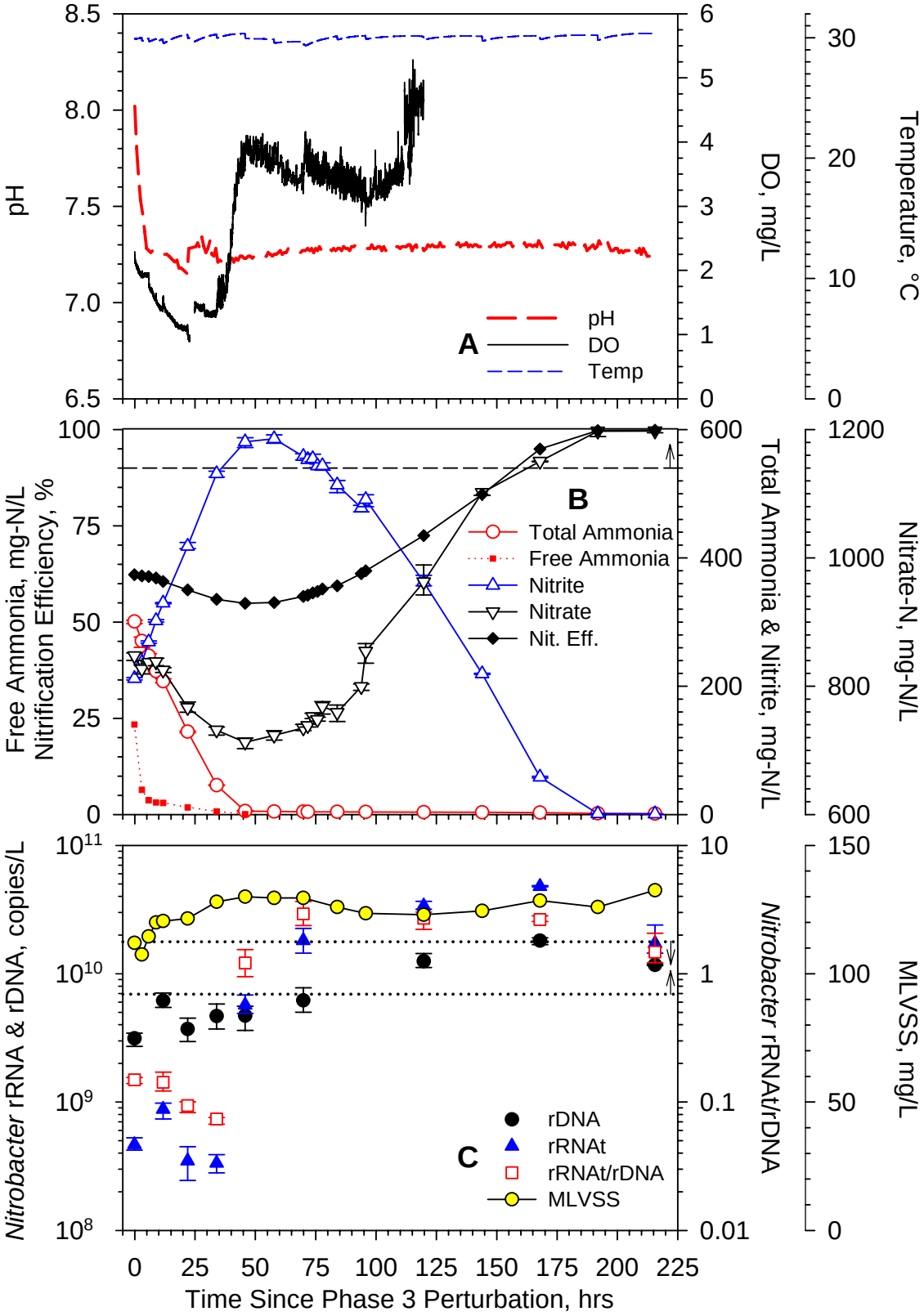
The pH dropped quickly after the control system setpoint was changed to 7.20, falling at a rate of 0.19 pH units/hr until pH 7.5 was attained after 2.7 hours (Figure 35-A). This rate of decline was similar to that observed after pH control was disabled to

Figure 35 The response of various operational parameters after changing the BSNR pH control system setpoint from 8.0 to 7.2 to initiate phase 3 of a staged inhibition experiment.

A. Temperature, pH, and DO data.

B. Soluble nitrogen data (as mg-N/L) are presented along with the nitrification efficiency. A horizontal reference line indicates 90% nitrification efficiency.

C. The MLVSS along with the *Nitrobacter* rDNA and rRNAt concentrations and the rRNAt/rDNA ratio. For the rDNA and rRNAt data, the median ± minimum/maximum assay mean are presented (Table 24). The rRNAt/rDNA ratio is displayed with error bars corresponding to the interquartile range of all possible ratio combinations of the rDNA and rRNAt assay means (Table 24). Horizontal reference lines (·····) indicate the upper (⇓) and lower (⇑) *Nitrobacter* rRNAt/rDNA ratio prediction intervals established in Section 5.2.


pH
DO, mg/L
Temperature, °C
A
pH
DO
Temp
Free Ammonia, mg-N/L
Nitrification Efficiency, %
Total Ammonia & Nitrite, mg-N/L
Nitrate-N, mg-N/L
B
Total Ammonia
Free Ammonia
Nitrite
Nitrate
Nit. Eff.
Nitrobacter rRNA & rDNA, copies/L
Nitrobacter rRNAt/rDNA
MLVSS, mg/L
C
rDNA
rRNAt
rRNAt/rDNA
MLVSS
Time Since Phase 3 Perturbation, hrs

initiate phase 1 (0.17 pH units/hr). Between 2.7 and 5.2 hours after the setpoint change, the rate of pH decline slowed to 0.10 pH units/hr. After 5.2 hours the pH control system became active and thereafter maintained the pH between 7.14 - 7.39 until the experiment ended.

The DO concentration decline that began in phase 2 (Figure 34-A) continued into phase 3 (Figure 35-A). During phase 3, the DO decreased from 2.3 to 0.9 mg/L after 22.7 hours had elapsed at pH setpoint 7.2. The DO concentration remained low (< 2.0 mg/L) until approximately 37.5 hours had elapsed. Between 37.5 and 44 hours after phase 3 began, the DO concentration increased sharply to approximately 3.8 mg/L. This suggested that a significant source of aerobic activity was eliminated during this time frame. Between 44 and 110 hours, the DO concentration was maintained between approximately 3 and 4 mg/L. After this point, the DO probe appeared to foul since the variability in the readings greatly increased. For this reason the remaining DO readings in phase 3 were discarded. However, it was clear from the reliable DO data collected that the concentration was much higher while excess nitrite was oxidized versus while excess ammonia was oxidized. This reflected the fact that nitrite oxidation consumes only 1/3 the oxygen required for ammonia oxidation.

As with phases 1 and 2, the reactor temperature was not significantly affected by the changing pH, DO, and biomass activities in phase 3 (30.0 ± 0.2 °C).

Soluble nitrogen

The free ammonia concentration was reduced from 23 mg-N/L at the end of phase 2 to 3.7 mg-N/L six hours after the pH setpoint was adjusted to 7.2 (Figure 35-B; Table 23). The concentration dropped below 1 mg-N/L between 6 and 34 hours into phase 3 due to ammonia oxidation, but the concentration at 6 hours (3.7 mg-N/L) did not significantly inhibit NOB activity in batch tests (Table 18). Thus, assuming that the relatively high free ammonia concentration (31 to 23 mg-N/L) was an important factor inhibiting nitrite oxidation in phase 2, the lower concentration established in the first six hours of phase 3 should have promoted NOB activity early in phase 3.

The drop in total ammonia that began in phase 2 (Figure 34-B) continued through the pH setpoint change in phase 3 (Figure 35-B). Between the end of phase 2 and 46 hours into phase 3, the total ammonia concentration decreased from 301 to 5 mg-N/L, confirming high AOB activity. Interestingly, this time period coincided with a DO concentration decline that began in phase 2 (Figure 34-B) and continued through phase 3 (Figure 35-B), while a sharp rise in DO concentration between 37.5 and 44 hours coincided with the disappearance of excess ammonia. This indicated that the loss in aerobic activity evident in the DO data was due to declining AOB activity as excess ammonia was exhausted.

Nitrite levels continued to increase with the declining ammonia concentration during the first 58 hours of phase 3, even though the free ammonia concentration had been significantly lowered (Figure 35-B). Thereafter, the concentration declined steadily. Thus, the recovery of NOB activity was coincidental with the removal of excess ammonia and the rise in DO concentration, rather than with the significant free ammonia reduction that occurred 40 hours earlier. This indicated free ammonia was not the principle inhibiting factor for nitrite oxidation in phase 2. Rather, based on the DO data and batch inhibition experiments in Chapter 7.0, it appeared that NOB inhibition was primarily due to poor competition for oxygen with highly active AOB, despite the bulk DO concentration remaining relatively high (≈ 1 - 4.5 mg/L from phase 2 into phase 3) compared with reported NOB oxygen half saturation constants (Table 3: ≈ 0.5 - 3 mg/L). However, other factors such as free hydroxylamine could have inhibited nitrite oxidation during phase 2 and the early part of phase 3 (Yang and Alleman, 1992). Once NOB activity resumed, nitrite was quickly removed from the reactor. Between 58 and 192 hours after the pH setpoint was changed to 7.2, the nitrite concentration decreased from 586 to 1.3 mg-N/L.

Nitrate data corroborate the assessment of AOB and NOB activity formulated based on the DO, ammonia, and nitrite data. Overall, the washout of nitrate that began in phase 1 (Figure 33-B) continued through phase 2 (Figure 34-B) and 46 hours into phase 3 (Figure 35-B). At this point the lowest nitrate concentration of the experiment occurred

(714 mg-N/L). Thereafter, nitrate increased for the first time since the experiment was initiated, indicating that NOB activity began between 46 - 58 hours into phase 3. As excess nitrite was removed over the next 134 hours, the nitrate concentration increased concomitantly to 1,198 mg-N/L, a concentration similar to that measured at the beginning of phase 1 (1,298 mg-N/L).

MLVSS

The MLVSS increased from 112 mg/L at the end of phase 2 to 130 mg/L 46 hours into phase 3 (Figure 35-C). Thereafter, the MLVSS was relatively constant until the experiment ended (127 ± 3 mg/L). The increase in suspended solids occurred while excess ammonia was removed, and the point at which the MLVSS stabilized coincided with final excess ammonia removal. Thus, it appeared that AOB growth occurred while excess ammonia was removed. However, a further rise in the MLVSS did not occur as excess nitrite was removed, though NOB growth could have been offset by declining AOB abundance once the excess ammonia had been removed. Given that the MLVSS varied considerably, even under steady state conditions (Figure 10), the link suggested between AOB and NOB populations trends and the MLVSS may not be warranted.

Nitrobacter rDNA

Nitrobacter rDNA did not increase during the first 46 hours of phase 3 as the MLVSS increased and excess ammonia was oxidized (Figure 35-C). A Tukey HSD analysis of the log transformed rDNA assay mean data confirmed that during this time the *Nitrobacter* rDNA concentrations were not significantly different (Table 24: group E). However, the Tukey HSD analysis did indicate that the *Nitrobacter* rDNA concentration 168 hours into phase 3 (Tukey group A: $1.84 \pm 0.1 \times 10^{10}$ copies/L) was significantly higher than in the first 70 hours of phase 3 ($3.80 - 6.32 \times 10^{9}$ copies/L). In addition, between 34 and 168 hours into phase 3, the *Nitrobacter* rDNA increased consecutively over 5 sample events, making the increasing rDNA trend statistically significant (Kendall's $\tau = 1$; p-value = 0.0083), which was hypothesized for phase 3 (Section 8.2.3). Thus, while the excess nitrite was removed, the *Nitrobacter* rDNA concentration increased.

Nitrobacter rRNAt

The *Nitrobacter* rRNAt concentration was low during the first 33 hours of phase 3 (Figure 35-C: 3.41 - 8.94 × 10^8 copies/L). However, the transcript abundance increased over an order of magnitude between 33 hours (3.41 ± 0.5 × 10^8 copies/L) and 46 hours (5.79 ± 1.0 × 10^9 copies/L) into phase 3. This sudden increase in transcript abundance was concomitant with excess ammonia removal and a significant increase in the DO concentration, and occurred immediately prior to a renewal in NOB activity based on the nitrite and nitrate data (between 46 - 58 hours into phase 3). Thereafter, the rRNAt concentration increased steadily until 168 hours after the pH setpoint change (4.88 ± 0.03 × 10^{10} copies/L), during which time the excess nitrite was removed. Further, between 34 and 168 hours into phase 3, the hypothesized trend for increasing *Nitrobacter* rRNAt abundance during NOB activity recovery was verified (Kendall's $\tau = 1$; p-value 0.0083; Section 8.2.3). In fact, the Tukey HSD analysis of the log transformed rRNAt assay mean data in Table 24 indicated that 168 hours into phase 3 the transcript abundance was significantly higher than at the beginning of phase 1 (Tukey group A and C, respectively). When the last sample was collected 24 hours later (after excess nitrite had been removed), the transcript abundance (1.79 × 10^{10} copies/L) had decreased significantly (Tukey group B/C) but was well above the abundance recorded at the beginning of phase 3. Thus, the *Nitrobacter* rRNAt abundance was low at the beginning of phase 3 when nitrite oxidation was inhibited, increased monotonically as excess nitrite was removed, and declined slightly after the excess nitrite was exhausted.

Nitrobacter rRNAt/rDNA ratio

As was observed in phase 1, the *Nitrobacter* rRNAt/rDNA ratio was controlled by the rRNAt abundance, so the general trends observed for transcript concentration were present for the ratio. However, a point of reference for the metric is the lower BSNR prediction interval established in Section 5.2 (Figure 35-C). The ratio was well below the lower prediction interval during the first 33 hours of phase 3 (range 0.07 - 0.12), confirming low NOB activity. Only 12 hours later, the ratio had increased above the lower prediction interval to 1.0, confirming that nitrite oxidation activity had significantly

increased. Thereafter, the ratio remained above the upper prediction interval (Figure 35-C: range 2.4 - 3.0) indicating that the NOB activity level was higher than would be expected in the BSNR when a steady state, high nitrification efficiency is maintained. After the excess nitrite was removed, the ratio returned to a range of expected values (1.5: between the upper and lower prediction intervals).

8.4 Summary

What could be described as a typical nitrification inhibition event was staged in the BSNR (Figure 36). NOB activity was clearly documented using a combination of pH, DO, and nitrogen data that could have substituted for the *Nitrobacter* rRNAt/rDNA ratio. However, the BSNR design (high influent ammonia, absence of reduced carbon, and aerobic environment), and the fact that nitrification is relatively simple ($NH_3 \rightarrow NO_2^- \rightarrow NO_3^-$), enhanced the effectiveness of these parameters in assessing activity. If the influent had contained organic substrates, or if more complicated N-conversion pathways were promoted, the effectiveness of these parameters would have been reduced.

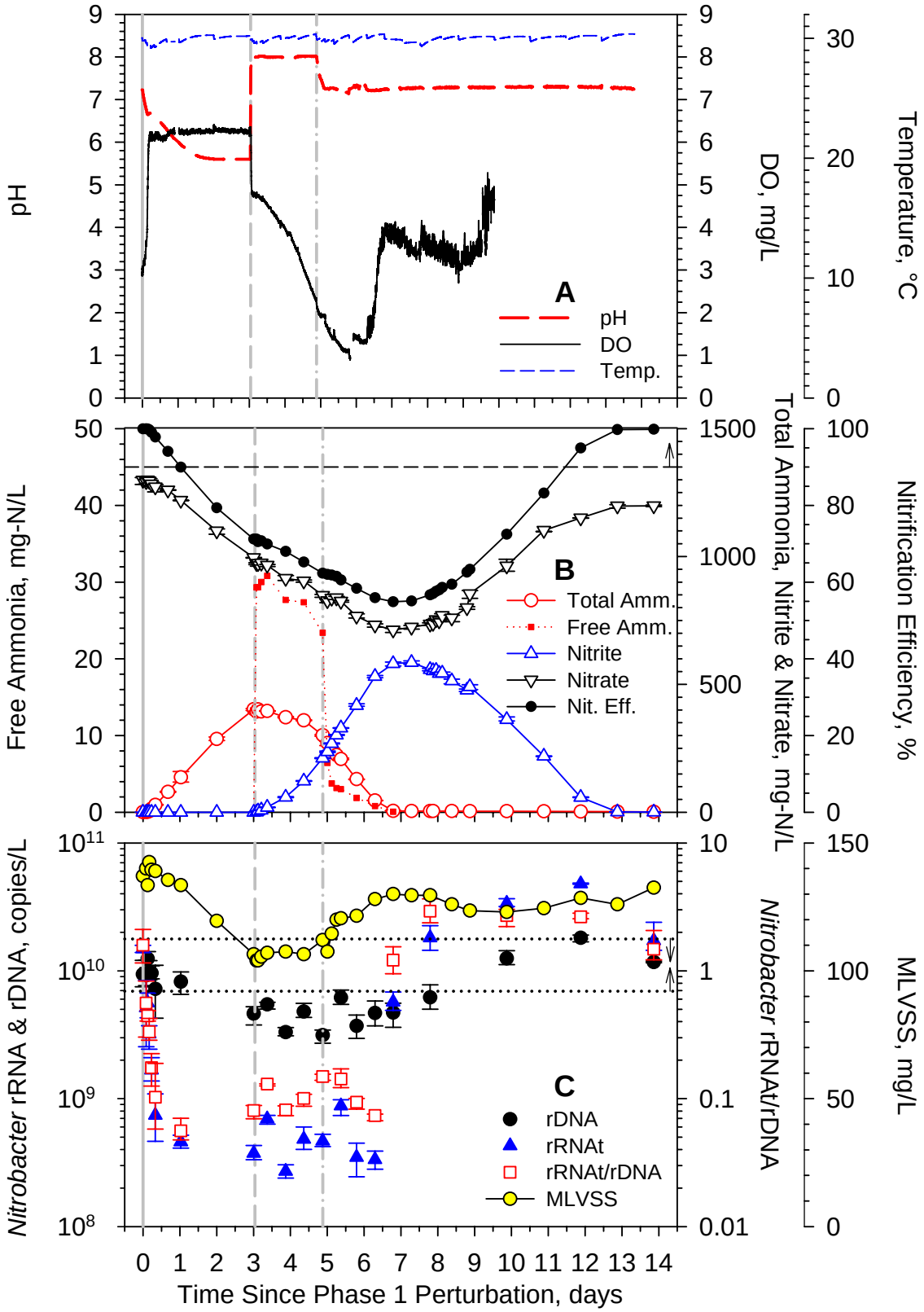
As hypothesized, the *Nitrobacter* rRNAt/rDNA ratio reflected NOB activity throughout the course of the staged inhibition experiment. In phase 1, the metric signaled an inhibition event 22 hours prior to the effects being realized as excessive ammonia accumulation. This demonstrated explicitly an application of rRNAt measurements first suggested by Cangelosi and Brabant (1997), and indicated that the ratio could be used proactively to ameliorate the effect of nitrification inhibition. Since the declining pH largely inhibited AOB activity, the results confirmed that the NOB rRNAt/rDNA ratio can be used in a dual role to monitor both AOB and NOB inhibition. In phase 2, the ratio remained below the lower BSNR prediction interval while nitrite oxidation was inhibited. In phase 3, a substantial increase in the metric value coincided with resumption of nitrite oxidation. In fact, the increase in the metric preceded clear evidence of increasing NOB activity in the nitrate data, indicating the metric can be used proactively to ameliorate the effects of NOB acclimation, for example in a denitritification reactor. Thereafter, the BSNR rRNAt/rDNA upper prediction interval was exceeded, indicating that higher than

Figure 36 The overall response of various operational parameters during a staged BSNR inhibition experiment. The being of phases 1, 2, and 3 of the experiment are indicated with vertical reference lines.

A. Temperature, pH, and DO data.

B. Soluble nitrogen data (as mg-N/L) are presented along with the nitrification efficiency. A horizontal reference line indicates 90% nitrification efficiency.

C. The MLVSS along with the *Nitrobacter* rDNA and rRNAt concentrations and the rRNAt/rDNA ratio. For the rDNA and rRNAt data, the median ± minimum/maximum assay mean are presented (Table 24). The rRNAt/rDNA ratio is displayed with error bars corresponding to the interquartile range of all possible ratio combinations of the rDNA and rRNAt assay means (Table 24). Horizontal reference lines (·····) indicate the upper (⇓) and lower (⇑) *Nitrobacter* rRNAt/rDNA ratio prediction intervals established in Section 5.2.


pH
DO, mg/L
Temperature, °C
A
pH
DO
Temp.
Free Ammonia, mg-N/L
Total Ammonia, Nitrite & Nitrate, mg-N/L
Nitrification Efficiency, %
B
Total Amm.
Free Amm.
Nitrite
Nitrate
Nit. Eff.
Nitrobacter rRNA & rDNA, copies/L
Nitrobacter rRNAt/rDNA
MLVSS, mg/L
C
rDNA
rRNAt
rRNAt/rDNA
MLVSS
Time Since Phase 1 Perturbation, days

normal nitrite oxidation activity was occurring in the BSNR. This was followed by a return to an expected range of values once excess nitrite was removed.

In phase 3, the *Nitrobacter* rRNAt/rDNA ratio emphasized a delayed return in NOB activity after the free ammonia concentration was lowered. The fact that a significant metric increase occurred concomitantly with a substantial increase in the DO concentration supported the hypothesis that poor competition for oxygen with highly active AOB can drive NOB inhibition (Chapter 7.0). It was evident in examining the nitrogen data in Figure 35 that the recovery event could have been misinterpreted as relief from free ammonia inhibition. This technique for estimating free ammonia inhibition (observing the point at which NOB activity recovers during an ammonia concentration decline) was used by Anthonisen et al (1976) who reported NOB free ammonia inhibition ranged from 0.08 - 0.8 mg-N/L. Though this work is widely referenced, the absence of controls in this and subsequent investigations to eliminate AOB activity and hold the free ammonia concentration constant (Table 2) indicates misinterpretations of the root cause of NOB inhibition could have been made when the ammonia concentration was high. However, it is also possible that hydroxylamine inhibited NOB during this experiment (Yang and Alleman, 1992).

In conclusion, the experimental results: (1) emphasized the usefulness of prediction intervals for the rRNAt/rDNA metric, (2) demonstrated the metric was sensitive to declining AOB activity, (3) demonstrated the metric could offer predictive capabilities that could be used to ameliorate the effects of undesired AOB/NOB inhibition or NOB acclimation by offering advanced warning of these events, and (4) suggested that free ammonia has only an ancillary inhibitory effect on nitrite oxidation.

CHAPTER 9.0

CONCLUSIONS AND IMPLICATIONS

9.1 Conclusions

The following conclusions were drawn from this study.

1. **The newly designed quantitative PCR detection systems for *Nitrobacter* rDNA and rRNAt were specific, accurate, and sensitive.** Even with less than optimal PCR protocol (low annealing temperatures), only *Nitrobacter* sequences appeared to be amplified in BSNR DNA and RNA extracts. The PCR/RT-PCR efficiency was similar for artificial standards and *Nitrobacter* rDNA and rRNAt in BSNR nucleic acid extracts; also, the extracts did not significantly inhibit the assays. A power analysis indicated only three replicate DNA/RNA extracts of two samples would be required to reliably detect a true ≥ 2-fold difference in *Nitrobacter* rDNA/rRNAt.

2. ***Nitrobacter* was a dominant NOB genus in the BSNR.** *Nitrobacter* rDNA constituted 5% of bacterial rDNA amplified in BSNR DNA extracts. *Nitrobacter* spp. were estimated to comprise between 11 to 22% of all bacteria in the reactor.

3. ***Nitrobacter* rDNA was useful for monitoring long term NOB population trends, but poorly reflected drastic short term nitrite oxidation activity changes.** When the BSNR was monitored over a 10 week time period, the *Nitrobacter* rDNA concentration declined significantly, even though high, steady state nitrification efficiency (> 90%) was continuously maintained. The *Nitrobacter* rDNA abundance dropped during NOB inhibition in the staged BSNR inhibition experiment, and increased after the inhibitory condition was removed.

However, the concentration changes were apparent only over the course of several days and were not evident in MLVSS variations. In a batch nitrite oxidation experiment and short term batch NOB inhibition experiments lasting several hours, *Nitrobacter* rDNA changes were not consistently detected, though nitrite oxidizing activity varied from complete inactivity to unlimited nitrite oxidation.

4. **The *Nitrobacter* rRNAt concentration varied tremendously after short term nitrite oxidizing activity changes.** In a nitrite oxidation experiment, the rRNAt concentration increased approximately 2 orders of magnitude after transition from nitrite starved to unlimited nitrite oxidizing activity. When nitrite oxidation was allowed to proceed several hours with excess nitrite present before being inhibited, the rRNAt concentration declined 1 to 2 orders of magnitude within 4.5 hours if the inhibition level was significant. The rRNAt/rDNA ratio was correlated with the rRNAt concentration, but not with the rDNA concentration, both in the BSNR at steady state nitrification efficiency and during the BSNR inhibition experiment. Since as noted above the *Nitrobacter* rDNA changed very little during short term activity changes, the *Nitrobacter* rRNAt abundance largely determined the metric value. These results also indicate that quantitative PCR is better suited to detect activity as opposed to population changes.

5. **Normalizing the rRNAt concentration to the rDNA concentration was valuable, since this made it possible to compare the relative rRNAt abundance with more precision.** The value in doing this was evident in the significant changes observed in the *Nitrobacter* rDNA concentration within the reactor, both at steady state, and during the staged inhibition experiment.

6. **The *Nitrobacter* rRNAt/rDNA ratio is at lower and upper limits during nitrite starvation and unlimited nitrite oxidation, respectively, and transitions between these limiting values over the course of several hours.** In

a batch experiment, the metric increased approximately two orders of magnitude from a lower limit of ≈ 0.05 to 0.10 during nitrite starvation to an upper limit of ≈ 3 to 6 after 8 hours of unlimited nitrite oxidation. Approximately 2 to 4 hours was required for the metric value to transition from the upper limit back to the lower limit once a starved state was resumed.

7. **BSNR *Nitrobacter* rRNAt/rDNA ratio prediction intervals were an effective means of interpreting variations in the metric value, adding the context and perspective of the reactor's treatment performance to experimental analyses.** The ratio varied between 0.68 and 1.8 during 10 weeks of steady state high nitrification efficiency (> 90%) in the BSNR. When compiled, this data was used to establish nonparametric lower (0.69) and upper (1.8) prediction intervals that were effectively used to interpret metric values generated under very different circumstances. For example, the ratio value during substrate starvation was below the lower prediction interval, and the ratio value during unlimited nitrite oxidation eventually exceeded the upper prediction interval. These results were predicted since in the BSNR NOB activity lies between these nitrite oxidizing activity extremes. During batch NOB inhibition experiments, the integration of the residual nitrite oxidizing activity data with the inhibited ratio results indicated that for two inhibitors studied (azide and H^+) the ratio would not likely decline below the reactor lower prediction interval unless the reactor treatment performance was in jeopardy. The best application for the intervals was in predicting, in an unbiased manner, near term reactor performance changes during the BSNR inhibition experiment.

8. **Free ammonia does not significantly inhibit *Nitrobacter*.** In batch experiments, nitrite oxidation was inhibited less than 60% at very high free ammonia concentrations when AOB were inhibited. In subsequent tests with uninhibited AOB at much lower free ammonia concentrations, nitrite oxidation was severely

inhibited. During the staged BSNR inhibition experiment, nitrite buildup occurred while excess ammonia was oxidized. Significantly reducing the free ammonia concentration in this experiment did not increase nitrite oxidizing activity; nitrite oxidizing activity recovered concomitantly with an increase in the bulk DO concentration and the exhaustion of excess ammonia.

9. **The *Nitrobacter* rRNAt/rDNA ratio response varies during exposure to mechanistically distinct inhibiting compounds.** For 3,5-DCP, the metric value declined significantly even when the ability to oxidize nitrite was unaffected. This indicated the ratio is particularly sensitive to growth inhibitors such as uncouplers. For azide and H^+, the metric declined appreciably only if nitrite oxidation was significantly inhibited. However, the expected decline in the ratio was absent when NOB activity was completely inhibited at pH 4.5. Conversely, when nitrite oxidation was completely inhibited after a pH change to 5.0, the metric significantly declined. This indicated that some inhibitors can arrest rRNAt processing and thereby remove the expected metric response during inhibition.

10. **The *Nitrobacter* rRNAt/rDNA ratio can be used as a species specific indicator of NOB activity to predict reactor performance changes, but is limited in this capacity by the methods currently available to quantify the ribosomal transcript and gene.** When pH control was eliminated in the BSNR, the metric value was significantly reduced within 2 hours, though the reactor nitrification efficiency did not appreciably decline until 1 day had elapsed. When NOB activity subsequently recovered, the metric value increased significantly before recovery was apparent as an increase in the nitrate concentration. However, the techniques used to quantify rDNA and rRNAt in this study (nucleic acid extraction followed by quantitative PCR), produce a lead time for the metric data ($\approx$ 8 hours) that reduces usefulness of the metric to predict performance changes.

9.2 Implications

The rRNAt/rDNA ratio can serve as a species specific in-situ indicator of nitrite oxidizing activity. For *Nitrobacter*, this parameter displays characteristics (a wide range of values and a relatively quick, consistent response to nitrite oxidizing activity changes) that would be useful in efforts to improve N-treatment efficiency, whether complete or partial nitrification is promoted. In reactors where complete nitrification is sought at 30°C, high *Nitrobacter* rRNAt/rDNA ratio values (> 2) will likely indicate that excess nitrite is present, intermediate values (0.7 - 2) will likely confirm that high nitrification efficiency can be maintained, while low values (< 0.7) could serve as a reliable indicator of NOB and/or AOB inhibition (Figure 37). However, high values can be misleading, since some inhibitors apparently destroy the ability to process existing ribosomal transcripts, which would adversely impact growth. In this case, long term NOB population changes (rDNA declines) would be useful in confirming this inhibitory condition. It is clear that other indicators of activity must be consulted in addition to the rRNAt/rDNA ratio (e.g. the OUR, trends in the NH_4^+N, NO_2^--N, and NO_3^--N concentrations, and H^+ production).

A mechanism for process improvement could be to use the metric to correlate influent sources and/or reactor operating conditions with NOB inhibition or adaptation, which may help isolate the sources or causes of these phenomena. A more advanced application would be to use the metric in a proactive remedial response. For example, in implementing complete nitrification reactor operators must now passively observe nitrification inhibition events as ammonia and nitrite accumulate, which makes a remedial response less effective. With advanced warning provided by the NOB rRNAt/rDNA metric, remedial measures could be taken before performance is impacted, perhaps preventing permit violations and downstream environmental damage. For example, the return sludge supply could be manipulated to increase the SRT, or commercial sources of nitrifying bacteria could be augmented into the reactor to prevent ammonia and/or nitrite buildup and nitrifier washout. Currently, the time required to quantify rDNA and rRNAt would limit, but not eliminate this metric application.

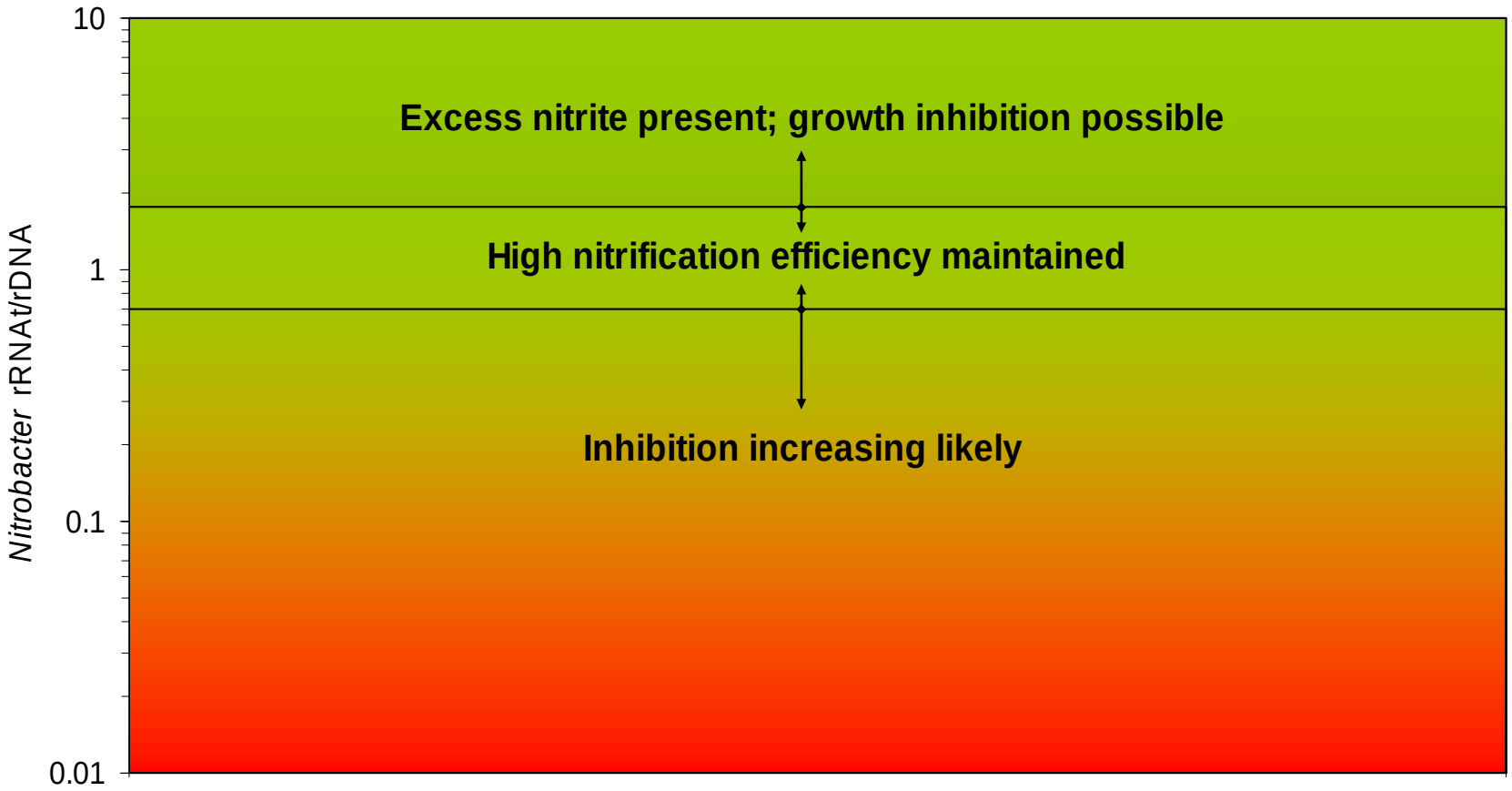


Figure 37 Schematic diagram illustrating inferences for the NOB activity level given different ranges of *Nitrobacter* rRNAt/rDNA ratio value when complete nitrification is promoted at 30°C.

Figure 37 is based on rRNAt/rDNA prediction intervals established in this study, though the general trend from the perspective of promoting complete nitrification should remain the same (declining treatment performance is likely as the ratio value drops). Establishing rRNAt/rDNA prediction intervals at high treatment efficiency should remain an effective way of interpreting metric values, but the thresholds presented in this figure will likely vary for other in which complete nitrification is promoted. For example, it is well known that NOB growth and nitrite oxidation rates vary with temperature, which may affect the threshold values presented in Figure 37. Also, the metabolic diversity of the *Nitrobacter* genera could affect the interpretation of specific ratio values in reactors where mixotrophic growth are possible, particularly since *Nitrobacter* spp. are capable of using both oxygen and nitrate as terminal electron acceptors. Of course, the ratio characteristics of *Nitrospira* need to be investigated and will likely differ from those measured for *Nitrobacter*. Also, the general perspective for treatment performance will likely be reversed from that shown in Figure 37 when partial nitrification is promoted; in this case, unusually high metric value may indicate a departure from high efficiency operating conditions as a result of NOB acclimation.

Wastewater research over the past 25 years has emphasized improved treatment efficiency through alternate N-conversion pathways. As reactors with increasingly complex consortiums of bacteria are utilized, there is more uncertainty in using N-cycle intermediates to quantify subpopulation activity. The rRNAt/rDNA ratio could help remedy this problem, since activity can be examined independently. A recent review of anammox (Stous and Jetten, 2004) reactors, in which both nitrite oxidation and reduction are possible, noted that it is not yet clear whether separate or integrated ammonia oxidation/anammox reactors will be most effective. The *Nitrobacter* rRNAt/rDNA metric could be used to study these alternative reactor configurations to determine which configuration most effectively inhibits nitrite oxidizing activity.

Energy intensive cellular functions such as motility (e.g. swarming) and production of extracellular polymers may impact rRNA levels or the rDNA transcription rate (Molin and Givskov, 1999). There is evidence that regulation of ribosomal transcription differs among bacteria (e.g. *Acinetobacter* vs. *E. coli*; Oerther et al., 2000)

and can be affected by the micronutrient composition of influent wastewater (Oerther et al., 2002). These factors could affect the usefulness of the rRNAt/rDNA ratio.

The implementation of similar ratios could be used for a variety of bacteria of interest in wastewater treatment and are not limited to the ribosomal gene. Examples include: filamentous strains to help identify and avoid sludge bulking and foaming, methanogens and acidogens to improve sludge digestion and/or methane production, poly-phosphate organisms to improve phosphate removal, and bacteria involved in N-conversion processes, such as heterotrophic denitrifiers and anaerobic ammonia oxidizers. Applications are not limited to wastewater treatment systems. For instance, the growth activity of various pathogens capable of blooming in drinking water supply systems could be monitored with rRNA/rDNA ratios (or mRNA/DNA ratios using virulence factor genes).

A caveat in applying the rRNAt/rDNA ratio to improve N-treatment efficiency is that the metric response varies across mechanistically distinct types of inhibition. While this somewhat obscures the interpretation of metric data, there is the possibility that the metric response could be used diagnoses different types of inhibition.

REFERENCES

1. Abeling, U. and Seyfried, C. F. 1992. Anaerobic-aerobic treatment of high-strength ammonium wastewater - nitrogen removal via nitrite. Water Science and Technology, 26:1007-1015.

2. Aleem, M. I. H. and Nason, A. 1960. Phosphorylation coupled to nitrite oxidation by particles from the chemoautotroph, *Nitrobacter agilis*. Proceedings of the National Academy of Science, 46:763-769.

3. Aleem, M. I. H. 1968. Mechanism of oxidative phosphorylation in the chemoautotroph *Nitrobacter agilis*. Biochimica et Biophysica Acta, 162:338-347.

4. Aleem, M. I. H. 1977. Coupling of energy with electron transfer reactions in chemolithotrophic bacteria. *In* B. A. Haddock and W. A. Hamilton (eds.), Microbial Energetics, pp. 351-381. Cambridge University Press, Cambridge.

5. Aleem, M. I. H. and Sewell, D. L. 1984. Oxidoreductase systems in *Nitrobacter agilis*. *In* W. R. Strohl and O. H. Tuovinen (eds.), Microbial Chemoautotrophy, pp. 185-210. Ohio State University Press, Columbus, OH.

6. Alleman, J. E. 1985. Elevated nitrite occurrence in biological waste-water treatment systems. Water Science and Technology, 17:409-419.

7. Altschul, S. F., Gish, W., Miller, W., Myers, E. W., and Lipman, D. J. 1990. Basic local alignment search tool. Journal of Molecular Biology, 215:403-410.

8. Altschul, S. F., Madden, T L., Schaffer A. A., Zhang J. H., Zhang, Z., Miller, W. and Lipman, D. J. 1997. Gapped BLAST and PSI-BLAST: a new generation of protein database search programs. Nucleic Acids Research, 25:3389-3402.

9. American Public Health Association (APHA). 1998. *Standard Methods for the Examination of Water and Wastewater*. 20th Edition. American Public Health Association, New York, New York.

10. Anthonisen, A. C., Loehr, R. C., Prakasam, T. B. S., and Srinath, E. G. 1976. Inhibition of nitrification by ammonia and nitrous acid. Journal of the Water Pollution Control Federation, 48:835-852.

11. Aoi, Y., Shiramasa, Y., Masaki, Y., Tsuneda, S., Hirata, A., Kitayama, A., and Nagamune, T. 2004a. Expression of *amoA* mRNA in wastewater treatment processes examined by competitive RT-PCR. Journal of Biotechnology, 111:111-120.

12. Aoi, Y., Masaki, Y., Tsuneda, S., and Hirata, A. 2004b. Quantitative analysis of amoA mRNA expression as a new biomarker of ammonia oxidizing activities in a complex microbial community. Letters in Applied Microbiology, 39(6):477-482.

13. Araki, N., Yamaguchi, T., Yamazaki, S., and Harada, H. 2004. Quantification of *amoA* gene abundance and their *amoA* mRNA levels in activated sludge by real-time PCR. Water Science and Technology, 50:1-8.

14. Arthur, J. W., West, C. W., Allen, K. N., and Hedtke, S. F. 1987. Seasonal toxicity of ammonia to 5 fish and 9 invertebrate species. Bulletin of Environmental Contamination and Toxicology, 38:324-331.

15. Atlas, R. M. and Bartha, R. 1997. *Microbial Ecology: Fundamentals and Applications*. Benjamin/Cummings Publishing Company, Inc., Menlo Park, CA.

16. Bach, H. J., Tomanova, J., Schloter, M., and Munch, J. C. 2002. Enumeration of total bacteria and bacteria with genes for proteolytic activity in pure cultures and in environmental samples by quantitative PCR mediated amplification. Journal of Microbiological Methods 49: 235-245.

17. Bach, H. J., Jessen, I., Schloter, M., and Munch, J. C. 2003. A TaqMan-PCR protocol for quantification and differentiation of the phytopathogenic *Clavibacter michiganensis* subspecies. Journal of Microbiological Methods 52: 85-91.

18. Bae, W., Baek, S., Chung, J., and Lee, Y. 2002. Optimal operational factors for nitrite accumulation in batch reactors. Biodegradation, 12:359-366.

19. Balmelle, B., Nguyen, K. M., Capdeville, B., Cornier, J. C., and Deguin, A. 1992. Study of factors controlling nitrite build-up in biological processes for water nitrification. Water Science and Technology, 26:1017-1025.

20. Bearson, S., Bradley, B., Foster, J. W. 1997. Acid stress responses in enterobacteria. FEMS Microbiology Letters, 147:173-180.

21. Bédard, C. and Knowles, R. 1989. Physiology, biochemistry, and specific inhibitors of CH_4, NH_4^+, and CO oxidation by methanotrophs and nitrifiers. Microbiological Reviews, 53:68-84.

22. Benefield, L. D. and Randall C. W. 1985. *Biological Process Design for Wastewater Treatment*, Inprint, Inc.

23. Bernet, N., Dangcong, P., Delgenès, J.-P., Moletta, R. 2001. Nitrification at low oxygen concentration in biofilm reactor. Journal of Environmental Engineering, 127:266-271.

24. Blum, D. J. W. and Speece, R. E. 1991. A database of chemical toxicity to environmental bacteria and its use in interspecies comparisons and correlations. Research Journal of the Water Pollution Control Federation, 63:198-207.

25. Bock, E. 1976. Growth of *Nitrobacter* in the presence of organic matter. II. Chemoorganotrophic growth of *Nitrobacter agilis*. Archives of Microbiology, 108:302-312.

26. Bock, E., Sundermeyer-Klinger, H. and Stackebrandt, E. 1983. New facultative lithoautotrophic nitrite-oxidizing bacteria. Archives of Microbiology, 136:281-284.

27. Bock, E., Wilderer, P. A., and Freitag, A. 1988. Growth of *Nitrobacter* in the absence of dissolved oxygen. Water Research, 22:245-250.

28. Bock, E., Koops, H.-P., and Möller, U. C., and Rudert, M. 1990. A new facultatively nitrite-oxidizing bacterium, *Nitrobacter vulgaris* sp. nov. Archives of Microbiology, 153:105-110.

29. Bock, E. and Koops, H.-P. 1992. The genus *Nitrobacter* and related genera. In: *The Prokaryotes*, 2nd edition, edited by Balows, A., Trüper, H. G., Dworkin, M., Harder, W., and Schleifer, K. H. Springer Verlag, New York, New York.

30. Bock, E., Schmidt, I., Stüven, R., and Zart, D. 1995. Nitrogen losses caused by denitrifying *Nitrosomonas* cell using ammonium or hydrogen as electron donors and nitrite as electron acceptor. Archives of Microbiology, 163:16-20.

31. Bock, E. and Wagner, M. 2001. Oxidation of inorganic nitrogen compounds as an energy source. In: Dworkin, M. ed., The Prokaryotes: an evolving electronic resource for the microbiology community, 3rd edition, release 3.7. Spinger-Verlag, New York, http://141.150.157.117:8080/prokPUB/index.htm.

32. Bollmann, A., Schmidt, I., Saunders, A. M., and Nicolaisen, M. H. 2005. Influence of starvation on potential ammonia-oxidizing activity and *amoA* mRNA levels of *Nitrosospira brensis*. Applied and Environmental Microbiology, 71:1276-1282.

33. Borneman, J., and E. W. Triplett. 1997. Molecular microbial diversity in soils from eastern Amazonia: evidence for unusual microorganisms and microbial population shifts associated with deforestation. Applied and Environmental Microbiology, 63:2647-2653.

34. Brosius, J., Dull, T. J., Sleeter, D. D., and Noller, H. F. 1981. Gene organization and primary structure of a ribosomal RNA operon from *Escherichia coli*. Journal of Molecular Biology, 148:107-127.

35. Bulich, A. A. 1986. Bioluminescence assays. Chapter 4 in: Toxicity testing using Microorganisms, Volume I. Editors Dutka, B. J. and Bitton, G. CRC Press, Inc., Boca Raton, FL.

36. Burrell, P. C., Keller, J., Blackall, L. L. 1998. Microbiology of a Nitrite-Oxidizing Bioreactor. Applied and Environmental Microbiology. 64:1878-1883.

37. Bustin, S. A. 2000. Absolute quantification of mRNA using real-time reverse transcription PCR assays. Journal of Molecular Endocrinology 25:169-193.

38. Bustin, S. A. 2002. Quantification of mRNA using real-time reverse transcription PCR: trends and problems. Journal of Molecular Endocrinology 29:23-29.

39. Calli, B., Tas, N., Mertoglu, B., Inanc, B., and Ozturk, I. 2003. Molecular analysis of microbial communities in nitrification and denitrification reactors treating high ammonia leachate. Journal of Environmental Science and Health, Part A - Toxic/Hazardous Substances & Environmental Engineering; 38:1997-2007.

40. Cangelosi, G. A., Brabant, W. H., Britschgi, T. B., and Wallis, C. K. 1996. Detection of rifampin- and ciprofloxacin-resistant *Mycobacterium tuberculosis* by using species-specific assays for precursor rRNA. Antimicrobial Agents and Chemotherapy, 40:1790-1795.

41. Cangelosi, G. A. and Brabant, W. H. 1997. Depletion of pre-16S rRNA in starved *Escherichia coli* cells. Journal of Bacteriology, 179:4457-4463.

42. Čech, J. S., Chudoba, J., and Grau, P. 1984. Determination of kinetic constants of activated sludge microorganisms. Water Science and Technology, 17:259-272.

43. Chain, P., Lamerdin, J., Larimer, F, Regala, W., Lao, V., Land, M., Hauser, L., Hooper, A., Klotz, M., Norton, J., Sayavedra-Soto, L., Arciero, D., Hommes, N., Whittaker, M., and Arp, D. 2003. Complete genome sequence of the ammonia oxidizing bacterium and obligate chemolithoautotrophic *Nitrosomonas europaea*. Journal of Bacteriology, 185:2759-2773.

44. Chandran, K. 1999. Biokinetic characterization of ammonia and nitrite oxidation by a mixed nitrifying culture using extant respirometry. Ph.D. Thesis, University of Connecticut, Storrs.

45. Chen, Y. and Suzuki, I. 2004. Effect of uncouplers on endogenous respiration and ferrous iron oxidation in a chemolithoautotrophic bacterium *Acidithiobacillus (Thiobacillus) ferrooxidans*. FEMS Microbiology Letters 237:139-145.

46. Chiocchia, G. and Smith, K. A. 1997. Highly sensitive method to detect mRNAs in individual cells by direct RT-PCR using *Tth* DNA polymerase. Biotechniques, 22:312-318.

47. Cho, J. C. and Kim, S. J. 2000. Increase in bacterial community diversity in subsurface aquifers receiving livestock wastewater input. Applied and Environmental Microbiology, 66:956-965.

48. Chudoba, P., Capdeville, B., and Chudoba, J. 1992. Explanation of the biological meaning of the S0/X0 ratio in batch cultivation. Water Science and Technology, 26:743.

49. Chun-Man, C., Waihung, L., Kwok-Yin, W., and Wai-Fun, C. 1999. Monitoring the toxicity of phenolic chemicals to activated sludge using a novel optical scanning respirometer. Chemosphere, 39:1421-1432.

50. Chung, J., Shim, H., Lee, Y. W., and Bae, W. 2005. Comparison of influence of free ammonia and dissolved oxygen on nitrite accumulation between suspended and attached cells. Environmental Technology, 26:21-33.

51. Cobley, J. B. 1976a. Energy conserving reactions in phosphorylating electron-transport particles from Nitrobacter winogradskyi. Activation of nitrite oxidation by the electrical component of the proton motive force. Biochemistry Journal. 156:481-491.

52. Cobley, J. B. 1976b. Reduction of cytochromes by nitrite in electron-transport particles from *Nitrobacter winogradskyi*. Biochemistry Journal, 156:493-498.

53. Copp, J. B. and Murphy, K. L. 1995. Estimation of the active nitrifying biomass in activated sludge. Water Research, 29:1855-1862.

54. Coskuner G. and Curtis T.P. 2002. In-situ characterization of nitrifiers in an activated sludge plant: detection of *Nitrobacter* spp. Journal of Applied Microbiology, 93:431-437.

55. Cotter, P. D. and Hill, C. 2003. Surviving the acid test: responses of gram-positive bacteria to low pH. Microbiology and Molecular Biology Reviews, 67:429-453.

56. Dalzell, D. J. B., Alte, S., Aspichueta, E., de la Sota, A., Etxebarria, J., Gutierrez, M., Hoffmann, C. C., Sales, D., Obst, U., and Christofi, N. 2002. A comparison of five rapid direct toxicity assessment methods to determine toxicity of pollutants to activated sludge. Chemosphere, 47:535-545.

57. Daims, H., Nielsen P.H., Nielsen, J.L., Juretschko, S., and Wagner, M. 2000. Novel *Nitrospira*-like bacteria as dominant nitrite-oxidizers in biofilms from wastewater treatment plants: diversity and in-situ physiology. Water Science and Technology, 41:85-90.

58. Daims, H., Nielsen, J. L., Nielsen, P. H., Schleifer, K. H., and Wagner, M. 2001. In-situ characterization of *Nitrospira*-like nitrite oxidizing bacteria active in wastewater treatment plants. Applied and Environmental Microbiology, 67:5273-5284.

59. Dapena-Mora, A., van Hulle, S. W. H., Campos, J. L., Mendez, R., and Jetten, M. S. M. 2004. Enrichment of anammox bacteria from activated sludge: experimental and modeling results. Journal of Chemical Technology and Biotechnology, 79:1421-1428.

60. Dawes, E. A. 1986. Microbial Energetics. Blackie & Sons, Glasgow.

61. de Boer, W., Gunnewiek, P. J. A., Veenhuis, M., Bock, E. and Laanbroek, H. G. 1991. Nitrification at low pH by aggregated chemolithotrophic bacteria. Applied and Environmental Microbiology, 57:3600-3604.

62. Dilworth, M. J. and Glenn, A. R. 1999. Problems of adverse pH and bacterial strategies to combat it. In: Chadwich, D. J. and Cardew (ed.), Bacterial responses to pH. Novartis Foundation Symposium 221. John Wiley & Sons, Brisbane, Australia.

63. Dionisi, H. M., Layton, A. C., Harms, G., Gregory, I. R., Robinson, K. G., and Sayler, G. S. 2002. Quantification of *Nitrosomonas oligotropha*-like ammonia oxidizing bacteria and *Nitrospira spp.* from full-scale wastewater treatment plants by competitive PCR. Applied and Environmental Microbiology, 68:245-253.

64. Dionisi, H. M., Harms, G., Layton, A. C., Gregory, I. R., Parker, J., Hawkins, S. A., Robinson, K. G., and Sayler, G. S. 2003. Power analysis for real-time PCR quantification of genes in activated sludge and analysis of the variability introduced by DNA extraction. Applied and Environmental Microbiology, 69:6597-6604.

65. Egli, K., Bossard, F., Werlen, C., Lais, P., Siegrist, H., Zehnder, A. J. B., and van der Meer, J. R. 1998. Microbial composition and structure of a rotating biological contactor biofilm treating ammonium-rich wastewater without organic carbon. Microbial Ecology, 45:419-432.

66. Egli, K., Fanger, U., Alvarez, P. J. J., Siegrist, H., van der Meer, J. R., Zehnder, A. J. B. 2001. Enrichment and characterization of an anammox bacterium from a

rotating biological contactor treating ammonium-rich leachate. Archives of Microbiology, 175:198-207.

67. Ehrich, S. D., Behrens, D., Lebedeva, E., Ludwig, W., and Bock, E. 1995. A new obligately chemolithoautotrophic, nitrite-oxidizing bacterium. *Nitrospira moscoviensis* sp. nov. and its phylogenetic relationship. Archives of Microbiology, 164:16-23.

68. Eigener, U. 1975. Adenine nucleotide pool variations in intact Nitrobacter winogradskyi cells. Archives of Microbiology, 102:233-240.

69. EPA. 1993. Process design manual for nitrogen control. EPA/625/R-93/010.

70. Escher, B. I., Snozzi, M., and Schwarzenbach, R. P. 1996. Uptake, speciation, and uncoupling activity of substituted phenols in energy transducing membranes. Environmental Science and Technology, 30:3071-3079.

71. Escher, B. I. and Schwarzenbach, R. P. 2002. Mechanistic studies on baseline toxicity and uncoupling of organic compounds as a basis for modeling effective membrane concentrations in aquatic organisms. Aquatic Sciences, 64:20-35.

72. Ferguson, S. J. 1982. Is a proton pumping cytochrome oxidase essential for energy conservation in *Nitrobacter*? FEBS Letters, 146:239-243.

73. Fernandez, A. S, Hashsham, S. A., Dollhopf, S. L., Raskin, L., Glagoleva, O., Dazzo, F. B., Hickey, R. F., Criddle, C. S., Tiedje, J. M. 2000. Flexible community structure correlates with stable community function in methanogenic bioreactor communities perturbed by glucose. Applied and Environmental Microbiology, 66:4058-4067.

74. Ferris, M. J., Muyzer, G., and Ward, D. M. 1996. Denaturing gradient gel electrophoresis profiles of 16S rRNA-defined populations inhabiting a hot spring microbial mat community. Applied and Environmental Microbiology, 62:340-346.

75. Finstein, M. S. and Delwitche, C. C. 1965. Molybdenum as a micronutrient for *Nitrobacter*. Journal of Bacteriology, 89:123-128.

76. Fischer-Le Saux, M., Hervio-Heath, D., Loaec, S., Colwell, R. R., and Pommepuy, M. 2002. Detection of cytotoxin-hemolysin mRNA in nonculturable populations of environmental and clinical *Vibrio vulnificus* strains in artificial seawater. Applied and Environmental Microbiology, 68:5641-5646.

77. Flaerdh, K., Cohen, P. S., and Kjelleberg, S. 1992. Ribosonme exist in large excess over the apparent demand in protein synthesis during carbon starvation in marin Vibri sp. Strin CCUG 15956. Journal of Bacteriology, 174:6780-6788.

78. Freeman, W. M., Vrana, S. L., Vrana, K. E. 1996. Use of elevated reverse transcription reaction temperatures in RT-PCR. Biotechniques, 20:782-783.

79. Freeman, W. M., Walker, S. J., and Vrana, K. E. 1999. Quantitative RT-PCR: Pitfalls and potential. Biotechniques, 26:112-125.

80. Freitag, A., Rudert, M., and Bock, E. 1987. Growth of *Nitrobacter* by dissimilatoric nitrate reduction. FEMS Microbiology Letters, 48:105-109.

81. Freitag, A. and Bock, E. 1990. Energy conservation in Nitrobacter. FEMS Microbiology Letters, 66:157-162.

82. Ford, D. L., Churchwell, R. L., and Kachtick, J. W. 1980. Comprehensive analysis of nitrification of chemical processing wastewaters. Journal of the Water Pollution Control Federation, 52:2726-2746.

83. Fouratt, M. A., Rhodes, J. S., Smithers, C. M., Love, N. G., and Stevens, A. M. 2003. Application of temperature gradient gel electrophoresis to the characterization of a nitrifying bioaugmentation product. FEMS Microbiology Ecology, 43:277-286.

84. Fukui, M., Suwa, Y., and Urushigawa, Y. 1996. High survival efficiency and ribosomal RNA decaying pattern of *Desulfobacter latus*, a highly specific acetate-utilizing organism, during starvation. FEMS Microbiology Ecology, 19:17-25.

85. Fukuoka, M. Fukumori, Y., and Yamanaka, T. 1987. *Nitrobacter winogradskyi* cytochrome a_1c_1 is an iron-sulfur molybdoenzyme having hemes a and c_1. Journal of Biochemistry, 102:525-530.

86. Fux, C., Boehler, M., Huber, P., Brunner, I., and Siegrist, H. 2002. Biological treatment of ammonium-rich wastewater by partial nitritation and subsequent anaerobic ammonium oxidation (anammox) in a pilot plant. Journal of Biotechnology, 99:295-306.

87. Fux, C., Lange, K., Faessler, A., Huber, P., Grueniger, B., and Siegrist, H. 2003. Nitrogen removal from digester supernatant via nitrite - SBR or SHARON? Water Science and Technology, 48:9-18.

88. Gaal, T., Bartlett, M. S., Ross, W., Turnbough, C. L., and Gourse, R. L. 1997. Transcription regulation by initiating NTP concentration: rRNA synthesis in bacteria. Science, 278:2092-2097.

89. García-Martínez, J., Acinas, S. G., Antón, A. I., and Rodríguez-Valera, F. 1999. Use of the 16S-23S ribosomal genes spacer region in studies of prokaryotic diversity. Journal of Microbiological Methods, 36:55-64.

90. Garrido, J. M. van Benthum, W. A. J., van Loosdrecht, M. C. M., and Heijnen, J. J. 1997. Influence of dissolved oxygen concentration on nitrite accumulation in a biofilm airlift suspension reactor. Biotechnology and Bioengineering, 53:168-178.

91. Gendig, C., Domogala, G., Agnoli, F., Pagga, U., Strotmann, U. J. 2003. Evaluation and further development of the activated sludge respiration inhibition test. Chemosphere, 52:143-149.

92. Georgellis, D., Arvidson, S., and von Gabain, A. 1992. Decay of ompA mRNA and processing of 9S RNA are immediately affected by shifts in growth rate, but in opposite manners. Journal of Bacteriology, 174:5382-5390.

93. Gernaey, K., Verschuere, L., Luyten, L., and Verstraete, W. 1997. Fast and sensitive acute toxicity detection with an enrichment nitrifying culture. Water Environment Research, 69:1163-1169.

94. Gernaey, K., Maffie, D., Vanrolleghem, P. and Verstraete, W. 1999. A new pH-based procedure to model toxic effects on nitrifiers in activated sludge. Journal of Chemical Technology and Biotechnology, 74:679-687.

95. Gibson, U. E. M., Heid, C. A., and Williams, P. M. 1996. A novel method for real time quantitative RT-PCR. Genome Research, 6:995-1001.

96. Ginestet, P., Audic, J.-M., Urbain, V., and Block, J.-C. 1998. Estimation of nitrifying bacterial activities by measuring oxygen uptake in the presence of the metabolic inhibitors allylthiourea and azide. Applied and Environmental Microbiology, 64:2266-2268.

97. Gourse, R. L., Gaal, T., Bartlett, M. S., Appleman, J. A., and Ross, W. 1996. rRNA transcription and growth rate-dependent regulation of ribosome synthesis in *Escherichia coli*. Annual Review of Microbiology, 50:645-677.

98. Grady, C. P. L., Daigger, G. T., and Lim, H. C. 1999. Biological Wastewater Treatment. 2nd Edition. Marcel Dekker, Inc., New York, New York.

99. Graja, S. and Wilderer. 2001. Characterization and treatment of the liquid effluents from the anaerobic digestion of biogenic solids waste. Water Science and Technology, 43:265-274.

100. Grunditz, C. and Dalhammer, G. 2001. Development of nitrification inhibition assays using pure cultures of *Nitrosomonas* and *Nitrobacter*. Water Research, 35:433-440.

101. Grundmann, G. L., Neyra, M. and Normand, P. 2000. High-resolution phylogenetic analysis of NO_2^--oxidizing *Nitrobacter* species using the *rrs-rrl* IGS sequence and *rrl* genes. International Journal of Systematic and Evolutionary Microbiology, 50:1893-1898.

102. Guisasola, A., Jubany, I., Baeza, J. A., Carrera, J., and Lafuente, J. 2005. Respirometric estimation of the oxygen affinity constants for biological ammonium and nitrite oxidation. Journal of Chemical Technology and Biotechnology, 80:388-396.

103. Gutiérrez, M., Etxebarria, J., and de las Fuentes, L. 2002. Evaluation of wastewater toxicity: comparative study between Microtox® and activated sludge oxygen uptake inhibition. Water Research, 36:919-924.

104. Hall, E. R. and Murphy, K. L. 1980. Estimation of nitrifying biomass and kinetics in wastewater. Water Research, 14:297-304.

105. Hamuda, H, Kiss, Z., Várady, G., Kuesma, N., Balázsy, S., and Kecskés, M. 1995. The influence of nitrapyrin and sodium azide on the growth and respiration of some *Rhizobium* strains. Microbiological Research, 150:247-251.

106. Hanaki, K. Wantawin, C. and Ohgaki, S. 1990. Nitrification at low levels of dissolved oxygen with and without organic loading in a suspended-growth reactor. Water Research, 24:297-302.

107. Hankinson, T. R. and Schmidt, E. L. 1988. An acidophilic and a neutrophilic *Nitrobacter* strain isolated from the numerically predominant nitrite-oxidizing population of an acid forest soil. Applied and Environmental Microbiology, 54:1536-1540.

108. Hara, T., Villalobos, A. P., Fukumori, Y., and Yamanaka, T. 1991. Purification and characterization of ATPase from *Nitrobacter winogradskyi*. FEMS Microbiology Letters, 82:49-54.

109. Harms, G., Layton, A. C., Dionisi, H. M., Gregory, I. R., Hawkins, S. A., Robinson, K. G., and Sayler, G. S. 2003. Real-time PCR quantification of nitrifying bacteria in a municipal wastewater treatment plant. Environmental Science and Technology, 37:343-351.

110. Hawkins, S. A. 2000. A bench scale activated sludge study of nitrification and carbon treatment using municipal wastewater. Masters Thesis, Department of Civil and Environmental Engineering, University of Tennessee, Knoxville, TN.

111. He, J. W. and Jiang, S. 2005. Quantification of enterococci and human adenoviruses in environmental samples by real-time PCR. Applied and Environmental Microbiology, 71:2250-2255.

112. Head, I.M., Hiorns, W. D., Embley, T. M., McCarthy, A. J., and Saunders, J. R. 1993. The phylogeny of autotrophic ammonia-oxidizing bacteria as determined by analysis of 16S ribosomal RNA gene sequences. Journal of General Microbiology, 139:1147-1153.

113. Heid, C. A., Stevens, J., Livak, K. J., and Williams, P. M. 1996. Real time Quantitative PCR. Genome Research, 6:986-994.

114. Hellinga, C., Schellen, A. A. J. C., Mulder, J. W., van Loosdrecht, M. C. M., and Heijnen, J. J. 1998. The SHARON process: an innovative method for nitrogen removal from ammonium-rich waste water. Water Science and Technology, 37:135-142.

115. Helsel, D. R. and Hirsch, R. M. 2002. Statistical Methods in Water Resources. U.S. Geologic Survey, U.S. Department of the Interior.

116. Henze, M., C. P. L. Grady, Fr., Gujer, W., Marais, G. v. R., and Matsuo, T. 1987. Activated Sludge Model No. 1. IAWQ Scientific and Technical Reports No. 1. IAWQ, London.

117. Henze, M. 1991. Capabilities of biological nitrogen removal processes from wastewater. Water Science and Technology, 23:669-679.

118. Hermansson, A. and Lindgren, P.-L. 2001 Quantification of ammonia-oxidizing bacteria in arable soil by real-time PCR. Applied and Environmental Microbiology, 67:972-976.

119. Higuchi, R., Fockler, C., Dollinger, G., and Watson, R. 1993. Kinetic PCR analysis: real-time monitoring of DNA amplification reactions. Bio/Technology, 11:1026-1030.

120. Hiorns, W. D., Hastings, R. C., Head, I. M., McCarthy, A. J., Saunders, J. R., Pickup, R. W., and Hall, G. H. 1995. Amplification of 16S ribosomal RNA genes of autotrophic ammonia-oxidizing bacteria demonstrates the ubiquity of *Nitrosospiras* in the environment. Microbiology (UK), 141:2793:2800.

121. Hirayama, H., Takai, K., Inagaki, F., Yamato, T., Suzuki, M., Nealson, K. H., and Horidoshi, K. 2005. Bacterial community shift along a subsurface geothermal water stream in a Japanese gold mine. Extremophiles, 9:169-184.

122. Hockenbury, M. R. and Grady, C. P. L. 1977. Inhibition of nitrification - effects of selected organic compounds. Journal of the Water Pollution Control Federation, 49:768-777.

123. Holland, P. M., Abramson, R. D., Watson, R., and Gelhard, D. H. 1991. Detection of specific polymerase chain reaction product by utilizing the 3′ → 5′ exonuclease activity of *Thermus aquaticus* DNA polymerase. Proceedings of the National Academy of Science, 88:7276-7280.

124. Hollocher, T. C., Kumar, S. and Nicholas, D. J. D. 1982. Respiration-dependent proton-translocation in *Nitrosomonas eutropaea* and its apparent absence in *Nitrobacter agilis* during inorganic oxidations. Journal of Bacteriology, 149:1013-1020.

125. Holmstrøm, K. Tolker-Nielsen, T., and Molen, S. 1999. Physiological states of individual *Salmonella typhimurium* cells monitored by in-situ reverse transcription-PCR. Journal of Bacteriology, 181:1733-1738.

126. Hooper, A. B., Vannelli, T., Bergmann, D. J., and Arciero, D. M. 1997. Enzymology of the oxidation of ammonia to nitrite by bacteria. Antoine van Leeuwenhoek, 71:59-67.

127. Hovanec, T. A., Taylor, L. T., Blakis, A. and Delong, E. F. 1998. *Nitrospira*-like bacteria associated with nitrite oxidation in freshwater aquaria. Applied and Environmental Microbiology, 64:258-264.

128. Hristova, K. R., Lutenegger, C. M., and Scow, K. M. 2001. Detection and quantification of methyl tert-butyl ether-degrading strain PM1 by real-time TaqMan PCR. Applied and Environmental Microbiology, 67:5154-5160.

129. Iman, R. L. 1994. A Data-Based Approach to Statistics. Wadsworth Publishing Company, Belmont, CA.

130. International Standards Organization (ISO). 1986. Test for inhibition of activated sludge by oxygen consumption. ISO 8192.

131. Jayamohan, S., Ohgaki, S., and Hanaki, K. 1988. Effect of DO on kinetics of nitrification. Water Supply, 6:141-150.

132. Jenson, M. A., Webster, J. A., and Staus, N. 1993. Rapid identification of bacteria on the basis of polymerase chain reaction-amplified ribosomal DNA spacer polymorphisms. Applied and Environmental Microbiology, 59:945-852.

133. Jetten, M. S. M., Strous, M., van de Pas-Schoonen, K. T., Schalk, J., van Dongen, U. G. J. M., van de Graff, A. A., Logemann, S., Muyzer, G., van Loosdrecht, M. C. M., and Kuenen, J. G. 1999. The anaerobic oxidation of ammonium. FEMS Microbiology Reviews, 22:421-437.

134. Jonsson, K., Grunditz, C., Dalhammar, G., and Jansen, J. L. 2000. Occurrence of nitrification inhibition in Swedish municipal wastewaters. Water Research, 34:2455-2462.

135. Juretschko, S., Timmermann, G., Schmid, M., Schleifer, K.-H., Pommerening-Röser, A., Koops, H.-P., and Wagner, M. 1998. Combined molecular and conventional analyses of nitrifying bacterium diversity in activated sludge: *Nitrosomonas mobilis* and *Nitrospira*-like bacteria as dominant populations. Applied and Environmental Microbiology, 64:3042-3051.

136. Ka, J. O., Yu, Z., and Mohn, W. W. 2001. Monitoring the size and metabolic activity of the bacterial community during biostimulation of fuel-contaminated soil using competitive PCR and RT-PCR. Microbial Ecology, 42:267-273.

137. Kämpfer, P., Erhart, R., Beimfohr, C., Bohringer, J., Wagner, M., and Amann, R. 1996. Characterization of bacterial communities from activated sludge: Culture-dependent numerical identification versus in situ identification using group- and genus-specific rRNA-targeted oligonucleotide probes. Microbial Ecology, 32:101-121.

138. Kerkhof, L. and Ward, B. B. 1993. Comparison of nucleic acid hybridization and fluorometry for measurement of the relationship between RNA/DNA Ratio and growth rate in a marine bacterium. Applied and Environmental Microbiology, 59:1303-1309.

139. Kiesow, L. 1964. On the assimilation of energy from inorganic sources in autotrophic forms of life. Proceedings of the National Academy of Science, 52:980-988.

140. Kikuchi, T., Iwasaki, K., Nishihara, H., Takamura, Y., and Yagi, O. 2002. Quantitative and rapid detection of the trichloroethylene-degrading bacterium *Methylocystis* sp M in groundwater by real-time PCR. Applied and Environmental Microbiology, 59:731-736.

141. King, E. F. and Dutka, B. J. 1986. Respirometric Techniques. Chapter 5 in: Toxicity testing using Microorganisms, Volume I. Editors Dutka, B. J. and Bitton, G. CRC Press, Inc., Boca Raton, FL.

142. Kim, J. S. and Chang, D. 1999. Evaluation of respirometric nitrification rate measurement technique. Journal of Industrial and Engineering Chemistry, 6:25-31.

143. Kirstein, K. and Bock, E. 1993. Close genetic relationship between Nitrobacter hamburgensis nitrite oxidoreductase and *Escherichia coli* nitrate reductase. Archives of microbiology, 160:447-453.

144. Klappenbach, J. A., Saxman, P. R., Cole, J. R., and Schmidt, T. M. 2001. rrndb: the ribosomal RNA operon copy number database. Nucleic Acids Research, 29:181-184.

145. Klečka, G. M. and Landi, L. P. 1985. Evaluation of the OECD activated sludge, respiration inhibition test. Chemosphere, 14:1239-1251.

146. Knowles, A. E. and Nagy, A. K. 1999. Inhibition of an ecto-ATP-diphosphohydrolase by azide. European Journal of Biochemistry, 262:349-357.

147. Koopman, B. and Bitton, G. 1986. Toxicity screening in wastewater treatment systems. Chapter 5 in: Toxicity testing using Microorganisms, Volume II. Editors Dutka, B. J. and Bitton, G. CRC Press, Inc., Boca Raton, FL.

148. Koops, H.-P., Böttcher, B., Möller, U. C., Pommerening-Röser, A., and Stehr, G. 1991. Classification of eight new species of ammonia-oxidizing bacteria: *Nitrosomonas communis* sp. nov., *Nitrosomonas urea* sp. nov., *Nitrosomonas aestuarii* sp. nov., *Nitrosomonas marina* sp. nov., *Nitrosomonas nitrosa* sp. nov., *Nitrosomonas eutropha* sp. nov., *Nitrosomonas oligotropha* sp. nov. and *Nitrosomonas halophila* sp. nov. Journal of General Microbiology, 137:1689-1699.

149. Koops, H.-P. and Pommerening-Röser, A. 2001. Distribution and ecophysiology of the nitrifying bacteria emphasizing cultured species. FEMS Microbiology Ecology, 37:1-9.

150. Kowalchuk, G. A., Naoumenko, Z. S., Derikx, P. J., L., Felske, A., Stephen, J. R., and Arkhipchenko, I. A. 1999. Molecular analysis of ammonia-oxidizing bacteria of the β-subdivision of the class *Proteobacteria* in compost and composted materials. Applied and Environmental Microbiology, 65:396-403.

151. Krüger, B., Meyer, O., Nagel, M., Andreesen, J. R., Meincke, M. and Bock, E., Blümle, S., and Zumft, W. G. 1987. Evidence for the presence of bactopterin in

the eubacterial molybdoenzymes nicotinic acid dehydrogenase, nitrite oxidoreductase, and respiratory nitrate reductase. FEMS Microbiology Letters, 48:225-227.

152. Kuenen, J. G. and Jetten, M. S. M. 2001. Extraordinary anaerobic ammonium-oxidizing bacteria. ASM News, 67:456-463.

153. Kumar, S. and Nicholas, D. J. D. 1981. Oxygen-dependent nitrite uptake and nitrate production by cells, spheroplasts and membrane vesicles of *Nitrobacter agilis*. FEMS Microbiology Letters, 11:201-206.

154. Kumar, S. and Nicholas, D. J. D. 1983. Proton electrochemical gradients in washed cells of *Nitrosomonas europaea* and *Nitrobacter agilis*. Journal of Bacteriology, 154:65-71.

155. Laanbroek, H. J. and Gerards, S. 1993. Competition for limiting amounts of oxygen between *Nitrosomonas europaea* and *Nitrobacter winogradskyi* grown in mixed continuous cultures. Archives of Microbiology, 159:453-459.

156. Laanbroek, H. J., Bodelier, P. L. E., and Gerards, S. 1994. Oxygen consumption kinetics of *Nitrosomonas europaea* and *Nitrobacter hamburgensis* grown in mixed continuous cultures at different oxygen concentrations. Archives of Microbiology, 161:156-162.

157. Lane, D. J. 1991. In *Nucleic Acid Techniques in Bacterial Systematics*, pp 115-148. Stackebrandt, E. and Goodfellow, M., Editors. John Wiley & Sons, Chichester, West Sussex.

158. Layton, A., C., Dionisi et al., H. B., Kwo, H.-W., Robinson, K. G., Garrett, V. M., Myers, A., Sayler, G. S. 2005. Emergence of competitive dominant ammonia-oxidizing bacterial populations in a full-scale industrial wastewater treatment plant. Applied and Environmental Microbiology, 71:1105-1108.

159. Leary, S. C., Battersby, B. J., Hansford, R. G., and Moyes, C. D. 1998. Interactions between bioenergetics and mitochondrial biogenesis. Biochimica et Biophysica Acta, 1365:522-530.

160. Licht, T. R., Tolker-Nielsen, T., Holmstrøm, K., Krogfelt, K. A., and Molin, S. 1999. Inhibition of *Escherichia coli* precursor-16S rRNA processing by mouse intestinal contents. Environmental Microbiology, 1:23-32.

161. Liu, D. 1981. A rapid biochemical test for measuring chemical toxicity. Bulletin of Environmental Contamination and Toxicology, 26:145-149.

162. Livak, K. J., Flood, S. J., Marmaro, J., Giusti, W., and Deetz, K. 1995. Oligonucleotides with fluorescent dyes at opposite ends provide a quenched probe system useful for detecting PCR product and nucleic acid hybridization. Genome Research, 4:357-362.

163. Logemann, S., Schantl, J., Bijvank, S., van Loosdrecht, M. C. M., Kuenen, J. G., and Jetten, M. 1998. Molecular microbial diversity in a nitrifying reactor system without sludge retention. FEMS Microbiology Ecology, 27:239-249.

164. López-Fiuza, J., Buys, B., Mosquera-Corral, A., Omil, F., and Méndez, R. 2002. Toxic effects exerted on methanogenic, nitrifying and denitrifying bacteria by chemicals used in a milk analysis laboratory. Enzyme and Microbial Technology, 31:976-985.

165. Lowe, T.M. and Eddy, S.R. 1997 tRNAscan-SE: a program for improved detection of transfer RNA genes in genomic sequence. Nucleic Acids Research, 25: 955-964.

166. Lyon, W. J. 2001. TaqMan PCR for detection of Vibrio *chlolerae* O1, O139, non-O1, and nonO-139 in pure cultures, raw oysters, and synthetic seawater. Applied and Environmental Microbiology, 67:4685-4693.

167. Madigan, M. T., Martinko, J. M., and Parker, J. 2000. *Brock Biology of Microorganisms*, 9th edition, Prentice Hall, Upper Saddle River, New Jersey.

168. Makino, S. I., Cheun, H. I., Watarai, M., Uchinda, I., and Takeshi, K. 2001. Detection of anthrax spores from the air by real-time PCR. Letters in Applied Microbiology, 33:237-240.

169. Maloney, P. and Wilson, T. H. 1996. Ion-coupled transport and transporters, p. 1130-1148. In: F. C. Neidhardt et al. (ed.) *Escherichia coli* and *Samonella*: cellular and molecular biology. ASM Press, Washington, D.C.

170. Marlowe, E. M., Wang, J. M., Pepper, I. L., and Maier, R. M. 2002. Application of a reverse transcription-PCR assay to monitor regulation of the catabolic *nahAc* gene during degradation of phenanthrene degradation. Biodegradation, 13:251-260.

171. McPherson, M. J. and Møller, S. G. 2000. *PCR*. Spinger-Verlag New York, Inc. New York, NY.

172. Meckenstock, R., Steinle, P., van der Meer, J., R., and Snozzi, M. 1998. Quantification of bacterial mRNA involved in degradation of 1,2,4-dichlorobenzene by Pseudomonas sp. strain P51 from liquid culture and from

river sediment by reverse transcriptase PCR (RT/PCR). FEMS Microbiology Letters, 167:123-129.

173. Milner, G. M., Saunders, J. R., and McCarthy, A. J. 2001. Relationship between nucleic acid ratios and growth in *Listeria monocytogenes*. Microbiology, 147:2689-2896.

174. Mobarry, B. K., Wagner, M., Urbain, V., Rittmann, B. E., and Stahl, D. A. 1996. Phylogenetic probes for analyzing abundance and spatial organization of nitrifying bacteria. Applied and Environmental Microbiology, 62:2156-2162.

175. Molecular Probes. 2001. Handbook of Fluorescent Probes and Research Products, 8th Edition. Molecular Probes, Inc. http://www.probes.com/handbook

176. Molin, S. and Givskov, M. 1999. Application of molecular tools for in-situ monitoring of bacterial growth activity. Environmental Microbiology 1:383-391.

177. Monod, J. 1949. The growth of bacterial cultures. Annual Review of Microbiology, 3:371-395.

178. Morgenroth, E., Obermayer, A., Arnold, E., Brühl, A., Wagner, M., and Wilderer, P. A. 2000. Effect of long term idle periods on the performance of sequencing batch reactors. Water Science and Technology, 41:105-113.

179. Morita, R. Y. 1993. Bioavailability of energy and starvation state. In Starvation in Bacteria. Kjelleberg, S. ed., © Plenum Press New York, New York.

180. Mulder, A., Van de Graaf, A. A., Robertson, L. A., and Kuenen, J. G. 1995. Anaerobic ammonia oxidation discovered in a denitrifying fluidized bed reactor. FEMS Microbiology Ecology, 16:177-184.

181. Mullis, K. B. 1990. The unusual origins of the polymerase chain reaction. Scientific American, 262:56-65.

182. Muttray, A. F. and Mohn, W. W. 1998. RNA/DNA ratio as an indicator of metabolic activity in resin acid-degrading bacteria. Water Science and Technology, 37:89-93.

183. Muttray, A. F. and Mohn, W. W. 2000. Quantitation of the population size and metabolic activity of a resin acid degrading bacterium in activated sludge using slot-blot hybridization to measure the rRNA:rDNA ratio. Microbial Ecology, 38:348-357.

184. Muttray, A. F., Yu, Z., and Mohn, W. W. 2001. Population dynamics and metabolic activity of *Pseudomonas abietaniphila* BKME-9 within pulp mill and

wastewater microbial communities assayed by competitive PCR and RT-PCR. FEMS Microbiology Ecology, 38:21-31.

185. Navarro, E. Simonet, P., Normand, P., and Bardin, R. 1992a. Characterization of natural populations of *Nitrobacter* spp. using PCR/RFLP analysis of the ribosomal intergenic spacer. Archives of Microbiology, 157:107-115.

186. Navarro, E., Fernandez, M. P., Grimont, F., Clays-Josserand, A., and Bardin, R. 1992b. Genomic heterogeneity of the genus *Nitrobacter*. International Journal of Systematic Bacteriology, 42:554-560.

187. Nogva, H. K., Rudi, K., Naterstad, K., Holck, A., and Lillehaug, D. 2000. Application of 5 '-nuclease PCR for quantitative detection of *Listeria monocytogenes* in pure cultures, water, skim milk, and unpasteurized whole milk. Applied and Environmental Microbiology, 66:4266-4271.

188. Oda, Y., Slagman, S. J., Meijer, W. G., Forney, L. J., and Gottschal, J. C. 2000. Influence of growth rate and starvation on fluorescent in-situ hybridization of *Rhodopseudomonas palustris*. FEMS Microbiology Ecology, 32:205-213.

189. Oerther, D. B., de le Reyes, F. L., and Raskin, L. 1999. Interfacing phylogenetic oligonucleotide probe hybridizations with representations of microbial populations and specific growth rates in mathematical models of activated sludge processes. Water Science and Technology, 39:11-20.

190. Oerther, D. B., Pernthaler, J., Schramm, A., Amann, R., and Raskin, L. 2000. Monitoring precursor 16S rRNAs of *Acinetobacter* spp. in activated sludge wastewater treatment systems. Applied and Environmental Microbiology, 66:2154-2165.

191. Oerther, D. B., de los Reyes, F. L., de los Reyes, M. F., and Raskin, L. 2001. Quantifying filamentous microorganisms in activated sludge before, during, and after an incident of foaming by oligonucleotide probe hybridizations and antibody staining. Water Research, 35:3325-3336.

192. Oerther, D. B., van Loosdrecht, M. C. M., and Raskin, L. 2002. Quantifying the impact of wastewater micronutrient composition on *in situ* growth activity of *Acinetobacter* spp. Water Science and Technology, 46:443-447.

193. Okabe, S., Satoh, H. and Watanabe, Y. 1999. In-situ analysis of nitrifying biofilms as determined by in-situ hybridization and the use of microelectrodes. Applied and Environmental Microbiology, 65:3182-3191.

194. O'Kelly, J. C., Becker, G. E., and Nason, A. 1970. Characterization of the particulate nitrite oxidase and its component activities from the chemoautotroph *Nitrobacter agilis*. Biochimica et biophsica acta, 205:409-425.

195. Orso, S., Gouy, M., Navarro, E., and Normand, P. 1994. Molecular phylogenetic analysis of *Nitrobacter* spp. International Journal of Systematic Bacteriology, 44:83-86.

196. Parker, J. J. 2001. The effects of dissolved oxygen concentration and biological solids retention time on activated sludge treatment performance. Masters Thesis, Department of Civil and Environmental Engineering, University of Tennessee, Knoxville, TN.

197. Peng, Y. Z., Chen, Y., Peng, C. Y., Liu, M., Wang, S. Y., Song, X., Q., and Cul, Y. W. 2004. Nitrite accumulation by aeration controlled in sequencing batch reactors treating domestic wastewater. Water Science and Technology, 50:35-43.

198. Philips, S. and Verstraete, W. 2000. Inhibition of activated sludge by nitrite in the presence of proteins or amino acids. Environmental Technology, 21:1119-1125.

199. Philips, S., Laanbroek, H. J., and Verstraete, W. 2002. Origin, causes, and effects of increased nitrite concentrations in aquatic environments. Re/Views in Environmental Science and Bio/Technology, 1:115 - 141.

200. Pollard, P. C., Steffens, M. A., Biggs, C. A., and Lant, P. A. 1998. Bacterial growth dynamics in activated sludge batch assays, Water Research, 32: 587-596.

201. Pollice, A., Tandoi, V., and Lestingi, C. 2002. Influence of aeration and sludge retention time on ammonium oxidation to nitrite and nitrate. Water Research, 36:2541-2546.

202. Pommerening-Röser, A., Rath, G., and Koops, H. P. 1996. Phylogenetic diversity within the genus *Nitrosomonas*. Systematic and Applied Microbiology, 19:344-351.

203. Poulsen, L. K., Ballard, G., and Stahl, D. A. 1993. Use of rRNA fluorescence in situ hybridization for measuring the activity of single cells in young and established biofilms. Applied and Environmental Microbiology, 59:1354-1360.

204. Poughon, L., Dussap, C.-G., and Gros, J.-B. 2001. Energy model and metabolic flux analysis for autotrophic nitrifiers. Biotechnology and Bioengineering, 72:416-433.

205. Prakasam, T. B. S. and Loehr, R. C. 1972. Microbial nitrification and denitrification in concentrated wastes. Water Research, 6:859-869.

206. Purkhold, U., Pommerening-Röser, A., Juretschko, S., Schmid, M. C., H.-P. Koops, and Wagner, M. 2000. Phylogeny of all recognized species of ammonia oxidizers based on comparative 16S rRNA and *amoA* sequence analysis: implications for molecular diversity studies. Applied and Environmental Microbiology, 66:5368-5382.

207. Qiagen. 2001a. RNAprotect™ Bacteria Reagent Handbook. 07/2001.

208. Qiagen. 2001b. RNeasy® Mini Handbook. 06/2001.

209. Qiagen. 2002. Quantitect™ Probe PCR Handbook. 01/2002.

210. Randall, C. W. and Buth, D. 1984a. Nitrite build-up in activated sludge resulting from temperature effects. Journal of the Water Pollution Control Federation, 56:1039-1044.

211. Randall, C. W. and Buth, D. 1984b. Nitrite build-up in activated sludge resulting from combined temperature and toxicity effects. Journal of the Water Pollution Control Federation, 56:1045-1049.

212. Rasmussen, R. 2001. Quantification on the LightCycler. In: Meuer, S., Wittwer, C., and Nakagawara, K. (eds) Rapid Cycle Real-Time PCR, Methods and Applications. Springer Press, Heidelberg, Germany; pp 21-34.

213. Rittmann, B. E. and McCarty, P. L. 2001. *Environmental Biotechnology: Principles and Applications*. McGraw Hill, New York, NY.

214. Rozen S. and Skaletsky, H. J. 2000. Primer3 on the WWW for general users and for biologist programmers. In: Krawetz, S. and Misener, S. (eds) *Bioinformatics Methods and Protocols: Methods in Molecular Biology*. Human Press, Totowa, NJ, pp 365-386.

215. Ruiz, G, Jeison, D., and Chamy, R. 2003. Nitrification with high nitrite accumulation for the treatment of wastewater with high ammonia concentration. Water Research, 37:1371-1377.

216. Saiki, R. K., Scharf, S., Faloona, F. A., Mullis, K. B., Horn, G. T., Erlich, H. A., and Arnheim, N. 1985. Enzymatic amplification of beta-globin genomic sequences and restriction site analysis for diagnosis of sickle-cell anemia. Science, 230:1350-1354.

217. Saiki, R. K., Gelfand, D. H., Stoffel, S., Scharf, S., Higuchi, R., Horn, G. T., Mullis, K. B., and Erlich, H. A. 1988. Primer-directed enzymatic amplification of DNA with a thermostable DNA-polymerase. Science, 239:487-491.

218. Sambrook, J. and Russell, D. W. 2001. *Molecular Cloning: A Laboratory Manual*. Cold Spring Harbor Press, Cold Spring Harbor, NY.

219. Samuels, M. L. 1989. *Statistics for the Life Sciences*. Dellen Publishing Company, Riverside, NJ.

220. Sánchez, O., Martí, M. C., Aspé, E., and Roeckel, M. 2001. Nitrification rates in a saline medium at different dissolved oxygen concentrations. Biotechnology Letters, 23:1597-1602.

221. Sandén, B. and Dalhammar, G. 1998. An amperometric enzyme-linked immunosensor for *Nitrobacter*. Applied Microbiology and Biotechnology, 50:710-716.

222. Sandén, B. and Dalhammar, G. 2000. Application of an amperometric immunosensor for the enumeration of *Nitrobacter* in activated sludge. Applied Microbiology and Biotechnology, 54:413-417.

223. Schalk, J., Oustad, H., Kuenen, J. G., and Jetten, M. S. M. 1998. The anaerobic oxidation of hydrazine: a novel reaction in microbial nitrogen metabolism. FEMS Microbiology Letters, 158:61-67.

224. Schalk, J., de Vries, S., Kuenen, J. G., and Jetten, M. S. M. 2000. Involvement of a novel hydroxylamine oxidoreductase in anaerobic ammonium oxidation. Biochemistry, 39:5405-5412.

225. Schmid, M. Twachtmann, U., Klein, M., Strous, M., Jureschko, S., Jetten, M., Metzger, J. W., Schleifer, K.-H., and Wagner, M. 2000. Molecular evidence for genus level diversity of bacteria capable of catalyzing anaerobic ammonium oxidation. Systematic and Applied Microbiology, 23:93-106.

226. Schmid, M. Schmitz-Esser, S., Jetten, M., and Wagner, M. 2001. 16S-23S rDNA intergenic spacer and 23S rDNA of anaerobic ammonium-oxidizing bacteria: implications for phylogeny and in-situ detection. Environmental Microbiology, 3:450-459.

227. Schmid, M., Walsh, K., Webb, R., Rijpstra, W. I. C., van de Pas-Schoonen, K., Verbruggen, M. J., Hill, T., Moffett, B., Fuerst, J., Schouten, S., Damste, J. S. S., Harris, J., Shaw, P., Jetten, M., and Strous, M. Candidatus "Scalindua brodae", sp nov., Candidatus "*Scalindua wagneri*", sp nov., two new species of anaerobic ammonia oxidizing bacteria. 2003. Systematic and Applied Microbiology, 26:529-538.

228. Schmidt, I., and Bock, E. 1997 Anaerobic ammonia oxidation with nitrogen dioxide by *Nitrosomonas eutropha*. Archives of Microbiology, 167:106-111.

229. Schmidt, I., and Bock, E. 1998. Anaerobic ammonia oxidation by cell-free extracts of Nitrosomonas eutropha. Antoine van Leeuwenhoek, 73:271-278.

230. Schmidt, I., Zart, D., and Bock, E. 2001. Gaseous NO_2 as a regulator for ammonia oxidation of *Nitrosomonas eutropha*. Antoine van Leeuwenhoek, 79:311-318.

231. Schmidt, I., Sliekers, O., Schmid, M., Bock, E., Fuerst, J., Kuenen, J. G., Jetten, M. S. M., and Strous, M. 2003. New concepts of microbial treatment processes for the nitrogen removal in wastewater. FEMS Microbiology Reviews, 27:481-492.

232. Schramm, A., Larsen, L. U., Revsbech, N. P., Ramsin, N. B., Amann,, R., Schleifer, K.-H. 1996. Structure and function of a nitrifying biofilm as determined by in-situ respirometry and the use of microelectrodes. Applied and Environmental Microbiology, 62:4641-4647.

233. Schramm, A., De Beer, D., Wagner, M., and Amann, R. 1998. Identification and activities in-situ of *Nitrosospira* and *Nitrospira* spp. as dominant populations in a nitrifying fluidized bed reactor. Applied and Environmental Microbiology, 64:3480-3485.

234. Schramm, A., De Beer, D., van den Heuvel, J. C., Otengraf, S., and Amann, R. 1999. Microscale distribution of populations and activities of *Nitrosospira* and *Nitrospira* spp. along a macroscale gradient in a nitrifying bioreactor: quantification by in-situ hybridization and the use of microsensors. Applied and Environmental Microbiology, 65:3690-3696.

235. Sellner, L. N. and Turbett, G. R. 1998. Comparison of three RT-PCR methods. Biotechniques, 25:230-234.

236. Sewell, D. L., Aleem, M. I. H., and Wilson, D. F. 1972. The oxidation-reduction potentials and rates of oxidation of the cytochromes of *Nitrobacter agilis*. Archives of Biochemistry and Biophysics, 152:312-319.

237. Shabala, L., Budde, Birgitte, Ross, T., Siegumfeldt, H., Jakobsen, M., and McMeekin, T. 2002. Responses of *Listeria monocytogenes* to acid stress and glucose availability revealed by a novel combination of fluorescence microscopy and microelectrode ion-selective techniques. Applied and Environmental Microbiology, 68:1794-1802.

238. Shammas, N. K. 1986. Interactions of temperature, pH, and biomass on the nitrification process. Journal of the Water Pollution Control Federation, 58:52-59.

239. Sharkey, F. H., Banat, I. M., and Marchant, R. 2004. Detection and quantification of gene expression in environmental bacteriology. Applied and Environmental Microbiology, 70:3795-3806.

240. Sharma, B. and Ahlert, R. C. 1977. Nitrification and nitrogen removal. Water Research, 11:897-925.

241. Siegrist, H. 1996. Nitrogen removal from digester supernatant - comparison of chemical and biological methods. Water Science and Technology, 34:399-406.

242. Siegrist, H., Reithaar, S., and Lais, P. 1998. Nitrogen loss in a nitrifying rotating contactor treating ammonium-rich wastewater without organic carbon. Water Science and Technology, 38:241-248.

243. Simkins, S. and Alexander, M. 1984. Models for mineralization kinetics with the variables of substrate concentration and population density. Applied and Environmental Microbiology, 47:1299-1306.

244. Sliekers, A. O., Dewort, N., Compos Gomez, J. L., Strous, M., Kuenen, J. G., and Jetten, M. S. M. 2002. Completely autotrophic nitrogen removal over nitrite in one singe reactor. Water Research, 36:2475-2482.

245. Sliekers, A. O., Third, K. A., Abma, W., Kuenen, J. G., and Jetten, M. S. M. 2003. CANON and Anammox in a gas-lift reactor. FEMS Microbiology Letters, 218:339-344.

246. Snyder, L. and Champness, W. 2003. Molecular Genetics of Bacteria. 2nd Edition. ASM Press, Washington, D.C., USA.

247. Snoeyink, V. L. and Jenkins, D. W. 1980. *Water Chemistry*. John Wiley & Sons.

248. Sone, N., Yanagita, Y., Hon-Nami, K., Fukumori, Y., and Yamanaka, T. 1983. Proton-pump activity of Nitrobacter agilis and Thermus thermophilus cytochrome c oxidases. Federation of European Biochemical Societes Letters, 155:150-154.

249. Sone, N. 1986. Measurement of proton pump activity of the thermophilic bacterium PS3 and Nitrobacter agilis at the cytochrome oxidase level using total membrane and heptyl thioglucoside. Journal of Biochemistry, 100:1465-1470.

250. Sorokin, D. Y, Muyzer, G., Brinkhoff, T., Kuenen, J. G., and Jetten, M. S. M. 1998. Isolation and characterization of a novel facultatively alkaliphilic

Nitrobacter species, *N. alkalicus* sp. nov. Archives of Microbiology, 170:345-352.

251. Srinath, E. G. and Loehr, R. C., and Prakasam, T. B. S. 1976. Nitrifying organism concentration and activity. Journal of the Environmental Engineering Division of the American Society of Civil Engineers, 102:449-463.

252. Stackbrandt, E. and Goebel, B. M. 1994. A place for DNA-DNA reassociation and 16S ribosomal-RNA sequence-analysis in the present species definition in bacteriology. International Journal of Systematic Bacteriology, 44:846-849.

253. Stein, L. Y. and Arp, D. J. 1998a. Ammonium limitation results in the loss of ammonia-oxidizing activity in *Nitrosomonas europaea*. Applied and Environmental Microbiology, 64:1514-1521.

254. Stein, L. Y. and Arp, D. J. 1998b. Loss of ammonia monooxygenase activity in *Nitrosomonas europaea* upon exposure to nitrite. Applied and Environmental Microbiology, 64:4098-4102.

255. Steinmüller, W. and Bock, E. 1977. Growth of Nitrobacter in the presence of organic matter. I. Mixotrophic growth. Archives of Microbiology, 108:299-304.

256. Sternberg, C., Christensen, B. B., Johansen, T., Nielsen, A. T., Anderson, J. B., Givskov, M., and Molin, S. 1999. Distribution of bacterial growth activity in flow-control chamber biofilms. Applied and Environmental Microbiology, 65:4108-4117.

257. Stevenson, B. S. and Schmidt, T. M. 1998. Growth rate-dependent accumulation of RNA from plasmid-borne rRNAt operons in *Escherichia coli*. Journal of Bacteriology, 180:1970-1972.

258. Stroot, P. G. and Oerther, D. B. 2003. Elevated precursor 16S rRNA levels suggest the presence of growth inhibitors in wastewater. Water Science and Technology, 47:241-250.

259. Strotmann, U. J. and Eglsäer, H. 1995. The toxicity of substituted phenols in the nitrification inhibition test and luminescent bacteria test. Ecotoxicology and Environmental Safety, 30:269-273.

260. Strotmann, U. J. and Pagga, U. 1996. A growth inhibition test with sewage bacteria - results of an international ring test 1995. Chemosphere, 32:921-933.

261. Strous, M., van Gerven, E., Zheng, P., Kuenen, J. G., and Jetten, M. S. M. 1997a. Ammonium removal from concentrated waste streams with the anaerobic

ammonium oxidation (Anammox) process in different reactor configurations. Water Science and Technology, 31:1955-1962.

262. Strous, M. van Gerven, E., Kuenen, J. G., and Jetten, M. 1997b. Effects of aerobic and microaerobic conditions on anaerobic ammonium-oxidizing (Anammox) sludge. Applied and Environmental Microbiology, 63:2446-2448.

263. Strous, M., Fuerst, J. A., Kramer, E. H. M., Logemann, S., Muyzer, G., van de Pas-Schoonen, K. T., Webb, R., Kuenen, J. G., and Jetten, M. S. M. 1999a. Missing lithotroph identified as new plactomycete. Nature. 400:446-449.

264. Strous, M., Kuenen, J. G., and Jetten, M. S. M. 1999b. Key physiology of anaerobic ammonium oxidation. Applied and Environmental Microbiology, 65:3248-50.

265. Strous, M. and Jetten, M. S. M. 2004. Anaerobic oxidation of methane and ammonium. Annual Review of Microbiology, 58:99-177.

266. Stryer, L. 1995. *Biochemistry*, 4th Ed. W. H. Freeman, New York, N.Y.

267. Sundermeyer, H. and Bock, E. 1981. Energy metabolism of autotrophically and heterotrophically grown cells of *Nitrobacter winogradskyi*. Archives of Microbiology, 130:250-254.

268. Suthersan, S. and Ganczarczyk, J. J. 1986. Inhibition of nitrite oxidation during nitrification: some observations. Water Pollution Research Journal of Canada, 21:257-266.

269. Suzuki, I., Dular, U., and Kwok, S. C. 1974. Ammonia or ammonium ion as substrate for oxidation by *Nitrosomonas europaea* cells and extracts. Journal of Bacteriology, 120:556-558.

270. Svenson, A., Sandén, B., Dalhammer, G., Remberger, M., and Kaj, L. 2000. Toxicity identification and evaluation of nitrification inhibitors in wastewaters. Environmental Toxicology, 15:527-532.

271. Tanaka, Y., Fukumori, Y., and Yamanaka, T. 1983. Purification of cytochrome a_1c_1 from *Nitrobacter agilis* and characterization of nitrite oxidation system of the bacterium. Archives of Microbiology, 135:265-271.

272. Tanaka, T. A., Fukumori, Y. and Yamanaka, T. 1993. Membrane-bound cytochrome c is an alternative electron donor for cytochrome aa3 in *Nitrobacter* winogradskyi. Journal of Bacteriology, 175:4400-4404.

273. Tang, N. H., Blum, D. J. W., Nirmalakhandan, N., and Speece, R. E. 1992. QSAR parameters for toxicity of organic chemicals to *Nitrobacter*. Journal of Environmental Engineering (ASCE), 118:17-37.

274. Tarre, S. and Green, M. 2004. High-rate nitrification at low pH in suspended- and attached-biomass reactors. Applied and Environmental Microbiology, 70:6481-6487.

275. Tatusova, T. A. and Madden, T. L. 1999. Blast 2 sequences - a new tool for comparing protein and nucleotide sequences. FEMS Microbiology Letters 174:247-250.

276. Tchobanoglous, G and Burton, F. L. 1991. *Wastewater Engineering: Treatment, Disposal, and Reuse*, 3rd Edition. McGraw-Hill.

277. Third, K. A., Sliekers, A. O., Kuenen, J. G., and Jetten, M. S. M. 2001. The CANNON (Completely Autotrophic Nitrogen-removal Over Nitrite) under ammonium limitation: Interaction and competition between three groups of bacteria. Systematic and Applied Microbiology, 24:588-596.

278. Thompson, J. D., Gibson, T. J., Plewniak, F., Jeanmougin, F., and Higgins, D. G. 1997. The ClustalX windows interface: flexible strategies for multiple sequence alignment aided by quality analysis tools. Nucleic Acids Research, 25:4876-4882.

279. Teske, A., Alm, E., Regan, J. M., Toze, S., Rittmann, B. E., and Stahl, D. A. 1994. Evolutionary relationships among ammonia- and nitrite-oxidizing bacteria. Journal of Bacteriology, 176:6623-6630.

280. Tomlinson, T. G., Boon, A. G., and Trotman, C. N. A. 1966. Inhibition of nitrification in the activated sludge process of sewage disposal. Journal of Applied Bacteriology, 29:266-291.

281. Tourova, T. G. 2003. Copy number of ribosomal operons in prokaryotes and its effect on phylogenetic analyses. Microbiology, 72:389-402.

282. Tseng, C.-C., Potter, T. G., and Koopman, B. 1998. Effect of influent chemical oxygen demand to nitrogen ratio on a partial nitrification/complete denitrification process. Water Research, 32:165-173.

283. Tsubaki, M. and Yoshikawa, S. 1993. Fourier-transform infared study of azide binding to the Fea3-CuB binuclear site of bovine heart cytochrome c oxidase: new evidence for a redox-linked conformational change at the binclear site. Biochemistry, 32:174-182.

284. Tsubaki, M., Mogi, T., and Mori, H. 1999. Azide- and cyanide-binding to the *Escherichia coli* bd-type ubiquinol oxidase studied by visible absorption, EPR, and FTIR, spectroscopies. Journal of Biochemistry (Tokyo), 126:510-19.

285. Turk, O. and Mavinic, D. 1987. Benefits of using selective inhibition to remove nitrogen from highly nitrogenous wastes. Environmental Technology Letters, 8:419-426.

286. Turk, O. and Mavinic, D. 1989a. Maintaining nitrite build-up in a system acclimated to free ammonia. Water Research, 23:1383-1388.

287. Turk, O. and Mavinic, D. 1989b. Stability of nitrite build-up in an activated sludge system. Journal of the Water Pollution Control Federation, 61:1440-1448.

288. USGS. 1999. The Quality of Our Nation's Waters – Nutrient and Pesticides. U.S. Geological Survey Circular 1225.

289. van de Graaf, A. A., Mulder, A., de Bruijn, P., Jetten, M. S. M., Robertson, L. A., and Kuenen, J. 1995. Anaerobic oxidation of ammonium is a biologically mediated process. Applied and Environmental Microbiology, 61:1246-1251.

290. van de Graaf, A. A., de Bruijn, P., Robertson, L. A., Jetten, M. S. M., and Kuenen, J. G. 1997. Metabolic pathway of anaerobic ammonium oxidation on the basis of ^{15}N studies in a fluidized bed reactor. Microbiology-UK, 143:2415-2421.

291. van Dongen, Jetten, M. S. M, and van Loosdrecht, M. C. M. 2001 The Sharon®-Anammox® process for treatment of ammonium rich wastewater. Water Science and Technology, 44:153-160.

292. Villaverde, S., Fdz-Polanco, F., and Garcia, P. A. 2000. Nitrifying biofilm acclimation to free ammonia in submerged biofilters. Start-up influence. Water Research, 34:602-610.

293. Voets, J. P., Vanstaen, H., and Verstraete, W. 1975. Removal of nitrogen from highly nitrogenous wastewaters. Journal of the Water Pollution Control Federation, 47:394-398.

294. Wagner, M., Amann, R., Lemmer, H., and Schleifer, K.H. 1993. Probing activated sludge with oligonucleotides specific for Proteobacteria: inadequacy of culture-dependent methods for describing microbial community structure. Applied and Environmental Microbiology, 59:1520-1525.

295. Wagner, M., Rath, G., Amann, R., Koops, H.-P., and Schleifer, K.-H. 1995. In-situ identification of ammonia-oxidizing bacteria. Systematic and Applied Microbiology, 18:251-264.

296. Wagner, M., Rath, G., Koops, H.-P., Flood, J., and Amann, R. 1996. In-situ analysis of nitrifying bacteria in sewage treatment plants. Water Science and Technology, 34:237-244.

297. Wagner, M., Noguera, D. R., Juretschko, S., Rath, G., Koops, H.-P., and Schleifer, K.-H. 1998. Combining fluorescent in-situ hybridization (fish) with cultivation and mathematical modeling to study population structure and function of ammonia-oxidizing bacteria in activated sludge. Water Science and Technology, 37:441-449.

298. Walter, B. Sidransky, E., Kristjansson, J. K., and Hollocher, T. C. 1978. Inhibition of denitrification by uncouplers of oxidative phophoylation. Biochemistry, 17:3039-3045.

299. Wang, W. and Reed, P. 1984. *Nitrobacter* bioassay for aquatic toxicity. In: Toxicity Screening Procedures Using Bacterial System. Edition by Liu, D. and Dutka, B. Marcel Dekker, Inc. © 1984, New York, New York.

300. Watson, S. W., Bock, E., Valois, F. W., Waterbury, J. B., and Schlosser, U. 1986. *Nitrospira marina*, gen.nov.,sp.nov.: a chemolithotrophic nitrite-oxidizing bacterium. Archives of Microbiology, 144:1-7.

301. Watson, S. W., Bock, E., Harms, H., Koops, H.-P., Hooper, A. B. 1989. Nitrifying bacteria , p. 1808–1834. In: Stayley, J. T., Bryant, M. P., Pfennig, N., and Holt, J. G. (ed.), Bergey's manual of systematic bacteriology, vol. 3. Williams and Wilkins Baltimore, USA.

302. Wetzstein, H.-G. and Ferguson, S. J. 1985. Respiration-dependent proton translocation and the mechanism of protonmotive force generation in *Nitrobacter winogradskyi*. FEMS Microbiology Letters, 30:87-92.

303. Widada, J., Nojiri, H., Kasuga, K., Yoshida, T., Habe, H., and Omori, T. 2001. Quantification of the carbazole 1,9a-dioxygenase gene by real-time competitive PCR combined with co-extraction of internal standards. FEMS Microbiology Letters, 202:51-57.

304. Wiesmann, U. 1994. Biological nitrogen removal from wastewater. Advances in Biochemical Engineering/Biotechnology, edition by A. Fiechter, Springer-Verlag Berlin, New York, 113-154.

305. Willems, A., Coopman, R., and Gillis, M. 2001. Comparison of sequence analysis of 16S-23S rDNA spacer regions, AFLP analysis and DNA-DNA hybridizations in *Bradyrhizobium*. International Journal of Systematic and Evolutionary Microbiology, 51:623-632.

306. Williamson, K. J. and Johnson, D. G. 1981. A bacterial bioassay for assessment of wastewater toxicity. Water Research, 15:383-390.

307. Winther-Nielsen, M. and Jansen, J. la C. 1996. The role of the sludge in nitrification inhibition tests. Water Science and Technology, 33:1333-1339.

308. Wong-Chong, G. M. and Loehr, R. C. 1978. Kinetics of microbial nitrification: nitrite-nitrogen oxidation. Water Research, 12:605-609.

309. Yang, L. and Alleman, J. E. 1992. Investigation of batchwise nitrite build-up by an enriched nitrification culture. Water Science and Technology, 26:997-1005.

310. Yang, S.-F., Tay, J.-H., and Liu, Y. 2004. Inhibition of free ammonia to the formation of aerobic granules. Biochemical Engineering Journal, 17:41-48.

311. Yamanaka, T., Kamita, Y., and Fukumori, Y. 1981. Molecular and enzymatic properties of "cytochrome aa3"-type terminal oxidase derived from *Nitrobacter agilis*. Journal of Biochemistry, 89:265-273.

312. Yamanaka, T. 1983. Effect of paraquat on growth of *Nitrosomonas europaea* and *Nitrobacter agilis*. Plant and Cell Physiology, 24:1349-1352.

313. Yamanaka, T., Fukumori, Y. and Tanaka, Y. 1984. A relationship between prokaryote and eukaryote observed in *Nitrobacter agilis* cytochrome aa3 and c. Origins of Life, 14:739-746.

314. Yoo, H., Ahn, K.-H., Lee, H.-J., Lee, K.-H., Kwak, Y.-J., and Song, K.-G. 1999. Nitrogen removal from synthetic wastewater by simultaneous nitrification and denitrification (SND) via nitrite in an intermittently aerated bioreactor. Water Research, 33:145-154.

315. Yun, H.-J. and Kim, D.-J. 2003. Nitrite accumulation characteristics of high strength ammonia wastewater in an autotrophic nitrifying biofilm reactor. Journal of Chemical Technology and Biotechnology, 78:377-383.

316. Zengel, J. M. and Lindahl, L. 1994. Diverse mechanisms for regulating ribosomal protein synthesis in *Escherichia coli*. Progress in Nucleic Acid Research and Molecular Biology, 47:331-370.

317. Zimmermann, K. and Mannhalter, J. W. 1996. Technical aspects of quantitative competitive PCR. Bio/Techniques, 21:268-279.

318. Zuker, M. 2003. Mfold web server for nucleic acid folding and hybridization prediction. Nucleic Acids Research, 31:3406-3415.

319. Zumft, W. G. 1997. Cell biology and molecular basis of denitrification. Microbiology and Molecular Biology Reviews, 61:533-616.

APPENDIXES

Appendix A

Quantitative PCR Primer and Probe Design Data

Table A-1 Cloned BSNR DNA sequences (clone library 1) generated with the conserved bacterial PCR primers 1055f and 23Sr. The clones are distinguished with numbers in the "ID" column. The sequences originated from BSNR DNA extracts collected either 50 or 163 days after the reactor was seeded: column "N" designates these cloning events as 1 and 2, respectively. The primer used to generate a partial sequence is noted in column "P": M13f (1), M13r (2), and 1492r (3). A "C" in column "P" indicates the insert sequence is complete. The 16S - 23S ISR sequence for clone 1-20 (*Nitrobacter* spp.) is underlined.

ID	N	P	FASTA formatted sequence (5′ → 3′ sense strand)
1-1	1	3	1 ATGGCTGTCGTCAGCTCGTGTCGTGAGATGTTGGGTTAAGTCCCGCAACGAGCGCAACCC 61 TCGCCTTTAGTTGCCATCATTTAGTTGGGCACTCTAGAGGGACTGCCGGTGATAAGCCGG 121 AGGAAGGTGGGGATGACGTCAAGTCCTCATGGCCCTTACGGGTTGGGCTACACACGTGCT 181 ACAATGGCGGCGACAATGGGCAGCGAAGGGGCGACCCGGTGCAAATCCCAAAAAGCCGTC 241 TCAGTTCGGATTGTTCTCTGCAACTCGAGAGCATGAAGGTGGAATCGCTAGTAATCGCGT 301 AACAGCATGACGCGGTGAATACGTTCCCGGGCCTTGTACACACCGCCCGTCACACCATGG 361 GAGTTGGTTTTACCCGAAGCTGGTGCGCTAACCGCAAGGAGGCAGCCAACCACGGTAAGG 421 TCA
1-2	1	3	1 ATGGCTGTCGTCAGCTCGTGCCGTGAGGTGTTGGGTTAAGTCCCGCAACGAGCGCAACCC 61 CTATCCCTAGTTGCCATCGAGTCAAGTCGGGCACTCTAGAGAGACTGCCTACGCAAGTAG 121 AGAGGAAGGTGGGGATGACGTCAAGTCATCATGGCCCTTACGTCTGGGGCTACACACGTG 181 ATACAATGGACGGTACAGTGGGCGAGGCTGCGAAGCCAAGGTAATCCCCAAAACCGTTCT 241 CAGTTCGGATTGGAGTCTGCAACTCGACTCCATGAAGGTGGAATCGCTAGTAATCGCGGA 301 TCAGCATGCCGCGGTGAATACGTTCCCGGGCCTTGTACACACCGCCCGTCAAGCCATGGG 361 AGCCGGGGGCGCCCGAAGCCGGCAGAGATGCCGTCGAAGGCGAAATCG
1-3	1	3	1 ATGGCTGTCGTCAGCTCGTGCCGTGAGGTGTTGGGTTAAGTCCCGCAACGAGCGCAACCC 61 CTATCTTTAGTTACCAGCGAGTCATGTCGGGAACTCTAAAGAAACTGCCTACGCAAGTAG 121 AGAGGAAGGCGGGGACGACGTCAAGTCATCACGGCCCTTACGTCCTGGGCCACACACGTG 181 CTACAATGGTCGGTACAGAGGGCAGCTACCTGGTGACAGGATGCGAATCTCGAAAGCCGA 241 TCTCAGTTCGGATTGGAGTCTGCAACTCGACTCTATGAAGCTGGAATCGCTAGTAATCGC 301 GCATCAGCCATGGCGCGGTGAATACGTTCCCGGGCCTTGTACACACCGCCCGTCAAACAA 361 TGGAAGCTGGGGGTACCTGAAGTCGGTAACCGAAAGGAGCTGCCTAGGGTAAAACTAGTA 421 AC
1-4	1	3	1 ATGGCTGTCGTCAGCTCGTGCCGTGAGGTGTTGGGTTAAGTCCCGCAACGAGCGCAACCC 61 CTATCCCTAGTTGCCATCGAGTCAAGTCGGGCACTCTAGAGAGACTGCCTACGCAAGTAG 121 AGAGGAAGGTGGGGATGACGTCAAGTCATCATGGCCCTTACGTCTGGGGCTACACACGTG 181 ATACAATGGACGGTACAGTGGGCGAGGCTGCGAAGCCAAGGTAATCCCCAAAACCGTTCT 241 CAGTTCGGATTGGAGTCTGCAACTCGACTCCATGAAGGTGGAATCGCTAGTAATCGCGGA 301 TCAGCACGCCGCGGTGAATACGTTCCCGGGCCTTGTACACACCGCCCGTCAAGCCATGGG 361 AGCCGGGGGCGCCCGAAGCCGGCAGAGATGCCGTCGAAGGCGAAATCGG
1-5	1	3	1 ATGGCTGTCGTCAGCTCGTGTCGTGAGATGTTGGGTTAAGTCCCGCAACGAGCGCAACCC 61 TCGCCTTTAGTTGCCATCATTTAGTTGGGCACTCTAGAGGGACTGCCGGTGATAAGCCGG 121 AGGAAGGTGGGGATGACGTCAAGTCCTCATGGCCCTTACGGGTTGGGCTACACACGTGCT 181 ACAATGGCGGCGACAATGGGCAGCGAAGGGGCGACCCGGTGCAAATCCCAAAAAGCCGTC 241 TCAGTTCGGATTGTTCTCTGCAACTCGAGAGCATGAAGGTGGAATCGCTAGTAATCGCGT 301 AACAGCATGACGCGGTGAATACGTTCCCGGGCCTTGTACACACCGCCCGTCACACCATGG 361 GAGTTGGTTTTACCCGAAGCTGGTGCGCTAACCGCAAGGAGGCAGCCAACCACGGTAAGG 421 TCAGCG

Table A-1 Continued.

ID	N	P	FASTA formatted sequence (5′ → 3′ sense strand)
1-6	1	3	1 ATGGCTGTCGTCAGCTCGTGTCGTGAGATGTTGGGTTAAGTCCCGCAACGAGCGCAACCC 61 TTGTCGCTAATTGCTATCATTTTAATGAGCACTTTAGCGAGACTGCCGGTGACAAACCGG 121 AGGAAGGTGGGGATGACGTCAAGTCCTCATGGCCCTTATGGGTAGGGCTTCACACGTAAT 181 ACAATGGCGCGTACAGAGGGTTGCCAATCCGCGAGGAGGAGCCAATCTCAGAAAGCGCGT 241 CGTAGTCCGGATCGGAGTCTGCAACTCGACTCCGTGAAGTCGGAATCGCTAGTAATCGCG 301 GATCAGCATGCCGCGGTGAATACGTTCCCGGGTCTTGTACACACCGCCCGTCACACCATG 361 GGAGTGATTTTCACCAGAAGCAGGTAGTTTAACCGCAAGGAGGGCGCTTGCCACGGTGGG 421 GGTCAG
1-7	1	3	1 ATGGCTGTCGTCAGCTCGTGTCGTGAGATGTTGGGTTAAGTCCCGCAACGAGCGCAACCC 61 TTGTCGCTAATTGCTATCATTTTAATGAGCACTTTAGCGAGACTGCCGGTGACAAACCGG 121 AGGAAGGTGGGGATGACGTCAAGTCCTCATGGCCCTTATGGGTAGGGCTTCACACGTAAT 181 ACAATGGCGCGTACAGAGGGTTGCCATCCGCGAGGAGGAGCCAATCTCAGAAAGCGCGTC 241 GTAGTCCGGATCGGAGTCTGCAACTCGACTCCGTGAAGTCGGAATCGCTAGTAATCGCGG 301 ATCAGCATGCCGCGGTGAATACGTTCCCGGGTCTTGTACACACCGCCCGTCACACCATGG 361 GAGTGATTTTCACCAGAAGCAGGTAGTTTAACCGCAAGGAGGGCGCTTGCCACGGTGGGG 421 GTCA
1-8	1	3	1 ATGGCTGTCGTCAGCTCGTGCCGTGAGGTGTTGGGTTAAGTCCCGCAACGAGCGCAACCC 61 CTATCCCTAGTTGCCATCGAGTCAAGTCGGGCACTCTAGAGAGACTGCCTACGCAAGTAG 121 AGAGGAAGGTGGGGATGACGTCAAGTCATCATGGCCCTTACGTCTGGGGCTACACACGTG 181 ATACAATGGACGGTACAGTGGGCGAGGCTGCGAAGCCAAGGTAATCCCCAAAACCGTTCT 241 CAGTTCGGATTGGAGTCTGCAACTCGACTCCATGAAGGTGGAATCGCTAGTAATCGCGGA 301 TCAGCATGCCGCGGTGAATACGTTCCCGGGCCTTGTACACACCGCCCGTCAAGCCATGGG 361 AGCCGGGGGCGCCCGAAGCCGGCAGAGATGCCGTCGAAGGCGAAATCGG
1-9	1	3	1 ATGGCTGTCGTCAGCTCGTGCCGTGAGGTGTTGGGTTAAGTCCCGCAACGAGCGCAACCC 61 CTATCTTTAGTTACCAGCGAGTCATGTCGGGAACTCTAAAGAAACTGCCTACGCAAGTAG 121 AGAGGAAGGCGGGGACGACGTCAAGTCATCACGGCCCTTACGTCCTGGGCCACACACGTG 181 CTACAATGGTCGGTACAGAGGGCAGCTACCTGGTGACAGGATGCGAATCTCGAAAGCCGA 241 TCTCAGTTCGGATTGGAGTCTGCAACTCGACTCTATGAAGCTGGAATCGCTAGTAATCGC 301 GCATCAGCCATGGCGCGGTGAATACGTTCCCGGGCCTTGTACACACCGCCCGTCAAACAA 361 TGGAAGCTGGGGGTACCTGAAGTCGGTAACCGAAAGGAGCTGCCTAGGGTAAAACTAGTA 421 AC
1-10	1	3	1 ATGGCTGTCGTCAGCTCGTGCCGTGAGGTGTTGGGTTAAGTCCCACAACGAGCGCAACCC 61 CTATTTTCAGTTGCCAACTGACAGTGATGTCAAGGGACTCTGGAGAGACTGCCTACGTAA 121 GTAGAGAGGAAGGCGGGGATGACGTCAAATCATCATGGCCTTTATGCCTAGGGCGACACA 181 CGTGCTACAATGGCCGGTACAGAGGGTTGCGAGACAGTGATGTTAAGCCAATCCCAAAAA 241 GCCGGTCCCAGTTCGGATTGGAGTCTGGAACTCGACTCCATGAAGGTGGAATCGCTAGTA 301 ATCGCGCATCAGCCATGGCGCGGTGAATACGTTCCCGGACCTTGTACACACCGCCCGTCA 361 AGCCATGGAAGCCGAGGGTGCCTGAAGATGGTGACTCTACAGGGAGCTATCTAAG
1-11	1	3	1 ATGGCTGTCGTCAGCTCGTGTCGTGAGATGTTGGGTTAAGTCCCGCAACGAGCGCAACCC 61 TTGTCCTTAGTTGCCAGCACGTAATGGTGGGAACTCTAGGGAGACTGCCGGTGACAAACC 121 GGAGGAAGGTGGGGATGACGTCAAGTCATCATGGCCCTTACGGCCAGGGCTACACACGTA 181 CTACAATGGTCGGGACAGAGGGCAGCGAGACCGCGAGGTGGAGCCAATCCCAGAAACCCG 241 ATCCCAGTCCGGATTGCAGTCTGCAACTCGACTGCATGAAGTCGGAATCGCTAGTAATCG 301 CAGATCAGCATTGCTGCGGTGAATACGTTCCCGGGCCTTGTACACACCGCCCGTCACACC 361 ATGGGAGTTGGTTGCTCCAGAAGCAGGTAGTCTAACCGCAAGGAGGACGCTTGCCACGGA 421 GTGGTCAA
1-12	1	3	1 ATGGCTGTCGTCAGCTCGTGTCGTGAGATGTTGGGTTAAGTCCCGCAACGAGCGCAACCC 61 TCGCCTTTAGTTGCCATCATTAAGTTGGGCACTCTAGAGGGACTGCCGATGATAAGTCGG 121 AGGAAGGTGGGGATGACGTCAAGTCCTCATGGCCCTTACGGGTTGGGCTACACACGTGCT 181 ACAATGGCGGCGACAATGGGCAGCGAAGGGGCGACCCGGTGCAAATCCCAAAAAGCCGTC 241 TCAGTTCGGATTGTACTCTGCAACTCGAGTGCATGAAGGTGGAATCGCTAGTAATCGCGT 301 AACAGCATGACGCGGTGAATACGTTCCCGGGCCTTGTACACACCGCCCGTCACACCATGG 361 GAGTTGGTTTTACCCGAAGCCGGTGCGCTAACCGCAAGGAGGCAGCCGACC

Table A-1 Continued.

ID	N	P	FASTA formatted sequence (5′ → 3′ sense strand)
1-13	1	3	1 ATGGCTGTCGTCAGCTCGTGTCGTGAGATGTTGGGTTAAGTCCCGCAACGAGCGCAACCC 61 TTGTCGCTAATTGCTATCATTTTAATGAGCACTTTAGCGAGACTGCCGGTGACAAACCGG 121 AGGAAGGTGGGGATGACGTCAAGTCCTCATGGCCCTTATGGGTAGGGCTTCACACGTAAT 181 ACAATGGCGCGTACAGAGGGTTGCCAATCCGCGAGGAGGAGCCAATCTCAGAAAGCGCGT 241 CGTAGTCCGGATCGGAGTCTGCAACTCGACTCCGTGAAGTCGGAATCGCTAGTAATCGCG 301 GATCAGCATGCCGCGGTGAATACGCTCCCGGGTCTTGTACACACCGCCCGTCACACCATG 361 GGAGTGATTTTCACCAGAAGCAGGTAGTTTAACCGCAAGGAGGGCGCTTGCCACGGTGGG 421 GGTCA
1-14	1	3	1 ATGGCTGTCGTCAGCTCGTGTCGTGAGATGTTGGGTTAAGTCCCGCAACGAGCGCAACCC 61 TTGTCCTTAGTTGCCAGCACGTAATGGTGGGAACTCTAGGGAGACTGCCGGTGACAAACC 121 GGAGGAAGGTGGGGATGACGTCAAGTCATCATGGCCCTTACGGCCAGGGCTACACACGTA 181 CTACAATGGTCGGGACAGAGGGCAGCGAGACCGCGAGGTGGAGCCAATCCCAGAAACCCG 241 ATCCCAGTCCGGATTGCAGTCTGCAACTCGACTGCATGAAGTCGGAATCGTCTAGTAATC 301 AGCAGATCAGCATTGCTGCGGTGAATACGTTCCCGGGCCTTGTACACACCGCCCGTCACA 361 CCATGGGAGTTGGTTGCTCCAGAAGCAGGTAGTCTAACCGCAAGGGGGACGCTTGCCACG 421 GAG
1-15	1	3	1 ATGGCTGTCGTCAGCTCGTGCCGTGAGGTGTTGGGTTAAGTCCCGCAACGAGCGCAACCC 61 CTATCTTTAGTTACCAGCGAGTCATGTCGGGAACTCTAAAGAAACTGCCTACGCAAGTAG 121 AGAGGAAGGCGGGGACGACGTCAAGTCATCACGGCCCTTACGTCCTGGGCCACACACGTG 181 CTACAATGGTCGGTACAGAGGGCAGCTACCTGGTGACAGGATGCGAATCTCGAAAGCCGA 241 TCTCAGTTCGGATTGGAGTCTGCAACTCGACTCTATGAAGCTGGAATCGCTAGTAATCGC 301 GCATCAGCCATGGCGCGGTGAATACGTTCCCGGGCCTTGTACACACCGCCCGTCAAACAA 361 TGGAAGCTGGGGGTACCTGAAGTCGGTAACCGAAAGGAGCTGCCTAGGGTAAAA
1-16	1	3	1 ATGGCTGTCGTCAGCTCGTGTGGTGAGATGTTGGGTTAAGTCCCGCAACGAGCGCAACCC 61 TCGCCTTTAGTTGCCATCATTAAGTTGGGCACTCTAGAGGGACTGCCGATGATAAGTCGG 121 AGGAAGGTGGGGATGACGTCAAGTCCTCATGGCCCTTACGGGTTGGGCTACACACGTGCT 181 ACAATGGCGGCGACAATGGGCAGCGAAGGGGCGACCCGGTGCAAATCCCAAAAAGCCGTC 241 TCAGTTCGGATTGTACTCTGCAACTCGAGTGCATGAAGGTGGAATCGCTAGGAATCGCGT 301 AACAGCATGACGCGGTGAATACGTTCCCGGGCCTTGTACACACCGCCCGTCACACCATGG 361 GAGTTGGTTTTACCCGAAGCCGGTGCGCTAACCGCAAGGAGGCAGCCGACCACGG
1-17	1	3	1 ATGGCTGTCGTCAGCTCGTGCCGTGAGGTGTTGGGTTAAGTCCCGCAACGAGCGCAACCC 61 CTATTTTCAGTTGCCAACTGACAGTGATGTCAAGGGACTCTGGAGAGACTGCCTACGTAA 121 GTAGAGAGGAAGGCGGGGATGACGTCAAATCATCATGGCCTTTATGCCTAGGGCGACACA 181 CGTGCTACAATGGCCGGTACAGAGGGTTGCGAGACAGTGATGTTAAGCCAATCCCAAAAA 241 GCCGGTCCCAGTTCGGATTGGAGTCTGGAACTCGACTCCATGAAGGTGGAATCGCTAGTA 301 ATCGCGCATCAGCCATGGCGCGGTGAATACGTTCCCGGACCTTGTACACACCGCCCGTCA 361 AGCCATGGAAGCCGAGGGTGCCTGAAGATGGTGACTCTACAGGGAGCTATCTAAGGTAAA 421 ATT
1-18	1	3	1 ATGGCTGTCGTCAGCTCGTGCCGTGAGGTGTTGGGTTAAGTCCCGCAACGAGCGCAACCC 61 CTATCTTTAGTTACCAGCGAGTCATGTCGGGAACTCTGAAGAAACTGCCTACGCAAGTAG 121 AGAGGAAGGCGGGGACGACGTCAAGTCATCACGGCCCTTACGTCCTGGGCCACACACGTG 181 CTACAATGGTCGGTACAGAGGGCAGCTACCTGGTGACAGGATGCGAATCTCGAAAGCCGA 241 TCTCAGTTCGGATTGGAGTCTGCAACTCGACTCTATGAAGCTGGAATCGCTAGTAATCGC 301 GCATCAGCCATGGCGCGGTGAATACGTTCCCGGGCCTTGTACCCACCGCCCGTCAAACAA 361 TGGAAGCTGGGGGTACCTGAAGTCGGTAACCGAAAGGAGC
1-19	1	3	1 ATGGCTGTCGTCAGCTCGTGCCGTGAGGTGTTGGGTTAAGTCCCGCAACGAGCGCAACCC 61 CTATCTTTAGTTACCAGCGAGTCATGTCGGGAACTCTGAAGAAACTGCCTACGCAAGTAG 121 AGAGGAAGGCGGGGACGACGTCAAGTCATCACGGCCCTTACGTCCTGGGCCACACACGTG 181 CTACAATGGTCGGTACAGAGGGCAGCTACCTGGTGACAGGATGCGAATCTCGAAAGCCGA 241 TCTCAGTTCGGATTGGAGTCTGCAACTCGACTCTATGAAGCTGGAATCGCTAGTAATCGC 301 GCATCAGCCATGGCGCGGTGAATACGTTCCCGGGCCTTGTACCCACCGCCCGTCAAACAA 361 TGGAAGCTGGGGGTACCTGAAGTCGGTAACCGAAAGGAGCTGCCTAGGGTAAAA

Table A-1 Continued.

ID	N	P	FASTA formatted sequence (5′ → 3′ sense strand)
1-20	1	C	1 ATGGCTGTCGTCAGCTCGTGTCGTGAGATGTTGGGTTAAGTCCCGCAACGAGCGCAACCC 61 CCGTCCTTAGTTGCTACCATTTAGTTGAGCACTCTAAGGAGACTGCCGGTGATAAGCCGC 121 GAGGAAGGTGGGGATGACGTCAAGTCCTCATGGCCCTTACGGGCTGGGCTACACACGTGC 181 TACAATGGCGGTGACAATGGGAAGCAAAGGGGTGACCCCTAGCAAATCTCAAAAAACCGT 241 CTCAGTACGGATTGGGCTCTGCAACCCGAGCCCATGAAGTTGGAATCGCTAGTAATCGTG 301 GATCAGCATGCCACGGTGAATACGTTCCCGGGCCTTGTACACACCGCCCGTCACACCATG 361 GGAGTTGGTTTTACCTGAAGGCGGTGCGCTAACCCGCAAGGGAGGCAGCCGACCACGGTA 421 GGGTCAGCGACTGGGGTGAAGTCGTAACAAGGTAGCCGTAGGGGAACCTGCGGCTGGATC 481 ACCTCCTTTATCACCTCCTTTCTAAGGATGACTCTTCAGAAGCGCTCACGCTCTTCTATC 541 GGGTTTCTTGGAAACATCAGTGGCCAATGATCGTCAGGATCGTTGAGCTGCATTGGCGGG 601 ATTTCGCCGTCTTCGTTTCTCTTTCTTCGCGGACGAACACGCGCCAGGGGCGGCGCTTGT 661 GCTCATGATCCGGTTAATCCGGTGGAGCGCGCTGTCCCTCGTCGTTAGGGGCTTGTAGCT 721 CAGTTGGTTAGAGCGCGCGCTTGATAAGCGTGAGGTCGGAAGTTCAAGTCTTCCCAGGCC 781 CACCATTCAATCAAGCGCAGCATTCGTCTTCTGGTACGGGGCCATAGCTCAGCTGAGAGA 841 GCGCGTGCTTTGCAAGCATGAGGTCGTCGGTTCGATCCCGTCTGGCTCCACCAGATGGTT 901 TGATTGACTGGCTTGATCGATGTTGCTCGATTAATTTCGTCCGCGGGAACAACGCTTCGC 961 ATGTCTCATTTATTACAGATGAGGTGTGCGGGATTTCTGACATCGTAAAGAGGAGATCGA 1021 TCCGAGTTTGGATCGCATGCCATGCCATGTGCGTGGTGAGCGTCCATTCACTATCTCCAG 1081 GTCATTTCGGCGCCCGTTCGGGTCGTGACGCAAGTTGCGATGTGTGCGGGTTGTGAATGA 1141 TCCTGTTAGCGAAGCATGACCGCCTCGCTATCGGTTCGATCTTACGAAGCAAGCTGGTCT 1201 TTCTAATCAATATCCGGCCGCATCAAGCATTCATCGAGGGTGCGTGCGTAAAAGGCTTTC 1261 GAGCTTTTGGCGCGTGGATGCGGACGACATTCTGTCGAGTGTGTGGATATTGATAATGAG 1321 AGCAATCAAGTGCCTTAAGGGTGTTCGGTGGATGCCTTGGCGCTGAGAGGCGACGAAGGA 1381 CGTACTACGCTGCGATAAGCCGTGGGGAGCTGCGAAGAAGCTTTGATCCACGGATTTCCG 1441 AATGGGGCAACCC
1-21	2	1	1 ATGGCTGTCGTCAGCTCGTGTCGTGAGATGTTGGGTTAAGTCCCGTAACGAGCGCAACCC 61 TTGTCCTTAGTTGCCAGCACGTAATGGTGGGAACTCTAAGGAGACTGCCGGTGACAAACC 121 GGAGGAAGGCGGGGACGACGTCAAGTCATCATGGCCCTTACGGGTAGGGCTACACACGTG 181 CTACAATGGGTGATACAGAGGGAAGCGAAGGGGTGACCTGGAGCTAATCTTAGAAAGTCG 241 CTCGTAGTCCGGATTGGAGTCTGCAACTCGACTCCATGAAGTCGGAATCGCTAGTAATCG 301 CGAATCAGCATGTCGCGGTGAATACGTTCCCGGGCCTTGTACACACCGCCCGTCACACCA 361 TGGGAGTGGGCTGCACCAGAAGTAGATAGTCTAACCTTCGGGAGGACGTTTACCACGGTG 421 TGGTTCATGACTGGGGTGAAGTCGTAACAAGGTAGCCGTAGGGGAACCTGCGGCTGGATC 481 ACCTCCTTAATTAGAGCACTAAAGATTTAAAGTGCCCACACAGTTTGTTTTCGAGATAAT 541 GAAGAGCCCG
1-22	2	1	1 ATGGCTGTCGTCAGCTCGTGTCGTGAGATGTTGGGTTAAGTCCCGCAACGAGCGCAACCC 61 TTACGGGCAGTTGCCATCATTAAGTTGGGAACTCTGCTCGGACTCCCGTTGATAAAACGG 121 AGGAAGGTGGGGATGATGTCAAGTCATCATGGCCTTTATGTTCAGGGCTACACACGTGCT 181 ACAATGGACGGTACAAAACGTTGCTATCCCGCGAGGGGGAGCTAATCGCAAAAACCGTTC 241 TCAGTTCGGATTGAAGTCTGCAACTCGACTTCATGAAGTTGGAATCGCTAGTAATCGCAG 301 ATCAGCATGCTGCGGTGAATACGTTCCCGGGTCTCGTACACACCGCCCGTCACATCACGA 361 AAGTAGGTTGTACTAGAAGTAGCTGGGCTAACCCGCAAGGGAGGCAGGTTACCACGGTAT 421 GATTTATGATTGGGGTGAAGTCGTAACAAGGTAGCTGTAGGAGAACCTGTGGCTGGATCA 481 CCTCCTTAAAACCATACGACACAGGTCAAGCCTTCTAACAAGATCGCGAGACCGACTTAC 541 ATATCTAGTT
1-23	2	3	1 ATGGCTGTCGTCAGCTCGTGTCGTGAGATGTTGGGTTAAGTCCCGCAACGAGCGCAACCC 61 TTACGGGCAGTTGCCATCATTAAGTTGGGAACTCTGCTCGGACTGCCGTTGATAAAACGG 121 AGGAAGGTGGGGATGATGTCAAGTCATCATGGCCTTTATGTTCAGGGCTACACACGTGCT 181 ACAATGGACGGTACAAAACGTTGCTATCCCGCGAGGGGGAGCTAATCGCAAAAACCGTTC 241 TCAGTTCGGATTGAAGTCTGCAACTCGACTTCATGAAGTTGGAATCGCTAGTAATCGCAG 301 ATCAGCATGCTGCGGTGAATACGTTCCCGGGTCTTGTACACACCGCCCGTCACATCACGA 361 AAGTAGGTTGTACTAGAAGTAGCTGGGCTAACCCGCAAGGGAGGCAGGTTACCAAGGTAT 421 GATTTATGGATTGGGG

Table A-1 Continued.

ID	N	P	FASTA formatted sequence (5′ → 3′ sense strand)
1-24	2	C	1 ATGGCTGTCGTCAGCTCGTGTCGTGAGATGTTCGGTTAAGTCCGGCAACGAGCGCAACCC 61 ACGTCCTTAGTTGCCATCCTTCAGTTGGGCACTCTAAGGAAACTGCCGGTGATAAGCCGG 121 AGGAAGGTGTGGATGACGTCAAGTCCTCATGGCCCTTACGGGTTGGGCTACACACGTGCT 181 ACAATGGTGGTGACAATGGGATAATCCCCAAAAGCCATCTCAGTTCGGATTGGGGTCTGC 241 AACTCGACCCCATGAAGTCGGAATCGCTAGTAATCGCGTAACAGCATGACGCGGTGAATA 301 CGTTCCCGGGCCTTGTACACACCGCCCGTCACACCATGGGAATTGGGTCTACCCGAAGGT 361 GGTGCGCTAACTCGCAAGAGAGGCAGCCAACCACGGTAGGCTCAGTGACTGGGGTGAAGT 421 CGTAACAAGGTAGCCGTAGGGGAACCTGCGGCTGGATCACCTCCTTTCTAAGGATGTTCC 481 TGGCAGCTTGAGCTTGCTTAAGCTCGTGGAACACTTAGCAGAAGTGCCAGTCAGGCACTT 541 CATATACGCCGAGTTCGTCTCGGCGTGGACCGGACCGTCCTCATATCCCTTCATGACAGA 601 ATGAGCAGGATGCGAACCACCTGTCGCGCTTTTGCGTGGCGCTCGTGTCCGTCCAGTGGA 661 CGGCCGCGTCCTGGCGAAGCCAGGCCGGCTTGCGGGTCGGTAGCTCAGGTGGTTAGAGCG 721 TACGCCTGATAAGCGTAAGGTCGGAGGTTCAAGTCCTCCTCGACCCACCATCGCTTGCCT 781 GGCGGCGCATCCCTTCGGGGCCTTAGCTCAGCTGGGAGAGCGCCTGATTTGCATTCAGGA 841 GGTCATCGGTTCGATCCCGATAGGCTCCACCACGTCGTGTTCGGCAAGCCGAACACGACG 901 CGCGCGCCGGCAGAAGATTGCGAAGCAATCTTCGAGAGGCGTCGCCCGGTCCCAAATGGC 961 TCACCCCACTATCCCCTGTCGTCATCATCCAAAGATCATCGGATCATCCAGGCCGTTTGC 1021 CATGGGTTGGGTCGTCCGATGGACGCGTGAAGCGAGCAAGTCGCTTCGTTTGACATCGTT 1081 GAGAGAGAAACACATCGGTTTCATGCCCAAAGATCATCGGATCATCCAGGCCGTTTGCCA 1141 TGGGTTGGGTCGTCCGATGGACGCGTGAAGCGAGCAAGTCGCTTCGTTTGACATCGTTGA 1201 GAGAGAAACACATCGGTTTCATGCCGATGGCCCCGCGTGAGGGGCACATCGCGCCGGTCT 1261 TCGGACCCGCAAGGCATGAAACTGTTCCAAGTCTAGTACAACTGACCGCGATACTCGTAT 1321 CGCATGGGAAATGTACAGCTTTCGACCGGGAAGCGGCTGCGCGAGAACAAAAGGCGCGCG 1381 GCCTTGCTCTTTCCGTGTCGAATCAAGCGCGATAAGGGCGTTTGGTGGATGCCTAGGCAG 1441 CAAGAGGCGATGAAGGACGTGATACCCTGCGATAAGCCATGGGGAGCCGGGAATAGGCTT 1501 TGATCCATGGATCTCCGAATGGGGCAACCC
1-25	2	1	1 ATGGCTGTCGTCAGCTCGTGTCGTGAGATGTTCGGTTAAGTCCGAAAACGAGCGCAACCC 61 CTAACATTAGTTACAAGTGTCTAATGTGACTGCCCGTGAGAAACGGGAGGAAGGTGGGGA 121 TGATGTCAAGTCAGCATGGCCTTTATATCTAGGGCTACACACACGCTACAATGGTCAGTA 181 CAAAGGGCAGCGAAACCGCGAGGTGGAGCGAATCCAAGAAAGCTGATCGAAGTTCGGATT 241 GCAGGCTGCAACTCGCCTGCATGAAGCTGGAGTTGCTAGTAACCGCGCGTCAGTGATAGT 301 GCGGTGAATACGTTCCCGGGCCTTGTACACACCGCCCGTCACGTCACGGGAGCTGGTCAC 361 GCCTGAAGTCGGTGAGCGAACCGCAAGGGAGCAACCGCCGAAGGCAGGGCTGGTGACTGG 421 GACGAAGTCGTAACAAGGTAGCAGTACCGGAAGGTGCGGCTGGATCACCTCCTTTCTAGA 481 ACAAGAAATAGTGCGAGTGTTGTAAAACGCTCAATGCACTCAAAAAAAAATCTGGTTCGC 541 TTTTTCTGTCACTAT
1-26	2	2	1 ATGGCTGTCGTCAGCTCGTGTCGTGAGATGTTGGGTTAAGTCCCGCAACGAGCGCAACCC 61 CTGTGAACAGTTGCTAATCGCAAGATGCACTCTGTTCAGACTGCCCTGTGAAACGGGGAG 121 GAAGGTGGGGACGACGTCAAGTCAGCATGGCCCTTACGGCCAGGGCTGCACACGTACTAC 181 AATGCCCACTACAGAATGAACCAATACCGCGAGGTGGAGGAAATCGATAAAAGTGGGCCC 241 AGTTCGGATTGAAGGCTGCAATTCGCCTTCATGAAGTCGGAATCGCTAGTAATGGCGCAT 301 CAGCTACGGCGCCGTGAATACGTTCCCGGGCCTTGTACACACCGCCCGTCACATCATGGA 361 AATCACTTGCACCCGAAGTCCGTGCGCTAACCCGCAAGGGAGGCAGCGGCCGAAGGTATG 421 AGTGGTAACTGGGATGAAGTCGTAACAAGGTAGCCGTAGGGGAACCTGCGGCTGGATCAC 481 CTCCTTTCTAAGGAGTAACTCCGATCCTCACGGATCGAAGTAGGTCGAGCGAATAAGAAC 541 CTGTTTTTAC
			1 TAGCTCAGCTGGTAGAGCGCCAGCTTTGCAAGCTGGATGTCAGGGGTTCGAATCCCCTTG 61 CCTCCATTCCAAATGCTATTCCATGCAAACCATGCGGATGCACGATTGGAAAATTGGCAA 121 GATTCTCATTGGAATATTATTTTGAATATTATTTTCAATAACGAATCTGCATATCCGGTC 181 GCAAATCCAATTGGGCCTGTAGCTCAGTTGGTTAGAGCATGCGCTTGATAAGCGCAGGGT 241 CACTGGTTCGAGTCCAGTCAGGCCCACCACCCAAATTCAGTGGGCAATGCACAGTGAAGT 301 CATTCACTAAACTTTTGCTCGCGTCGAACGTTTCGACAGTCAACCTGTTCTTTGATATCT 361 GCATACAGAAAGAGAATACAACTAAACGCTGAGAATCTGTAAAACTCACGGAGGTTTTAG 421 ATTTCAAGCTACTAAGAGCGCATGATGAATGCCTTGGTGTCAGTAGGCGATGAAGGACGT 481 GATAAGCTGCGATAAGTCACGGAGAGCGGCAAATACGCTTTGACCCGTGAATGTCCGAAT 541 GGGGCAACCC

Table A-1 Continued.

ID	N	P	FASTA formatted sequence (5′ → 3′ sense strand)
1-27	2	1	1 ATGGCTGTCGTCAGCTCGTGTCGTGAGATGTTGGGTTAAGTCCCGCAACGAGCGCAACCC 61 TCGTCCTTAGTTGCCATCATTCAGTTGGGCACTCTAAGGAAACCGCCGGTGATAAGCCGG 121 AGGAAGGTGGGGATGACGTCAAGTCCTCATGGCCCTTACGCGCTGGGCTACACACGTGCT 181 ACAATGGCGGTGACAGTGGGCAGCAAACCCGCGAGGGTGAGCTAATCTCCAAAAGCCGTC 241 TCAGTTCGGATTGTTCTCTGCAACTCGAGAGCATGAAGGCGGAATCGCTAGTAATCGCGG 301 ATCAGCATGCCGCGGTGAATACGTTCCCAGGCCTTGTACACACCGCCCGTCACACCATGG 361 GAGTTGGTTTCACCCGAAGGCTGTGCGCTAACCGCAAGGAGGCAGCAGACCACGGTGGGA 421 TCAGCGACTGGGGTGAAGTCGTAACAAGGTAGCCGTAGGGGAACCTGCGGCTGGATCACC 481 TCCTTTCTAAGGATAGCTTGCGGATCAACTCCTCGAACCCCGGTTCGGGCAAGTTTCCGC 541 GACTTCCATAGACATT
1-28	2	1	1 ATGGCTGTCGTCAGCTCGTGTCGTGAGATGTTGGGTTAAGTCCCGCAACGAGCGCAACCC 61 CTGTGAACAGTTGCTAATCGCAAGATGCACTCTGTTCAGACTGCCCTGTGAAACGGGGAG 121 GAAGGTGGGGACGACGTCAAGTCAGCATGGCCCTTACGGCCAGGGCTGCACACGTACTAC 181 AATGCCCACTACAGAATGAACCAATACCGCGAGGTGGAGGAAATCGATAAAAGTGGGCCC 241 AGTTCGGATTGAAGGCTGCAATTCGCCTTCATGAAGTCGGAATCGCTAGTAATGGCGCAT 301 CAGCTACGGCGCCGTGAATACGTTCCCGGGCCTTGTACACACCGCCCGTCACATCATGGA 361 AATCACTTGCACCCGAAGTCCGTGCGCTAACCCGCAAGGGAGGCAGCGGCCGAAGGTATG 421 AGTGGTAACTGGGATGAAGTCGTAACAAGGTAGCCGTAGGGGAACCTGCGGCTGGATCAC 481 CTCCTTTCTAAGGAGTAACTCCGATCCTCACGGATCGAAGTAGGTCGAGCGAATAAGAAC 541 CTGTTTTTAC
1-29	2	1	1 ATGGCTGTCGTCAGCTCGTGTCGTGAGATGTTGGGTTAAGTCCCGCAACGAGCGCAACCC 61 TTGTCGCTAATTGCTATCATTTTAATGAGCACTTTAGCGAGACTGCCGGTGACAAACCGG 121 AGGAAGGTGGGGATGACGTCAAGTCCTCATGGCCCTTATGGGTAGGGCTTCACACGTAAT 181 ACAATGGCGCGTACAGAGGGTTGCCAATCCGCGAGGAGGAGCCAATCTCTGAAAGCGCGT 241 CGTAGTCCGGATCGGAGTCTGCAACTCGACTCCGTGAAGTCGGAATCGCTAGTAATCGCG 301 GATCAGCATGCCGCGGTGAATACGTTCCCGGGTCTTGTACACACCGCCCGTCACACCATG 361 GGAGTGATTTTCACCAGAAGCAGGTAGTTTAACCGCAAGGAGGGCGCTTGCCACGGTGGG 421 GGTCATGACTGGGGTGAAGTCGTAACAAGGTAGCCGTAGGGGAACCTGCGGCTGGATCAC 481 CTCCTTTCATAAATTATTGTCAAGTGTTCACACTTATTGGTTATTTGAATAAATAAATAT 541 AAATTTGGG
		2	1 ATGGCTGTCGTCAGCTCGTGTCGTGAGATGTTGGGTTAAGTCCCGCAACGAGCGCAACCC 61 TTGTCGCTAATTGCTATCATTTTAATGAGCACTTTAGCGAGACTGCCGGTGACAAACCGG 121 AGGAAGGTGGGGATGACGTCAAGTCCTCATGGCCCTTATGGGTAGGGCTTCACACGTAAT 181 ACAATGGCGCGTACAGAGGGTTGCCAATCCGCGAGGAGGAGCCAATCTCTGAAAGCGCGT 241 CGTAGTCCGGATCGGAGTCTGCAACTCGACTCCGTGAAGTCGGAATCGCTAGTAATCGCG 301 GATCAGCATGCCGCGGTGAATACGTTCCCGGGTCTTGTACACACCGCCCGTCACACCATG 361 GGAGTGATTTTCACCAGAAGCAGGTAGTTTAACCGCAAGGAGGGCGCTTGCCACGGTGGG 421 GGTCATGACTGGGGTGAAGTCGTAACAAGGTAGCCGTAGGGGAACCTGCGGCTGGATCAC 481 CTCCTTTCATAAATTATTGTCAAGTGTTCACACTTATTGGTTATTTGAATAAATAAATAT 541 AAATTTGGG
1-30	2	1	1 ATGGCTGTCGTCAGCTCGTGCCGTGAGGTGTCAGGTTAAGTCCTATAACGAGCGCAACCC 61 TTATCGCTAGTTGCCAGCGTTTCAAGACGGGGACTCTAGCGAGACTGCCAACGCAAGTTG 121 CGAGGAAGGTGGGGACGACGTCAAGTCATCACGGCCCTTACGTCTTGGGCGACACACGTG 181 CTACAATGGCCGGTACAGAGGGCAGCTACCACGCGAGTGGATGCGAATCTCGAAAACCGG 241 TCTCAGTTCGGATTGGAGTCTGCAACTCGACTCTATGAAGCTGGAATCGCTAGTAATCGC 301 ATATCAGCCATGATGCGGTGAATACGTTCCCGGGCCTTGTACACACCGCCCGTCAAGCCA 361 TGGAAGCCGGGGGTACCTGAAGTCGGTGACCGTCAAAGGAGCTGCCTAGGGTAAAACTGG 421 TAACTAGGGCTAAGTCGTAACAAGGTAGCCGTACCGGAAGGTGCGGCTGGAACATCTCTT 481 ATATAGAGTACGACGAATCAAACTTGTCAATTAAAGGGATTGGCTGTTTTTTTTAGGTTT 541 TTTTTTCTTC

Table A-1 Continued.

ID	N	P	FASTA formatted sequence (5′ → 3′ sense strand)
1-31	2	1	1 CAGGCCCACCATCCACTTCACCTAAAGGGGCCGTAGCTCAGCTGGGAGAGCACCTGCTTT 61 GCAAGCAGGGGGTCGTCGGTTCGATCCCGTCCGGCTCCACCAAATGGTGTCGAGTGGACG 121 GATCAGTCATTCGCTGGGAAAACAAGTTTGCGCCGGACCTTTGGTCCTGCGCCTGTTCTG 181 TATGACATCGTAAAGAGAAGATTTGTTCGGGCTCCATCGTCGGAGCCTGGCCTTGAAGGG 241 TCCATAACCCTTCGTAATCGGCCGGGCATCGATGGCGGTGATTCGTCGCGCGGGACGCTC 301 AATCCTGCGCATATGATTGGCCTGCCTAACCGCGGCCATCGGACAGATCTCGAGAAGCTG 361 GTCTTTTTGTTGCCAGTACTCTTTCGGGGCTTGCCCCGGATGGGCATTGGCAATGTGAAC 421 AATCAAGTGTCTTAAGGGCAATTGGTGGATGCCTTGGCATGCACAGGCGATGAAGGACGT 481 GATACGCTGCGATAAGCGTCGGGGAGGTGCGAATACCCTTTGATCCGACGATTTCCGAAT 541 GGGGCAACCC
		2	1 ATGGCTGTCGTCAGCTCGTGTCGTGAGATGTTGGGTTAAGTCCCGCAACGAGCGCAACCC 61 TCGCCCTTAGTTGCCAGCATTCAGTTGGGCACTCTAAGGGGACTGCCGGTGATAAGCCGA 121 GAGGAAGGTGGGGATGACGTCAAGTCCTCATGGCCCTTACGGGCTGGGCTACACACGTGC 181 TACAATGGTGGTGACAGTGGGCAGCGAGACCGCGAGGTCGAGCTAATCTCCAAAAGCCAT 241 CTCAGTTCGGATTGCACTCTGCAACTCGAGTGCATGAAGTTGGAATCGCTAGTAATCGCG 301 GATCAGCATGCCGCGGTGAATACGTTCCCGGGCCTTGTACACACCGCCCGTCACACCATG 361 GGAGTTGGCTTTACCCGAAGGTCGTGCGCTAACCGCAAGGAGGCAGCGAACCACGGTAGG 421 GTCAGCGACTGGGGTGAAGTCGTAACAAGGTAGCCGTAGGGGAACCTGCGGCTGGATCAC 481 CTCCTTTCTAAGGATGAACCCTAATGGAAACGCTTCTTCATGAAGCCTCTGCCTTTCGGT 541 TCTCTTCAGA
1-32	2	2	1 CTTGCACGCAGGGGGTCAAGGGTTCGAATCCCTTATTCTCCACAGGGTTGATTTTAGATA 61 TCGGATTTAAGATTTAAGATTGAAAAAATTTAAAATCTAAAATCTAAAATTTAAAATCAT 121 CAAAGAAGAGTTCATAAAAATAAGAAAGGAAATTAGCATCGCCTATAAAGCGAAGGGCTG 181 GATCATCCCGATTTGACATCGGGAGGGTCAAGGGTTCGAATCCCTTATTCTCCACAGGGT 241 TGATTTTAGATATCGGATTTAAGATTTAAGATTGAAAAAATTTAAAATCTAAAATTTAAA 301 ATTTAAAATCGGCAAAGAAGAGTTCATTGACATATTGGAAGAAAAATAACGAAAGAAATC 361 GAAAACAACTTTAAAAAGTTCATAACGAAATACAATAACCGAACACGAGAGCGGCGGTTA 421 GAAAAAAGTTACAAAGAGCGTATGGCGGATGCCTAGGCTTCGAGAGGCGATGAAGGACGT 481 GATAAGCTGCGATAAGCTGCGGGGACTGGCACATACAGATTGATCCGCAGATTTCCGAAT 541 GGGGCAACCC
		1	1 ATGGCTGTCGTCAGCTCGTGCCGTGAGGTGTCAGGTTAAGTCCTATAACGAGCGCAACCC 61 TTATCGCTAGTTGCCAGCGTTTCAAGACGGGGACTCTAGCGAGACTGCCAACGCAAGTTG 121 CGAGGAAGGTGGGGACGACGTCAAGTCATCACGGCCCTTACGTCTTGGGCGACACACGTG 181 CTACAATGGCCGGTACAGAGGGCAGCTACCACGCGAGTGGATGCGAATCTCGAAAACCGG 241 TCTCAGTTCGGATTGGAGTCTGCAACTCGACTCTATGAAGCTGGAATCGCTAGTAATCGC 301 ATATCAGCCATGATGCGGTGAATACGTTCCCGGGCCTTGTACACACCGCCCGTCAAGCCA 361 TGGAAGCCGGGGGTACCTGAAGTCGGTGACCGTCAAAGGAGCTGCCTAGGGTAAAACTGG 421 TAACTAGGGCTAAGTCGTAACAAGGTAGCCGTACCGGAAGGTGCGGCTGGAACATCTCTT 481 ATATAGAGTACGACGAATCAAACTTGTCAATTAAAGGGATTGGCTGTTTTTTTTAGGTTT 541 TTTTTTCTTC
1-33	2	1	1 TAGCTCAGCTGGTAGAGCGCCAGCTTTGCAAGCTGGATGTCAGGGGTTCGAATCCCCTTG 61 CCTCCATTCCAAATGCTATTCCATGCAAACCATGCGGATGCACGATTGGAAAATTGGCAA 121 GATTCTCATTGAAATATTATTTTGAATATTATTTTCAATAACGAATCTGCATATCCGGTC 181 GCAAATCCAATTGGGCCTGTAGCTCAGTTGGTTAGAGCATGCGCTTGATAAGCGCAGGGT 241 CACTGGTTCGAGTCCAGTCAGGCCCACCACCCAAATTCAGTGGGCAATGCACAGTGAAGT 301 CATTCACTAAACTTTTGCTCGCGTCGAACGTTTCGACAGTCAACCTGTTCTTTGATATCT 361 GCATACAGAAAGAGAATACAACTAAACGCTGAGAATCTGTAAAACTCACGAAGGTCTTAG 421 ATTTCAAGCTACTAAGAGCGCATGATGAATGCCTTGGTGTCAGTAGGCGATGAAGGACGT 481 GATAAGCTGCGATAAGTCACGGAGAGCGGCAAATACGCTTTGACCCGTGAATGTCCGAAT 541 GGGGCAACCC
		2	1 ATGGCTGTCGTCAGCTCGTGTCGTGAGATGTTGGGTTAAGTCCCGCAACGAGCGCAACCC 61 CTGTGAACAGTTGCTAATCGCAAGATGCACTCTGTTCAGACTGCCCTGTGAAACGGGGAG 121 GAAGGTGGGGACGACGTCAAGTCAGCATGGCCCTTACGGCCAGGGCTGCACACGTACTAC 181 AATGCCCACTACAGAATGAACCAATACCGCGAGGTGGAGGAAATCGATAAAAGTGGGCCC 241 AGTTCGGATTGAAGGCTGCAATTCGCCTTCATGAAGTCGGAATCGCTAGTAATGGCGCAT 301 CAGCTACGGCGCCGTGAATACGTTCCCGGGCCTTGTACACACCGCCCGTCACATCATGGA 361 AATCACTTGCACCCGAAGTCCGTGCGCTAACCCGCAAGGGAGGCAGCGGCCGAAGGTATG 421 AGTGGTAACTGGGATGAAGTCGTAACAAGGTAGCCGTAGGGGAACCTGCGGCTGGATCAC 481 CTCCTTTCTAAGGAGTAACTCCGATCCTCACGGATCGAAGTAGGTCGAGCGAATAAGAAC 541 CTGTTTTTAC

Table A-1 Continued.

ID	N	P	FASTA formatted sequence (5′ → 3′ sense strand)
1-34	2	2	1 ATGGCTGTCGTCAGCTCGTGTCGTGAGATGTTGGGTTAAGTCCCGCAACGAGCGCAACCC 61 TTGTCGCTAATTGCTATCATTTTAATGAGCACTTTAGCGAGACTGCCGGTGACAAACCGG 121 AGGAAGGTGGGGATGACGTCAAGTCCTCATGGCCCTTATGGGTAGGGCTTCACACGTAAT 181 ACAATGGCGCGTACAGAGGGTTGCCAATCCGCGAGGAGGAGCCAATCTCAGAAAGCGCGT 241 CGTAGTCCGGATCGGAGTCTGCAACTCGACTCCGTGAAGTCGGAATCGCTAGTAATCGCG 301 GATCAGCATGCCGCGGTGAATACGTTCCCGGGTCTTGTACACACCGCCCGTCACACCATG 361 GGAGTGATTTTCACCAGAAGCAGGTAGTTTAACCGCAAGGAGGGCGCTTGCCACGGTGGG 421 GGTCA
1-35	2	3	1 ATGGCTGTCGTCAGCTCGTGTCGTGAGATGTTCGGTTAAGTCCGGCAACGAGCGCAACCC 61 ACACCCTTAGTTGCCAGCATTCAGTTGGGCACTCTAGGGGAACTGCCGGTGATAAGCCGG 121 AGGAAGGTGTGGATGACGTCAAGTCCTCATGGCCCTTACGGGTTGGGCTACACACGTGCT 181 ACAATGGTGGTGACAATGGGTTAATCCCCAAAAGCCATCTCAGTTCGGATTGGGGTCTGC 241 AACTCGACCCCATGAAGTCGGAATCGCTAGTAATCGCGTAACAGCATGACGCGGTGAATA 301 CGTTCCCGGGCCTTGTACACACCGCCCGTCACACCATGGGAGTTGGGTCTACCCGACGAC 361 GGTGCGCTAACCCTTACGGGAGGCAGCCGGCCACGGTAGGCTCAGCGGA
1-36	2	1	1 AAAGGGTCTGTAGCTCAGTTGGTTAGAGCACCGTCTTGATAAGGCGGGGGTCGTTGGTTC 61 GAGACCAACCAGACCCACCATCTTCATGGGGGATTAGCTCAGCTGGGAGAGCACCTGCTT 121 TGCAAGCAGGGGGTCGTCGGTTCGATCCCGTCATCCTCCACCACGTTGACGCACATCGCT 181 GACCCGAAAGGCTGTCTGGCTTTTCGGGTCAGCGATTCGAGAGGATCGGCTGAAGTTCTT 241 TAACAATTCGTAGAGTCGAATCAGCGTTGCCCTTGAGCTTACGATCACTGATCGTGCGCG 301 CAAGAGGCGATATTTGATTGCGTCACCAATATTCAACTCGTAAGAGTTTGAACAACGGCA 361 TAACGCGAATACTCTAAATTGTCCTTGACGATGCTTCGAGCAGAGGCGTCAAAGTTATAG 421 GGTCAAGTGACTAAGTGCATGTGGTGGATGCCTTGGCGATTACAGGCGATGAAGGACGTG 481 ATAGCCTGCGATAAGCTTCGGGGAGCTGGCAAATTAGCTTTGATCCGGAGATTTCCGAAT 541 GGGGCAACCC
		2	1 ATGGCTGTCGTCAGCTCGTGTCGTGAGATGTTGGGTTAAGTCCCGCAACGAGCGCAACCC 61 TTATCATTAGTTGCTACGCAAGGGCACTCTAATGAGACTGCCGGTGACAAACCGGAGGAA 121 GGTGGGGATGACGTCAGGTCATCATGGCCCTTATGGGTAGGGCTACACACGTCATACAAT 181 GGCCGGTACAGAGGGCTGCCAACCCGCGAGGGGGAGCTAATCTCATAAAGCCGGTCGTAG 241 TCCGGATCGCAGTCTGCAACTCGACTGCGTGAAGTCGGAATCGCTAGTAATCGCGGATCA 301 GCTTGCCGCGGTGAATACGTTCCCGGGTCTTGTACACACCGCCCGTCACACCATGGGAGC 361 GGGTTCTGTCAGAAGTAGTTAGCCTAACCGCAAGGAGGGCGATTACCACGGCAGGGTTCG 421 TGACTGGGGTGAAGTCGTAACAAGGTAGCCGTATCGGAAGGTGCGGCTGGATCACCTCCT 481 TTCTGGAAAACGCACTCAAATTCTTGCGCCCACACTTATCGGCTGTAGTTGAACACAGCG 541 TGTGAAACGT
1-37	2	3	1 ATGGCTGTCGTCAGCTCGTGTCGTGAGATGTTGGGTTAAGTCCCGCAACGAGCGCAACCC 61 TTACCCTTAGTTGCCAGCATTCAGTTGGGAACTCTAAGGGGACCGCCGGTGACAAACCGG 121 AGGAAGGTGGGGATGACGTCAAGTCATCATGGCCCTTATGACCAGGGCTACACACGTGCT 181 ACAATGGCCGGTACAAAGGGTTGCCAACCCGCGAGGGGGAGCCAATCCCATAAAGCCGGT 241 CGTAGTCCGGATCGCAGTCTGCAACTCGGCTGCGTGAAGTCGGAATCGCTAGTAATCGTG 301 AATCAGCATTGTCACGGTGAATACGTTCCCGGGTCTTGTACACACCGCCCGTCACACCAT 361 GGGAGTTGATTGCACCAGAAGTAGGTAGCCTAACCGCAAGGAGGGCGCTTACCACGGTGG 421 GTCAATG
1-38	2	1	1 CCTGCGGCTGGATCACCTCCTTTCATAAATTATTGTCAAGTGTTCACACTTATTGGTTAT 61 TTGAATAAATAAATATAAATTTGGGTTTGAGGTGTGGGGTTAAACTTGGACTCGTAAGGG 121 TCTGTAGCTCAGTTGGTTAGAGCACACGCTTGATAAGCGTGGGGTCGGTGGTTCAAGTCC 181 ACCCAGACCCACCATAGGGGGTGTAGCTCAGCTGGGAGAGCACCTGCTTTGCAAGCAGGG 241 GGTCATCGGTTCGATCCCGTTCACCTCCACCATTAAGAATGGAAATTTAATTTATTTATT 301 GCTCTTTAAAAATAAAAAATGGGTAAGATTGTGCTTAAAGCATAATTAAAGTAACTATAA 361 GAGTGATGACAAAGCACCAATCTTTTTTGTGAGGGTGGTGGTAAGTTTTCAAGATTATAG 421 GATCAAGCGAACAAGTGCATGTGGTGGATGCCTTGGCGATTACANNGCGATGAAGGACGT 481 GGCACGCTGCGATAAGCTGCGGTGAGGTGTGAGCAACCTTTGACCCGCAGATTTCCGAAT 541 GGGGCAACCC
		2	1 ATGGCTGTCGTCAGCTCGTGTCGTGAGATGTTGGGTTAAGTCCCGCAACGAGCGCAACCC 61 TTGTCGCTAATTGCTATCATTTTAATGAGCACTTTAGCGAGACTGCCGGTGACAAACCGG 121 AGGAAGGTGGGGATGACGTCAAGTCCTCATGGCCCTTATGGGTAGGGCTTCACACGTAAT 181 ACAATGGCGCGTACAGAGGGTTGCCAATCCGCGAGGAGGAGCCAATCTCAGAAAGCGCGT 241 CGTAGTCCGGATCGGAGTCTGCAACTCGACTCCGTGAAGTCGGAATCGCTAGTAATCGCG 301 GATCAGCATGCCGCGGTGAATACGTTCCCGGGTCTTGTACACACCGCCCGTCACACCATG 361 GGAGTGATTTTCACCAGAAGCAGGTAGTTTAACCGCAAGGAGGGCGCTTGCCACGGTGGG 421 GGTCATGACTGGGGTGAAGTCGTAACAAGGTAGCCGTAGGGGAACCTGCGGCTGGATCAC 481 CTCCTTTCATAAATTATTGTCAAGTGTTCACACTTATTGGTTATTTGAATAAATAAATAT 541 AAATTTGGGT

Table A-1 Continued.

ID	N	P	FASTA formatted sequence (5′ → 3′ sense strand)
1-39	2	1	1 ATGGCTGTCGTCAGCTCGTGTCGTGAGATGTTGGGTTAAGTCCCGCAACGAGCGCAACCC 61 TCGCTACTAGTTGCCAGCAGGTTGAGCTGGGCACTCTAGTGGAACTGCCGGTGGCAAGCC 121 GGAGGAAGGTGGGGATGACGTCAAGTCCTCATGGCCCTTACGCGTGGGGCTACACACGTG 181 CTACAATGGTGGTGACAGAGGGATAATCCCTAAAAACCATCTCAGTTCGGATTGTCCTCT 241 GCAACTCGAGGGCATGAAGTTGGAATCGCTAGTAATCGCGGATCAGCATGCCGCGGTGAA 301 TACGTTCCCGGGCCTTGTACACACCGCCCGTCACACCATGGGAGTTGGTTCTACCCGAAG 361 GCGCTGCGCTAACCGCAAGGGGGCAGGCGACCACGGTAGGGTCAGCGACTGGGGTGAAGT 421 CGTAACAAGGTAGCCGTAGGGGAACCTGCGGCTGGATCACCTCCTTTCTAAGGAAGATCA 481 CGATTGGATATCGGCGCGAAAGCCCGATCCTCGCGATCGACTTGGACAAGCCCCAGATCT 541 TCGGATCTGA
1-40	2	1	1 ATGGCTGTCGTCAGCTCGTGTCGTGAGATGTTGGGTTAAGTCCCGCAACGAGCGCAACCC 61 TCGCTACTAGTTGCCAGCAGGTTAAGCTGGGCACTCTAGTGGAACTGCCGGTGGCAAGCC 121 GGAGGAAGGTGGGGATGACGTCAAGTCCTCATGGCCCTTACGCGTGGGGCTACACACGTG 181 CTACAATGGTGGTGACAGAGGGATAATCCCTAAAAACCATCTCAGTTCGGATTGTCCTCT 241 GCAACTCGAGGGCATGAAGTTGGAATCGCTAGTAATCGCGGATCAGCATGCCGCGGTGAA 301 TACGTTCCCGGGCCTTGTACACACCGCCCGTCACACCATGGGAGTTGGTTCTACCCGAAG 361 GCGCTGCGCTAACCGCAAGGGGGCAGGCGACCACGGTAGGGTCAGCGACTGGGGTGAGTC 421 GTAACAAGGTAGCCGTAGGGGAACCTGCGGCTGGATCACCTCCTTTCTAAGGAAGATCAC 481 GATTGGATATCGGCGCGAAAGCCCGATCCTCGCGATCGACTTGGACAAGCCCCAGATCTT 541 CGGATCTGAG

Table A-2 Blastn (Altschul et al., 1990; Altschul et al., 1997) sequence analysis results for Table A-1. GenBank® database matches (typically an environmental clone and/or the closest cultured organism) are described. Blastn results for Clones 1-26, 1-31, 1-32, 1-33, 1-36, and 1-38 are for the 16S portion of the cloned sequence.

ID	Accession Number	Similarity Score	Database Description	Taxonomic Association
1-1	AJ318134.1	Score = 815 bits (411), Expect = 0.0 Identities = 421/423 (99%) Gaps = 1/423 (0%)	Uncultured alpha proteobacterium 16S rDNA, clone BIfdii32	α-Proteobacteria
	AF227160.1	Score = 694 bits (350), Expect = 0.0 Identities = 402/418 (96%) Gaps = 1/418 (0%)	*Achromobacter* sp. LMG5430 16S rDNA	β-Proteobacteria
1-2	AF097828.1	Score = 628 bits (317), Expect = e^{-177} Identities = 382/405 (94%) Gaps = 1/405 (0%)	Unidentified bacterium clone 4955 16S rDNA	Eubacteria
	U10877.1	Score = 396 bits (200), Expect = e^{-107} Identities = 327/366 (89%) Gaps = 5/366 (1%)	*Riemerella anatipestifer* ATCC 11845 16S rDNA	CFB group bacteria
1-3	AF428833.1	Score = 733 bits (370), Expect = 0.0 Identities = 409/422 (96%)	Uncultured bacterium clone CR98-24-27 16S rDNA	Eubacteria
	U87104.1	Score = 622 bits (314), Expect = e^{-176} Identities = 395/422 (93%)	*Ornithobacterium rhinotracheale* 16S rDNA	CFB group bacteria
1-4	AF097828.1	Score = 636 bits (321), Expect = e^{-180} Identities = 383/405 (94%) Gaps = 1/405 (0%)	Unidentified bacterium clone 4955 16S rDNA	Eubacteria
	U10877.1	Score = 389 bits (196), Expect = e^{-105} Identities = 326/366 (89%) Gaps = 5/366 (1%)	*Riemerella anatipestifer* ATCC 11845 16S rDNA	CFB group bacteria

Table A-2 Continued.

ID	Accession Number	Similarity Score	Database Description	Taxonomic Association
1-5	AJ318134.1	Score = 821 bits (414), Expect = 0.0 Identities = 424/426 (99%) Gaps = 1/426 (0%)	Uncultured alpha proteobacterium 16S rDNA	α-Proteobacteria
	AF227160.1|	Score = 696 bits (351), Expect = 0.0 Identities = 409/427 (95%) Gaps = 1/427 (0%)	*Achromobacter* sp. LMG5430 16S rDNA	β-Proteobacteria
1-6	AF353161.1	Score = 842 bits (425), Expect = 0.0 Identities = 425/425 (100%)	*Nitrosomonas* sp. CNS326 16S rDNA	β-Proteobacteria - *Nitrosomonas* sp.
	AF353160.1	Score = 757 bits (382), Expect = 0.0 Identities = 416/426 (97%) Gaps = 1/426 (0%)	*Nitrosomonas europaea* 16S rDNA	
1-7	AF353161.1	Score = 827 bits (417), Expect = 0.0 Identities = 424/425 (99%) Gaps = 1/425 (0%)	*Nitrosomonas* sp. CNS326 16S rDNA	β-Proteobacteria - *Nitrosomonas* sp.
	AF353160.1	Score = 741 bits (374), Expect = 0.0 Identities = 415/426 (97%) Gaps = 2/426 (0%)	*Nitrosomonas europaea* 16S rDNA	
1-8	AF097828.1	Score = 628 bits (317), Expect = e^{-177} Identities = 382/405 (94%) Gaps = 1/405 (0%)	Unidentified bacterium clone 4955 16S rDNA	Eubacteria
	U10877.1	Score = 396 bits (200), Expect = e^{-107} Identities = 327/366 (89%) Gaps = 5/366 (1%)	*Riemerella anatipestifer* ATCC 11845 16S rDNA	CFB group bacteria

Table A-2 Continued.

ID	Accession Number	Similarity Score	Database Description	Taxonomic Association
1-9	AF428833.1	Score = 733 bits (370), Expect = 0.0 Identities = 409/422 (96%)	Uncultured bacterium clone CR98-24-27 16S rDNA	Eubacteria
	U87104.1	Score = 622 bits (314), Expect = e^{-176} Identities = 395/422 (93%)	*Ornithobacterium rhinotracheale* 16S rDNA	CFB group bacteria
1-10	AJ318154.1	Score = 700 bits (353), Expect = 0.0 Identities = 398/413 (96%)	Uncultured *Bacteroides* bacterium 16S rDNA	CFB group bacteria
	M58790.1	Score = 414 bits (209), Expect = e^{-113} Identities = 293/322 (90%)	*Haliscomenobacter hydrossis* 16S rDNA	
1-11	AF332262.1	Score = 712 bits (359), Expect = 0.0 Identities = 404/419 (96%)	Uncultured bacterium clone C12-25 16S rDNA	Eubacteria
	AF479790.1	Score = 706 bits (356), Expect = 0.0 Identities = 407/424 (95%)	*Pseudoxanthomonas taiwanensis* strain CB-225 16S rDNA	γ-Proteobacteria
1-12	AY007683.1	Score = 795 bits (401), Expect = 0.0 Identities = 408/411 (99%)	Unknown marine alpha proteobacterium JP57 16S rDNA	α-Proteobacteria
	AF227160.1	Score = 634 bits (320), Expect = e^{-179} Identities = 387/408 (94%) Gaps = 1/408 (0%)	*Achromobacter* sp. LMG5430 16S rDNA	β-Proteobacteria
1-13	AY123795.1	Score = 835 bits (421), Expect = 0.0 Identities = 424/425 (99%)	*Nitrosomonas eutropha* 16S rDNA	β-Proteobacteria - *Nitrosomonas* sp.
	AF353161.1	Score = 835 bits (421), Expect = 0.0 Identities = 424/425 (99%)	*Nitrosomonas* sp. CNS326 16S rDNA	

Table A-2 Continued.

ID	Accession Number	Similarity Score	Database Description	Taxonomic Association
1-14	AF332262.1	Score = 676 bits (341), Expect = 0.0 Identities = 403/421 (95%) Gaps = 2/421 (0%)	Uncultured bacterium clone C12-25 16S rDNA	Eubacteria
	AF479790.1	Score = 668 bits (337), Expect = 0.0 Identities = 402/421 (95%) Gaps = 2/421 (0%)	*Pseudoxanthomonas taiwanensis* strain CB-225 16S rDNA	γ-Proteobacteria
1-15	AF428833.1	Score = 718 bits (362), Expect = 0.0 Identities = 401/414 (96%)	Uncultured bacterium clone CR98-24-27 16S rDNA	Eubacteria
	U87104.1	Score = 607 bits (306), Expect = e^{-171} Identities = 387/414 (93%)	*Ornithobacterium rhinotracheale* 16S rDNA	CFB group bacteria
1-16	AY007683.1	Score = 787 bits (397), Expect = 0.0 Identities = 410/415 (98%)	Unknown marine alpha proteobacterium 16S rDNA	α-Proteobacteria
	AF227160.1	Score = 626 bits (316), Expect = e^{-177} Identities = 392/416 (94%) Gaps = 1/416 (0%)	*Achromobacter* sp. LMG5430 16S rDNA	β-Proteobacteria
1-17	AJ318154.1	Score = 720 bits (363), Expect = 0.0; Identities = 408/423 (96%)	Uncultured *Bacteroidetes* bacterium 16S rRNA gene	CFB group bacteria
	M58790.1	Score = 426 bits (215), Expect = e^{-116} Identities = 299/328 (91%)	*Haliscomenobacter hydrossis* 16S rDNA	
1-18	AF428833.1	Score = 674 bits (340), Expect = 0.0 Identities = 385/400 (96%)	Uncultured bacterium clone CR98-24-27 16S rDNA	Eubacteria
	U87106.1	Score = 563 bits (284), Expect = e^{-158} Identities = 371/400 (92%)	*Ornithobacterium rhinotracheale* 16S rDNA	CFB group bacteria

Table A-2 Continued.

ID	Accession Number	Similarity Score	Database Description	Taxonomic Association
1-19	AF428833.1	Score = 686 bits (346), Expect = 0.0 Identities = 391/406 (96%)	Uncultured bacterium clone CR98-24-27 16S rDNA	Eubacteria
	U87104.1	Score = 575 bits (290), Expect = e^{-161} Identities = 377/406 (92%)	*Ornithobacterium rhinotracheale* 16S rDNA	CFB group bacteria
1-20	AJ005009.1	Score = 1532 bits (773), Expect = 0.0 Identities = 875/905 (96%); Gaps = 3/905 (0%)	*Nitrobacter agilis* 23S rDNA gene	α-Proteobacteria - *Nitrobacter* sp.
1-21	X73400.1	Score = 844 bits (426), Expect = 0.0 Identities = 435/438 (99%)	*L.steigerwaltii* (ATCC 35302) 16S rDNA	γ-Proteobacteria - Legionellaceae group
	X73394.1	Score = 844 bits (426), Expect = 0.0 Identities = 435/438 (99%)	*L.anisa* (ATCC 35292) gene for 16S rDNA	β-Proteobacteria
1-22	AF234751.1	Score = 791 bits (399), Expect = 0.0 Identities = 465/487 (95%)	Uncultured sludge bacterium S6 16S rDNA	Fibrobacteres/Acidobacteria group
	X70954.1	Expect = e^{-110}; could not retrieve precise score	*Pelobacter propionicus* (closest organism in culture)	CFB group bacteria
1-23	AF097780.1	Score = 726 bits (366) Expect = 0.0 Identities = 409/424 (96%)	Unidentified bacterium clone 29524 16S rDNA	Unclassified Bacteria
1-24	X53855.1	Score = 809 bits (408), Expect = 0.0 Identities = 470/488 (96%) Gaps = 2/488 (0%)	*R. sphaeroides* ribosomal RNA operon rrnC	α-Proteobacteria
1-25	AF234705.1	Score = 636 bits (321), Expect = e^{-180} Identities = 438/477 (91%)	Uncultured sludge bacterium H8 16S rDNA	Plactomycetales

Table A-2 Continued.

ID	Accession Number	Similarity Score	Database Description	Taxonomic Association
1-26	AF217462.1	Score = 553 bits (279), Expect = e^{-155} Identities = 419/463 (90%) Gaps = 2/463 (0%)	*Candidatus Xiphinematobacter* brevicolli 16S rDNA	Verrucomicrobia
1-27	AJ001344.1	Score = 898 bits (453), Expect = 0.0 Identities = 477/485 (98%)	Star-like microcolonies 16S rDNA	α-Proteobacteria
	AB084247.1	Score = 894 bits (451), Expect = 0.0 Identities = 454/455 (99%)	*Sphingomonas* sp. Y2 gene for 16S rDNA	α-Proteobacteria *Sphingomonas* sp.
1-28	AF217462.1	Score = 553 bits (279), Expect = e^{-155} Identities = 419/463 (90%) Gaps = 2/463 (0%)	*Candidatus Xiphinematobacter* brevicolli 16S rDNA	Verrucomicrobia
1-29	AB031960.1	Score = 957 bits (483), Expect = 0.0 Identities = 486/487 (99%)	*Nitrosomonas* sp. TK794 gene for 16S rRNA	β-Proteobacteria - *Nitrosomonas* sp.
	NZ_AAAY01000001.1	Score = 936 bits (472), Expect = 0.0 Identities = 515/528 (97%) Gaps = 1/528 (0%)	*Nitrosomonas europaea* Neur_1, whole genome shotgun sequence	
1-30	AJ318191.1	Score = 823 bits (415), Expect = 0.0 Identities = 439/447 (98%)	Uncultured *Bacteroidetes* bacterium 16S rDNA	CFB group bacteria
	U87100.1	Score = 676 bits (341), Expect = 0.0 Identities = 419/444 (94%) Gaps = 2/444 (0%)	*Ornithobacterium rhinotracheale* 16S rDNA	

Table A-2 Continued.

ID	Accession Number	Similarity Score	Database Description	Taxonomic Association
1-31	U45329.1	Score = 955 bits (482), Expect = 0.0 Identities = 491/494 (99%)	*Agrobacterium vitis* ribosomal operon	α-Proteobacteria
	AL591792.1	Score = 932 bits (470), Expect = 0.0 Identities = 488/494 (98%)	*Sinorhizobium meliloti* 1021	
1-32	AJ318191.1	Score = 823 bits (415), Expect = 0.0 Identities = 439/447 (98%)	Uncultured *Bacteroidetes* bacterium 16S rDNA	CFB group bacteria
	U87100.1	Score = 676 bits (341), Expect = 0.0 Identities = 419/444 (94%) Gaps = 2/444 (0%)	*Ornithobacterium rhinotracheale* 16S rDNA	
1-33	AF217462.1	Score = 553 bits (279), Expect = e^{-155} Identities = 419/463 (90%) Gaps = 2/463 (0%)	Candidatus *Xiphinematobacter brevicolli* 16S rDNA	Chlamydiae/Verrucomicrobia group - Verrucomicrobia
1-34	AY123795.1	Score = 842 bits (425), Expect = 0.0 Identities = 425/425 (100%)	*Nitrosomonas eutropha* 16S rDNA	β-Proteobacteria *Nitrosomonas* sp.
1-35	AB041770.1	Score = 708 bits (357), Expect = 0.0 Identities = 393/405 (97%)	*Paracoccus kawasakiensis* gene for 16S rDNA	α-Proteobacteria
	AF434674.2	Score = 688 bits (347), Expect = 0.0 Identities = 392/407 (96%)	*Silicibacter pomeroyi* strain DSS-10 16S rDNA	
1-36	AF176594.1	Score = 940 bits (474), Expect = 0.0 Identities = 513/526 (97%)	MTBE-degrading bacterium PM1 16S ribosomal RNA gene	β-Proteobacteria
	X97071.1	Score = 884 bits (446), Expect = 0.0 Identities = 473/482 (98%)	*Leptothrix mobilis* 16S rDNA	

Table A-2 Continued.

ID	Accession Number	Similarity Score	Database Description	Taxonomic Association
1-37	AF507743.1	Score = 722 bits (364), Expect = 0.0 Identities = 414/428 (96%) Gaps = 2/428 (0%)	Uncultured soil bacterium clone S175 16S rDNA	Unclassified Bacteria
	AF173169.1	Score = 607 bits (306), Expect = e^{-171} Identities = 393/421 (93%) Gaps = 2/421 (0%)	*Thiobacillus neapolitanus* DSM 581 16S rDNA	Gamma Proteobacteria
1-38	AB031960.1	Score = 965 bits (487), Expect = 0.0 Identities = 487/487 (100%)	*Nitrosomonas* sp. TK794 gene for 16S rDNA	β-Proteobacteria *Nitrosomonas* sp.
	NZ_AAAY01000001.1	Score = 944 bits (476), Expect = 0.0 Identities = 516/528 (97%) Gaps = 1/528 (0%)	*Nitrosomonas europaea* Neur_1, whole genome shotgun sequence	
1-39	AF234756.1	Score = 825 bits (416), Expect = 0.0 Identities = 461/472 (97%) Gaps = 3/472 (0%)	Uncultured sludge bacterium S36 16S rDNA	α-Proteobacteria
	AJ227782.1	Score = 678 bits (342), Expect = 0.0 Identities = 423/449 (94%) Gaps = 2/449 (0%)	*Brevundimonas bacteroides* DNA for 16S rDNA	
1-40	AF234756.1	Score = 817 bits (412), Expect = 0.0 Identities = 461/472 (97%) Gaps = 4/472 (0%)	Uncultured sludge bacterium S36 16S rDNA	α-Proteobacteria
	AJ227782.1	Score = 662 bits (334), Expect = 0.0 Identities = 422/449 (93%) Gaps = 3/449 (0%)	*Brevundimonas bacteroides* DNA for 16S rDNA	

Table A-3 A ClustalX percent identify matrix for the 16S portion of the sequences in Table A-1 and the major phylogenic branches of the nitrifiers (from approximately the 1055f up to the 1492r primer annealing sequences). *Nitrobacter*, *Nitrococcus*, *Nitrosococcus*, *Nitrosomonas*, *Nitrospira*, and *Nitrospina* sequence data corresponded to GenBank® accession numbers L11661, L35510, M96395, AF037106, X82558, and L35504, respectively. The matrix was created after an alignment of the sequences was completed by constructing an NJ tree. Sequences with similarities ≥ 97% are boxed to emphasize the relatively close phylogenic relationship. A "*" indicates ≈ 100% sequence similarity.

	1-1	1-5	1-12	1-16	1-20	*Nitrobacter*	1-24	1-35	1-27	1-31	1-39	1-40	1-11	1-14	1-21	*Nitrosococcus*	*Nitrococcus*	1-37	1-6	1-13	1-34	1-7	1-38	1-29	*Nitrosomonas*	1-36	1-22	1-23	1-26	1-28	1-33	1-25	*Nitrospira*	*Nitrospina*	1-4	1-8	1-2	1-3	1-9	1-15	1-19	1-18	1-30	1-32	1-10	1-17
1-1	*	*	98	98	91	92	92	91	91	92	91	91	84	84	83	84	84	84	81	81	81	81	81	81	81	81	82	82	76	76	76	76	80	81	81	81	81	79	79	79	79	80	78	78	79	79
1-5	*	*	98	98	92	92	91	91	91	92	91	91	84	84	83	83	84	83	81	81	81	81	81	81	81	81	81	81	76	76	76	76	80	81	81	81	81	78	78	79	79	80	78	78	79	79
1-12	98	98	*	*	91	91	91	91	91	91	91	92	84	84	84	84	84	83	82	82	82	82	82	82	82	81	83	83	77	77	77	77	81	83	84	84	84	81	81	81	81	81	81	81	80	80
1-16	98	98	*	*	91	91	90	91	91	91	91	91	84	84	84	84	84	83	82	82	82	82	82	82	82	81	82	83	77	77	77	77	81	82	83	83	83	81	81	81	80	81	80	80	79	80
1-20	91	92	91	91	*	*	91	89	91	91	91	91	82	82	84	83	83	82	81	81	81	81	82	81	82	81	80	80	76	76	76	75	81	81	80	80	80	78	78	79	78	79	76	76	77	77
Nitrobacter	92	92	91	91	*	*	91	90	91	91	91	91	82	82	84	82	83	82	81	81	81	81	81	81	82	81	80	80	76	76	76	75	81	81	80	80	80	78	78	79	79	80	76	76	77	77
1-24	92	91	91	90	91	91	*	95	92	93	89	89	83	83	84	82	84	82	80	80	80	80	81	81	81	82	81	81	77	77	77	76	80	81	82	82	82	80	80	80	80	81	77	77	79	79
1-35	91	91	91	91	89	90	95	*	89	91	89	89	84	84	82	82	84	84	81	81	81	81	80	80	80	80	80	81	75	75	75	75	79	82	82	82	82	80	80	81	80	81	78	78	79	79
1-27	91	91	91	91	91	91	92	89	*	94	91	91	85	85	83	84	85	85	82	82	82	82	82	82	83	83	82	82	78	78	78	75	81	82	81	81	81	78	78	79	78	79	76	76	77	77
1-31	92	92	91	91	91	91	93	91	94	*	93	93	87	87	84	85	86	85	81	81	82	82	82	82	82	83	83	83	78	78	78	77	79	84	81	81	81	79	79	79	79	80	76	76	79	79
1-39	91	91	91	91	91	91	89	89	91	93	*	*	84	85	83	85	85	83	81	81	81	81	81	81	81	83	83	83	77	77	77	76	82	83	82	82	82	79	79	80	79	80	77	77	78	78
1-40	91	91	92	91	91	91	89	89	91	93	*	*	85	85	83	85	85	83	81	81	81	81	81	81	81	83	83	83	77	77	77	76	83	83	83	83	83	79	79	80	79	80	77	77	78	78
1-11	84	84	84	84	82	82	83	84	85	87	84	85	*	*	89	89	90	90	87	87	87	87	87	87	86	87	83	83	77	77	77	78	80	83	82	83	83	79	79	80	79	81	78	78	80	80
1-14	84	84	84	84	82	82	83	84	85	87	85	85	*	*	89	89	90	89	87	87	87	88	87	87	87	87	83	83	78	78	78	79	81	83	83	84	84	80	80	80	80	81	79	79	80	80
1-21	83	83	84	84	84	84	84	82	83	84	83	83	89	89	*	88	88	87	85	85	85	85	85	85	85	86	81	81	77	77	77	75	79	83	80	80	80	80	80	80	80	81	76	76	78	78
Nitrosococcus	84	83	84	84	83	82	82	82	84	85	85	85	89	89	88	*	92	90	86	86	87	87	87	87	87	87	84	84	77	77	77	77	82	85	84	84	84	80	80	81	80	81	78	78	81	81
Nitrococcus	84	84	84	84	83	83	84	84	85	86	85	85	90	90	88	92	*	91	86	86	86	86	86	86	87	87	84	84	78	78	78	77	84	87	82	83	83	80	80	81	80	82	78	78	82	81
1-37	84	83	83	83	82	82	82	84	85	85	83	83	90	89	87	90	91	*	88	88	88	88	88	88	88	90	84	85	75	75	75	77	79	84	79	79	79	78	78	79	78	80	77	77	79	79
1-6	81	81	82	82	81	81	80	81	82	81	81	81	87	87	85	86	86	88	*	*	*	*	*	*	97	89	80	80	77	77	77	75	76	79	78	78	78	74	74	75	74	75	75	75	77	76
1-13	81	81	82	82	81	81	80	81	82	81	81	81	87	87	85	86	86	88	*	*	*	*	*	*	97	89	80	80	77	77	77	75	76	79	78	78	78	74	74	74	74	75	75	75	76	76

Table A-3 Continued.

	1-1	1-5	1-12	1-16	1-20	*Nitrobacter*	1-24	1-35	1-27	1-31	1-39	1-40	1-11	1-14	1-21	*Nitrosococcus*	*Nitrococcus*	1-37	1-6	1-13	1-34	1-7	1-38	1-29	*Nitrosomonas*	1-36	1-22	1-23	1-26	1-28	1-33	1-25	*Nitrospira*	*Nitrospina*	1-4	1-8	1-2	1-3	1-9	1-15	1-19	1-18	1-30	1-32	1-10	1-17
1-34	81	81	82	82	81	81	80	81	82	82	81	81	87	87	85	87	86	88	*	*	*	*	*	*	98	89	80	80	77	77	77	75	76	80	78	78	78	74	74	75	74	75	76	76	77	76
1-7	81	81	82	82	81	81	80	81	82	82	81	81	87	88	85	87	86	88	*	*	*	*	*	*	98	89	80	80	77	77	77	75	76	80	78	78	79	74	74	75	74	75	76	76	77	76
1-38	81	81	82	82	82	81	81	80	82	82	81	81	87	87	85	87	86	88	*	*	*	*	*	*	98	90	80	80	77	77	77	75	77	80	78	78	78	74	74	75	74	75	75	75	77	76
1-29	81	81	82	82	81	81	81	80	82	82	81	81	87	87	85	87	86	88	*	*	*	*	*	*	97	89	80	80	77	77	77	75	77	79	78	78	78	74	74	75	74	75	75	75	76	76
Nitrosomonas	81	81	82	82	82	82	81	80	83	82	81	81	86	87	85	87	87	88	97	97	98	98	98	97	*	90	80	81	77	77	77	75	77	80	78	78	78	74	74	75	75	76	75	75	76	76
1-36	81	81	81	81	81	81	82	80	83	83	83	83	87	87	86	87	87	90	89	89	89	89	90	89	90	*	82	82	77	77	77	78	80	82	80	80	80	78	78	78	78	79	77	77	79	78
1-22	82	81	83	82	80	80	81	80	82	83	83	83	83	83	81	84	84	84	80	80	80	80	80	80	80	82	*	99	78	78	78	77	83	85	78	78	78	76	76	77	77	78	77	77	78	78
1-23	82	81	83	83	80	80	81	81	82	83	83	83	83	83	81	84	84	85	80	80	80	80	80	80	81	82	99	*	79	79	79	78	84	85	78	78	79	76	76	77	77	78	77	77	79	79
1-26	76	76	77	77	76	76	77	75	78	78	77	77	77	78	77	77	78	75	77	77	77	77	77	77	77	77	78	79	*	*	*	80	79	78	75	75	75	74	74	74	74	75	74	74	76	76
1-28	76	76	77	77	76	76	77	75	78	78	77	77	77	78	77	77	78	75	77	77	77	77	77	77	77	77	78	79	*	*	*	80	79	78	75	75	75	74	74	74	74	75	74	74	76	76
1-33	76	76	77	77	76	76	77	75	78	78	77	77	77	78	77	77	78	75	77	77	77	77	77	77	77	77	78	79	*	*	*	80	79	78	75	75	75	74	74	74	74	75	74	74	76	76
1-25	76	76	77	77	75	75	76	75	75	77	76	76	78	79	75	77	77	77	75	75	75	75	75	75	75	78	77	78	80	80	80	*	77	78	76	76	76	75	75	75	74	75	74	74	77	76
Nitrospira	80	80	81	81	81	81	80	79	81	79	82	83	80	81	79	82	84	79	76	76	76	76	77	77	77	80	83	84	79	79	79	77	*	84	81	80	80	80	80	81	81	82	79	79	82	81
Nitrospina	81	81	83	82	81	81	81	82	82	84	83	83	83	83	83	85	87	84	79	79	80	80	80	79	80	82	85	85	78	78	78	78	84	*	82	82	82	82	82	83	82	83	79	79	82	82
1-4	81	81	84	83	80	80	82	82	81	81	82	83	82	83	80	84	82	79	78	78	78	78	78	78	78	80	78	78	75	75	75	76	81	82	*	*	*	85	85	86	85	86	85	85	86	86
1-8	81	81	84	83	80	80	82	82	81	81	82	83	83	84	80	84	83	79	78	78	78	78	78	78	78	80	78	78	75	75	75	76	80	82	*	*	*	86	86	86	86	87	85	85	86	86
1-2	81	81	84	83	80	80	82	82	81	81	82	83	83	84	80	84	83	79	78	78	78	79	78	78	78	80	78	79	75	75	75	76	80	82	*	*	*	86	86	86	86	87	85	85	86	86
1-3	79	78	81	81	78	78	80	80	78	79	79	79	79	80	80	80	80	78	74	74	74	74	74	74	74	78	76	76	74	74	74	75	80	82	85	86	86	*	*	*	*	*	91	91	86	86
1-9	79	78	81	81	78	78	80	80	78	79	79	79	79	80	80	80	80	78	74	74	74	74	74	74	74	78	76	76	74	74	74	75	80	82	85	86	86	*	*	*	*	*	91	91	86	86
1-15	79	79	81	81	79	79	80	81	79	79	80	80	80	80	80	81	81	79	75	74	75	75	75	75	75	78	77	77	74	74	74	75	81	83	86	86	86	*	*	*	*	*	91	91	86	86
1-19	79	79	81	80	78	79	80	80	78	79	79	79	79	80	80	80	80	78	74	74	74	74	74	74	75	78	77	77	74	74	74	74	81	82	85	86	86	*	*	*	*	*	90	90	86	86
1-18	80	80	81	81	79	80	81	81	79	80	80	80	81	81	81	81	82	80	75	75	75	75	75	75	76	79	78	78	75	75	75	75	82	83	86	87	87	*	*	*	*	*	90	90	86	86
1-30	78	78	81	80	76	76	77	78	76	76	77	77	78	79	76	78	78	77	75	75	76	76	75	75	75	77	77	77	74	74	74	74	79	79	85	85	85	91	91	91	90	90	*	*	83	83
1-32	78	78	81	80	76	76	77	78	76	76	77	77	78	79	76	78	78	77	75	75	76	76	75	75	75	77	77	77	74	74	74	74	79	79	85	85	85	91	91	91	90	90	*	*	83	83
1-10	79	79	80	79	77	77	79	79	77	79	78	78	80	80	78	81	82	79	77	76	77	77	77	76	76	79	78	79	76	76	76	77	82	82	86	86	86	86	86	86	86	86	83	83	*	*
1-17	79	79	80	80	77	77	79	79	77	79	78	78	80	80	78	81	81	79	76	76	76	76	76	76	76	78	78	79	76	76	76	76	81	82	86	86	86	86	86	86	86	86	83	83	*	*

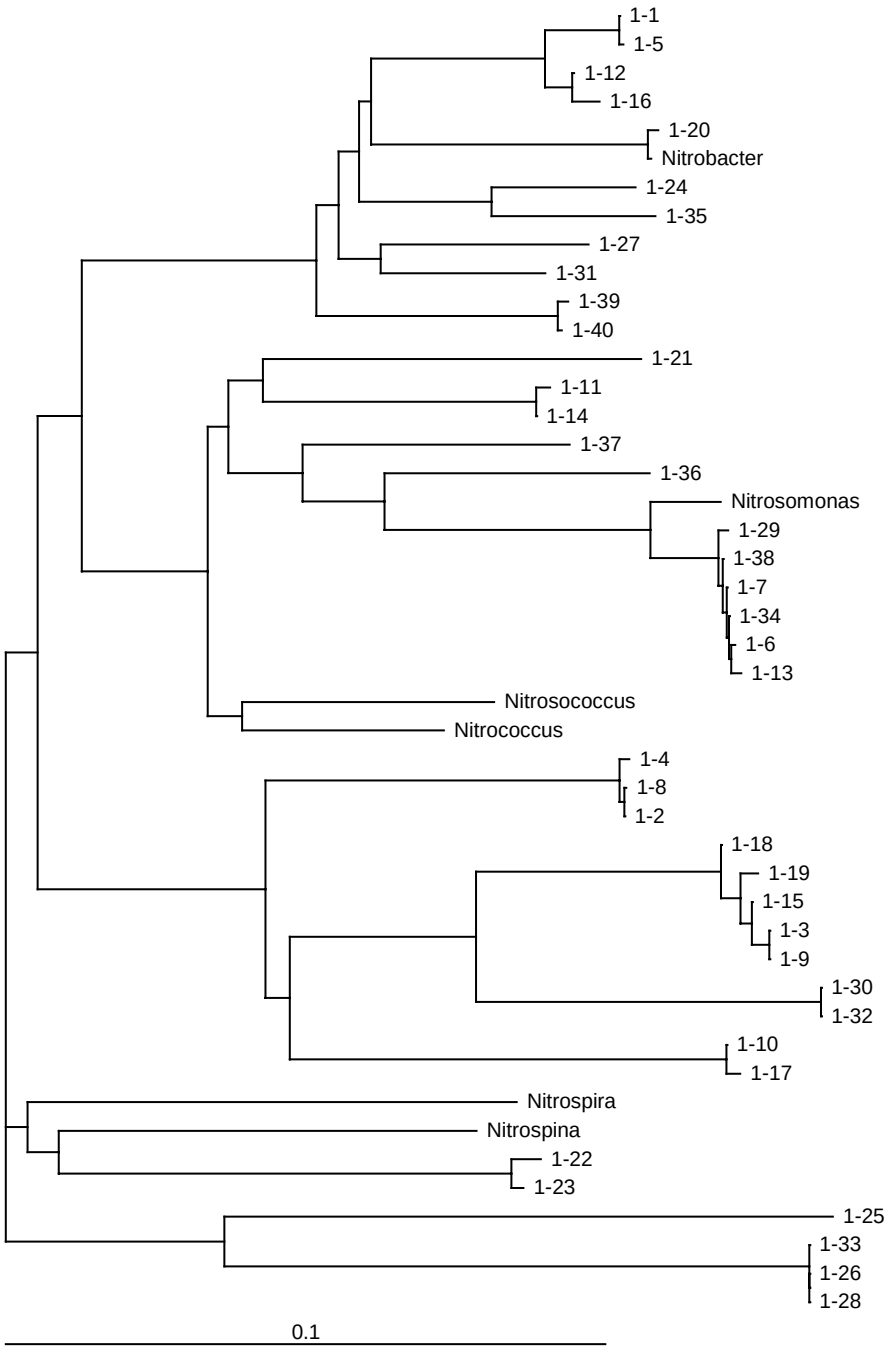
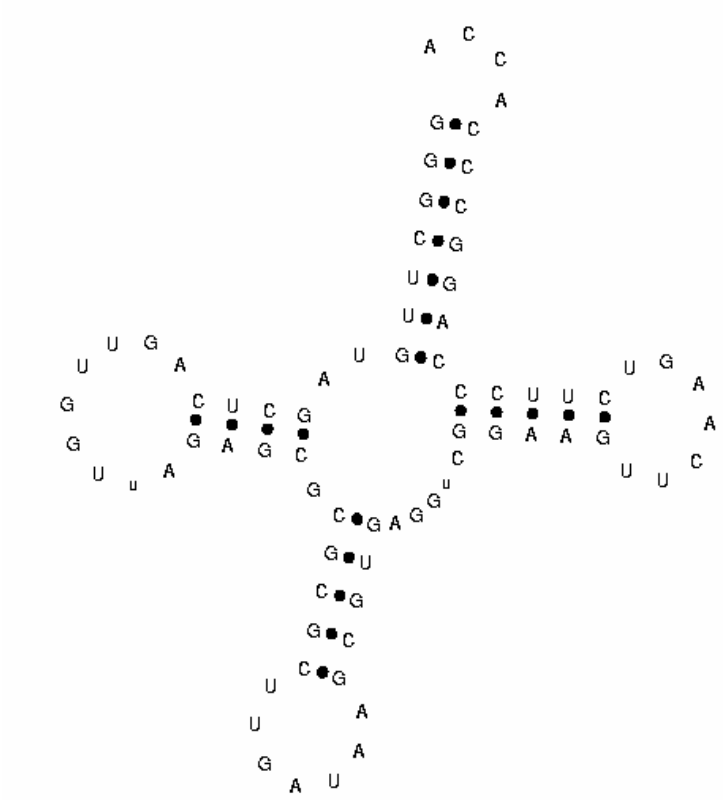


Figure A-1 A phylogram of clone library 1 (Table A-1) that includes the major phylogenic branches of nitrifying bacteria as outgroups (see Table A-3). After the alignment was complete, an NJ tree was bootstrapped with the default program settings to generate the final tree groupings. The scale indicates 0.1 nucleotide substitution per site.

Isoleucine (GAU), 93.43 bits, 109-185



Alanine (UGC), 78.39 bits, 218-293

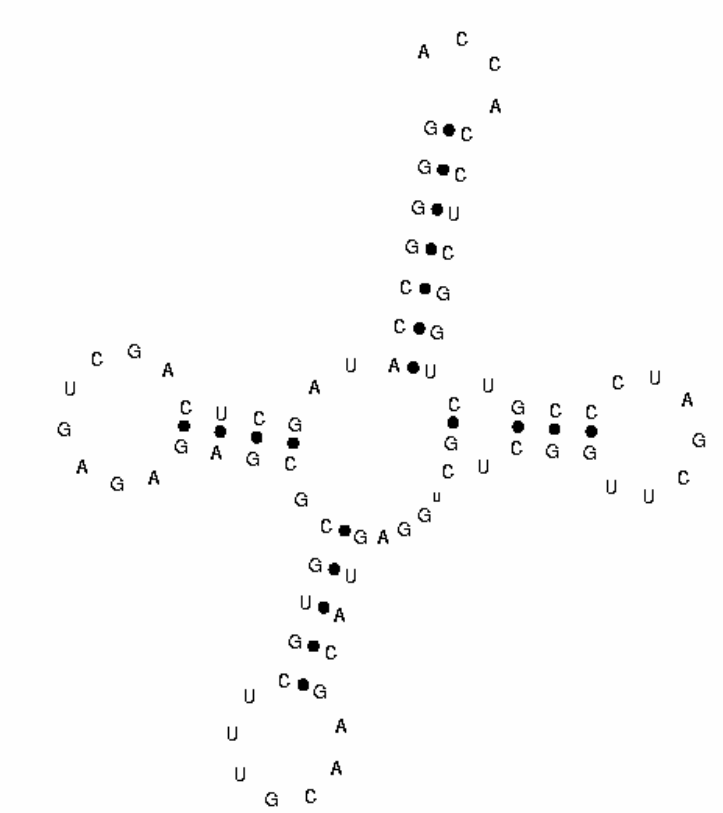


Figure A-2 Two tRNA sequences identified in the clone 1-20 DNA sequence (Table A-1) using tRNAscan-SE version 1.21 (Lowe and Eddy, 1997; http://www.genetics.wustl.edu/eddy/tRNAscan-SE/). The default search mode was utilized for bacterial sources of DNA. Figure captions indicate the target amino acid (anticodon sequence), the cove score, and the beginning and ending base pairs within the 16S - 23S ISR sequence of clone 1-20.

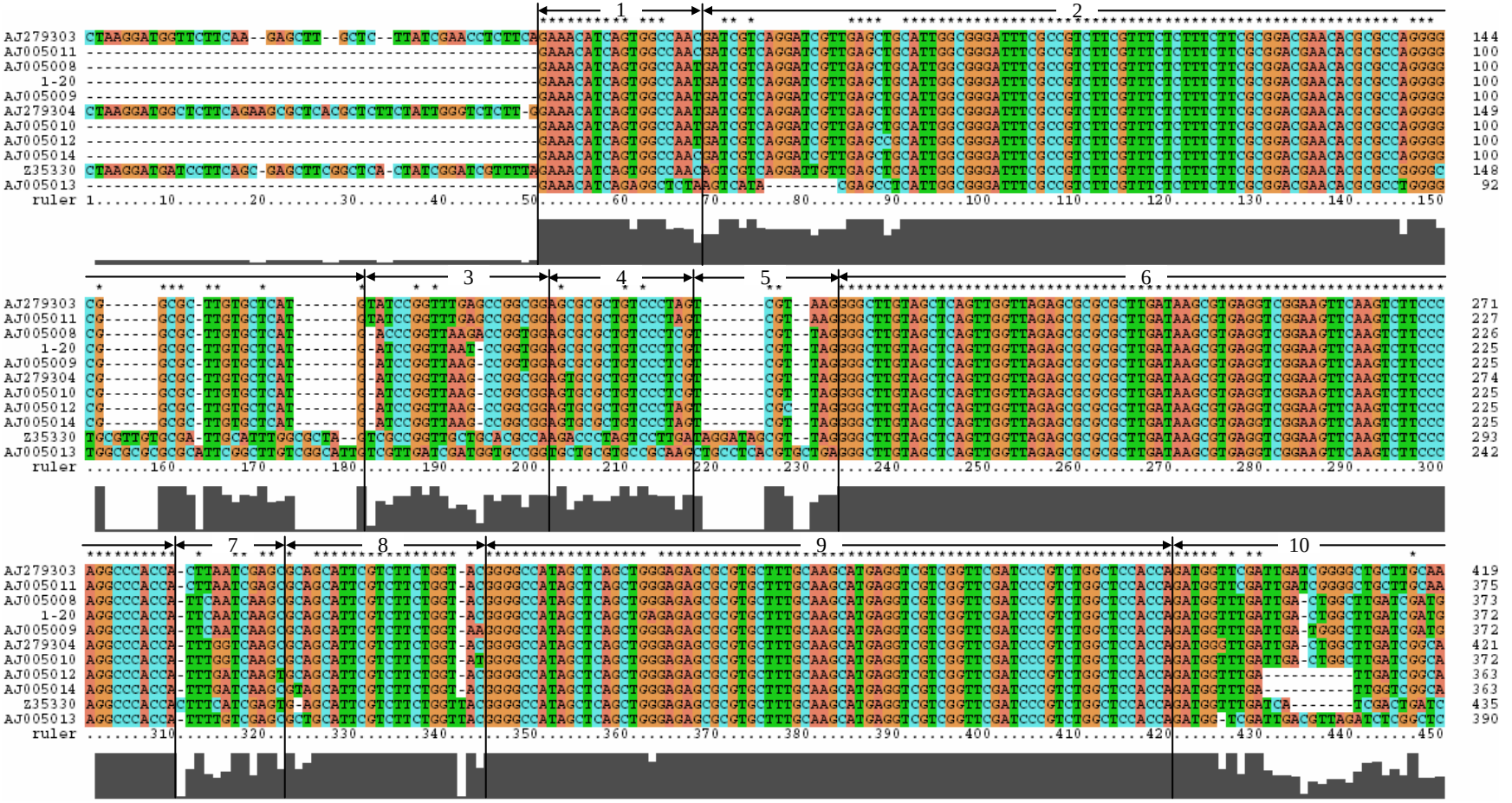


Figure A-3 A ClustalX alignment of the 16S - 23S ISRs for clone 1-20 (Table A-1), *Nitrobacter* spp., and two closely related α-Proteobacteria. GenBank® accession numbers are provided for the *Nitrobacter* and α-Proteobacteria sequences. The alignment was divided into twenty regions to design a quantitative PCR detection system.

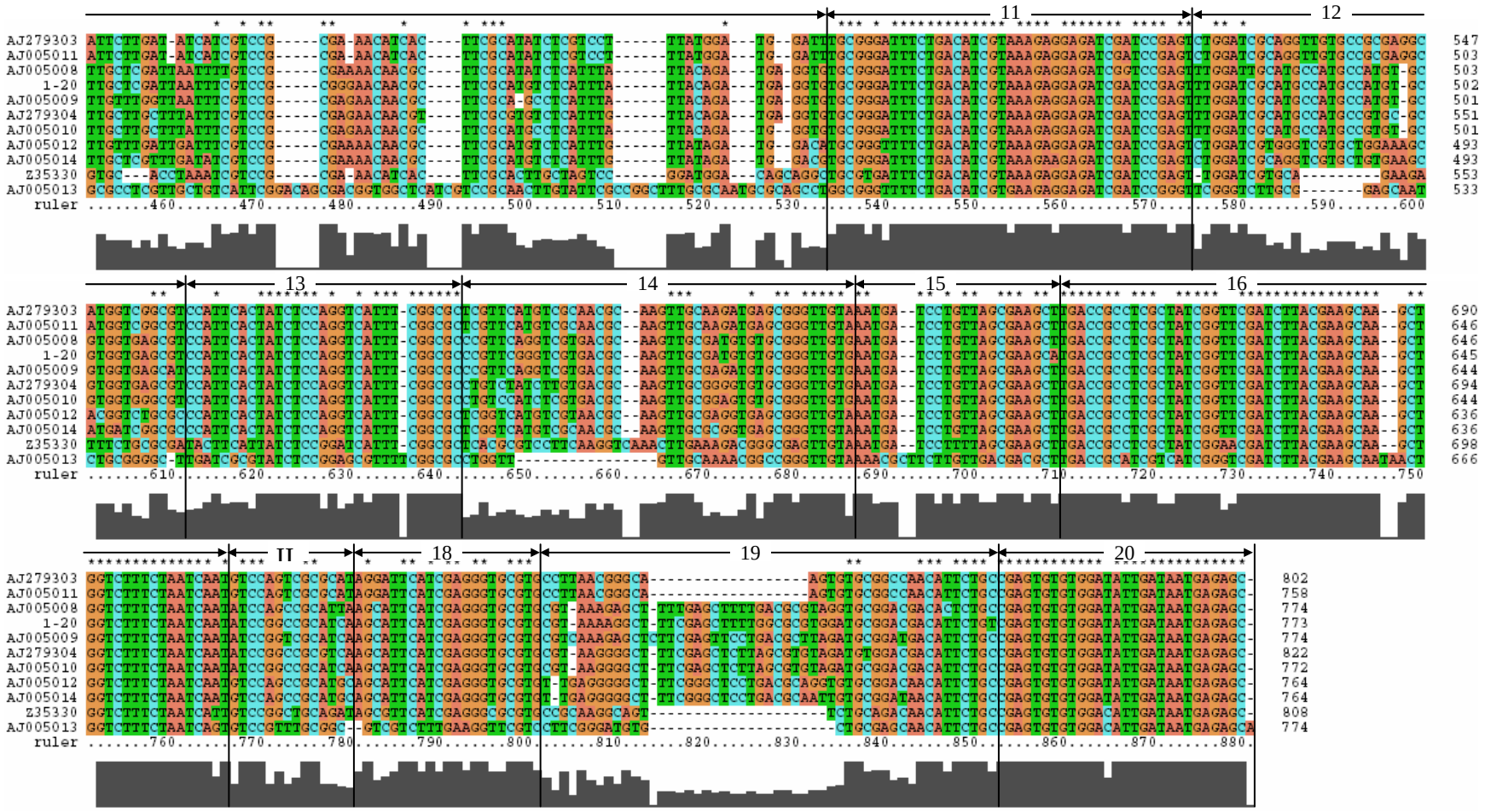


Figure A-3 Continued.

Table A-4 Cloned *Nitrobacter hamburgensis* DNA sequences generated with the conserved bacterial primers 1055f and 23Sr (clone library 2). The clones are distinguished with numbers in the "ID" column. Column "P" indicates if the sequence is complete (C) or was partially generated using 23Sr (1).

ID	P	FASTA formatted sequence (5′ → 3′ sense strand)
2-1	C	1 ATGGCTGTCGTCAGCTCGTGTCGTGAGATGTTGGGTTAAGTCCCGCAACGAGCGCAACCC 61 CCGTCCTTAGTTGCTACCATTTAGTTGAGCACTCTAAGGAGACTGCCGGTGATAAGCCGC 121 GAGGAAGGTGGGGATGACGTCAAGTCCTCATGGCCCTTACGGGCTGGGCTACACACGTGC 181 TACAATGGCGGTGACAATGGGAAGCAAAGGGGCAACCCCTAGCAAATCTCAAAAAACCGT 241 CTCAGTTCGGATTGGGCTCTGCAACTCGAGCCCATGAAGTTGGAATCGCTAGTAATCGTG 301 GATCAGCATGCCACGGTGAATACGTTCCCGGGCCTTGTACACACCGCCCGTCACACCATG 361 GGAGTTGGTTTTACCTGAAGGCGGTGCGCTAACCCGCAAGGGAGGCAGCCGACCACGGTA 421 GGGTCAGCGACTGGGGTGAAGTCGTAACAAGGTAGCCGTAGGGGAACCTGCGGCTGGATC 481 ACCTCCTTTCTAAGGATGGTTCTTCAAGAGCTTGCTCTTATCGAACCTCTTCAGAAACAT 541 CAGTGGCCAACGATCGTCAGGACCGTTGAGCTGCATTGGCGGGATTTCGCCGTCTTCGTT 601 TCTCTTTCTTCGCGGACGAACACGCGCCAGGGGCGGCGCTTGTGCTCATGTATCCGGTTT 661 GAGCCGGCGGAGCGCGCTGTCCCTAGTCGTAAGGGGCTTGTAGCTCAGTTGGTTAGAGCG 721 CGCGCTTGATAAGCGTGAGGTCAGAAGTTCAAGTCTTCCCAGGCCCACCACTTAATCGAG 781 CGCAGCATTCGTCTTCTGGTACGGGGCCATAGCTCAGCTGGGAGAGCGCGTGCTTTGCAA 841 GCATGAGGTCGTCGGTTCGATCCCGTCTGGCTCCACCAGATGGTTCGATTGATCGGGGCT 901 GCTTGCAAATTCTTGATATCATCGTCCGCGAAACATCACTTCGCATATCTCGTCCTTTAT 961 GGATGGATTTGCGGGATTTCTGACATCGTAAAGAGGAGATCGATCCGAGTCTGGATCGCA 1021 GGTTGTGCCGCTCCACCAGATGGTTCGATTGATCGGGGCTGCTTGCAAATTCTTGATATC 1081 ATCGTCCGCGAAACATCACTTCGCATATCTCGTCCTTTATGGATGGATTTGCGGGATTTC 1141 TGACATCGTAAAGAGGAGATCGATCCGAGTCTGGATCGCAGGTTGTGCCGCGAGGCATGG 1201 TCGGCGTCCATTCACTATCTCCAGGTCATTTCGGCGCTCGTTCATGTCGCAACGCAAGTT 1261 GCAAGATGAGCGGGTTGTAAATGATCCTGTTAGCGAAGCTTGACCGCCTCGCTATCGGTT 1321 CGATCTTACGAAGCAAGCTGGTCTTTCTAATCAATGTCCAGTCGCGCATAGGATTCATCG 1381 AGGGTGCGTGCCTTAACGGGCAAGTGTGCGGCCAACATTCTGCCGAGTGTGTGGATATTG 1441 ATAATGAGAGCAATCAAGTGCCTTAAGGGTGTTCGGTGGATGCCTTGGCGCTGAGAGGCG 1501 ATGAAGGACGTACTACGCTGCGATAAGCCGTGGGGAGCTGCGAAGAAGCTTTGATCCACG 1561 GATTTCCGAATGGGGCAACCC
2-2	1	1 AAGCATGAGGTCGTCGGTTCGATCCCGTCTGGCTCCACCAGATGGTTCGATTGATCGGGG 61 CTGCTTGCAAATTCTTGATATCATCGTCCGCGAAACATCACTTCGCATATCTCGTCCTTT 121 ATGGATGGATTTGCGGGATTTCTGACATCGTAAAGAGGAGATCGATCCGAGTCTGGATCG 181 CAGGTTGTGCCGCGAGGCATGGTCGGCGTCCATTCACTATCTCCAGGTCATTTCGGCGCT 241 CGTTCATGTCGCAACGCAAGTTGCAAGATGAGCGGGTTGTAAATGATCCTGTTAGCGAAG 301 CTTGACCGCCTCGCTATCGGTTCGATCTTACGAAGCAAGCTGGTCTTTCTAATCAATGTC 361 CAGTCGCGCATAGGATTCATCGAGGGTGCGTGCCTTAACGGGCAAGTGTGCGGCCAACAT 421 TCTGCCGAGTGTGTGGATATTGATAATGAGAGCAATCAAGTGCCTTAAGGGTGTTCGGTG 481 GATGCCTTGGCGCTGAGAGGCGATGAAGGACGTACTACGCTGCGATAAGCCGTGGGGAGC 541 TGCGAAGAAG
2-3	1	1 AAGCATGAGGTCGTCGGTTCGATCCCGTCTGGCTCCACCAGATGGTTCGATTGATCGGGG 61 CTGCTTGCAAATTCTTGATATCATCGTCCGCGAAACATCACTTCGCATATCTCGTCCTTT 121 ATGGATGGATTTGCGGGATTTCTGACATCGTAAAGAGGAGATCGATCCGAGTCTGGATCG 181 CAGGTTGTGCCGCGAGGCATGGTCGGCGTCCATTCACTATCTCCAGGTCATTTCGGCGCT 241 CGTTCATGTCGCAACGCTAGTTGCAAGATGAGCGGGTTGTAAATGATCCTGTTAGCGAAG 301 CTTGACCGCCTCGCTATCGGTTCGATCTTACGAAGCAAGCTGGTCTTTCTAATCAATGTC 361 CAGTCGCGCATAGGATTCATCGAGGGTGCGTGCCTTAACGGGCAAGTGTGCGGCCAACAT 421 TCTGCCGAGTGTGTGGATATTGATAATGAGAGCAATCAAGTGCCTTAAGGGTGTTCGGTG 481 GATGCCTTGGCGCTGAGAGGCGATGAAGGACGTACTACGCTGCGATAAGCCGTGGGGAGC 541 TGCGAAGAAG
2-4	1	1 AAGCATGAGGTCGTCGGTTCGATCCCGTCTGGCTCCACCAGATGGTTCGATTGATCGGGG 61 CTGCTTGCAAATTCTTGATATCATCGTCCGCGAAACATCACTTCGCATATCTCGTCCTTT 121 ATGGATGGATTTGCGGGATTTCTGACATCGTAAAGAGGAGATCGATCCGAGTCTGGATCG 181 CAGGTTGTGCCGCGAGGCATGGTCGGCGTCCATTCACTATCTCCAGGTCATTTCGGCGCT 241 CGTTCATGTCGCAACGCAAGTTGCAAGATGAGCGGGTTGTAAATGATCCTGTTAGCGAAG 301 CTTGACCGCCTCGCTATCGGTTCGATCTTACGAAGCAAGCTGGTCTTTCTAATCAATGTC 361 CAGTCGCGCATAGGATTCATCGAGGGTGCGTGCCTTAACGGGCAAGTGTGCGGCCAACAT 421 TCTGCCGAGTGTGTGGATATTGATAATGAGAGCAATCAAGTGCCTTAAGGGTGTTCGGTG 481 GATGCCTTGGCGCTGAGAGGCGATGAAGGACGTACTACGCTGCGATAAGCCGTGGGGAGC 541 TGCGAAGAAG

Table A-4 Continued.

ID	P	FASTA formatted sequence (5′ → 3′ sense strand)
2-5	1	1 AAGCATGAGGTCGTCGGTTCGATCCCGTCTGGCTCCACCAGATGGTTCGATTGATCGGGG 61 CTGCTTGCAAATTCTTGATATCATCGTCCGCGAAACATCACTTCGCATATCTCGTCCTTT 121 ATGGATGGATTTGCGGGATTTCTGACATCGTAAAGAGGAGATCGATCCGAGTCTGGATCG 181 CAGGTTGTGCCGCGAGGCATGGTCGGCGTCCATTCACTATCTCCAGGTCGTTTCGGCGCT 241 CGTTCATGTCGCAACGCAAGTTGCAAGATGAGCGGGTTGTAAATGATCCTGTTAGCGAAG 301 CTTGACCGCCTCGCTATCGGTTCGATCTTACGAAGCAAGCTGGTCTTTCTAATCAATGTC 361 CAGTCGCGCATAGGATTCATCGAGGGTGCGTGCCTTAACGGGCAAGTGTGCGGCCAACAT 421 TCTGCCGAGTGTGTGGATATTGATAATGAGAGCAATCAAGTGCCTTAAGGGTGTTCGGTG 481 GATGCCTTGGCGCTGAGAGGCGATGAAGGACGTACTACGCTGCGATAAGCCGTGGGGAGC 541 TGCGAAGAAG
2-6	1	1 AAGCATGAGGTCGTCGGTTCGATCCCGTCTGGCTCCACCAGATGGTTCGATTGATCGGGG 61 CTGCTTGCAAATTCTTGATATCATCGTCCGCGAAACATCACTTCGCATATCTCGTCCTTT 121 ATGGATGGATTTGCGGGATTTCTGACATCGTAAAGAGGAGATCGATCCGAGTCTGGATCG 181 CAGGTTGTGCCGCGAGGCATGGTCGGCGTCCATTCACTATCTCCAGGTCATTTCGGCGCT 241 CGTTCATGTCGCAACGCAAGTTGCAAGATGAGCGGGTTGTAAATGATCCTGTTAGCGAAG 301 CTTGACCGCCTCGCTATCGGTTCGATCTTACGAAGCAAGCTGGTCTTTCTAATCAATGTC 361 CAGTCGCGCATAGGATTCATCGAGGGTGCGTGCCTTAACGGGCAAGTGTGCGGCCAACAT 421 TCTGCCGAGTGTGTGGATATTGATAATGAGAGCAATCAAGTGCCTTAAGGGTGTTCGGTG 481 GATGCCTTGGCGCTGAGAGGCGATGAAGGACGTACTACGCTGCGATAAGCCGTGGGGAGC 541 TGCGAAGAAG
2-7	1	1 AAGCATGAGGTCGTCGGTTCGATCCCGTCTGGCTCCACCAGATGGTTCGATTGATCGGGG 61 CTGCTTGCAAATTCTTGATATCATCGTCCGCGAAACATCACTTCGCATATCTCGTCCTTT 121 ATGGATGGATTTGCGGGACTTCTGACATCGTAAAGAGGAGATCGATCCGAGTCTGGATCG 181 CAGGTTGTGCCGCGAGGCATGGTCGGCGTCCATTCACTATCTCCAGGTCATTTCGGCGCT 241 CGTTCATGTCGCAACGCAAGTTGCAAGATGAGCGGGTTGTAAATGATCCTGTTAGCGAAG 301 CTTGACCGCCTCGCTATCGGTTCGATCTTACGAAGCAAGCTGGTCTTTCTAATCAATGTC 361 CAGTCGCGCATAGGATTCATCGAGGGTGCGTGCCTTAACGGGCAAGTGTGCGGCCAACAT 421 TCTGCCGAGTGTGTGGATATTGATAATGAGAGCAATCAAGTGCCTTAAGGGTGTTCGGTG 481 GATGCCTTGGCGCTGAGAGGCGATGAAGGACGTACTACGCTGCGATAAGCCGTGGGGAGC 541 TGCGAAGAAG
2-8	1	1 AAGCATGAGGTCGTCGGTTCGATCCCGTCTGGCTCCACCAGATGGTTCGATTGATCGGGG 61 CTGCTTGCAAATTCTTGATATCATCGTCCGCGAAACATCACTTCGCATATCTCGTCCTTT 121 ATGGATGGATTTGCGGGATTTCTGACATCGTAAAGAGGAGATCGATCCGAGTCTGGATCG 181 CAGGTTGTGCCGCGAGGCATGGTCGGCGTCCATTCACTATCTCCAGGTCATTTCGGCGCT 241 CGTTCATGTCGCAACGCAAGTTGCAAGATGAGCGGGTTGTAAATGATCCTGTTAGCGAAG 301 CTTGACCGCCTCGCTATCGGTTCGATCTTACGAAGCAAGCTGGTCTTTCTAATCAATGTC 361 CAGTCGCGCATAGGATTCATCGAGGGTGCGTGCCTTAACGGGCAAGTGTGCGGCCAACAT 421 TCTGCCGAGTGTGTGGATATTGATAATGAGAGCAATCAAGTGCCTTAAGGGTGTTCGGTG 481 GATGCCTTGGCGCTGAGAGGCGATGAAGGACGTACTACGCTGCGATAAGCCGTGGGGAGC 541 TGCGAAGAAG
2-9	1	1 AAGCATGAGGTCGTCGGTTCGATCCCGTCTGGCTCCACCAGATGGTTCGATTGATCGGGG 61 CTGCTTGCAAATTCTTGATATCATCGTCCGCGAAACATCACTTCGCATATCTCGTCCTTT 121 ATGGATGGATTTGCGGGATTTCTGACATCGTAAAGAGGAGATCGATCCGAGTCTGGATCG 181 CAGGTTGTGCCGCGAGGCATGGTCGGCGTCCATTCACTATCTCCAGGTCATTTCGGCGCT 241 CGTTCATGTCGCAACGCAAGTTGCAAGATGAGCGGGTTGTAAATGATCCTGTTAGCGAAG 301 CTTGACCGCCTCGCTATCGGTTCGATCTTACGAAGCAAGCTGGTCTTTCTAATCAATGTC 361 CAGTCGCGCATAGGATTCATCGAGGGTGCGTGCCTTAACGGGCAAGTGTGCGGCCAACAT 421 TCTGCCGAGTGTGTGGATATTGATAATGAGAGCAATCAAGTGCCTTAAGGGTGTTCGGTG 481 GATGCCTTGGCGCTGAGAGGCGATGAAGGACGTACTACGCTGCGATAAGCCGTGGGGAGC 541 TGCGAAGAAG
2-10	1	1 AAGCATGAGGTCGTCGGTTCGATCCCGTCTGGCTCCACCAGATGGTTCGATTGATCGGGG 61 CTGCTTGCAAATTCTTGATATCATCGTCCGCGAAACATCACTTCGCATATCTCGTCCTTT 121 ATGGATGGATTTGCGGGATTTCTGACATCGTAAAGAGGAGATCGATCCGAGTCCGGATCG 181 CAGGTTGTGCCGCGAGGCATGGTCGGCGTCCATTCACTATCTCCAGGTCATTTCGGCGCT 241 CGTTCATGTCGCAACGCAAGTTGCAAGATGAGCGGGTTGTAAATGATCCTGTTAGCGAAG 301 CTTGACCGCCTCGCTATCGGTTCGATCTTACGAAGCAAGCTGGTCTTTCTAATCAATGTC 361 CAGTCGCGCATAGGATTCATCGAGGGTGCGTGCCTTAACGGGCAAGTGTGCGGCCAACAT 421 TCTGCCGAGTGTGTGGATATTGATAATGAGAGCAATCAAGTGCCTTAAGGGTGTTCGGTG 481 GATGCCTTGGCGCTGAGAGGCGATGAAGGACGTACTACGCTGCGATAAGCCGTGGGGAGC 541 TGCGAAGAAG

Table A-5 A melting temperature analysis for potential forward and reverse primers from regions 13 and 16, respectively, of the *Nitrobacter* 16S - 23S ISR (Figure A-3). The primers chosen for a *Nitrobacter* specific quantitative PCR detection system are underlined.

Primer Description				Melting Temperature (°C)[3]									
Delineation[1]	Sequence[2] (length base pairs)			1 mMMg^{+2}		2 mMMg^{+2}		3 mMMg^{+2}		4 mMMg^{+2}		5 mMMg^{+2}	
				DNA DNA	RNA DNA	DNA DNA	RNA DNA	DNA DNA	RNA DNA	DNA DNA	RNA DNA	DNA DNA	RNA DNA
NITISRf 514 532	CCATTCACTATCTCCAGGT		(19)	55.0	-	56.9	-	58.0	-	58.9	-	59.6	-
NITISRf 514 533	CCATTCACTATCTCCAGGTC		(20)	57.0	-	58.8	-	60.0	-	60.9	-	61.5	-
NITISRr 630 647	CCAGCTTGCTTCGTAAGA		(18)	55.7	52.9	57.5	54.8	58.7	56.0	59.6	56.8	60.2	57.5
NITISRr 630 648	ACCAGCTTGCTTCGTAAGA		(19)	57.5	54.0	59.4	55.9	60.5	57.0	61.4	57.9	62.1	58.6
NITISRr 631 648	ACCAGCTTGCTTCGTAAG		(18)	55.6	52.1	57.5	54.0	58.7	55.2	59.5	56.0	60.2	56.7
NITISRr 631 649	GACCAGCTTGCTTCGTAAG		(19)	57.5	54.0	59.4	55.9	60.5	57.0	61.4	57.9	62.1	58.6
NITISRr 632 649	GACCAGCTTGCTTCGTAA		(18)	56.0	53.3	57.9	55.2	59.1	56.3	59.9	57.2	60.6	57.9
NITISRr 632 650	AGACCAGCTTGCTTCGTAA		(19)	57.5	54.0	59.4	55.9	60.5	57.0	61.4	57.9	61.1	58.6
NITISRr 632 651	AAGACCAGCTTGCTTCGTAA		(20)	58.2	52.3	60.0	54.1	61.2	55.3	62.1	56.2	62.7	56.8
NITISRr 633 650	AGACCAGCTTGCTTCGTA		(18)	56.7	56.0	58.6	57.9	59.7	59.1	60.6	59.9	61.3	60.6
NITISRr 633 651	AAGACCAGCTTGCTTCGTA		(19)	57.5	54.0	59.4	55.9	60.5	57.0	61.4	57.9	62.1	59.6
NITISRr 633 652	AAAGACCAGCTTGCTTCGTA		(20)	58.2	52.3	60.0	54.1	61.2	55.3	62.1	56.2	62.7	56.8
NITISRr 634 650	AGACCAGCTTGCTTCGT		(17)	56.8	56.3	58.0	58.2	59.8	59.4	60.7	60.2	61.4	60.9
NITISRr 634 651	AAGACCAGCTTGCTTCGT		(18)	57.6	54.2	59.5	56.1	60.6	57.2	61.5	58.1	62.2	58.8
NITISRr 634 652	AAAGACCAGCTTGCTTCGT		(19)	58.3	52.4	60.2	54.2	61.4	55.4	62.2	56.3	62.9	56.9

Table A-5 Continued.

Primer Description			Melting Temperature (°C)[3]									
Delineation[1]	Sequence[2] (length base pairs)		1 mM Mg^{+2}		2 mM Mg^{+2}		3 mM Mg^{+2}		4 mM Mg^{+2}		5 mM Mg^{+2}	
			DNA DNA	RNA DNA	DNA DNA	RNA DNA	DNA DNA	RNA DNA	DNA DNA	RNA DNA	DNA DNA	RNA DNA
NITISRr 635 651	AAGACCAGCTTGCTTCG	(17)	55.7	50.2	57.6	52.0	58.7	53.2	59.6	54.1	60.3	54.7
NITISRr 635 652	AAAGACCAGCTTGCTTCG	(18)	56.6	48.6	58.4	50.5	59.6	51.6	60.5	52.5	61.1	53.2
NITISRr 635 653	GAAAGACCAGCTTGCTTCG	(19)	58.4	50.5	60.3	52.4	61.4	53.6	62.3	54.4	63.0	55.1
NITISRr 636 654	AGAAAGACCAGCTTGCTTC	(19)	56.5	50.4	58.4	52.2	59.5	53.4	60.4	54.2	61.1	54.9
NITISRr 636 655	TAGAAAGACCAGCTTGCTTC	(20)	56.4	50.4	58.3	52.2	59.5	53.4	60.3	54.3	61.0	54.9
NITISRr 636 656	TTAGAAAGACCAGCTTGCTTC	(21)	57.2	51.2	59.0	53.1	60.2	54.3	61.1	55.1	61.7	55.8
NITISRr 636 657	ATTAGAAAGACCAGCTTGCTTC	(22)	57.3	51.7	59.1	53.6	60.3	54.7	61.2	55.6	61.8	56.3
NITISRr 637 657	TTAGAAAGACCAGCTTGCTT	(21)	55.4	49.3	57.3	51.2	58.5	52.3	59.3	53.2	60.0	53.9
NITISRr 637 658	GATTAGAAAGACCAGCTTGCTTC	(22)	57.3	51.6	59.1	53.4	60.3	54.6	61.2	55.5	61.8	56.0
NITISRr 638 657	GATTAGAAAGACCAGCTTGCT	(20)	57.6	50.8	58.5	52.6	59.6	53.8	60.5	54.7	61.2	55.3
NITISRr 639 659	TGATTAGAAAGACCAGCTTGC	(21)	57.7	49.8	59.6	51.6	60.7	52.8	61.6	53.7	62.3	54.3
NITISRr 639 660	TTGATTAGAAAGACCAGCTTGC	(22)	57.7	49.8	59.6	51.6	60.7	52.8	61.6	53.7	62.3	54.3
NITISRr 639 661	ATTGATTAGAAAGACCAGCTTGC	(23)	57.8	50.3	59.7	52.1	60.8	53.3	61.7	52.2	62.4	54.8

1 The delineation is given to distinguish particular sequences: *NIT*robacter Intergenic Spacer Region forward/reverse primer, followed by numbers that designate the initial and final base pair numbers within the clone 1-20 sequence underlined in Table A-1 (base pair 1 = the first base pair within the ISR, following the 3′ end of the 16S gene).

2 The forward primer is listed as the 5′ to 3′ *Nitrobacter* rDNA sense strand sequence; the reverse primer is listed as the 5′ to 3′ antisense sequence.

3 The melting temperature was evaluated at the indicated Mg^{2+} concentration at Na^{+} = 50 mM (Oligonucleotide Analyzer: http://www.rnature.com/oligonucleotide.html).

Table A-6 The results of a secondary structure and specificity analysis of primers from regions 13 and 16 of the *Nitrobacter* 16S - 23S ISR (Figure A-3). The potential for stable secondary structures was investigated with two calculators at 37°C and 60°C. *Nitrobacter* specificity was analyzed with a GenBank® search (Altschule et al., 1997). The primers chosen for a *Nitrobacter* specific quantitative PCR detection system are underlined.

Primer[1]	Oligonucleotide Analyzer[2]		MFOLD 3.1[3]			BLASTn search results for GenBank® matches[4]	
	Hairpin	Self-Dimer	N	ΔG	T_m	Accession Number	Description
NITISRf 514 532	-1.36	-2.22	8	2.2	-17.2	None	-
NITISRf 514 533	-1.36	-2.22	8	2.2	-17.2	None	-
NITISRr 630 647	-1.68	-3.99	4	0.5	47.5	Many	α-Proteobacteria
				0.7	42.9		
				0.8	40.1		
NITISRr 630 648	-1.68	-3.99	4	0.5	47.5	Many	α-Proteobacteria
				0.7	42.9		
				0.8	40.1		
NITISRr 631 648	-1.68	-3.99	1	0.8	40.1	Many	α-Proteobacteria
NITISRr 631 649	-1.68	-3.99	1	0.8	40.1	Many	α-Proteobacteria
NITISRr 632 649	-0.96	-3.99	1	0.8	40.1	Many	α-Proteobacteria
NITISRr 632 650	-0.96	-3.99	1	0.8	40.1	Many	α-Proteobacteria
NITISRr 632 651	-1.68	-3.99	3	0.8	40.1	Many	α-Proteobacteria
NITISRr 633 650	-0.96	-3.99	1	0.8	40.1	Many	α-Proteobacteria
NITISRr 633 651	-1.68	-3.99	3	0.8	40.1	Many	α-Proteobacteria
NITISRr 633 652	-1.68	-3.99	2	0.8	40.1	Many	α-Proteobacteria

Table A-6 Continued.

Primer[1]	Oligonucleotide Analyzer[2]		MFOLD 3.1[3]			BLASTn search results for GenBank® matches[4]	
	Hairpin	Self-Dimer	N	ΔG	T_m	Accession Number	Description
NITISRr 634 650	-0.96	-3.99	1	0.8	40.1	Many	α-Proteobacteria
NITISRr 634 651	-1.68	-3.99	3	0.8	40.1	Many	α-Proteobacteria
NITISRr 634 652	-1.68	-3.99	2	0.8	40.1	Many	α-Proteobacteria
NITISRr 635 651	-1.68	-3.99	3	0.8	40.1	Many	α-Proteobacteria
NITISRr 635 652	-1.98	-3.99	2	0.8	40.1	Many	α-Proteobacteria
NITISRr 635 653	-1.98	-3.99	2	0.8	40.1	Many	α-Proteobacteria
NITISRr 636 654	-1.98	-3.99	3	0.8	40.1	Many	α-Proteobacteria
NITISRr 636 655	-1.98	-3.99	3	0.8	40.1	Many	α-Proteobacteria
NITISRr 636 656	-1.98	-3.99	3	0.8	40.1	Many	α-Proteobacteria
NITISRr 636 657	-1.98	-3.99	3	0.8	40.1	Many	α-Proteobacteria
NITISRr 637 657	-1.78	-3.99	3	0.8	40.1	Many	α-Proteobacteria
NITISRr 637 658	-1.78	-3.99	3	0.8	40.1	Many	α-Proteobacteria
NITISRr 638 657	-1.78	-3.99	3	1.1	41.3	Many	α-Proteobacteria
NITISRr 639 659	-0.91	-3.99	1	1.1	41.3	Many	α-Proteobacteria
NITISRr 639 660	-0.91	-3.99	1	1.1	41.3	AF338161	Bradyrhizobium sp. USDA 4435
NITISRr 639 661	-0.91	-3.99	1	1.1	41.3	AF338161	Bradyrhizobium sp. USDA 4435

1 See Table A-5.

2 The free energy for formation (kcal/mol) of stable hairpins and dimers at 37°C (Oligonucleotide Analyzer: http://www.rnature.com/oligonucleotide.html).

3 The number of stable hairpin structures (N), free energy (ΔG) for their formation at 60°C (kcal/mol), and the hairpin melting temperature (Mfold Version 3.1) (Zucker, 2003: http://www.bioinfo.rpi.edu/applications/mfold).

4 The specificity of the primers was evaluated with BLASTn searches (Altschule et al., 1997) of GenBank®.

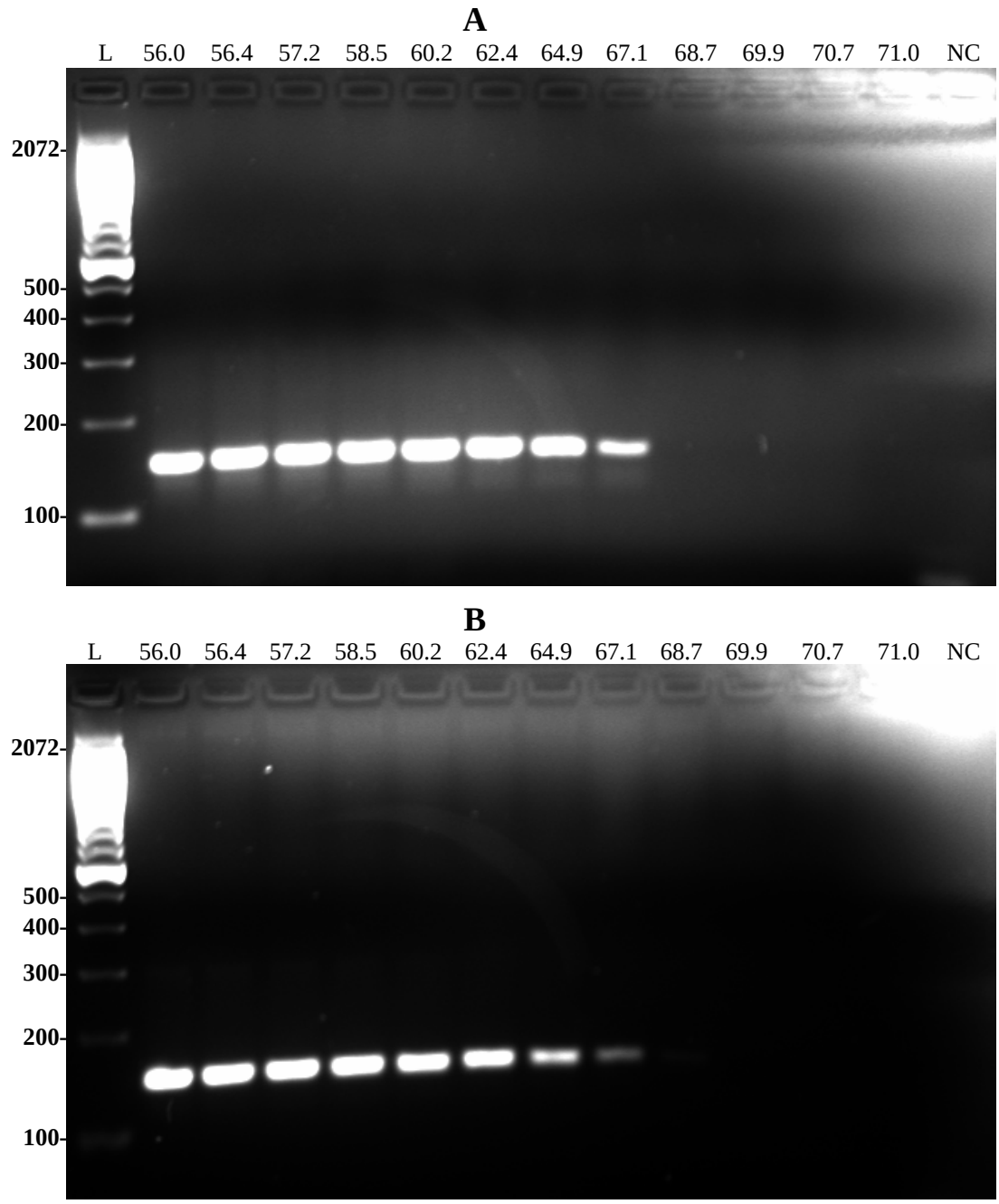


Figure A-4 Electrophoresis gel images of temperature gradient PCR products using *Nitrobacter* specific primers (Table A-5) and DNA extracts from either the BSNR mixed liquor (A) or a *N. hamburgensis* mixotrophic culture (B). Wells are labeled with the annealing temperature in °C for the PCR products. Well "L" contained a 100 bp ladder (Invitrogen; Carlsbad, CA); distinct and the largest bands are labeled. Well "NC" contained a negative control reaction.

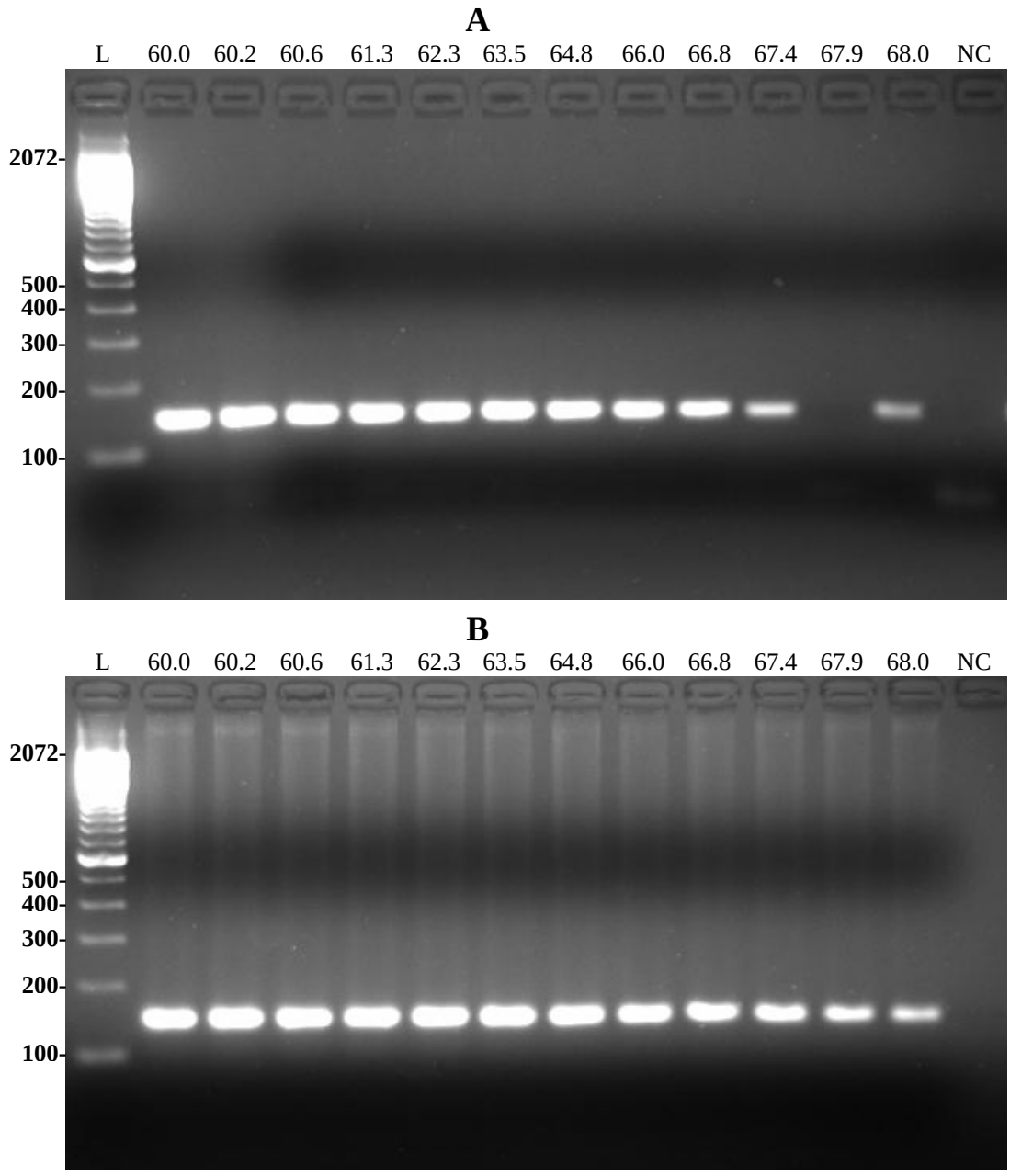


Figure A-5 Electrophoresis gel images of temperature gradient PCR products using *Nitrobacter* specific primers (Table A-5) and DNA extracts from either the BSNR mixed liquor (A) or a *N. hamburgensis* mixotrophic culture (B). Wells are labeled with the annealing temperature in °C for the PCR products. Well "L" contained a 100 bp ladder (Invitrogen, Carlsbad, CA); distinct and the largest bands are labeled. Well "NC" contained a negative control reaction.

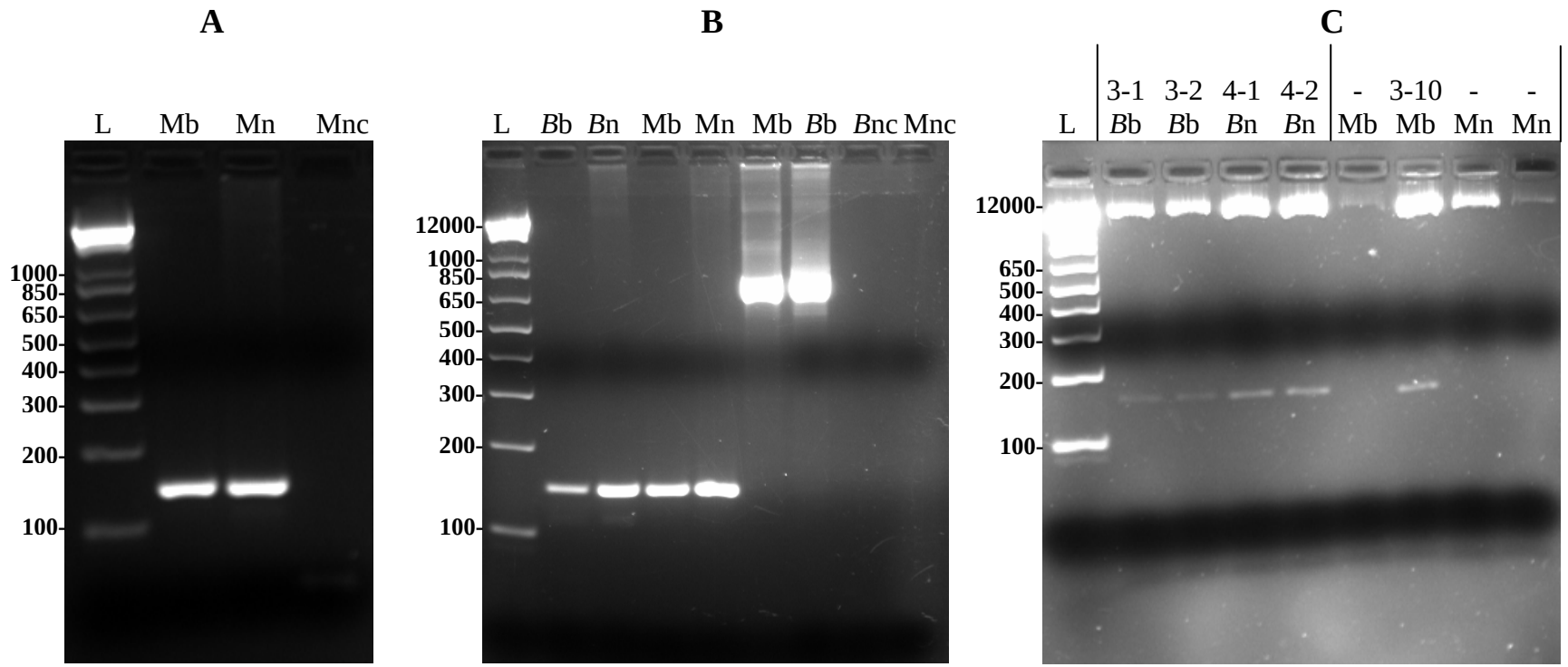


Figure A-6 Electrophoresis gel images documenting cloning of PCR products obtained with *Nitrobacter* specific primers (Table A-5) and either BSNR (b) or *N. hamburgensis* (n) DNA extracts. A. PCR products obtained at an annealing temperature of 62°C using Quantitect Probe PCR mastermix (M). A negative control reaction (Mnc) was performed. B. PCR products obtained at an annealing temperature of 62°C using M or PCR Ready-To-Go™ beads (*B*). A control reaction (c) generated single 750 bp amplicons with M and *B* PCR media. Negative control reactions (*B*nc and Mnc) were performed. C. The results for a restriction enzyme digest of cloned plasmids (library numbers provided) using the PCR reactions documented in gel images A and B with M or *B* PCR media. For all gels, well "L" contained a ladder; distinct and the largest bands are labeled.

Table A-7 Cloned BSNR DNA sequences generated with *Nitrobacter* specific primers (Table A-5) (clone library 3). The clones are distinguished with numbers in the "ID" column.

ID	FASTA formatted sequence (5′ → 3′ sense strand)
3-1	1 CCATTCACTATCTCCAGGTCATTTCGGCGCCCGTTCGGGTCGTGACGCAAGTTGCGATGT 61 GTGCGGGTTGTGAATGATCCTGTTAGCGAAGCATGACCGCCTCGCTACCGGTTCGATCTT 121 ACGAAGCAAGCTGGTCTTTCTAATCAA
3-2	1 CCATTCACTATCTCCAGGTCATTTCGGCGCCCGTTCAGGTCGTGACGCAAGTTGCGATGT 61 GTGCGGGTTGTGAATGATCCTGTTAGCGAAGCTTGACCGCCTCGCTATCGGTTCGATCTT 121 ACGAAGCAAGCTGGTCTTTCTAATCAA
3-3	1 CCATTCACTATCTCCAGGTCATTTCGGCGCCCGTTCGGGTCGTGACGCAAGTTGCGATGT 61 GTGCGGGTTGTGAACGATCCTGTTAGCGAAGCTTGACCGCCTCGCTATCGGTTCGATCTT 121 ACGAAGCAAGCTGGTCTTTCTAATCAA
3-4	1 CCATTCACTATCTCCAGGTCATTTCGGCGCCCGTTCAGGTCGTGACGCAAGTTGCGATGT 61 GTGCGGGTTGTGAATGATCCTGTTAGCGAAGCTTGACCGCCTCGCTATCGGTTCGATCTT 121 ACGAAGCAAGCTGGTCTTTCTAATCAA
3-5	1 CCATTCACTATCTCCAGGTCATTTCGGCGCCCGTTCAGGTCGTGACGCAAGTTGCGATGT 61 GTGCGGGTTGTGAATGATCCTGTTAGCGAAGCTTGACCGCCTCGCTATCGGTTCGATCTT 121 ACGAAGCAAGCTGGTCTTTCTAATCAA
3-6	1 CCATTCACTATCTCCAGGTCATTTCGGCGCCCGTTCAGGTCGTGACGCAAGTTGCGATGT 61 GTGCGGGTTGTGAATGATCCTGTTAGCGAAGCTTGACCGCCTCGCTATCGGTTCGATCTT 121 ACGAAGCAAGCTGGTCTTTCTAATCAA
3-7	1 CCATTCACTATCTCCAGGTCATTTCGGCGCCCGTTCGGGTCGTGACGCAAGTCGCGATGT 61 GTGCGGGTTGTGAATGATCCTGTTAGCGAAGCATGACCGCCTCGCTATCGGTTCGATCTT 121 ACGAAGCAAGCTGGTCTTTCTAATCAA
3-8	1 CCATTCACTATCTCCAGGTCATTTCGGCGCCTGTCCATCTCGTGACGCAAGTTGCGGAGT 61 GTGCGGGTTGTGAATGATCCTGTTAGCGAAGCTTGACCGCCTCGCTATCGGTTCGATCTT 121 ACGAAGCAAGCTGGTCTTTCTAATCA
3-9	1 CCATTCACTATCTCCAGGTCATTTCGGCGCCCGTTCNGGTCGTGACGCAAGTTGCGATGT 61 GTGCGGGTTGTGAATGATCCTGTTAGCGAAGCTTGACCGCCTCGCTATCGGTTCGATCTT 121 ACGAAGCAAGCTGGTCTTTCTAATCA
3-10	1 CCATTCACTATCTCCAGGTCATTTCGGCGCCCGTTCGGGTCGTGACGCAAGTTGCGATGT 61 GTGCGGGTTGTGAATGATCCTGTTAGCGAAGCATGACCGCCTCGCTATCGGTTCGATCTT 121 ACGAAGCAAGCTGGTCTTTCTAATCAA

Table A-8 Cloned *Nitrobacter hamburgensis* DNA sequences generated with *Nitrobacter* specific primers (Table A-5) (clone library 4). The clones are distinguished with numbers in the "ID" column.

ID	FASTA formatted sequence (5′ → 3′ sense strand)
4-1	1 CCATTCACTATCTCCAGGTCATTTCGGCGCTCGTTCATGTCGCAACGCAAGTTGCAAGAT 61 GAGCGGGTTGTAAATGATCCTGTTAGCGAAGCTTGACCGCCTCGCTATCGGTTCGATCTT 121 ACGAAGCAAGCTGGTCTTTCTAATCA
4-2	1 CCATTCACTATCTCCAGGTCATTTCGGCGCTCGTTCATGTCGCAACGCAAGTTGCAAGAT 61 GAGCGGGTTGTAAATGATCCTGTTAGCGAAGCTTGACCGCCTCGCTATCGGTTCGATCTT 121 ACGAAGCAAGCTGGTCTTTCTAATCA
4-3	1 CCATTCACTATCTCCAGGTCATTTCGGCGCTCGTTCATGTCGCAACGCAAGTTGCAAGAT 61 GAGCGGGTTGTAAATGATCCTGTTAGCGAAGCTTGACCGCCTCGCTATCGGTTCGATCTT 121 ACGAAGCAAGCTGGTCTTTCTAATCA
4-4	1 CCATTCACTATCTCCAGGTCATTTCGGCGCTCGTTCATGTCGCAACGCAAGTTGCAAGAT 61 GAGCGGGTTGTAAATGATCCTGTTAGCGAAGCTTGACCGCCTCGCTATCGGTTCGATCTT 121 ACGAAGCAAGCTGGTCTTTCTAATCA
4-5	1 CCATTCACTATCTCCAGGTCATTTCGGCGCTCGTTCATGTCGCAACGCAAGTTGCAAGAT 61 GAGCGGGTTGTAAATGATCCTGTTAGCGAAGCTTGACCGCCTCGCTATCGGTTCGATCTT 121 ACGAAGCAAGCTGGTCTTTCTAATCAA

Table A-9 A melting temperature analysis of potential real-time PCR antisense probe sequences within region 16 of the *Nitrobacter* 16S - 23S ISR (Figure A-3).

Probe				Melting Temperature (°C)[3]									
Delineation[1]	Description[2]			1 mMMg^{+2}		2 mMMg^{+2}		3 mMMg^{+2}		4 mMMg^{+2}		5 mMMg^{+2}	
	5′→3′ Antisense Sequence	L	D	DNA DNA	RNA DNA	DNA DNA	RNA DNA	DNA DNA	RNA DNA	DNA DNA	RNA DNA	DNA DNA	RNA DNA
NITISRp 607 627	GAACCG**A**TAGCGAGGCGGTCA	21	12	67.0	63.5	68.9	65.4	70.1	66.6	70.9	67.4	71.6	68.1
NITISRp 607 628	CGAACCG**A**TAGCGAGGCGGTCA	22	11	69.3	63.3	71.2	65.2	72.4	66.3	73.2	67.2	73.9	67.9
NITISRp 607 629	TCGAACCG**A**TAGCGAGGCGGTCA	23	10	70.3	64.3	72.2	66.2	73.4	67.3	74.2	68.2	74.9	68.9
NITISRp 607 630	ATCGAACCG**A**TAGCGAGGCGGTCA	24	9	69.9	66.2	71.8	66.1	73.0	67.2	73.8	68.1	74.5	68.8
NITISRp 607 631	GATCGAACCG**A**TAGCGAGGCGGTCA	25	8	70.8	65.4	72.7	67.3	73.9	68.4	74.7	69.3	75.4	70.0
NITISRp 607 632	AGATCGAACCG**A**TAGCGAGGCGGTCA	26	7	71.5	66.7	73.4	68.5	74.5	69.7	75.4	70.6	76.1	71.2
NITISRp 608 633	AAGATCGAACCG**A**TAGCGAGGCGGTCA	27	6	71.4	66.8	73.3	68.7	74.5	69.8	75.3	70.7	76.0	71.4
NITISRp 608 628	CGAACCG**A**TAGCGAGGCGGTC	21	11	68.2	63.5	70.0	65.4	71.2	66.5	72.0	67.4	72.7	68.1
NITISRp 608 629	TCGAACCG**A**TAGCGAGGCGGTC	22	10	69.2	64.5	71.1	66.4	77.3	67.6	73.1	68.4	73.8	69.1
NITISRp 608 630	ATCGAACCG**A**TAGCGAGGCGGTC	23	9	68.9	64.4	70.8	66.3	71.9	67.4	72.8	68.3	73.5	69.0
NITISRp 608 631	GATCGAACCG**A**TAGCGAGGCGGTC	24	8	69.8	65.7	71.7	67.5	72.9	68.7	73.7	69.6	74.4	70.2
NITISRp 608 632	AGATCGAACCG**A**TAGCGAGGCGGTC	25	7	70.5	67.0	72.4	68.8	73.6	70.0	74.4	70.9	75.1	71.5
NITISRp 608 633	AAGATCGAACCG**A**TAGCGAGGCGGTC	26	6	70.5	67.1	72.4	69.0	73.6	70.1	74.4	71.0	75.1	71.7
NITISRp 608 634	TAAGATCGAACCG**A**TAGCGAGGCGGTC	27	5	70.0	66.5	71.9	68.4	73.1	69.6	73.9	70.4	74.6	71.1
NITISRp 609 628	CGAACCG**A**TAGCGAGGCGGT	20	11	67.0	62.4	68.9	64.2	70.0	65.4	70.9	66.2	71.6	66.9
NITISRp 609 629	TCGAACCG**A**TAGCGAGGCGGT	21	10	68.2	63.5	70.0	65.4	71.2	66.5	72.0	67.4	72.7	68.1

Table A-9 Continued.

Probe				Melting Temperature (°C)[3]									
Delineation[1]	Description[2]			1 mMMg^{+2}		2 mMMg^{+2}		3 mMMg^{+2}		4 mMMg^{+2}		5 mMMg^{+2}	
	5′→3′ Antisense Sequence	L	D	DNA DNA	RNA DNA	DNA DNA	RNA DNA	DNA DNA	RNA DNA	DNA DNA	RNA DNA	DNA DNA	RNA DNA
NITISRp 609 630	ATCGAACCG**A**TAGCGAGGCGGT	22	9	67.8	63.4	69.7	65.3	70.9	66.4	71.7	67.3	72.4	68.0
NITISRp 609 631	GATCGAACCG**A**TAGCGAGGCGGT	23	8	68.8	64.7	70.8	66.6	71.9	67.8	72.8	68.6	73.5	69.3
NITISRp 609 632	AGATCGAACCG**A**TAGCGAGGCGGT	24	7	69.6	66.1	71.5	68.0	72.7	69.2	73.5	70.0	74.2	70.7
NITISRp 609 633	AAGATCGAACCG**A**TAGCGAGGCGGT	25	6	69.7	66.3	71.5	68.1	72.7	69.3	73.6	70.2	74.2	70.8
NITISRp 609 634	TAAGATCGAACCG**A**TAGCGAGGCGGT	26	5	69.2	65.7	71.1	67.6	72.2	68.8	73.1	69.6	73.8	70.3
NITISRp 609 635	GTAAGATCGAACCG**A**TAGCGAGGCGGT	27	4	69.9	66.0	71.8	67.9	73.0	69.1	73.8	70.0	74.5	70.6
NITISRp 610 629	TCGAACCG**A**TAGCGAGGCGG	20	10	67.1	63.0	69.0	64.9	70.1	66.0	71.0	67.0	71.7	67.6
NITISRp 610 630	ATCGAACCG**A**TAGCGAGGCGG	21	9	66.8	62.9	68.7	64.8	69.9	66.0	70.7	66.9	71.4	67.5
NITISRp 610 631	GATCGAACCG**A**TAGCGAGGCGG	22	8	68.0	64.3	69.8	66.2	71.0	67.4	71.8	68.2	72.5	68.9
NITISRp 610 632	AGATCGAACCG**A**TAGCGAGGCGG	23	7	68.8	65.8	70.6	67.7	71.8	68.8	72.7	69.7	73.3	70.4
NITISRp 610 633	AAGATCGAACCG**A**TAGCGAGGCGG	24	6	68.8	66	70.7	67.8	71.9	69.0	72.7	69.8	74.4	70.5
NITISRp 610 634	TAAGATCGAACCG**A**TAGCGAGGCGG	25	5	68.3	65.4	70.2	67.3	71.4	68.4	72.3	69.3	72.9	70.0
NITISRp 610 635	GTAAGATCGAACCG**A**TAGCGAGGCGG	26	4	69.2	65.7	71.1	67.6	72.2	68.8	73.1	69.6	73.8	70.3
NITISRp 610 636	CGTAAGATCGAACCG**A**TAGCGAGGCGG	27	3	71.0	65.4	72.8	67.2	74.0	68.4	74.9	69.3	75.5	69.9
NITISRp 611 632	AGATCGAACCG**A**TAGCGAGGCG	22	7	66.3	63	68.2	64.9	69.4	66.0	70.2	66.9	70.9	67.6
NITISRp 611 633	AAGATCGAACCG**A**TAGCGAGGCG	23	6	66.5	63.3	68.4	65.1	69.6	66.3	70.4	67.2	71.1	67.8
NITISRp 611 634	TAAGATCGAACCG**A**TAGCGAGGCG	24	5	66.1	62.8	68.0	64.7	69.1	65.8	70.0	66.7	70.7	67.4
NITISRp 611 635	GTAAGATCGAACCG**A**TAGCGAGGCG	25	4	67.0	63.2	68.9	65.1	70.1	66.3	70.9	67.1	71.6	67.8

Table A-9 Continued.

Probe				Melting Temperature (°C)[3]									
Delineation[1]	Description[2]			1 mMMg^{+2}		2 mMMg^{+2}		3 mMMg^{+2}		4 mMMg^{+2}		5 mMMg^{+2}	
	5′→3′ Antisense Sequence	L	D	DNA DNA	RNA DNA	DNA DNA	RNA DNA	DNA DNA	RNA DNA	DNA DNA	RNA DNA	DNA DNA	RNA DNA
NITISRp 611 636	CGTAAGATCGAACCG**A**TAGCGAGGCG	26	3	69.0	63.0	70.9	64.9	72.0	66.1	72.9	66.9	73.6	67.6
NITISRp 611 637	TCGTAAGATCGAACCG**A**TAGCGAGGCG	27	2	69.8	63.9	71.7	65.8	72.9	66.9	73.2	67.8	74.4	68.5
NITISRp 612 636	CGTAAGATCGAACCGAT**A**GCGAGGC	25	3	67.0	63.2	68.9	65.1	70.1	66.3	70.9	67.1	71.6	67.8
NITISRp 612 637	TCGTAAGATCGAACCGAT**A**GCGAGGC	26	2	68.0	64.1	69.9	66.0	71.0	67.2	71.9	68.0	72.6	68.7
NITISRp 612 638	TTCGTAAGATCGAACCGAT**A**GCGAGGC	27	1	68.1	62.4	70	64.2	71.1	65.4	72	66.3	73	66.9
NITISRp 613 637	TCGTAAGATCGAACCG**A**TAGCGAGG	25	2	66	61	67.9	62.9	69.1	64	69.9	64.9	70.6	66
NITISRp 613 637	TTCGTAAGATCGAACCG**A**TAGCGAGG	26	1	66.2	59.3	68.1	61.2	69.3	62.4	70.1	63.2	70.8	64

1 The delineation is given to distinguish particular probe sequences: *NITrobacter* Intergenic Spacer Region probe, followed by numbers that designate the initial and final base pair numbers within the clone 1-20 sequence underlined in Table A-1 (base pair 1 = the first base pair within the ISR, following the 3′ end of the 16S gene). A mismatching base with one of the BSNR clones (3-1: Table A-7) is shown in bold. Probe sequences with a 5′ G are emphasized with a double underline.

2 The probe is listed as the 5′ to 3′ *Nitrobacter* rDNA antisense sequence; L = probe length in base pairs; D = distance from reverse primer in base pairs.

3 The melting temperature was evaluated at the indicated Mg^{2+} concentration at Na^{+} = 50 mM (Oligonucleotide Analyzer: http://www.rnature.com/oligonucleotide.html).

Table A-10 A secondary structure and specificity analysis of potential real-time PCR antisense probe sequences (Table A-9). The potential for stable secondary structures was investigated with two T_m calculators at 37°C and 60°C. *Nitrobacter* specificity was analyzed with a GenBank® search (Altschule et al., 1997); exact database matches are listed for structurally sound probe sequences (hairpin T_m < 50°C).

Probe[1]	Oligonucleotide Analyzer[2]		MFOLD 3.1[3]			BLASTn search results for GenBank® matches[4]	
	Hairpin	Self-Dimer	N	ΔG	T_m	Accession Number	Description
NITISRp 607 628	-5.01	-5.01	1	-0.3	63.6	-	-
NITISRp 607 629	-5.01	-5.01	1	-0.3	63.6	-	-
NITISRp 607 630	-5.01	-5.01	1	-0.3	63.6	-	-
NITISRp 607 632	-5.01	-5.01	2	-0.3	63.6	-	-
				0.6	52.4		
NITISRp 607 633	-5.01	-5.01	2	-0.3	63.6	-	-
				0.6	52.4		
NITISRp 608 628	-5.01	-5.01	1	-0.3	63.6	-	-
NITISRp 608 629	-5.01	-5.01	1	-0.3	63.6	-	-
NITISRp 608 630	-5.01	-5.01	1	-0.3	63.6	-	-
NITISRp 608 632	-5.01	-5.01	2	-0.3	63.6	-	-
				0.6	52.4		
NITISRp 608 633	-5.01	-5.01	2	-0.3	63.6	-	-
				0.6	52.4		
NITISRp 608 634	-5.01	-5.01	2	-0.3	63.6	-	-
				0.6	52.4		
NITISRp 609 628	-5.01	-5.01	2	0.1	58.8	-	-
				0.9	46.0		
NITISRp 609 629	-5.01	-5.01	2	0.1	58.8	-	-
				0.9	46.0		

Table A-10 Continued.

Probe[1]	Oligonucleotide Analyzer[2]		MFOLD 3.1[3]			BLASTn search results for GenBank® matches[4]	
	Hairpin	Self-Dimer	N	ΔG	T_m	Accession Number	Description
NITISRp 609 630	-5.01	-5.01	2	0.1	58.8	-	-
				0.9	46.0		
NITISRp 609 632	-5.01	-5.01	3	0.1	58.8	-	-
				0.6	52.4		
				0.9	46.0		
NITISRp 609 633	-5.01	-5.01	3	0.1	58.8	-	-
				0.6	52.4		
				0.9	46.0		
NITISRp 609 634	-5.01	-5.01	3	0.1	58.8	-	-
				0.6	52.4		
				0.9	46.0		
NITISRp 610 629	-3.55	-3.55	5	0.9	46.0	AY187818; AF338160	*Bradyrhizobium* sp. Tv2a-2; *Bradyrhizobium* sp. USDA 4409
				1.0	48.6		
NITISRp 610 630	-3.55	-3.55	5	0.9	46.0	-	-
				1.0	48.6		
NITISRp 610 632	-3.55	-4.49	3	0.6	52.4	-	-
				0.9	46.0		
				1.0	48.6		
NITISRp 610 633	-3.55	-4.49	3	0.6	52.4	AY187818; AF338160	*Bradyrhizobium* sp. Tv2a-2; *Bradyrhizobium* sp. USDA 4409
				0.9	46.0		
				1.0	48.6		
NITISRp 610 634	-3.55	-4.49	3	0.6	52.4	AY187818; AF338160	*Bradyrhizobium* sp. Tv2a-2; *Bradyrhizobium* sp. USDA 4409
				0.9	46.0		
				1.0	48.6		

Table A-10 Continued.

Probe[1]	Oligonucleotide Analyzer[2]		MFOLD 3.1[3]			BLASTn search results for GenBank® matches[4]	
	Hairpin	Self-Dimer	N	ΔG	T_m	Accession Number	Description
NITISRp 610 636	-3.55	-4.49	3	0.6	52.4	AF338160	*Bradyrhizobium* sp. USDA 4409
				0.9	46.0		
				1.0	48.6		
NITISRp 611 632	-3.09	-4.49	2	0.6	52.4	AY187818; AF338160	*Bradyrhizobium* sp. Tv2a-2; *Bradyrhizobium* sp. USDA 4409
				0.9	46.0		
NITISRp 611 633	-3.09	-4.49	2	0.6	52.4	AY187818; AF338160	*Bradyrhizobium* sp. Tv2a-2; *Bradyrhizobium* sp. USDA 4409
				0.9	46.0		
NITISRp 611 634	-3.09	-4.49	2	0.6	52.4	AY187818; AF338160	*Bradyrhizobium* sp. Tv2a-2; *Bradyrhizobium* sp. USDA 4409
				0.9	46.0		
NITISRp 611 636	-3.09	-4.49	2	0.6	52.4	-	-
				0.9	46.0		
NITISRp 611 637	-3.09	-4.49	5	0.5	47.5	AY187818	*Bradyrhizobium* sp. Tv2a-2
				0.6	52.4		
				0.7	46.4		
				0.9	46.0		
NITISRp 612 636	-3.09	-4.49	2	0.6	52.4	AY187818	*Bradyrhizobium* sp. Tv2a-2
				0.9	46.0		
NITISRp 612 637	-3.09	-4.49	5	0.5	47.5	AY187818	*Bradyrhizobium* sp. Tv2a-2
				0.6	52.4		
				0.7	46.4		
				0.9	46.0		

Table A-10 Continued.

Probe[1]	Oligonucleotide Analyzer[2]		MFOLD 3.1[3]			BLASTn search results for GenBank® matches[4]	
	Hairpin	Self-Dimer	N	ΔG	T_m	Accession Number	Description
NITISRp 612 638	-4.17	-4.49	5	0.5	47.5	AY187818	*Bradyrhizobium* sp. Tv2a-2
				0.6	52.4		
				0.7	46.4		
				0.9	46.0		
NITISRp 613 637	-4.17	-4.49	5	0.5	47.5	AY187818	*Bradyrhizobium* sp. Tv2a-2
				0.6	52.4		
				0.7	46.4		
				0.9	46.0		
NITISRp 613 637	-3.09	-4.49	5	0.5	47.5	AY187818	*Bradyrhizobium* sp. Tv2a-2
				0.6	52.4		
				0.7	46.4		
				0.9	46.0		

1 See Table A-9. The probe sequence used in this study is underlined.

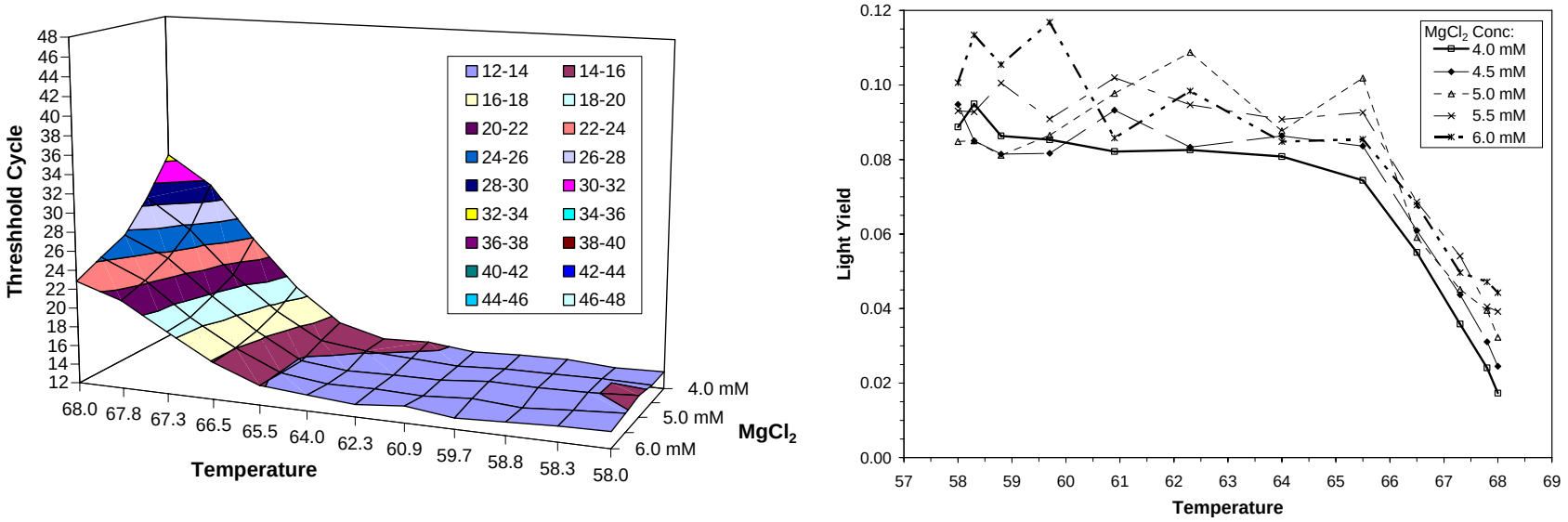
2 The free energy for formation (kcal/mol) of stable hairpins and self-dimers at 37°C (Oligonucleotide Analyzer: http://www.rnature.com/oligonucleotide.html).

3 The number of stable hairpin structures (N), free energy (ΔG) for formation at 60°C (kcal/mol), and the hairpin melting temperature (Mfold Version 3.1) (Zucker, 2003: http://www.bioinfo.rpi.edu/applications/mfold).

4 The specificity of the probe sequence was evaluated with BLASTn searches (Altschule et al., 1997) of GenBank®.

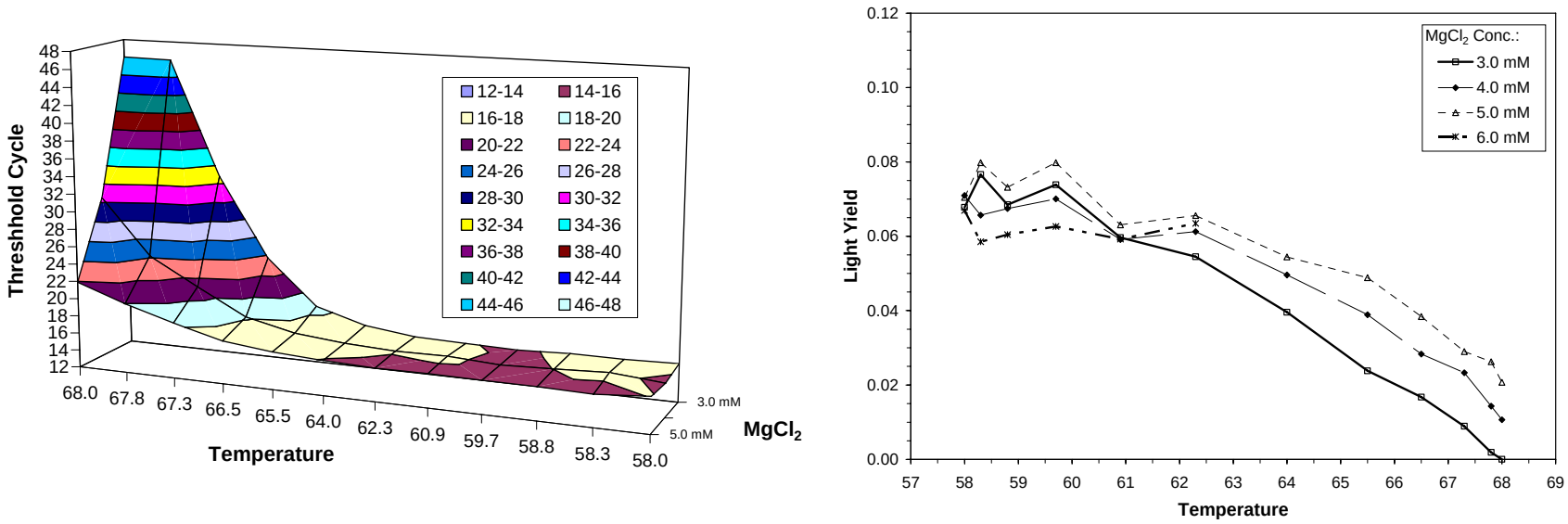
Appendix B

Quantitative PCR Optimization Data



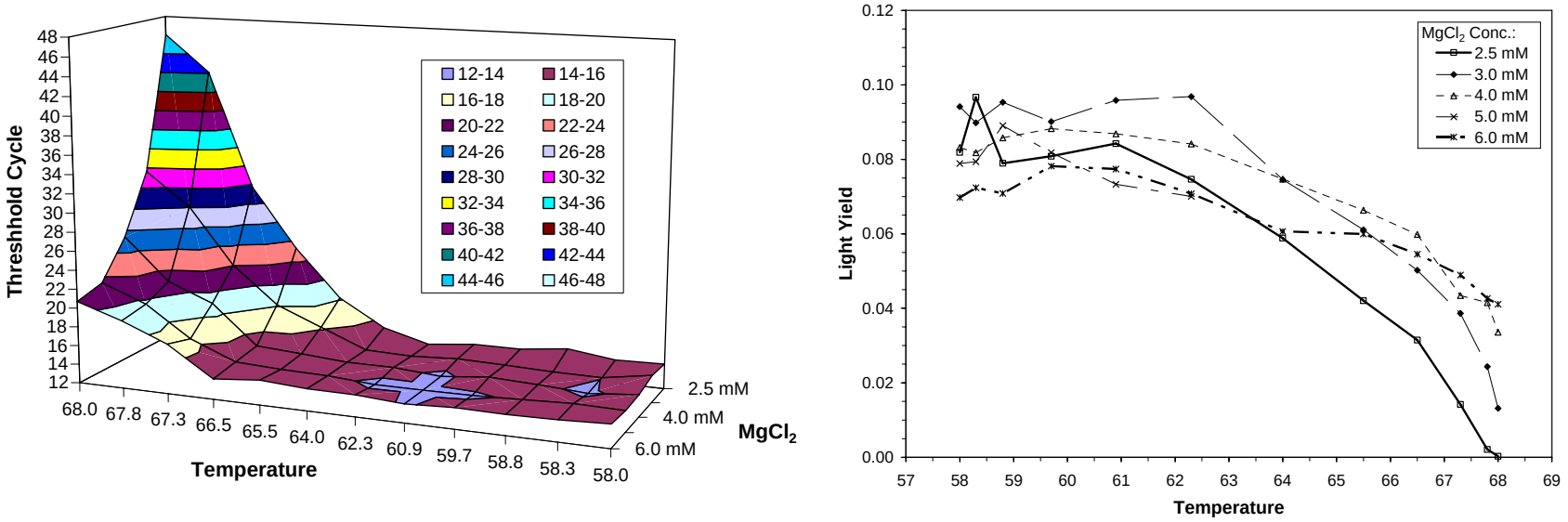
A **B**

Figure B-1 Threshold cycle (A) and light yield (B) versus annealing temperature/Mg^{2+} gradients for real-time PCR reactions using the *Nitrobacter* detection system with Quantitect® Probe PCR mastermix (Qiagen; Valencia, CA). Temperature protocol: 50°C for 2 minutes, 95°C *Taq* activation for 15 minutes, 45 cycles with 94°C melting for 15 seconds and an annealing/extension temperature gradient from 58 to 68°C for 1 minute. Reaction recipe (25 µl): 12.5 µl mastermix, 400 nM primers (1µl) , 150 nM probe (0.375 µl), $MgCl_2$ gradient (4 - 6 mM × 0.5 mM; 0 - 1.00 µl of a 20 µM stock), 0.2 µm fHPLC dilution water (to 20 µl volume), and 5 µl of a 10^6 copies/µl *Nitrobacter* rDNA standard.



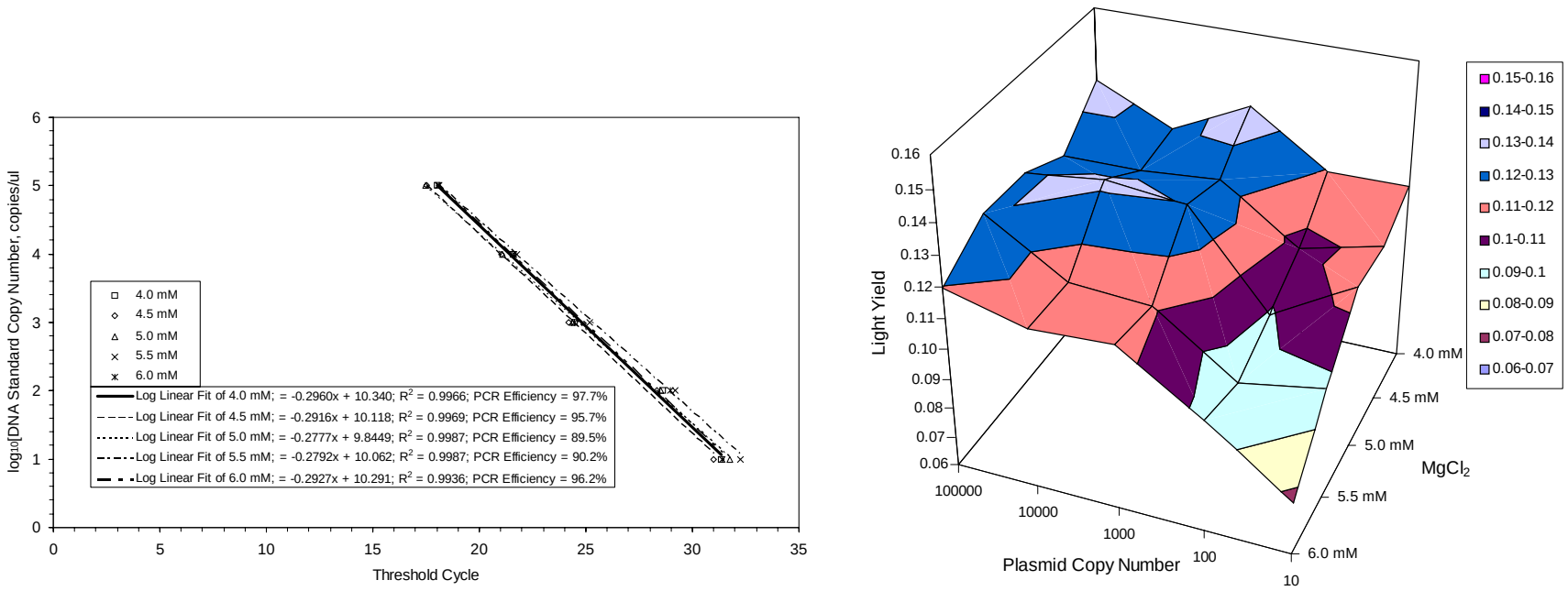
A **B**

Figure B-2 Threshold cycle (A) and light yield (B) versus annealing temperature/Mg^{2+} gradients for real-time PCR reactions using the *Nitrobacter* detection system with Platinum® Quantitative PCR SuperMix-UDG (Invitrogen; Carlsbad, CA). Temperature protocol: 50°C for 2 minutes, 95°C *Taq* activation for 2 minutes, 45 cycles with melting 95°C for 15 seconds and an annealing/extension temperature gradient from 58 to 68°C for 1 minute. Reaction recipe (25 µl): 12.5 µl mastermix, 400 nM primers (1µl) , 150 nM probe (0.375 µl), $MgCl_2$ gradient (3 - 6 mM × 1.0 mM; 0 - 1.00 µl of a 20 µM stock), 0.2 µm fHPLC dilution water (to 20 µl volume), and 5 µl of a 10^6 copies/µl *Nitrobacter* rDNA standard.



A **B**

Figure B-3 Threshold cycle (A) and light yield (B) versus annealing temperature/Mg^{2+} gradients for real-time PCR reactions using the *Nitrobacter* detection system with HotMasterMix (Eppendorf; Hamburg, Germany). Temperature protocol: preheat block to 94°C, 94°C initial melting for 1.5 minutes, 45 cycles with 94°C melting for 15 seconds and annealing/extension temperature gradient 58 to 68°C for 1 minute. Reaction recipe (25 µl): 10 µl mastermix, 400 nM primers (1µl) , 150 nM probe (0.375 µl), $MgCl_2$ gradient (3 - 6 mM × 1.0 mM; 0 - 1.00 µl of a 20 µM stock), 0.2 µm fHPLC dilution water (to 20 µl volume), and 5 µl of a 10^6 copies/µl *Nitrobacter* rDNA standard.



A **B**

Figure B-4 Threshold cycle (A) and light yield (B) versus plasmid copy number/Mg^{2+} gradients for real-time PCR reactions using the *Nitrobacter* detection system with Quantitect® Probe PCR mastermix (Qiagen; Valencia, CA). Temperature protocol: 50°C incubation for 2 minutes, 95°C *Taq* activation for 15 minutes, 45 cycles with 94°C melting for 15 seconds and a 61°C annealing/extension temperature for 1 minute. Reaction recipe (25 µl): 12.5 µl mastermix, 400 nM primers (1µl) , 150 nM probe (0.375 µl), $MgCl_2$ gradient (4 -6 mM × 0.5 mM; 0 - 1.00 µl of a 20 µM stock), 0.2 µm fHPLC dilution water (to 20 µl volume), and 5 µl of a 10^6 copies/µl *Nitrobacter* rDNA standard.

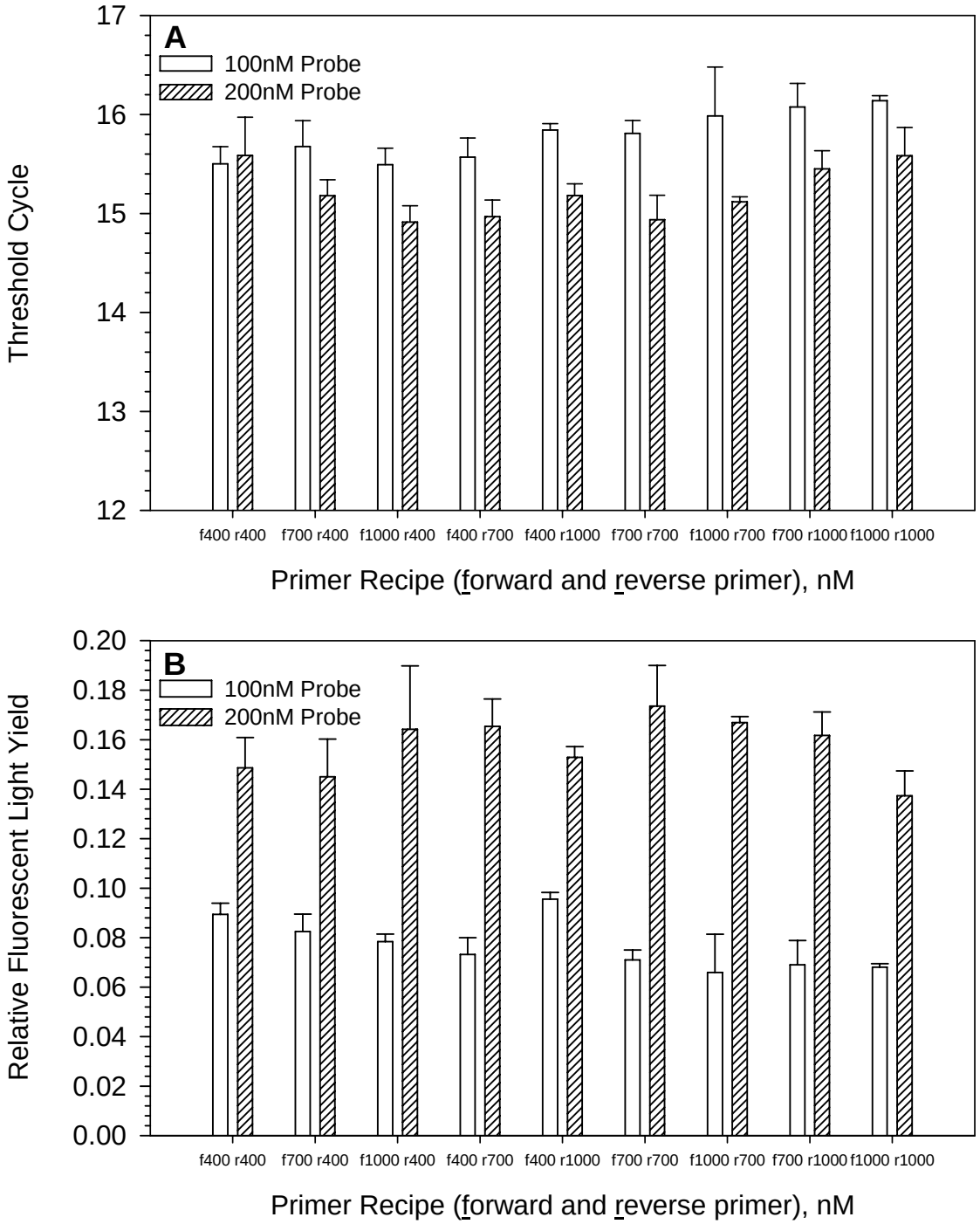


Figure B-5 Threshold cycle (A) and fluorescent light yield (B) for real-time PCR reactions (mean ± standard deviation of 3 reactions) with the *Nitrobacter* rDNA detection system and a 10^6 copies/µL standard. Quantitect® Probe PCR mastermix (Qiagen; Valencia, CA) was used at a 61°C annealing/extension temperature at different primer and probe concentrations.

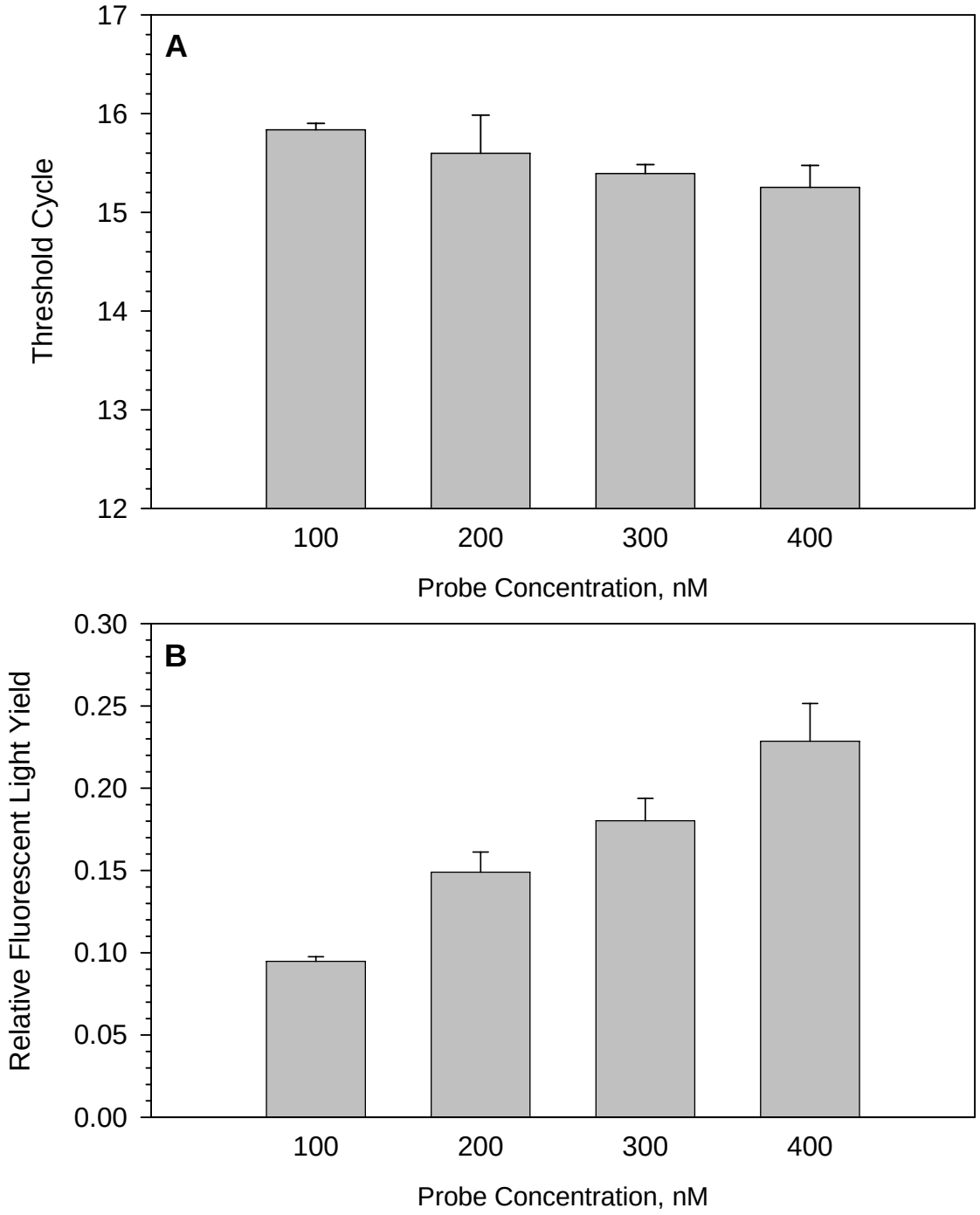


Figure B-6 Threshold cycle (A) and fluorescent light yield (B) for real-time PCR reactions (mean ± standard deviation of 3 reactions) with the *Nitrobacter* rDNA detection system and a 10^6 copies/µL standard. Quantitect® Probe PCR mastermix (Qiagen; Valencia, CA) was used at a 61°C annealing/extension temperature with 400 nM of each primer and between 100 and 400 nM of probe.

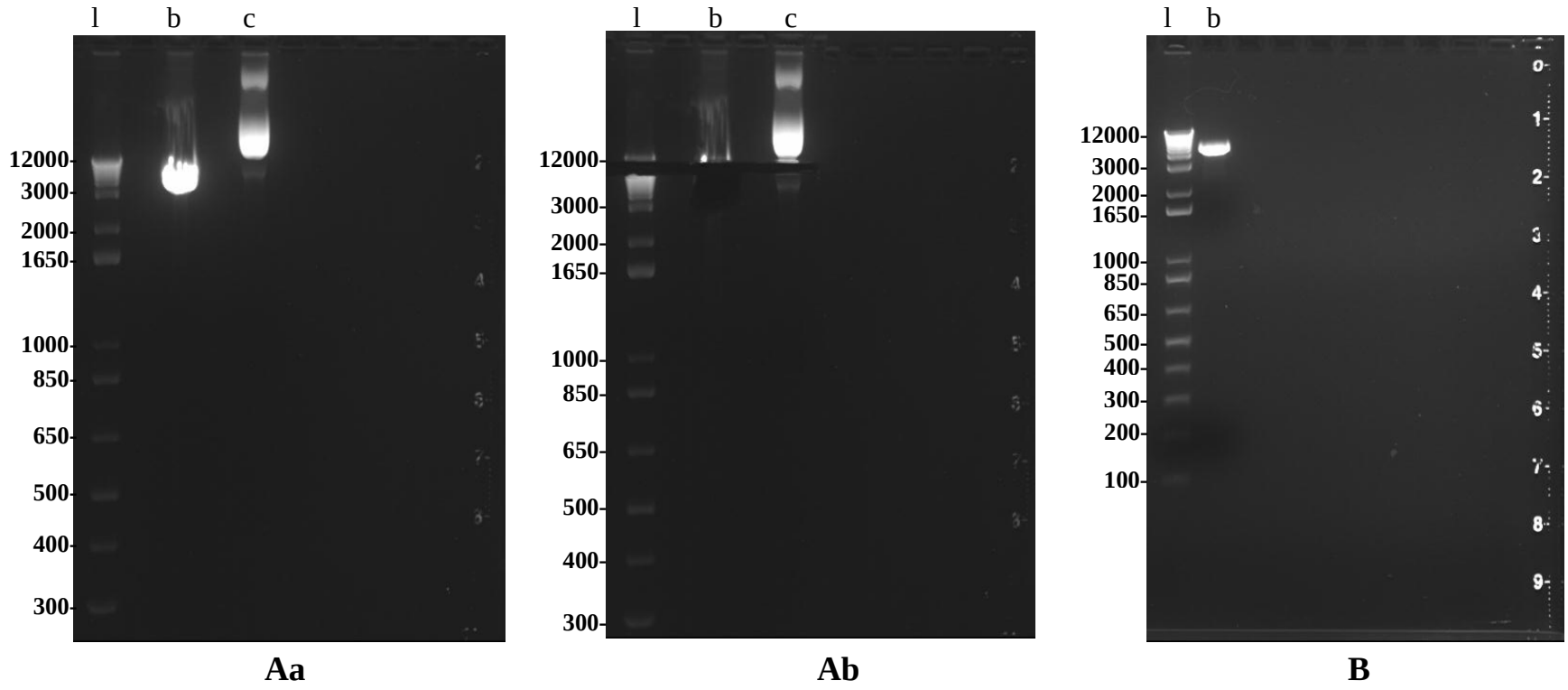


Figure B-7 Electrophoresis gel images that document linearization of a plasmid containing a BSNR *Nitrobacter* clone. A. Images that document separation (Aa) and removal (Ab) of the linear plasmid following *SpeI* digestion: lane "b" contained the 40 µl digest reaction, lane "c" contained a 36 µl control reaction. B. An image that documents the integrity and size of the linear plasmid (lane "b") following gel purification of the excised linear plasmid. For each gel, lane "l" contained the 1 Kb Plus Ladder (Promega; Madison, WI); distinct and the largest bands are annotated.

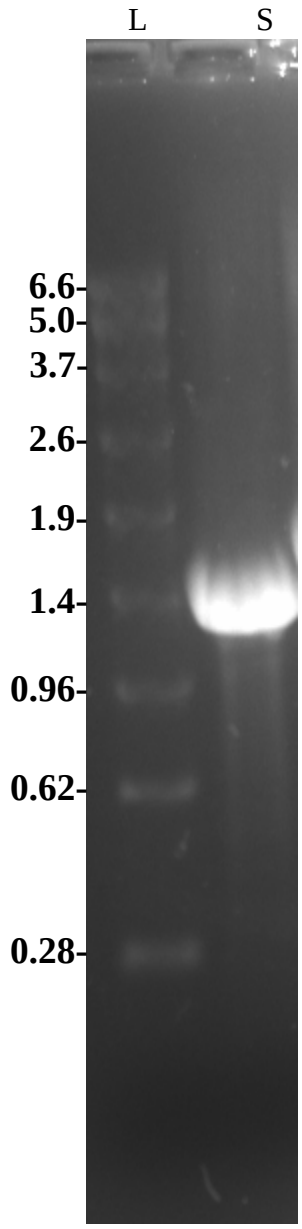


Figure B-8 Electrophoresis gel image used to evaluate the integrity of an artificial *Nitrobacter* rRNAt stock solution. Lane "L" contained an RNA ladder (Promega; Madison, WI); bands are annotated. Lane "S" contained the artificial transcript preparation.

Appendix C

Quantitative PCR Quality Control Data

Table C-1 Quantitative PCR results for dilutions of a BSNR DNA and RNA extract.

Dilution	*Nitrobacter* rDNA					*Nitrobacter* rRNAt				
	C_T	copies/(µl dilution)		copies/(L mixed liquor)		C_T	copies/(µl dilution)		copies/(L mixed liquor)	
		Assay	Mean	Assay	Mean		Assay	Mean	Assay	Mean
1:2	19.75	6.61E+04	7.91E+04	5.29E+09	6.33E+09	18.19	2.77E+05	3.28E+05	1.33E+10	7.87E+09
	19.40	8.22E+04		6.58E+09		17.85	3.45E+05		1.66E+10	
	19.27	8.90E+04		7.12E+09		17.77	3.62E+05		1.74E+10	
1:4	20.77	3.54E+04	3.66E+04	5.66E+09	5.85E+09	19.26	1.39E+05	1.63E+05	1.33E+10	7.81E+09
	20.74	3.61E+04		5.77E+09		18.95	1.70E+05		1.63E+10	
	20.65	3.82E+04		6.11E+09		18.86	1.80E+05		1.72E+10	
1:8	21.75	1.94E+04	2.05E+04	6.20E+09	6.57E+09	19.96	8.87E+04	9.43E+04	1.70E+10	9.05E+09
	21.51	2.24E+04		7.18E+09		19.77	1.00E+05		1.93E+10	
	21.72	1.98E+04		6.33E+09		19.87	9.39E+04		1.80E+10	
1:16	23.17	8.11E+03	9.07E+03	5.19E+09	5.81E+09	20.89	4.90E+04	4.97E+04	1.88E+10	9.54E+09
	23.13	8.30E+03		5.31E+09		20.82	5.10E+04		1.96E+10	
	22.71	1.08E+04		6.91E+09		20.88	4.91E+04		1.89E+10	
1:32	24.72	3.15E+03	4.38E+03	4.03E+09	5.61E+09	21.45	3.41E+04	3.31E+04	2.62E+10	1.27E+10
	24.04	4.77E+03		6.11E+09		21.42	3.47E+04		2.66E+10	
	23.89	5.23E+03		6.69E+09		21.62	3.06E+04		2.35E+10	
1:64	24.38	3.87E+03	3.67E+03	9.92E+09	9.40E+09	22.39	1.87E+04	1.47E+04	2.87E+10	1.13E+10
	24.51	3.56E+03		9.12E+09		23.04	1.23E+04		1.89E+10	
	24.50	3.59E+03		9.18E+09		22.94	1.31E+04		2.02E+10	
1:128	25.57	1.87E+03	1.57E+03	9.56E+09	8.04E+09	23.35	1.00E+04	7.42E+03	3.09E+10	1.14E+10
	25.79	1.63E+03		8.34E+09		24.14	6.05E+03		1.86E+10	
	26.27	1.21E+03		6.22E+09		24.11	6.16E+03		1.89E+10	

Table C-1 Continued.

Dilution	*Nitrobacter* rDNA					*Nitrobacter* rRNAt				
	C_T	copies/(µl dilution)		copies/(L mixed liquor)		C_T	copies/(µl dilution)		copies/(L mixed liquor)	
		Assay	Mean	Assay	Mean		Assay	Mean	Assay	Mean
1:256	26.69	9.40E+02	7.72E+02	9.62E+09	7.91E+09	25.04	3.41E+03	3.17E+03	2.09E+10	9.72E+09
	27.16	7.04E+02		7.21E+09		25.11	3.26E+03		2.00E+10	
	27.23	6.73E+02		6.89E+09		25.33	2.83E+03		1.74E+10	
1:512	27.86	4.57E+02	4.15E+02	9.36E+09	8.50E+09	25.70	2.23E+03	1.94E+03	2.74E+10	1.19E+10
	28.14	3.85E+02		7.88E+09		25.99	1.85E+03		2.27E+10	
	28.06	4.04E+02		8.26E+09		26.080	1.74E+03		2.14E+10	
1:1024	29.22	1.99E+02	1.95E+02	8.15E+09	8.01E+09	26.80	1.10E+03	9.83E+02	2.70E+10	1.21E+10
	29.22	1.98E+02		8.11E+09		26.87	1.05E+03		2.57E+10	
	29.30	1.89E+02		7.76E+09		27.29	8.01E+02		1.97E+10	

Table C-2 Quantitative PCR results for BSNR DNA and RNA extracts from different mixed liquor sample volumes.

Nitrobacter rDNA						*Nitrobacter* rRNAt					
Volume (ml)	C_T	copies/(µl extract)		copies/(L mixed liquor)		Volume (ml)	C_T	copies/(µl extract)		copies/(L mixed liquor)	
		Assay	Mean	Assay	Mean			Assay	Mean	Assay	Mean
0.47	27.24	7.03E+03	7.77E+03	2.99E+09	3.31E+09	-	-	-	-	-	-
	26.97	8.27E+03		3.52E+09			-	-		-	
	27.04	7.93E+03		3.37E+09			-	-		-	
	27.02	8.01E+03		3.41E+09			-	-		-	
	27.11	7.61E+03		3.24E+09			-	-		-	
0.96	24.20	4.39E+04	5.07E+04	9.10E+09	1.05E+10	0.94	21.78	2.37E+05	2.39E+05	1.52E+10	1.53E+10
	24.16	4.49E+04		9.31E+09			21.60	2.66E+05		1.70E+10	
	23.95	5.09E+04		1.06E+10			21.56	2.73E+05		1.74E+10	
	23.64	6.13E+04		1.27E+10			21.96	2.12E+05		1.35E+10	
	23.89	5.27E+04		1.09E+10			21.97	2.09E+05		1.34E+10	
1.77	22.21	1.45E+05	1.40E+05	1.63E+10	1.58E+10	1.95	20.85	4.34E+05	4.66E+05	1.34E+10	1.43E+10
	22.40	1.29E+05		1.46E+10			20.37	5.92E+05		1.82E+10	
	22.20	1.46E+05		1.65E+10			20.72	4.72E+05		1.45E+10	
	22.20	1.46E+05		1.65E+10			20.85	4.33E+05		1.33E+10	
	22.35	1.34E+05		1.51E+10			20.99	3.96E+05		1.22E+10	
4.78	21.11	2.82E+05	2.71E+05	1.18E+10	1.13E+10	4.63	19.39	1.12E+06	1.05E+06	1.45E+10	1.36E+10
	21.12	2.80E+05		1.17E+10			19.84	8.37E+05		1.08E+10	
	21.55	2.16E+05		9.03E+09			19.47	1.06E+06		1.38E+10	
	21.03	2.96E+05		1.24E+10			19.34	1.16E+06		1.50E+10	
	21.13	2.79E+05		1.17E+10			19.48	1.06E+06		1.37E+10	

Table C-2 Continued.

Nitrobacter rDNA						*Nitrobacter* rRNAt					
Volume (ml)	C_T	copies/(µl extract)		copies/(L mixed liquor)		Volume (ml)	C_T	copies/(µl extract)		copies/(L mixed liquor)	
		Assay	Mean	Assay	Mean			Assay	Mean	Assay	Mean
0.46	26.51	1.15E+04	1.24E+04	4.95E+09	5.34E+09	-	-	-	-	-	-
	26.29	1.31E+04		5.64E+09			-	-		-	
	26.16	1.41E+04		6.08E+09			-	-		-	
	26.38	1.24E+04		5.36E+09			-	-		-	
	26.62	1.08E+04		4.66E+09			-	-		-	
0.97	26.12	1.45E+04	1.85E+04	2.99E+09	3.82E+09	0.98	22.09	1.62E+05	1.70E+05	9.94E+09	1.05E+10
	25.79	1.76E+04		3.63E+09			21.90	1.85E+05		1.13E+10	
	25.45	2.16E+04		4.44E+09			22.03	1.69E+05		1.04E+10	
	25.51	2.07E+04		4.27E+09			21.98	1.74E+05		1.07E+10	
	25.73	1.82E+04		3.76E+09			22.09	1.62E+05		9.97E+09	
1.98	23.32	7.54E+04	9.14E+04	7.63E+09	9.25E+09	1.75	20.59	4.38E+05	4.45E+05	1.50E+10	1.53E+10
	23.28	7.72E+04		7.81E+09			20.68	4.12E+05		1.42E+10	
	22.63	1.13E+05		1.15E+10			20.39	4.99E+05		1.71E+10	
	22.63	1.14E+05		1.15E+10			20.76	3.91E+05		1.34E+10	
	23.27	7.76E+04		7.85E+09			20.43	4.87E+05		1.67E+10	
4.87	21.43	2.30E+05	2.87E+05	9.45E+09	1.18E+10	4.65	19.69	7.96E+05	9.48E+05	1.03E+10	1.22E+10
	21.08	2.83E+05		1.16E+10			19.49	9.07E+05		1.17E+10	
	20.86	3.22E+05		1.32E+10			19.50	8.99E+05		1.16E+10	
	20.79	3.35E+05		1.38E+10			19.15	1.14E+06		1.47E+10	
	21.20	2.64E+05		1.08E+10			19.33	1.00E+06		1.30E+10	

Table C-2 Continued.

Nitrobacter rDNA						*Nitrobacter* rRNAt					
Volume (ml)	C_T	copies/(µl extract)		copies/(L mixed liquor)		Volume (ml)	C_T	copies/(µl extract)		copies/(L mixed liquor)	
		Assay	Mean	Assay	Mean			Assay	Mean	Assay	Mean
0.50	26.97	9.19E+03	1.12E+04	3.68E+09	4.47E+09	-	-	-	-	-	-
	26.69	1.09E+04		4.37E+09			-	-		-	
	26.61	1.14E+04		4.57E+09			-	-		-	
	26.58	1.16E+04		4.66E+09			-	-		-	
	26.45	1.26E+04		5.06E+09			-	-		-	
0.94	23.70	6.64E+04	7.08E+04	1.41E+10	1.50E+10	0.95	21.39	2.12E+05	2.33E+05	1.34E+10	1.48E+10
	23.84	6.11E+04		1.30E+10			21.37	2.14E+05		1.36E+10	
	23.52	7.44E+04		1.58E+10			21.11	2.55E+05		1.62E+10	
	23.48	7.59E+04		1.61E+10			21.13	2.53E+05		1.60E+10	
	23.48	7.62E+04		1.62E+10			21.25	2.33E+05		1.48E+10	
1.84	22.45	1.42E+05	1.26E+05	1.54E+10	1.37E+10	1.83	20.47	3.92E+05	4.34E+05	1.28E+10	1.42E+10
	22.81	1.14E+05		1.24E+10			20.25	4.56E+05		1.49E+10	
	22.56	1.33E+05		1.44E+10			20.23	4.61E+05		1.51E+10	
	22.60	1.30E+05		1.41E+10			20.25	4.53E+05		1.48E+10	
	22.86	1.11E+05		1.20E+10			20.42	4.06E+05		1.33E+10	
4.90	20.79	3.87E+05	3.85E+05	1.58E+10	1.57E+10	4.57	19.45	7.74E+05	9.17E+05	1.02E+10	1.20E+10
	20.92	3.59E+05		1.46E+10			19.41	7.96E+05		1.04E+10	
	20.85	3.74E+05		1.52E+10			19.22	9.09E+05		1.19E+10	
	20.64	4.23E+05		1.72E+10			19.04	1.02E+06		1.34E+10	
	20.81	3.83E+05		1.56E+10			18.95	1.08E+06		1.42E+10	

Table C-3 A statistical summary of the *Nitrobacter* rDNA and rRNAt data in Table C-2. The mean, standard deviation (SD), and coefficient of variation (CV) are provided for five replicate log transformed assay results (intra-assay replicates) and for the mean log transformed results across the approximate (gross) sample volumes (inter-extract replicates). The overall results apply across the inter-extract means.

Assay	Sample Volume (ml)		Log[copies/(L mixed liquor)]								
			Intra-Assay Replicates			Inter-Extract Replicates			Overall		
	Gross	Exact	Mean	SD	CV	Mean	SD	CV	Mean	SD	CV
Nitrobacter rDNA Real-Time PCR	0.5	0.47	9.52	0.03	0.29%	9.63	0.10	1.08%	9.92	0.25	2.47%
		0.46	9.73	0.05	0.47%						
		0.50	9.65	0.05	0.53%						
	1	0.96	10.02	0.06	0.59%	9.92	0.30	3.12%			
		0.97	9.58	0.07	0.71%						
		0.94	10.18	0.04	0.42%						
	2	1.77	10.20	0.02	0.24%	10.04	0.13	1.37%			
		1.98	9.96	0.09	0.93%						
		1.91	9.96	0.01	0.06%						
	5	4.78	10.05	0.05	0.54%	10.10	0.07	0.78%			
		4.87	10.07	0.07	0.66%						
		4.90	10.20	0.03	0.26%						
Nitrobacter rRNAt Real-Time RT-PCR	1	0.94	10.18	0.05	0.53%	10.12	0.09	0.90%	10.13	0.03	0.90%
		0.98	10.02	0.02	0.23%						
		0.95	10.17	0.04	0.38%						
	2	1.95	10.15	0.07	0.65%	10.16	0.02	0.17%			
		1.75	10.18	0.05	0.45%						
		1.83	10.15	0.03	0.32%						
	5	4.63	10.13	0.06	0.55%	10.10	0.03	0.28%			
		4.63	0.00	0.00	0.00%						
		4.57	10.08	0.06	0.57%						

Table C-4 ANOVA comparisons of the *Nitrobacter* rDNA and rRNAt data in Table C-2 and Table C-3.

Assay	Group	Parameters	Sum of Squares		Degrees of Freedom	Mean Square	Evaluation	
							F	Sig.
Nitrobacter rDNA Real-Time PCR	Exact sample volume (Table C-2)	log[copies *Nitrobacter* rDNA/(L mixed liquor)] (Table C-2)	Between Groups	3.499	11	0.318	109.94	0.000
			Within Groups	0.139	48	0.0029		
			Total	3.638	59			
	2 and 5 ml sample volume (Table C-3)	log[copies *Nitrobacter* rDNA/(L mixed liquor)] (Table C-3)	Between Groups	0.0001	1	0.0001	0.009	0.928
			Within Groups	0.0433	4	0.0108		
			Total	0.0434	5			
Nitrobacter rRNAt Real-Time RT-PCR	Exact sample volume (Table C-2)	log[copies *Nitrobacter* rRNAt/(L mixed liquor)] (Table C-2)	Between Groups	0.1256	8	0.0157	6.13	0.000
			Within Groups	0.0922	36	0.0026		
			Total	0.2178	44			
	Gross sample volume (Table C-3)	log[copies *Nitrobacter* rRNAt/(L mixed liquor)] (Table C-3)	Between Groups	0.006	1	0.006	10.62	0.031
			Within Groups	0.002	4	0.001		
			Total	0.008	5			

Table C-5 Total bacterial rDNA and *Nitrobacter* rDNA gene copy number in replicate BSNR DNA extracts.

Replicate BSNR DNA Extract		Bacterial rDNA					*Nitrobacter* rDNA				
		C_T	copies/(µl extract)		copies/(L mixed liquor)		C_T	copies/(µl extract)		copies/(L mixed liquor)	
Number	Dilution		Assay	Mean	Assay	Mean		Assay	Mean	Assay	Mean
1	1:5	25.12	2.09E+06	2.73E+06	8.74E+10	1.14E+11	21.36	2.51E+05	2.54E+05	1.05E+10	1.06E+10
		24.99	2.26E+06		9.43E+10		21.41	2.43E+05		1.01E+10	
		24.16	3.83E+06		1.60E+11		21.25	2.68E+05		1.12E+10	
	1:50	23.48	5.88E+06	5.78E+06	2.50E+11	2.46E+11					
		23.07	7.62E+06		3.24E+11		-	-	-	-	-
		24.15	3.86E+06		1.64E+11						
	1:500	24.12	3.92E+06	3.13E+06	1.69E+11	1.35E+11					
		24.60	2.90E+06		1.25E+11		-	-	-	-	-
		24.79	2.57E+06		1.11E+11						
2	1:5	28.40	2.62E+06	3.55E+06	1.09E+11	1.48E+11	20.55	4.16E+05	3.88E+05	1.77E+10	1.65E+10
		28.05	3.26E+06		1.36E+11		20.68	3.82E+05		1.63E+10	
		27.46	4.75E+06		1.99E+11		20.76	3.66E+05		1.56E+10	
	1:50	26.37	9.47E+06	9.56E+06	4.03E+11	4.07E+11					
		26.35	9.58E+06		4.08E+11		-	-	-	-	-
		26.35	9.61E+06		4.09E+11						
	1:500	27.09	6.00E+06	4.82E+06	2.58E+11	2.08E+11					
		27.35	5.08E+06		2.19E+11		-	-	-	-	-
		28.00	3.39E+06		1.46E+11						
3	1:5	31.58	3.51E+06	3.60E+06	1.47E+11	1.51E+11	21.01	3.12E+05	3.03E+05	1.34E+10	1.31E+10
		31.67	3.31E+06		1.38E+11		21.12	2.91E+05		1.25E+10	
		31.38	3.99E+06		1.67E+11		21.03	3.08E+05		1.32E+10	
	1:50	29.33	1.46E+07	1.46E+07	6.21E+11	6.20E+11					
		29.19	1.59E+07		6.78E+11		-	-	-	-	-
		29.49	1.32E+07		5.62E+11						
	1:500	30.69	6.16E+06	5.07E+06	2.65E+11	2.18E+11					
		30.91	5.35E+06		2.30E+11		-	-	-	-	-
		31.50	3.69E+06		1.59E+11						

Appendix D

Nitrobacter rRNAt/RNA Ratio Range and Rate of Change Data

Table D-1 Soluble nitrogen, nitrification efficiency, and MLVSS in the BSNR over the 11 week time period used to establish *Nitrobacter* rRNAt/rDNA upper and lower prediction intervals.

Day	BSNR Soluble Nitrogen, mg-N/L			Nitrification Efficiency, %[1]	MLVSS, mg/L
	Ammonia	Nitrite	Nitrate		
1	21.9	386.3	1005	71.12	114
3	7.0	221.0	1141	83.34	116
5	8.0	1.3	1344	99.31	118
8	10.4	0.4	1348	99.21	126
10	11.1	0.3	1343	99.16	135
12	14.7	17.2	1379	97.74	123
15	1.1	0.5	1306	99.88	148
17	4.3	0.0	1341	99.68	154
19	8.1	0.0	1306	99.38	168
22	5.5	0.0	1330	99.59	169
24	9.7	0.0	1366	99.30	168
26	6.9	0.0	1340	99.48	159
29	6.1	0.0	1336	99.54	167
31	7.7	0.5	1308	99.38	155
33	7.6	0.0	1272	99.40	157
36	1.4	0.6	1261	99.84	153
38	1.2	0.7	1278	99.85	156
40	1.2	1.1	1395	99.84	155
43	1.2	1.5	1379	99.81	182
45	0.3	0.4	1316	99.95	172
47	0.2	0.3	1378	99.96	162
50	0.1	0.3	1354	99.97	150
52	0.2	0.4	1401	99.96	165
54	-	-	-	-	-
57	0.2	0.2	1455	99.97	149
59	0.3	0.0	1348	99.98	145
61	0.2	0.0	1387	99.98	152
66	0.2	0.0	1436	99.99	136
68	0.3	0.0	1439	99.98	149
71	0.2	0.0	1422	99.99	131
73	0.2	0.2	1298	99.97	131

1 Calculated as: nitrate-N/(ammonia-N + nitrite-N + nitrate-N) × 100%

Table D-2 Quantitative PCR results for the 11 week period used to establish BSNR *Nitrobacter* rRNAt/rDNA prediction intervals.

Sample[1]		*Nitrobacter* rDNA					*Nitrobacter* rRNAt				
		C_T	copies/(µl extract)		copies/L		C_T	copies/(µl extract)		copies/L	
Day	N		Assay	Mean	Assay	Mean		Assay	Mean	Assay	Mean
3	1	20.06	6.67E+05	6.62E+05	2.53E+10	2.52E+10	17.80	4.57E+06	4.14E+06	9.20E+10	8.33E+10
		20.09	6.55E+05		2.49E+10		17.98	4.07E+06		8.18E+10	
		20.06	6.66E+05		2.53E+10		18.09	3.78E+06		7.60E+10	
	2	20.39	5.48E+05	5.71E+05	2.31E+10	2.41E+10	18.18	3.57E+06	4.04E+06	6.89E+10	7.79E+10
		20.41	5.40E+05		2.27E+10		17.96	4.13E+06		7.96E+10	
		20.17	6.26E+05		2.64E+10		17.85	4.41E+06		8.52E+10	
	3	20.53	5.03E+05	5.31E+05	2.01E+10	2.12E+10	18.36	3.17E+06	3.66E+06	6.43E+10	7.41E+10
		20.42	5.39E+05		2.15E+10		17.91	4.25E+06		8.61E+10	
		20.39	5.50E+05		2.19E+10		18.19	3.55E+06		7.19E+10	
10	1	20.46	5.26E+05	5.43E+05	2.10E+10	2.17E+10	19.32	1.69E+06	1.72E+06	3.36E+10	3.42E+10
		20.24	5.98E+05		2.39E+10		19.31	1.70E+06		3.39E+10	
		20.53	5.05E+05		2.02E+10		19.26	1.76E+06		3.50E+10	
	2	20.27	5.88E+05	6.18E+05	2.39E+10	2.52E+10	19.08	1.97E+06	2.01E+06	3.64E+10	3.71E+10
		20.26	5.92E+05		2.41E+10		19.20	1.83E+06		3.38E+10	
		20.04	6.75E+05		2.75E+10		18.90	2.23E+06		4.10E+10	
	3	20.55	4.99E+05	5.59E+05	1.93E+10	2.17E+10	19.36	1.65E+06	1.89E+06	2.90E+10	3.31E+10
		20.28	5.87E+05		2.27E+10		19.09	1.97E+06		3.46E+10	
		20.26	5.91E+05		2.29E+10		19.03	2.04E+06		3.58E+10	
17	1	20.80	4.30E+05	4.58E+05	1.74E+10	1.85E+10	-	-	-	-	-
		20.71	4.53E+05		1.83E+10		-	-		-	
		20.57	4.92E+05		1.99E+10		-	-		-	
	2	20.54	5.02E+05	4.96E+05	1.89E+10	1.86E+10	19.40	1.60E+06	1.25E+06	3.09E+10	2.40E+10
		20.66	4.67E+05		1.76E+10		20.03	1.06E+06		2.04E+10	
		20.48	5.19E+05		1.95E+10		20.02	1.07E+06		2.07E+10	
	3	20.69	4.59E+05	4.33E+05	1.81E+10	1.70E+10	20.11	1.01E+06	1.01E+06	1.91E+10	1.92E+10
		20.80	4.29E+05		1.69E+10		20.21	9.43E+05		1.78E+10	
		20.87	4.11E+05		1.62E+10		20.00	1.09E+06		2.05E+10	

Table D-2 Continued.

Sample[1]		*Nitrobacter* rDNA					*Nitrobacter* rRNAt				
		C_T	copies/(µl extract)		copies/L		C_T	copies/(µl extract)		copies/L	
Day	N		Assay	Mean	Assay	Mean		Assay	Mean	Assay	Mean
24	1	20.45	5.29E+05	4.69E+05	2.10E+10	1.86E+10	20.26	9.17E+05	8.26E+05	1.66E+10	1.50E+10
		20.58	4.88E+05		1.94E+10		20.90	6.04E+05		1.10E+10	
		20.96	3.91E+05		1.55E+10		20.19	9.55E+05		1.73E+10	
	2	20.59	4.86E+05	4.54E+05	1.97E+10	1.84E+10	20.69	6.91E+05	5.13E+05	1.30E+10	9.63E+09
		20.70	4.57E+05		1.85E+10		21.24	4.84E+05		9.07E+09	
		20.84	4.20E+05		1.70E+10		21.66	3.66E+05		6.86E+09	
	3	20.56	4.94E+05	4.82E+05	1.85E+10	1.81E+10	20.30	8.95E+05	7.46E+05	1.57E+10	1.31E+10
		20.65	4.69E+05		1.76E+10		21.00	5.64E+05		9.89E+09	
		20.61	4.82E+05		1.81E+10		20.51	7.79E+05		1.37E+10	
31	1	20.38	5.51E+05	5.12E+05	2.26E+10	2.10E+10	20.45	8.11E+05	7.03E+05	1.44E+10	1.25E+10
		20.38	5.52E+05		2.26E+10		20.78	6.53E+05		1.16E+10	
		20.78	4.34E+05		1.78E+10		20.80	6.45E+05		1.14E+10	
	2	20.75	4.43E+05	4.26E+05	1.81E+10	1.74E+10	20.34	8.69E+05	7.72E+05	1.55E+10	1.38E+10
		20.68	4.62E+05		1.89E+10		20.60	7.31E+05		1.30E+10	
		21.04	3.71E+05		1.52E+10		20.64	7.16E+05		1.28E+10	
	3	21.32	3.15E+05	3.24E+05	1.23E+10	1.27E+10	20.28	9.04E+05	7.42E+05	1.60E+10	1.31E+10
		21.09	3.61E+05		1.41E+10		20.93	5.93E+05		1.05E+10	
		21.43	2.96E+05		1.16E+10		20.61	7.30E+05		1.29E+10	
38	1	20.85	4.18E+05	4.72E+05	1.71E+10	1.93E+10	19.91	1.15E+06	1.07E+06	2.14E+10	1.99E+10
		20.53	5.04E+05		2.06E+10		19.89	1.16E+06		2.16E+10	
		20.57	4.93E+05		2.02E+10		20.29	9.00E+05		1.67E+10	
	2	20.74	4.44E+05	4.03E+05	1.78E+10	1.61E+10	20.00	1.08E+06	1.10E+06	1.97E+10	2.01E+10
		20.96	3.90E+05		1.56E+10		19.72	1.31E+06		2.38E+10	
		21.02	3.76E+05		1.50E+10		20.25	9.22E+05		1.68E+10	
	3	21.25	3.29E+05	3.38E+05	1.34E+10	1.38E+10	19.48	1.52E+06	1.45E+06	2.64E+10	2.53E+10
		21.23	3.33E+05		1.36E+10		19.59	1.42E+06		2.47E+10	
		21.14	3.51E+05		1.43E+10		19.59	1.42E+06		2.47E+10	

Table D-2 Continued.

Sample[1]		*Nitrobacter* rDNA					*Nitrobacter* rRNAt				
		C_T	copies/(µl extract)		copies/L		C_T	copies/(µl extract)		copies/L	
Day	N		Assay	Mean	Assay	Mean		Assay	Mean	Assay	Mean
45	1	20.97	3.88E+05	3.70E+05	1.55E+10	1.48E+10	20.24	1.38E+06	1.34E+06	2.50E+10	2.44E+10
		20.96	3.91E+05		1.56E+10		20.19	1.42E+06		2.58E+10	
		21.23	3.32E+05		1.33E+10		20.40	1.23E+06		2.24E+10	
	2	21.23	3.32E+05	3.11E+05	1.31E+10	1.23E+10	20.12	1.48E+06	1.35E+06	2.66E+10	2.42E+10
		21.45	2.92E+05		1.15E+10		20.31	1.31E+06		2.35E+10	
		21.35	3.09E+05		1.22E+10		20.39	1.25E+06		2.24E+10	
	3	20.99	3.84E+05	3.74E+05	1.50E+10	1.46E+10	20.24	1.10E+06	1.40E+06	1.97E+10	2.51E+10
		21.05	3.70E+05		1.44E+10		19.90	1.37E+06		2.45E+10	
		21.06	3.69E+05		1.44E+10		19.54	1.73E+06		3.11E+10	
52	1	21.20	3.38E+05	3.14E+05	1.23E+10	1.14E+10	20.46	9.49E+05	9.21E+05	1.70E+10	1.65E+10
		21.44	2.94E+05		1.07E+10		20.50	9.26E+05		1.66E+10	
		21.35	3.09E+05		1.13E+10		20.57	8.87E+05		1.59E+10	
	2	21.12	3.55E+05	3.16E+05	1.43E+10	1.28E+10	20.84	7.42E+05	7.69E+05	1.29E+10	1.34E+10
		21.38	3.04E+05		1.23E+10		20.66	8.37E+05		1.45E+10	
		21.46	2.90E+05		1.17E+10		20.87	7.29E+05		1.27E+10	
	3	21.27	3.24E+05	2.99E+05	1.23E+10	1.14E+10	21.43	6.30E+05	6.85E+05	1.09E+10	1.19E+10
		21.37	3.06E+05		1.17E+10		21.23	7.16E+05		1.24E+10	
		21.60	2.68E+05		1.02E+10		21.25	7.09E+05		1.23E+10	
59	1	21.59	2.71E+05	2.66E+05	9.96E+09	9.79E+09	20.94	8.70E+05	8.58E+05	1.62E+10	1.60E+10
		21.52	2.81E+05		1.03E+10		20.97	8.49E+05		1.58E+10	
		21.74	2.47E+05		9.09E+09		20.96	8.56E+05		1.59E+10	
	2	21.53	2.79E+05	2.52E+05	1.02E+10	9.22E+09	20.84	9.28E+05	9.03E+05	1.70E+10	1.66E+10
		21.84	2.32E+05		8.52E+09		20.78	9.62E+05		1.76E+10	
		21.77	2.43E+05		8.92E+09		21.03	8.18E+05		1.50E+10	
	3	21.87	2.29E+05	2.28E+05	8.34E+09	8.32E+09	21.09	7.86E+05	7.94E+05	1.59E+10	1.61E+10
		21.89	2.26E+05		8.24E+09		21.20	7.30E+05		1.48E+10	
		21.87	2.30E+05		8.37E+09		20.95	8.65E+05		1.75E+10	

Table D-2 Continued.

Sample[1]		*Nitrobacter* rDNA					*Nitrobacter* rRNAt				
		C_T	copies/(µl extract)		copies/L		C_T	copies/(µl extract)		copies/L	
Day	N		Assay	Mean	Assay	Mean		Assay	Mean	Assay	Mean
66	1	21.53	2.80E+05	2.54E+05	1.11E+10	1.01E+10	20.41	9.82E+05	7.92E+05	1.76E+10	1.42E+10
		21.74	2.47E+05		9.79E+09		20.84	7.43E+05		1.33E+10	
		21.83	2.35E+05		9.33E+09		21.04	6.51E+05		1.17E+10	
	2	21.98	2.15E+05	2.08E+05	8.56E+09	8.29E+09	20.81	7.56E+05	7.28E+05	1.31E+10	1.26E+10
		21.91	2.24E+05		8.92E+09		20.82	7.51E+05		1.31E+10	
		22.23	1.85E+05		7.38E+09		20.98	6.77E+05		1.18E+10	
	3	21.99	2.14E+05	2.05E+05	8.49E+09	8.15E+09	21.07	6.38E+05	7.56E+05	1.14E+10	1.35E+10
		22.03	2.09E+05		8.31E+09		21.04	6.52E+05		1.17E+10	
		22.17	1.92E+05		7.65E+09		20.42	9.78E+05		1.75E+10	
73	1	21.28	1.66E+05	1.91E+05	6.55E+09	7.53E+09	20.24	8.39E+05	9.15E+05	1.46E+10	1.59E+10
		20.97	2.01E+05		7.91E+09		20.20	8.60E+05		1.49E+10	
		20.93	2.06E+05		8.12E+09		19.90	1.05E+06		1.82E+10	
	2	20.83	2.18E+05	2.49E+05	8.06E+09	9.20E+09	20.39	7.64E+05	8.51E+05	1.36E+10	1.51E+10
		20.63	2.46E+05		9.10E+09		20.30	8.10E+05		1.44E+10	
		20.41	2.82E+05		1.04E+10		20.00	9.79E+05		1.74E+10	
	3	20.14	3.31E+05	3.27E+05	1.23E+10	1.21E+10	-	-	8.61E+05	-	1.39E+10
		20.29	3.03E+05		1.12E+10		20.20	8.63E+05		1.39E+10	
		20.08	3.45E+05		1.28E+10		20.21	8.59E+05		1.39E+10	

1 See Figure 10; N = a number assigned to replicate DNA/RNA extracts for each sample.

Table D-3 Quantitative PCR results for an experiment that evaluated the *Nitrobacter* rRNAt/rDNA ratio range and dynamics.

Sample[1]			*Nitrobacter* rDNA					*Nitrobacter* rRNAt				
			C_T	copies/(µl extract)		copies/L		C_T	copies/(µl extract)		copies/L	
Vessel	Time, hrs	N		Assay	Mean	Assay	Mean		Assay	Mean	Assay	Mean
1	-0.03	1	22.58	1.57E+05	1.69E+05	6.18E+09	6.65E+09	26.36	1.19E+04	1.29E+04	2.32E+08	2.51E+08
			22.38	1.76E+05		6.94E+09		26.30	1.25E+04		2.42E+08	
			22.41	1.73E+05		6.83E+09		26.07	1.44E+04		2.80E+08	
		2	22.37	1.78E+05	1.91E+05	6.67E+09	7.17E+09	25.81	1.71E+04	1.73E+04	2.86E+08	2.89E+08
			22.22	1.94E+05		7.26E+09		26.03	1.48E+04		2.48E+08	
			22.15	2.02E+05		7.58E+09		25.57	2.00E+04		3.34E+08	
		3	22.69	1.46E+05	1.47E+05	5.87E+09	5.91E+09	24.87	3.15E+04	3.03E+04	6.47E+08	6.21E+08
			22.72	1.44E+05		5.77E+09		24.89	3.12E+04		6.39E+08	
			22.63	1.51E+05		6.08E+09		25.04	2.82E+04		5.78E+08	
2	0.75	1	-	-	-	-	-	23.95	5.75E+04	5.49E+04	1.20E+09	1.14E+09
			-	-		-		24.14	5.07E+04		1.06E+09	
			-	-		-		23.97	5.66E+04		1.18E+09	
		2	22.53	1.61E+05	1.72E+05	6.01E+09	6.41E+09	23.03	1.05E+05	1.07E+05	1.88E+09	1.92E+09
			22.40	1.74E+05		6.48E+09		23.04	1.03E+05		1.86E+09	
			22.33	1.81E+05		6.75E+09		22.92	1.12E+05		2.02E+09	
		3	23.80	7.51E+04	1.02E+05	2.87E+09	3.89E+09	22.90	1.13E+05	1.11E+05	2.10E+09	2.06E+09
			23.11	1.14E+05		4.33E+09		22.79	1.22E+05		2.27E+09	
			23.06	1.18E+05		4.48E+09		23.14	9.71E+04		1.80E+09	
3	1.58	1	22.42	1.52E+05	1.74E+05	6.00E+09	6.87E+09	23.63	7.05E+04	6.51E+04	1.13E+09	1.05E+09
			22.07	1.86E+05		7.36E+09		23.71	6.72E+04		1.08E+09	
			22.10	1.84E+05		7.26E+09		23.94	5.77E+04		9.27E+08	
		2	22.44	1.51E+05	1.67E+05	6.11E+09	6.78E+09	22.95	1.10E+05	1.25E+05	2.00E+09	2.28E+09
			22.20	1.74E+05		7.02E+09		22.77	1.24E+05		2.26E+09	
			22.16	1.78E+05		7.19E+09		22.56	1.42E+05		2.58E+09	
		3	22.29	1.64E+05	1.81E+05	6.62E+09	7.29E+09	22.84	1.18E+05	1.07E+05	2.14E+09	1.93E+09
			22.09	1.84E+05		7.44E+09		23.16	9.59E+04		1.73E+09	
			22.01	1.93E+05		7.80E+09		23.01	1.06E+05		1.91E+09	

Table D-3 Continued.

Sample[1]			*Nitrobacter* rDNA					*Nitrobacter* rRNAt				
			C_T	copies/(µl extract)		copies/L		C_T	copies/(µl extract)		copies/L	
Vessel	Time, hrs	N		Assay	Mean	Assay	Mean		Assay	Mean	Assay	Mean
4	2.33	1	22.42	1.52E+05	1.59E+05	5.63E+09	5.87E+09	24.60	3.67E+04	3.91E+04	6.34E+08	6.75E+08
			22.40	1.54E+05		5.70E+09		24.54	3.84E+04		6.63E+08	
			22.24	1.69E+05		6.27E+09		24.39	4.23E+04		7.30E+08	
		2	22.79	1.23E+05	1.48E+05	4.96E+09	5.98E+09	22.55	1.41E+05	1.41E+05	2.84E+09	2.83E+09
			22.52	1.44E+05		5.80E+09		22.68	1.30E+05		2.60E+09	
			22.16	1.77E+05		7.16E+09		22.45	1.51E+05		3.04E+09	
		3	23.34	8.90E+04	1.22E+05	3.53E+09	4.85E+09	22.72	1.27E+05	1.26E+05	2.54E+09	2.52E+09
			22.62	1.36E+05		5.39E+09		22.76	1.23E+05		2.47E+09	
			22.54	1.42E+05		5.64E+09		22.71	1.27E+05		2.55E+09	
5	3.83	1	22.02	1.92E+05	2.03E+05	7.20E+09	7.61E+09	22.68	1.30E+05	1.28E+05	2.45E+09	2.42E+09
			21.96	1.99E+05		7.45E+09		22.67	1.31E+05		2.47E+09	
			21.80	2.19E+05		8.20E+09		22.77	1.23E+05		2.32E+09	
		2	22.50	1.46E+05	1.56E+05	5.76E+09	6.15E+09	21.04	3.80E+05	3.40E+05	7.10E+09	6.34E+09
			22.45	1.50E+05		5.90E+09		21.30	3.21E+05		5.99E+09	
			22.21	1.72E+05		6.80E+09		21.31	3.18E+05		5.94E+09	
		3	22.07	1.87E+05	1.72E+05	7.17E+09	6.60E+09	21.20	3.42E+05	3.10E+05	6.09E+09	5.53E+09
			22.41	1.54E+05		5.89E+09		21.34	3.13E+05		5.57E+09	
			22.17	1.76E+05		6.74E+09		21.52	2.77E+05		4.93E+09	
6	6.33	1	21.49	2.61E+05	2.14E+05	9.34E+09	7.63E+09	20.71	4.71E+05	4.23E+05	9.43E+09	8.46E+09
			22.03	1.91E+05		6.82E+09		20.98	3.96E+05		7.91E+09	
			22.05	1.89E+05		6.75E+09		20.95	4.02E+05		8.04E+09	
		2	22.21	1.72E+05	1.72E+05	6.86E+09	6.85E+09	20.16	6.77E+05	6.70E+05	1.53E+10	1.52E+10
			22.31	1.62E+05		6.47E+09		20.19	6.62E+05		1.50E+10	
			22.13	1.81E+05		7.21E+09		20.18	6.70E+05		1.52E+10	
		3	22.75	1.26E+05	1.23E+05	5.19E+09	5.09E+09	19.40	1.12E+06	1.07E+06	2.22E+10	2.13E+10
			22.80	1.22E+05		5.04E+09		19.46	1.07E+06		2.13E+10	
			22.80	1.22E+05		5.04E+09		19.52	1.03E+06		2.05E+10	

Table D-3 Continued.

Sample[1]			*Nitrobacter* rDNA					*Nitrobacter* rRNAt				
			C_T	copies/(µl extract)		copies/L		C_T	copies/(µl extract)		copies/L	
Vessel	Time, hrs	N		Assay	Mean	Assay	Mean		Assay	Mean	Assay	Mean
1	8.57	1	21.45	2.69E+05	2.27E+05	9.80E+09	8.30E+09	20.65	4.92E+05	4.73E+05	9.64E+09	9.27E+09
			21.88	2.08E+05		7.60E+09		20.53	5.34E+05		1.04E+10	
			21.91	2.06E+05		7.50E+09		20.99	3.94E+05		7.72E+09	
		2	21.52	2.58E+05	2.13E+05	9.87E+09	8.18E+09	19.01	1.43E+06	1.49E+06	2.76E+10	2.86E+10
			21.84	2.14E+05		8.19E+09		19.06	1.38E+06		2.66E+10	
			22.24	1.69E+05		6.47E+09		18.80	1.64E+06		3.16E+10	
		3	22.03	1.91E+05	1.99E+05	7.72E+09	8.05E+09	19.12	1.33E+06	1.76E+06	2.53E+10	3.34E+10
			21.86	2.11E+05		8.51E+09		18.44	2.08E+06		3.95E+10	
			21.99	1.96E+05		7.92E+09		18.60	1.87E+06		3.55E+10	
2	9.98	1	22.25	1.69E+05	1.79E+05	6.74E+09	7.13E+09	23.73	6.64E+04	6.95E+04	1.29E+09	1.35E+09
			22.01	1.94E+05		7.75E+09		23.72	6.67E+04		1.30E+09	
			22.20	1.73E+05		6.91E+09		23.53	7.56E+04		1.47E+09	
		2	21.89	2.08E+05	1.97E+05	8.44E+09	8.00E+09	21.96	2.10E+05	1.79E+05	4.23E+09	3.62E+09
			21.85	2.12E+05		8.61E+09		22.75	1.26E+05		2.53E+09	
			22.22	1.71E+05		6.94E+09		22.01	2.03E+05		4.10E+09	
		3	22.09	1.84E+05	1.93E+05	7.28E+09	7.60E+09	22.41	1.57E+05	1.49E+05	2.93E+09	2.78E+09
			21.85	2.12E+05		8.37E+09		22.53	1.45E+05		2.71E+09	
			22.12	1.81E+05		7.16E+09		22.53	1.45E+05		2.70E+09	
3	11.08	1	22.47	1.48E+05	1.12E+05	5.85E+09	4.45E+09	25.40	2.23E+04	1.85E+04	4.55E+08	3.77E+08
			23.09	1.03E+05		4.09E+09		25.81	1.71E+04		3.49E+08	
			23.40	8.62E+04		3.41E+09		25.91	1.60E+04		3.27E+08	
		2	22.03	1.91E+05	1.38E+05	7.05E+09	5.08E+09	23.35	8.50E+04	7.73E+04	1.48E+09	1.35E+09
			23.01	1.08E+05		3.97E+09		23.58	7.29E+04		1.27E+09	
			22.92	1.14E+05		4.21E+09		23.56	7.39E+04		1.29E+09	
		3	22.85	1.18E+05	1.25E+05	4.54E+09	4.78E+09	23.15	9.67E+04	8.16E+04	1.83E+09	1.54E+09
			22.44	1.51E+05		5.77E+09		23.46	7.91E+04		1.49E+09	
			23.06	1.05E+05		4.03E+09		23.67	6.90E+04		1.30E+09	

Table D-3 Continued.

Sample[1]			*Nitrobacter* rDNA					*Nitrobacter* rRNAt				
			C_T	copies/(µl extract)		copies/L		C_T	copies/(µl extract)		copies/L	
Vessel	Time, hrs	N		Assay	Mean	Assay	Mean		Assay	Mean	Assay	Mean
4	12.08	1	22.95	1.12E+05	9.32E+04	4.43E+09	3.69E+09	24.98	2.87E+04	2.81E+04	6.20E+08	6.09E+08
			23.56	7.87E+04		3.12E+09		24.91	3.01E+04		6.51E+08	
			23.34	8.91E+04		3.53E+09		25.15	2.56E+04		5.55E+08	
		2	22.41	1.53E+05	1.30E+05	6.09E+09	5.17E+09	23.74	6.47E+04	6.48E+04	1.19E+09	1.19E+09
			22.57	1.40E+05		5.55E+09		23.93	5.70E+04		1.04E+09	
			23.19	9.75E+04		3.87E+09		23.56	7.26E+04		1.33E+09	
		3	22.45	1.50E+05	1.25E+05	5.62E+09	4.69E+09	23.70	6.62E+04	6.42E+04	1.21E+09	1.17E+09
			22.87	1.17E+05		4.39E+09		23.67	6.80E+04		1.24E+09	
			23.01	1.08E+05		4.05E+09		23.89	5.85E+04		1.07E+09	
5	13.58	1	22.40	1.75E+05	1.76E+05	6.43E+09	6.47E+09	25.28	2.36E+04	2.20E+04	4.41E+08	4.13E+08
			22.37	1.77E+05		6.54E+09		25.48	2.07E+04		3.87E+08	
			22.39	1.75E+05		6.45E+09		25.39	2.19E+04		4.10E+08	
		2	22.41	1.73E+05	1.71E+05	6.82E+09	6.72E+09	24.53	3.85E+04	3.51E+04	7.22E+08	6.59E+08
			22.54	1.60E+05		6.29E+09		24.96	2.90E+04		5.45E+08	
			22.35	1.79E+05		7.05E+09		24.56	3.78E+04		7.10E+08	
		3	22.55	1.60E+05	1.50E+05	6.48E+09	6.10E+09	25.33	2.28E+04	2.73E+04	4.36E+08	5.23E+08
			22.72	1.44E+05		5.83E+09		25.00	2.83E+04		5.43E+08	
			22.68	1.48E+05		5.99E+09		24.87	3.08E+04		5.91E+08	
6	15.63	1	22.75	1.41E+05	1.24E+05	5.39E+09	4.75E+09	25.49	2.06E+04	1.87E+04	3.65E+08	3.31E+08
			23.03	1.20E+05		4.58E+09		25.78	1.69E+04		3.00E+08	
			23.14	1.12E+05		4.28E+09		25.64	1.86E+04		3.30E+08	
		2	22.58	1.56E+05	1.67E+05	6.22E+09	6.64E+09	24.84	3.15E+04	2.79E+04	5.83E+08	5.17E+08
			22.52	1.63E+05		6.48E+09		25.17	2.53E+04		4.69E+08	
			22.33	1.81E+05		7.22E+09		25.08	2.70E+04		4.99E+08	
		3	22.99	1.22E+05	1.22E+05	4.64E+09	4.62E+09	24.77	3.29E+04	3.01E+04	5.99E+08	5.48E+08
			22.89	1.30E+05		4.94E+09		25.04	2.77E+04		5.03E+08	
			23.13	1.12E+05		4.26E+09		24.92	2.98E+04		5.42E+08	

1 Time is relative to a nitrite spike illustrated in Figure 12; N = a number assigned to replicate DNA/RNA extracts for each sample.

Appendix E

Batch Respirometric Inhibition Experiment Data

Table E-1 Results for batch respirometric inhibition experiments using the inhibitor 3,5-DCP.

Experiment[1]	Vessel		OUR1 (mg/L/hr)[3]			3,5-DCP (mg/L)	OUR2 (mg/L/hr)[3]			Inhibition[4]	
	Number	Type[2]	Slope	Fit	OUR1V		Slope	Fit	OUR2V	OUR	NOR
Preliminary (Figure 15)	1	C	9.96	0.9992	22.1	0.00	9.77	0.9991	21.71	0.02	-
	2	I	10.54	0.9992	23.4	2.00	9.77	0.9987	21.70	0.07	-
	3	I	10.03	0.9978	22.8	4.07	9.51	0.9992	21.61	0.05	-
	4	I	10.81	0.9988	24.0	7.94	0.36	0.6683	0.79	0.97	-
	5	I	9.53	0.9974	21.2	15.75	0.17	0.2784	0.37	0.98	-
	6	I	8.72	0.9987	19.4	31.01	0.58	0.8090	1.28	0.93	-
Preliminary	1	I	10.58	0.9990	23.5	2.99	10.11	0.9996	22.46	0.04	-
	2	I	10.73	0.9991	23.8	4.98	9.24	0.9984	20.53	0.14	-
	3	I	11.80	0.9991	26.2	6.95	1.46	0.9321	3.24	0.88	-
	4	I	10.42	0.9992	23.2	8.92	0.42	0.6094	0.92	0.96	-
	5	I	11.38	0.9990	25.3	10.88	0.29	0.4797	0.66	0.97	-
Preliminary	1	I	9.90	0.9997	22.0	5.96	7.46	0.9992	16.58	0.25	-
	2	I	9.99	0.9997	22.2	6.95	1.66	0.9767	3.69	0.83	-
	3	I	10.03	0.9997	22.3	7.94	0.42	0.9096	0.93	0.96	-
	4	I	10.52	0.9987	23.4	8.92	0.10	0.3283	0.23	0.99	-
	5	I	10.30	0.9991	22.9	9.90	0.32	0.7598	0.71	0.97	-
Preliminary	1	I	10.30	0.9989	22.9	3.98	9.87	0.9996	21.94	0.04	-
	2	I	10.55	0.9991	23.5	4.98	9.59	0.9997	21.30	0.09	-
	3	I	10.33	0.9980	23.0	5.96	7.79	0.9971	17.31	0.25	-
	4	I	9.77	0.9983	21.7	6.95	1.09	0.8911	2.41	0.89	-
	5	I	10.77	0.9994	23.9	7.94	0.44	0.5715	0.98	0.96	-
Preliminary	1	I	10.36	0.9983	23.0	4.98	9.87	0.9994	21.92	0.05	-
	2	I	9.76	0.9982	21.7	5.96	7.26	0.9989	16.12	0.26	-
	3	I	9.73	0.9981	21.6	6.95	1.39	0.9953	3.09	0.86	-
	4	I	6.98	0.9967	15.5	7.94	0.35	0.9221	0.78	0.95	-

Table E-1 Continued.

Experiment[1]	Vessel		OUR1 (mg/L/hr)[3]			3,5-DCP (mg/L)	OUR2 (mg/L/hr)[3]			Inhibition[4]	
	Number	Type[2]	Slope	Fit	OUR1V		Slope	Fit	OUR2V	OUR	NOR
Preliminary	1	C	9.57	0.9998	19.3	0.00	9.38	0.9976	18.95	0.02	-0.02
	2	I	10.33	0.9998	20.9	6.09	8.54	0.9982	17.25	0.17	0.17
	3	I	9.74	0.9998	19.7	6.59	4.78	0.9953	9.65	0.51	0.50
	4	I	9.72	0.9999	19.6	7.09	1.12	0.9430	2.27	0.88	0.90
	5	I	9.36	0.9997	18.9	8.10	0.21	0.5859	0.42	0.98	0.97
Experiment I (Figure 17)	1	C	10.89	0.9987	23.9	0.00	11.05	0.9984	24.28	-0.01	-0.05
	2	I	10.50	0.9993	23.1	4.95	10.23	0.9998	22.49	0.03	-0.04
	3	I	10.20	0.9994	22.4	5.93	9.12	0.9998	20.05	0.11	0.12
	4	I	10.72	0.9997	23.6	6.92	-	-	5.74	-	0.77
	5	I	9.80	0.9994	21.5	7.90	0.53	0.9616	1.17	0.95	0.98
Experiment II (Figure 17)	1	C	10.52	0.9999	21.2	0.00	10.81	0.9997	21.83	-0.03	0.01
	2	I	10.28	0.9998	20.8	0.50	10.62	0.9999	21.45	-0.03	-0.01
	3	I	10.19	0.9997	20.6	3.00	10.04	0.9999	20.28	0.01	0.07
	4	I	10.26	0.9993	20.7	6.48	3.83	0.9982	7.73	0.63	0.64
	5	I	9.66	0.9995	19.5	14.82	0.35	0.9169	0.71	0.96	0.99

1 See Section 6.1.2 for a description of the respirometric inhibition assay. Preliminary experiments were used to construct a dose response curve for the inhibitor (Figure 16) that was used as a guide for Experiments I and II that included DNA and RNA extractions.

2 Control vessels (C) received no inhibitor. Inhibited vessels (I) received the prescribed inhibitor dose.

3 Oxygen uptake rates were determined using regression line slopes of ≈ 4 hours of cumulative oxygen uptake and time data before (OUR1) and after (OUR2) the prescribed inhibitor dose. Fit is the regression R^2. OUR1V and OUR2V are OUR1 and OUR2, respectively, corrected for the BSNR mixed liquor sample dilution factor and were used to estimate what constituted "significant" inhibition (Section 6.5).

4 Inhibition is the fraction inhibition value calculated with either respirometric (OUR - Equation 13) or nitrite (NOR - Equation 14) data.

Table E-2 Quantitative PCR results for a 3,5-DCP respirometric inhibition experiment (Experiment I) (Figure 17-A).

Sample[1]			*Nitrobacter* rDNA					*Nitrobacter* rRNAt				
			C_T	copies/(µl extract)		copies/L		C_T	copies/(µl extract)		copies/L	
Time	Vessel	N		Assay	Mean	Assay	Mean		Assay	Mean	Assay	Mean
Before Inhibitor Dose	1	1	23.13	1.09E+05	1.22E+05	4.39E+09	4.90E+09	20.23	1.38E+06	1.58E+06	2.72E+10	3.11E+10
			22.85	1.29E+05		5.18E+09		19.83	1.79E+06		3.53E+10	
			22.86	1.28E+05		5.14E+09		20.05	1.56E+06		3.07E+10	
		2	23.28	1.00E+05	1.02E+05	3.74E+09	3.81E+09	20.84	9.28E+05	1.03E+06	1.82E+10	2.02E+10
			23.31	9.78E+04		3.66E+09		20.65	1.05E+06		2.06E+10	
			23.16	1.07E+05		4.02E+09		20.56	1.11E+06		2.18E+10	
		3	22.88	1.26E+05	1.27E+05	4.47E+09	4.48E+09	20.25	1.37E+06	1.32E+06	3.00E+10	2.89E+10
			22.78	1.34E+05		4.75E+09		20.21	1.40E+06		3.07E+10	
			22.98	1.19E+05		4.23E+09		20.46	1.19E+06		2.61E+10	
After Inhibitor Dose	1	1	23.61	8.24E+04	8.72E+04	3.35E+09	3.55E+09	20.05	1.56E+06	1.47E+06	2.90E+10	2.73E+10
			23.32	9.74E+04		3.96E+09		20.01	1.60E+06		2.97E+10	
			23.62	8.18E+04		3.33E+09		20.38	1.26E+06		2.34E+10	
		2	23.31	9.81E+04	1.00E+05	3.92E+09	4.01E+09	20.56	1.12E+06	1.21E+06	2.22E+10	2.41E+10
			23.41	9.23E+04		3.69E+09		20.49	1.17E+06		2.33E+10	
			23.11	1.10E+05		4.41E+09		20.26	1.35E+06		2.69E+10	
		3	23.31	9.80E+04	1.15E+05	3.97E+09	4.66E+09	20.76	9.74E+05	1.18E+06	1.53E+10	1.86E+10
			22.90	1.25E+05		5.06E+09		20.49	1.17E+06		1.84E+10	
			22.94	1.22E+05		4.94E+09		20.21	1.40E+06		2.21E+10	
After Inhibitor Dose	2	1	23.15	1.08E+05	1.05E+05	4.28E+09	4.17E+09	23.30	1.85E+05	1.76E+05	3.66E+09	3.49E+09
			23.26	1.01E+05		4.00E+09		23.36	1.77E+05		3.50E+09	
			23.17	1.06E+05		4.22E+09		23.44	1.68E+05		3.32E+09	
		2	23.05	1.15E+05	1.10E+05	4.25E+09	4.08E+09	24.20	1.02E+05	9.50E+04	1.85E+09	1.72E+09
			23.07	1.13E+05		4.20E+09		24.25	9.84E+04		1.78E+09	
			23.25	1.02E+05		3.78E+09		24.49	8.42E+04		1.52E+09	
		3	22.97	1.20E+05	1.06E+05	4.68E+09	4.15E+09	23.77	1.35E+05	1.17E+05	2.44E+09	2.10E+09
			23.15	1.08E+05		4.20E+09		24.12	1.08E+05		1.94E+09	
			23.43	9.14E+04		3.57E+09		24.13	1.07E+05		1.93E+09	

Table E-2 Continued.

Sample[1]			*Nitrobacter* rDNA					*Nitrobacter* rRNAt				
			C_T	copies/(µl extract)		copies/L		C_T	copies/(µl extract)		copies/L	
Time	Vessel	N		Assay	Mean	Assay	Mean		Assay	Mean	Assay	Mean
After Inhibitor Dose	3	1	23.96	6.68E+04	6.17E+04	2.72E+09	2.52E+09	25.31	4.93E+04	4.52E+04	9.85E+08	9.02E+08
			24.10	6.17E+04		2.52E+09		25.43	4.56E+04		9.11E+08	
			24.24	5.66E+04		2.31E+09		25.61	4.05E+04		8.10E+08	
		2	-	-	9.83E+04	-	3.93E+09	26.23	2.70E+04	2.49E+04	5.37E+08	4.95E+08
			23.11	1.10E+05		4.41E+09		26.27	2.62E+04		5.22E+08	
			23.53	8.63E+04		3.45E+09		26.58	2.14E+04		4.27E+08	
		3	23.59	8.31E+04	8.27E+04	3.24E+09	3.23E+09	27.68	1.03E+04	9.49E+03	2.17E+08	1.99E+08
			23.51	8.75E+04		3.41E+09		27.86	9.20E+03		1.93E+08	
			23.71	7.77E+04		3.03E+09		27.91	8.93E+03		1.87E+08	
After Inhibitor Dose	4	1	23.49	8.82E+04	7.86E+04	3.37E+09	3.00E+09	26.63	2.06E+04	2.11E+04	3.11E+08	3.18E+08
			23.82	7.26E+04		2.77E+09		26.49	2.27E+04		3.42E+08	
			23.77	7.50E+04		2.86E+09		26.68	2.00E+04		3.01E+08	
		2	24.26	5.61E+04	5.65E+04	2.26E+09	2.28E+09	27.33	1.31E+04	1.37E+04	2.07E+08	2.17E+08
			24.23	5.69E+04		2.29E+09		27.16	1.46E+04		2.32E+08	
			24.25	5.63E+04		2.27E+09		27.28	1.35E+04		2.14E+08	
		3	23.94	6.76E+04	7.48E+04	2.69E+09	2.98E+09	27.94	8.77E+03	1.03E+04	1.60E+08	1.88E+08
			23.51	8.74E+04		3.48E+09		27.46	1.20E+04		2.19E+08	
			23.90	6.94E+04		2.76E+09		27.70	1.02E+04		1.86E+08	
After Inhibitor Dose	5	1	24.08	6.25E+04	6.77E+04	2.51E+09	2.71E+09	28.22	7.26E+03	8.67E+03	1.44E+08	1.72E+08
			23.82	7.26E+04		2.91E+09		27.90	8.98E+03		1.78E+08	
			23.93	6.80E+04		2.73E+09		27.77	9.78E+03		1.94E+08	
		2	23.65	8.05E+04	7.12E+04	3.17E+09	2.81E+09	28.45	6.26E+03	6.55E+03	1.27E+08	1.33E+08
			24.01	6.50E+04		2.56E+09		28.32	6.83E+03		1.39E+08	
			23.93	6.81E+04		2.68E+09		28.38	6.55E+03		1.33E+08	
		3	23.80	7.36E+04	6.91E+04	2.92E+09	2.74E+09	29.36	3.44E+03	3.76E+03	7.03E+07	7.70E+07
			24.01	6.51E+04		2.58E+09		29.24	3.73E+03		7.63E+07	
			23.92	6.86E+04		2.72E+09		29.08	4.13E+03		8.44E+07	

1 Samples were collected immediately before or ≈ 4.5 hours after the inhibitor was added (Table E-1); N = a number assigned to replicate DNA/RNA extracts for each sample.

Table E-3 Quantitative PCR results for a 3,5-DCP respirometric inhibition experiment (Experiment II) (Figure 17-B).

Sample[1]			*Nitrobacter* rDNA					*Nitrobacter* rRNAt				
			C_T	copies/(µl extract)		copies/L		C_T	copies/(µl extract)		copies/L	
Time	Vessel	N		Assay	Mean	Assay	Mean		Assay	Mean	Assay	Mean
Before Inhibitor Dose	1	1	23.27	8.67E+04	9.24E+04	3.42E+09	3.64E+09	21.30	7.79E+05	8.71E+05	1.39E+10	1.56E+10
			23.03	9.99E+04		3.94E+09		21.04	9.27E+05		1.66E+10	
			23.20	9.04E+04		3.57E+09		21.07	9.06E+05		1.62E+10	
		2	23.38	8.09E+04	9.08E+04	3.08E+09	3.45E+09	21.06	9.10E+05	1.10E+06	1.27E+10	1.53E+10
			23.20	9.04E+04		3.44E+09		20.90	1.01E+06		1.41E+10	
			23.01	1.01E+05		3.84E+09		20.43	1.37E+06		1.90E+10	
		3	27.11	8.83E+04	9.58E+04	3.55E+09	3.85E+09	20.84	1.05E+06	9.61E+05	1.63E+10	1.49E+10
			26.98	9.53E+04		3.83E+09		21.04	9.26E+05		1.44E+10	
			26.84	1.04E+05		4.17E+09		21.07	9.05E+05		1.41E+10	
After Inhibitor Dose	1	1	23.11	9.50E+04	9.01E+04	3.85E+09	3.65E+09	21.76	5.82E+05	6.18E+05	1.22E+10	1.30E+10
			23.33	8.37E+04		3.39E+09		21.69	6.09E+05		1.28E+10	
			23.18	9.15E+04		3.71E+09		21.56	6.62E+05		1.39E+10	
		2	22.87	1.10E+05	1.17E+05	4.47E+09	4.78E+09	20.69	1.16E+06	1.21E+06	1.73E+10	1.80E+10
			22.43	1.43E+05		5.83E+09		20.70	1.15E+06		1.71E+10	
			23.04	9.93E+04		4.05E+09		20.49	1.32E+06		1.96E+10	
		3	28.22	4.55E+04	5.58E+04	1.83E+09	2.24E+09	21.75	5.85E+05	8.62E+05	9.43E+09	1.39E+10
			27.79	5.89E+04		2.37E+09		21.11	8.86E+05		1.43E+10	
			27.68	6.30E+04		2.53E+09		20.75	1.11E+06		1.79E+10	
After Inhibitor Dose	2	1	22.45	1.41E+05	1.26E+05	5.70E+09	5.10E+09	21.09	8.96E+05	9.29E+05	1.59E+10	1.64E+10
			22.81	1.14E+05		4.60E+09		21.06	9.13E+05		1.62E+10	
			22.67	1.24E+05		5.00E+09		20.95	9.78E+05		1.73E+10	
		2	23.06	9.82E+04	9.18E+04	3.94E+09	3.68E+09	20.86	1.04E+06	9.16E+05	1.76E+10	1.55E+10
			23.36	8.21E+04		3.29E+09		21.20	8.32E+05		1.41E+10	
			23.11	9.51E+04		3.81E+09		21.12	8.80E+05		1.49E+10	
		3	27.11	8.83E+04	9.58E+04	3.57E+09	3.88E+09	20.70	1.15E+06	1.05E+06	2.16E+10	1.98E+10
			26.98	9.53E+04		3.86E+09		20.94	9.88E+05		1.86E+10	
			26.84	1.04E+05		4.20E+09		20.88	1.02E+06		1.92E+10	

Table E-3 Continued.

Sample[1]			*Nitrobacter* rDNA					*Nitrobacter* rRNAt				
			C_T	copies/(µl extract)		copies/L		C_T	copies/(µl extract)		copies/L	
Time	Vessel	N		Assay	Mean	Assay	Mean		Assay	Mean	Assay	Mean
After Inhibitor Dose	3	1	23.48	7.63E+04	7.09E+04	3.11E+09	2.89E+09	21.76	5.81E+05	5.14E+05	1.00E+10	8.89E+09
			23.81	6.28E+04		2.55E+09		22.12	4.61E+05		7.98E+09	
			23.54	7.36E+04		3.00E+09		21.99	5.01E+05		8.66E+09	
		2	23.56	7.27E+04	8.61E+04	2.94E+09	3.49E+09	22.23	4.28E+05	4.56E+05	8.06E+09	8.58E+09
			23.26	8.69E+04		3.52E+09		22.19	4.41E+05		8.29E+09	
			23.05	9.89E+04		4.01E+09		22.00	4.99E+05		9.39E+09	
		3	22.89	1.09E+05	1.13E+05	4.45E+09	4.65E+09	22.96	2.69E+05	2.71E+05	4.88E+09	4.91E+09
			22.76	1.17E+05		4.80E+09		22.85	2.89E+05		5.24E+09	
			22.80	1.15E+05		4.70E+09		23.05	2.54E+05		4.60E+09	
After Inhibitor Dose	4	1	23.42	7.93E+04	7.38E+04	3.14E+09	2.92E+09	27.75	1.23E+04	1.16E+04	2.37E+08	2.23E+08
			23.66	6.86E+04		2.71E+09		27.92	1.11E+04		2.12E+08	
			23.54	7.36E+04		2.91E+09		27.86	1.14E+04		2.20E+08	
		2	23.78	6.37E+04	5.83E+04	2.49E+09	1.85E+09	27.73	1.25E+04	1.25E+04	2.45E+08	2.46E+08
			24.03	5.52E+04		2.16E+09		27.74	1.24E+04		2.44E+08	
			24.00	5.61E+04		2.19E+09		27.71	1.27E+04		2.49E+08	
		3	23.80	6.31E+04	6.63E+04	2.46E+09	2.28E+09	28.00	1.05E+04	1.24E+04	1.91E+08	2.27E+08
			23.59	7.17E+04		2.80E+09		27.52	1.43E+04		2.62E+08	
			23.77	6.41E+04		2.50E+09		27.72	1.25E+04		2.29E+08	
After Inhibitor Dose	5	1	23.80	6.31E+04	6.63E+04	2.46E+09	2.59E+09	29.05	5.35E+03	6.77E+03	1.04E+08	1.31E+08
			23.59	7.17E+04		2.80E+09		28.60	7.11E+03		1.38E+08	
			23.77	6.41E+04		2.50E+09		28.45	7.85E+03		1.52E+08	
		2	21.10	6.30E+04	5.36E+04	2.51E+09	2.14E+09	28.47	7.77E+03	8.47E+03	1.29E+08	1.41E+08
			21.41	5.24E+04		2.09E+09		28.23	9.04E+03		1.50E+08	
			21.64	4.55E+04		1.82E+09		28.31	8.61E+03		1.43E+08	
		3	21.10	6.30E+04	5.36E+04	2.51E+09	2.14E+09	27.89	1.12E+04	1.18E+04	1.89E+08	1.98E+08
			21.41	5.24E+04		2.09E+09		27.83	1.17E+04		1.97E+08	
			21.64	4.55E+04		1.82E+09		27.74	1.24E+04		2.08E+08	

1 Samples were collected immediately before or ≈ 4.5 hours after the inhibitor was added (Table E-1); N = a number assigned to replicate DNA/RNA extracts for each sample.

Table E-4 Results for batch respirometric inhibition experiments using the inhibitor azide.

Experiment[1]	Vessel		OUR1 (mg/L/hr)[3]			Azide (M)	OUR2 (mg/L/hr)[3]			Inhibition[4]	
	Number	Type[2]	Slope	Fit	OUR1V		Slope	Fit	OUR2V	OUR	NOR
Preliminary	1	C	5.99	0.9997	-	0	5.40	0.9995	-	0.10	-
	2	I	5.84	0.9985	-	5.00E-05	0.77	0.7705	-	0.87	-
	3	I	5.81	0.9984	-	9.99E-05	0.38	0.8662	-	0.93	-
	4	I	5.84	0.9986	-	5.00E-04	0.52	0.8818	-	0.91	-
	5	I	5.85	0.9984	-	9.99E-04	0.29	0.7336	-	0.95	-
Preliminary	1	C	8.13	0.9984	20.3	0	8.50	0.9986	21.24	-0.04	-
	2	I	7.71	0.9963	19.3	8.88E-07	5.67	5.6688	14.17	0.26	-
	3	I	9.20	0.9977	20.4	3.00E-05	1.12	0.9528	2.48	0.88	-
	4	I	9.08	0.9984	20.2	3.75E-05	1.01	0.8676	2.24	0.89	-
	5	I	8.16	0.9981	20.4	4.44E-05	0.82	0.8330	2.04	0.90	-
Preliminary	1	C	7.67	0.9971	17.0	0	8.20	0.9995	18.22	-0.07	-
	2	I	7.92	0.9972	17.6	1.00E-05	1.33	0.9868	2.95	0.83	0.76
	3	I	8.16	0.9964	18.1	1.51E-05	1.05	0.9598	2.32	0.87	0.82
	4	I	7.95	0.9928	17.7	2.01E-05	0.81	0.9277	1.81	0.90	0.87
	5	I	7.74	0.9971	17.2	5.02E-05	0.58	0.8174	1.28	0.93	0.91
Preliminary	1	C	9.78	0.9992	21.7	0	9.67	0.9998	21.48	0.01	0.05
	2	I	9.92	0.9979	22.0	5.02E-06	2.34	0.9855	5.19	0.76	0.81
	3	I	10.42	0.9989	23.2	7.53E-06	1.92	0.9767	4.27	0.82	0.83
	4	I	9.37	0.9969	20.8	1.00E-05	1.53	0.9738	3.41	0.84	0.87
	5	I	10.00	0.9988	22.2	2.51E-05	1.02	0.8576	2.27	0.90	0.94
Preliminary	1	C	9.53	0.9987	21.2	0	9.72	0.9993	21.61	-0.02	0.08
	2	I	9.48	0.9986	21.1	1.11E-07	9.37	0.9992	20.83	0.01	0.06
	3	I	11.03	0.9987	24.5	5.02E-07	8.12	0.9987	18.05	0.26	0.26
	4	I	10.48	0.9994	23.3	1.00E-06	6.99	0.9967	15.54	0.33	0.37
	5	I	10.34	0.9991	23.0	5.02E-06	3.19	0.9810	7.10	0.69	0.81
	6	I	10.21	0.9997	22.7	1.00E-05	1.52	0.9435	3.37	0.85	0.89

Table E-4 Continued.

Experiment[1]	Vessel		OUR1 (mg/L/hr)[3]			Azide (M)	OUR2 (mg/L/hr)[3]			Inhibition[4]	
	Number	Type[2]	Slope	Fit	OUR1V		Slope	Fit	OUR2V	OUR	NOR
Preliminary	1	I	11.81	0.9997	23.6	2.02E-07	11.42	0.9993	22.85	0.03	-0.03
	2	I	12.23	0.9990	24.5	3.03E-07	11.26	0.9992	22.52	0.08	0.06
	3	I	12.09	0.9993	24.2	4.04E-07	10.75	0.9998	21.51	0.11	0.07
	4	I	11.63	0.9997	23.3	2.02E-06	5.72	0.9963	11.44	0.51	0.52
	5	I	11.69	0.9988	23.4	3.03E-06	4.27	0.9990	8.54	0.63	0.67
Preliminary	1	I	12.50	0.9989	25.0	1.01E-06	8.08	0.9980	16.15	0.35	0.32
	2	I	11.97	0.9995	23.9	2.02E-06	5.52	0.9992	11.05	0.54	0.53
	3	I	11.50	0.9985	23.0	1.01E-05	1.94	0.9467	3.88	0.83	0.85
	4	I	12.30	0.9988	24.6	1.51E-05	1.41	0.9437	2.82	0.89	0.88
Experiment III (Figure 20)	1	C	10.59	0.9998	21.2	0	11.13	0.9994	22.26	-0.05	-0.01
	2	I	10.65	0.9997	21.3	1.01E-07	10.98	0.9992	21.97	-0.03	0.02
	3	I	10.43	0.9995	20.9	7.04E-07	10.73	0.9993	21.47	-0.03	0.00
	4	I	10.33	0.9998	20.7	2.01E-06	5.30	0.9982	10.59	0.49	0.53
	5	I	10.16	0.9993	20.3	4.02E-06	3.20	0.9943	6.39	0.69	0.71
Experiment IV (Figure 20)	1	C	10.22	0.9995	20.4	0	10.97	0.9997	21.93	-0.07	-0.06
	2	I	9.69	0.9997	19.4	1.00E-06	6.96	0.9995	13.93	0.28	0.30
	3	I	9.48	0.9998	19.0	3.01E-06	3.55	0.9990	7.09	0.63	0.67
	4	I	9.68	0.9997	19.4	6.02E-06	2.40	0.9956	4.80	0.75	0.76
	5	I	9.83	0.9997	19.7	2.01E-05	1.13	0.9799	2.27	0.88	0.89

1 See Section 6.1.2 for a description of the respirometric inhibition assay. Preliminary experiments were used to construct a dose response curve for the inhibitor (Figure 19) that was used as a guide for Experiments III and IV that included DNA and RNA extractions.

2 Control vessels (C) received no inhibitor. Inhibited vessels (I) received the prescribed inhibitor dose.

3 Oxygen uptake rates were determined using regression line slopes of ≈ 4 hours of cumulative oxygen uptake and time data before (OUR1) and after (OUR2) the prescribed inhibitor dose. Fit is the regression R^2. OUR1V and OUR2V are OUR1 and OUR2, respectively, corrected for the BSNR mixed liquor sample dilution factor and were used to estimate what constituted "significant" inhibition (Section 6.5).

4 Inhibition is the fraction inhibition value calculated with either respirometric (OUR - Equation 13) or nitrite (NOR - Equation 14) data.

Table E-5 Quantitative PCR results for an azide respirometric inhibition experiment (Experiment III) (Figure 20-A).

Sample Event[1]			Real-Time PCR (*Nitrobacter* rDNA)					Real-Time RT-PCR (*Nitrobacter* rRNAt)				
			Threshold Cycle	copies/[µl extract]		copies/L		Threshold Cycle	copies/[µl extract]		copies/L	
Time	Vessel	N		assay	mean	assay	mean		Assay	Mean	Assay	Mean
Before Inhibitor Dose	1	1	22.02	1.10E+05	1.38E+05	4.34E+09	5.44E+09	19.75	1.26E+06	1.26E+06	2.39E+10	2.40E+10
			21.54	1.46E+05		5.76E+09		19.74	1.26E+06		2.40E+10	
			21.42	1.57E+05		6.21E+09		19.74	1.26E+06		2.40E+10	
		2	22.14	1.03E+05	1.27E+05	3.97E+09	4.92E+09	19.27	1.71E+06	1.62E+06	2.63E+10	2.49E+10
			21.77	1.28E+05		4.95E+09		19.41	1.56E+06		2.41E+10	
			21.50	1.50E+05		5.82E+09		19.40	1.57E+06		2.42E+10	
		3	21.44	1.56E+05	1.51E+05	6.11E+09	5.92E+09	19.97	1.09E+06	1.13E+06	2.10E+10	2.18E+10
			21.63	1.39E+05		5.46E+09		19.87	1.17E+06		2.25E+10	
			21.42	1.57E+05		6.18E+09		19.91	1.14E+06		2.19E+10	
After Inhibitor Dose	1	1	21.44	1.56E+05	1.51E+05	5.77E+09	5.59E+09	19.28	1.71E+06	1.44E+06	2.95E+10	2.49E+10
			21.63	1.39E+05		5.16E+09		19.62	1.37E+06		2.37E+10	
			21.42	1.57E+05		5.84E+09		19.77	1.24E+06		2.15E+10	
		2	21.69	1.34E+05	1.41E+05	5.16E+09	5.43E+09	19.49	1.48E+06	1.62E+06	2.79E+10	3.05E+10
			21.53	1.47E+05		5.69E+09		19.43	1.55E+06		2.91E+10	
			21.60	1.41E+05		5.45E+09		19.17	1.83E+06		3.44E+10	
		3	22.27	9.51E+04	1.19E+05	3.63E+09	4.53E+09	19.33	1.65E+06	1.50E+06	3.00E+10	2.71E+10
			21.84	1.23E+05		4.69E+09		19.43	1.54E+06		2.80E+10	
			21.64	1.38E+05		5.27E+09		19.70	1.30E+06		2.35E+10	
After Inhibitor Dose	2	1	21.11	1.89E+05	2.05E+05	7.00E+09	7.59E+09	19.68	1.32E+06	1.34E+06	2.52E+10	2.56E+10
			21.03	1.98E+05		7.34E+09		19.68	1.32E+06		2.53E+10	
			20.79	2.28E+05		8.45E+09		19.61	1.37E+06		2.63E+10	
		2	21.36	1.63E+05	1.58E+05	6.08E+09	5.89E+09	20.05	1.04E+06	1.03E+06	2.04E+10	2.02E+10
			21.49	1.51E+05		5.63E+09		20.07	1.02E+06		2.00E+10	
			21.39	1.60E+05		5.96E+09		20.07	1.02E+06		2.01E+10	
		3	21.16	1.83E+05	1.80E+05	7.34E+09	7.20E+09	19.33	1.65E+06	1.68E+06	3.02E+10	3.07E+10
			21.35	1.64E+05		6.58E+09		19.34	1.64E+06		3.00E+10	
			21.08	1.92E+05		7.68E+09		19.24	1.75E+06		3.20E+10	

Table E-5 Continued.

Sample Event[1]			Real-Time PCR (*Nitrobacter* rDNA)					Real-Time RT-PCR (*Nitrobacter* rRNAt)				
			Threshold Cycle	copies/[µl extract]		copies/L		Threshold Cycle	copies/[µl extract]		copies/L	
Time	Vessel	N		assay	mean	assay	mean		Assay	Mean	Assay	Mean
After Inhibitor Dose	3	1	21.22	1.77E+05	1.58E+05	6.26E+09	5.60E+09	20.25	9.09E+05	1.03E+06	1.76E+10	1.99E+10
			21.60	1.41E+05		4.99E+09		20.09	1.01E+06		1.95E+10	
			21.42	1.57E+05		5.55E+09		19.87	1.16E+06		2.25E+10	
		2	21.53	1.47E+05	1.79E+05	5.44E+09	6.64E+09	19.19	1.81E+06	1.48E+06	3.00E+10	2.46E+10
			21.09	1.91E+05		7.07E+09		19.65	1.34E+06		2.22E+10	
			21.01	2.00E+05		7.40E+09		19.70	1.30E+06		2.15E+10	
		3	22.40	8.80E+04	9.49E+04	3.51E+09	3.79E+09	19.90	1.14E+06	1.04E+06	1.92E+10	1.75E+10
			22.14	1.03E+05		4.11E+09		20.29	8.85E+05		1.49E+10	
			22.30	9.37E+04		3.74E+09		19.96	1.10E+06		1.85E+10	
After Inhibitor Dose	4	1	21.30	1.68E+05	1.49E+05	6.38E+09	5.64E+09	20.80	6.38E+05	5.26E+05	1.13E+10	9.34E+09
			21.60	1.42E+05		5.36E+09		21.15	5.09E+05		9.04E+09	
			21.65	1.37E+05		5.19E+09		21.40	4.30E+05		7.65E+09	
		2	21.91	1.18E+05	1.03E+05	4.50E+09	3.91E+09	20.91	5.91E+05	5.00E+05	1.02E+10	8.65E+09
			22.14	1.03E+05		3.91E+09		21.49	4.06E+05		7.03E+09	
			22.42	8.73E+04		3.33E+09		21.17	5.02E+05		8.69E+09	
		3	21.74	1.30E+05	1.22E+05	5.16E+09	4.83E+09	20.81	6.31E+05	6.25E+05	9.28E+09	9.19E+09
			21.86	1.21E+05		4.81E+09		20.66	6.97E+05		1.02E+10	
			21.96	1.14E+05		4.53E+09		21.03	5.47E+05		8.04E+09	
After Inhibitor Dose	5	1	21.87	1.21E+05	1.15E+05	4.63E+09	4.39E+09	22.24	2.51E+05	2.35E+05	3.58E+09	3.35E+09
			22.08	1.07E+05		4.08E+09		22.37	2.31E+05		3.30E+09	
			21.93	1.16E+05		4.46E+09		22.42	2.23E+05		3.18E+09	
		2	21.88	1.20E+05	1.12E+05	4.44E+09	4.15E+09	22.46	2.16E+05	2.15E+05	3.24E+09	3.22E+09
			22.07	1.07E+05		3.97E+09		22.36	2.31E+05		3.47E+09	
			22.03	1.09E+05		4.05E+09		22.61	1.97E+05		2.96E+09	
		3	21.98	1.13E+05	1.05E+05	4.36E+09	4.06E+09	22.42	2.22E+05	1.95E+05	3.32E+09	2.91E+09
			22.16	1.01E+05		3.92E+09		22.88	1.66E+05		2.47E+09	
			22.17	1.01E+05		3.90E+09		22.61	1.97E+05		2.94E+09	

1 Samples were collected immediately before or ≈ 4.5 hours after the inhibitor was added (Table E-4); N = a number assigned to replicate DNA/RNA extracts for each sample.

Table E-6 Quantitative PCR results for an azide respirometric inhibition experiment (Experiment IV) (Figure 20-B).

Sample[1]			*Nitrobacter* rDNA					*Nitrobacter* rRNAt				
			C_T	copies/(µl extract)		copies/L		C_T	copies/(µl extract)		copies/L	
Time	Vessel	N		Assay	Mean	Assay	Mean		Assay	Mean	Assay	Mean
Before Inhibitor Dose	1	1	22.05	1.50E+05	1.38E+05	5.41E+09	4.98E+09	19.14	1.21E+06	1.15E+06	2.17E+10	2.05E+10
			22.16	1.41E+05		5.09E+09		19.26	1.12E+06		2.00E+10	
			22.40	1.23E+05		4.42E+09		19.28	1.11E+06		1.98E+10	
		2	22.19	1.38E+05	1.20E+05	5.26E+09	4.58E+09	19.39	1.03E+06	9.39E+05	2.15E+10	1.96E+10
			22.39	1.24E+05		4.70E+09		19.80	7.81E+05		1.63E+10	
			22.76	9.90E+04		3.77E+09		19.42	1.01E+06		2.10E+10	
		3	-	-	-	-	-	19.30	1.09E+06	1.14E+06	1.67E+10	1.73E+10
			-	-		-		19.20	1.17E+06		1.79E+10	
			-	-		-		19.24	1.14E+06		1.74E+10	
After Inhibitor Dose	1	1	22.25	1.34E+05	1.41E+05	4.50E+09	4.76E+09	19.26	1.13E+06	1.11E+06	1.99E+10	1.97E+10
			22.01	1.54E+05		5.20E+09		19.42	1.01E+06		1.79E+10	
			22.23	1.35E+05		4.56E+09		19.15	1.21E+06		2.14E+10	
		2	22.37	1.25E+05	1.33E+05	5.10E+09	5.41E+09	18.85	1.47E+06	1.85E+06	2.34E+10	2.93E+10
			22.15	1.42E+05		5.80E+09		18.56	1.80E+06		2.85E+10	
			22.29	1.31E+05		5.34E+09		18.20	2.28E+06		3.61E+10	
		3	-	-	-	-	-	19.28	1.11E+06	1.14E+06	1.71E+10	1.75E+10
			-	-		-		19.13	1.23E+06		1.89E+10	
			-	-		-		19.33	1.07E+06		1.65E+10	
After Inhibitor Dose	2	1	22.39	1.23E+05	1.19E+05	5.06E+09	4.88E+09	19.56	9.17E+05	9.32E+05	1.47E+10	1.50E+10
			22.43	1.21E+05		4.94E+09		19.67	8.55E+05		1.37E+10	
			22.53	1.13E+05		4.65E+09		19.40	1.02E+06		1.64E+10	
		2	22.55	1.13E+05	1.14E+05	4.64E+09	4.69E+09	19.50	9.60E+05	8.83E+05	1.66E+10	1.52E+10
			22.49	1.16E+05		4.78E+09		19.70	8.38E+05		1.45E+10	
			22.54	1.13E+05		4.66E+09		19.68	8.51E+05		1.47E+10	
		3	-	-	-	-	-	19.75	8.12E+05	7.58E+05	1.49E+10	1.39E+10
			-	-		-		19.79	7.91E+05		1.45E+10	
			-	-		-		20.03	6.70E+05		1.23E+10	

Table E-6 Continued.

Sample[1]			*Nitrobacter* rDNA					*Nitrobacter* rRNAt				
			C_T	copies/(µl extract)		copies/L		C_T	copies/(µl extract)		copies/L	
Time	Vessel	N		Assay	Mean	Assay	Mean		Assay	Mean	Assay	Mean
After Inhibitor Dose	3	1	23.06	8.32E+04	6.98E+04	3.17E+09	2.66E+09	21.33	2.82E+05	3.24E+05	4.89E+09	5.61E+09
			23.42	6.77E+04		2.58E+09		20.92	3.72E+05		6.46E+09	
			23.67	5.84E+04		2.22E+09		21.16	3.16E+05		5.48E+09	
		2	22.39	1.23E+05	9.86E+04	4.65E+09	3.72E+09	20.33	5.49E+05	4.61E+05	8.51E+09	7.15E+09
			22.93	9.00E+04		3.40E+09		20.87	3.84E+05		5.95E+09	
			23.07	8.26E+04		3.12E+09		20.63	4.50E+05		6.98E+09	
		3	-	-	-	-	-	21.14	3.22E+05	3.36E+05	6.25E+09	6.52E+09
			-	-		-		21.04	3.43E+05		6.66E+09	
			-	-		-		21.04	3.42E+05		6.65E+09	
After Inhibitor Dose	4	1	23.31	7.18E+04	7.05E+04	2.61E+09	2.56E+09	22.25	1.53E+05	1.31E+05	2.83E+09	2.41E+09
			23.16	7.85E+04		2.85E+09		22.59	1.22E+05		2.26E+09	
			23.59	6.11E+04		2.22E+09		22.66	1.16E+05		2.15E+09	
		2	23.52	6.38E+04	5.25E+04	2.45E+09	2.02E+09	21.45	2.61E+05	2.09E+05	4.56E+09	3.65E+09
			24.01	4.78E+04		1.83E+09		22.18	1.60E+05		2.79E+09	
			24.07	4.61E+04		1.77E+09		21.80	2.07E+05		3.61E+09	
		3	-	-	-	-	-	22.16	1.62E+05	1.65E+05	2.62E+09	2.66E+09
			-	-		-		22.04	1.76E+05		2.84E+09	
			-	-		-		22.21	1.57E+05		2.52E+09	
After Inhibitor Dose	5	1	23.15	7.92E+04	7.20E+04	2.99E+09	2.72E+09	23.34	7.41E+04	6.44E+04	1.36E+09	1.19E+09
			23.18	7.78E+04		2.93E+09		23.66	5.97E+04		1.10E+09	
			23.65	5.90E+04		2.23E+09		23.67	5.95E+04		1.10E+09	
		2	23.24	7.52E+04	6.50E+04	2.73E+09	2.36E+09	23.04	9.01E+04	9.81E+04	1.36E+09	1.49E+09
			23.53	6.33E+04		2.30E+09		22.65	1.17E+05		1.77E+09	
			23.72	5.65E+04		2.05E+09		23.10	8.70E+04		1.32E+09	
		3	-	-	-	-	-	22.78	1.07E+05	9.76E+04	1.72E+09	1.57E+09
			-	-		-		22.96	9.54E+04		1.53E+09	
			-	-		-		23.04	9.02E+04		1.45E+09	

1 Samples were collected immediately before or ≈ 4.5 hours after the inhibitor was added (Table E-4); N = a number assigned to replicate DNA/RNA extracts for each sample.

Table E-7 Results for batch respirometric inhibition experiments using the inhibitor H^+ (sudden acidic pH changes).

Experiment[1]	Vessel		OUR1 (mg/L/hr)[3]			pH	OUR2 (mg/L/hr)[3]			Inhibition[4]	
	Number	Type[2]	Slope	Fit	OUR1V		Slope	Fit	OUR2V	OUR	NOR
Preliminary	1	I	10.35	0.9992	20.8	7.57	10.12	0.9996	20.35	0.02	0.03
	2	I	9.96	0.9991	20.0	7.83	8.53	0.9996	17.15	0.14	0.16
	3	I	10.08	0.9993	20.3	8.13	3.10	0.9983	6.23	0.69	0.65
	4	I	9.83	0.9991	19.8	8.61	2.27	0.9977	4.57	0.77	0.78
	5	I	7.16	0.9781	14.4	8.90	1.36	0.9920	2.74	0.81	0.87
Preliminary	1	I	10.04	0.9999	20.2	7.81	7.39	0.9984	14.84	0.26	0.32
	2	I	9.83	0.9999	19.8	8.95	1.30	0.9932	2.62	0.87	0.89
	3	I	9.83	1.0000	19.8	9.65	0.65	0.9844	1.31	0.93	1.01
	4	I	9.24	0.9998	18.6	10.10	0.42	0.9373	0.85	0.95	1.00
	5	I	8.94	0.9999	18.0	10.89	0.24	0.8889	0.48	0.97	0.91
Preliminary	1	C	9.86	0.9995	19.8	7.28	10.61	0.9994	21.33	-0.08	-0.08
	2	I	9.72	0.9997	19.5	7.00	10.83	0.9987	21.76	-0.11	-0.10
	3	I	9.48	0.9998	19.1	6.72	10.28	0.9992	20.65	-0.08	-0.03
	4	I	9.23	0.9998	18.6	6.51	9.32	0.9978	18.74	-0.01	0.06
	5	I	6.61	0.9996	-	4.38	0.00	0.0001	-	1.00	0.91
Preliminary	1	C	11.30	0.9993	22.7	7.21	11.21	0.9985	22.52	0.01	0.06
	2	I	10.65	0.9995	21.4	6.38	10.71	0.9997	21.53	-0.01	0.04
	3	I	10.53	0.9995	21.2	6.00	8.24	0.9956	16.56	0.22	0.31
	4	I	10.46	0.9993	21.0	5.36	1.94	0.9919	3.89	0.81	0.81
	5	I	9.93	0.9994	20.0	4.87	-0.03	0.0658	-0.07	1.00	0.97
Preliminary	1	I	10.16	0.9988	20.4	6.08	9.27	0.9948	18.63	0.09	0.15
	2	I	10.22	0.9998	20.5	5.84	6.00	0.9951	12.06	0.41	0.38
	3	I	10.08	0.9992	20.3	5.57	3.25	0.9928	6.53	0.68	0.65
	4	I	10.12	0.9998	20.3	5.22	0.11	0.3447	0.22	0.99	0.87
	5	I	10.12	0.9990	20.3	5.04	0.13	0.2288	0.26	0.99	1.00

Table E-7 Continued.

Experiment[1]	Vessel		OUR1 (mg/L/hr)[3]			pH	OUR2 (mg/L/hr)[3]			Inhibition[4]	
	Number	Type[2]	Slope	Fit	OUR1V		Slope	Fit	OUR2V	OUR	NOR
Preliminary	1	C	10.89	0.9999	21.8	7.27	11.06	0.9998	22.11	-0.02	-0.05
	2	I	10.65	0.9998	21.3	6.03	5.03	0.9816	10.06	0.53	0.49
	3	I	9.47	0.9997	18.9	5.50	1.12	0.9521	2.24	0.88	0.88
	4	I	10.29	0.9999	20.6	5.36	1.00	0.9130	2.01	0.90	0.88
	5	I	10.22	0.9998	20.4	5.01	0.27	0.7530	0.54	0.97	0.97
Experiment V (Figure 23)	1	C	12.09	0.9935	24.2	7.41	11.70	0.9999	23.41	0.03	-
	2	I	10.38	0.9989	20.8	5.81	2.99	0.9715	5.98	0.71	0.67
	3	I	11.40	0.9990	22.8	5.57	2.64	0.9904	5.29	0.77	0.76
	4	I	10.30	0.9991	20.6	5.15	1.09	0.9058	2.18	0.89	0.90
	5	I	11.25	0.9994	22.5	4.56	-0.01	0.0000	-0.01	1.00	0.98
Experiment VI (Figure 23)	1	C	12.61	0.9962	25.1	7.28	12.43	0.9994	24.73	0.01	-
	2	I	12.34	0.9991	24.6	5.66	6.43	0.9921	12.79	0.48	0.44
	3	I	12.65	0.9993	25.2	5.25	1.60	0.8824	3.19	0.87	0.81
	4	I	12.70	0.9990	25.3	4.98	0.13	0.5436	0.26	0.99	0.99
	5	I	12.60	0.9992	25.1	4.42	0.00	0.0000	0.00	1.00	0.94

1 See Section 6.1.2 for a description of the respirometric inhibition assay. Preliminary experiments were used to construct a dose response curve for the inhibitor (Figure 22) that was used as a guide for Experiments V and VI that included DNA and RNA extractions.

2 Control vessels (C) received no inhibitor. Inhibited vessels (I) received the prescribed inhibitor dose.

3 Oxygen uptake rates were determined using regression line slopes of ≈ 4 hours of cumulative oxygen uptake and time data before (OUR1) and after (OUR2) the prescribed inhibitor dose. Fit is the regression R^2. OUR1V and OUR2V are OUR1 and OUR2, respectively, corrected for the BSNR mixed liquor sample dilution factor and were used to estimate what constituted "significant" inhibition (Section 6.5).

4 Inhibition is the fraction inhibition value calculated with either respirometric (OUR - Equation 13) or nitrite (NOR - Equation 14) data.

Table E-8 Quantitative PCR results for an H^+ (acid) respirometric inhibition experiment (Experiment V) (Figure 24-A).

Sample[1]			*Nitrobacter* rDNA					*Nitrobacter* rRNAt				
			C_T	copies/(µl extract)		copies/L		C_T	copies/(µl extract)		copies/L	
Time	Vessel	N		Assay	Mean	Assay	Mean		Assay	Mean	Assay	Mean
Before Inhibitor Dose	1	1	22.37	1.61E+05	1.62E+05	6.32E+09	6.35E+09	20.63	8.49E+05	7.49E+05	1.56E+10	1.37E+10
			22.17	1.81E+05		7.09E+09		20.90	7.14E+05		1.31E+10	
			22.56	1.44E+05		5.65E+09		20.97	6.82E+05		1.25E+10	
		2	22.47	1.52E+05	1.57E+05	5.57E+09	5.74E+09	20.71	8.08E+05	7.90E+05	1.42E+10	1.39E+10
			22.42	1.56E+05		5.74E+09		20.93	6.98E+05		1.23E+10	
			22.36	1.61E+05		5.92E+09		20.60	8.65E+05		1.52E+10	
		3	22.83	1.23E+05	1.29E+05	4.34E+09	4.57E+09	20.69	8.16E+05	8.74E+05	1.48E+10	1.59E+10
			22.68	1.34E+05		4.74E+09		20.64	8.47E+05		1.54E+10	
			22.72	1.31E+05		4.63E+09		20.44	9.60E+05		1.74E+10	
After Inhibitor Dose	1	1	22.10	1.89E+05	1.84E+05	6.89E+09	6.72E+09	20.10	1.20E+06	1.17E+06	1.46E+10	1.42E+10
			22.09	1.90E+05		6.94E+09		20.02	1.27E+06		1.54E+10	
			22.24	1.73E+05		6.34E+09		20.33	1.04E+06		1.26E+10	
		2	22.36	1.62E+05	1.83E+05	5.17E+09	5.83E+09	20.61	8.61E+05	8.62E+05	1.41E+10	1.41E+10
			22.06	1.93E+05		6.18E+09		20.60	8.66E+05		1.42E+10	
			22.06	1.93E+05		6.16E+09		20.61	8.60E+05		1.41E+10	
		3	22.39	1.59E+05	1.78E+05	5.19E+09	5.82E+09	20.12	1.18E+06	1.18E+06	1.65E+10	1.64E+10
			22.09	1.90E+05		6.20E+09		20.15	1.16E+06		1.62E+10	
			22.12	1.86E+05		6.07E+09		20.12	1.18E+06		1.65E+10	
After Inhibitor Dose	2	1	21.86	2.18E+05	1.96E+05	7.35E+09	6.62E+09	21.82	3.92E+05	3.84E+05	8.43E+09	8.26E+09
			22.00	2.00E+05		6.77E+09		21.91	3.69E+05		7.95E+09	
			22.28	1.70E+05		5.74E+09		21.82	3.91E+05		8.41E+09	
		2	22.58	1.43E+05	1.34E+05	5.69E+09	5.36E+09	19.96	1.32E+06	7.55E+05	2.76E+10	1.58E+10
			22.46	1.52E+05		6.09E+09		21.45	4.97E+05		1.04E+10	
			23.05	1.08E+05		4.30E+09		21.60	4.51E+05		9.45E+09	
		3	22.63	1.38E+05	1.41E+05	5.06E+09	5.15E+09	22.03	3.42E+05	4.39E+05	7.26E+09	9.32E+09
			22.47	1.52E+05		5.56E+09		21.50	4.82E+05		1.02E+10	
			22.71	1.32E+05		4.83E+09		21.47	4.92E+05		1.05E+10	

Table E-8 Continued.

Sample[1]			*Nitrobacter* rDNA					*Nitrobacter* rRNAt				
			C_T	copies/(µl extract)		copies/L		C_T	copies/(µl extract)		copies/L	
Time	Vessel	N		Assay	Mean	Assay	Mean		Assay	Mean	Assay	Mean
After Inhibitor Dose	3	1	22.54	1.46E+05	1.47E+05	5.60E+09	5.64E+09	22.19	3.08E+05	3.20E+05	5.57E+09	5.78E+09
			22.52	1.48E+05		5.68E+09		22.23	3.00E+05		5.43E+09	
			22.53	1.47E+05		5.64E+09		21.98	3.52E+05		6.36E+09	
		2	22.90	1.18E+05	1.13E+05	4.68E+09	4.50E+09	22.31	2.84E+05	2.87E+05	4.43E+09	4.47E+09
			23.03	1.09E+05		4.35E+09		22.25	2.95E+05		4.60E+09	
			22.98	1.12E+05		4.46E+09		22.32	2.82E+05		4.39E+09	
		3	23.23	9.69E+04	9.87E+04	4.37E+09	4.46E+09	21.88	3.77E+05	4.32E+05	6.93E+09	7.93E+09
			23.21	9.83E+04		4.44E+09		21.73	4.15E+05		7.62E+09	
			23.16	1.01E+05		4.56E+09		21.43	5.04E+05		9.25E+09	
After Inhibitor Dose	4	1	22.07	1.92E+05	1.83E+05	6.66E+09	6.33E+09	23.51	1.30E+05	1.21E+05	1.96E+09	1.82E+09
			22.11	1.87E+05		6.47E+09		23.61	1.22E+05		1.84E+09	
			22.29	1.69E+05		5.85E+09		23.76	1.10E+05		1.66E+09	
		2	22.23	1.75E+05	1.85E+05	6.45E+09	6.82E+09	23.19	1.60E+05	1.40E+05	2.25E+09	1.96E+09
			22.02	1.98E+05		7.29E+09		23.38	1.42E+05		1.98E+09	
			22.15	1.83E+05		6.73E+09		23.67	1.17E+05		1.64E+09	
		3	22.97	1.13E+05	1.28E+05	4.91E+09	5.55E+09	23.67	1.17E+05	1.16E+05	1.77E+09	1.75E+09
			22.59	1.42E+05		6.15E+09		23.47	1.33E+05		2.01E+09	
			22.75	1.29E+05		5.58E+09		23.95	9.75E+04		1.47E+09	
After Inhibitor Dose	5	1	21.89	2.13E+05	2.30E+05	7.80E+09	8.45E+09	20.16	1.16E+06	1.06E+06	1.99E+10	1.82E+10
			21.76	2.30E+05		8.43E+09		20.33	1.03E+06		1.77E+10	
			21.63	2.49E+05		9.12E+09		20.39	9.97E+05		1.71E+10	
		2	22.39	1.59E+05	1.63E+05	5.69E+09	5.82E+09	20.60	8.66E+05	8.11E+05	1.48E+10	1.38E+10
			22.37	1.61E+05		5.76E+09		20.51	9.21E+05		1.57E+10	
			22.29	1.69E+05		6.02E+09		21.05	6.45E+05		1.10E+10	
		3	21.99	2.01E+05	1.87E+05	7.16E+09	6.67E+09	20.37	1.01E+06	1.01E+06	1.74E+10	1.73E+10
			22.13	1.85E+05		6.58E+09		20.41	9.80E+05		1.68E+10	
			22.22	1.76E+05		6.27E+09		20.33	1.03E+06		1.78E+10	

1 Samples were collected immediately before or ≈ 4.5 hours after the inhibitor was added (Table E-7); N = a number assigned to replicate DNA/RNA extracts for each sample.

Table E-9 Quantitative PCR results for an H^+ (acid) respirometric inhibition experiment (Experiment VI) (Figure 24).

Sample[1]			*Nitrobacter* rDNA					*Nitrobacter* rRNAt				
			C_T	copies/(µl extract)		copies/L		C_T	copies/(µl extract)		copies/L	
Time	Vessel	N		Assay	Mean	Assay	Mean		Assay	Mean	Assay	Mean
Before Inhibitor Dose	1	1	22.99	1.86E+05	1.94E+05	7.15E+09	7.47E+09	20.18	1.11E+06	1.11E+06	1.68E+10	1.69E+10
			22.74	2.15E+05		8.27E+09		20.06	1.21E+06		1.82E+10	
			23.03	1.82E+05		7.00E+09		20.30	1.02E+06		1.55E+10	
		2	22.81	2.06E+05	2.22E+05	7.94E+09	8.53E+09	21.01	6.44E+05	6.79E+05	1.24E+10	1.31E+10
			22.62	2.30E+05		8.86E+09		21.00	6.47E+05		1.25E+10	
			22.63	2.28E+05		8.78E+09		20.78	7.46E+05		1.44E+10	
		3	23.23	1.62E+05	1.66E+05	6.29E+09	6.43E+09	20.23	1.08E+06	1.18E+06	1.72E+10	1.89E+10
			23.15	1.70E+05		6.58E+09		19.93	1.32E+06		2.10E+10	
			23.19	1.66E+05		6.43E+09		20.12	1.16E+06		1.85E+10	
After Inhibitor Dose	1	1	22.81	2.07E+05	2.16E+05	7.35E+09	7.69E+09	19.83	1.40E+06	1.26E+06	2.04E+10	1.84E+10
			22.52	2.43E+05		8.64E+09		19.95	1.29E+06		1.89E+10	
			22.87	1.99E+05		7.08E+09		20.21	1.09E+06		1.59E+10	
		2	22.87	1.99E+05	2.23E+05	7.15E+09	8.03E+09	20.20	1.10E+06	9.91E+05	1.78E+10	1.61E+10
			22.49	2.47E+05		8.88E+09		20.51	8.95E+05		1.45E+10	
			22.66	2.25E+05		8.08E+09		20.37	9.80E+05		1.59E+10	
		3	22.86	2.00E+05	2.16E+05	7.79E+09	8.40E+09	20.24	1.07E+06	1.13E+06	1.59E+10	1.68E+10
			22.60	2.32E+05		9.03E+09		20.14	1.14E+06		1.70E+10	
			22.74	2.15E+05		8.38E+09		20.10	1.17E+06		1.75E+10	
After Inhibitor Dose	2	1	22.38	2.63E+05	2.66E+05	9.20E+09	9.28E+09	20.41	9.52E+05	8.50E+05	1.72E+10	1.54E+10
			22.48	2.48E+05		8.68E+09		20.77	7.54E+05		1.36E+10	
			22.24	2.85E+05		9.95E+09		20.60	8.43E+05		1.52E+10	
		2	22.73	2.16E+05	2.38E+05	8.33E+09	9.19E+09	20.19	1.10E+06	1.01E+06	1.65E+10	1.51E+10
			22.61	2.31E+05		8.89E+09		20.34	1.00E+06		1.50E+10	
			22.35	2.68E+05		1.03E+10		20.45	9.30E+05		1.39E+10	
		3	22.54	2.41E+05	2.19E+05	9.36E+09	8.52E+09	20.62	8.30E+05	8.37E+05	1.37E+10	1.38E+10
			22.80	2.07E+05		8.04E+09		20.58	8.55E+05		1.41E+10	
			22.78	2.10E+05		8.16E+09		20.63	8.25E+05		1.37E+10	

Table E-9 Continued.

Sample[1]			*Nitrobacter* rDNA					*Nitrobacter* rRNAt				
			C_T	copies/(µl extract)		copies/L		C_T	copies/(µl extract)		copies/L	
Time	Vessel	N		Assay	Mean	Assay	Mean		Assay	Mean	Assay	Mean
After Inhibitor Dose	3	1	22.71	2.18E+05	2.20E+05	7.53E+09	7.57E+09	23.00	1.71E+05	1.61E+05	2.56E+09	2.40E+09
			22.67	2.24E+05		7.71E+09		23.12	1.59E+05		2.37E+09	
			22.72	2.17E+05		7.47E+09		23.18	1.52E+05		2.28E+09	
		2	23.02	1.83E+05	2.03E+05	6.97E+09	7.73E+09	23.13	1.57E+05	1.47E+05	2.30E+09	2.15E+09
			22.63	2.28E+05		8.69E+09		23.30	1.40E+05		2.06E+09	
			22.89	1.97E+05		7.51E+09		23.28	1.42E+05		2.08E+09	
		3	22.70	2.19E+05	2.21E+05	7.92E+09	7.97E+09	23.39	1.33E+05	1.19E+05	2.26E+09	2.02E+09
			22.66	2.24E+05		8.09E+09		23.64	1.12E+05		1.91E+09	
			22.70	2.19E+05		7.91E+09		23.65	1.11E+05		1.90E+09	
After Inhibitor Dose	4	1	23.00	1.85E+05	1.77E+05	7.29E+09	6.97E+09	23.78	1.02E+05	1.21E+05	1.92E+09	2.27E+09
			23.16	1.69E+05		6.66E+09		23.58	1.16E+05		2.19E+09	
			23.08	1.77E+05		6.97E+09		23.27	1.44E+05		2.71E+09	
		2	23.17	1.68E+05	1.50E+05	7.99E+09	7.14E+09	23.61	1.15E+05	1.03E+05	1.94E+09	1.75E+09
			23.46	1.42E+05		6.77E+09		23.97	9.00E+04		1.52E+09	
			23.49	1.40E+05		6.66E+09		23.73	1.05E+05		1.78E+09	
		3	-	-	-	-	-	-	-	-	-	-
			-	-		-		-	-		-	
			-	-		-		-	-		-	
After Inhibitor Dose	5	1	22.33	2.70E+05	2.31E+05	9.12E+09	7.81E+09	20.44	9.36E+05	9.33E+05	1.45E+10	1.45E+10
			22.59	2.34E+05		7.90E+09		20.42	9.48E+05		1.47E+10	
			22.96	1.89E+05		6.40E+09		20.48	9.14E+05		1.42E+10	
		2	23.22	1.63E+05	1.41E+05	6.17E+09	5.33E+09	20.35	9.94E+05	1.07E+06	1.41E+10	1.52E+10
			23.28	1.58E+05		5.98E+09		20.16	1.13E+06		1.60E+10	
			24.06	1.01E+05		3.83E+09		20.21	1.09E+06		1.55E+10	
		3	23.20	1.65E+05	1.52E+05	5.89E+09	5.41E+09	21.06	6.22E+05	8.18E+05	9.22E+09	1.21E+10
			23.22	1.63E+05		5.81E+09		20.48	9.12E+05		1.35E+10	
			23.66	1.27E+05		4.53E+09		20.46	9.21E+05		1.37E+10	

1 Samples were collected immediately before or ≈ 4.5 hours after the inhibitor was added (Table E-7); N = a number assigned to replicate DNA/RNA extracts for each sample.

Table E-10 Quantitative PCR results for an ammonia respirometric inhibition experiment (Experiment VII) (Figure 29).

Sample[1]			*Nitrobacter* rDNA)					*Nitrobacter* rRNAt				
			C_T	copies/(µl extract)		copies/L		C_T	copies/(µl extract)		copies/L	
Time, hrs	Vessel	N		Assay	Mean	assay	mean		Assay	Mean	Assay	Mean
4.5	1	1	23.41	1.44E+05	1.42E+05	1.05E+10	1.04E+10	21.56	9.00E+05	8.93E+05	1.55E+10	1.54E+10
			23.55	1.32E+05		9.69E+09		21.43	9.82E+05		1.69E+10	
			23.35	1.49E+05		1.09E+10		21.74	7.99E+05		1.38E+10	
		2	24.17	9.09E+04	9.39E+04	6.47E+09	6.68E+09	21.52	9.21E+05	7.32E+05	1.66E+10	1.32E+10
			23.97	1.03E+05		7.30E+09		22.11	6.21E+05		1.12E+10	
			24.22	8.81E+04		6.27E+09		22.04	6.52E+05		1.17E+10	
		3	23.55	1.32E+05	1.54E+05	8.16E+09	9.48E+09	21.70	8.18E+05	8.32E+05	1.43E+10	1.45E+10
			23.42	1.42E+05		8.79E+09		21.73	8.00E+05		1.40E+10	
			22.98	1.86E+05		1.15E+10		21.60	8.77E+05		1.53E+10	
4.5	2	1	24.40	7.91E+04	8.76E+04	5.42E+09	6.01E+09	22.04	6.52E+05	6.20E+05	1.18E+10	1.12E+10
			24.22	8.84E+04		6.06E+09		22.08	6.35E+05		1.15E+10	
			24.09	9.53E+04		6.53E+09		22.23	5.74E+05		1.04E+10	
		2	24.76	6.40E+04	6.99E+04	4.73E+09	5.17E+09	23.38	2.66E+05	2.74E+05	5.80E+09	5.99E+09
			24.46	7.63E+04		5.65E+09		23.23	2.95E+05		6.44E+09	
			24.62	6.94E+04		5.14E+09		23.40	2.63E+05		5.74E+09	
		3	24.10	9.50E+04	1.03E+05	5.53E+09	5.98E+09	24.65	1.14E+05	-	2.23E+09	-
			23.85	1.10E+05		6.43E+09		24.44	1.31E+05		2.56E+09	
			23.97	1.03E+05		5.98E+09		24.47	1.29E+05		2.52E+09	
4.5	3	1	23.18	1.20E+05	1.16E+05	5.62E+09	5.43E+09	22.87	2.85E+05	3.19E+05	5.92E+09	6.63E+09
			23.18	1.19E+05		5.62E+09		22.57	3.48E+05		7.24E+09	
			23.36	1.08E+05		5.06E+09		22.68	3.23E+05		6.72E+09	
		2	23.29	1.12E+05	1.09E+05	5.36E+09	5.18E+09	22.02	5.00E+05	4.93E+05	9.24E+09	9.11E+09
			23.50	9.91E+04		4.73E+09		22.23	4.36E+05		8.05E+09	
			23.26	1.14E+05		5.45E+09		21.90	5.44E+05		1.00E+10	
		3	23.25	1.15E+05	1.23E+05	5.95E+09	6.39E+09	21.29	8.15E+05	8.11E+05	1.34E+10	1.34E+10
			23.10	1.26E+05		6.51E+09		21.33	7.95E+05		1.31E+10	
			23.04	1.30E+05		6.72E+09		21.27	8.25E+05		1.36E+10	

Table E-10 Continued.

Sample[1]			*Nitrobacter* rDNA)					*Nitrobacter* rRNAt				
			C_T	copies/(µl extract)		copies/L		C_T	copies/(µl extract)		copies/L	
Time, hrs	Vessel	N		Assay	Mean	assay	mean		Assay	Mean	Assay	Mean
4.5	4	1	23.70	8.78E+04	9.19E+04	4.77E+09	4.99E+09	21.32	7.99E+05	8.79E+05	1.33E+10	1.47E+10
			23.65	9.08E+04		4.93E+09		20.98	1.00E+06		1.67E+10	
			23.54	9.69E+04		5.26E+09		21.25	8.38E+05		1.40E+10	
		2	23.30	1.11E+05	1.10E+05	5.52E+09	5.47E+09	22.16	4.57E+05	4.46E+05	1.06E+10	1.04E+10
			23.21	1.18E+05		5.85E+09		22.05	4.90E+05		1.14E+10	
			23.46	1.02E+05		5.05E+09		22.39	3.92E+05		9.12E+09	
		3	22.51	1.77E+05	1.69E+05	1.04E+10	9.91E+09	21.23	8.45E+05	8.28E+05	1.44E+10	1.41E+10
			22.52	1.76E+05		1.03E+10		21.23	8.46E+05		1.44E+10	
			22.74	1.54E+05		9.05E+09		21.33	7.93E+05		1.35E+10	
4.5	5	1	23.21	1.18E+05	1.23E+05	7.34E+09	7.66E+09	23.40	2.00E+05	3.00E+05	4.04E+09	6.05E+09
			23.07	1.28E+05		7.97E+09		22.56	3.49E+05		7.04E+09	
			23.13	1.23E+05		7.68E+09		22.56	3.50E+05		7.06E+09	
		2	-	-	9.42E+04	-	6.21E+09	-	-	3.53E+05	-	6.78E+09
			23.52	9.80E+04		6.47E+09		22.45	3.76E+05		7.23E+09	
			23.66	9.03E+04		5.96E+09		22.65	3.29E+05		6.32E+09	
		3	23.36	1.08E+05	1.18E+05	6.50E+09	7.10E+09	22.16	4.57E+05	5.21E+05	8.12E+09	9.26E+09
			23.10	1.25E+05		7.55E+09		21.97	5.16E+05		9.17E+09	
			23.17	1.20E+05		7.27E+09		21.77	5.90E+05		1.05E+10	
9	3	1	23.49	9.98E+04	1.04E+05	6.43E+09	6.72E+09	23.16	2.34E+05	2.54E+05	4.40E+09	4.76E+09
			23.30	1.11E+05		7.18E+09		22.86	2.87E+05		5.38E+09	
			23.45	1.02E+05		6.56E+09		23.13	2.40E+05		4.49E+09	
		2	23.83	8.16E+04	8.92E+04	4.95E+09	5.41E+09	22.01	5.03E+05	5.76E+05	8.78E+09	1.01E+10
			23.58	9.48E+04		5.74E+09		21.68	6.27E+05		1.10E+10	
			23.64	9.13E+04		5.54E+09		21.75	5.99E+05		1.05E+10	
		3	24.21	6.53E+04	6.97E+04	4.08E+09	4.35E+09	23.25	2.21E+05	2.40E+05	4.28E+09	4.63E+09
			24.09	7.02E+04		4.38E+09		23.17	2.33E+05		4.50E+09	
			24.00	7.36E+04		4.60E+09		22.97	2.66E+05		5.13E+09	

Table E-10 Continued.

Sample[1]			*Nitrobacter* rDNA)					*Nitrobacter* rRNAt				
			C_T	copies/(µl extract)		copies/L		C_T	copies/(µl extract)		copies/L	
Time, hrs	Vessel	N		Assay	Mean	assay	mean		Assay	Mean	Assay	Mean
9	4	1	23.20	1.18E+05	1.08E+05	7.63E+09	6.98E+09	21.77	5.92E+05	5.48E+05	1.08E+10	1.00E+10
			23.26	1.14E+05		7.35E+09		21.75	5.99E+05		1.09E+10	
			23.62	9.21E+04		5.95E+09		22.17	4.55E+05		8.31E+09	
		2	22.71	1.58E+05	1.53E+05	1.04E+10	1.00E+10	22.78	3.03E+05	2.85E+05	5.66E+09	5.33E+09
			22.86	1.44E+05		9.46E+09		22.89	2.82E+05		5.26E+09	
			22.73	1.56E+05		1.02E+10		22.94	2.71E+05		5.07E+09	
		3	23.50	9.92E+04	9.48E+04	6.37E+09	6.09E+09	22.05	4.90E+05	5.43E+05	9.33E+09	1.03E+10
			23.56	9.54E+04		6.13E+09		21.55	6.86E+05		1.31E+10	
			23.67	8.98E+04		5.77E+09		22.17	4.53E+05		8.63E+09	
9	5	1	23.67	8.97E+04	9.26E+04	5.54E+09	5.72E+09	24.20	1.18E+05	1.19E+05	2.05E+09	2.08E+09
			23.61	9.31E+04		5.75E+09		24.34	1.07E+05		1.87E+09	
			23.57	9.50E+04		5.87E+09		24.00	1.34E+05		2.34E+09	
		2	23.52	9.79E+04	9.34E+04	6.84E+09	6.52E+09	24.31	1.09E+05	1.18E+05	2.07E+09	2.23E+09
			23.72	8.71E+04		6.08E+09		24.25	1.14E+05		2.16E+09	
			23.57	9.52E+04		6.65E+09		24.04	1.30E+05		2.46E+09	
		3	23.59	9.40E+04	9.73E+04	5.31E+09	5.49E+09	23.72	1.62E+05	1.93E+05	2.84E+09	3.38E+09
			23.48	1.00E+05		5.67E+09		23.40	2.01E+05		3.52E+09	
			23.53	9.74E+04		5.50E+09		23.29	2.16E+05		3.79E+09	
26	5	1	23.16	1.21E+05	1.10E+05	6.82E+09	6.19E+09	26.14	3.23E+04	3.03E+04	6.83E+08	6.42E+08
			23.34	1.09E+05		6.15E+09		26.28	2.94E+04		6.22E+08	
			23.49	9.94E+04		5.62E+09		26.29	2.94E+04		6.21E+08	
		2	23.29	1.12E+05	1.03E+05	5.64E+09	5.16E+09	26.67	2.27E+04	1.84E+04	4.28E+08	3.47E+08
			23.34	1.09E+05		5.46E+09		27.32	1.48E+04		2.78E+08	
			23.72	8.70E+04		4.36E+09		27.04	1.78E+04		3.35E+08	
		3	23.60	9.36E+04	9.03E+04	5.34E+09	5.16E+09	26.84	2.04E+04	2.05E+04	3.61E+08	3.64E+08
			23.73	8.63E+04		4.93E+09		27.08	1.73E+04		3.07E+08	
			23.64	9.11E+04		5.20E+09		26.59	2.40E+04		4.24E+08	

Table E-10 Continued.

Sample[1]			*Nitrobacter* rDNA)					*Nitrobacter* rRNAt				
			C_T	copies/(µl extract)		copies/L		C_T	copies/(µl extract)		copies/L	
Time, hrs	Vessel	N		Assay	Mean	assay	mean		Assay	Mean	Assay	Mean
67	5	1	23.46	1.01E+05	9.78E+04	5.16E+09	4.98E+09	23.83	1.50E+05	1.51E+05	2.57E+09	2.59E+09
			23.48	1.00E+05		5.10E+09		23.65	1.69E+05		2.90E+09	
			23.63	9.20E+04		4.69E+09		24.00	1.34E+05		2.30E+09	
		2	22.87	1.44E+05	1.35E+05	6.97E+09	6.57E+09	26.51	2.52E+04	-	4.69E+08	-
			22.87	1.44E+05		6.97E+09		26.57	2.42E+04		4.50E+08	
			23.19	1.19E+05		5.77E+09		26.82	2.06E+04		3.83E+08	
		3	23.69	8.85E+04	8.88E+04	3.86E+09	3.88E+09	23.78	1.55E+05	1.60E+05	2.89E+09	2.98E+09
			23.62	9.24E+04		4.04E+09		23.83	1.51E+05		2.80E+09	
			23.75	8.55E+04		3.73E+09		23.61	1.74E+05		3.24E+09	

1 N = a number assigned to replicate DNA/RNA extracts for each sample.

Appendix F

BSNR Inhibition Experiment Data

Table F-1 Quantitative PCR results for a BSNR inhibition experiment (Figure 36).

Sample[1]			*Nitrobacter* rDNA					*Nitrobacter* rRNAt				
			C_T	copies/(µl extract)		copies/L		C_T	copies/(µl extract)		copies/L	
Phase	Time	N		Assay	Mean	Assay	Mean		Assay	Mean	Assay	Mean
1	-0.1	1	21.28	1.66E+05	1.91E+05	6.55E+09	7.53E+09	20.24	8.39E+05	9.15E+05	1.46E+10	1.59E+10
			20.97	2.01E+05		7.91E+09		20.20	8.60E+05		1.49E+10	
			20.93	2.06E+05		8.12E+09		19.90	1.05E+06		1.82E+10	
		2	20.83	2.18E+05	2.49E+05	8.06E+09	9.20E+09	20.39	7.64E+05	8.51E+05	1.36E+10	1.51E+10
			20.63	2.46E+05		9.10E+09		20.30	8.10E+05		1.44E+10	
			20.41	2.82E+05		1.04E+10		20.00	9.79E+05		1.74E+10	
		3	20.14	3.31E+05	3.27E+05	1.23E+10	1.21E+10	-	-	8.61E+05	-	1.39E+10
			20.29	3.03E+05		1.12E+10		20.20	8.63E+05		1.39E+10	
			20.08	3.45E+05		1.28E+10		20.21	8.59E+05		1.39E+10	
1	2.1	1	20.14	3.31E+05	3.27E+05	1.23E+10	1.21E+10	20.92	5.39E+05	5.05E+05	9.02E+09	8.46E+09
			20.29	3.03E+05		1.12E+10		21.27	4.29E+05		7.18E+09	
			20.08	3.45E+05		1.28E+10		20.90	5.49E+05		9.18E+09	
		2	20.97	2.01E+05	2.25E+05	7.52E+09	8.42E+09	23.03	1.37E+05	1.59E+05	2.21E+09	2.56E+09
			20.77	2.27E+05		8.50E+09		22.76	1.64E+05		2.65E+09	
			20.63	2.47E+05		9.26E+09		22.66	1.75E+05		2.82E+09	
		3	21.34	1.60E+05	2.08E+05	6.03E+09	7.80E+09	21.98	2.71E+05	3.89E+05	4.56E+09	6.54E+09
			20.90	2.09E+05		7.86E+09		21.18	4.58E+05		7.70E+09	
			20.59	2.53E+05		9.52E+09		21.24	4.38E+05		7.36E+09	
1	3.1	1	20.20	3.20E+05	3.66E+05	1.25E+10	1.42E+10	21.15	4.65E+05	4.23E+05	7.37E+09	6.71E+09
			20.08	3.43E+05		1.34E+10		21.41	3.93E+05		6.23E+09	
			19.70	4.33E+05		1.69E+10		21.34	4.11E+05		6.52E+09	
		2	20.11	3.39E+05	3.28E+05	1.32E+10	1.28E+10	21.58	3.52E+05	3.79E+05	5.83E+09	6.27E+09
			20.29	3.03E+05		1.18E+10		21.67	3.31E+05		5.48E+09	
			20.09	3.42E+05		1.33E+10		21.19	4.53E+05		7.50E+09	
		3	20.38	2.88E+05	2.71E+05	1.12E+10	1.06E+10	21.81	3.03E+05	2.68E+05	4.86E+09	4.31E+09
			20.58	2.54E+05		9.93E+09		22.15	2.43E+05		3.90E+09	
			20.47	2.72E+05		1.06E+10		22.05	2.59E+05		4.15E+09	

Table F-1 Continued.

Sample[1]			*Nitrobacter* rDNA					*Nitrobacter* rRNAt				
			C_T	copies/(µl extract)		copies/L		C_T	copies/(µl extract)		copies/L	
Phase	Time	N		Assay	Mean	Assay	Mean		Assay	Mean	Assay	Mean
1	4.0	1	20.40	2.84E+05	2.29E+05	1.10E+10	8.87E+09	22.11	2.49E+05	2.37E+05	3.89E+09	3.71E+09
			20.99	1.99E+05		7.70E+09		22.22	2.32E+05		3.63E+09	
			20.95	2.03E+05		7.87E+09		22.23	2.31E+05		3.62E+09	
		2	20.28	3.04E+05	3.01E+05	1.21E+10	1.20E+10	22.34	2.15E+05	2.25E+05	3.51E+09	3.67E+09
			20.33	2.96E+05		1.18E+10		22.35	2.13E+05		3.48E+09	
			20.29	3.03E+05		1.21E+10		22.13	2.46E+05		4.01E+09	
		3	20.64	2.45E+05	2.20E+05	9.51E+09	8.54E+09	22.76	1.63E+05	1.57E+05	2.54E+09	2.45E+09
			20.91	2.08E+05		8.08E+09		22.99	1.41E+05		2.19E+09	
			20.92	2.07E+05		8.02E+09		22.72	1.67E+05		2.60E+09	
1	5.5	1	21.68	1.87E+05	2.16E+05	7.52E+09	8.69E+09	24.09	7.54E+04	1.03E+05	1.23E+09	1.68E+09
			21.27	2.38E+05		9.55E+09		23.25	1.30E+05		2.12E+09	
			21.37	2.24E+05		9.01E+09		23.59	1.04E+05		1.70E+09	
		2	21.38	2.23E+05	2.45E+05	8.50E+09	9.34E+09	23.65	1.00E+05	1.35E+05	1.58E+09	2.13E+09
			21.23	2.43E+05		9.27E+09		23.05	1.48E+05		2.34E+09	
			21.06	2.69E+05		1.02E+10		22.97	1.56E+05		2.47E+09	
		3	21.40	2.20E+05	2.44E+05	9.90E+09	1.10E+10	24.10	7.51E+04	9.04E+04	1.16E+09	1.39E+09
			21.23	2.43E+05		1.10E+10		23.85	8.82E+04		1.36E+09	
			21.06	2.69E+05		1.21E+10		23.54	1.08E+05		1.66E+09	
1	8.1	1	21.56	2.00E+05	2.03E+05	7.92E+09	8.02E+09	25.66	2.72E+04	2.90E+04	4.37E+08	4.65E+08
			21.59	1.97E+05		7.80E+09		25.55	2.94E+04		4.71E+08	
			21.47	2.11E+05		8.34E+09		25.50	3.03E+04		4.86E+08	
		2	21.14	2.56E+05	2.94E+05	9.65E+09	1.11E+10	24.28	6.66E+04	6.79E+04	1.07E+09	1.09E+09
			20.84	3.06E+05		1.15E+10		24.39	6.23E+04		1.00E+09	
			20.75	3.21E+05		1.21E+10		24.10	7.47E+04		1.20E+09	
		3	22.71	1.02E+05	1.26E+05	3.50E+09	4.30E+09	25.20	3.68E+04	5.25E+04	5.84E+08	8.34E+08
			22.26	1.33E+05		4.54E+09		24.74	4.96E+04		7.88E+08	
			22.15	1.42E+05		4.85E+09		24.18	7.12E+04		1.13E+09	

Table F-1 Continued.

Sample[1]			*Nitrobacter* rDNA					*Nitrobacter* rRNAt				
			C_T	copies/(µl extract)		copies/L		C_T	copies/(µl extract)		copies/L	
Phase	Time	N		Assay	Mean	Assay	Mean		Assay	Mean	Assay	Mean
1	24.7	1	20.57	2.55E+05	2.37E+05	1.06E+10	9.83E+09	25.44	2.86E+04	3.12E+04	4.77E+08	5.19E+08
			20.65	2.44E+05		1.01E+10		25.25	3.25E+04		5.41E+08	
			20.88	2.13E+05		8.81E+09		25.25	3.24E+04		5.39E+08	
		2	20.47	2.72E+05	2.16E+05	1.11E+10	8.83E+09	25.72	2.38E+04	2.45E+04	4.00E+08	4.11E+08
			20.88	2.13E+05		8.68E+09		25.60	2.59E+04		4.34E+08	
			21.30	1.65E+05		6.72E+09		25.73	2.38E+04		3.99E+08	
		3	21.17	1.78E+05	1.62E+05	7.25E+09	6.57E+09	25.44	2.86E+04	2.86E+04	4.60E+08	4.60E+08
			21.48	1.47E+05		5.99E+09		25.40	2.94E+04		4.72E+08	
			21.35	1.59E+05		6.47E+09		25.48	2.79E+04		4.47E+08	
1	72.1	1	21.43	1.52E+05	1.34E+05	5.70E+09	5.03E+09	25.51	2.74E+04	2.86E+04	4.13E+08	4.31E+08
			21.93	1.12E+05		4.19E+09		25.47	2.81E+04		4.23E+08	
			21.58	1.39E+05		5.20E+09		25.35	3.03E+04		4.56E+08	
		2	21.38	1.57E+05	1.38E+05	6.01E+09	5.28E+09	25.60	2.58E+04	2.39E+04	3.94E+08	3.66E+08
			21.57	1.40E+05		5.37E+09		25.66	2.48E+04		3.80E+08	
			21.87	1.17E+05		4.47E+09		25.91	2.11E+04		3.24E+08	
		3	22.21	9.48E+04	9.32E+04	3.83E+09	3.77E+09	26.13	1.83E+04	2.24E+04	2.75E+08	3.36E+08
			22.17	9.75E+04		3.94E+09		25.71	2.40E+04		3.61E+08	
			22.35	8.73E+04		3.53E+09		25.66	2.48E+04		3.72E+08	
2	7.9	1	22.23	1.35E+05	1.46E+05	5.26E+09	5.69E+09	24.18	4.23E+04	4.75E+04	6.41E+08	7.20E+08
			22.16	1.41E+05		5.49E+09		23.96	4.90E+04		7.42E+08	
			21.92	1.63E+05		6.32E+09		23.89	5.13E+04		7.78E+08	
		2	22.10	1.46E+05	1.50E+05	5.50E+09	5.68E+09	24.27	3.98E+04	5.25E+04	5.70E+08	7.53E+08
			22.04	1.51E+05		5.72E+09		23.77	5.56E+04		7.97E+08	
			22.01	1.54E+05		5.82E+09		23.60	6.21E+04		8.90E+08	
		3	22.14	1.43E+05	1.36E+05	5.26E+09	5.03E+09	24.32	3.86E+04	4.15E+04	5.89E+08	6.34E+08
			22.33	1.28E+05		4.72E+09		24.08	4.52E+04		6.90E+08	
			22.19	1.39E+05		5.12E+09		24.24	4.06E+04		6.21E+08	

Table F-1 Continued.

Sample[1]			*Nitrobacter* rDNA					*Nitrobacter* rRNAt				
			C_T	copies/(µl extract)		copies/L		C_T	copies/(µl extract)		copies/L	
Phase	Time	N		Assay	Mean	Assay	Mean		Assay	Mean	Assay	Mean
2	20.0	1	21.90	1.14E+05	8.49E+04	4.51E+09	3.35E+09	25.73	2.38E+04	1.69E+04	3.58E+08	2.54E+08
			22.65	7.29E+04		2.87E+09		27.05	1.01E+04		1.52E+08	
			22.77	6.74E+04		2.65E+09		26.26	1.68E+04		2.52E+08	
		2	21.79	1.23E+05	9.55E+04	4.70E+09	3.66E+09	25.75	2.35E+04	1.90E+04	3.81E+08	3.08E+08
			22.41	8.40E+04		3.22E+09		26.23	1.72E+04		2.79E+08	
			22.49	8.00E+04		3.06E+09		26.31	1.63E+04		2.64E+08	
		3	22.35	8.69E+04	8.42E+04	3.22E+09	3.12E+09	26.24	1.71E+04	1.76E+04	2.66E+08	2.73E+08
			22.27	9.17E+04		3.39E+09		26.03	1.95E+04		3.04E+08	
			22.62	7.39E+04		2.73E+09		26.32	1.62E+04		2.51E+08	
2	31.7	1	22.39	1.23E+05	1.07E+05	4.97E+09	4.34E+09	24.92	2.58E+04	2.45E+04	4.91E+08	4.66E+08
			22.72	1.02E+05		4.11E+09		25.07	2.34E+04		4.44E+08	
			22.79	9.74E+04		3.93E+09		25.00	2.44E+04		4.64E+08	
		2	22.24	1.35E+05	1.41E+05	5.33E+09	5.57E+09	24.34	3.79E+04	3.71E+04	6.18E+08	6.05E+08
			22.13	1.44E+05		5.67E+09		24.17	4.25E+04		6.94E+08	
			22.12	1.45E+05		5.71E+09		24.65	3.08E+04		5.03E+08	
		3	22.42	1.21E+05	1.15E+05	4.84E+09	4.61E+09	25.31	1.98E+04	2.52E+04	3.21E+08	4.07E+08
			22.49	1.16E+05		4.64E+09		24.89	2.62E+04		4.24E+08	
			22.61	1.08E+05		4.33E+09		24.72	2.94E+04		4.75E+08	
2	44.1	1	22.25	9.26E+04	8.51E+04	3.59E+09	3.30E+09	25.35	3.03E+04	2.80E+04	4.99E+08	4.62E+08
			22.38	8.57E+04		3.33E+09		25.33	3.07E+04		5.06E+08	
			22.55	7.70E+04		2.99E+09		25.77	2.31E+04		3.80E+08	
		2	22.04	1.05E+05	9.10E+04	4.03E+09	3.47E+09	25.49	2.78E+04	2.79E+04	5.28E+08	5.31E+08
			22.27	9.13E+04		3.48E+09		25.28	3.18E+04		6.05E+08	
			22.57	7.63E+04		2.91E+09		25.70	2.42E+04		4.59E+08	
		3	22.52	7.86E+04	6.78E+04	3.17E+09	2.73E+09	25.66	2.48E+04	2.51E+04	4.18E+08	4.23E+08
			22.81	6.60E+04		2.66E+09		25.75	2.34E+04		3.94E+08	
			23.00	5.89E+04		2.37E+09		25.52	2.71E+04		4.57E+08	

Table F-1 Continued.

Sample[1]			*Nitrobacter* rDNA					*Nitrobacter* rRNAt				
			C_T	copies/(μl extract)		copies/L		C_T	copies/(μl extract)		copies/L	
Phase	Time	N		Assay	Mean	Assay	Mean		Assay	Mean	Assay	Mean
3	11.7	1	21.72	1.12E+05	1.37E+05	4.51E+09	5.51E+09	24.52	4.22E+04	5.43E+04	7.35E+08	9.46E+08
			21.32	1.44E+05		5.80E+09		24.02	5.86E+04		1.02E+09	
			21.21	1.55E+05		6.22E+09		23.94	6.21E+04		1.08E+09	
		2	21.19	1.56E+05	1.88E+05	5.94E+09	7.17E+09	24.34	4.75E+04	6.00E+04	7.89E+08	9.98E+08
			20.94	1.82E+05		6.94E+09		24.01	5.91E+04		9.82E+08	
			20.60	2.26E+05		8.62E+09		23.68	7.35E+04		1.22E+09	
		3	21.30	1.46E+05	1.54E+05	5.77E+09	6.06E+09	24.46	4.39E+04	4.40E+04	7.36E+08	7.38E+08
			21.23	1.53E+05		6.03E+09		24.44	4.45E+04		7.47E+08	
			21.14	1.62E+05		6.37E+09		24.47	4.36E+04		7.32E+08	
3	22.0	1	21.62	1.20E+05	1.20E+05	4.53E+09	4.53E+09	25.06	2.95E+04	2.52E+04	5.31E+08	4.54E+08
			21.82	1.06E+05		4.00E+09		25.63	2.01E+04		3.62E+08	
			21.44	1.34E+05		5.05E+09		25.24	2.61E+04		4.71E+08	
		2	22.09	8.92E+04	9.34E+04	3.66E+09	3.84E+09	25.83	1.76E+04	2.22E+04	3.08E+08	3.89E+08
			22.06	9.09E+04		3.73E+09		25.40	2.35E+04		4.11E+08	
			21.90	1.00E+05		4.12E+09		25.27	2.56E+04		4.48E+08	
		3	22.91	5.36E+04	7.37E+04	2.20E+09	3.03E+09	26.38	1.22E+04	1.50E+04	2.02E+08	2.49E+08
			22.27	7.96E+04		3.27E+09		26.12	1.45E+04		2.40E+08	
			22.11	8.79E+04		3.61E+09		25.77	1.84E+04		3.04E+08	
3	33.9	1	21.38	1.39E+05	1.46E+05	5.50E+09	5.80E+09	25.34	2.45E+04	2.29E+04	4.18E+08	3.91E+08
			21.31	1.45E+05		5.76E+09		25.34	2.44E+04		4.16E+08	
			21.20	1.55E+05		6.14E+09		25.66	1.98E+04		3.38E+08	
		2	21.35	1.41E+05	1.22E+05	5.52E+09	4.79E+09	25.73	1.89E+04	1.83E+04	3.58E+08	3.46E+08
			21.77	1.09E+05		4.26E+09		26.07	1.50E+04		2.85E+08	
			21.65	1.17E+05		4.59E+09		25.58	2.08E+04		3.94E+08	
		3	21.93	9.84E+04	8.82E+04	4.16E+09	3.73E+09	25.44	2.28E+04	1.81E+04	3.60E+08	2.86E+08
			22.08	8.97E+04		3.79E+09		25.91	1.68E+04		2.64E+08	
			22.34	7.64E+04		3.23E+09		26.09	1.48E+04		2.33E+08	

Table F-1 Continued.

Sample[1]			*Nitrobacter* rDNA					*Nitrobacter* rRNAt				
			C_T	copies/(µl extract)		copies/L		C_T	copies/(µl extract)		copies/L	
Phase	Time	N		Assay	Mean	Assay	Mean		Assay	Mean	Assay	Mean
3	45.8	1	21.18	1.57E+05	1.34E+05	6.11E+09	5.21E+09	21.47	3.19E+05	2.81E+05	5.58E+09	4.92E+09
			21.71	1.13E+05		4.39E+09		21.81	2.55E+05		4.46E+09	
			21.47	1.31E+05		5.11E+09		21.73	2.69E+05		4.70E+09	
		2	21.41	1.36E+05	1.50E+05	5.08E+09	5.60E+09	21.25	3.70E+05	4.29E+05	5.92E+09	6.87E+09
			21.31	1.45E+05		5.42E+09		20.95	4.53E+05		7.24E+09	
			21.07	1.69E+05		6.30E+09		20.91	4.65E+05		7.44E+09	
		3	22.17	8.50E+04	8.55E+04	3.60E+09	3.62E+09	21.35	3.47E+05	3.46E+05	5.61E+09	5.58E+09
			22.08	9.01E+04		3.82E+09		21.27	3.67E+05		5.92E+09	
			22.24	8.13E+04		3.44E+09		21.46	3.23E+05		5.22E+09	
3	69.9	1	20.78	2.02E+05	1.93E+05	8.16E+09	7.79E+09	19.61	1.10E+06	1.04E+06	2.40E+10	2.26E+10
			20.89	1.88E+05		7.61E+09		19.93	8.90E+05		1.93E+10	
			20.89	1.88E+05		7.60E+09		19.57	1.13E+06		2.46E+10	
		2	21.07	1.68E+05	1.56E+05	6.61E+09	6.13E+09	19.74	1.01E+06	8.53E+05	1.74E+10	1.46E+10
			21.12	1.63E+05		6.41E+09		20.07	8.14E+05		1.40E+10	
			21.41	1.36E+05		5.36E+09		20.23	7.31E+05		1.25E+10	
		3	21.58	1.23E+05	1.33E+05	4.65E+09	5.03E+09	19.53	1.16E+06	1.06E+06	2.03E+10	1.86E+10
			21.21	1.54E+05		5.85E+09		20.07	8.11E+05		1.42E+10	
			21.60	1.21E+05		4.60E+09		19.46	1.22E+06		2.13E+10	
3	120	1	20.23	2.83E+05	2.96E+05	1.16E+10	1.22E+10	18.59	2.18E+06	2.32E+06	3.49E+10	3.72E+10
			20.15	2.97E+05		1.22E+10		18.78	1.91E+06		3.06E+10	
			20.11	3.06E+05		1.26E+10		18.17	2.87E+06		4.60E+10	
		2	19.72	3.90E+05	3.69E+05	1.52E+10	1.44E+10	18.89	1.78E+06	1.81E+06	3.14E+10	3.19E+10
			19.68	3.99E+05		1.56E+10		19.01	1.64E+06		2.89E+10	
			20.05	3.18E+05		1.24E+10		18.70	2.02E+06		3.55E+10	
		3	20.29	2.73E+05	2.85E+05	1.07E+10	1.12E+10	18.84	1.84E+06	1.83E+06	3.32E+10	3.30E+10
			20.19	2.91E+05		1.14E+10		18.96	1.70E+06		3.05E+10	
			20.19	2.91E+05		1.14E+10		18.75	1.96E+06		3.53E+10	

Table F-1 Continued.

Sample[1]			*Nitrobacter* rDNA					*Nitrobacter* rRNAt				
			C_T	copies/(µl extract)		copies/L		C_T	copies/(µl extract)		copies/L	
Phase	Time	N		Assay	Mean	Assay	Mean		Assay	Mean	Assay	Mean
3	168	1	18.93	6.37E+05	4.68E+05	2.37E+10	1.74E+10	17.83	3.60E+06	2.74E+06	6.40E+10	4.87E+10
			19.67	4.02E+05		1.49E+10		18.55	2.23E+06		3.96E+10	
			19.83	3.65E+05		1.35E+10		18.44	2.40E+06		4.26E+10	
		2	18.98	6.18E+05	4.80E+05	2.43E+10	1.88E+10	17.68	3.98E+06	2.91E+06	6.73E+10	4.91E+10
			19.66	4.05E+05		1.59E+10		18.35	2.54E+06		4.30E+10	
			19.61	4.17E+05		1.64E+10		18.58	2.19E+06		3.71E+10	
		3	19.23	5.30E+05	5.05E+05	2.00E+10	1.91E+10	18.19	2.82E+06	2.81E+06	4.88E+10	4.86E+10
			19.17	5.47E+05		2.07E+10		18.12	2.98E+06		5.15E+10	
			19.53	4.38E+05		1.66E+10		18.30	2.63E+06		4.55E+10	
3	216	1	19.81	3.68E+05	3.14E+05	1.41E+10	1.20E+10	19.45	1.23E+06	9.44E+05	1.92E+10	1.48E+10
			20.06	3.16E+05		1.21E+10		20.08	8.07E+05		1.26E+10	
			20.39	2.56E+05		9.82E+09		20.09	8.00E+05		1.25E+10	
		2	20.00	3.27E+05	2.92E+05	1.31E+10	1.17E+10	20.13	7.78E+05	9.09E+05	1.29E+10	1.51E+10
			20.11	3.06E+05		1.23E+10		19.54	1.16E+06		1.92E+10	
			20.48	2.43E+05		9.76E+09		20.11	7.93E+05		1.31E+10	
		3	19.97	3.33E+05	2.93E+05	1.32E+10	1.16E+10	19.36	1.30E+06	1.36E+06	2.29E+10	2.39E+10
			20.19	2.91E+05		1.15E+10		19.29	1.36E+06		2.39E+10	
			20.40	2.56E+05		1.01E+10		19.22	1.43E+06		2.51E+10	

1 See Table 22 for a full description of the experiment sample events; N = a number assigned to replicate DNA/RNA extracts for each sample.

VITA

Shawn Allen Hawkins was born in South Pittsburg, Tennessee June 16th, 1969. He graduated from South Pittsburg High School in 1987. He received a Bachelor of Science in Engineering with a Minor in Chemistry in 1994 from the University of Tennessee at Chattanooga. Mr. Hawkins worked 5 years in the hazardous waste remediation field before entering the graduate program full time at the University of Tennessee at Knoxville in June, 1999. He graduated with a Master of Science in Environmental Engineering in December, 2000 and completed the requirements for a Doctor of Philosophy degree in Civil Engineering in August, 2005.